Identification of signalling pathways involved in the oxidative stress response triggered by Low Temperature Plasma in prostate epithelial cells and the assessment of tumour-associated allelic expression in Prostate Cancer

John Packer BSc. (Hons)

Ph.D

University of York

Biology

June 2018

Abstract

Pairing of cancer genome and transcriptome data has revealed that heterozygous mutations aren't always expressed in cells. The potential for point mutation or genomic rearrangement to alter tumour allelic expression has implications for understanding cellular heterogeneity and application of treatments. Mutation of SPOP, PTEN and IDH-1 was assessed in 51 primary prostate cancer cultures to establish allelic heterozygosity and ascertain whether oncogenic change to coding regions altered allelic expression. No mutations were detected in the three genes, although 18% of tested cultures had loss of heterozygosity in PTEN. The TMPRSS2-ERG fusion, present in half of all prostate cancers, is selectively expressed at an allelic level by cancer stem cells. Monoallelic expression didn't correlate with TMPRSS2 promoter hypermethylation. Prostate cultures expressed fusion transcript, however epigenetic features of monoallelically expressed genes were not investigated in the epithelial subpopulations. Understanding of allelic chromatin states may inform treatment strategies that permit tumour suppressor expression or oncogenic protein repression.

Inability to predict indolent or aggressive progression of organ-confined prostate cancers has created the problem of surgical overtreatment. Focal therapies targeting the tumour core are being met with increasing rates of recurrence, necessitating development of novel treatments. The anti-cancer properties of Low Temperature Plasma (LTP) are being explored in prostate models where it produces autophagy and necrosis through generation of reactive species. Initial gene expression response to LTP and the activation of upstream transcription factors were analysed. LTP activated Nrf2, AP-1 and Notch signalling in patient matched prostate normal and cancer cultures. The progenitor-containing cell fraction was more responsive to LTP than differentiated epithelial cells in both transcription of response genes and nuclear accumulation of active Notch1. When linked to cell-fate outcomes, these immediate molecular responses of prostate cancer to LTP could be used as hallmarks of resistance or treatment efficacy in patients.

Thesis Contents

Abstract 2

Thesis Contents 3

List of Tables 8

List of Figures 9

Acknowledgements 13

Author's Declaration 14

1.1 - The Prostate; Anatomy and Cellular Hierarchy 15

1.1.1 – Prostate Anatomy 15

1.1.2 – Prostate Development 15

1.1.3 - Cells of the Prostate 18

1.1.4 - Prostate Epithelial Stem Cells 21

1.2 - Disorders of the Prostate 26

1.2.1 - Benign Prostatic Hyperplasia 26

1.2.2 - Prostatitis 26

1.2.3 - Inflammatory Aetiology of Prostate Cancer 26

1.2.4 - Proliferative Inflammatory Atrophy 30

1.2.5 - Prostatic Intraepithelial Neoplasia 31

1.2.6 - General Attributes of Prostate Cancer 33

1.2.7 - Prostate Cancer Epidemiology 33

1.3 - Tumour Heterogeneity and Cancer Stem Cells 36

1.3.1 - Clonal Evolution Model 36

1.3.2 - Linear step carcinogenesis 39

1.3.3 - Field Cancerisation 39

1.3.4 - Cancer Stem Cell Model 40

1.3.5 - Pre-tumour development 44

1.3.6 - The stem cell niche 45

1.3.7 - The immortal strand hypothesis 45

1.3.8 - Cancer relapse; a stem cell triggered event? 46

1.3.9 - Prostate Cancer Stem Cells 47
1.4 - Prostate Cancer Diagnosis 50
1.4.1 - Prostate Specific Antigen Testing 50
1.4.2 - The Gleason Grading System 51
1.4.3 – Treatment of Low Grade Prostate Cancer 54
1.4.4 - Treatment of Advanced Prostate Cancer 57
1.5 – The Genetic Background of Primary Prostate Cancer 61
1.6 - Castrate Resistant Prostate Cancer (CRPC) 65
1.6.1 - Androgen signalling in end-stage disease 65
1.6.2 - Involvement of Basal Cancer Stem Cells in Metastatic disease 67
1.6.3 - Neuroendocrine Prostate Cancer 68
1.6.4 - Genetic heterogeneity in Castrate Resistant Prostate Cancer 69
1.6.5 - Prostate Cancer Invasion and Metastasis 70
1.7 - Prostate Cancer Models 75
1.7.1 - Cell Lines and Primary Cultures 75
1.7.2 - Mouse Models; Xenograft and Transgenic lines 79
1.7.3 - Cancer Stem Cells in Mice 82
1.8 - Alterations of Allelic expression in Prostate Cancer 83
1.8.1 - Classical monoallelic expression 83
1.8.2 - Random monoallelic expression; involvement in cancer? 87
1.8.3 - Epigenetic regulation of random monoallelic expression and perturbation in cancer 89
1.8.4 - Epigenetic modifiers as cancer treatments 94
1.8.5 - PTEN and Prostate Cancer 95
1.8.6 - SPOP and Prostate Cancer 100
1.8.7 - Isocitrate Dehydrogenase-1 and Prostate Cancer 106
1.8.8 - TMPRSS2-ERG; a defining rearrangement in Prostate Cancer 112
1.9 - Low Temperature Plasma and Oxidative Stress 117
1.9.1 - Low Temperature Plasma as an anticancer therapy 117
1.9.2 - Oxidative Stress – Antioxidant and Transcriptional Response 117

1.9.3 - Cell Fate in LTP induced Oxidative Stress 120

1.9.4 - Oxidative Stress in Prostate Cancer 121

2. Thesis Aims.....123

3. Materials and Methods.....124

3.1 –Cell and Tissue Culture.....124

3.2 – Molecular Analyses 126

3.3 - Low Temperature Plasma Treatments.....138

3.4 - Allelic Expression Experiments 142

4. Results – Determination if common tumourigenic alterations to genes in prostate cancers alters their allelic expression 143

4.1 – Heterozygosity in TMPRSS2 is common in primary prostate epithelial cultures.....143

4.2 – The TMPRSS2-ERG fusion is expressed in primary prostate epithelial cultures 144

4.3 – Mutations observed in primary prostate cancers aren't represented in current cell lines 155

4.4 – PTEN heterozygous deletion is represented in primary prostate cancer cultures 155

4.5 – Mutations observed in primary tumours aren't observed in primary prostate cancer cultures 155

5. Results– Oxidative stress response signalling in LTP treated primary prostate basal epithelial cells 163

5.1 – Optimisation of plasma dose and post-treatment assessment of gene expression.....163

5.2 – A central oxidative stress response is triggered by LTP in cultures, regardless of pathology 164

5.3 – LTP stimulated the respective activation and accumulation of AP-1 and Nrf2 transcription factors in prostate epithelial cells.....183

5.4 – Development of a cell line model of primary LTP stress response 183

6. Results– Microarray analysis revealed rapid activation of Notch and AP-1 by LTP.....192

6.1 – Microarray data identified activation of multiple signalling pathways by LTP in prostate primary cultures.....192

6.2 – Upstream transcription factors Notch1 and Jun are activated by plasma 193

6.3 – Stem and transit amplifying cells are the plasma-responsive fraction in primary cultures 201

7.1 Discussion – Alterations in allelic expression of genes involved in the molecular pathogenesis of prostate cancer 208

7.1 – Do current cell lines and the primary prostate basal epithelial cultures adequately represent modern prostate cancers? 208

7.1.1 - Cell lines 208

7.1.2 - Primary basal epithelial cultures 208

7.2 Discussion - Stress signalling in LTP treated primary prostate basal epithelial cells 211

7.2.1 - Primary cultures respond more rapidly to plasma treatment than prostate cell lines ...211

7.2.2 - Oxidative stress is initiated by LTP in prostate primary cultures 211

7.2.3 - Gleason 7 cultures have elevated expression of oxidative stress genes over their normal counterparts 213

7.2.4 - The HMOX1 SmartFlare fluorescence doesn't match transcript levels of its target 213

7.2.5 - The transcription factors Nrf2 and AP-1 are activated by Low Temperature Plasma in patient cultures 214

7.2.6 - Interpatient heterogeneity, and not tissue pathology, is the main generator of variability between the oxidative stress transcriptional response in primary cultures 217

7.2.7 - A model of a model; using P4E6 to map LTP induced stress responses in the prostate .218

7.3 Discussion - Microarray analysis reveals rapid activation of Notch and AP-1 by LTP.....221

7.3.1 - Microarray analysis reveals that Low Temperature Plasma significantly alters the expression of multiple genes involved in stress response and cellular fate.....221

7.3.2 – Low Temperature Plasma activates Notch-directed gene expression in primary prostate cultures 222

7.3.3 - Further evidence of AP-1 signalling in plasma treated primary cultures 232

7.3.4 - Activation of NF-kB is not consistently observed in plasma treated cultures 233

7.3.5 – Gene Ontology and KEGG metadata confirms pathway activation and highlights the unfolded protein response, ER stress and a balancing of apoptotic signalling processes in LTP treated prostate epithelia.....238

7.3.6 - Plasma responsive genes of biological interest highlighted by LIMMA analysis.....243

7.3.7 - Basal epithelial subpopulations differ in their molecular responses to plasma.....243

7.3.8 - Stem and transit amplifying cells selectively activate Notch signalling in response to plasma treatment 245

8. Future work.....251

8.1 – Determination of allelic expression changes in prostate cancer 251

8.2 – LTP induced signalling and cell fate outcomes in prostate epithelial subpopulations 254

Appendices.....256

A.1 – Complete Sanger sequence traces of all samples; TMPRSS2, SPOP, PTEN & IDH1 256

A.2 - Development of P4E6 as a stress signalling model of prostate cancer 270

List of Abbreviations used.....274

References 282

List of Tables

TABLE 1 – Cancer Stem Cells of solid tumours.....43

TABLE 2 – Prostate cell lines 76

TABLE 3 – All known PTEN mutations in prostate cancer.....98

TABLE 4 – Location of prostate cancer associated mutations in the PTEN gene.....99

TABLE 5 – All known SPOP mutations in prostate cancer.....104

TABLE 6 – Location of prostate cancer associated mutations in the SPOP gene 105

TABLE 7 – All known IDH-1 mutations in prostate cancer 111

TABLE 8 – TaqMan probes used in study. 130

TABLE 9 – Antibodies used in study. 132

TABLE 10 – PCR information 136

TABLE 11 – Primary samples with known rs12329760 status. 146

TABLE 12 - Primary samples selected for further study of TMPRSS2 allelic expression in fractionated populations. 152

TABLE 13 – Sample information of all patient cultures used in LTP study. 165

TABLE 14 – Summary of conditions and samples used for Oxidative Stress Profiler Arrays 170

TABLE 15 – Signalling Pathway upregulated genes indicated by initial microarray analysis.....228

TABLE 16 – LIMMA-specified and range-separated LTP-upregulated genes.....241

TABLE 17 – Gene Ontology and KEGG Pathway annotations of microarray data 242

List of Figures

FIGURE 1 – Zonal anatomy and situation of the prostate 16

FIGURE 2 - Organisation of the normal prostate epithelium.....20

FIGURE 3 – The stem cell niche and the role it can play in division choice 22

FIGURE 4 – Factors influencing prostate inflammation in carcinogenesis. 29

FIGURE 5 – Proposed staged progression of prostatic disease into prostate cancer.....32

FIGURE 6 – Age as a disease risk-factor in prostate cancer.....34

FIGURE 7 – Linear step, clonal evolution and field cancerisation.....38

FIGURE 8 – CSC model and metastatic relapse.....42

FIGURE 9 – Molecular markers of prostate cancer stem cells.....48

FIGURE 10 - The Gleason grading system. 52

FIGURE 11 – Focal therapies of prostate cancer.....56

FIGURE 12 – Androgen Deprivation Therapy.....59

FIGURE 13 – Defective DNA damage repair response in prostate cancer.....62

FIGURE 14 – Common genetic alterations in primary and castrate resistant prostate cancer. 64

FIGURE 15 – Androgen Receptor aberration in CRPC.....66

FIGURE 16 – Metastatic cascade of prostate cancer 72

FIGURE 17 - Generation of primary prostate epithelial cultures from tissue.....78

FIGURE 18 – Mouse models of prostate cancer 81

FIGURE 19 - X chromosome inactivation 84

FIGURE 20 – Models of Imprinting.....86

FIGURE 21 - Resolution of bivalent chromatin to RME chromatin 91

FIGURE 22 – Literature examples of normal to cancer allelic alterations 93

FIGURE 23 – PTEN signalling and disturbances in Prostate Cancer 96

FIGURE 24 – SPOP signalling in prostate cancer.....101

FIGURE 25 – IDH-1 mutation in prostate cancer 109

FIGURE 26 – Generation of the TMPRRS2-ERG fusion in prostate cancer. 114

FIGURE 27 –Low Temperature Plasma and Reactive Oxygen Species.....118

FIGURE 28 – Allelic expression of TMPRSS2 study structure and the primary cultures assessed for heterozygosity of the gene. 145

FIGURE 29 – Analysis of TMPRSS2 exon 6 DNA from primary prostate cultures for the SNP rs12329760. 147

FIGURE 30 - Sanger sequencing traces of rs12329760 heterozygotes in TMPRSS2 exon 6 of primary cultures. 148

FIGURE 31 – Selection of prostate basal epithelial subpopulations by collagen I adhesion. 149

FIGURE 32 – Confirmation of rs12329760 SNP status in fractionated primary culture samples. ..150

FIGURE 33 – Identification of TMPRSS2-ERG fusion expression in primary prostate cultures.....151

FIGURE 34 – Study plan - Does point mutation in prostate cancer genes affect allelic expression? 153

FIGURE 35 – SPOP, PTEN and IDH-1 aren't mutated in prostate cell lines. 154

FIGURE 36 – Detection of PTEN Loss of Heterozygosity in prostate cancer primary cultures. 157

FIGURE 37 – Primary prostate culture SPOP exon 6+7, PTEN exon 5 and IDH1 exon 6 PCR products. 158

FIGURE 38 – SURVEYOR detection of primary prostate culture SPOP heterozygotes. 159

FIGURE 39 – SPOP Sanger sequence traces of heterozygote primary prostate cancer cultures. ..160

FIGURE 40 – PTEN Sanger sequence traces of heterozygote primary prostate cancer cultures....161

FIGURE 41- IDH1 Sanger sequence traces of primary prostate cancer cultures. 162

FIGURE 42 – Prostate cell line expression of SOD2 in response to LTP is varied.....166

FIGURE 43 - Primary culture stress response gene expression following oxidative treatment. 167

FIGURE 44 - Oxidative stress response array time-point optimisation using the H329/13 LB primary culture. 168

FIGURE 45 - Oxidative stress response array dose optimisation using the H209/12 LA primary culture. 169

FIGURE 46 - Oxidative stress gene response in the H434/14 patient matched pair. 173

FIGURE 47 - Oxidative stress gene response in the H329/13 patient matched pair. 174

FIGURE 48 - Oxidative stress gene response in the H209/12 patient matched pair. 175

FIGURE 49 - Tissue pathology average of oxidative stress response gene expression at 0.5 hours post-LTP. 176

FIGURE 50 - Tissue pathology average of oxidative stress response gene expression at 2 hours post-LTP. 177

FIGURE 51 - Oxidative stress response genes are expressed at higher basal levels in Gleason 7 cultures of patient matched pairs. 178

FIGURE 52 - Oxidative stress gene response in three BPH primary cultures. 179

FIGURE 53 - Oxidative stress gene response in three Gleason 9 primary cultures. 180

FIGURE 54 - Oxidative stress gene expression qRT-PCR array data was reproducible and robust. 181

FIGURE 55 - SmartFlares do not accurately represent transcriptional changes in HMOX1 gene expression. 182

FIGURE 56 - LTP caused accumulation of Nrf2 and activation of AP-1 within 0.5 hours of treatment. 185

FIGURE 57 - Nrf2 is located in the nucleus of primary prostate basal epithelial cultures. 187

FIGURE 58 -pJun is nuclear in primary prostate cultures and phosphorylation was increased by LTP treatment. 188

FIGURE 59 - Arsenite dose response in P4E6 and PNT1a prostate cell lines. 190

FIGURE 60 - HMOX1 and JUN transcript levels in Arsenite and Plasma treated P4E6 and PNT1a prostate cell lines. 191

FIGURE 61 - Microarray RNA sample integrity and initial microarray data shows that LTP treatment alters gene expression. 194

FIGURE 62 - Heatmap of annotated gene expression changes following LTP treatment. 195

FIGURE 63 - Linear Models for Microarray Data (LIMMA) analysis found 89 transcripts were significantly altered by LTP in primary prostate cultures. 196

FIGURE 64 - Validation of 12 genes from initial analysis confirmed robustness of the microarray dataset. 198

FIGURE 65 - LTP activated Notch and AP-1 signalling in primary prostate epithelial cultures. 199

FIGURE 66 - Densitometry analysis of LTP treatment time-course showed activation of Notch, AP-1 and non-canonical NF-kB signalling. 200

FIGURE 67 - Canonical NF-kB signalling in primary prostate cultures is unaffected by LTP. 202

FIGURE 68 - Notch1 is activated by LTP in primary prostate epithelial cultures. 203

FIGURE 69 - NR4A isoform upregulation by LTP was more potent in the SC/TA subpopulation of primary prostate cultures. 204

FIGURE 70 - Epithelial subpopulation analysis of LTP-induced AP-1 and Notch signalling. 205

FIGURE 71 - Notch1 is nuclear in LTP-treated SC/TA cells. 207

FIGURE 72 – Stress induced Nrf2 and AP-1 signalling.....215

FIGURE 73 - Notch signalling.....224

FIGURE 74 – Notch signalling molecule mRNA expression in prostate basal epithelial subpopulations. 225

FIGURE 75 - Inhibition of Notch signalling in primary prostate cultures promoted epithelial differentiation. 227

FIGURE 76 – Canonical and Non-canonical NF-kB signalling elements. 234

FIGURE 77 – Prostate epithelial progenitors express JUN to greater levels than differentiated committed basal cells. 247

FIGURE 78 – Notch signalling and the balance of prostate epithelial stem cell decision. 248

FIGURE 79 – TMPRSS2 exon 6 Sanger sequence traces. 257

FIGURE 80 – SPOP exon 6 and 7 Sanger sequence traces of all samples. 258

FIGURE 81 – PTEN exon 5 Sanger sequence traces of all samples. 262

FIGURE 82 – IDH1 exon 6 Sanger sequence traces of all samples. 266

FIGURE 83 - Stress-reporter Luciferase vector preparation and optimisation of P4E6 transfection. 272

FIGURE 84 - Optimisation of P4E6 chromatin sonication. 273

Acknowledgements

This work was compiled over the course of four years and wouldn't have been finished without the contribution and help of the following people.

To Norman, Fiona, Leanne, Adam and the rest of the Cancer Research Unit. Thank you for your patience, expertise and teaching. You all helped immensely in the writing of this manuscript and in developing me into a "proper" scientist! Thank you for asking the right questions.

To Em. Thank you for keeping me sane when I doubted myself the most.

To Jack, Ben, Gal & Jesse. Thank you for doing life with me, for always making me laugh.

To Matty, Hatty, Dom, Kat, Cam, Mel. Thank you for being family and reminding me what I am capable of.

To Greg. Thank you for showing me who a man can be and should aspire to be. Your kindness and leadership have formed who I am today.

To Ellen & Stu. You guys are home and I'm so proud of you both.

To Mum. Thank you for being so strong when the rest of us weren't. You always know what to say and when to say it. I don't think I would have done this justice without your love and belief.

To Dad. Thank you for being my friend and for showing me the open spaces where I found the most joy and comfort when work got hard. Your wisdom and laughter led the way when I didn't know what to do.

To Amy. My love and wife. Thank you for your patience and sacrifice while I got this done. The knowledge of your love kept me going when things got tough. Thank you for taking me as I am and sharing life with me. I adore you.

To God. Thank you for being my Rock and comforting me when no one else could. With you nothing was and is impossible.

One day this will all stop, and I won't have to rush, or push, or pull, or try. I'll give back everything I took and kiss everyone I love. And I will fall asleep, and not wake up for weeks and weeks.

Reuben, Dusk

Author's Declaration

Work published during the formation of this thesis is listed below;

Packer, JR. & Maitland, NJ. (2016) 'The molecular and cellular origin of human prostate cancer', *Biochimica et Biophysica Acta (BBA) - Molecular Cell Research*, 1863(6, Part A), pp. 1238-1260 [Online]. Available at*: ISSN 0167-4889. https://doi.org/10.1016/j.bbamcr.2016.02.016. (http://www.sciencedirect.com/science/article/pii/S0167488916300416)*

Packer, J R. Hirst, A M. Frame, F M. Maitland, N J. O'Connell, D. (2018) 'Microarray analysis identifies activation of multiple signalling pathways in primary prostate epithelial cells by Low Temperature Plasma.', *Clinical Plasma Medicine*, 9(2-48), pp. 20-21 [Online]. Available at: *http://dx.doi.org/10.1016/j.cpme.2017.12.033*

The following manuscript is currently under consideration for publication;

Packer, J.R. Hirst, A.M. Droop, A. P. Adamson, R. Frame, F. M. O'Connell, D. Maitland, N. J. (2018) 'Activation of Stem Cell Identity and Oxidative Stress Response pathways by Low Temperature Plasma in primary prostate cells.'

Work was presented as posters at the following Conferences and Meetings;

- Yorkshire Cancer Research Annual Research Meeting, July 2015. Pavillions of Harrogate, Harrogate, Yorkshire, United Kingdom.
  "Low Temperature Plasma; A Novel Prostate Cancer Therapy"
- American Association of Cancer Research Developmental Biology and Cancer, November-December 2015. Seaport Hotel, Boston, Massachusetts, United States of America.
  "Epigenetic control of prostate epithelial stem cell differentiation"
- YorkTalks 2017, PhD Research Spotlight Final. January 2017. Spring Lane Building, University of York, York, United Kingdom.
- International Conference of Plasma Medicine, March 2018. University of Greifswald, Greifswald, Germany.
  "Low Temperature Plasma treatment of primary prostate cancer cultures initiates Notch, AP-1 and Nrf2 signalling"

I declare that this thesis is a presentation of original work and I am the sole author. This work has not previously been presented for an award at this, or any other, University. All sources are acknowledged as References.

1.1 - The Prostate; Anatomy and Cellular Hierarchy

1.1.1 – Prostate Anatomy

Situated below the bladder, the prostate is a walnut sized organ that surrounds the descending urethra **(Figure 1)**. In the adult male, the prostate is an accessory sex organ that secretes proteolytic fluid into the ejaculatory duct. This exocrine exudation contains classical markers of the luminal epithelial cell population such as prostatic acid phosphatase (PAP) and prostate specific antigen (PSA), alongside proteases and nutrients that afford sperm greater motility. The alkaline nature of the fluid neutralises the acidic environment of the vaginal canal to increase sperm viability **(1)**.

The prostate itself is made up of distinct heterogeneous tissues surrounded by a vascularised stromal capsule. Four separate prostatic zones have been classified **(Figure 1)**;

- Peripheral Zone (PZ) – makes up ~70% of the glandular prostate and is situated at the posterior of the gland. This is the region where prostatic intraepithelial neoplasia (PIN), (the supposed precursor to cancer) and the majority of adenocarcinomas form.
- Central Zone (CZ) – ~25% of the glandular prostate tissue. The CZ surrounds the vesicular seminalis ductal tube to where it meets the urethra (verumontanum). This section of the prostate is rarely implicated in disease with ~3% of tumours originating in the CZ **(2)**.
- Transitional Zone (TZ) – constitutes ~5% of the glandular prostate and is found at the anterior of the gland. It surrounds the transitional urethra, immediately below the bladder. This region continually grows in a hormone dependent manner and is the tissue in which benign prostatic hyperplasia (BPH) arises. Population studies have indicated that ~25% of prostate cancers initiate in this zone of tissue **(3)**.
- Anterior Zone (AZ) - lacks any glandular structure and consists of fibromuscular stroma **(1, 4)**.

1.1.2 – Prostate Development

The generation of this anatomically complex organ begins with coordinated tissue development from the urogenital sinus (UGS) in a process called branching morphogenesis. Here, epithelial buds from the UGS invade the surrounding mesenchyme with subsequent elongation and branching, forming the epithelial ducts and acini of the adult prostate **(5)**.

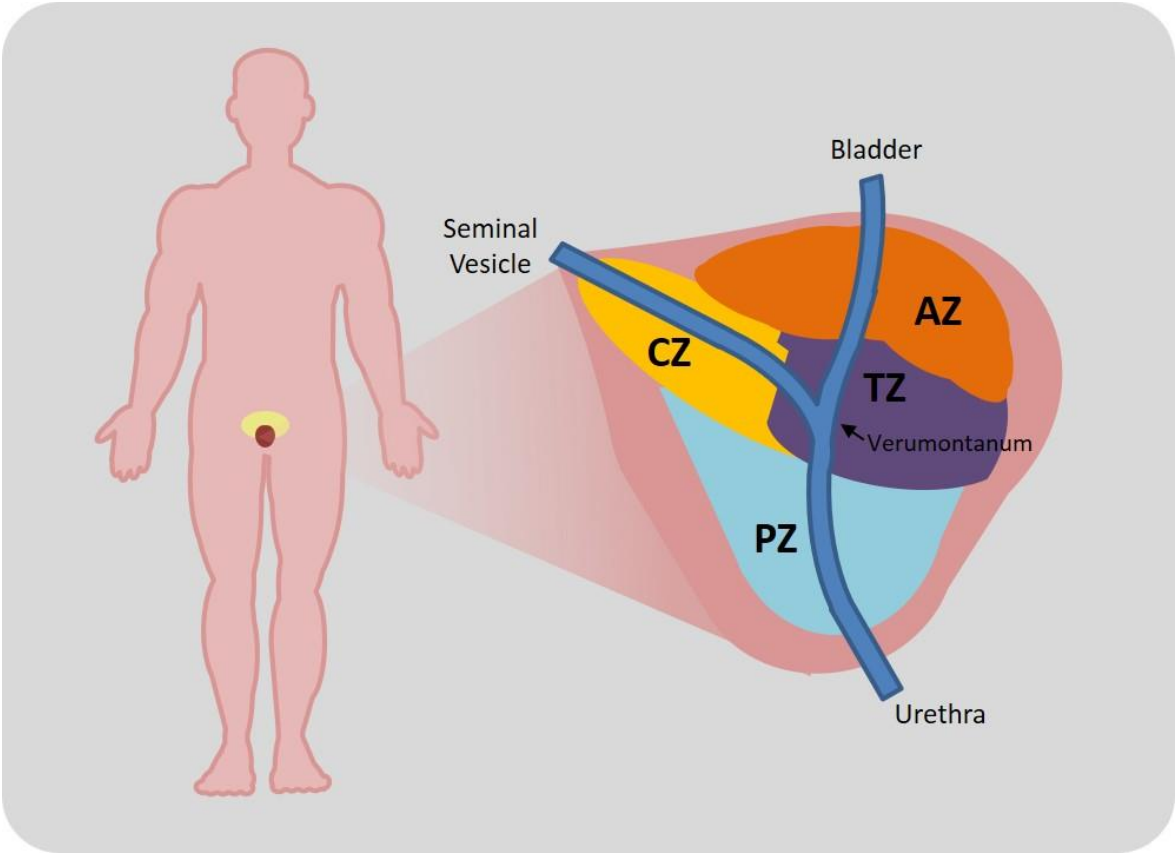

FIGURE 1 – Zonal anatomy and situation of the prostate

The prostate is situated directly below the male bladder, and surrounds both the descending urethra and the junction with the ejaculatory duct from the seminal vesicles. The human prostate can be divided into four zones; peripheral (PZ), central (CZ), transitional (TZ) and anterior (AZ).

Morphogenesis proceeds through paired differentiation of the UGM (mesenchyme) and UGE (epithelia). This occurs upon contact and in conjunction with the seminal vesicle epithelia and mesenchyme **(6)**.

Initial development of the prostate is hormone dependent **(7)**. Transduction of proliferative signalling through binding of androgens to the androgen receptor (AR) is well characterised in the somatic luminal cells of the prostate, however AR also plays a role in early prostatic development. Both the UGM and UGE are AR^+ yet only the mesenchymal component *requires* the nuclear receptor for synchronous development of both tissues into the characteristic acinar structure. This suggests that an enforced paracrine signalling loop is established which transmits the downstream proliferative effects of AR from the mesenchyme to the epithelium **(8, 9)**. The UGE progresses into the hierarchal basal and luminal epithelia whilst the UGM forms the surrounding stromal capsule of smooth muscle cells and fibroblasts **(10)**. It would be reasonable to hypothesise that due to the distinct nature and phenotype of the UGM and UGE, both tissues have separate stem cell populations which are heavily involved in the early stages of branching morphogenesis.

The initial surge of androgens in the neonatal prostate mirrors that of pubescent hormone levels in the organ, and has the effect of "imprinting" a proliferative response to androgens. Consequently this may explain the androgen-dependence of early cancers in the adult prostate. Imprinting effects have also been shown with estrogens. In the early prostate; variance in estrogen levels have long term consequences on both adult organ size and function **(5)**. Estrogen receptor (ER) expression in the early prostate follows after the initial spike in AR levels. This transient ER peak temporally coincides with a rise in the levels of progesterone (PR) and retinoid receptors (RAR/RXR) hinting at a hormonal switch in development. Exposure of rat prostate to estrogen caused down-regulation of genes that promote epithelial differentiation. Among these were the homeobox genes; NKX3.1 and HOXB13, as well as SHH (sonic hedgehog) and FGF-10 (fibroblast growth factor). Elevated neonatal estrogen also maintained anti-proliferative BMP4 levels. Typically, expression of BMP4 becomes reduced in the post-natal prostate to allow for branching morphogenesis **(11)**. Hormonal control of organ development is thus extremely important, with imprinting of the tissue influencing latter malignancy.

To understand prostate cancer aetiology and development it is first necessary to understand the cellular components and the hierarchical organisation of the glandular prostate epithelium.

1.1.3 - Cells of the Prostate

The glandular prostate of transitional, peripheral and central zones is further organised into bundles of exocrine acini. These structures are composed of stroma and epithelium separated by the basement membrane (BM). This is a complex mesh of cellular adhesion molecules (CAMs) and structural proteins including; collagen IV, laminin and heparin sulphate proteoglycans **(12, 13)**.

The stroma originates from the UGM and is composed of smooth muscle cells, myo-fibroblasts and fibroblasts **(Figure 2F)**. These cells aid epithelial growth and differentiation through androgen-dependent expression of a range of growth factors (GFs) including; epidermal (EGF), insulin-like (IGF1), platelet-derived (PDGF) and vascular endothelial (VEGF) **(14)**. The composition of stromal cell-types is altered in malignancy, with almost complete loss of smooth muscle **(15)**. In prostate cancer, the stroma exhibits genetic instability alongside aberrant epigenetic regulation of genes involved in stress response and cellular growth **(16-18)**.

The prostate epithelium itself contains 3 cell types; neuroendocrine, secretory luminal and undifferentiated basal cells. The latter two are organised into distinct luminal and basal layers **(Figure 2A-D)**. These cells are classically characterised by immunophenotypic markers such as cytokeratins (CK), with the normal prostate showing a 60:40 luminal to basal cell ratio **(Figure 2G)(19)**.

Luminal cells are the largest cellular population in the prostate and are terminally differentiated, existing in a state of senescence. They function as secretory cells that exocytose PSA and PAP into the prostatic ducts. Classic luminal cytokeratin markers are CK8 and CK18, and these cells also express AR, CD24, CD57 and ALOX15B **(Figure 2D)(20, 21)**. Luminal hyperplasia results in the precursor lesion PIN, and a continued expansion of this epithelial layer in cancer skews the epithelial hierarchy to a stage where the tumour cell population is typically ~99% luminal **(22)**. These cells are dependent upon androgens for survival.

Neuroendocrine cells are the other terminally differentiated cell-type in the adult prostate and exist scattered throughout the epithelium. Cellular function is unclear but they canonically lack AR and are identified through staining for chromogranin A **(23)**. Expression of another marker; neuropeptide Y, which is thought to promote angiogenesis through mitogen activated protein kinases (MAPKs), has been used to show increased numbers of neuroendocrine cells in tumours. The enrichment of this cell-type suggests a role in cancer progression, supported by findings that the cells also secrete VEGF, another angiogenic protein **(24, 25)**. These neuroendrocrine or anaplastic prostate cancers arise in late-stage disease. They are innately castrate resistant due to the cells lacking AR, and are therefore androgen-independent pre-ablation therapy **(Figure 2E)(26)**. Androgen blockade may therefore select for the neuroendocrine lineage or development

of this neuroendocrine phenotype from the resistant cells could be a reflexive adaptation following treatment **(27)**.

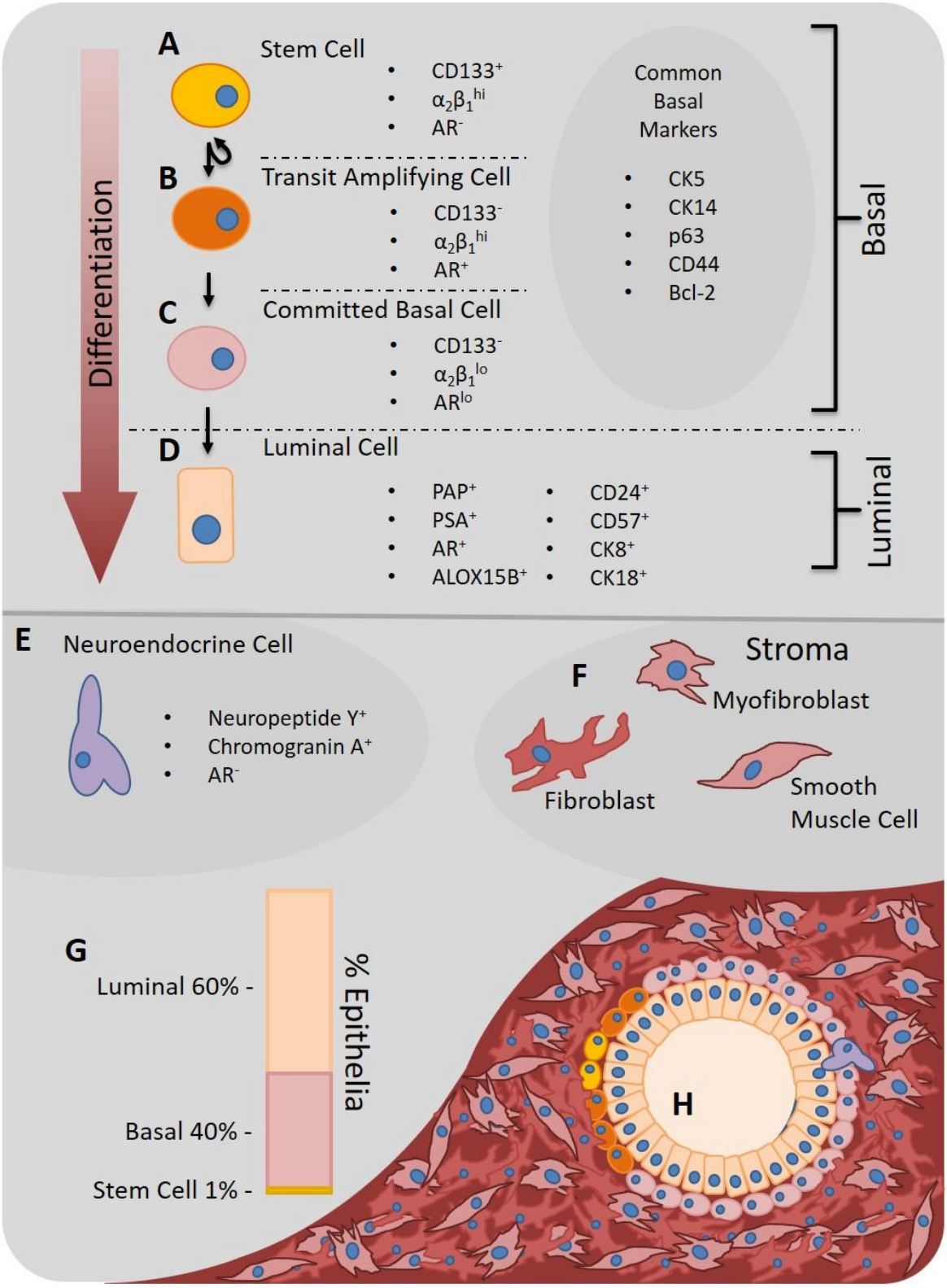

FIGURE 2 - Organisation of the normal prostate epithelium

A-F) The cell populations of the prostate, with identifying immunophenotypic markers **(13, 20, 21, 23, 28)**. **G)** Constituent representation of the prostate epithelial cells in a normal gland. **H)** Diagrammatic schematic of a normal acinus with epithelial bilayer surrounded by fibromuscular stroma.

The basal cellular compartment is heterogeneous and contains several distinct populations **(Figure 2A-C)**. Canonical basal cell markers include; CK5, CK14, p63, CD44 and Bcl-2 **(29)**. These cells adhere to the BM as their name suggests and contain ~70% of total proliferating cells in the prostate **(30)**. This, along with other compelling evidence, suggests that the adult epithelial stem cells reside in the basal layer of the human prostate. Prospective populations of these stem cells (SC) ($CD133^{+}$ $\alpha_2\beta_1^{hi}$ AR^{-}), alongside transit amplifying (TA) ($CD133^{-}$ $\alpha_2\beta_1^{hi}$ AR^{+}) and committed basal (CB) cells ($CD44^{+}$ $\alpha_2\beta_1^{lo}$ AR^{lo}) have been identified within this monolayer **(13, 20, 28)**. Low levels of AR protein have been observed in the $CD133^{+}$ population **(31)**, yet this report conflicts with work in which no AR transcript or protein were detectable in the epithelial stem cells **(13)**. Basal populations can focally express other hormonal nuclear receptors such as ER and PR that aid the androgen independence of the epithelial layer **(32)**.

Other groups have also identified markers that define prostate epithelial stem cells and cancerous equivalents. CD166/ALCAM is found to enrich for murine progenitors **(33)** and enhances metastatic potential in end-stage disease **(34)**. Like CD166, ALDH1 was initially identified as a marker for murine prostate stem populations (both normal and cancerous) **(35)** and has been significantly associated with human prostate cancer through large patient cohort studies **(36, 37)**.

1.1.4 - Prostate Epithelial Stem Cells

Stem cells are defined by both their ability to produce cells that are committed to separate lineages of differentiation and their enhanced self-renewal capacity. A single adult stem cell thus has the innate ability to reconstitute and populate its originating organ or cellular lineage.

Self-renewal is the maintenance of stem cell population number whilst also generating non-stem daughter cells that are committed to a differentiation path, a phenomenon that occurs by asymmetric mitosis. Stem cells can also commit to symmetrical division to produce either two stem daughter or two non-stem daughter cells, **(Figure 3) (38)** allowing for expansion or deletion of the stem cell pool respectively.

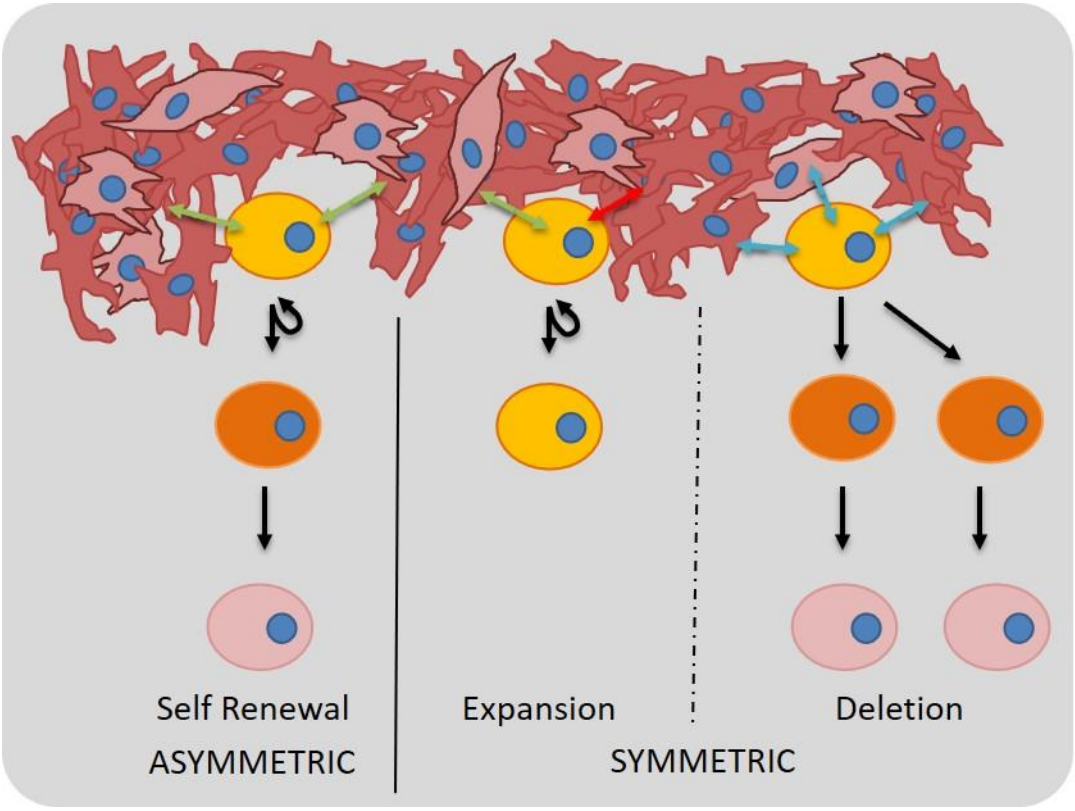

FIGURE 3 – The stem cell niche and the role it can play in division choice

The prostate epithelial stem cell niche is likely to reside on the basement membrane in close proximity to the stromal compartment. Heterotypic signalling in this environment is likely to determine self-renewal decisions.

Replication choice is dependent upon both intrinsic and niche-related factors. Intrinsic effectors that govern stem cell asymmetric division include transcription factors (such as Notch, Hedgehog and Wnt) and other cellular proteins/nucleic acids within the progenitors themselves that produce asymmetric accumulation of fate determining polypeptides and mRNA transcripts that subsequently promote asymmetric division **(38, 39)**.

The niche or microenvironment is the cocktail of GFs and cellular contacts that surround a stem cell **(Figure 3)**. In the prostate, the niche is probably situated on the basement membrane of acini due to high stem cell expression of $\alpha_2\beta_1$ integrin that binds collagen **(40, 41)**. This positions the stem cells in close proximity to the underlying stromal compartment that through heterotypic signalling may play an important role in stem cell self-renewal choices. TGFβ and Wnt are examples of ligands that are consistently present in niches that self-renew tissues through stem cell asymmetric division and are seen to be dysregulated in prostate cancer to promote tumourigenesis **(38, 42)**. Cell surface molecules are the other determining extrinsic factor that governs division choice. An example of this would be Notch signalling; Numb regulation of Notch receptors facilitates exclusive formation of asymmetric contacts to promote self-renewal of the stem cell **(43)**.

Adult or somatic stem cells are found in all tissues where they have an important role in population homeostasis and in situations of wound healing or tissue replacement **(38)**. Haematopoietic stem cells are the most studied of these somatic populations and are well characterised, ($CD34^+$ Lin^- $CD38^+$) giving rise to the myeloid and lymphoid lineages of the blood **(44, 45)**. Adult stem cells have a number of defining features. They exist as a minute subpopulation in the tissue, situated in a specific niche. They have a large nuclear to cytoplasmic ratio, are structurally unspecialised with few organelles, are slow cycling yet have a rapid (and inducible) proliferative ability and give rise to a population of TA cells that proliferate clonally to ultimately yield a terminally differentiated cell population **(46)**. Stem cells of epithelial tissues, such as the prostate, are characterised by a heightened in vitro and in vivo proliferative capacity and exist within a well-protected niche that is in contact with a mesenchymal compartment **(46)**.

The case for a basally situated prostate epithelial stem cell pool began with the androgen depletion and replacement experiments in the rat prostate performed in the 1980s. Here, castration caused apoptosis of the androgen-dependent luminal cells whilst leaving an intact basal layer. Re-introduction of androgen at a later stage caused regeneration of the luminal cell layer **(47)**. This lead to the hypothesis of a basal stem cell that produces an androgen-responsive TA population capable of self-expansion and reproduction of the terminally differentiated secretory layer **(48)**. The relapse of human prostate cancer after hormonal castration by androgen deprivation therapy (ADT) mirrors this response, and highlights the phenotypic plasticity of the

progenitor basal compartment. Prospective prostate epithelial stem cells were isolated from within the total $CD44^+$ basal population **(49)** on the basis of high $\alpha_2\beta_1$ integrin expression. **(21, 41)**. This $\alpha_2\beta_1^{hi}$ population was later found to contain both stem and TA cell subpopulations, with further enrichment of stem cells achieved by selection using the CD133 marker **(28, 50)**. Biochemical evidence, further supporting the initial hypothesis proposed by Isaacs and Coffey in 1989, **(48)** was obtained by interrogating AR expression in these fractionated cell populations. Prostate epithelial stem cells were found to be AR^- or AR^{lo}, TA cells had relatively high amounts of the nuclear receptor whilst CB cells had low to undetectable protein levels **(13)**. This molecular evidence highlights the plausibility of the original hypothesis and strongly suggests that the somatic stem cells of the prostate may play a more sinister role in cancer development.

In vitro cell growth experiments also suggest a basal stem cell. Spheroid culture of prostate epithelial cells only permitted clonal growth from cells of a basal phenotype, characterised by CK5, integrin α_6, CD44 and p63 expression **(51)**. These prostaspheres lacked AR and PSA luminal markers and could be formed from either $CD133^+$ or $CD133^-$ fractions. Basal epithelia are also easier to grow in organoid culture systems. Organoids generated from single basal cells have a 70% growth efficiency compared to those of luminal origin. Luminal cells could only successfully generate organoids in 1-2% of cases **(52)**. The stark difference in clonogenicity of the epithelial populations in the normal prostate is clear. However, current work does suggest that a rare luminal progenitor also exists in the prostate, but that its contribution to the normal epithelial hierarchy and, by association, the initiation of cancer is comparably negligible to that of the basal stem cell **(52, 53)**.

Lineage analysis of these cells has further supported their status at the root of the epithelial hierarchy in the prostate **(Figure 2)**. One study used lineage-tracking lentiviral vectors to incorporate fluorescent PSA reporter genes into basal epithelial cells. These cultures were then stimulated to differentiate and fluorescence was observed, as expected, as the cells developed into secretory luminal cells **(54)**. Other studies have used mitochondrial DNA mutations to map cytochrome c oxidase (COX) deficiency in prostatic acini. These mutations are reasoned to accumulate in stem cells and become observable through lateral clonal propagation throughout the acinus. This can be tracked by immunohistochemical staining of COX deficient cells through sequential tissue sections. Deficiency presented in all three cell types; basal, luminal and neuroendocrine, dictating that a common originating cell must exist within the epithelium **(55)**. Further in-depth tissue sectioning of COX deficiency in prostates located multipotent basal progenitor cells **(53)**. These were situated in a niche proximal to the urethra and gave rise to bipotent basal cells from which the mitochondrial mutation could be simultaneously inherited; laterally, by the basal epithelia and through differentiation, by the luminal monolayer. These

multipotent basal progenitors expressed high levels of Delta homolog 1, DLK, integrin α_6 and Notch1 and could generate differentiated spheroids. Like the generation of organoid cultures **(52)**, this lineage tracing approach also identified a minor population of luminal epithelial stem cells **(53)**.

Telomeres are extended sequences of hexanucleotide repeats found at the end of the chromosomes and buffer the loss of genetic material caused by the end-replication problem after every mitotic S-phase. Telomeric regions get shorter as the cell ages, causing genomic instability and eventually replicative cell senescence **(56, 57)**. These repeats are maintained in the germline by the telomerase enzyme (TERT) which is later silenced in development. Analysis of telomere lengths and congruent activation of telomerase allows for tracking of cell population progression. In BPH, the basal stem cell population may be either bipotent or produce an early progenitor that can resolve down both the basal or luminal lineages. Here *only* the SC and TA populations have telomerase activation yet luminal cells have longer telomere lengths than CB cells. Progression down a linear route of epithelial differentiation of SC to TA, TA to CB and CB to luminal cell in this model does not account for this sequential loss and gain of telomere length, therefore the luminal cells must be produced directly from the SC or TA populations **(58)**.

TERT is silenced in the normal prostate epithelial subpopulations **(59)** including the stem cells, but becomes active during PIN and in the luminal cells of prostate cancers with both RNA and protein levels increasing in primary to metastatic disease **(60, 61)**. The telomere lengths of cancer cells however are lower than that of surrounding normal tissue epithelium, **(60-63)** suggesting that an expansion of the $TERT^-$ stem cell pool occurred during tumorigenesis that resulted in telomere reduction of its more differentiated progeny **(59)**. By extrapolating the findings in BPH there may be a root for the aberrant differentiation seen in prostate cancer. The burst of stem cell differentiation may “exhaust” the basal cell lineage as TERT reactivation doesn’t occur, however the telomere length can be maintained in the cancerous luminal cells that have active telomerase and thus the imbalance observed in luminal to basal epithelial populations is created **(58)**.

1.2 - Disorders of the Prostate

1.2.1 - Benign Prostatic Hyperplasia

Normal postnatal prostatic growth occurs due to a rise in circulating testosterone levels during puberty, however the organ can also undergo abnormal growth later in life due to BPH; a chronic disease that affects the TZ of the prostate. Here hormone-dependent micronodular hyperplasia of the glandular and stromal tissue enlarges the TZ to constrict the descending urethra, resulting in lower urinary tract symptoms such as acute urinary retention. The restriction of urinary flow and obvious discomfort can be alleviated by transurethral resection of the prostate (TURP) where the tissue overgrowth is surgically removed. An increase in prostate volume due to BPH has been linked to elevated PSA levels, which may contribute to false positive cancer diagnoses through use of the canonical diagnostic test (discussed further in **Section 1.4**) **(64)**. Future growth of the prostate in BPH can be predicted using baseline prostate volume and assessing internal prostatic architecture. For example; if a patient has a clearly defined TZ with an obvious stromal border, a larger endpoint prostatic volume can be expected **(65)**.

Microarray data has highlighted the divergence of BPH and cancer at the transcriptional level **(66)**. The diseases are also phenotypically distinct in the fact that BPH has hyperproliferation of both layers of prostate epithelium rather than an exclusively luminal expansion **(58, 67)**.

1.2.2 - Prostatitis

Tissue inflammation is the most common disorder of the prostate and occurs at a higher incidence than both BPH and cancer **(68)**. Bacterial and viral infection, along with chemical exposure all cause prostatitis **(69, 70)**. The disease can be split into four separate classes; I – acute bacterial prostatitis, II – chronic bacterial prostatitis, III – chronic pelvic pain syndrome, and IV – asymptomatic prostatitis **(70)**. It is estimated that ~16% of US males will suffer symptomatic prostatitis (I-III) during their lifetime. Surprisingly, asymptomatic prostatitis is much more prevalent in the population and high percentages of both BPH and cancer biopsies show signs of surrounding tissue inflammation **(70)**. Prostatitis, like BPH, can raise serum PSA levels - thought to be linked to destruction of tissue architecture causing “leakage” of the protein into the circulation, with levels of the antigen decreasing concordantly upon application of antibiotics **(71)**.

1.2.3 - Inflammatory Aetiology of Prostate Cancer

Inflammation has been postulated as a triggering event or accelerating factor for prostate cancer development for many years **(68, 72, 73)**. Inflammation, produced by an initial infection, can then trigger immune cell infiltration of the tissue; creating a disruptive chemical environment that can result in prolonged exposure of epithelial cells to a cocktail of transforming cyto- and chemokines.

Our lab has identified that prostate cancers do exhibit a reliance on inflammatory pathways centred about NF-kB, IFNGR and IL-6 signalling **(66)** which may have been cultivated in a situation not dissimilar to that described above.

The initial (or combination of) infectious or chemical insult that triggers the cascade of inflammation and immune activation can come from a wide array of sources.

Inflammation; Infectious Agents

Many infectious organisms that produce prostatic inflammation are sexually transmitted, owing to the close proximity of the gland to the male genitalia. Sexually transmitted infections (STI) of *Chlamydia trachomatis* (Chlamydia), **(74)** *Neisseria gonorrhoeae* (Gonorrhoea), **(75)** *Treponema pallidum* (Syphilis), Herpes Simplex Virus, Human Papillomaviruses (HPV), Human Herpes Virus and Cytomegalovirus **(76)** have all been detected in prostate tissue.

Meta-analysis linking STI data to prostate cancer has shown that past history of any STI increases later disease incidence. In particular, gonorrhoea infection heightens risk of malignancy development by 20% **(77)**.

Propionibacterium acnes, as the name suggests, is more commonly associated with the skin condition acne, **(78)** yet is recurrently discovered in inflamed prostate tissue **(79, 80)**. Studies, both in vitro and in vivo, that position the bacterium in this prostatic niche have identified similar molecular activations and defects seen in human prostate tumours. Culturing the bacterium with the prostate epithelial cell line RPWE-1, caused activation of STAT3 and NF-kB with secretion of the IL-6 cytokine **(81)** and in a mouse model; infection stimulated epithelial hyperproliferation, inflammation and downregulation of the tumour suppressor, NKX3.1 **(82)(Figure 4A)**.

HPV infection has been correlated with increased Gleason grading of tumours and also with lower survival rates **(83, 84)**. However, several studies have also found no correlation with infection and many tumour tissues display absence of any genetic material attributable to the virus **(85-87)**. This suggests that further studies with larger patient cohorts and sequencing depth would be required to ascertain the involvement of HPV in prostate cancer development.

Another virus that has been recurrently found in the prostate is Epstein-Barr virus (EBV). This pathogen has historical ties to epithelial and blood cancers **(88)** and is proposed to collaborate with HPV infection to initiate prostate carcinogenesis **(89)**.

Human BK polyomavirus has been detected in cancer and associated proliferative inflammatory atrophy (PIA) lesions, suggesting a role for the virus in disease development. Interestingly the virulent BK T antigen can abrogate both p53 and Rb protein function (both usually intact in early prostate cancers **(90)**, marking a path for non-mutagenic removal of two key tumour suppressing

genes by the virus **(91, 92)**. Conversely, BK sero-positivity in patients with prostate cancer is linked to a reduction in rates of biochemical recurrence – meaning that presence of the virus may be a good prognostic factor – yet again, studies with larger sample sizes will hopefully ascertain if the virus plays a role in the development of prostate cancer **(93)(Figure 4B)**.

Deep sequencing of homogenised tissue can now identify the presence of bacterial and viral genetic information in prostate samples, **(79)** a feat only previously achievable through targeted PCRs – a sensitive yet blinkered approach **(94-96)**. This opens a gateway leading to possible identification of new pathogenic species, that previously couldn't be sustained in ex vivo culture, and any subsequent involvement in prostate carcinogenesis that they may have.

Inflammation; Dietary Compounds

Epidemiology has linked the increase of prostate cancer incidence in a population with high intake of animal fat and red meats **(97, 98)**. The active chemicals cited to trigger carcinogenesis are heterocyclic amines (HCA). Supplementing the diet of rats with an HCA; 2-amino 1-methyl-6-phenylimidazo[4,5-b]pyridine (PhIP) caused spontaneous cancer formation in the breast, intestinal and prostate tissue of the animals **(99)**. This HCA also increased the mutation rate in the rodent prostate cancers and was observed to have lobe-specific effects – similar to the high zonal specificity seen in human disease. The rats also had a marked progression of disease; with stages of PIA and PIN existing prior to full adenocarcinoma **(72, 100, 101)**. Dietary PhIP has also been observed to enhance bacterial prostatitis with congruent IL-6 signalling activation and development of prostate cancer **(102, 103)**.

Dietary compounds have also been linked to a reduced risk of prostate cancer development and progression. These have mainly been associated through large cohort studies and include; green tea, **(104)** tomatoes (lycopenes), **(105)** cruciferous vegetables, **(106)** soy, **(107)** and pomegranates **(108)**. Specific chemicals in these foodstuffs have been shown in isolation to halt cancer cell growth in vitro and protect against oxidative stress – a key mediator of inflammatory damage in this early stage of disease **(Figure 4C)**.

Inflammation; Immune Cell Infiltration

There is also considerable evidence suggesting that tissue infiltrates of immune cells contribute towards BPH and cancer **(68-70, 109)**.

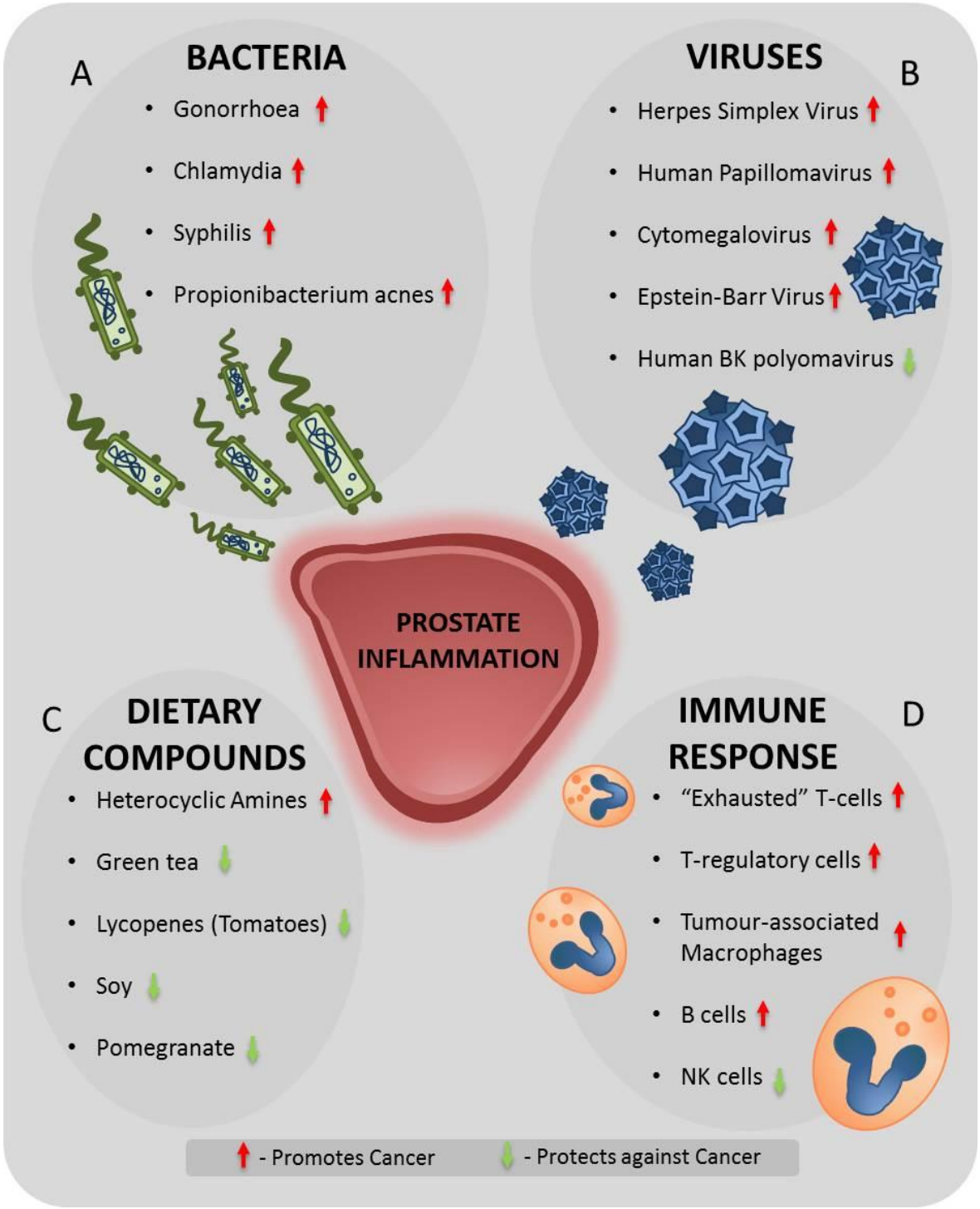

FIGURE 4 – Factors influencing prostate inflammation in carcinogenesis.

A) Bacterial and **B)** viral infections, alongside **C)** diet and the individual's immune **D)** response all affect prostate inflammation and the outcome of disease initiation and progression.

Against initial thought, an increased number of intratumoural immune cells can, in fact, promote disease progression **(110)**. T cell infiltrates of prostate tumours are regularly found to be "exhausted" (non-active) due to expression of the PD-1 receptor and cognate ligand PD-L1 **(111)**. These infiltrates also contain a high percentage of T_{reg} cells, suggesting further dampening of the T-cell directed immune response against the tumour **(111, 112)**. Other immune cells also have correlative incidences with prostate tumours. An increase in tumour associated macrophages and B cells **(113, 114)** can promote disease whilst the reverse is true of Natural Killer (NK) cell numbers **(115)**. B cells also contribute towards cancer cell self-renewal processes through heterotypic signalling; something that may be harnessed, and misappropriated, by the stem cell compartment of the organ in disease **(116)(Figure 4D)**.

Inflammation; Further Aetiological Evidence

Suppression, by pharmacological "dampening", of a patient's immune system following organ transplant, increases the risk of prostate adenocarcinoma developing, suggesting that infectious agents or a lack of immune surveillance plays a role in the initiation of disease **(117)**. Several studies have found that a recurrent dose of non-steroidal anti-inflammatories reduces prostate cancer incidence **(72, 118-120)** and that higher grade cancers often have inflammation in the surrounding normal tissue. This also provides further evidence in favour of inflammation playing a role in disease initiation and progression **(121)**.

1.2.4 - Proliferative Inflammatory Atrophy

PIA is thought to occur as a precursor to PIN, manifesting as regenerative hyperproliferation of the epithelia in response to an initiating inflammatory insult. PIA is most commonly found in the PZ and has been seen here to merge with PIN and cancerous epithelial tissue **(72, 122)** – providing correlative evidence towards a hierarchical progression of disease **(Figure 5A)**. Interestingly, similar molecular defects can be tracked across these overlaying lesions. Loss and gain of genetic material, commonly observed in prostate cancer, doesn't occur in PIA lesions **(123)** yet there are several notable changes in gene expression. GSTπ1, a protector against oxidative stress, and Bcl-2, an apoptosis suppressor, are both upregulated whilst tumour suppressor genes commonly deleted in prostate cancers are downregulated **(70, 124, 125)**. Progression of PIA to PIN is likely, however there is also evidence that disputes this hypothesis; a study that processed over 1000 biopsies from 98 patients suggests that PIA has links to prostatitis yet it is unlikely the lesion develops into PIN based on tissue architecture and proximity **(126)**. Further evidence is therefore required to ascertain if there is a true development of PIN from PIA.

1.2.5 - Prostatic Intraepithelial Neoplasia

PIN is suspected to be a precancerous lesion, characterised by hyperplasia of the luminal cell population into the acinar lumen. It is biochemically, genetically and phenotypically similar to prostate adenocarcinoma, however there is no disruption of the basement membrane **(127)(Figure 5B)**. Other key differences include the reduction of basal cells (still present in PIN, whereas in cancer the basal population is proportionally negligible) and the surrounding stromal tissue isn't completely reactive **(128)**. In PIN the relative mitotic rates of cells in the bilayer switch and the luminal cells become more proliferative, causing the observed hyperplasia. This overgrowth can present as tufting, micropapillary projection, cribiform or flat growth into the lumen **(127)**. PIN is a chronic disease that has been identified in men as early as in their twenties. Prostate cancer foci can be detected within a decade later, with percentages of both diseases increasing as population cohorts grow older. This implies that prostate cancer initiates relatively early in men yet doesn't present clinically until much later in life **(129)**. Anatomically PIN, like cancer, occurs dominantly in the PZ and is thought to give rise to the malignant phenotype via a "field" effect, a hypothesis supported by common reports of high-grade PIN (hgPIN) and cancer tissue merging **(127, 130)**.

In terms of their expression profiles, PIN and cancer are significantly similar. The ETV and ERG gene fusions specific to prostate adenocarcinomas are foreshadowed in PIN, where the neoplasia presents with active transcriptional networks reliant upon the very same ETS transcription factors **(123)**. A recent study exposing clonal dynamics in tissue by means of unique TMPRSS2-ERG fusion breakpoints observed that some hgPIN lesions were actually retrograde carcinomas that also harboured PTEN deletions **(131)**. These presented, in tissue pathology, as PIN yet were actually cancers. In similar cases, hgPIN has been shown to harbour primary genetic defects of prostate cancer such as the TMPRSS2-ERG fusion, **(132)** SPOP mutation **(133)** and NKX3.1 loss **(127)**, highlighting a possible hierarchy of multi-step carcinogenic development through neoplasia or cancer mimicry of PIN tissue patterns.

Development of adenocarcinoma from PIN has also been assessed using temporally separated biopsies taken from the same patient's prostate **(134)**. A study of just under 800 patients that were diagnosed with PIN at first biopsy and then re-biopsied within a year of initial diagnosis, found that there was an increase in the amount of cancers sampled. However, the authors attributed this to the poor initial sampling of the patients i.e. the cancer was present yet undetected the first time, rather than a progression of PIN into carcinoma.

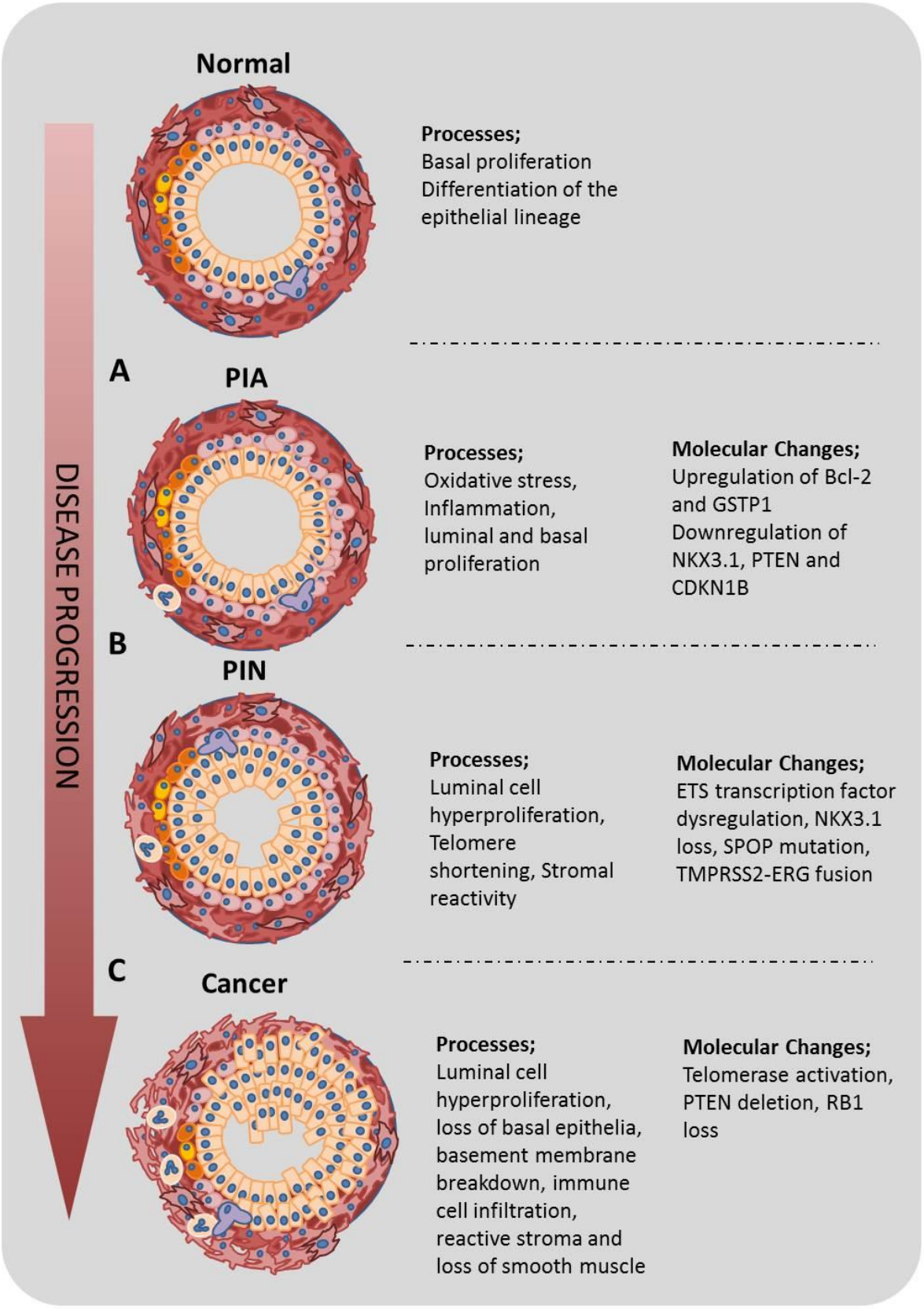

FIGURE 5 – Proposed staged progression of prostatic disease into prostate cancer.

Disease progression, highlighting the cellular and molecular changes through **A)** PIA, **B)** PIN and **C)** Cancer.

1.2.6 - General Attributes of Prostate Cancer

Prostate cancer is the most commonly diagnosed cancer in men of the United Kingdom **(135)**. The prevailing risk factor for disease seems to be age, with diet and infection also thought to play important roles in disease aetiology. The most striking phenotypic feature of ductal carcinoma is the apparent breakdown of acinar tissue architecture. The skewing of epithelial cell populations seen in hgPIN is further exaggerated in cancer with luminal expansion, twinned with loss of basal cells, causing a >99% to <1% luminal-basal split **(22)**. The BM is degraded and cells migrate into the reactive stroma where heterotypic signalling facilitates further invasion of the tissue **(14)**. The disruption of normal acinar morphology is thought to be what leads to higher circulating levels of PSA, the canonical diagnostic marker of the cancer **(136)**.

Tissue architecture is histopathologically defined by the Gleason grading system, upon which patient disease can be stratified and prognostic severity estimated **(128)**. Prostate cancer is also classified by the TNM (tumour, nodes, metastases) scale. T1-4 stratifies the local primary tumour growth and invasion, N0-3 infers level of lymph node metastases, and finally M0-1 signifying the presence of any distant metastases **(137)**. Localised disease can be treated by surgical removal of prostate tissue, an array of focal therapies and, in advanced cases, ADT. ADT is used to target the AR-dependent luminal cells of the tumour to result in initial remission of the cancer **(136)**. As prostate cancer is distinctly heterogeneous, treating tumours as a homogeneous collection of cells (as ADT does) ultimately fails as the reduced basal compartment, and possibly a small percentage of luminal cells that have escaped androgen dependence, can regenerate the tumour. Relapse of castration-resistant prostate cancer (CRPC) typically presents 12-24 months following hormone therapy **(26)**. Advanced prostate cancer either rapidly metastasises following treatment or may have spread to secondary sites prior to hormonal therapy. This catastrophic stage of disease leads rapidly to patient mortality. This end-stage disease is currently inefficiently treated with broad-spectrum cytotoxic chemotherapeutic drugs or second generation anti-androgens that extend life by a few months. All therapies at this point are palliative **(26)**.

1.2.7 - Prostate Cancer Epidemiology

In the United Kingdom and United States, prostate cancer has the greatest annual incidence of diagnosis in males, accounting for approximately 1 in 4 male cancer cases **(138)**. The most up to date figures in the UK state that there were around 47,000 new diagnoses of disease in 2014 **(138)**. It is also the second most common cause of male cancer death in both countries with just over 11,000 mortalities in the UK and 30,000 in the USA **(139)**. Age is the major obvious risk factor; over 50% of cases are diagnosed after the age of 70 **(138)(Figure 6)**.

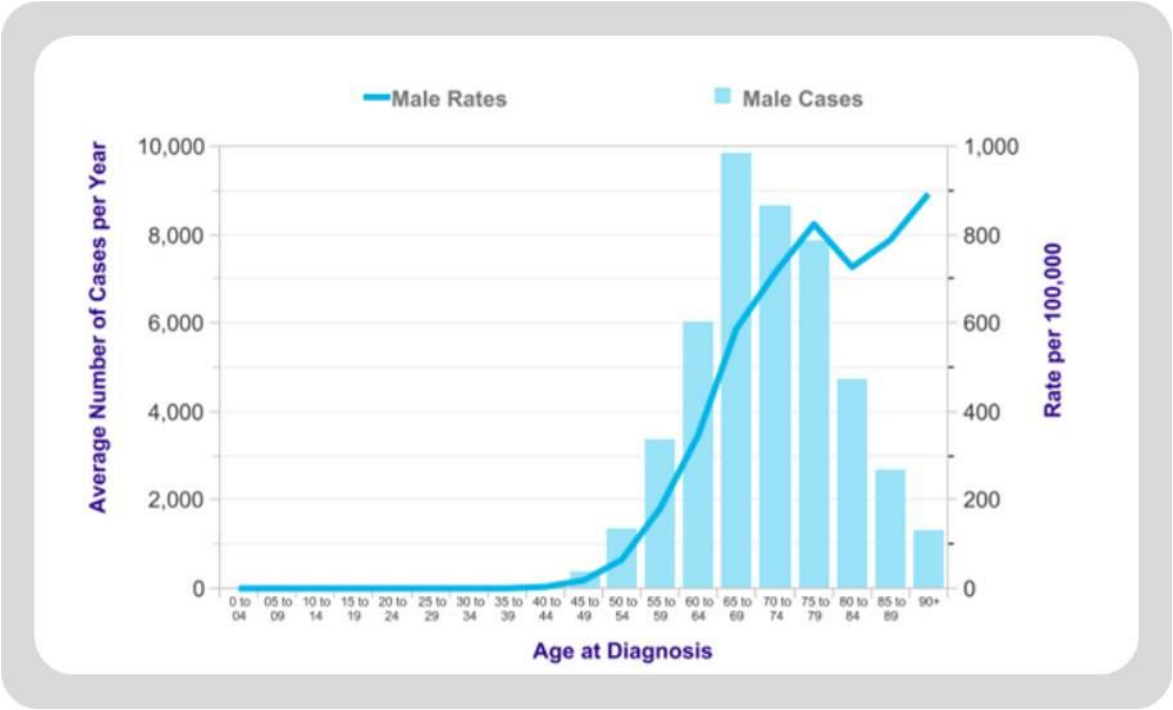

FIGURE 6 – Age as a disease risk-factor in prostate cancer

Data from 2012-2014 compiled by CRUK indicating peak incidence of disease in 65-70yr old men and >50% diagnoses coming after 70yrs of age. http://www.cancerresearchuk.org/health-professional/cancer-statistics/statistics-by-cancer-type/prostate-cancer/incidence#heading-One

Familial prostate cancer accounts for 10-20% of population cases. It is defined in a family that has disease incidence in two first-degree relatives (father, brother or son) or in one first-degree and at least 2 second-degree relatives (uncle, cousin, nephew, half-brother) **(140)**.

Hereditary prostate cancer has stricter criteria than that of familial cases;

1. Prostate cancer in three or more first-degree relatives
2. Prostate cancer in three consecutive generations
3. Early diagnosis of prostate cancer (~50 years old) in two siblings **(140)**

It is notable that, whilst not fully understood, there is a racial predisposition to prostate cancer with Asian men having the lowest rick of mortality from disease and African-Americans, the highest **(141-143)**.

Aside from genetic factors, other compelling epidemiological evidence highlights that environmental factors also significantly contribute towards disease. As previously mentioned, the incidence of prostate cancer in the Asian population is lower than that observed in Westerners. However, in Japanese who migrated to Hawaii it was observed that previously low rates of prostate cancer development in the population rose to match that of the American indigenous **(144)**. This suggests that a change in diet, or habit, **(145)** or possibly an endemic infection may have caused the rise in incidence and also infers there may be an underlying connection of prostate cancer to an environmental influence that supersedes any current observation of racial predisposition to the disease.

Recent statistics show the extent of the impact that prostate cancer has in the male population. With current treatments unable to combat advanced prostate cancers that have become castrate resistant, better understanding of cancer cell type of origin and the development of the disease is required to produce new and effective therapies**.**

1.3 - Tumour Heterogeneity and Cancer Stem Cells

Tumours present a complex microenvironment due to heterogeneity of constituent and recruited cells. Tumour cell phenotypic variance can be observed both histopathologically and within proliferation and differentiation states **(146-148)**. Unfortunately, most cancer treatments assume that tumours are close to a homogeneous cellular mass which can be killed within the spectrum of singular agent or combination therapies. These treatments can cause initial regression of tumour bulk yet the cancer often relapses in a more advanced form, suggesting selection of a more aggressive phenotype. This raises several questions. Is resistance adaptive or pre-existing? How is tumour heterogeneity generated presuming a clonal origin of cancer, and, do all cells have an equal capacity for tumour regeneration?

Heterogeneity observed in blood malignancies **(149)** and solid tumours **(150)** has shown that cancers consist of genetically and phenotypically diverse cells. This variance within tumours can be accounted for, and generated by two theories which are not entirely mutually exclusive **(19, 151)**.

1.3.1 - Clonal Evolution Model

In this model, all cells have an equal propensity to become tumourigenic, with transformation occurring through a stochastic mutational or epigenetic event. This transformed cell then gives rise to other like-cells via mitosis, which have similar tumour forming ability. The tumour cells can then acquire subsequent mutation/s, giving them a selective advantage that allows for disease progression **(19, 151)**.

The first cell (and the clonal expansion of cells it produces) to incur the epigenetic or genetic change can be thought of as the “trunk” of the cancer (tree), with all further sub-clones branching off as the tumour develops **(Figure 7A)**. Initiating genetic events, so called trunk mutations, have been classically modelled, by transformation of cell lines through introduction or removal of single genes that are altered across human cancers **(152-156)**. Assimilation of cancer genomic data has allowed around 150 carcinogenic “driver” genes which operate in 12 central signalling pathways to be identified **(157)**.

A driver is a gene that, when “favourably” altered, gives the cell a proliferative edge over its neighbours, causing the cell to behave selfishly. The transformed cell abandons its role in the tissue and competes to survive and divide. Drivers can be further subclassified as tumour suppressors (when disease is promoted by gene loss or inactivation) and oncogenes (when disease is promoted by gene gain or activation). However, cancers usually harbour many more mutations than would be required to transform a single cell. These additional mutations are called

passengers. They accumulate in the clone with the advantageous driver mutation/s and are selected alongside during clonal evolution. In a very small fraction of cancers, these passenger mutations may become adaptive in a different microenvironment (such as that encountered in a new treatment regime or secondary metastatic site) and aid tumour survival. The majority of current sequencing studies use late stage tumours loaded with an overwhelming amount of mutational changes. From this end-point it is difficult to decipher which order the mutations occurred in, and also which alterations are critical to cancer initiation, development and progression **(157)**.

Epigenetic events can also drive cancer progression. Epigenetically altered tumour progenitor cells do not have inflexible fixed mutations but instead, and more elegantly, fluctuate the expression of critical genes. Control of transcript levels through methylation of the DNA or histone tails allows the cell a heightened plasticity over that of a mutational change, as it can adapt within a mitotic cycle to microenvironmental alteration **(158)**.

A study that highlights the feasibility of the clonal evolution model in prostate cancer was conducted by Goldstein *et al*. Sequential lentiviral introduction of the oncogenes ERG and AKT (mimicking TMPRSS2-ERG fusion and PTEN loss respectively) into basal cells caused formation of PIN-like disease in mice. Addition of AR into these activated cells then produced various tumours; some of which presented with outgrowth of an AR^+ population and “loss” of the basal cells that were initially transformed, a situation not dissimilar to the presentation of human prostate cancers in situ **(159)**. This challenges current thought that prostate tumours at diagnosis are the same at initiation, progression and presentation. The same group has repeated this study of serial gene alteration in human cell derived organoid cultures that were subsequently transplanted into mice. Transformation of basal cells produced a more aggressive disease phenotype than that of a luminal origin. Formation of luminal cell derived tumours show that these secretory cells can initiate cancer in this specific context with the study also observing divergent histology and heterogeneity of cancers (that were representative of human disease) stemmed by cells of the different epithelial populations **(160)**. However, the study failed to address which particular subpopulation in the broad basal and luminal epithelial classes was the cell of origin. The organoids were also not serially transplanted in mice, only cultured in vitro, meaning that further interrogation of cell of origin is required for human prostate cancer.

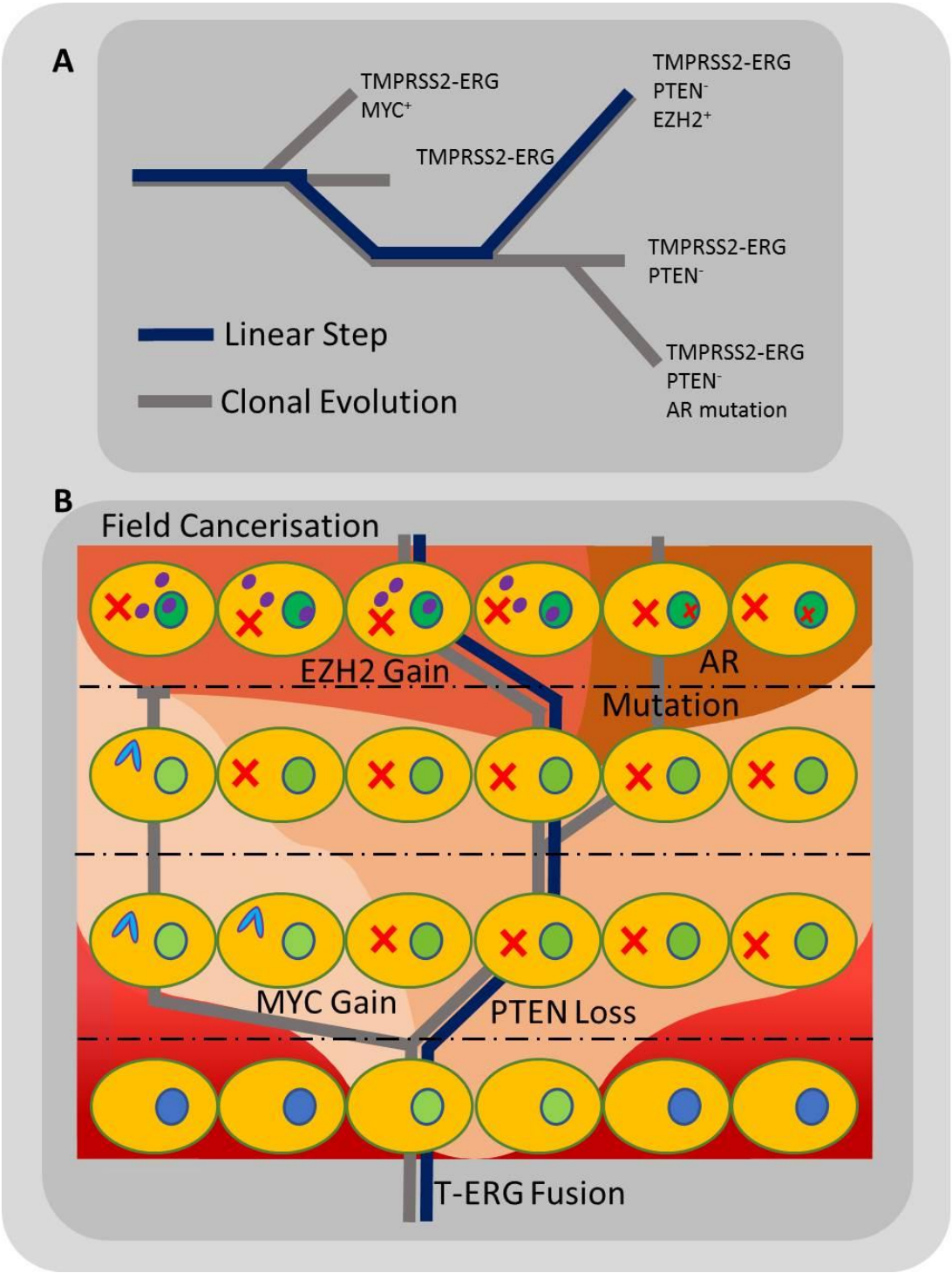

FIGURE 7 – Linear step, clonal evolution and field cancerisation.

A) A schematic of a fictional tumour, the dark blue line traces the route of a linear progression with mutation gained step by step, the dark grey line shows the network of clonal evolution in the tumour with continuation of route lineages and branching of less "successful" sub clones. **B)** The associated diagram showing the field cancerisation effect of the tumour schematic in **A** – here any cell in the field can gain a mutational change that allows for development of successful sub-clones.

1.3.2 - Linear step carcinogenesis

Proposed by Fearon & Vogelstein in 1990, **(152)** step-wise carcinogenesis implies the sequential accumulation of driver mutations in a single cell **(Figure 7A)**. The mutational burden, upon reaching a certain number, transforms the cell into the initiating clone. The number of mutations required to create a cancer cell appears to be tissue specific with initial estimates placing the number of specific aberrations to be around 7 **(161)**. However, recent analytical modelling suggests that this number is more likely to be ~3 specific mutations in the majority of solid tumours **(162)**. Leukaemias usually present in childhood, where the early onset is thought to be driven by the minimal requirement of a single transformative event such as well characterised BCR-ABL and RUNX1-ETV5 gene fusions **(146, 163)**. In the case of prostate cancer, sequential mutagenesis in mouse models suggests that 1-3 mutational events are needed to form the initiating cell **(128)**.

Linear step carcinogenesis however has two main criticisms;

- Metastatic potential

  The original model places cellular acquisition of metastatic potential as a final step immediately prior to patient death, however metastasis is now known to occur early in cancer development yet remain undetectable. This is due to inefficiency in secondary-site seeding and the variable latency of micro-metastases **(164-166)**.

- Immune surveillance and apoptosis evasion

  Step-wise accrual of mutations that drastically affect cell growth pathways would usually cause cell death or elimination by the immune system; the body's quality control mechanisms. There would need to be a mutational protection from self-initiated cell death before other proliferative mutations could occur. The HPV oncogenes; E6 and E7, give a perfect example of this. E7 binds cellular Rb and causes cell cycle dysregulation yet requires E6 to bind p53 the prevent the destruction of the transformed cell. Both are needed for survival and growth advantage. Therefore, the step-wise gain of mutation has to be coordinated and well timed to transform a cell without simultaneously inducing apoptosis **(167-169)**.

1.3.3 - Field Cancerisation

Field cancerisation (FC) is similar to the linear-step model but considers that the entire tissue or "field", rather than just a single cell, is pre-disposed to carcinogenesis **(Figure 7B)**. It was proposed due to the multi-focal nature of primary oral cancers that formed in extreme proximity to one another, yet were entirely separate **(170)**. Here, in the "activated" field, a cell can incur an

epi/genetic change and then divide; producing a sub-field of clonal cells in which further change can accumulate until a tumourigenic profile is achieved and cancer forms **(171)**.

There is evidence of this effect, both epigenetically and genetically, in prostate cancer; that exists commonly as multi-focal disease **(172)**. Methylation ratios of two genes; APC and RARβ2, across both tumour and surrounding benign prostate tissue, highlighted a previously undetected underlying field of heritable epigenetic defect **(173)**. Similarly, deep-sequencing of sectioned tissue from three prostates and their associated cancers found an unexpectedly (due to previously reported low mutation rates in prostate cancer **(90, 174)**) high incidence of background somatic mutations in "normal" tissue. The authors themselves proposed that this was representative of an activated mutational field that then stemmed the multifocal prostate tumours they were studying **(175)**.

1.3.4 - Cancer Stem Cell Model

The Cancer Stem Cell (CSC) theory stipulates that only some cells have an ability to initiate and regenerate a cancer. They are thought to arise from somatic stem cells or a transformational event in a near progenitor that affords the cell stem-like attributes. Heterogeneity is then generated through aberrant differentiation from the clonal CSC origin which produces the dysfunctional lineage **(28, 176-178)(Figure 8A)**. Accumulation of mutations and epigenetic defects in the stem cell is thought to occur in pre-tumour development **(179)**.

CSCs were predicted long before their eventual discovery. In 1938, Furth & Kahn discovered that a single cell was sufficient to transmit leukaemia between mice from a common genetic background **(180)**. Twenty years later, Chury and Tobiska described a leukaemia observed in a human patient as a stem cell disease **(181)**. John Cairns then discussed the potential role of stem cells in human cancers, as tumours arise primarily in epithelial tissues sustained by a somatic progenitor population **(182)**. Culture of extracted human patient tumour stem cells in vitro was then pioneered and suggested that it would, in future, permit assessment of metastatic potential and allow for targeted personalised medicine to be applied against the individual's cancer **(183)**. In 1988, Pierce & Speers proposed that tumours mirrored dysfunctional tissues and were therefore sustained by a small population of, in this instance, malignant stem cells **(147)**.

Once technology had advanced sufficiently to allow isolation of cells by expression of surface molecules, the first tumour progenitors to be identified were the leukaemic stem cells of the acute myeloid leukaemia (AML) initiating population by Bonnet and Dick in 1997 **(184)**. These cells shared the immunophenotype of Haematopoietic Stem Cells (HSCs), possessed an enhanced self-renewal capability and were able to generate the entirety of the leukaemic blast lineage.

Fractionation of tumour cells has now allowed for the identification of many tumour initiating populations in solid cancers, listed in **Table 1**.

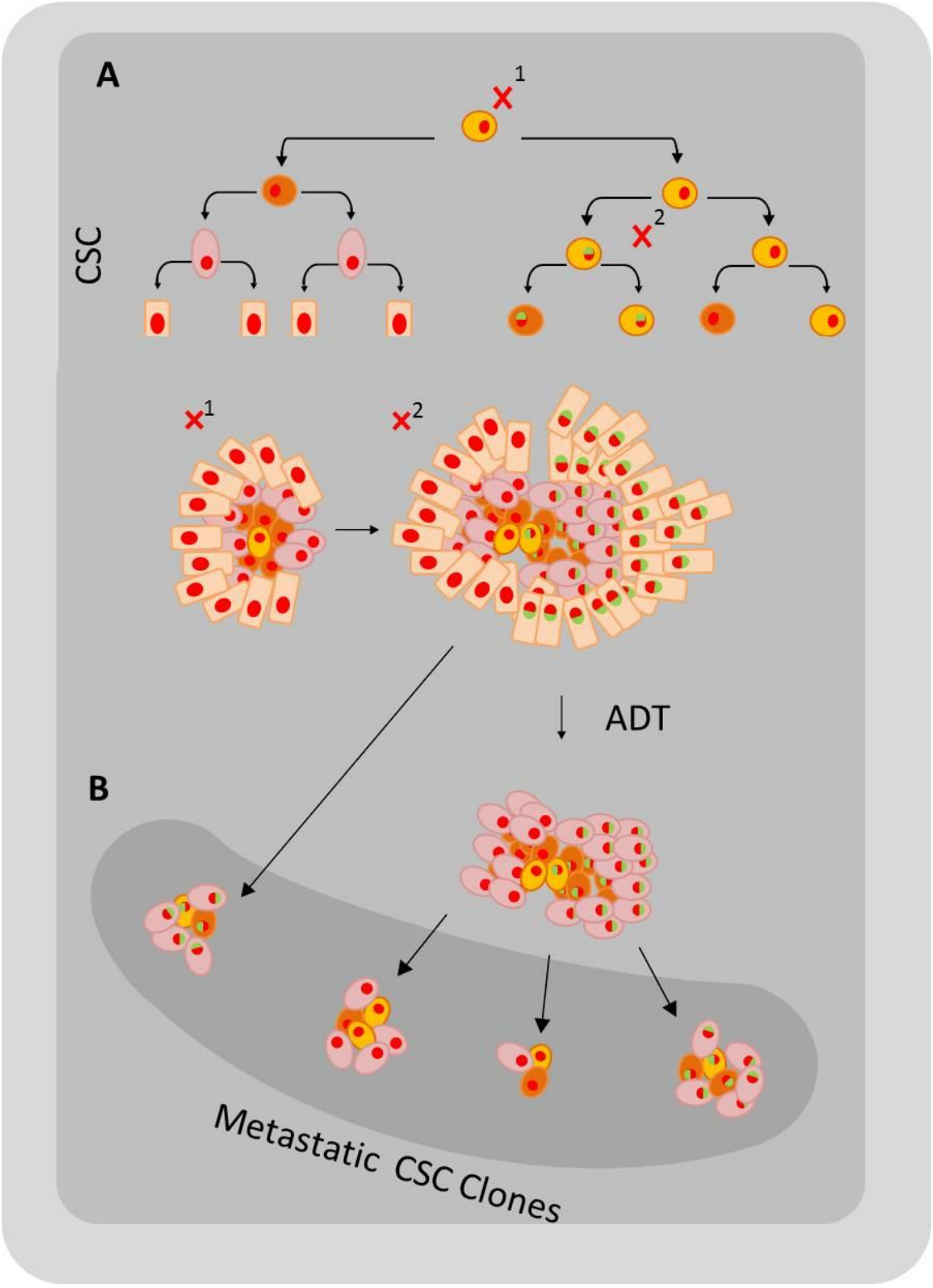

FIGURE 8 – CSC model and metastatic relapse

A) The CSC model of heterogeneity generation. A mutated (X1) progenitor or CSC can both give rise to a more differentiated lineage and create stem cell clones by asymmetric division. The CSC clones can then incur further mutation (X2) to produce another CSC derived mutated lineage and generate the heterogeneity observed in tumours. **B)** Following ADT the basal CSCs, which are innately resistant to castration, can trigger relapse and metastatic spread of the cancer.

Tissue	Phenotype	Reference
Haematopoietic System	$CD34^{+}$ $CD38^{-}$	(Bonnet & Dick 1997)**(184)**
Breast	$CD44^{+}$ $CD24^{-/lo}$	(Al-Hajj 2003)**(185)**
Brain	$CD133^{+}$	(Singh 2003)**(186)**
Multiple Myeloma	$CD138^{-}$	(Matsui 2004)**(187)**
Prostate	$CD44^{+}$ $CD133^{+}$ $\alpha_2\beta_1^{hi}$	(Collins 2005, Patrawala 2007)**(21, 28)**
Melanoma	$CD20^{+}$	(Fang 2005)**(188)**
Pancreas	$CD44^{+}$ $CD24^{+}$ ESA^{+}	(Li 2009)**(189)**
Liver	$CD133^{+}$	(Ma 2007)**(190)**
Colon	$CD133^{+}$	(Ricci-Vitiani 2007)**(191)**
Head and Neck Squamous Carcinoma	$CD44^{+}$ $BMI1^{+}$	(Prince 2007)**(192)**
Lung	$CD133^{+}$	(Eramo 2008)**(193)**
Ovary	$CD44^{+}$ $CD117^{+}$	(Zhang 2008)**(194)**
Endometrium	$CD133^{+}$	(Rutella 2009)**(195)**
Bladder	$67LR^{+}$ $CEACAM6^{+}$ $CK17^{+}$	(He 2009)**(196)**
Cervix	$CD44^{+}$ $CK17^{+}$	(Feng 2009)**(197)**

TABLE 1 – Cancer Stem Cells of solid tumours.

The CSC fraction is characterised much in the same way as adult stem cells. They must be able to self-renew, to maintain the CSC pool, and have differentiation capacity to produce the more differentiated tumour cell lineage. They also display similar cell surface markers (or immunophenotype) to that of their normal tissue counterparts **(19)**. The exact origin of CSCs in a tumour's natural history isn't definitively known, yet current thought is that they arise from a transformative event in a tissue stem cell or near progenitor. The best evidence of this is from colorectal cancers. Here adenocarcinomas were induced in mice *only* upon stem cell transformation and not in the case of attempted initiation by transformed TA cells **(176)**.

The gold standard for CSC validation remains the initiation of cancer by xenotransplantation of enriched cells (preferably a single cell) into immunocompromised mice **(151)**. However, the degree to which each recipient mice strain's immune system is deficient can complicate the interpretation; some may permit CSC growth whilst others may not, based solely on the complement of endogenous immune cells left intact in the mouse **(198)**. Existence of a rare CSC population (apart from in melanomas, where all cells have CSC properties **(198)**) has huge implications for existing therapies that target tumour bulk, yet leave this resistant fraction unscathed to act as minimal residual disease **(44, 199)**. CSCs can be selected and expanded by chemotherapy **(200, 201)** as depletion of tumour bulk causes CSC activation; the root of the cancerous lineage dividing to replace differentiated tumour cells lost to treatment. This could make tumour progenitors susceptible to correctly timed therapies and gives a possible explanation to immediate relapse of cancer following "successful" treatment.

1.3.5 - Pre-tumour development

Pre-tumour development describes a period that occurs well before visible emergence of cancer. The adult or somatic stem cell pool of the prostate isn't depleted by differentiation, development or apoptosis and is maintained throughout the course of an individual's life-span. The long-life and constancy of this cell pool is afforded by the relative quiescence and slow-turnover of the stem cells. This means that, in the case of the prostate, pre-tumour development can take place over decades. The increased emergence of disease in older men does suggest that the stem cell population has a role in disease **(146, 179)**.

However, this is perhaps an oversimplification of the many factors that contribute to carcinogenesis. Recently, the number of life-long stem cell divisions was correlated with cancer incidence in several tissues **(202)**. This analysis however drew widespread criticism as the authors; neglected to use data from major cancers including breast and prostate, **(203)** didn't account for known environmental influences which aid tumourigenesis, **(204)** only used data from the USA

and suggested that cancer is “bad luck” **(205-207)** which flies in the face of current evidence that lifestyle choices play a critical deterministic factor in disease initiation and progression **(208)**.

The vast number of mutations harboured by late-stage solid tumours cannot be plausibly accrued using random multi-hit mutational modelling **(209, 210)** without the early development of a mutator phenotype **(68, 179, 211)**. This is more suggestive of microevolutionary processes that select for advantageous mutation in the stem cells **(212)**. Mathematical modelling implementing cancer genome deep sequencing data has been used to support this theory; identifying that the necessary drivers are present in the first cell with heterogeneity then being derived after initiating events to create the passenger mutation noise that then masks the foundational signature. Here lineages can develop neutrally with passenger mutations becoming adaptive later in progression **(213)**.

1.3.6 - The stem cell niche

Adult and cancer stem cells are maintained by, and contribute to, a niche. The niche is a protective microenvironment that surrounds the stem cell population in the tissue and is constituted by the necessary cell-cell, cell-structure contacts alongside immersion in growth factors and other soluble compounds that can alter stem cell fate and division choice **(38, 214)**. The best evidence for an independent CSC niche is from glioblastoma. Here a hypoxic microenvironment maintains the stem cells **(215)** yet there also exists a sub-clone that can act through trans-differentiation as an endothelial progenitor if the niche requires oxygen **(216, 217)**. The prostate epithelial stem cell niche is most likely located at the basement membrane of acini due to high expression of the collagen-binding integrin $\alpha_2\beta_1$ (CD49b) **(28, 41)**. More research is required into establishing the exact location **(218)** and determining what factors separate the normal and cancerous niches, as specific disruption of the CSC niche would likely amount to an efficacious treatment of prostate cancer. This may also extend to treatments of metastatic disease as niche-mimicry and secondary site seeding by CSCs remain a distinct possibility in prostate cancer **(219)**.

1.3.7 - The immortal strand hypothesis

Stem cell asymmetric division may also protect the population from fixing mutations. The immortal strand hypothesis stipulates that, in mitosis, the stem cell non-randomly retains its template genetic material so that any mutation incurred in DNA replication is segregated to the non-stem daughter. This facilitates both the survival of the stem cell and the serial creation of mutated and differentiated progeny through asymmetric division **(19, 44, 148, 220, 221)**. Initial evidence suggested that the hypothesis may be founded in truth, with selective retention of template strands observed in embryonic fibroblasts **(222)** and by the stem cells of skeletal muscle

(223) and mouse intestine **(224)**. Recent observations however dispute existence of an immortal strand as both HSCs **(225)** and mouse intestinal stem cells **(226)** randomly segregate DNA upon asymmetric division, experiments that are in agreement with current modelling of somatic stem cell mutational accumulation **(227)**. This meta-analysis does have shortcomings in that it compares normal stem cell divisions with cancer genome data and also fails to take into account that CSCs may purposefully disrupt strand segregation mechanisms **(228)** to create an environment more favourable to mutational accumulation.

1.3.8 - Cancer relapse; a stem cell triggered event?

A CSC does not have to increase its proliferative capabilities to be "successful", indeed the ability to enter and re-emerge from a quiescent state is far more advantageous to a cancerous progenitor. This renders treatments such as radio- and chemotherapy ineffective as both rely on cell division to have a toxic effect. Indeed, normal somatic HSCs evade DNA damage through this mechanism **(229)**.

In prostate cancer, targeted treatment of androgen deprivation therapy causes tumour volume to decrease as cells dependent on the hormone develop regressive morphology, stop growing and in some instances, undergo apoptosis **(230-233)**. However, in the following 36 months, the cancer usually reappears and often does so in the advanced and catastrophic spread of metastasis. Dormant CSCs coming out of their quiescent state are a likely perpetrator for the sudden emergence of disease, however little is known about successful metastatic founder clones of prostate cancers **(165, 178, 234)(Figure 8B)**. The targeting of dormant cells with therapy is a difficult challenge in which there are two possible treatment options. The first, and most risky due to the possibility of cellular evasion over time, is enforcing the dormancy of the CSC subpopulation so that they can't re-enter mitosis and bring about relapsed disease. The other acts upon the opposite end of the same signalling axis and actively triggers the CSCs into a cycling state. This would be tailored so that the CSCs have a preference for symmetrical division to produce non-stem daughters, allowing depletion of the cell pool. This so-called differentiation therapy hopes to shift the cancerous cells to a phenotype that then also becomes targetable by the spectrum of conventional chemotherapies **(235-237)**. Differentiation therapy does have one major challenge to overcome, that is; the selective nature of inducing CSC-specific mitotic entry and not that of normal tissue somatic stem cells. This off-target effect in treatment of prostate cancer would result in drastic loss of glandular and acinar architecture – and may also affect other somatic stem cell pools.

1.3.9 - Prostate Cancer Stem Cells

Prostate cancer is slow growing and has been observed histologically in men as young as forty, in whom the disease becomes clinically apparent in later life **(129)**. This suggests a model of accumulated mutations in the stem cell population, rather than cancer arising in the senescent luminal cells. The dominant luminal phenotype in prostate adenocarcinoma **(22)** also hints at an aberrant differentiation program produced by the CSC.

Mouse models have evidence for both basal **(33, 238)** and luminal **(239, 240)** CSCs whereas in the human prostate, overwhelming current evidence points towards a prostate epithelial and cancerous stem cell of basal phenotype **(21, 28, 49, 52, 160, 241-243)**. Isaacs & Coffey predicted existence of these malignant progenitors **(48)** before Collins *et al.* identified the $CD44^{+}$ $CD133^{+}$ $\alpha_2\beta_1^{hi}$ CSC population **(28)**. Subsequent studies using similar basal molecular markers as a base for fractionation and enrichment of this prostate CSCs have independently verified existence of this rare cell type **(21, 244)**. Interestingly, experiments attempting to initiate cancer from benign human basal epithelial subpopulations found that the $CD133^{+}$ cells were protected from tumourigenesis and it was the $CD133^{-}$ $\alpha_2\beta_1^{hi}$ TA population that was susceptible to transformation **(245)**. This suggests that prostate cancers may initiate in a $CD133^{-}$ basal cell that then adapts into a $CD133^{+}$ cell to sustain tumour growth.

The biochemistry of this $CD133^{+}$ CSC population has been further investigated. These cells express the basal epithelial markers; p63, CK5 and CK14, and lack canonical luminal markers; AR, PSA and PAP. The invasive nature noted by Collins *et al.* was further confirmed in microarray data, by identification of an epithelial to mesenchymal transition (EMT) signature, with loss of E-cadherin and gain of both vimentin and osteonectin **(13, 28)**. Common genetic alterations in prostate cancer, such as the TMPRRS2-ERG fusion and PTEN deletions, are confirmed to be present in this tumourigenic population **(66, 246, 247)**.

Notch signalling, classically observed in epithelial cell fate decision making and in the maintenance of the stem cell compartment, is active in prostate epithelial stem cells and their cancerous equivalents **(Rachel Adamson, unpublished data).** Notch is context dependent; invoking varying responses in different cell types and disease stages **(248)**. Active signalling is maintained by cell-cell contact in which a ligand receptor; Jagged 1 (JAG1), JAG2 or Delta-like 1 (DLL1), DLL2 or DLL3, binds the Notch receptor, of which there are four isoforms (NOTCH1-4). Notch receptors are comprised of an extracellular and an intracellular domain (NICD). Binding of ligand receptor to NOTCH begins a series of proteolytic cleavage events, releasing the NICD into the cytosol whereupon it acts as a transcription factor (alongside RBPJ) for a number of canonical downstream genes such as the HES1 and HEY1 transcriptional repressors, MYC and CCND1 **(248)**.

This maintains a dedifferentiated state and facilitates asymmetrical divisions through the polarisation of cell-cell contacts **(249)**.

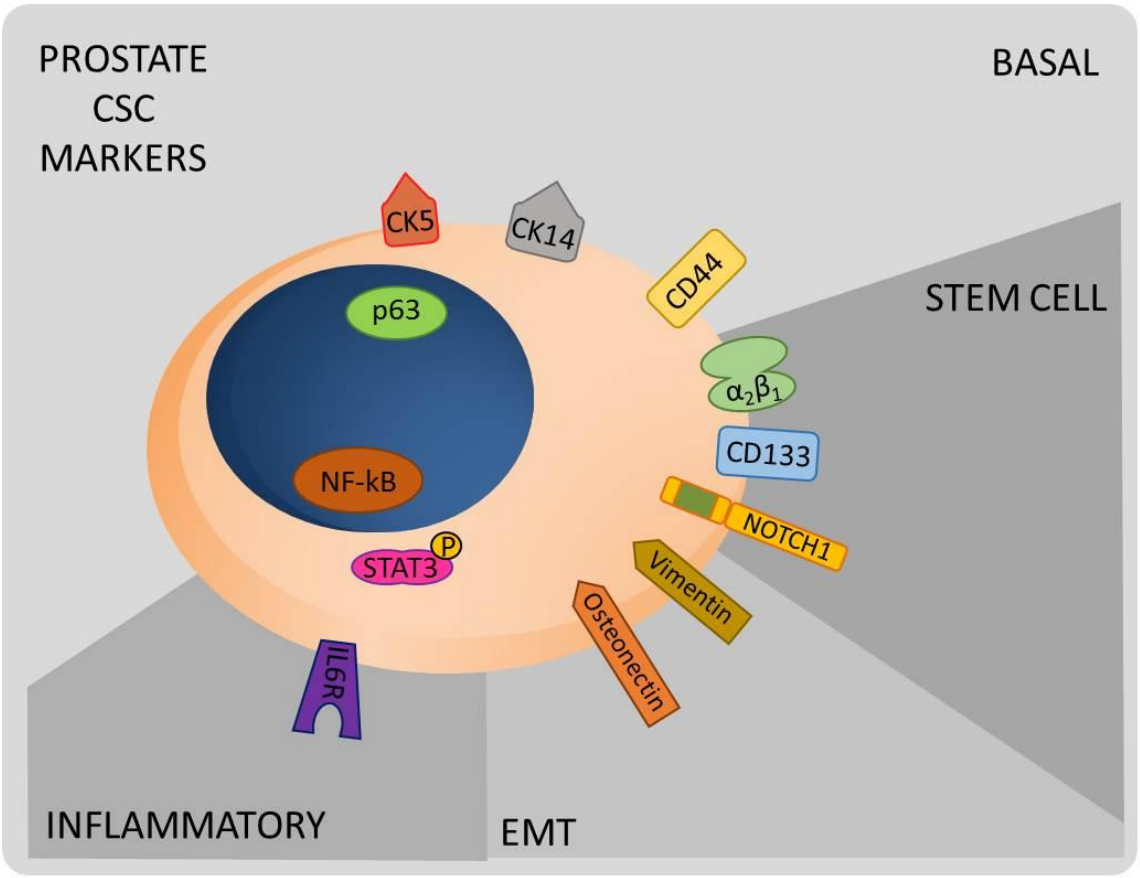

FIGURE 9 – Molecular markers of prostate cancer stem cells.

Combination of basal epithelial, stem cell, epithelial to mesenchymal transition and inflammatory proteins can be used to identify and isolate the cancer stem cells of prostate cancer.

The suspected inflammatory aetiology of prostate cancer may also have roots in the CSC pool. Microarray data distinguished a CSC expression signature with an enrichment in JAK-STAT signalling and NF-kB activation with involvement of IL-6 **(66)**. IL-6 is highly expressed in prostate cancers and serum concentration of the cytokine becomes elevated in metastatic disease **(250-252)**. CSCs have also been shown to express high levels of IL-6 and its cognate receptor (IL-6R), reinforcing an autocrine signalling loop to promote JAK-STAT activation. Disruption of this pathway by STAT3 phosphorylation inhibitor LLL12 resulted in reduced CSC colony forming efficiency and viability as a result of differentiation **(253)**. IL-6 positive feedback via NF-kB has also been shown to act as a transforming and cancer-sustaining event in a breast epithelial cell line, enhancing sphere forming ability and induction of a breast CSC phenotype **(254)**. Activation of STAT3 signalling also affords prostate cancers an androgen independence mechanism in castrate-disease, **(255)** and has been implicated in maintenance of glioblastoma stem cell self-renewal ability **(256)**. The pervasive nature of the STAT3 pathway throughout prostate cancers has led to the development of phosphorylation **(253, 255, 257)** and DNA-binding inhibitors as future treatments of advanced disease **(258)(Figure 9)**.

As alluded to at the beginning of this section, both CSC and clonal evolution theories are likely to co-exist in cancers. For prostate cancer, the slow progression and almost inevitable relapse after hormone therapy can readily be attributed to the CSC pool, whilst the runaway nature of metastatic castrate disease looks to be a CSC-derived dominant clonal expansion of cells **(259)**.

1.4 - Prostate Cancer Diagnosis

1.4.1 - Prostate Specific Antigen Testing

Screening and diagnosis of prostate cancer is currently centred upon serum levels of PSA, a serine protease that aids seminal fluid liquification. PSA in the blood is indicative of cancer, where higher levels correlate with more advanced disease **(260)**. In disease, characteristic degradation of the basement membrane allows escape of this protein into the vasculature, **(136)** increasing circulating concentrations by up to 10^5 fold. The normal adult male blood concentration of PSA is ~0.6ng/ml **(261)** and the threshold value for prostate cancer diagnosis has been set at 4ng/ml. The Prostate Cancer Prevention Trial required all 5519 participants in the placebo group to undergo prostate biopsy after PSA test and digital rectal exam (DRE). The trial found that a PSA value of >4ng/ml has a selectivity of 93% and sensitivity of 24% in correct prostate cancer diagnosis **(136, 262)**. PSA exists in the blood either as free PSA (fPSA) or more commonly, bound to protease inhibitors, as complexed PSA (cPSA). The availability of epitopes on fPSA allows the quantification of fPSA and thus cPSA, in coordination with the normal PSA test that measures total PSA levels **(136)**. The percentage of fPSA seems to be a more specific diagnostic factor than total PSA levels; <25% fPSA has a reported 95% selectivity and 20% sensitivity for correct prostate cancer diagnosis **(263)**.

However, PSA testing, like many biomarker diagnostic tools, does have problems in which false positives are detected and true positives missed. PSA is detectable in other tissues including the lungs and salivary glands, **(264)** other disease states such as prostatitis can elevate circulating levels **(71)** and some men with cancer have normal (<4ng/ml) PSA levels, all of which complicate diagnosis **(262)**.

Several other diagnostic alternatives to PSA have been developed. The next generation urinary biomarkers for prostate cancer are PCA3 and TMPRSS2-ERG **(265, 266)**. PCA3 is a non-coding transcript that is overexpressed, relative to normal tissue, in nearly all prostate cancers. There is significant data which suggests that PCA3 is more selective for prostate cancers than the PSA test **(265, 267)**. This biomarker can also be utilised in combination with urinary TMPRSS2-ERG RNA – an extremely selective prostate cancer transcript, to stratify patient disease **(266, 268)**. Currently, rapid detection colorimetric tests have been developed for TMPRSS2-ERG breakpoints that would allow assessment of fusion status from a post-DRE urine sample in less than two hours **(269)**.

Another powerful diagnostic platform is the Stockholm-3 (STHLM3) model developed by researchers in the Swedish capital **(270)**. The diagnosis of clinically relevant cancers is based upon several plasma protein biomarkers, a genetic profile of 232 single nucleotide polymorphisms

(SNPs) and clinical variables of the individual patients. With the same sensitivity for cancer detection as the standard 3ng/ml PSA test; STHLM3 could reduce total biopsies taken by half and the number of unnecessary biopsies taken of benign disease by 76% **(271)**.The model has recently been improved for the Swedish male cohort by inclusion of further SNPs, specifically a HOXB13 variant and the removal of intact PSA as a serum biomarker, to further reduce unnecessary biopsies **(272)**.

Multi-parametric magnetic resonance imaging (mpMRI) can be used to direct single biopsies of prostate cancer foci through combination of several imaging techniques. These include; T2-weighted imaging which can distinguish between the four tissue zones of the prostate and has high signal intensity in the PZ that is disrupted by tumours, diffusion weighted MRI which measures water movement parameters in tissue, particularly its restriction in tumours, and dynamic contrast enhanced MRI, in which a contrast agent is used to map tissue and tumour vasculature **(273)**. mpMRI has been shown through several large cohort studies to be extremely accurate in detecting clinically significant prostate cancers, is far superior to standard transrectal ultrasound (TRUS) -guided biopsy (that takes 10-12 tissue cores) and is able to stratify disease that requires treatment or active surveillance **(274-276)**.

1.4.2 - The Gleason Grading System

Detection of high circulating levels of PSA in a patient is followed by multiple prostate tissue biopsies to allow for disease stratification by the Gleason grading system **(277)**. This system, based on tissue pathology, was reported in 1966 by Donald Gleason and remains the greatest tool of prognostic value in prostate cancer **(278)** over PSA levels, biomarkers and genetic profiling **(128)**. It works by establishing and rating relative tumour architectural patterns that are scored 1-5; one representing normal acinar morphology and five being anaplastic sheets of undifferentiated tissue. The two most commonly observed grade patterns present in the individual's sample are added together to give a final score between two and ten that is then assigned to the cancer **(Figure 10A)**.

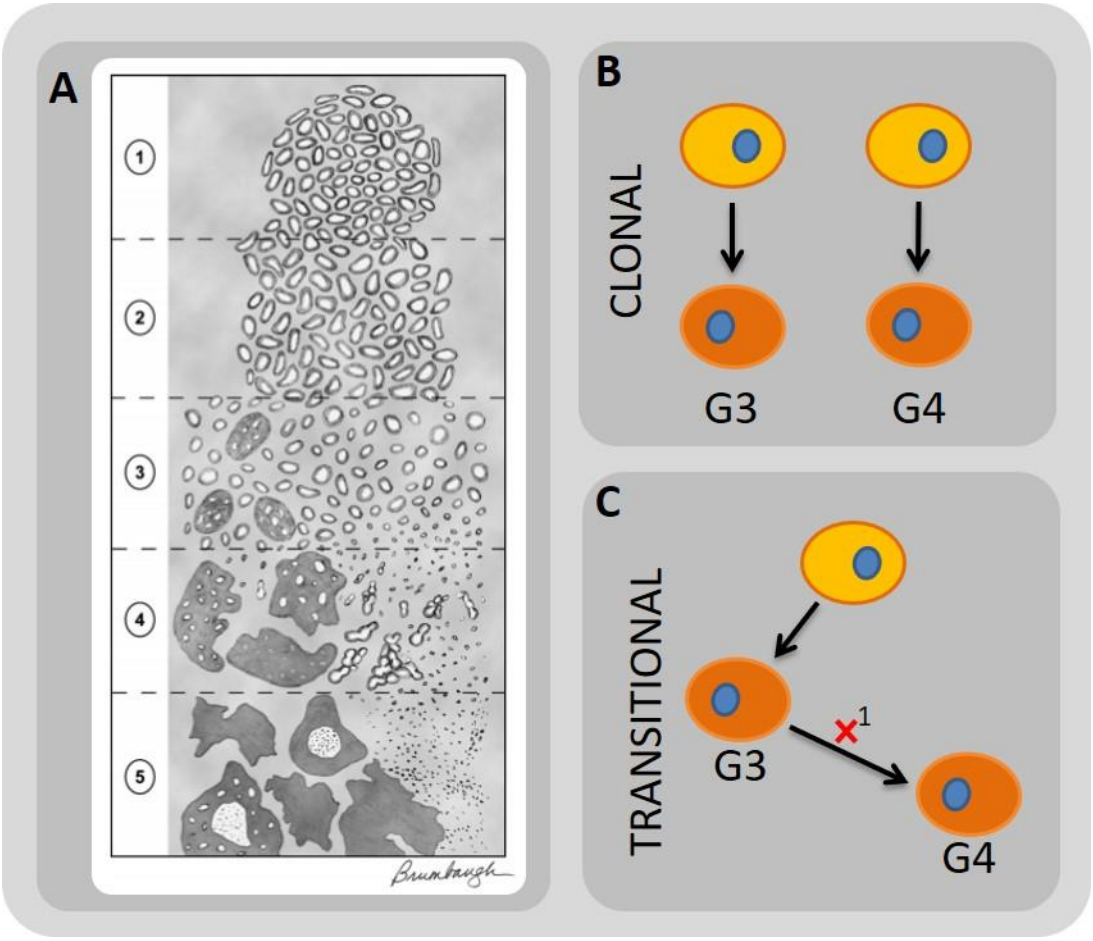

FIGURE 10 - The Gleason grading system.

A) The Gleason grading system chart of tissue pathology – 1 shows normal prostate acini and 5 anaplastic undifferentiated sheets of tissue observed in advanced prostate cancer. Figure taken from **Epstein 2005 (279)**. **B)** Clonal model of Gleason progression – divergent clones "stem" the Gleason 3 and 4 tissues. **C)** Transitional model of Gleason progression – the Gleason 3 cell incurs a molecular change that permits progression to the more advanced Gleason 4 tissue.

The system was revised in 2005, and again in 2014 by the International Society of Urological Pathology, with changes to protocol and additions to classification including; inclusion of cribiform cancer as grade 4, the reporting of negligible secondary lower grade cancer, final grade decision in the presence of tertiary pattern high grade cancer and the consideration of the benign nature of Gleason 3 tissue **(279-282)**.

The major problem that faces diagnosis of localised prostate cancer is that no current biomarker can distinguish between indolent and aggressive disease. This is particularly important when a patient presents with intermediate Gleason grade cancer (6-7); immediate treatment could be life-saving if the cancer is aggressive but over-treatment of indolent cancer has serious implications on the patient's quality of life **(128)**.

There is a notable molecular difference between pattern 3 and 4 tissues, whereas Gleason scores of 4 and 5 are indistinguishable in gene expression studies **(283)**. Gleason 6 and 7 transcriptomic differences were used to construct a gene signature with the ability to separate these tissues. Interestingly, inclusion of the Gleason 6 tumours in total analysis (comparing cancer to BPH) removed any previously observed separation of benign and cancerous tissue **(66)**. Another similar study couldn't produce such a divisive expressional signature; however this may have been due to domination of any underlying gene changes by the majority luminal cell cDNA input of the microarray **(123)**.

Detectable differences between the two tissues bearing separate Gleason grades opens another question facing both clinicians and scientists; do Gleason tissue patterns share a common or divergent ancestral clone? Namely, does the Gleason 3 cell progress into a pattern 4 cell, the transitional model, or are there separate clones for Gleason 3 and 4+ tissues, the clonal model?

The most obvious way to conduct this research is to perform repeat biopsy on patient prostates to track if there is any progression or if development is stemmed from separate cancer clones. However, this approach is hampered by several factors, including; the heterogeneity of prostate tissue, the common multi-focal presentation of cancer and the inherent sampling error of needle biopsies **(284-286)**.

Clonal Model of Gleason Scores

The widespread use of PSA testing has allowed earlier detection of tumours, in the natural history of the individual's cancer, than before clinical adaptation of the biomarker. If Gleason grade progressed over time, this would mean that earlier detection would have reduced the number of higher grade tumours observed at diagnosis. A large study of over 1200 patients found that this wasn't the case and that incidence of Gleason 7+ tumours has not changed post-PSA testing **(286)**. Another piece of evidence supporting the clonal theory is the fact that Gleason 6 (3+3) patterns

rarely advance to lethal disease **(287, 288)** whereas presence of secondary, or even tertiary Gleason 4 tissue predicts cancer progression **(289)(Figure 10B)**.

Transitional Model of Gleason Scores

Supporting a transitional advancement of Gleason grading, is the positive correlation of Gleason grade magnitude with age of detection; older men are diagnosed with increasingly aberrant tissue architecture **(286)**. There is also extremely compelling molecular evidence in favour of the transitional model. Upon tumour tissue isolation, adjacent Gleason 3 and 4 patterns were separated by laser capture microdissection. The tissues were then processed and sequenced. This identified that a small population of the Gleason 3 pattern had stemmed the Gleason 4 tissue due to shared lineage of unique chromothriptic and TMPRSS2-ERG breakpoints **(290)**. Either the tumour had progressed transitionally, or a common progenitor (containing the trunk chromothripsis and fusion genomic alterations) produced both the linked 3 and 4 patterns **(Figure 10C)**.

1.4.3 – Treatment of Low Grade Prostate Cancer

Treatment strategies for prostate cancer are very much dependent on the stage of disease. Low Gleason grade cancers are still differentiated and may require a more conservative approach such as active surveillance. Over-detection of cancers by PSA testing has resulted in treatment of some patients that would never have progressed to a clinically troubling disease. Protocols have been put in place to mark cancer progression rather than treat first, ask questions later. This applies to low Gleason grade tumours with a combined score no greater than 6. PSA is measured every 3 months and biopsies are repeated annually over a 2 year period to monitor tumour status **(291)**.

The surgical approach towards advanced local disease, radical prostatectomy, can prove an effective treatment before local invasion and metastasis have occurred. The benefits of this surgery were observed in a clinical trial of patients that had T0-T2 stage disease, a negative bone scan and PSA <50ng/ml. After 10 years of follow up, deaths due to prostate cancer in the watchful waiting cohort were up 5.3% and incidence of distant metastasis increased by 10.2% over that of the radical prostatectomy arm of the trial **(292)**.

Focal Treatments

Other options for the treatment of localised prostate cancer are focal therapies. This may be preferable to radical surgery in cases where progression of the cancer is low-risk. The chief aim of these therapies is to maximise cancer cell death whilst simultaneously minimising damage to the surrounding tissues **(293)**.

High-Intensity Focused Ultrasound (HIFU) causes intensification of ultrasonic waves, allowing high energies to be delivered into a localised area whilst leaving the tissue along its path-length unaffected. This heats the target tissue rapidly to $80^{O}C$; denaturing their cellular protein content and facilitating necrotic cell death **(294)**. HIFU is applied trans-rectally and is monitored carefully to ensure that the tumour is targeted for the entirety of treatment duration. This issue has been aided by the recent advances in real-time magnetic resonance imaging **(295)(Figure 11A)**.

Cryotherapy allows for rapid freezing and thawing of tissue to result in localised cellular necrosis and cell death, again by protein denaturation. Treatment of the tumour with either liquid nitrogen or argon gas is administered by transperineal cryoprobes under direction of TRUS **(296)**. Freezing of surrounding tissue is monitored using temperature sensors and a warming catheter is applied to the urethra to limit any adverse damage **(297)(Figure 11C)**.

Radiotherapy (RT) delivers targeted ionising radiation to the tumour to cause DNA damage. Damage can occur indirectly; through formation of reactive oxygen species (ROS) that attack the genetic material, or directly; by inducing single or double strand breaks of the phosphodiester backbone. Extensive DNA damage leads to cell cycle arrest and apoptosis. The most common RT applied to prostate cancers is external beam radiotherapy (EBRT), where 5-7 beams are targeted to the tumour mass core. EBRT has recently been improved through use of Cyberknife, a technology that monitors movement of the prostate during treatment and corrects radiation targeting (of 150-200 beams) so that the focal point of radiation remains within a 2mm target area **(298, 299)(Figure 11E)**. Brachytherapy is a variation on traditional RT. Here trans-perineal placement of radioactive seeds such as ^{103}Pd, ^{125}I and ^{131}Cs into the prostate itself allow for localised administration of an internal radioactive dose. Both TRUS and MRI are used to achieve optimal placement **(300)(Figure 11D)**.

Photo-Dynamic Therapy (PDT) produces extremely localised tissue damage through photo-activation of a targeted drug molecule. Energy provided by the light source is transferred to oxygen molecules resulting in formation of single delta oxygen (SDO). SDO creates a hypoxic environment surrounding the tumour and also cause apoptosis/necrosis of the cancer cells **(301)**. Trans-perineal and trans-urethral insertions of fibres for photo-activation have been used in PDT treatment of prostate cancer **(302)(Figure 11B)**. Recently, a Phase III clinical trial targeting low-grade prostate cancers found PDT to be advantageous over active surveillance **(303)**.

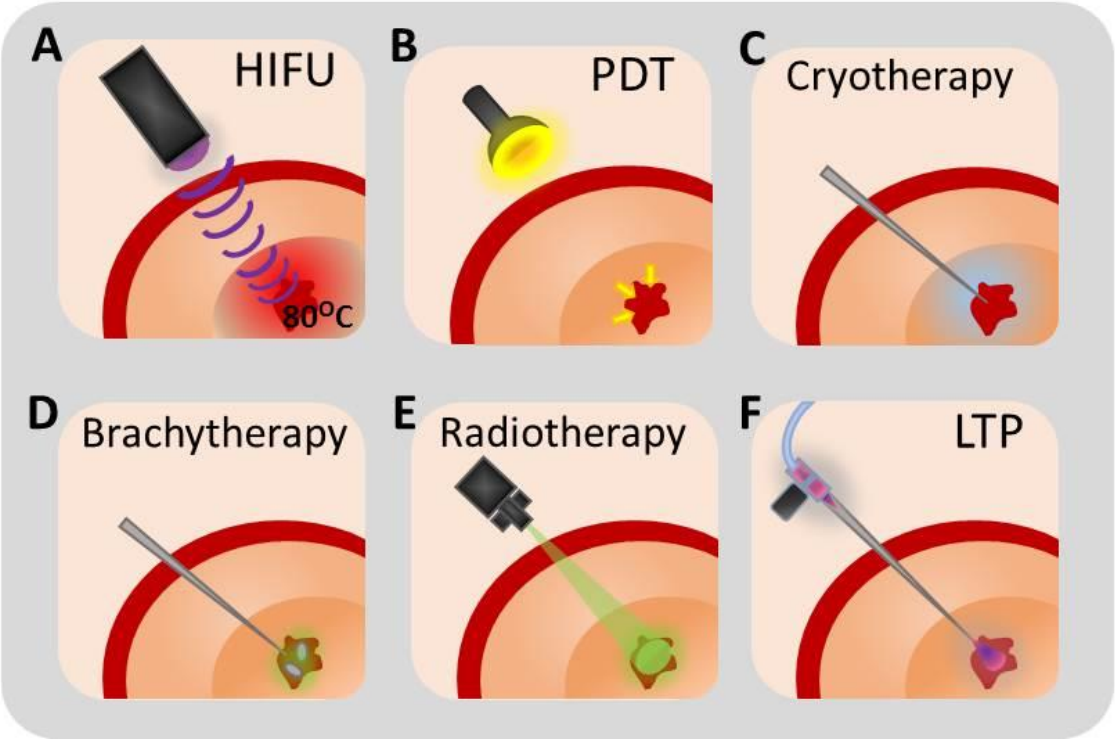

FIGURE 11 – Focal therapies of prostate cancer.

A) High intensity focused ultrasound – heats cells to cause necrosis. **B)** Photodynamic therapy – activates targeted drug molecules using light to cause specific cancer cell death. **C)** Cryotherapy – rapidly freezes tissues to cause cell death by necrosis. **D)** Brachytherapy – planting of radioactive "seeds" in the prostate tumour to exert killing effect. **E)** Radiotherapy – targeted ionising radiation that causes extensive DNA damage and cell death **F)** Low Temperature Plasma – ionised gas injection that facilitates massive oxidative stress and cell death by necrosis and apoptosis. This focal therapy has not yet been tested in patients.

Pre-clinical studies in our laboratory have shown that application of Low Temperature Plasma (LTP) is also effective at killing primary prostate epithelial cells **(304)**. Plasma is formed by the stripping of electrons from gas molecules, achieved by application of a high voltage across an oxygen-helium admixture. The background gases form the dominating species yet the accelerated free electrons drive a unique reactive environment that produces interconverting reactive oxygen and nitrogen species (RNS), UV radiation and charged particles **(293)**. LTP treatment of primary prostate tumour cultures found that plasma reduced cell viability and induced DNA damage, leading to cellular necrosis **(304, 305)(Figure 11F)**. Elucidating the mechanisms behind the killing effects of LTPs on tissues, considerations of safety, practical means of applying the plasma to the tumour site and the establishment an of optimal dose for individual patient treatments are all required before the devices can be implemented in a clinical setting. The full extent of LTP use as a potential anti-cancer strategy will be discussed further in **Section 1.9**.

1.4.4 - Treatment of Advanced Prostate Cancer

Cancers of higher Gleason grade have a less differentiated appearance, and this breakdown of the normal prostate structure hints at the invasive and metastatic potential of the cancer. In this event, the treatment is ADT. These therapies target the androgen signalling axis upon which the majority of prostate cancer cells are dependent **(Figure 12)**.

Androgens are produced mainly in the testes, where expression of testosterone is stimulated by luteinising hormone (LH). LH itself is released from the pituitary in response to hypothalamic luteinising-hormone releasing hormone (LHRH). Pharmacological castration can be achieved through use of LHRH antagonists such as Zoladex, which circumvents androgen production through restriction of circulating LH **(306)**.

Serum testosterone is further processed in prostate cells by the enzyme; 5α-reductase, into the more potent metabolite dihydrotestosterone (DHT) that directly binds AR. Inhibitors of 5α-reductase testosterone metabolism such as finasteride **(262)** and dutasteride **(307)** are known to decrease intraprostatic DHT levels and subsequently reduce androgen signalling in the organ.

ADT can also directly target AR through anti-androgens (molecules that act as AR antagonists). The anti-androgens hydroxyflutamide **(308)** and bicalutamide **(309, 310)** initially have similar efficacies to surgical castration (orchiectomy), showing the specificity these inhibitors have for AR upon first exposure. However, development of resistance to these drugs has prompted the production of second generation molecules.

One such molecule, enzalutamide binds almost irreversibly to AR, reducing its ligand-dependent nuclear translocation and the receptor's ability to bind androgen response elements to recruit coactivators and stimulate transcription **(311)**. A phase 3 clinical trial observed that enzalutamide

increased survival in post-chemotherapy CRPC patients by 5.4 months over that of the placebo group. No direct comparisons with previously used anti-androgens were made, however enzalutamide extended median overall survival by 4.8 months **(312)**. Androgens are produced in the testes, adrenal glands and, in some cases, the prostate by intra-tumoural expression of the CYP17 enzyme. Abiraterone is a selective inhibitor of CYP17 and blocks testosterone synthesis. The drug performed similarly to enzalutamide in post-chemotherapy CRPC patients, improving their overall survival by 3.9 months **(313)**. These drugs represent the current forefront of prostate cancer treatment. Although a modest extension of expected lifespan is granted to these patients **(312, 313)** underlying tumoural resistance at the molecular level arises; with discovery of AR splice-variant (AR-V) upregulation **(314, 315)** and novel AR mutations in relapsed patients **(316, 317)** which allow for promiscuous activation of AR, that can now bind hormones other than androgens **(318)**.

Cytotoxic therapies used in prostate cancer are palliative as they are restricted to the inevitably fatal metastatic patient cohort. The main chemotherapeutic agent used is docetaxel **(319)** which is utilised in a wide range of combination therapies **(26)**. The drug has obvious toxicities as a microtubule stabiliser, yet resistance has developed through involvement of several proteins such as STAT1, **(320)** PIM-1 **(321)** and ABCB1 **(322)**.

Both ADT and chemotherapy assume that the tumour is a mass of homogenous cells that are respectively androgen-dependent and mitotically cycling. In this scenario the heterogeneity evident in prostate tumours is unaccounted for. This oversight is particularly relevant to the prostate CSC population, as they don't express AR and are quiescent or at least extremely slow-cycling. These cells have already been shown to be radio-resistant, **(323)** with other solid tumour CSCs noted to possess an efficient DNA damage response, **(324)** high levels of detoxifying enzymes **(200)** and drug efflux transporters, **(325)** making them extremely resilient targets **(19)**. The most efficient possibility of targeting the CSC population is through use of differentiation therapies, discussed earlier in **Section 1.3**. In the case of prostate cancer this would deplete the stem cell pool through eventual production of more differentiated luminal cells that are then susceptible to ADT. Such differentiation therapies have been observed to work in gliobastoma **(326)**, breast cancer **(68, 327)** and leukaemia **(328)**.

The targeting of the secretory luminal cells in prostate cancer by the ADT regimen is thought to select for the more advanced CRPC phenotype. This disease stage is irreconcilable and leads, eventually, to patient death.

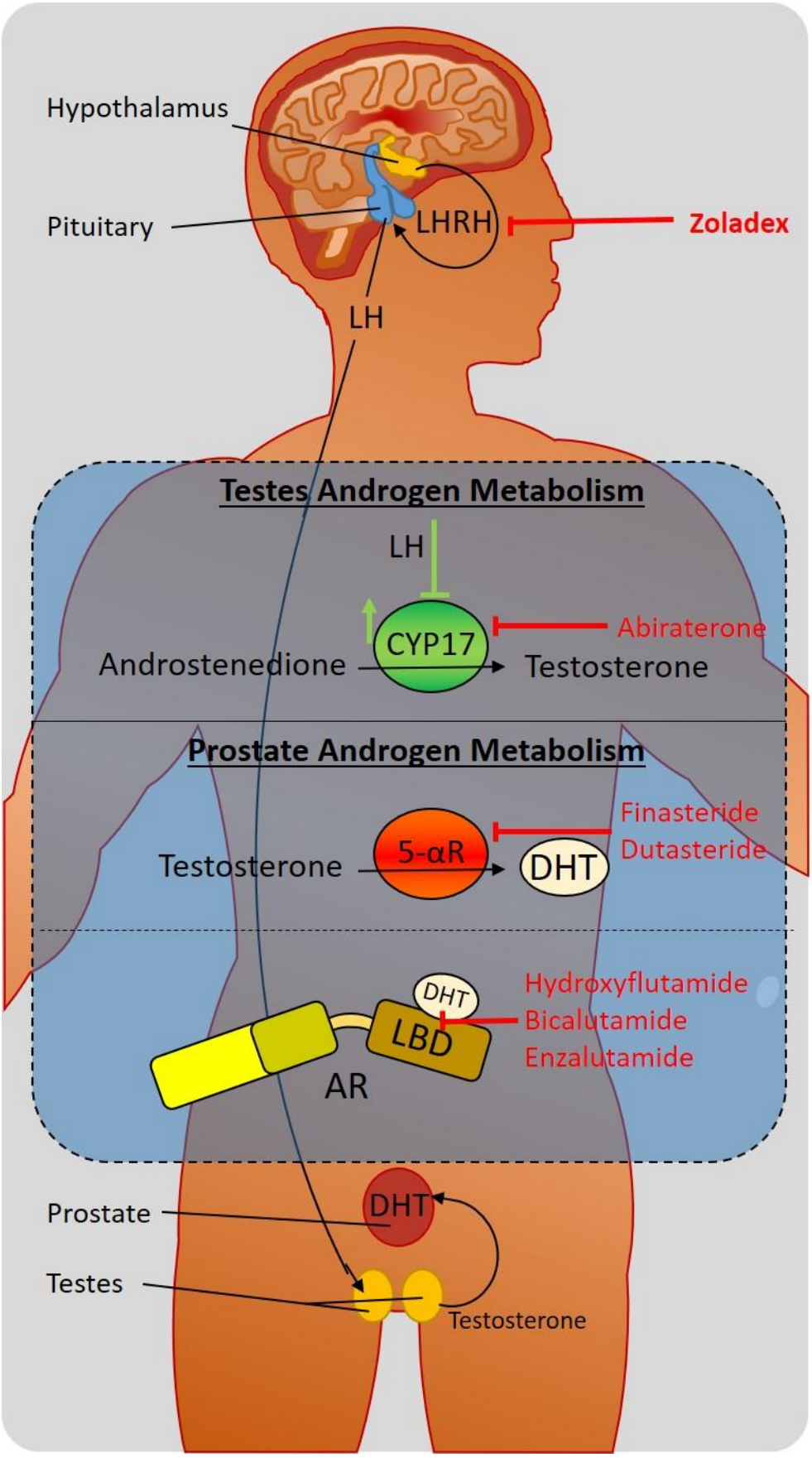

FIGURE 12 – Androgen Deprivation Therapy

The pharmacological targeting of the androgen axis in prostate cancer. The prevention of Luteinising Hormone Releasing Hormone (LHRH) stimulating Luteinising Hormone (LH) induced

production of testosterone in the testes, and the intraprostatic processing of testosterone to Dihydrotestosterone (DHT) by 5-alpha Reductase (5-αR), alongside antagonising DHT binding to the ligand binding domain (LBD) of AR all minimise the pro-proliferative effects of androgens on prostate cancers.

1.5 – The Genetic Background of Primary Prostate Cancer

Current targeted treatments of prostate cancer focus on the androgen-axis, in part due to the work of Huggins **(329)** and the importance of AR in prostate development,**(7)** but also as relatively few other targetable defects have been identified through genetic studies. The profound heterogeneity between patient's prognoses and corresponding genetic profiles of tumours has hampered progress **(330, 331)**. Recent studies have attempted to define genetic subtypes that could be used to profile; cancer indolence/aggressiveness, Gleason scores and, in advanced cancers, separation of CRPC and neuroendocrine prostate cancer (NEPC) **(27, 66, 283, 332, 333)**. The ultimate aim is to offer accurate prognosis to individual patients based on the genetic make-up of their cancer.

Prostate cancers differ from most solid tumours, as they rely almost entirely upon copy number variations, rather than specific mutation, to facilitate cellular transformation and disease progression **(90, 133, 174, 175, 334, 335)**. With tumours of so-called "hypermutator" phenotype, regularly observed in primary cancers of other tissues, only presenting following advanced treatment **(336, 337)**. Scrambling of the prostate cancer genome is achieved by chromoplexy; chained rearrangement events that are notably convergent between individual patient tumours. Temporally, it isn't known when these patterned translocations and deletions occur in a cancer's natural history. Due to clonality of founder or "trunk" events (fusion of TMPRSS2-ERG and NKX3.1 deletion) and sub-clonality of further common genetic aberrations (PTEN and CDKN1B deletions) chromoplexy is presumably a staged event that occurs over a long time. Deletions of RB1 and TP53 are also linked to chromoplectic chains, yet only present in advanced prostate cancers **(334, 338)**. It is thought that defective DNA repair machinery, a common defect in prostate tumours, aids the chromoplectic re-shuffling of the genome. It is relevant that hallmark chromoplectic deletions and fusions are present in the prostate CSCs **(66, 246, 247)**.

As a hallmark of cancer, **(148)** genomic instability can both predispose and accelerate tumourigenesis, becoming particularly relevant to prostate cancer, in the light of common mass genomic rearrangement. Instability afforded by the reduction of telomere lengths and aberrations to DNA maintenance and damage response pathways in prostate cancer contribute towards a less favourable prognosis **(339)**.

Prostate cancer frequently presents with attenuated DNA damage response and repair networks **(338, 340)(Figure 13)**. Studies of both familial and sporadic disease have identified predisposing genetic alterations in these pathways. The well-known BRCA1 and 2 mutations most commonly associated with ovarian and breast cancers, also heighten risk of prostate cancer development in men **(341, 342)**. Families with hereditary prostate cancer show an enrichment of Chk2 mutations;

with the defective enzyme unable to cause G_1 arrest and prevent the accumulation of genetic aberration, upon detection of DNA damage **(343)**. Risk alleles for DNA repair genes PARP1, ATM and XRCC1 have been identified by multiple independent population studies **(344)**. Whilst these mutations and variants do increase risk of developing cancer, they typically present in less than 5% of the total population. Observation of further recurrent ATM and p53 mutations in advanced prostate tumours show that DNA damage response is an important signalling axis in the initiation and progression of prostate cancers **(27)**. These defects mainly affect the homologous recombination repair (HRR) pathway making prostate cancer cells more reliant on the error prone non-homologous end joining (NHEJ) pathway to fix double strand breaks (DSBs); a situation that lends itself to the production of chromoplexy. **(Figure 13)**

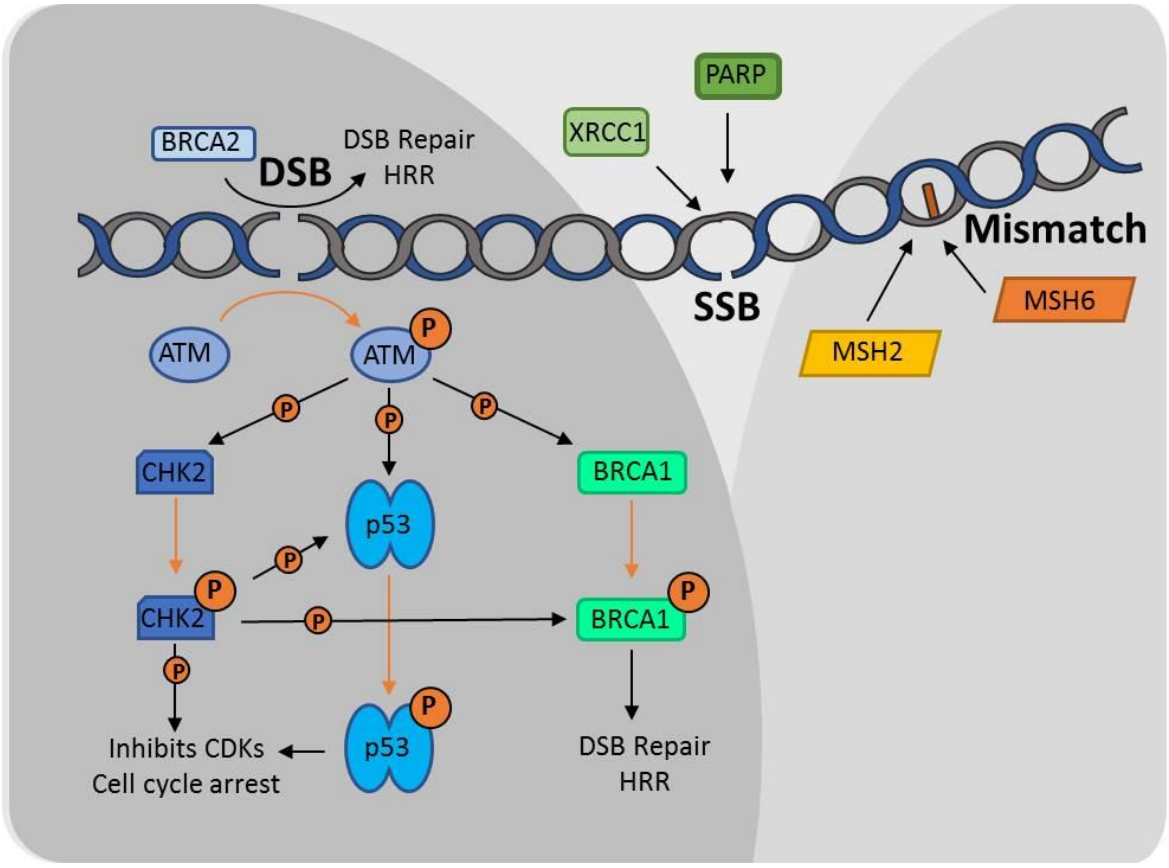

FIGURE 13 – Defective DNA damage repair response in prostate cancer.

The genes of all proteins depicted in the diagram are recurrently mutated or deleted in prostate tumours. Arrows depict phosphorylation (P) events that activate the recipient protein.

Replicative stress triggered by runaway oncogene activation also contributes towards genomic instability. In the prostate, ungated activation of AKT and the PI3K pathway; due to catalytic subunit mutations of PI3K **(90, 133)** and the more common PTEN deletion, **(345)** alongside proliferative signals supplied by dysregulated MYC increase the mitotic index and thus replicative stress of affected cells **(346)**. AKT can promote the NHEJ DNA repair pathway, creating an environment more favourable for chromoplectic rearrangements **(340)**. AR also has a role in DNA damage response as the nuclear receptor relies upon PARP1 to enforce its basal transcriptional program **(347)**. Upon DNA damage; AR stimulates upregulation of DNA-PK_{CS}, XRCC2 and XRCC3, proteins that have a role in the DSB repair pathways of homologous recombination repair and NHEJ **(348)**.

Tumours of the prostate that present with a mutator phenotype are attributed to genomic rearrangement and mutation of the mismatch repair pathway enzymes, specifically MSH2 and MSH6 **(90, 133, 336, 337)**. Current evidence suggests that genetic insult to these enzymes, and thus tumour hypermutation, is created by the genotoxicity of cancer treatments. Therefore this phenotype is observed more prevalently in advanced disease; however mutation of MSH6 has been identified in primary prostate cancer **(133, 337)**.

Linkage studies relating ETS^{+} tumours to DNA repair gene variants have identified risk alleles encoding ESCO1, POLI1 and BRCA2 that form a genetic background inductive of fusion formation **(349)**. In a culture environment of genotoxic stress, and a lineage-dependent manner; prostate cells form de novo TMPRSS2-ERG fusions, an event attributable to AR-mediated transcriptional proximity of involved loci **(350)**.

Distinct molecular subtypes of prostate cancer have now been assigned to tumours due to the frequent identification of genomic changes, in both primary and metastatic disease **(334, 335)(Figure 14)**. One classification paradigm is the ETS factor fusion status of the tumour. Now commonly and recurrently observed, ERG and ETV1 fusion events were discovered as prostate cancer specific aberrations in 2005 **(351)** and the TMPRSS2-ERG fusion has now been established by many large population cohort studies to occur in half of all primary tumours **(90, 330, 331, 334)**. These fusion positive tumours often have linked chromoplectic deletions of PTEN, TP53 and 3p14 (a locus encompassing several tumour suppressor genes) **(90, 133, 334)**. A divergent subclass of prostate tumours are those that harbour CHD1 deletions **(133, 352)**. CHD1 is an ATP-dependent chromatin remodelling factor that facilitates availability of transcriptionally active chromatin. CHD1 deletion is often mutually exclusive of ETS fusions, as loss of the remodelling protein results in an increase in condensed chromatin. The open chromatin structure usually observed at the fusion loci therefore no longer forms – meaning that there is a reduced chance of damage, inappropriate repair and thus fusion formation **(353)**. SPOP mutation, the most

frequently observed mutation in primary cancers, **(133, 330)** co-segregates with CHD1 deletions to give an ETS^- $CHD1^-$ $SPOP^-$ subclass. Through combining prostate cancer transcriptomes with matched genome data, detailed signatures can be used to stratify prostate tumours on prognosis and outcome using this advanced molecular data **(90, 331, 338, 354, 355)**.

The genetic heterogeneity of primary prostate cancer was highlighted by a study conducted by the Cancer Genome Atlas (TCGA) which extensively mapped over 300 primary prostate cancers and, using the comprehensive information gained by several sequencing platforms, was unable to group one in four of the tumours into a molecular signature. This genetic heterogeneity in the initial stages of localised cancer will impact the response to treatment of these tumours as well as their progression into more advanced and castrate disease **(330)**. Another recent multi-centre sequencing study of prostate cancers identified novel coding and non-coding driving events in primary tumours that had remained undetected in previous datasets and their subsequent analysis **(338)**. This highlights that there are still important molecular alterations which remain to be uncovered, aberrations that may play pivotal roles in the initiation and progression of select sub-groups of prostate cancer.

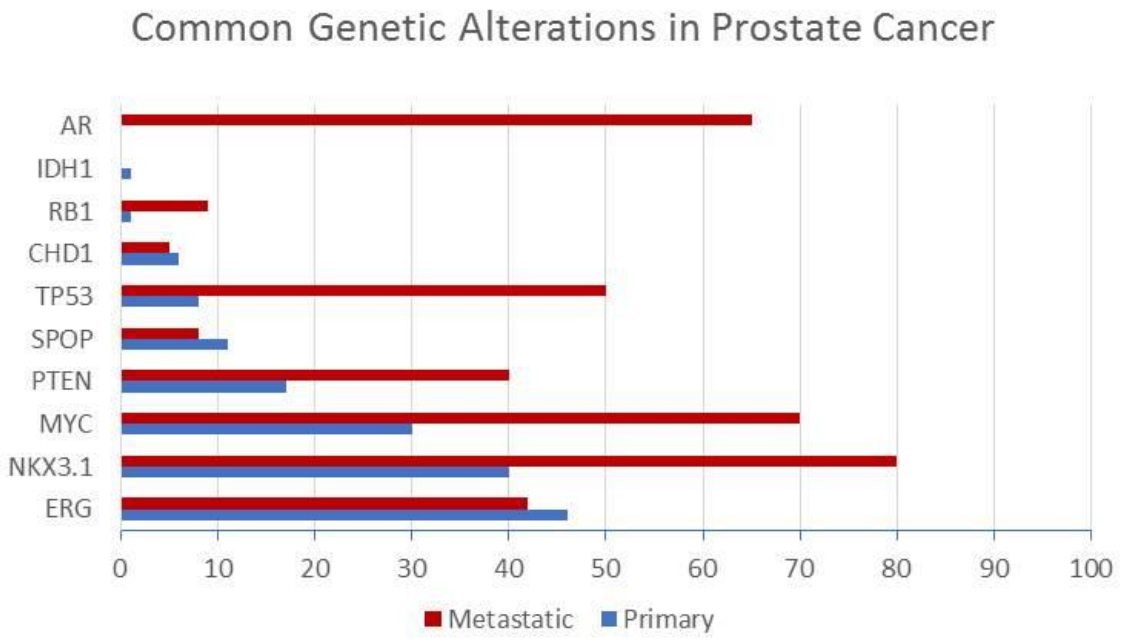

FIGURE 14 – Common genetic alterations in primary and castrate resistant prostate cancer.

Graph compiled using data from Taylor 2010 **(90)**, Robinson 2015 **(331)** and TCGA 2015 **(330).** The scale represents the percentage of the sequencing cohort with genetic aberration in the labelled gene.

1.6 - Castrate Resistant Prostate Cancer (CRPC)

1.6.1 - Androgen signalling in end-stage disease

The first line of chemotherapy for advanced prostate cancer is ADT, which is achieved by chemical ablation of the androgen axis as discussed in **Section 1.4.** Specific targeting of the AR by anti-androgens leads to the clonal expansion of cells that have AR aberrations. These cells can function in extremely low levels of androgen through dysregulation of the androgen signalling axis.

Before the CRPC terminology, this end-stage of disease was referred to as androgen independent prostate cancer as the pharmaceutically imposed androgen blockade was thought to have nullified AR signalling. However in castrate conditions, tumours and metastases have been identified to possess residual, and augmented, androgen signalling. Here the cancer switches from androgen-dependent stromal paracrine signalling to a more autocrine pattern **(356)**. The most common genetic alterations specific to CRPC, found in 50-60% of patients, are those that influence AR signalling and the receptor itself **(331, 357, 358)(Figure 15)**. This is likely due to treatment-mediated selection of cellular subpopulations in which AR alteration confers survival advantages in castrate levels of androgen. Hormone naïve cancers rarely exhibit any detectable AR changes apart from a few exceptions, suggesting that the aggressive latter stage of disease may be induced by ADT **(359, 360)**. Overexpression **(361)** (via possible autoregulation **(362)**) and transcription factor dysregulation **(363-365)**, locus amplification **(366, 367)** and mutations that reduce ligand-specificity **(368-373)** of the receptor all manifest in CRPC tumours. A similar effect is seen in methotrexate resistance, where amplification or overexpression of dihydrofolate reductase is frequently observed in leukaemia **(374)**.

A recent study investigating patient-matched metastatic and non-metastatic tumours observed that AR amplification and mutation were; mutually exclusive, and absent in hormone-naïve cancers **(27)**. It is now widely accepted that ADT profoundly alters prostate cancer genomes and transcriptomes **(375)**. AR promotes a divergent transcriptional program in CRPC, to that of the nuclear receptor in localised disease, supporting cellular survival in castrate conditions **(376)**. Thus AR maintains a role in the development of CRPC.

Another ADT-circumvention mechanism upon which CRPC relies is the constituent action of AR splice variants (or AR-V). These divergent transcripts are created through aberrant splicing of cryptic exons early in the AR gene **(377-380)**. The majority of the variants also exhibit absence of latter exons encoding the nuclear receptors' hinge region and ligand-binding domain (LBD) **(381)** that allow for degradation **(382)** and activation of the receptor respectively. AR-Vs show constitutive nuclear localisation, that is not reliant upon canonical importation pathways **(383,**

384) and are able to activate transcription of the full-length AR gene portfolio independently of androgen binding, ablation therapy and indeed presence of the full-length transcript **(315, 378, 383, 384)**.

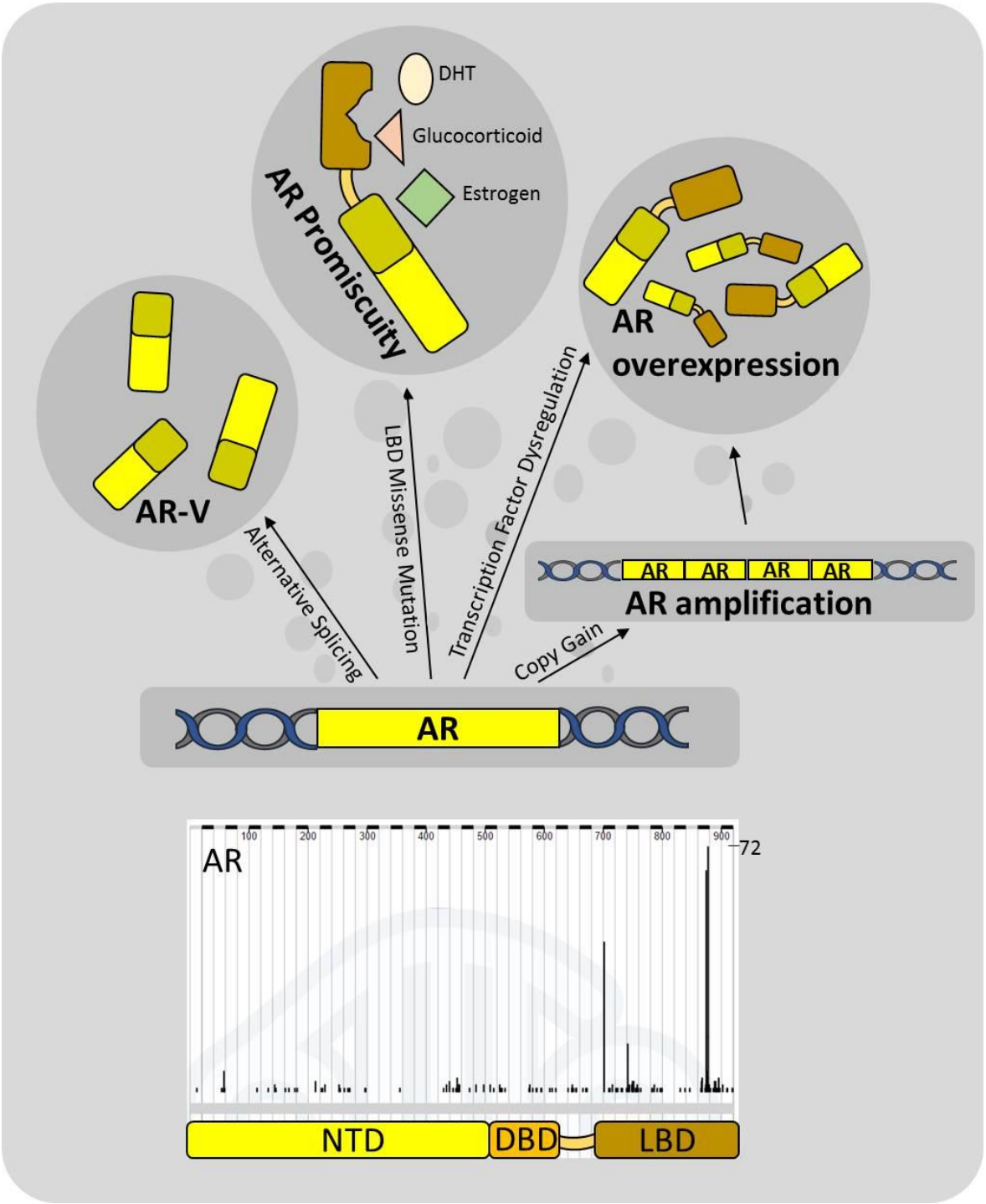

FIGURE 15 – Androgen Receptor aberration in CRPC

AR changes through splice variation, ligand binding domain mutation, overexpression and amplification in advanced castrate disease. Mutational plot highlighting clustering of LBD mutations was adapted from COSMIC website **(385)**.

Variants activate gene transcription networks divergent from those of full-length AR such as STAT3, AP-1/Jun **(384)** and AKT **(378)**. However not all studies are in agreement with this altered profile **(315)**. As most anti-androgens including bicalutamide and next generation treatments such as enzalutamide target the LBD of AR **(315)**, AR-Vs are not susceptibility to these therapies. Instead this innately conferred resistance allows the variants to proceed unaffected; directing the independent growth of cancer cells. They are observed to be upregulated and selected in castrate conditions both in culture **(315, 381)** and in tumours **(378, 379)**. However, there is opposition to these findings that state the variants rely on full-length AR for effect, and this renders them sensitive to enzalutamide **(381)**. In benign prostate tissues, presence of the splice variants in stromal and basal populations, but not in the luminal epithelia, may contribute towards the androgen independent growth of these cells **(378)**. It is still unknown whether the epigenetic changes resulting in AR-V production are a driver of late stage disease or an adaptive change.

Most studies interrogating the molecular workings of CRPC focus on AR. Whilst the nuclear receptor is an important driver, it does not completely account for the "efficacy" of end-stage disease. Indeed, recent studies have shown that small cellular populations of AR^- neuroendocrine and AR independent basal cells are left untouched by hormonal treatment **(241)**. Currently it is unknown whether CRPC is a natural progression of prostate cancer or if it is selected by ADT. Supporting evidence for CRPC as an inevitable stage of disease include; 10-20% patients have no biochemical response to ADT **(386)** and the identification of AR alterations prior to treatment **(387)**. Castration selecting for CRPC has been suggested in the sudden appearance of androgen signalling defects in tumours and in studies in mice models **(388)**. This selection could hypothetically be of a luminal cell that has already acquired therapy resistance attributes and/or of an androgen independent basal TIC.

1.6.2 - Involvement of Basal Cancer Stem Cells in Metastatic disease

Selection of the CSC pool is entirely plausible, as they are therapy resistant and would expand in response to the castration-induced apoptosis and growth arrest of the secretory luminal epithelia **(232)**. Androgen-independent cells (existing at low frequencies; 1 in 10^5-10^6 cells) in a prostate cancer xenograft were able to re-initiate tumour growth by clonal expansion **(389)**. These cells, although uncharacterised, were very probably the CSC population.

In the recent generation of organoid cell lines which accurately represent metastatic prostate cancer, one of these models PCa6 presented with cytokeratin 5 and p63 expression and a genetic background of PTEN deletion and MLL2 mutation suggesting a metastatic outgrowth of basal cell origin **(241)**. This is supported by another study which developed a comprehensive and congruent expression profile between primary basal stem cells and advanced neuroendocrine metastatic

cancer datasets from multiple studies – suggesting that the progenitors may be at the root of advanced disease **(390)**.

Dysregulation of micro RNAs (miRNAs), key post-transcriptional regulatory molecules dictating gene expression, in prostate cancer has been recognised for almost a decade **(391-394)** with implication of specific miRNA networks in castrate resistance **(395-398)**. It has recently been shown that the miRNA profile of prostate CSCs is conserved between different disorders and tumour grades suggesting that miRNAs are critical in stem cell maintenance throughout disease progression. Forced expression of miR-548c-3p, upregulated in the progenitor population, reverted the CB cells to a more stem-like state, both phenotypically and functionally. Interestingly, the prostate CSC miRNA expression profile is closest to that of unfractionated CRPC cells **(399)** with the signature confirmed by other studies that noted miR-548c-3p elevation in advanced prostate cancers **(400)** and the overlap of EMT/CSC miRNA expression networks **(401)**.

CRPC is predominantly viewed as a progression of disease, yet a dedifferentiation phenotype is becoming more apparent. Whether this is an acquired plasticity of malignant cells or an expansion of the CSC pool is yet to be determined. There also exists the possibility that a subset of CSCs is more metastatic than others amongst the tumour initiating population, like that observed in pancreatic cancers **(402)**. The reappearance of prostate CSC markers and molecular subtypes in advanced disease will hopefully be incorporated into the development of treatments which consider the difficulty of killing malignant stem cells.

1.6.3 - Neuroendocrine Prostate Cancer

The castrate levels of androgens also permit emergence of a distinct tumour phenotype. Anaplastic or NEPC is often seen focally in advanced prostate cancer and represents a truly androgen-independent form of disease as these cells do not express AR **(27)**. NEPC correlates with a more aggressive clinical onset, progressing to death <6 months post-diagnosis **(403-405)**. It is thought that neuroendocrine cell differentiation may be occurring during CRPC; thus cases of NEPC may benefit from docetaxel and carboplatin combination chemotherapy that would have obvious toxicity on the dividing cells **(26)**.

Neuroendocrine cells are found primarily in the PZ of the organ, scattered throughout the basal epithelium. They are terminally differentiated, canonically lack AR, release mitogenic compounds, and are classically identified through staining for chromogranin A **(404)**. The functions of this cell type are unclear but it is thought that neuroendocrine cells assist prostate epithelial differentiation through secreted factors and may possibly affect the constitution of seminal fluid **(396)**. Inflammatory stimuli also play a role in neuroendocrine differentiation; cooperativity between IL-6 and STAT3, like that reported in CSCs, has also been shown to cause neuroendocrine

differentiation in prostate cancer cell lines **(406)**. Recent sequencing of cancers with neuroendocrine features identified upregulation of EZH2 and co-amplification of N-Myc and Aurora kinase. Molecular hallmarks that distinguish this disease stage over primary epithelial tumours **(26)**.

Neuroendocrine prostate cancer has clonal origins in prostatic adenocarcinoma as shown by a study investigating p53 mutation **(407)**, a finding which is corroborated by exome sequencing efforts to disseminate the heterogeneity of advanced cancer. Postulation that the neuroendocrine phenotype may arise through divergent clonal evolution from the original adenocarcinoma following hormonal treatment rather than a linear progression into androgen independence **(333, 375)** suggests that either an aberrant differentiation pathway or trans-differentiation may be promoted in castrate conditions.

1.6.4 - Genetic heterogeneity in Castrate Resistant Prostate Cancer

Considerable effort has been made to map the specific genomic landscape of CRPC **(27, 335, 408-410)**. Recurrent fusion of TMPRSS2-ERG, deletion of PTEN, NKX3.1 and BRCA2 with amplification of Myc are inherited from earlier stage tumours **(27, 133, 174, 334, 335)**. Post-ADT tumours have additional AR mutation and amplification (not observed in hormone-naïve cancers), but also increased p53 mutation, RB1 loss and defects in DNA damage repair and response enzymes **(27, 335, 408, 409)**. SPOP mutation, although present, **(27, 155, 331, 411)** is not seen at the same level as observed in primary tumours, **(133, 174)** with mutation percentage dropping below 10% in advanced disease **(330)**.

Pathway analysis of CRPC also identified similar defects to these found in primary cancer, such as disruption of the PI3K signalling network, **(90, 174, 335, 409)**, deregulation of ETS factors,**(123, 334, 335, 351)** and AR cofactors including; NCOA2 **(90, 409)** and FOXA1 **(334, 335)**. The Wnt/β-catenin pathway is selectively activated in CRPC tissues over hormone-naïve cancers and is linked to a dedifferentiated phenotype in these castrate conditions **(410)**. The Wnt and Glucocorticoid Receptor (GR) pathways are mutually exclusive in circulating tumour cell (CTC) subsets, suggesting that variant androgen-independence mechanisms develop side-by-side in metastatic cancers **(411, 412)**. The shift in hormonal synthesis under low androgen conditions also creates an environment that selects for promiscuous AR mutant clones which can be activated by glucocorticoids **(413)**. WNT5A, upregulated in CRPC, has also been shown to confer heightened cancer cell resistance to the anti-androgen enzalutamide **(412)** showing that these pathways not only allow more effective growth of cancer cells but also protect them from cell death.

As discussed above, treatment of CRPC is palliative as no current drug combination can dissect the genetic heterogeneity of metastatic disease **(reviewed in (414))**. Heterogeneity regarding cell-

type has again not been addressed to a sufficient level in these studies as most sequencing efforts employ, at best, epithelial cell mixtures from tissue microdissections or needle biopsies which also contain stromal and haematopoietic cells. However, the improved depth of sequencing does allow for visualisation of clonality – especially in metastatic polyclonal abundance **(411, 412, 415)**. The mutation rate in non mutator phenotype tumours **(331, 335-337)** is very low in CRPC tumours, suggesting a non-obvious inductive aetiology.

Alterations found in DNA repair and response genes are found in 20% of CRPCs. Loss of BRCA2, which also exhibits germline predisposition of prostate cancer, becomes apparent in castrate resistant over treatment naïve cancers **(331)**.

Targeting the androgen axis has proven to be effective in the short term, yet as resistance continually develops in response to next generation therapeutics, novel treatments that act upon other actionable defects in end-stage disease are required. Currently, the most promising among these is PARP inhibition **(416-418)**. This utilises the defective DNA damage response and repair pathways against the cancer, and kills cells due to synthetic lethality. Synthetic lethality is where one mutational event has no effect as a variant bypass pathway can rescue the damage but a secondary event in (or inhibition of) said salvage pathway becomes lethal for the cell **(340)**.

PARP is involved in the repair of single-strand breaks with inhibition proving lethal to cells that have DSB processing defects – a common phenotype in advanced prostate cancer with recurrent identification of loss of or mutation to BRCA2 and ATM genes **(331)**. Several studies have highlighted the potential of PARP inhibitors in cancer **(416, 418)**. These insights have produced the TOPARP clinical trial of olaparib in prostate cancer patients which has confirmed the predicted enhanced response in patients that present with disrupted DNA response and repair **(417)**.

Aside from sequencing efforts to gain insight into how prostate cancer genomes are rearranged, studies have also identified dysregulation of multiple chromatin modifying enzymes that further impact upon the epigenetic state of tumours in advanced disease. These include alterations to the histone methyltransferases (HMTs) ; EZH2, **(90, 123)** MLL2, SMYD, **(335)** and demethylases; JMJD3, **(419)** KDM4C **(420)** and JARID1B to name a few. The epigenome of prostate cancer and indeed the significance of the alterations to both DNA and histones in the initiation, progression and prognosis of disease is only just beginning to be uncovered **(421-423)**.

1.6.5 - Prostate Cancer Invasion and Metastasis

Metastasis is the process in which the primary cancer spreads to anatomically-distant secondary sites utilising body cavities or the circulatory and lymphatic systems. In prostate cancer, patient metastasis represents a terminal diagnosis. Only ~5% of patients initially present with metastases yet this percentage rises to 40% after treatment **(26)**. Like other cancers, prostate metastases

have particular secondary tissue tropisms; - 90% of patients have bone metastases upon autopsy, highlighting the extreme bone tropism of prostate CTCs. Other common metastatic sites are the lungs (46%), liver (25%), pleural cavity (21%) and adrenal glands (13%) **(424)(Figure 16A)**.

The metastatic cascade is a series of steps that cancers must pass through to establish and form "successful" secondary cancers throughout the body, outlined in **(Figure 16B)**.This process is extraordinarily inefficient, with estimates that fewer than 0.01% of CTCs actually form macrometastases **(425)**. Certain steps such as final metastatic colonisation of the foreign tissue also have higher attrition rates than others **(426)**. Most metastases have a clonal route from one locally confined cancer focus, showing a selection process of "successful" cancers.

1. **Local Invasion**

   Breakdown of the BM by secreted proteases, such as matrix metallo-proteinases (MMPs), **(427)** releases extracellular matrix GF ligands that enhance an invasive phenotype. Destruction of the BM affords greater access to the reactive stroma that further contribute to invasion through heterotypic signalling **(14)**. Here, EMT plays a critical role. Reduced E-cadherin expression through miRNA and transcription factor interplay causes dissolution of epithelial structures and allows cells to collectively invade local tissue. At the cellular level two distinct invasive programs have been identified; mesenchymal (protease, stress fibre and integrin dependent) and amoeboid (Rho/ROCK signalling dependent). Plasticity exists between these two states to optimise invasiveness in different microenvironments **(164, 428)**.

2. **Intravasation**

   Intravasation is the process by which tumour cells access the vasculature or lymph. The main route of metastasis is through the circulatory system with acquisition of traits that allow passage through the pericyte and endothelial cell layers which surround blood vessels. The vessels stimulated to grow within tumours however aren't "normal". Angiogenesis initiated by the hypoxic microenvironment creates an irregular neo-vasculature. These vessels have incomplete pericyte coverage and are also prone to leaks due to weak endothelial cell interactions, both of which make intravasation a much easier process **(429)**.

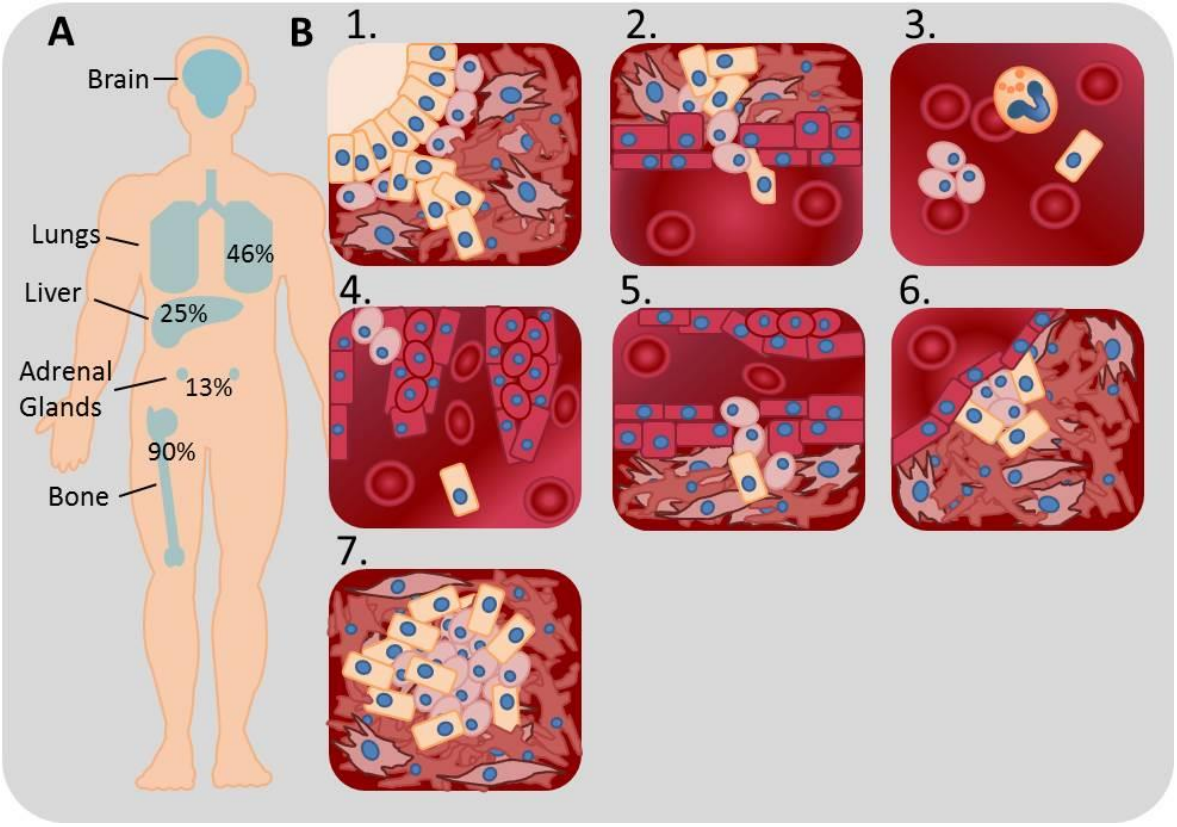

FIGURE 16 – Metastatic cascade of prostate cancer

A) Common secondary sites for metastatic prostate cancer colonisation. **B)** The metastatic cascade of prostate cancer; 1. Invasion, 2. Intravasation, 3. Circulation, 4. Secondary site arrest, 5. Extravasation, 6. Survival in secondary site microenvironment, 7. Secondary site colonisation

3. **Circulatory Survival**

CTCs are spread via venous and arterial blood flow to distant secondary sites. PSA expression has been used to detect prostate cancer CTCs in the peripheral circulation **(430)**. CTC number has also been used in prognosis of castrate resistant disease. Identification of >5 cells in 7.5ml of blood correlated with a 10 month reduction in overall survival **(431)**. These circulating cells have been characterised, showing the presence of TMPRSS2-ERG fusions with heterogeneous AR amplification and PTEN loss **(432)**. As a survival requirement, these cells must suppress anoikis (apoptosis provoked by loss of anchorage to the substratum) mechanisms, **(433)** and assuage other problems, such as immune surveillance and shearing forces within the blood vessels. Expression of certain cell surface molecules allows the CTCs to complex with platelets and form metastatic emboli. These bodies can thus evade both fates through the binding of other circulatory cells **(434)**.

4. **Arrest at Secondary site**

Cancer cells have preferable adhesion sites, evident in their individual tissue tropism profiles. It is thought that this process is dependent on both the physical restrictions of CTC passage through micro-vessels and differential expression of cellular adhesion molecules that allow selective attachment in certain capillary beds **(164)**.

5. **Extravasation**

Upon vascular arrest, the cells move by the process of extravasation through the vessel walls. Extravasation is an exceedingly more difficult proposition than intravasation as secondary site vasculature is healthy and is likely to be of low permeability. This does have exceptions such as at the fenestrated sinusoids of the liver and bone **(435)**.

6. **Survival in the Secondary site microenvironment**

Initial survival at the secondary site is obviously critical for metastasis formation. To achieve this, cells must adapt to the variant microenvironment that is composed of different stromal cell constitution, ECM ligands, GFs, cytokines and tissue architecture. There is evidence of preparation of secondary sites as pre-metastatic niches, with the aim to reduce the differences between the distant tissue and the primary tumour. This is thought to be achieved through tissue remodelling instigated by secreted systemic factors from the original tumour and would also explain cases of tissue tropism **(436)**. This challenge also shows that cells involved in establishing secondary site metastases cannot be terminally differentiated, as some plasticity must be retained. In prostate cancer it has been shown that the β_1 integrin is involved in interactions with bone stroma that enhance survival and colonisation **(437)**. This includes $\alpha_2\beta_1$, a surface marker of prostate CSC and

TA cell populations, **(28)** citing possible involvement of these progenitor cells in seeding metastases.

7. **Secondary site colonisation**

   Survival at the secondary site is no guarantee of "successful" metastases, as the cells can remain viable but may not be able to produce any net gain in numbers due to either; entry into a quiescent state or simply a balance between proliferative and apoptotic indices. Tissue-specific tropism has been observed in divergent metastatic gene-sets identified in breast cancer for bone, lung, brain and liver colonisation **(164)**. Success in sustaining prolonged growth however depends on the self-renewal capabilities of the cells establishing the secondary site, again implicating CSC involvement.

An interesting study followed a single patient from diagnosis to death, tracking the genetic trail of the complete metastatic cascade. Sequencing of the patient's multi-focal primary cancer and biopsied/autopsied metastases revealed a monoclonal origin with acquired genetic changes throughout staged progression **(155)**. This approach has previously identified clonal origin of metastases in primary pancreatic tumours, **(438)** and indeed reflects the intra-tumoural heterogeneity of the primary cancer itself **(439)**.

1.7 - Prostate Cancer Models

1.7.1 - Cell Lines and Primary Cultures

Cell lines are the primary model of studying prostate cancer as a disease. They are able to be easily manipulated and transfected over repeated passages and can be grown in varying culture conditions. There are now well established lines representative of normal tissue, benign, malignant and metastatic forms of disease. These cells also range across basal and luminal phenotypes to give a more complete picture of disease, in which the appropriate mode can be chosen for further study **(Table 2)**.

Cell lines are useful models in preliminary studies of the disease yet do not accurately represent prostate cancer *in vivo*. Long term culture of cells has been shown to cause divergence from the original phenotype and genotype of the once physiologically relevant disease at initial isolation **(440)**. This includes chromosomal alterations, changes in gene expression **(441)** and promoter hypermethylation **(442)**. There have also been cases of misrepresentation; due to cell line cross-contamination **(443)** or laboratory introduction of an infectious agent **(444)**. Current problems facing prostate cancer cell lines are; the relatively low number of them (which have been made widely available), their failure to recapitulate all of the molecular phenotypes of disease and the lack of lines produced from a current disease state, with the majority of cells having been isolated from tissue over 20 years ago **(Table 2)**. Culturing of primary cells, taken with patient approval, provides a better disease model. Primary cells still have slight changes imposed upon them by culture conditions yet afford a close and relevant model of patient disease when kept at a low passage **(445)**. These prostate cancer primary cultures display relevant molecular defects including TMPRSS2-ERG **(66, 246)** and PTEN deletion **(247)**. Primary culture is not without its practical limitations. Cells are often slow growing and in some instances patient tissue doesn't propagate in culture at all. The restriction of keeping cells at low passage also means that the high cell numbers required for some molecular techniques, and readily achievable through growth of cell lines, cannot be reached using primary cultures.

Cell line	Tissue Derivation	Immortalisation Method	Phenotype	Stage of Disease	Disease Features	Derivation Reference
PNT2-C2	Primary epithelial culture	SV40 large T and small t antigen	Luminal	Normal	Express CK19	Berthon 1995 **(446)**
PNT1-A	Primary epithelial culture	SV40 large T and small t antigen	Luminal	Normal	Luminal CK Expression	Cusenot 1991 **(447)**
BPH-1	TURP primary epithelial cell culture	SV40 large T antigen	Intermediate	Benign	Luminal CK expression, AR^-, PSA^-, PAP^-	Hayward 1995 **(448)**
P4E6	Primary epithelial culture	HPV-16 E6 gene	Intermediate	Malignant	Luminal and basal CK expression, $CD44^+$, β_1^+, AR^-	Maitland 2001 **(449)**
Du145	Brain metastasis	/	Basal	Metastatic	Androgen insensitive PTEN Heterozygous Deletion **(451)**	Stone 1978 **(450)**
PC3	Bone metastasis	/	Basal	Metastatic	Androgen insensitive PTEN Homozygous deletion **(453)**	Kaighn 1979 **(452)**
22Rv1	CWR22 xenograft	/	Luminal	Metastatic	Contains AR splice variants **(454)**	Sramkoski 1999 **(455)**
LNCaP	Lymph node metastasis	/	Luminal	Metastatic	Mutant AR **(456)** TMPRSS2-ETV1 fusion **(351)** PTEN frameshift **(453)**	Horoszewicz 1980 **(457)**
VCaP	Bone metastasis	/	Luminal	Metastatic	$TMPRSS2\text{-}ERG^+$ **(458)**	Korenchuk 2001 **(459)**

TABLE 2 – Prostate cell lines

Derivation, phenotype and molecular features of prostate epithelial cell lines.

Four years after characterisation of prostate epithelial stem cells in 2001, **(41, 50)** the same surface markers of $CD44^{+}$ $\alpha_2\beta_1^{hi}$ $CD133^{+}$ were used to isolate the tumourigenic fraction from prostate cancers of varying Gleason grades. The selected population constituted ~0.1% of total tumour cells, exhibited self-renewal with high secondary colony forming efficiency, displayed enhanced proliferative potential over that of non-malignant prostate epithelial stem cells and were also extremely invasive **(28)**. Selection of the tumour subpopulations is described in further detail in **Figure 17 (50)**.

There is also another problem that the current, and limited, repertoire of prostate cell lines doesn't fully address; the genetic background of disease for both primary and advanced cancers. The metastatic cell lines, as indicated in **Table 2**, do have some common features of disease such as PTEN deletion, AR mutation and ETS factor fusions yet other subtypes of disease such as SPOP mutation, CHD1 deletion and SPINK1 overexpression aren't represented **(460)**. A study in 2014 attempted to expand this cohort of lines by successfully generating seven fully-characterised organoid cultures **(241)**. These cultures encapsulate the molecular phenotypes listed above as well as harbouring other common genetic alterations seen in advanced disease such as RB1 loss and TP53 mutation **(335)**. These representative and more relevant models can hopefully be more widely distributed, to facilitate discovery of treatment strategies and further current understanding of the molecular underpinnings governing advanced prostate cancers.

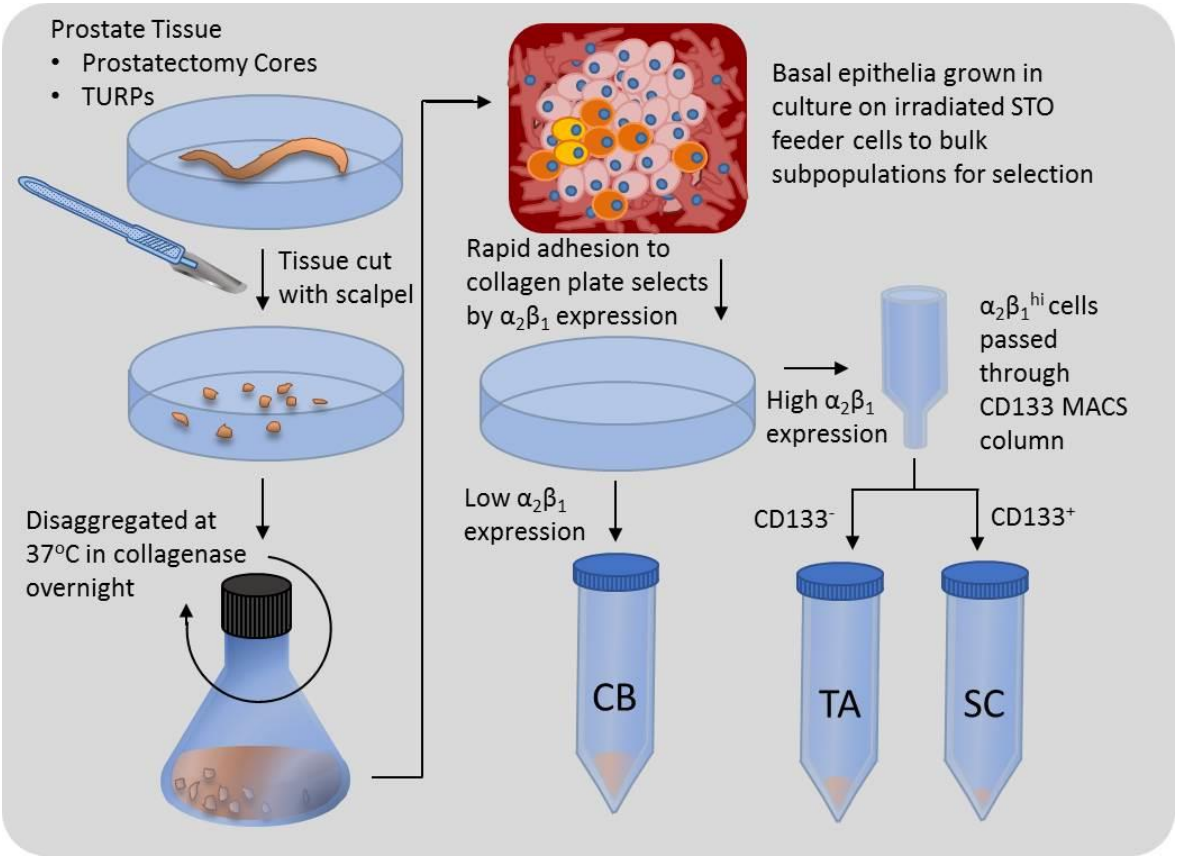

FIGURE 17 - Generation of primary prostate epithelial cultures from tissue

Tissue from patients is cultured using this process stream. Molecular markers can then be used to isolate individual cell populations from the heterogeneous epithelial cultures.

1.7.2 - Mouse Models; Xenograft and Transgenic lines

For any theory or treatment option to be clinically accepted, results of in vitro studies must be validated in vivo. The greatest in vivo tool used in prostate cancer is the mouse. These are either generated as transgenic models or are recipients of human prostate cancer tissue xenografts **(128)**.

Studies using transgenic mice have been pivotal in uncovering the precise biology of many human diseases, however there are many anatomical differences between the prostates of mice and humans. Firstly, mouse prostate tissue atrophies with increasing age, a situation contrasted to the spontaneous neoplastic growth of both BPH and cancer in humans **(461)**. Anatomical organisation also differs; the mouse organ comprises of four lobes surrounding the urethra whereas humans have an alobular prostate that envelopes the descending urethra **(462)**. The glandular structure of the tissue is similarly divergent. Human acini are composed of distinct, yet contiguous, luminal and basal epithelial layers in comparison to the single mixed layer of epithelial cells of the mouse prostate **(463)(Figure 18B)**.Tumours do not naturally initiate in the mouse prostate, meaning that any parallels drawn between cancer in the mouse to that in the human have to be carefully considered. The very act of promoting a non-naturally occurring scenario on a model system will produce artefacts, some of which may be open to misinterpretation.

Since mice do not spontaneously develop prostate cancer, transgenic models have been generated to mimic disease development. The two classic transgenic lines are TRAMP and Lady, with other more specialised models subsequently generated to investigate gain or loss of specific proteins. Such mice include $PTEN^{+/-}$, $TMPRSS2\text{-}ERG^{+}$ and $TMPRSS2\text{-}ERG^{+}/PTEN^{+/-}$ mice that have given useful insights into the process of carcinogenesis **(464, 465)(Figure 18A)**.

Xenografts can be established from cell lines or primary human tissue. Cell line xenografts have major limitations as they do not recapitulate the heterogeneity of prostate cancer. As previously mentioned, these cells have genetic and phenotypic changes induced by culture that aren't representative of tumours. Grafting of human tissue provides a better model of true cancer yet proves even more challenging than primary tissue culture, with initial grafts only having a 0-20% "take" rate. Xenograft lines, established from successful primary tissue grafts, can be serially transferred between mice. In prostate cancer, these include the well-established LAPC and CWR22 lines. Again, the value of these models has been questioned due to lack of AR and PSA expression in most lines and the lack of physiological similarity due to tissue adaptation to the environment of the mouse. Efficacy of this process is dependent on the site of engraftment; subcutaneous, in the renal capsule or orthotopic. Each has relative survival advantages and mimicry of tumour microenvironment yet each is met with increasing procedural challenge. Other additional aids such as testosterone implant and mouse mesenchymal tissue recombination have

been shown to improve xenograft survival rates **(466)**. Patient derived xenografts (PDX) are notoriously difficult to grow due to inefficient take rates and complication in that human T and B cell lymphocytic tumours spontaneously develop in the immune-deficient PDX models and mimic solid tissue derived cancer **(467)**. Report of 21 novel and characterised PDXs, representative of metastatic prostate cancer, that both encapsulate the genetic heterogeneity of advanced disease and respond in similar fashion to conventional treatments (docetaxel and ADT), is promising news in the search for more efficacious CRPC therapies **(468)**.

Xenografting is performed in immunocompromised mice to stop the rejection of foreign tissue. The best emerging model are the NOD mice, these lack T and B cells and have NK cell and macrophages with impaired function. The addition of mutation-inactivated ILR2γ to these mice causes further depletion of NK cells and dendritic cell dysfunction. This augmentation to the original model has produced the NSG (NOD-SCID-ILR2$\gamma^{-/-}$) and NRG (NOD-Rag1$^{-/-}$-ILR2$\gamma^{-/-}$) mice which, due to lack of an effective immune response, allow for improved xenograft take efficiency **(466)(Figure 18C)**.

However, the lack of immune system in the mice can permit development of spontaneous human lymphomas in the mice from tumour-infiltrating immune cells with latent EBV infection. This is particularly common in prostate cancer PDXs which both decreases successful take rates and requires further diagnostic screening to remove these “false positives” **(469, 470)**.

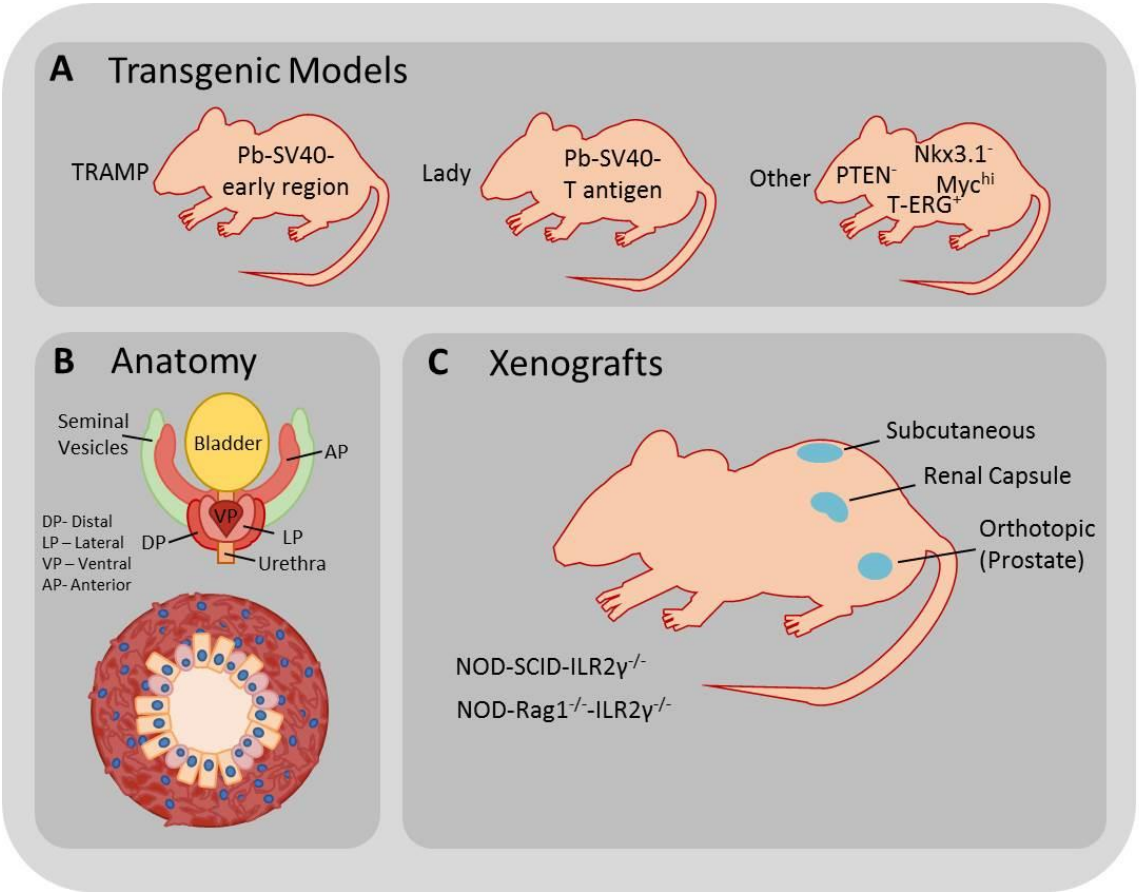

FIGURE 18 – Mouse models of prostate cancer

A) Transgenic mouse models of prostate cancer, Lady and TRAMP represent early models and the latter highlighting the prostate specific expression (or lack) of known disease genes. **B)** Organ and gland anatomy of the mouse prostate. **C)** Xenograft mouse lines and engraftment sites for modelling prostate cancer

1.7.3 - Cancer Stem Cells in Mice

Both basal **(33, 238, 471)** and luminal **(239, 240)** CSC models of disease are supported in the mouse prostate; a scenario that frustrates the search for the origin of an epithelial stem cell progenitor in human prostate cancer, adding more confusion than clarification.

In terms of CSC dynamics during xenotransplantation, the niche in mouse tissue will not re-capitulate that of the cell in culture or indeed that of epithelia in the human prostate. Hypothetically, xenografting of cancer cells may select for a previously non-dominant CSC clone that is better adapted in supporting tumour growth in the mouse **(245)**. The stromal compartment is extremely important in prostate tumourigenesis; xenografting of cancer cells with human stroma enhances their tumourigenicity, implying that the CSC pool interacts with the stromal compartment to enhance intrinsic self-renewal and proliferative capabilities **(472, 473)**.

As discussed, mice are important in deciphering the development and mechanisms of prostate cancer. However, limitations are due to the physiological differences compared to the human prostate gland; both cellularly and anatomically **(474, 475)**. The lack of immune response and non-endogenous heterotypic stromal interaction also adds further variables that must be accounted for in the modelling of disease **(466)**.

1.8 - Alterations of Allelic expression in Prostate Cancer

PTEN and SPOP are two tumour suppressor genes (TSGs) that are recurrently mutated, at modest frequencies, in primary prostate tumours. Genetic aberrations of both genes are typically heterozygous; meaning that a functional allele is still present in affected cells. Cancers may exploit this "opportunity" and silence the remaining gene copy epigenetically. The IDH-1 proto-oncogene is also observed to be heterozygously mutated in a small percentage of prostate tumours. The effects of mutation are pleiotropic in different cell backgrounds and thus the mutated allele may be silenced for reactivation in a more "favourable" setting by cancer cells to maximise the selective advantage of the enzyme's neomorphic capabilities.

Allelic regulation of gene expression has, over the last decade, been shown to affect many autosomal disease genes, a possible explanation for the variable penetrance of several neurodegenerative disorders, but hasn't yet been interrogated in prostate cancer. Recent work conducted in the Maitland laboratory observed monoallelic expression of the TMPRSS2-ERG fusion gene in prostate CSCs. The finding highlights the importance of allelic perturbation in cancer and suggests that selection of ERG is beneficial for stem-like properties of these malignant progenitors. Identification of higher order regulatory mechanisms in allelic expression may allow therapeutic targeting of epigenetic insults in prostate cancer.

1.8.1 - Classical monoallelic expression

Mendelian genetics assumes that inherited alleles, paternal and maternal, are congruently expressed and contribute in equal parts to progeny phenotype. This is termed biallelic expression, where transcription of both alleles occurs in equivalent frequencies **(476)**. However, for some gene sets; expression only occurs from a single allele. To date, there are three distinct examples of monoallelic expression; X chromosome inactivation (XCI), imprinting and random monoallelic expression (RME).

X-inactivation is a mammalian female-specific dosage compensation event in which one of the X chromosomes is enveloped in heterochromatin and silenced. This creates cellular X monosomy, meaning that there is only one active copy of each X-linked gene present. The initial selection for silencing of the chromosome; X^M (maternal) or X^P (paternal) is random and propagates clonally, yielding a mosaic pattern of X inactivation across tissues **(477)**. The mechanism of XCI is well studied and involves Xist (X-inactive silencing transcript), a long non-coding RNA (lncRNA) **(478)** produced from the X inactivation centre (XIC). Xist achieves this by recruiting the Polycomb repressive complex 2 (PRC2), containing EZH2, that directs trimethylation of H3K27 along the

chosen X chromosome **(479)**. Silencing the majority of genes on a single X chromosome facilitates, by default, monoallelic expression of the partner alleles on the active X **(Figure 19)**.

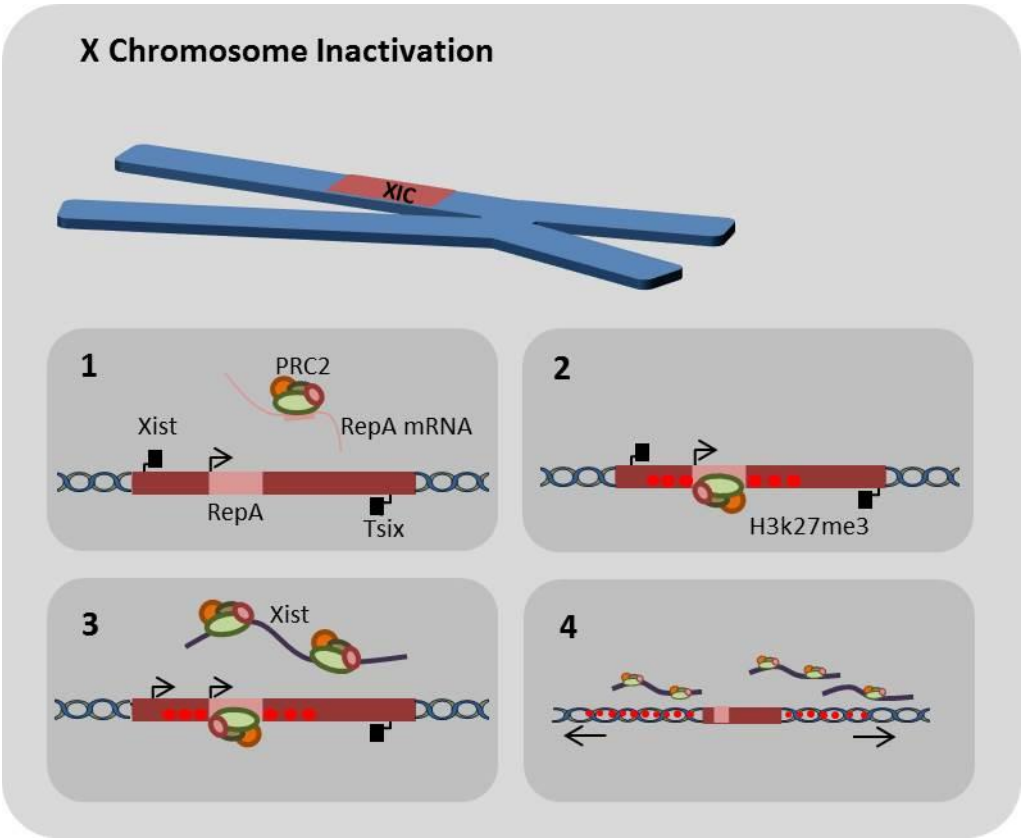

FIGURE 19 - X chromosome inactivation

1. RepA mRNA recruits PRC2 to the X inactivation centre (XIC)
2. PRC2 directs trimethylation of H3K27 of XIC
3. This activates Xist lncRNA expression that recruits PRC2
4. Xist directs the repressive trimethylation of the whole X chromosome through PRC2

Imprinting is non-random monoallelic expression. Here, silencing is dictated by parent-of-origin-dependent expression in gene clusters. This phenomenon accounts for observations that both paternal and maternal chromosomes are required in the development of viable progeny **(480)**. These clusters all contain a regulatory element, or imprinting control region (ICR), that enforces the monoallelic expression of a local gene or genes. lncRNA genes also found at the loci further enforce silencing of one of the alleles.

Gene imprinting has several models describing the regulation of allelic expression. Currently, these can be divided into insulator and lncRNA regulated imprinting. In the insulator mechanism; a protein coding and lncRNA gene (separated by a common ICR) share downstream enhancer sequences. The maternal allele ICR is bound to by a CTCF insulator protein which restricts access of the protein coding gene to the enhancer as they are now in disparate genomic neighbourhoods. At the paternal allele; the ICR is methylated thus CTCF cannot bind to the element. The paternal epigenetic alteration also seeds secondary methylation of the lncRNA gene resulting in paternal allele expression of the protein coding gene, as the enhancer regions are accessible and maternal-specific expression of the lncRNA. This is canonically observed at the Igf2 – H19 locus **(481)(Figure 20A)**.

Currently the lncRNA model of imprinting has no definitive universal consensus, and indeed seems unique in both a cellular context and the nature of the individual lncRNA. There is evidence to show that the sense transcript may anneal to the antisense of the adjacent allele's promoter causing, initially, transcriptional disruption followed by a proximal accumulation of repressive chromatin and DNA methylation, or loss of active histone marks **(482)**. Another possibility is that the imprinting lncRNAs mimic Xist and package the other gene copy into repressive chromatin structures. Indeed, lncRNAs have been shown to interact with several epigenetic modifiers. These include; PRC2, the H3K9me3 HMT G9a, DNMT1 and KDM1B (H3K4 demethylase) offering plausible correlating evidence **(481, 483, 484)(Figure 20B)**.

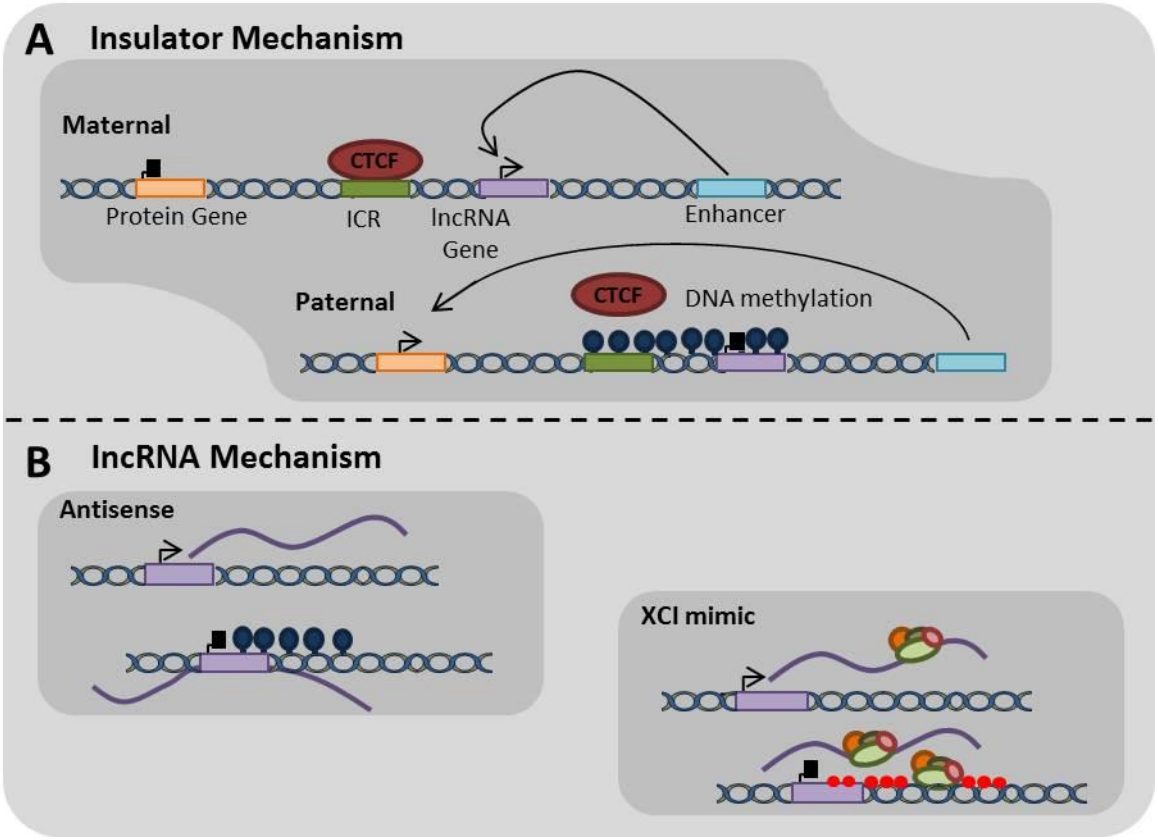

FIGURE 20 – Models of Imprinting

A) Insulator mechanism of gene imprinting. **B)** The antisense and XCI mimic models of lncRNA mediated gene imprinting

1.8.2 - Random monoallelic expression; involvement in cancer?

RME is unlike XCI and imprinting as it doesn't occur at distinct loci but is observed to be widespread across autosomes **(476, 485)**. It is established in development **(486-488)** and regulated through conserved epigenetic mechanisms **(489, 490)**. There is an extremely high probability that RME is perturbed in cancer i.e. that pathogenic heterozygous mutation or deletion of a gene can trigger a switching of allelic expression at an epigenetic level that silences the remaining gene copy. In a cancer cell, this would cause complete removal of protein expression and, thus, tumour suppressor activity. Similarly, observation of epigenetic selection and activation of oncogenes remains plausible in this setting.

Disease genes known to be affected by RME include those associated with neurodevelopmental disorders; **(491)** such as the amyloid precursor protein in Alzheimer's **(485)** and α-synuclein in Parkinson's **(492)**. Death-associated protein kinase (DAPK1) in chronic lymphoblastic leukaemia (CLL), **(485, 493)** the Eya transcriptional co-factors implicated in brachio-otic/brachio-oto-renal syndromes **(487)** are other RME disease genes. The altering of expression occurs at a transcriptional level and typically reduces total transcriptional output although some genes do exhibit transcriptional compensation **(487, 494)**. Haploinsufficiency and the variance produced by monoallelic expression produces intra-clonal diversity at the transcriptomic level in tissues. This is hypothesised to contribute towards the differing penetrance seen in many disease states **(495)**. Some studies show that selective allelic expression can reduce the dosage of the mutant allele and presumably protect the cell from pathologic effects **(496, 497)**.

Cellular populations, due to stochastic choice upon development, will express an RME gene both monoallelically and biallelically. This generates a further layer of heterogeneity amongst genetically identical clones **(485, 487, 494)**. In colorectal cancer xenografts, intra-clonal diversity has been observed to alter cellular proliferation and response to chemotherapy. Population variance couldn't be attributed to genetic differences and therefore must be propagated by epigenetic alterations (including RME) and/or niche placement in the tumour microenvironment **(498)**. Indeed, recent developments in single-cell transcriptomic sequencing **(499, 500)** has further revealed that both normal **(501)** and cancerous **(502-504)** cell clones vary greatly in their expression profiles and the levels of transcript expressed. The increased diversity allows tumour cells a wider field to enable survival upon tackling the selective pressures of microenvironmental changes and during treatment; meaning that they are more prepared, as a collective, for the adaptive changes required for progression into a "successful" cancer **(212, 505)**.

It has also been observed that most cells exhibit dynamic RME due to transcriptional bursting. This term is used to describe the temporally asynchronous production of mRNA transcript from paternal and maternal alleles. Dynamic RME is widespread across the human genome and affects

a significant percentage of transcribed loci **(506)**. These episodic bursts complicate studies which evaluate stable monoallelic expression as most techniques, such as RNA-seq and RNA-FISH, only afford a snapshot of cellular mRNA expression at a single time-point. For a biallelically expressed gene, the alternate transient production of a single allele's mRNA due to transcriptional bursting, as visualised by the aforementioned methods, will appear as stable monoallelic expression – resulting in a false positive result for allelic imbalance.

This problem has been highlighted in an almost perfect case study. In 2012, a group reported monoallelic expression of the pluripotency factor nanog in the early stages of embryonic development using RNA-FISH **(507)**. This allelic restriction however was shown to be due to transcriptional bursting by another study the following year. Fluorescent protein labelling was used to mark the two nanog alleles to show biallelic expression of the gene in real-time **(508)**. It is therefore necessary to evaluate several time-points when looking at allelic expression, preferably using multiple analytic methods **(486)**.

This is both to prevent incorrect claims of stable monoallelic expression and also to reduce the number of false positives due to transcriptional bursts. Use of RNA-seq to determine allelic frequency ratios in mouse embryonic, liver and fibroblast cells detected global transcriptional bursting. This, as expected, gave a much higher than usual percentage of monoallelically expressed transcripts due to the dynamic nature of the bursting **(509, 510)**. A follow-up study using single-cell RNA-seq that accounted for the clonal dynamics of cells, observed that the majority of cellular RME is due to transcriptional bursting with very few genes stably and clonally monoallelically expressed **(511)**.

RME genes differ between cellular lineages yet there appears to be a core group conserved across cell types. The observation at present is that the overlap is greater between biologically related and functionally similar cells **(489, 510)**. This has impact on cancers, as, like their mutational content, they will most likely have variant monoallelically expressed gene-sets that may compromise important pathogenic alleles. However, as the field is in its infancy, the extent to which the phenomenon impacts upon the state of cancer is relatively unknown with only a select few "driving" genes having been linked to RME. The epigenetic regulatory mechanisms of monoallelic expression are known **(489, 490)** yet their timing, resolution and whether there are any key upstream players above the HMTs involved is still a mystery. All of the aforementioned may be perturbed in cancer leading to a state where allelic expression at a global level is affected.

It is also worth noting that, although discovered in cell culture, RME has now been shown to exist *in vivo* by multiple studies and is not an artefact of the artificial growth environment **(487, 489, 511-513)**.

1.8.3 - Epigenetic regulation of random monoallelic expression and perturbation in cancer

The regulation of allelic choice, in the majority of RME genes **(487)** is not controlled by correlative methylation of promoter CpG islands **(246, 514, 515)** as originally postulated. Strand-specific methylation could account for switching in active alleles at mitosis, however analysis of published ChIP-seq datasets implies that RME is defined by an asymmetric chromatin signature **(516)**.

Gene body histones of the active allele are tri-methylated at H3K36 and the nucleosomes of the silenced allele are trimethylated at H3K27 **(489)**. This fingerprint has been shown to be predictive of monoallelic expression and is orthologically conserved in both mice **(490)** and chimpanzees **(517)** suggesting that the unknown upstream regulation of allelic expression is encoded into our DNA. The recent compilation of many transcriptional and ChIP-seq datasets has led to the creation of a monoallelic expression database that has both mouse and human cell and tissue records **(518)**. In reference to the evolutionarily conserved nature of RME; Matthew Thayer's laboratory have identified loci, found on chromosomes 6 and 15, which produce autosomal equivalents of the *Xist* lncRNA called ASARs (asynchronous replication and autosomal RNAs). These molecules direct monoallelic expression in *cis* along their chromosomes, placing ASARs in a possible higher order of regulatory mechanisms for RME. These regions may provide ICR activity as they act akin to the lncRNAs identified in imprinted gene clusters. It is likely there are other, as yet undiscovered, loci which dictate autosomal monoallelic expression **(519, 520)**.

The majority of genes encompassed by the characteristic RME chromatin structure are bivalently marked in embryonic stem cells (ESCs) **(489)**. Bivalent or "poised" chromatin is formed by dual deposition of respective activating and repressive trimethylations, H3K4me3 and H3K27me3, on the same nucleosome **(521-524)**, in gene promoter regions which, although antagonistic, maintains a low level of gene transcription. Removal of one of the marks by a specific histone demethylase **(525)** results in the rapid activation or repression upon stem cell differentiation **(526)(Figure 21)**. Resolution of somatic stem cell bivalent marks into those observed in RME gene bodies is plausible theory **(489, 527)**. It has been observed that promoter elements of RME genes are regulated by allelic accessibility in differentiated cells, and that this is pre-marked by deposition of H3K4me3, K27me3 and K9me3 in ESCs **(528)**. Bivalent genes, like RME gene-sets, are lineage specific **(529)** and are perturbed in cancers of various tissues **(530-537)** including the prostate **(423)**. The bivalent histone state of normal tissue and progenitor cell gene promoters has high predictive value for the subsequent methylation of these regions in tissue matched cancer cells **(538, 539)**. These regions also exhibit microenvironmental plasticity and have been observed to respond to hypoxia **(540)**. Breast cancer cells increase bivalent domains during EMT, to reduce transcript levels of epithelial identity genes, and resolve them during the reverse mesenchymal to

epithelial transition (MET) via expression of the H3K27me3 demethylase, JMJD3 **(541)**. This permits successful secondary site seeding and the establishment of metastases.

Sequencing has also identified an enrichment of events that dysregulate chromatin modifying enzymes involved in deposition of these trimethylations in prostate tumours. In advanced cancers, the H3K27 methyltransferase EZH2 is upregulated and its locus frequently amplified **(90, 123)**. EZH2 expression can be activated by ERG, a developmental transcription factor frequently dysregulated in prostate cancer, an interplay that promotes a de-differentiation program **(542)** by epigenetic silencing of critical genes such as NKX3.1 **(543)**. H3K4 methyltransferases SMYD3 and MLL2 are also perturbed in prostate cancer. The first enzyme is seen to be frequently overexpressed in cancer tissues, **(422)** whilst MLL2, that interacts with and facilitates epigenetic transactivation of AR, is recurrently mutated **(335)**. Interestingly these HMTs are involved in maintenance of bivalent chromatin;**(526)** that, in the prostate, marks a gene-set which becomes dysregulated during cancer development **(423)**. Studies in prostate cancer cell lines have observed the alterations at bivalent loci from benign to cancerous states and also during EMT **(421, 422)** yet work of this nature needs to be undertaken in primary cells and tissues to ascertain closer to physiological correlations of these histone trimethylations.

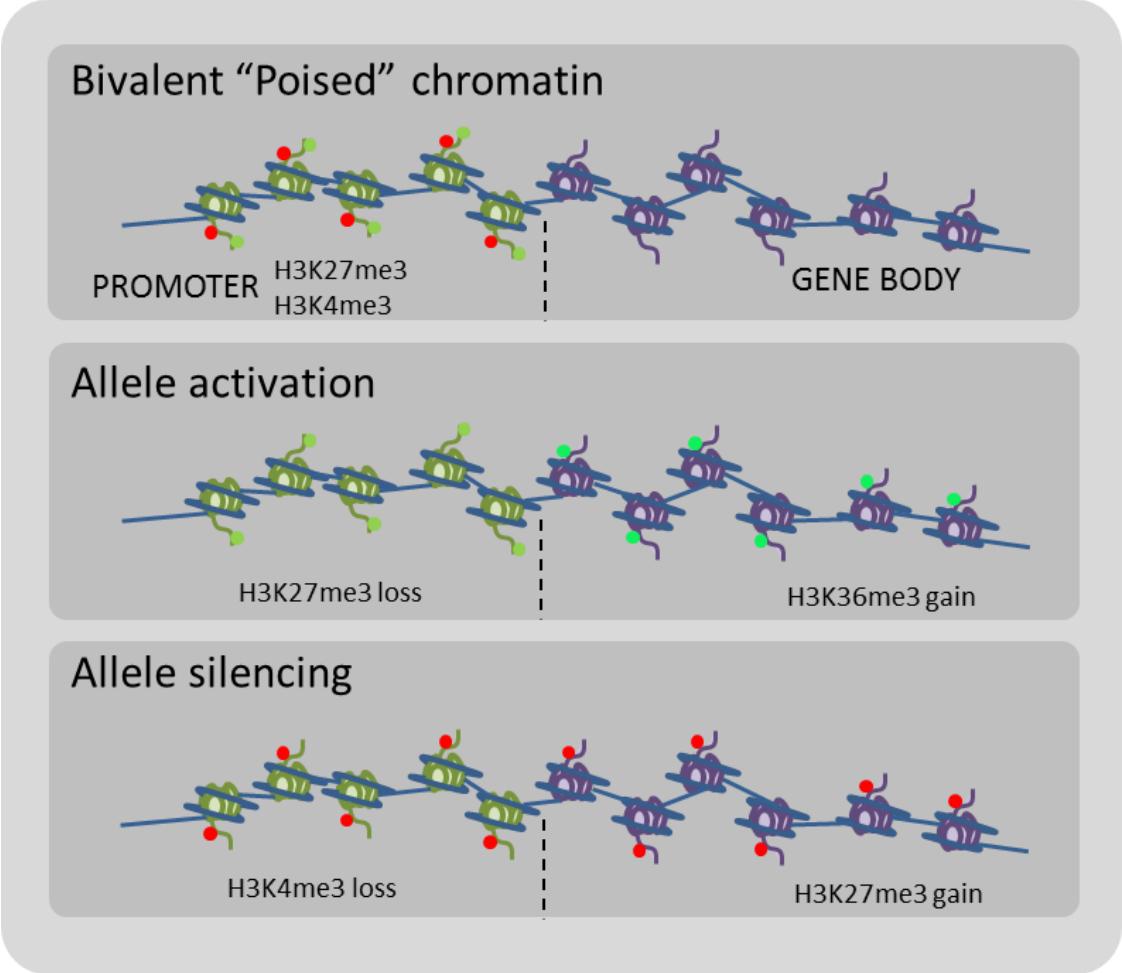

FIGURE 21 - Resolution of bivalent chromatin to RME chromatin

The original bivalent or poised state of the allele allows for rapid activation or silencing of the gene copy by promoter loss of a histone trimethylation and gene body gain of another.

Apart from obvious alterations to gene copy number by deletion and amplification, nucleotide changes that lead to an epigenetic switch of allelic expression have been identified in cancer.

DAPK1 is a mediator of apoptosis that is monoallelically expressed in peripheral blood mononuclear cells **(485)**. The gene promoter is recurrently hypermethylated in CLL, allowing the cells to become more resistant to apoptotic cell death. A rare germline mutation has also been discovered in a suppressor sequence of the gene that increases the binding affinity of the transcriptional repressor HOXB7, further reducing output of DAPK1 transcript from the mutant allele **(493)(Figure 22A)**.

In T-ALL, microinsertions upstream of the TAL1 oncogene disrupt normal deposition of silencing H3K27me3 and cause monoallelic reactivation of the gene that is usually silenced in the T-cell lineage. The nucleotide insertion was initially observed in the Jurkat cell line and has now been recurrently identified in primary samples – this monoallelic defect correlates with worse overall survival and higher blast counts in patients **(544)(Figure 22B)**.

Allele-specific upregulation of FGFR2 has been observed in breast cancers. Here a haplotype of 2 specific minor SNPs confers abnormal binding of RUNX2 to the oncogenic allele – stimulating a disproportionate activation of FGFR2 expression in breast cancer cells. Allelic upregulation of the mitogenic receptor tyrosine kinase confers a growth advantage to cells which is exploited by the cancer **(545, 546)(Figure 22C)**.

TERT promoter mutations are always heterozygous, and have been observed in a number of cancers, but not in the prostate **(547-549)**. This molecular defect can actually drive expression of telomerase more efficiently than the wild-type promoter **(550)**. The mutant allele binds the GABPA ETS factor, causing a switch from the usual H3K27me3 to an active chromatin structure. The silent allele also becomes associated with repressive marks such as H3K27me3 and EZH2 **(551)**. This allele-specific binding event presumably allows for the deposition of H3K4me3 and the subsequent monoallelic expression of telomerase – granting replicative immortality to the cancer cell **(552)(Figure 22D)**.

The most comprehensive study of the proportion of mutated alleles expressed in cancer has come from multiple myeloma **(497)**. Contrary to the assumptions of most genome sequencing studies that all mutations are expressed and affect protein; it was shown, through combination of matched patient RNA and DNA-seq datasets, that the majority of mutations in the cancer weren't expressed. This phenomenon has also been previously observed in studies of breast, lung and brain cancers **(553-555)**.

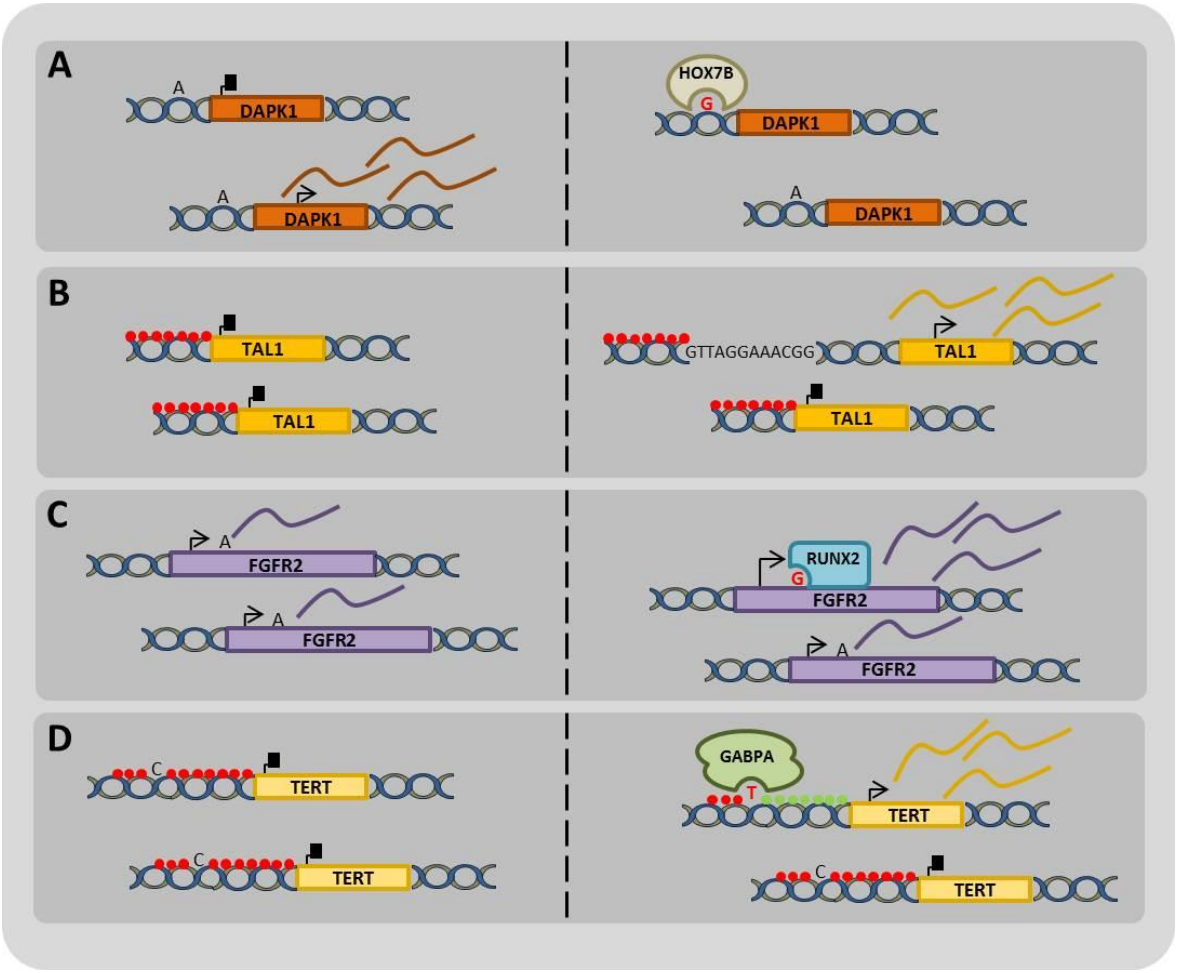

FIGURE 22 – Literature examples of normal to cancer allelic alterations

Red circles – repressive epigenetic marks. Green circles – activating epigenetic marks.

A) DAPK1 methylation in CLL. The gene is hypermethylated in chronic lymphoblastic leukaemia and a mutation upstream of the gene can provide a novel binding site for the HOX7B transcriptional repressor protein that further decreases transcriptional output.

B) TAL1 chromatin changes in T cell lymphoma. Micro-insertions disrupt deposition of repressive histone modifications to cause allelic activation of the TAL1 oncogene.

C) FGFR2 transcription factor binding in breast cancer. SNP variants create a RUNX2 binding site in an allele of FGRF2 and cause a hyperactivation of allelic transcription.

D) TERT promoter mutation in several cancers. Promoter mutation produces a biding site for the GABPA ETS factor and a switch from silencing to active chromatin signature that permits telomerase expression from the single allele.

1.8.4 - Epigenetic modifiers as cancer treatments

The switching on and off of allelic expression in disease can be related to dynamic chromatin restructuring. Prostate cancer itself has an enrichment of mutation and rearrangements in chromatin modifying enzymes such as CHD1, **(174)** MLL2 **(335)** and EZH2, among others **(90)**. The polycomb group protein EZH2 is up-regulated by TMPRSS2-ERG, **(542)** and creates the chromatin structures seen to envelope bivalent and RME genes **(489)**. Treating cancer cells that are epigenetically aberrant with small molecule inhibitors of specific DNA or histone modifying enzymes may cause a reversal of either the deposition or removal of the epigenetic mark – resulting in a regression of the cancer phenotype.

CSCs of the prostate have heightened levels of heterochromatin that offers greater protection from radiotherapy. Co-application of an Histone Deacetylase (HDAC) inhibitor sensitised the stem cells to the radiation dose leading to formation of open chromatin structures and exposing DNA vulnerable to damage by the treatment **(323)**. Promoter hypermethylation is another commonly observed epigenetic event in prostate cancer differentiation. Affected genes are first downregulated and *then* methylated to lock them in the repressed state. Interestingly these differentiation associated hypermethylated (DAH) genes were identified to have previously been associated with bivalent chromatin earlier in development. The DAH genes, in 3D cultured prostatic acini, showed a non-significant methylation increase with a significant decrease of the H3K4me3 mark throughout differentiation. Promoter H3K4 trimethylation permits the expression of the genes in the stem cells, yet this chromatin signature is lost upon development, causing gene downregulation and subsequent methylation **(423)**. The identification of this gene-set in prostate cancer and its initial bivalent status suggest that RME may also play a genome-wide role in tumours through reduction of transcript levels and producing subsequent heterogeneity of gene expression during the aberrant differentiation of the prostate epithelia.

Inhibition of DNA methyltransferases is used to facilitate epigenetic reactivation of TSGs. The reversible nature of methylation marks it as an attractive anti-cancer therapeutic target. Commonly used inhibitors are azacitidine and decitabine which have seen use in myeloid leukaemias with some effect **(556)**. Azacitidine decreased PSA levels in correlation with reduced LINE methylation in pre-chemotherapy CRPC patients **(557)** suggesting possible application of the drug earlier in prostate cancer progression may reduce biochemical symptoms and slow progression of disease. In relation to RME, regular treatment of the Raji CLL cell line with decitabine caused a steady rise in DAPK1 expression while untreated cells had no response in expression levels as the tumour suppressor remained epigenetically silenced **(493)**.

Targeting DNA methylation as a viable treatment option is possible yet it seems that in the case of prostate cancer, histone modifications are the more important regulators; advocating possible use of HDAC and HMT inhibitors in combination with other therapies.

1.8.5 - PTEN and Prostate Cancer

Phosphatase and tensin homologue deleted on chromosome ten (PTEN) is a dual-specificity protein tyrosine phosphatase (PTP) that has both lipid and protein targets **(558)**. The enzyme itself was discovered due to frequent loss of heterozygosity (LOH) at chromosome 10q23 in prostate, breast and brain cancers; implicating the gene as a probable tumour suppressor **(558)**. The major cellular role of PTEN is to antagonise PI3K phosphorylation at the 3' position of PIP2 (phosphatidylinositol 3,4 bisphosphate) and PIP3 (phosphatidylinositol 3,4,5 triphosphate) **(559)**. Depletion of these specific phospholipid signalling molecules prevents binding of proteins with Pleckstrin homology (PH) domains, such as AKT; a central growth signalling kinase **(560-562)**.

In prostate cancer, PTEN deletion is among the most common genetic alterations in both primary and metastatic tumours. Deletion of the phosphatase is seen in ~40% of localised cancers with incidence rising to 70-80% in metastatic disease **(345)**. This pattern suggests that PTEN plays a role in both initiation and progression of prostate cancers.

Disruption of the phosphatase gene allows for unchecked AKT activity – sustained proliferative signalling, increased protein synthesis through MTORC1, enhanced cellular survival, angiogenesis and tumour progression **(148, 563-565)**. PTEN also has caretaker functions as it promotes genomic stability, both through nuclear and cytosolic localisation, and aids the DNA damage response **(565-568)**. The enzyme has protein targets, independent of its lipid phosphatase activity in the PI3K pathway. These include FAK (Focal Adhesion Kinase) **(569)** an enzyme involved in cell motility, the transcription factor CREB **(570)** and the non-receptor tyrosine kinase; Src **(571)**. Alterations in the PI3K/AKT signalling pathway are a common occurrence in prostate cancer, with PI3K mutations and other regulators also being disrupted in the disease state **(90, 174, 331, 345, 572)(Figure 23)**.

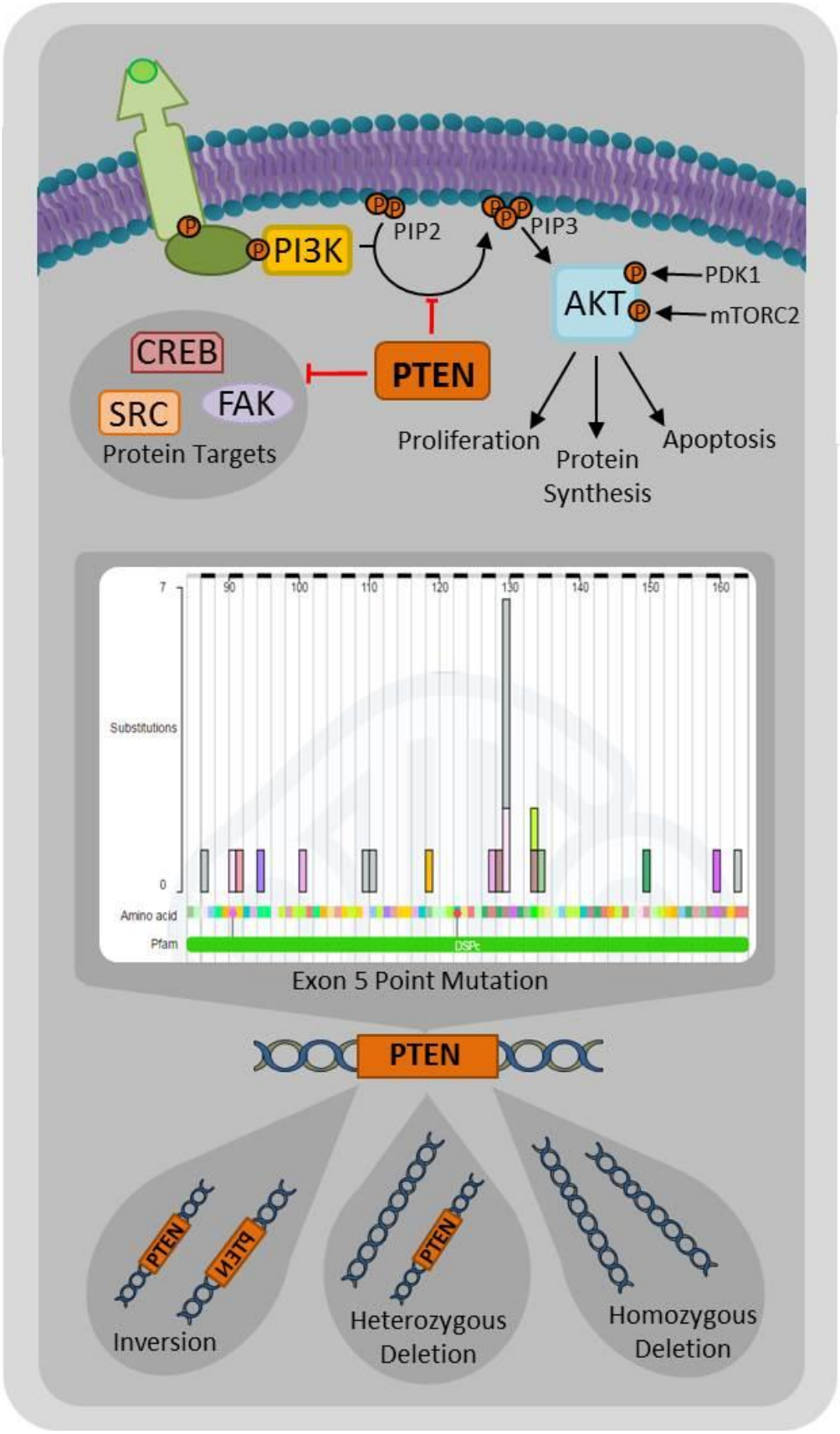

FIGURE 23 – PTEN signalling and disturbances in Prostate Cancer

Normal PTEN signalling and the molecular alterations to the gene frequently observed in prostate cancers. Mutational chart of exon 5 taken from COSMIC website **(573).**

The deletion of the 10q23 locus is commonly seen in TMPRSS2-ERG^{+} tumours **(90)** created by coordinated chromoplectic chain events **(334)**. It has been shown that PTEN deletion also causes staged cancer progression; prostate specific homozygous deletion of the gene in transgenic mice causes accelerated development of PIN, adenocarcinoma and metastatic disease. The murine PTEN null tumours were hypersensitive to ADT, yet upon autopsy it was found that AR^{+} cells were still present. This suggests that if observation time had been extended, the PTEN$^{-/-}$ tumours may have advanced into a state of CRPC **(574)**. The prevalence of genetic insults to the PTEN gene in prostate cancer has been used to map heterogeneity in tumours. Multifocal disease in the prostate is common and PTEN status at each focus varies, suggesting that loss of the phosphatase is a later sub-clonal event. Increased heterogeneity of PTEN deletion has also been shown to directly correlate with Gleason grade and thus cancer aggressiveness **(345)**.

Classically, for cancer to arise from mutated TSGs, inactivation of both alleles must occur according to Knudson's two-hit hypothesis **(575)**. The other PTEN allele in cancer has been observed to be deleted (homozygous removal of PTEN), mutated and epigenetically silenced (although promoter hypermethylation of the gene isn't observed in prostate tumours) **(174, 576, 577)**. TMPRSS2-ERG^{+} tumours can also repress PTEN expression via ERG, highlighting that a convergent molecular outcome in prostate cancers is a reduction of PTEN protein **(578)**. Thus the gene dosage of PTEN is critical in the prostate, as cancer can result from haploinsufficiency of the gene **(579, 580)**. If RME affects the PTEN gene, then reduced dose through monoallelic expression in cancer will enhance tumourigenesis.

The metastatic prostate cancer cell lines; PC3, LNCaP and Du145 represent the importance of PTEN aberrations in disease. PC3 cells completely lack PTEN due to homozygous deletion, Du145 have heterozygous deletion and exon 5 point mutation to the remaining allele whilst LNCaPs have an exon 1 indel that creates a frameshift **(451, 558)**. In prostate tumours it is observed that PTEN mutation typically targets the PTP domain of the enzyme (exon 5 of the gene), with the ^{123}HCKAGKGR^{130} catalytic loop being the most frequently mutated region of the phosphatase domain **(565)(Tables 3 & 4)**. Although frequency varies between population studies; in prostate cancer, PTEN mutation is not a commonly observed event relative to deletions of the gene **(133, 330, 335, 558, 581-584)**. Recently, a recurrent inversion of the whole PTEN gene has been observed in hormone naïve localised prostate cancers that decreases PTEN mRNA production and, surprisingly, reduces pathway activity below that seen in cases of heterozygous deletion **(332)(Figure 23)**.

Codon Nucleotide Change	Amino Acid Change	Location (Exon/Domain)	Consequence	Reference
19G>C	E7Q	Exon 1	Missense	Haffner 2013 **(155)**
58G>T	G20Stop	Exon 1	Nonsense	Dong 2001**(585)**
70G>A	D24N	Exon 1	Missense	COSMIC – UK **(586)**
144C>A	N48K	Exon 2	Missense	TCGA 2015 **(330)**
163A>G	R55G	Exon 2	Missense	Dong 2001 **(585)**
202T>C	Y68H	Exon 3	Missense	COSMIC – UK **(586)**
259C>T	Q87Stop	Exon 5/PTPc	Nonsense	Vliestra 1998 **(453)**
271G>C	E91Q	Exon 5/PTPc	Missense	Suzuki 1998 **(584)**
276C>A	D92E	Exon 5/PTPc	Missense	COSMIC – UK **(586)**
283C>T	P95S	Exon 5/PTPc	Missense	de Muga 2010 **(581)**
302T>A	I101N	Exon 5/PTPc	Missense	Dong 2001 **(585)**
328C>T	Q110Stop	Exon 5/PTPc	Nonsense	Dong 2001 **(585)**
332G>A	W111Stop	Exon 5/PTPc	Nonsense	Kan 2010 **(583)**
355G>T	V119F	Exon 5/PTPc	Missense	TCGA 2015 **(330)**
384G>C	K128N	Exon 5/PTPc	Missense	Barbieri 2012 **(66)**
385G>A	G129R	Exon 5/PTPc	Missense	Li 1997 **(558)**
388C>T	R130Stop	Exon 5/PTPc	Nonsense	Vliestra 1998 **(453)**
400A>T	M134L	Exon 5/PTPc	Missense	Li 1997 **(558)**
401T>G	M134R	Exon 5/PTPc	Missense	COSMIC – UK **(586)**
403A>G	I135V	Exon 5/PTPc	Missense	Dong 2001 **(585)**
449A>G	E150G	Exon 5/PTPc	Missense	Dong 2001 **(585)**
480C>T	T160T	Exon 5/PTPc	Silent	Dong 1998 **(582)**
487A>T	K163Stop	Exon 5/PTPc	Nonsense	Grasso 2012 **(335)**
517C>T	R173C	Exon 6	Missense	COSMIC – UK **(586)**
518G>A	R173H	Exon 6	Missense	Barbieri 2012 **(133)**
520T>A	Y174N	Exon 6	Missense	Feilotter 1998 **(587)**
638C>G	P213R	Exon 7/C2	Missense	Grasso 2012 **(335)**
697C>T	R233Stop	Exon 7/C2	Nonsense	Barbieri 2012 **(133)**
758T>A	I253N	Exon 7/C2	Missense	COSMIC – UK **(586)**
814C>T	H272Y	Exon 8/C2	Missense	Dong 2001 **(585)**
977A>G	D326G	Exon 8/C2	Missense	TCGA 2015 **(330)**
1008C>A	Y336Stop	Exon 8/C2	Nonsense	Barbieri 2012 **(133)**
1031A>G	K344R	Exon 9/C2	Missense	Dong 2001 (585)
1043C>T	T348I	Exon 9/C2	Missense	Dong 2001 **(585)**
1102T>G	V369G	Exon 9	Missense	Dong 1998 **(582)**
1144A>T	T382S	Exon 9	Missense	Dong 2001 **(585)**

TABLE 3 – All known PTEN mutations in prostate cancer

Exon Number	mRNA/Protein	Sequence
1	mRNA	ATGACAGCCATCATCAAAGAGATCGTTAGCAGAAACAAAAGGAGATATCAAGAGGATGGATTCGAC TTAGACTTGACCT
	Protein	M T A I I K E I V S R N K R R Y Q E D G F D L D L T
2	mRNA	ATATTTATCCAAACATTATTGCTATGGGATTTCCTGCAGAAAGACTTGAAGGCGTATACAGGAACAA TATTGATGATGTAGTAA
	Protein	Y I Y P N I I A M G F P A E R L E G V Y R N N I D D V V R
3	mRNA	GGTTTTTGGATTCAAAGCATAAAAACCATTACAAGATATACAATCT
	Protein	F L D S K H K N H Y K I Y N
4	mRNA	TTGTGCTGAAAGACATTATGACACCGCCAAATTTAATTGCAGAG
	Protein	L C A E R H Y D T A K F N C R
5	mRNA	TTGCACAATATCCTTTTGAAGACCATAACCCACCACAGCTAGAACTTATCAAACCCTTTTGTGAAGAT CTTGACCAATGGCTAAGTGAAGATGACAATCATGTTGCAGCAATTCACTGTAAAGCTGGAAAGGGA CGAACTGGTGTAATGATATGTGCATATTTATTACATCGGGGCAAATTTTTAAAGGCACAAGAGGCCC TAGATTTCTATGGGGAAGTAAGGACCAGAGACAAAAAG
	Protein	V A Q Y P F E D H N P P Q L E L I K P F C E D L D Q W L S E D D N H V A A I H C K A G K G R T G V M I C A Y L L H R G K F L K A Q E A L D F Y G E V R T R D K K
6	mRNA	GGAGTAACTATTCCCAGTCAGAGGCGCTATGTGTATTATTATAGCTACCTGTTAAAGAATCATCTGG ATTATAGACCAGTGGCACTGTTGTTTCACAAGATGATGTTTGAAACTATTCCAATGTTCAGTGGCGG AACTTG
	Protein	G V T I P S Q R R Y V Y Y Y S Y L L K N H L D Y R P V A L L F H K M M F E T I P M F S G G T
7	mRNA	CAATCCTCAGTTTGTGGTCTGCCAGCTAAAGGTGAAGATATATTCCTCCAATTCAGGACCCACACGAC GGGAAGACAAGTTCATGTACTTTGAGTTCCCTCAGCCGTTACCTGTGTGTGGTGATATCAAAGTAGA GTTCTTCCACAAACAGAACAAGATGCTAAAAAAG
	Protein	C N P Q F V V C Q L K V K I Y S S N S G P T R R E D K F M Y F E F P Q P L P V C G D I K V E F F H K Q N K M L K K
8	mRNA	GACAAAATGTTTCACTTTTGGGTAAATACATTCTTCATACCAGGACCAGAGGAAACCTCAGAAAAAG TAGAAAATGGAAGTCTATGTGATCAAGAAATCGATAGCATTTGCAGTATAGAGCGTGCAGATAATG ACAAGGAATATCTAGTACTTACTTTAACAAAAAATGATCTTGACAAAGCAAATAAAGACAAAGCCAA CCGATACTTTTCTCCAAATTTTAAG
	Protein	D K M F H F W V N T F F I P G P E E T S E K V E N G S L C D Q E I D S I C S I E R A D N D K E Y L V L T L T K N D L D K A N K D K A N R Y F S P N F K
9	mRNA	GTGAAGCTGTACTTCACAAAAACAGTAGAGGAGCCGTCAAATCCAGAGGCTAGCAGTTCAACTTCT GTAACACCAGATGTTAGTGACAATGAACCTGATCATTATAGATATTCTGACACCACTGACTCTGATCC AGAGAATGAACCTTTTGATGAAGATCAGCATACACAAATTACAAAAGTCTG
	Protein	V K L Y F T K T V E E P S N P E A S S S T S V T P D V S D N E P D H Y R Y S D T T D S D P E N E P F D E D Q H T Q I T K V **Stop**

TABLE 4 – Location of prostate cancer associated mutations in the PTEN gene

1.8.6 - SPOP and Prostate Cancer

The primary role of Speckled-type POZ protein (SPOP) is that of a substrate-specific adaptor protein for the Cullin3-RING E3 ligase (CRL3) **(588, 589)**. SPOP owes its strange name to the roundabout way in which it was discovered. Application of autoimmune antibodies from a schleroderma patient onto COS7 cells created a confined speckled pattern in cell nuclei. Immuno-screening of a HeLa library identified the epitope-containing protein that was found to contain a POZ (pox virus and zinc finger) domain by subsequent BLAST search. The protein was thus named speckled-type POZ protein **(590)**.

In complex with CRL3, SPOP marks a plethora of protein substrates for targeted proteasomal degradation by poly and multi-mono ubiquitination **(591, 592)**. The adaptor protein is equipped for this function through MATH (meprin and TRAF homology) and BTB (Bric-a-brac/Tramtrack/Broad, also known as POZ) domains. The MATH domain sequesters substrate protein whilst the BTB domain facilitates activation of SPOP-CRL3 dimerisation/oligomerisation, and the binding of the Cullin 3 complex, to bring the substrate into close proximity to the E3 Ligase catalytic core **(593-595)**. Substrate proteins contain an SPOP binding consensus (SBC) consisting of a 5 amino acid motif **(595)**. SBCs are found in BMI1, macroH2A, Daxx, Gli2/3, DEK, TRIM24, AR, NCOA3, SETD2, BRD4 and ERG, to name a few of SPOP's targets **(382, 591, 592, 596-603)(Figure 24A)**. Whilst this binding typically confers ubiquitin-mediated degradation, it has been shown to have other effects; such as aiding macroH2A deposition on the inactivated X chromosome **(598)** and antagonising INF2-mediated regulation of mitochondrial fission **(604)**. SPOP also plays a role in the DNA damage response **(605, 606)** and in cellular senescence, suggestive of a caretaker role for the gene **(607)**. The presence of SPOP in an E3 ligase complex, one of the largest human enzyme classes, opens the potential for dysregulation of widespread protein targets in cancer, some of which won't have yet been identified as SPOP substrates.

SPOP is the most commonly mutated gene in primary prostate cancer (settling at around 10%) **(330-332, 608)**. Mutations of the gene have been identified in colorectal, **(609, 610)** hepatocellular, **(611)** thyroid **(612)** and endometrial **(592)** carcinomas. Allelic loss is also evident in breast cancer **(613)**. SPOP can have an oncogenic role, inconsistent with its tumour supressing capabilities in several cancers. This is due to the fact that dysregulation of cellular ubiquitination is entirely context dependent. For example; in clear cell renal cell carcinoma, SPOP is seen to be consistently overexpressed. Here, SPOP upregulation shifts protein localisation to the cytosol, favouring the increased degradation of tumour suppressing CRL3 substrates – including PTEN **(614, 615)**. The context dependent cancer promoting role for SPOP has led to the development of small-molecule inhibitors of SPOP-substrate interactions that promote renal cell death in vitro and in vivo **(616)**.

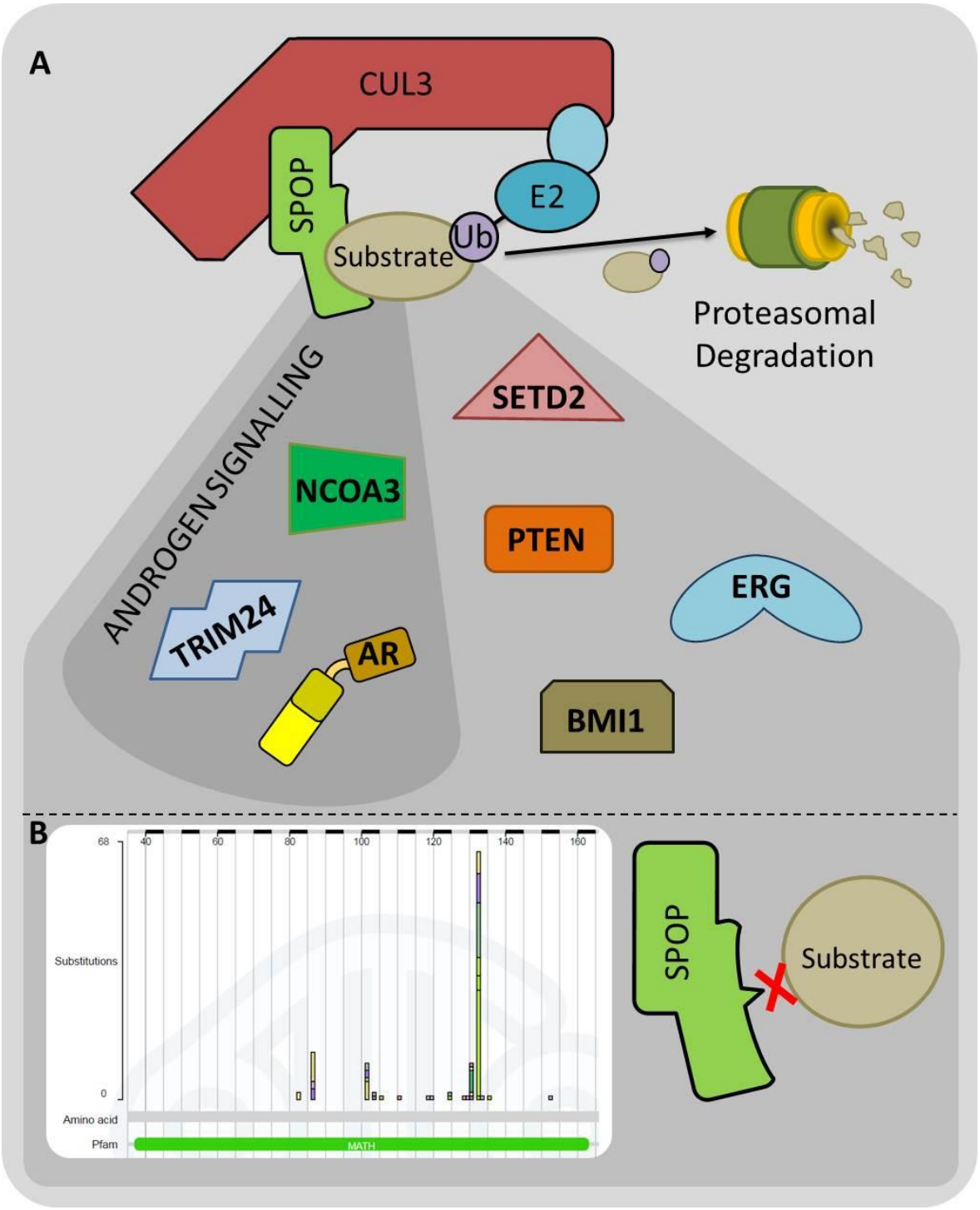

FIGURE 24 – SPOP signalling in prostate cancer

A) SPOP as a substrate binding adaptor protein of the Cullin3 E3 ligase – involved in the turnover of oncogenic proteins in the prostate – especially those involved in AR signalling. **B)**Mutational clustering in the substrate binding domain of SPOP (taken from COSMIC **(617)**) prevents substrate binding and degradation

Prostate cancer-associated SPOP mutations cluster exclusively in the MATH domain of the protein and affect amino acids required for substrate binding **(382, 592, 596, 597, 605, 607)**. Currently, 17 amino acid residues in the MATH domain **(See Figure 24B, Tables 5 & 6)(133, 174, 330, 335, 583, 593, 618-623)** are affected by missense mutation in prostate cancer; with all tested point mutations abrogating the ability to bind substrate protein **(596, 597, 605, 607, 624)**. Mutations in SPOP are mutually exclusive from ETS fusions and PI3K pathway alterations, yet correlate with CHD1 deletions in tumours and occur early in the cancer's natural history **(90, 330, 334, 605, 618)**. SPOP mutation has also been reported in hgPIN tissues adjacent to cancerous foci, marking it as a possible tumour-initiating event **(133, 335)**. A study that tracked metastases, based on genetic alterations, back to their source in the prostate showed that SPOP mutation occurred early in progression of the cancer as the metastatic molecular signature could be linked to an originating sub-clonal focus within the primary tumour **(155, 338)**.

Disruption of SPOP-specific Cullin 3 substrate degradation in prostate cancer impacts the cellular ubiquitylome and causes inappropriate protein accumulation **(592)**. Whilst in dimeric conformation with the wildtype protein, mutant SPOP is theorised to completely abrogate substrate protein ubiquitination – possibly explaining the complete effect of heterozygous mutation **(592)**. This so-called dominant-negative effect was seen in prostate epithelial cells (hPREC, PC3 and LNCaP) to affect NCOA3 **(625)** (AR co-factor), TRIM24 **(626)** (androgen-independent AR activator and degrades p53) and DEK (proto-oncogene) protein levels. Reduced degradation of these proteins that promote prostate epithelial cell growth and invasiveness correlated with increased tumourigenic potential of cells. SPOP's regulation of androgen signalling is extensive as even the AR itself has an SBC located the hinge region of the protein. This has implications in CRPC as AR splice variants, for example; V7, lack this domain and therefore cannot be affected through wildtype SPOP-CRL3 ubiquitination, allowing the AR transcriptional program to be constitutively enforced **(382)**. SPOP mediated degradation of AR is further supported by the fact that protein levels of closely related nuclear receptors; ERα **(627)** and PR **(241)** are also regulated by SPOP.

The adaptor protein has also been observed to degrade ERG, through binding to an N-terminal SBC. Again mutation of the adaptor protein fails to cause degradation of the transcription factor and, depending on the location of the breakpoint, truncated ERG is partially or fully resistant to SPOP-mediated ubiquitination **(596, 597)**. This means that in prostate cancer, the two dominant molecular subtypes; TMPRSS2-ERG fusion and SPOP mutation both achieve a congruent molecular endpoint; inappropriate accumulation of ERG. However, a recent study has observed that, in SPOP mutant prostate cancers; ERG is not expressed **(628)**. This means that, although MATH

domain mutations can stabilise ERG, SPOP defects drive prostate cancer with a complete separate molecular aetiology from ERG-high prostate cancers.

Recently, SPOP has been shown to aid degradation of PD-L1 which is involved in immune response suppression **(629)**. Mutation of the adaptor protein in prostate cancers abrogates the proteasomal turnover of PD-L1, and is thus linked to high PD-L1 protein levels with reduced immune cell infiltration in tumours.

SPOP has a wide repertoire of protein targets that are relevant to prostate cancer **(382, 596, 597, 614)**. This however isn't complete and there is potential for important links to be made in future which broaden the effect of mutations to the E3 ligase adaptor protein. SPOP mutants cause activation of mTOR, PI3K and AR signalling in transgenic mice. Data that aligns with paired previously obtained DNA and RNA sequencing efforts of localised human prostate cancer, highlighting that the diverse range of SPOP targets influence critical growth pathways **(630)**. If the SPOP gene is under regulation at an allelic level then there is the possibility that heterozygous mutation, with the functional allele silenced by histone trimethylations, can lead to complete loss of protein function as observed in multiple studies.

Codon Nucleotide Change	Amino Acid Change	Location (Exon; Domain)	Consequence	Reference
248A>G	Y83C	Exon 6/MATH	Missense	Saar 2014 **(620)**
259T>A	Y87N	Exon 6/MATH	Missense	Blattner 2014 **(618)**
260A>G	Y87C	Exon 6/MATH	Missense	Barbieri 2012 **(133)**
260A>C	Y87S	Exon 6/MATH	Missense	Grasso 2012 **(335)**
304T>A	F102I	Exon 6/MATH	Missense	COSMIC – CA **(621)**
304T>G	F102V	Exon 6/MATH	Missense	TCGA 2015 **(330)**
305T>G	F102C	Exon 6/MATH	Missense	Barbieri 2012 **(133)**
305T>C	F102S	Exon 6/MATH	Missense	Buckles 2014 **(619)**
310T>G	F104V	Exon 6/MATH	Missense	Garcia-Flores 2014 **(622)**
311T>C	F104S	Exon 6/MATH	Missense	TCGA 2015 **(330)**
318C>T	I106I	Exon 6/MATH	Silent	Buckles 2014 **(619)**
332G>A	G111E	Exon 6/MATH	Missense	Buckles 2014 **(619)**
356G>A	S119N	Exon 7/MATH	Missense	Barbieri 2012 **(133)**
358C>T	Q120Stop	Exon7/MATH	Nonsense	Garcia-Flores 2014 **(622)**
373T>G	F125V	Exon 7/MATH	Missense	Kan 2010 **(583)**
375T>A	F125L	Exon 7/MATH	Missense	Barbieri 2012 **(133)**
385A>G	K129E	Exon 7/MATH	Missense	Barbieri 2012 **(133)**
388G>A	D130N	Exon 7/MATH	Missense	Garcia-Flores 2014 (622)
391T>G	W131G	Exon 7/MATH	Missense	Garcia-Flores 2014 **(622)**
391T>C	W131R	Exon 7/MATH	Missense	TCGA 2015 **(330)**
392G>C	W131S	Exon 7/MATH	Missense	TCGA 2015 **(330)**
393G>C	W131C	Exon 7/MATH	Missense	TCGA 2015 **(330)**
397T>G	F133V	Exon 7/MATH	Missense	Berger 2011 **(174)**
398T>G	F133C	Exon 7/MATH	Missense	Barbieri 2012 **(133)**
398T>C	F133S	Exon 7/MATH	Missense	Barbieri 2012 (133)
399C>G	F133L	Exon 7/MATH	Missense	Barbieri 2012 (133)
397T>A	F133I	Exon 7/MATH	Missense	TCGA 2015 **(330)**
402G>C	K134N	Exon 7/MATH	Missense	Barbieri 2012 **(133)**
N/A	K135X	Exon 7/MATH	Missense	Blattner 2014 **(618)**
406T>C	F136L	Exon 7/MATH	Missense	COSMIC – UK **(586)**
457G>A	D153N	Exon 7/MATH	Missense	Garcia-Flores 2014 **(622)**
887A>T	N296I	Exon 11/BTB	Missense	Zuhlke 2014 **(631)**
1103G>A	R368H	Exon 12	Missense	TCGA 2015 **(330)**

TABLE 5 – All known SPOP mutations in prostate cancer

Exon Number	mRNA/ Protein	Sequence
1	mRNA	GGGGAGGAGGCCGCGCGGGGTGGGGTCTGGCGGTACGCGCTGGCTGCGTCGACGTGCTGACGCCATGA CGCCCCGGCTGGTGTGTGTCGGTGTGTATGTGTGTGTGTGAGTGTGCGCGCTCCGAGTGTGTGTGTATTT GTGTATCGGCGGTCCCGCAGGTCCCGGATGTTGCGGACAGTATGAGGCAAGCGCAGGGGGACGGGGAC CAGCAGCTGTCGCCGCCGCTCTCAG
	Protein	Non coding
2	mRNA	ATCGAGTCTTGCTCTGTCACCCAGGCTGGAGTGCAGTGGCGCGATCTCAGCTCACTGCCACCTTTGCCTCC TGGGTTCAAGCGATTCTTCTGCCTCAGCCTCCCGAGTAGCTGGGATTACAG
	Protein	Non coding
3	mRNA	GCTCTGGGAACCACCCTTCTACTTTCTGTCTCTAGGAATTTCACTACTCTAG
	Protein	Non coding
4	mRNA	GGTGAAGAGGGAACAGAAATCTTTGCCCCCTGACTTTGGAAATCTCGTTTAACCTTCAAACTGGCG**ATG**TC AAGGGTTCCAAGTCCTCCACCTCCGGCAGAAATGTCGAGTGGCCCCGTAGCTGAGAGTTGGTGCTACACA CAG
	Protein	M S R V P S P P P P A E M S S G P V A E S W C Y T Q
5	mRNA	ATCAAGGTAGTGAAATTCTCCTACATGTGGACCATCAATAACTTTAGCTTTTGCCGGGAGGAAATGGGTGA AGTCATTAAAAGTTCTACATTTTCATCAGGAGCAAATGATAAACTGAAATG
	Protein	I K V V K F S Y M W T I N N F S F C R E E M G E V I K S S T F S S G A N D K L K
6	mRNA	GTGTTTGCGAGTAAACCCCAAAGGGTTAGATGAAGAAAGCAAAGATT**A**CCTGTCACTT**TA**CCTGTTACTG GTCAGCTGTCCAAAGAGTGAAGTTCGGGCAAAA**TT**CAAA**TT**CTCCAT**C**CTGAATGCCAAGG**G**AGAAGAAA CCAAAGCTATGG
	Protein	W C L R V N P K G L D E E S K D **Y** L S L **Y** L L L V S C P K S E V R A K **F** K **F** S **I** L N A K **G** E E T K A M
7	mRNA	AGA**G**T**C**AACGGGCATATAGG**T**TT**T**GTGCAAGGC**A**AA**G**AC**TGG**GGA**TTC**AA**G**AAA**T**TCATCCGTAGAGATTT CTTTTGGATGAGGCCAACGGGCTTCTCCCTGAT**G**ACAAGCTTACCCTCTTCTGCGAG
	Protein	E **S** **Q** R A Y R **F** V Q G **K** **D** **W** G **F** **K** **K** **F** I R R D F L L D E A N G L L P D **D** K L T L F C E
8	mRNA	GTGAGTGTTGTGCAAGATTCTGTCAACATTTCTGGCCAGAATACCATGAACATGGTAAAGGTTCCTGAGTG CCGGCTGGCAGATGAGTTAGGAGGACTGTGGGAGAATTCCCGGTTCACAGACTGCTGCTTGTGTGTTGCC GGCCAGGAATTCCAGGCTCACAAGGCTATCTTAGCAG
	Protein	V S V V Q D S V N I S G Q N T M N M V K V P E C R L A D E L G G L W E N S R F T D C C L C V A G Q E F Q A H K A I L A
9	mRNA	CTCGTTCTCCGGTTTTTAGTGCCATGTTTGAACATGAAATGGAGGAGAGCAAAAAG
	Protein	A R S P V F S A M F E H E M E E S K K
10	mRNA	AATCGAGTTGAAATCAATGATGTGGAGCCTGAAGTTTTTAAGGAAATGATGTGCTTCATTTACACGGGAA GGCTCCAAACCTCGACAAAATGGCTGATGATTTGCTGGCAGCTGCTGACAAG
	Protein	N R V E I N D V E P E V F K E M M C F I Y T G K A P N L D K M A D D L L A A A D K
11	mRNA	TATGCCCTGGAGCGCTTAAAGGTCATGTGTGAGGATGCCCTCTGCAGTA**A**CCTGTCCGTGGAGAACGCTG CAGAAATTCTCATCCTGGCCGACCTCCACAGTGCAGATCAGTTGAAAACTCAGGCAGTGGATTTCATCAAC TA
	Protein	Y A L E R L K V M C E D A L C S **N** L S V E N A A E I L I L A D L H S A D Q L K T Q A V D F I N
12	mRNA	TCATGCTTCGGATGTCTTGGAGACCTCTGGGTGGAAGTCAATGGTGGTGTCACATCCCCACTTGGTGGCTG AGGCATACCGCTCTCTGGCTTCAGCACAGTGCCCTTTTCTGGGACCCCCAC**G**CAAACGCCTGAAGCAATCC TAAGATCCTGCTTGTTGTAAGACTCCGTTTAATTTCCAGAAGCAGCAGCCACTGTTGCTGCCACTGAC
	Protein	Y H A S D V L E T S G W K S M V V S H P H L V A E A Y R S L A S A Q C P F L G P P **R** K R L K Q S **Stop**

TABLE 6 – Location of prostate cancer associated mutations in the SPOP gene

1.8.7 - Isocitrate Dehydrogenase-1 and Prostate Cancer

IDH-1 is the cytoplasmic and peroxisomal isoform of Isocitrate Dehydrogenase, an enzyme that catalyses forward and reverse conversions of α-ketogluturate (α-KG) to iso-citrate. The mitochondrial IDH-2 supports the same reaction in the tricarboxylic acid cycle, a major pathway in aerobic respiration that fuels ATP production via oxidative phosphorylation. Besides aiding metabolism, the reaction which produces α-KG is one of the major contributors to the cellular NADPH pool. NADPH is a necessary reducing co-factor in redox regulation (both thioredoxin and glutathione require it) as well as being extensively utilised in several major biosynthetic pathways **(632)**.

Mutation of the IDH1 gene was first reported in glioblastoma, shortly followed by acute myeloid leukaemia. Whilst these cancers have the largest prevalence of IDH-1 mutation, the enzyme has now been found to be affected in many solid tumour types, albeit at much lower frequencies **(633)**. Mutation of the IDH-1 enzyme is postulated to be an early or founder event, as noted in brain cancer sequencing studies that predict occurrence prior to cellular transformation **(634, 635)**. These mutations affect a key active site arginine residue, R132, to alter the reaction performed by the enzyme. Instead of producing isocitrate, mutant IDH-1 forms the oncometabolite 2-hydroxygluturate (2-HG) that, due to the mutation-induced imbalance in the molecule's metabolism, builds to extraordinarily high intracellular concentrations **(636)**. As 2-HG closely resembles α-KG, (the C2 carbonyl group of α-KG is replaced by a hydroxyl group) the molecule competitively inhibits α-KG-dependent dioxygenases, that rely on the molecule as an essential co-factor in catalysis. This is an extremely diverse enzyme class with over eighty members in human cells, thus the effects of inhibitory 2-HG concentrations are extensive. Instead of a single pathway being defective, the 2-HG mediated dysregulation of both metabolism and chromatin structure means that disease phenotype is pleiotropic between cell types, with the true pathological molecular origin difficult to pinpoint amidst other background alterations **(632, 637)(Figure 25A)**.

Oxidative Stress

The reaction facilitated by IDH-1 boosts the NAPDH pool to indirectly protect the cell from oxidative stress. However, in gaining the neomorphic ability to create 2-HG, mutant IDH-1 depletes rather than increases cellular NADPH. In doing so the mutation promotes a redox environment with a decreased buffer from the harmful effects of ROS **(632)**. As expected IDH-1 mutation increases oxidative stress within glioma cells; a state, depending on the genetic background of the tumour, that may promote or inhibit cancer growth **(638)**.

DNA Methylation

DNA hypermethylation is a hallmark of IDH-1 mutant tumours. The ten-eleven translocase (TET) dioxygenases are a family of proteins that begin the process of DNA demethylation by converting 5-methyl-cytosine moieties to 5-hydroxymethyl-cytosines. IDH-1 mutant gliomas present with this methylated phenotype due to TET2 inhibition by 2-HG **(639)**. Aside from the expected gene silencing by promoter methylation,**(640)** reduced clearance of 5-methyl-cytosine has been observed to disrupt CTCF insulator binding sites across the genome. In particular, a restrictive boundary point between a super-enhancer element and the PDGFRA oncogene was shown to be defective in mutant IDH-1 patient gliomas; facilitating overexpression of the growth factor receptor and conferring subsequent proliferative advantage to mutant cells **(641)**. This discovery highlights the effects of inappropriate hypermethylation, not just at promoter CpG islands but, at an epi-genomic level whilst also presenting a case that IDH-1 mutation may promote similar deregulatory effects in other cancers.

Histone Methylation

The Jumonji-C (JmjC) domain histone demethylase family are another class of α-KG-dependent dioxygenases affected in IDH-1 mutant cells. The JmjC domain has been crystallised with 2-HG in the active site pocket typically occupied by α-KG. This particular protein structure was further associated with increased global histone methylation **(642)**. The complete effect and impact of IDH-1 mutation on chromatin organisation is only just beginning to be investigated. A recent study **(643)** using IDH-1 R132H knock-in mice, linked decreased protein expression of ATM in progenitor blood cells (but not in more differentiated progeny) to an increase of H3K9me3 at the gene's promoter. ATM reduction increased HSC DNA damage that the authors suggested could initiate transformation of the myeloid lineage, yet investigation in a human system or patient samples is required to observe whether the same phenotype prevails. The above study **(643)** highlights the need for cellular heterogeneity to be taken into account, due to the pleiotropic effects of the mutation in cells with variant genetic backgrounds and differentiation states.

Extracellular Matrix Composition

Collagen synthesis through the critical hydroxylation of proline and lysine residues by α-KG dependent prolyl hydroxylase domain containing proteins (PHDs) **(644, 645)** is an anabolic process affected by IDH-1 mutation. This has been observed to cause basement membrane disruption and also promotes ER stress through accumulation of the immature collagen proteins in the organelle **(646)**. Chondrosarcoma, the second most prevalent form of bone cancer, has an enrichment of IDH-1 mutations that are often combinatorial with aberrations to the COL2A1 cartilage collagen gene – suggesting that the molecular pathology of this cancer is to achieve disruption of collagen

synthesis **(647)**. Breakdown of the ECM, a hallmark of prostate cancers, alters cellular adherence; with associated growth and cell death signalling subsequently changing – all of which may promote transformation or indeed invasion and metastasis.

Hypoxia Inducible Factor Signalling

PHDs also regulate the hydroxylation of HIF1 and 2 in normoxic conditions to allow for recognition and subsequent proteasomal degradation via the VHL ubiquitin ligase. IDH-1 mutation would therefore hypothetically increase HIF levels due to PHD inhibition. This has been observed in glioma cells both in vitro **(642)** and ex vivo **(648, 649)**. However, regulation of HIF stability relies on several other factors, and HIF protein levels have been observed to be decreased **(650)** and subsequent signalling pathways inhibited **(651)** in the context of IDH mutation. HIF regulation by the EGLN prolyl-4 hydroxylases therefore classically marks the context dependence of IDH-1 mutations between and even within cancers.

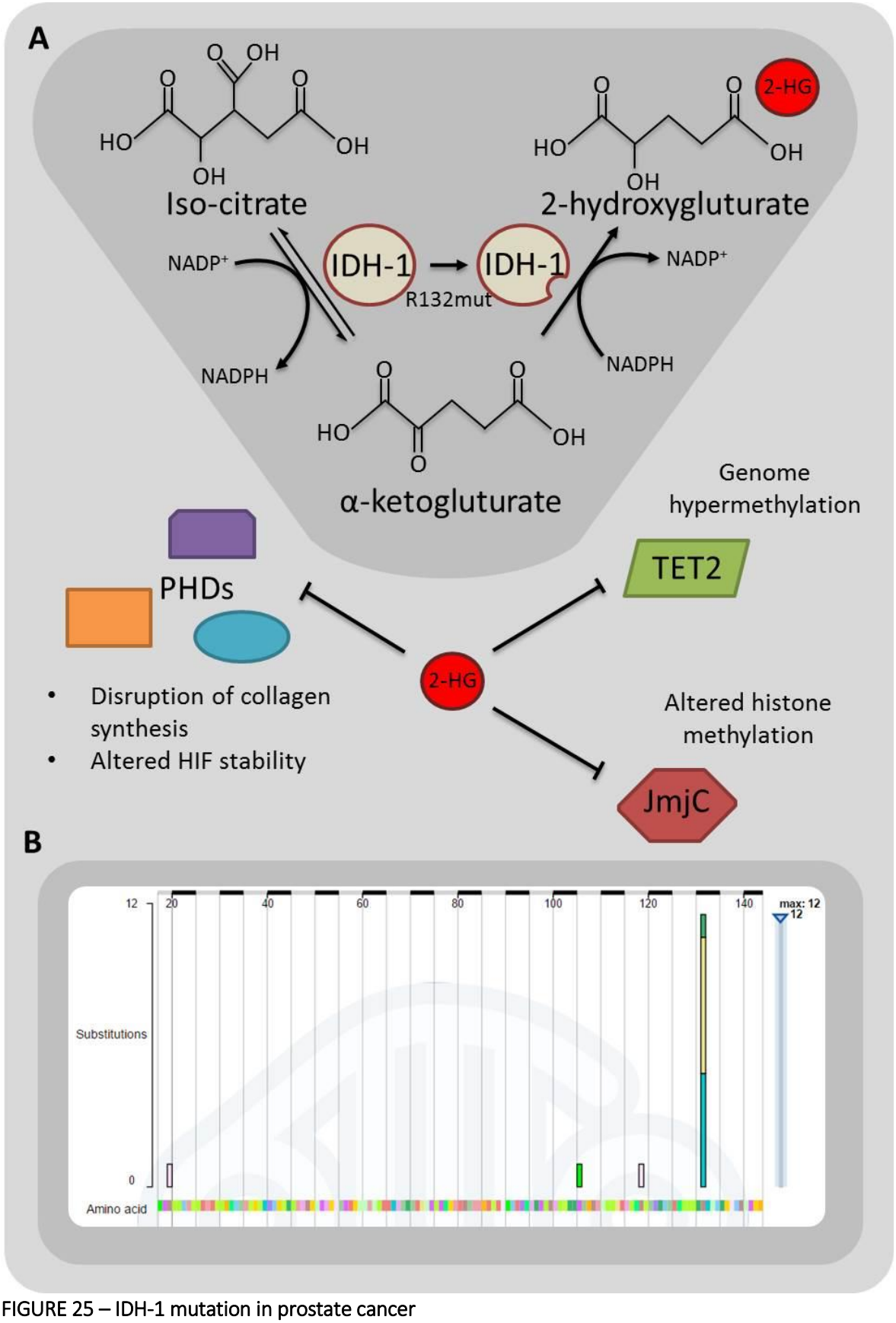

FIGURE 25 – IDH-1 mutation in prostate cancer

A) IDH1 gains a neomorphic capability via R132 mutation to create 2-hydroxygluturate (2-HG). 2-HG levels build in mutant cells and inhibit prolyl-hydroxylases (PHDs) and chromatin modifiers to disrupt critical cellular processes. **B)** Prostate cancer IDH-1 mutations taken from COSMIC **(652)**.

A multi-tissue sequencing project led to discovery of low frequency IDH-1 R132 point mutations in prostate cancer **(653)**. These mutations have now been recurrently identified in many cohorts of prostate cancer patients **(330, 608, 654-656)(Figure 25B & Table 7)**.

IDH-1 R132 mutant tumours appear to present in early-onset prostate cancers yet the mutation doesn't appear to track linearly through cancer progression **(330)**. Mutation of the enzyme isn't detected in sequencing studies of metastatic disease meaning; i) IDH-1 mutation is at too low a frequency to observe transition to "successful" metastasis, ii) IDH-1 mutant tumours never progress to an advanced stage, or iii) a cancerous progenitor clone without IDH-1 mutation stems the aggressive lineage, after the growth of the primary IDH-1 mutant tumour has acted as a "gateway" event. The low percentage of IDH-1 mutation in the total patient population probably does mask progression of primary to metastatic cancer. To date a single study has observed IDH-1 mutation in a lung metastases, but again there are too few known incidences of mutation to make a conclusion from current data **(657)**.

These prostate tumours also exhibit extensive hypermethylation of their genomes, to an extent greater than that previously documented in IDH mutant gliomas and leukaemias **(330)**. As hypermethylation in IDH-1 mutant cells also presents in prostate cancers, it would be expected that there are similar disruptive effects on transcriptional neighbourhood organisation seen in gliomas that may play an active role in disease **(641)**. Metabolic alterations would also be expected in these tumours, as observed in glioblastoma, however low incidence has hampered investigation into the mutation's effects in prostate cancer. Disruption of collagen synthesis in IDH-1 mutants may have effects on the CSC population of the prostate that typically express high levels of collagen's cognate integrin; $\alpha_2\beta_1$. How this population is affected with regard to collagen anabolism and the hypothesised increase of stem cell symmetrical division observed in IDH-1 mutant mice models are important future questions **(632, 639, 658)**. The convergent nature of IDH-1 R132 mutations has allowed several selective inhibitors to be developed that reduce 2-HG levels and genome hypermethylation in mutant cells. Interestingly allosteric inhibitors of the mutant enzyme have been observed to induce differentiation of leukaemic stem like cells and implementation of these inhibitors in the small patient cohort affected in prostate cancer is a realistic future exploitation of patient specific medicine **(659, 660)**.

Codon Nucleotide Change	Amino Acid Change	Location (Exon/Domain)	Consequence	Reference
59G>A	R20Q	5	Missense	COSMIC UK - COSU538
356G>A	R119Q	6	Missense	Barbieri 2012 **(133)**
395G>A	R132H	6	Missense	Barbieri 2012 **(133)**
395G>T	R132L	6	Missense	Barnett 2014 **(655)**
394C>A	R132S	6	Missense	Barnett 2014 **(655)**
394C>T	R132C	6	Missense	Barnett 2014 **(655)**
394C>G	R132G	6	Missense	Barnett 2014 **(655)**

TABLE 7 – All known IDH-1 mutations in prostate cancer

1.8.8 - TMPRSS2-ERG; a defining rearrangement in Prostate Cancer

In men, TMPRSS2 is almost exclusively expressed in prostate tissue under canonical activation of the AR **(661)** and in 2005 the gene was shown to be commonly fused to members of the ETS TF family in prostate cancers; establishing a novel role in carcinogenesis and the possibility that ETS factor expression is driven by androgen signalling **(351)**. The most common of the ETS fusions; TMPRSS2-ERG, is consistently observed in ~50% of all prostate tumours **(90, 330, 662)**.

The ERG gene is located at 21q22.3, downstream of TMPRSS2 at 21q22.2 meaning that a fusion can be created as a result of a deletion event or through a series of translocations **(174, 351)**. The chromosomal alteration places the 5' untranslated region (UTR) of TMPRSS2 upstream of ERG, causing inappropriate expression of the transcription factor, now under control of an active promoter region. A recent study also found that ERG alters the global chromatin state in prostate cancer and creates super-enhancers; regions of high transcriptional activity characterised by elevated H3K27 acetylation **(663)**. One of these regions extends through the TMPRSS2-ERG locus to further promote ERG expression. TMPRSS2-ERG fusions are unique to each patient's tumour at a genomic nucleotide level and are thought to be generated through regions of micro-homology by NHEJ following DSB formation **(664)**. Higher levels of the NHEJ master-regulator BRD4 associate with fusion positive cancers and the BET (bromodomain and extraterminal) protein regulates formation of TMPRSS2-ERG **(665)**. The transcriptional activity of TMPRSS2 and the accessibility of ERG intronic chromatin also determines fusion formation **(666)**.

Next generation sequencing can capitalise on the unique genomic nature of the fusion breakpoints; and employ them as highly specific trunk mutation clonal markers. TMPRSS2-ERG can thus be used to track cell population origin, development and location in prostate cancers **(131, 667)**. The variety of fusion transcripts (and thus protein products) between and within samples are diverse, however the most commonly observed exon-exon fusions are those between TMPRSS2 exon 1 and ERG exons 4 (as seen classically in the VCaP cell line) and 5 **(351, 596)**. Distinct fusions show focal heterogeneity in prostate tumour biopsy samples demonstrating that different fusions can exist side-by-side and are independently generated through separate initiating events within the same prostate **(668)**.

Fusions generated by deletion of the region between the two genes are heterogeneous within and between patients, with variant start sites leading to production of different fusions. The deletions, rather than the rearrangement events, can be correlated with cancers that have higher biochemical recurrence (PSA levels) after treatment **(662)**. The deletion also removes ETS2, an ETS family member that is observed to be mutated in fusion negative prostate cancers **(335, 662)**. This gene is a candidate tumour suppressor **(669)** and overexpression of ETS2 in VCaP decreased cellular proliferation, migration and invasion **(335)**. Chromoplexy acts as a factory for

chromosomal rearrangements in prostate cancer and recurrently produces TMPRSS2-ERG fusions **(334)**. TMPRSS2-ERG^{+} tumours have greater inter-chromosomal rearrangements than those that lack a fusion event suggesting that TMPRSS2-ERG-centred chromoplexy has wider carcinogenic effects on the genome; such as coordinated loss of tumour suppressing loci including PTEN and 3p14; an area containing three potential TSGs **(90, 334)**. Analysis of separate tumours found that different chromoplectic chains can still produce the necessary genetic rearrangements required for fusion formation.

Creation of TMPRSS2-ERG involves interphase co-localisation of the genes and topoisomerase II recruitment **(350, 670, 671)**. It has been hypothesised that androgen signalling is responsible for the close proximity of the loci and thus facilitates the chain of translocations leading to TMPRSS2-ERG **(174)**. Exposure of LNCaP to androgens does cause *de novo* fusion formation, an event that remains specific to cells of prostatic origin.

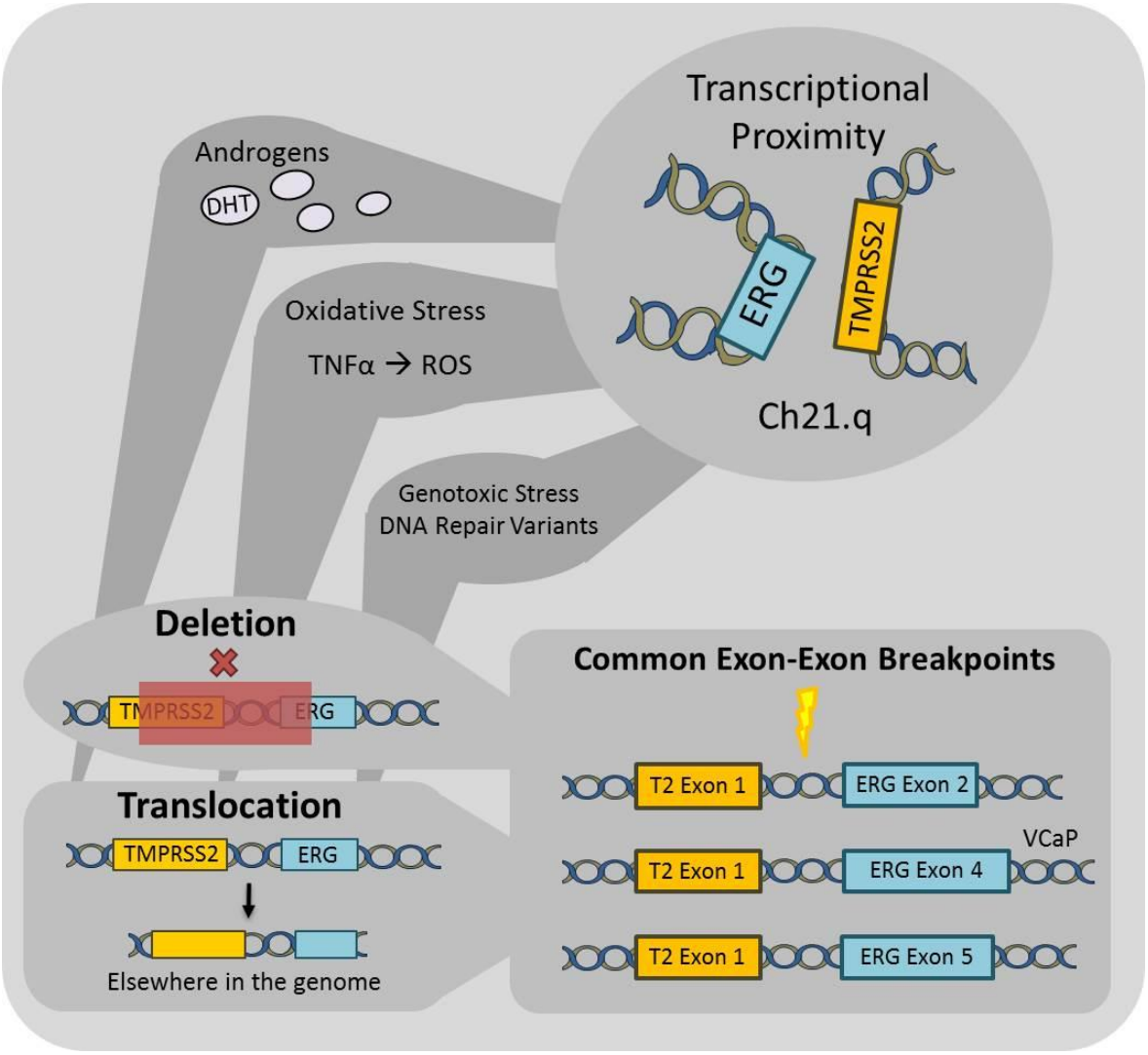

FIGURE 26 – Generation of the TMPRRS2-ERG fusion in prostate cancer.

Transcriptional proximity of the loci and the addition of micro-environmental stressors produce the fusion either by deletion or translocation of the intervening genetic material. The fusions are always produced in intronic regions and align early TMPRSS2 exons with later ERG exons.

This effect is enhanced by the presence of inflammation, which itself, in absence of androgen, can generate *de novo* fusions as modelled by TNF-α exposure **(666)**. Inflammation mediated by ROS has been observed to create fusions in LNCaP, both in vitro and in vivo. Interestingly, the in vivo study highlighted critical involvement of macrophage cytokines and the role of the innate immune system in TMPRSS2-ERG formation. As the supposed aetiology of human prostate cancer is rooted in inflammation of the organ, these findings give molecular evidence for the initial transformation of prostate cells. Repetition of these experiments in cells of a "normal" genetic background would add further and necessary weight to this theory **(Figure 26)**.

DNA repair gene variants, including BRCA2, ESCO1 and POLI, have been identified in population linkage studies to be significantly associated with fusion positive cancers, suggesting that they produce a genetic background conducive to TMPRSS2-ERG fusion production **(349)**. Interestingly genotoxic stress – like androgen and TNF-α exposure – also causes creation of the fusion in prostate cells **(350)**.

Expression profiles of the precursor lesion PIN and prostate cancer itself are extremely similar. The transition of PIN into malignancy correlates with increased expression of ERG, ETV1 and ETV4, all known fusion partners; suggesting that TMPRSS2 rearrangements act as founder events in prostate cancer **(123)**. ERG fusions are observed in hgPIN with incidence correlating with a faster rate of progression into prostate cancer over fusion negative PIN patients **(132)**. As the fusion is assumed to be an early event in the development of prostate cancer, it can be used to trace metastases back to their focal origin in the primary tumour **(662)**. TMPRSS2-ERG is present in the CSC fraction of the prostate, postulating a self-renewing root for widespread fusion presence in prostate tumours **(246)** and, in a genetically manipulated mouse model of the prostate, the fusion has indeed been shown to increase the self-renewal and invasiveness of basal progenitor (Sca-1^{hi}, $EpCAM^{+}$) cells, **(672)** again suggesting TMPRSS2-ERG plays a role in maintenance of the CSC population and allows for the subsequent mutational accumulation.

Transgenic TMPRSS2-ERG^{+} mice developed PIN with selective ERG overexpression at disease foci and not in benign glands, suggesting that enhanced protein levels induce a neoplastic phenotype rather than initiate the cancer. Further investigation using cell lines found that the fusion also facilitated an invasive phenotype through overexpression of MMPs and urokinase plasminogen activator (uPA). ERG knockdown in these cells raised expression of canonical luminal cell markers suggesting that overexpression of the ETS factor sequesters prostate epithelial cells in a dedifferentiated state **(427)**. The invasive phenotype has also been noted in patient samples where fusion positivity co-segregated with an increase in TGF-β signalling, a hallmark of EMT **(673, 674)**.

ERG in this context has been shown to upregulate PIM1. This kinase is an oncogene overexpressed in both haematological and epithelial malignancies and is implicated in docetaxel resistance of prostate cancer. PIM1 increases cyclin B levels to cause destabilisation of the G_2/M checkpoint, resulting in aneuploidy and genomic instability in pre-malignant prostate cells **(675)**. ERG regulation by AR also creates a wider network of cross talk between the two important TFs. Overlap of AR and ERG binding sites in VCaP cells found that ERG is co-recruited to around half of all AR-bound loci. One of the most enriched sites, identified by ERG ChIP-seq, was the AR gene itself. siRNA targeting of ERG caused an increase in AR protein levels highlighting that ERG has repressive effects on the androgen signalling axis, a finding that may have wider implications in CRPC **(542)**.

The recent development of ERG inhibitory peptides that reduce transcriptional activity, increase degradation of the transcription factor and suppress cancer progression in vitro and in vivo marks a promising and novel treatment strategy for the 50% of patients that present with the fusion **(676)**.

In primary prostate epithelial cells, a SNP-based pyrosequencing strategy was utilised to show RME of TMPRSS2 in the basal cell populations of cancer and BPH samples. The strongest allelic restriction of TMPRSS2 was seen in the stem cells, yet in most cases this was relaxed or even switched to the other allele upon asymmetric division in clonal TA cells. However, in TMPRSS2-ERG$^+$ cancers the fusion is solely expressed in the stem cell population with no expression of TMPRSS2 from the unfused “wildtype” allele. This doesn’t follow the random pattern of expression in the fusion negative samples and implies that the fused allele is somehow selected for in the stem cell, the allelic expression of which wasn’t correlative with promoter hypermethylation **(246)**.

Identification of genetic defects in SPOP, PTEN, IDH-1 and presence of the TMPRSS2-ERG fusion gene in primary prostate epithelial cultures will allow for allelic expression analysis to observe; i) whether mutant alleles are expressed, and ii) if there is any non-random selection of allelic expression in prostate cancers. This will inform whether mutations are actionable and, if observed, will introduce another layer of heterogeneity needed to be addressed and accounted for in the diagnosis and treatment of prostate cancer.

1.9 - Low Temperature Plasma and Oxidative Stress

1.9.1 - Low Temperature Plasma as an anticancer therapy

Treatments of localised **(293)** and metastatic prostate cancer **(26)** have improved over recent years, yet there remains the problem of overtreatment during the early stages of disease due to a lack of clinical biomarkers that can determine indolent or aggressive cancer **(283, 677)**. Current focal treatments of organ-confined disease such as radiotherapy have high rates of recurrence that can be attributed to sub-clonal cell populations in the prostate **(323, 678)**. Novel therapies are required to maximise treatment-options, increase overall success and effectively ablate the tumour initiating cell pool as discussed in **Section 1.4.**

The ability to generate plasma at ambient air temperatures has allowed biomedical implementation of LTP devices and subsequently, the technology has been postulated as an anti-cancer therapy **(293)**. Plasma is formed through application of a sufficiently high voltage across a gas-flow; causing removal and subsequent acceleration of gas molecule electrons into the surrounding atoms and molecules. A reactive cascade of interconverting neutral and charged species is created in the plasma effluent, alongside the emission of UV radiation. Mixing of LTP with gas molecules in the air is known to produce high concentrations of ROS and RNS **(679-684)** that can cause subsequent oxidative stress, DNA damage, protein oxidation and lipid peroxidation in living cells **(685, 686)**.

LTP based treatment has now been applied to a wide range of cell line models including those representative of; prostate cancer, **(304, 305)** cervical cancer, **(687)** melanoma, **(688, 689)** leukaemia, **(690)** ovarian cancer, **(691)** breast cancer, **(692, 693)** head and neck cancer, **(679)** glioblastoma, **(694, 695)** lung cancer, **(696, 697)** colorectal cancer **(698)** and liver cancer **(699)**.

1.9.2 - Oxidative Stress – Antioxidant and Transcriptional Response

In vitro studies, including our own **(304)**, have examined the effect of LTP upon cancer cell cultures and arrived at congruent conclusions; plasma is able to generate ROS and RNS in both the medium and the cells **(304, 679, 687, 695-697, 699)**. This in turn causes oxidative damage of lipids, **(699)** proteins **(692)** and DNA **(305, 679, 688, 689, 692, 695, 700)** to ultimately produce loss of viability and cell death in cultures **(304, 679, 687, 688, 692)**.

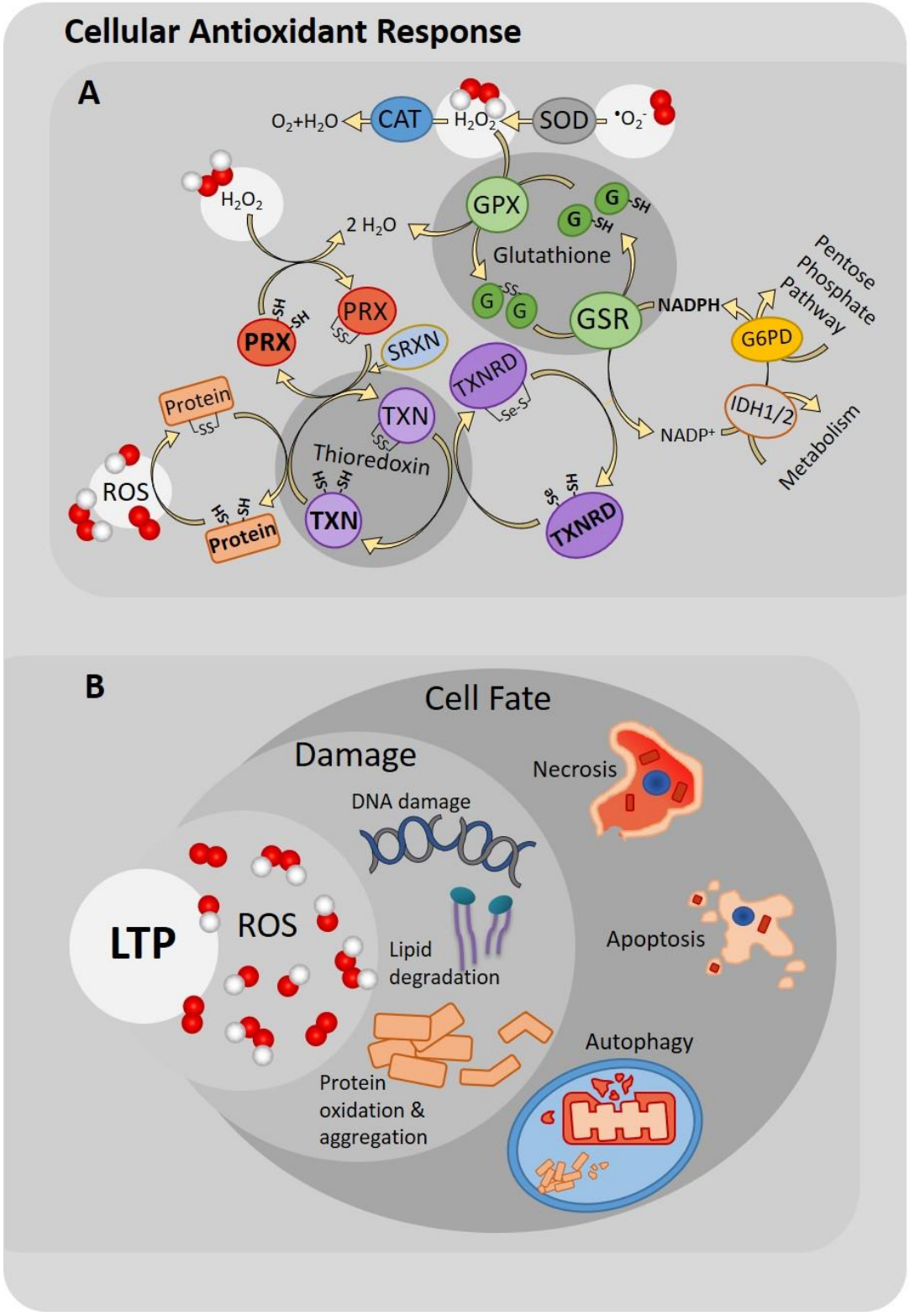

FIGURE 27 –Low Temperature Plasma and Reactive Oxygen Species.

A) The basal antioxidant defence network of a cell. The cellular NADPH pool maintains the Glutathione and Thioredoxin cycles that redox enzymes require to mount an effective response to oxidative stress and damaged proteins. **B)** The induction of ROS by LTP causes varied molecular and cellular damage that impacts cell fate decisions.

Oxidative stress is defined by the imbalance of ROS and cellular antioxidants; a state induced by LTP treatment and experimentally demonstrated by skewing of reduced and oxidised forms of cellular antioxidants and co-factors such as glutathione (GSH) and NADPH **(696, 701, 702)**. Antioxidants limit ROS induced damage and include both scavenging proteins and ROS-converting enzymes. Non-enzymatic antioxidants can donate electrons to neutralise ROS. GSH is the primary cellular antioxidant and can prevent damage caused by free radicals and peroxides. Enzymatic antioxidants include many well-studied proteins such as the superoxide dismutases (SOD), thioredoxins (TXN), glutathione peroxidases (GPX), haem oxygenases (HMOX) and peroxiredoxins (PRDX). Haem oxygenase 1 is an inducible enzyme that exerts an antioxidant effect by creation of biliverdin from haem. Biliverdin is subsequently entered into a cycle that scavenges and depletes cellular ROS **(703)**. The peroxiredoxins are involved in removal of hydrogen peroxide from cells, with their native reduced state being regenerated by GSH, TXN and sulfiredoxin (SRXN) **(704-706)(Figure 27A).**

Whilst oxidative stress response occurs rapidly through alterations in enzymatic activities, transcriptional programs are also augmented, to give cells a survival advantage in prolonged exposure. Gene expression response to ROS is mediated by a plethora of transcription factors such as Nrf2, HIF, NF-kB and AP-1 **(686, 707)**.

Nrf2 is restricted to the cytosol by dimers of Keap1, an adaptor protein of the Cullin 3 E3 Ligase that facilitates constitutive degradation of the transcription factor in non-stress conditions. Keap1 is redox sensitive at several cysteine residues and modification of these thiols by ROS causes dissociation from Nrf2. Nrf2 then translocates to the nucleus whereupon it forms heterodimers with small Maf proteins. These dimers act as transcriptional activators for genes downstream of Antioxidant Response Elements (AREs) including; glutathione reductase (GSR), PRDX, TXN, TXNRD1 (thioredoxin reductase 1), CAT, SOD1, HMOX1, NQO1 and GPXs **(708-713)**. Nrf2 is also phosphorylated by kinases, such as PKC and ERK, during oxidative stress which is also thought to aid the transcription factor's dissociation from Keap1 **(686)**. Recent studies have indicated the involvement of Nrf2-mediated anti-oxidant signalling in the cellular response to plasma. Application of LTP, and even plasma activated media, is adequate to promote nuclear translocation, cause upregulation of target genes and enhance ARE binding of the transcription factor **(714-716)**.

Previous studies have also shown that LTP triggers MAPKs such as JNK, p38 and ERK (JNK and p38 are also termed stress-activated protein kinases, SAPKs) through canonical phosphorylation of these proteins, allowing for activation of downstream apoptotic and response pathways **(679, 687, 715, 716)**. A microarray based approach in a lung cancer cell line identified increased expression of Jun and Fos transcription factors alongside increased activation of JNK in response

to LTP **(717)**. Activator Protein 1 (AP-1) is a collection of several dimeric basic leucine zipper proteins belonging to the Jun, Fos, Maf and ATF families; although, classically, AP-1 is formed by Jun-Fos heterodimers. Transcriptional activity can be induced by ROS through phosphorylation of Jun by JNK and p38 **(718)**. JNK phosphorylation can be induced by many upstream activators. Among these are ASK1, another kinase that is activated by hydrogen peroxide induced TXN oxidation, and the redox sensing GST(μ/π) to which JNK, and ASK1, are associated with in non-stress conditions **(414, 686, 719, 720)**.

Activation of these TFs would allow cells to respond at a molecular level to the oxidative stress induced by LTP. Differential gene targets between normal and cancerous cells may have potential to be pharmacologically exploited to sensitise prostate cancers to plasma treatment over surrounding normal tissue.

1.9.3 - Cell Fate in LTP induced Oxidative Stress

Our own studies using primary prostate epithelial cells have shown that, instead of the usual apoptosis observed in cell line studies, the mechanism of cell death is necrosis **(304)**. This can be interpreted as an abortive action when a cell has sustained a level of damage that cannot be salvaged. ROS excess switches cell death from apoptosis to necrosis as mitochondrial dysfunction reduces cellular ATP level, whilst ROS and RNS can inhibit caspases through oxidative modification or S-nitrosylation of the reactive thiol **(721, 722)**.

Oxidative stress can also lead to senescence through stalling of the cell cycle, which occurs as lipid peroxides prolong G_1 phase, with aldehyde oxidation products also causing CDK and DNA polymerase inhibition. Oxidative DNA damage further contributes to stabilise p53 through JNK and p38 phosphorylations causing either restriction point stalling or apoptosis **(414, 722)**.

Interestingly we also noted an enhanced autophagy response – an increased level of mature LC3-B - in the primary prostate cultures treated by LTP, suggesting that this salvage pathway may play a role in the survival of certain cells **(304)**. Autophagy allows for absorption of defective organelles, such as mitochondria, and abnormal protein aggregates in stressed cells. This process relies on the double membrane formation of the autophagosome that degrades interred organelles or cellular bodies upon lysosomal fusion. Autophagy is induced by superoxide and hydrogen peroxide and is thought to be mediated through lipid peroxidation and specific Cys81 thiol modification of Atg4, a key protein in autophagosome formation. Active Atg4 is critical in the formation of LC3-BII that coats the inner surface of the autophagosome whereupon it acts as a binding site for poly-ubiquitinated protein aggregates under the escort of the p62/SQSTM1 chaperone protein **(723, 724)**. Sequestosome 1 (SQSTM1) is an Nrf2, NF-kB and AP-1 target gene

(725, 726). Dysfunctional autophagy increases cellular oxidative stress as recycling of mitochondria, the major source of endogenous ROS, becomes defective **(727)(Figure 27B)**.

1.9.4 - Oxidative Stress in Prostate Cancer

Cancer cells generally have a higher ROS threshold that allows them to dampen cell death signals normally induced by higher ROS concentrations and allows further aberrant signalling to be mediated by the oxygen species. For example, GSH levels are higher in some cancers to buffer the excess ROS and transcriptional changes seen in oxidative stress are enhanced, allowing for aberrant activation of these signalling pathways such as AKT-mediated apoptosis inhibition and cellular proliferation **(702)**.

Various cancers contain mutations in genes involved in ROS management and stress response. Antioxidant enzymes SOD2 and GPX are mutated in prostate and other cancers along with the oxidative DNA damage repair enzymes OGG1 and APE1 **(686)**. The same is true of the transcription factor Nrf2 and its antagonising protein Keap1 **(728)**. Epigenetic regulation of genes can also be disturbed by oxidative stress; ROS can increase DNMT expression leading to gene (BRCA1, RB1, MDM2, MLH1 and KEAP1) silencing and genome hypermethylation **(702, 728)**. As mitochondria are the primary source of endogenous ROS, tumours can redirect their metabolic pathways into glycolysis, a change called the Warburg effect. This activates anaerobic hypoxic respiration, and also sets up a miniature Cori cycle with recruited cells. In oxidative stress, the process of oxidative phosphorylation becomes restricted, leading to pyruvate kinase inhibition and pentose phosphate pathway (G6PD) activation. The resultant increased production of NADPH is able to maintain GSH in a reduced state, facilitating ROS scavenging **(729, 730)** and contributing to tumour cell ROS resistance.

ROS resistance is enhanced in CSCs. The tumourigenic cell fraction in breast cancer was shown to have lower levels of ROS and higher levels of antioxidant proteins and enzymes. The importance of the antioxidant levels was demonstrated through the depletion of GSH which caused a significant reduction in colony forming efficiency of the CSCs **(731)**. The majority of cancer treatments induce ROS; upregulation of the antioxidant network in the tumour initiating cells would aid their commonly observed radio- and chemoresistance.

As part of the ROS-induced transcriptional response, mutations to KEAP1 that affect Nrf2 binding have been observed in prostate cancer cell lines and tumour samples; with epigenetic silencing, via DNA methylation of the gene, observed in Du145 cells **(732)**. However, most studies investigating Nrf2 in prostate cancer report a reduction in levels of the TF, **(733)** with promoter methylation perhaps reducing transcript levels **(734)**. Decreased Nrf2 presumably facilitates an

environment of oxidative stress to aid chromoplectic genome rearrangements and cellular transformation **(734)**.

AP-1 has context-dependent effects in prostate cancer due to its dual role in promoting both cell proliferation and apoptosis. Whilst the AP-1 axis isn't notably affected by mutation or rearrangement, levels of the transcription factors in the various stages of disease appear to contribute towards clinical outcome.

JUNB (cJun homologue) mRNA and protein levels decrease during cancer progression, where JUNB loss synergises with PTEN deletion mutants to promote invasive prostate cancer in transgenic mice **(735)**. However, another study found PTEN loss caused JNK, and subsequent Jun, activation through PI3K. Positive correlation of pAKT and pJun levels in human prostate cancer tissue microarrays were then identified as a supposed result of common PTEN phosphatase deletion **(736)**. AP-1 is elevated in more advanced prostate cancers with JNK driving disease progression from adenocarcinoma to metastatic disease in mouse models **(737)**. Expression of both Fos and Jun increases throughout disease. Incidence peaks in metastases where significant co-expression is also observed. Activation of Jun, in particular, is predictive of decreased patient survival following relapse from ADT, suggesting that the AP-1 pathway may act as a driver of androgen independent disease **(738, 739)**.

By identifying the transcriptional networks activated following plasma treatment of primary prostate epithelial cultures, derived from multiple disease contexts, the upstream transcription factors can be identified. An increased understanding of how prostate epithelia react to LTP will afford insight to how resistant populations can survive the oxidative stress induced by treatment whist also informing on possible sensitising treatments for cancerous cells over that of adjacent normal tissue to maximise the killing effect of the focal therapy.

2. Thesis Aims

AIM 1

To identify if genes commonly altered in prostate cancer are monoallelically expressed and, if so, whether mutation of the gene affects allelic expression.

Random monoallelic expression provides a source of expression heterogeneity. In the knowledge that allelic imbalances are molecular determinants of prostate cancers the phenomenon was thus investigated in primary prostate epithelial cultures. The study had two goals, to;

- Determine if silent and expressed TMPPRSS2 alleles are marked by histone trimethylations associated with monoallelic expression in primary prostate epithelial subpopulations. Ascertain whether these also correlate with allele specific expression of TMPRSS2-ERG fusion in prostate cancer samples.

- Analyse allelic expression of SPOP, PTEN and IDH1 and assess whether mutation of these commonly altered genes changes allelic expression.

AIM 2

To identify the molecular signalling events in prostate epithelia after Low Temperature Plasma exposure that are associated with the resistant population.

LTP is a promising novel focal therapy for prostate cancer. Our previous work has identified a potent killing effect; however, a viable population of cells remained after treatment. This resistant population may cause regrowth and relapse of the tumour. By identifying the immediate signalling events that contribute to post-LTP survival it may be possible to sensitise the resistant population using combination therapy. The study had the following goals;

- Identify whether oxidative stress response signalling was initiated by LTP.

- Find altered signalling pathways after treatment using whole transcriptome analysis.

- Identify active signalling intermediates and transcription factors upstream of gene expression.

- Connect gene expression and transcription factor response to the resistant population.

3. Materials and Methods

3.1 –Cell and Tissue Culture

Primary Cell Culture

Primary epithelial cells were dissociated from patient prostate tissue as previously described **(Collins 2005)(28)**. For matched Gleason 7 and Normal cells, tissue was obtained through needle biopsy immediately following surgical removal of the prostate. Biopsy sites were informed by previous pathology, imaging and palpitation. BPH and Gleason 9 tissue were obtained through trans-urethral resection of the prostate. All tissues were transported in RPMI-1640 supplemented with 5% foetal calf serum (FCS) and 100U/ml antibiotic/anti-mycotic solution at 4^{o}C and processed within 6 hours of surgery. All tissue was obtained with full ethical permission and consent of the patient through agreement with Hull Hospital - REC ref 07/H1304/121. Patient samples were anonymised before receipt at the York Cancer Research Unit.

Primary cells were grown on Collagen I coated 10cm dishes (Corning) in 5ml stem cell media (SCM). This is based upon keratinocyte serum free media supplemented with L-glutamine, stem cell factor, granulocyte macrophage colony stimulating factor, cholera toxin, bovine pituitary extract (Gibco), epidermal grown factor (Gibco) and leukaemia inhibitory factor, see **Collins 2005 (28)**. Primary cells were cultured in the presence of irradiated STO mouse feeder cells. No antibiotic/anti-mycotics were used to treat the cultures.

STOs were grown in D10 media [DMEM (Gibco) supplemented with 10% FCS and L-glut]. Batches of STOs, for use as feeder cultures of primary cells, were irradiated (60Gy) and resuspended in KSFM to be used within 4-5 days and kept at 4^{o}C. STOs were depleted by outgrowth of the epithelial cells before any plasma treatments so as to remove any mouse cell artefacts **(19)**.

Cell stocks were centrifuged to form pellets at 1500rpm for 5 minutes in the IEC CL30R centrifuge (Thermo Scientific). The pellet was then re-suspended in 1ml of filtered Freezing Media (7 parts RPMI 1640, 2 parts FCS and 1 part DMSO), transferred to a Cryo S cryovial (Greiner) and labelled. The sample was frozen in CoolCell LX foam freezing chamber (Biocision) from room temperature to -80^{o}C and then transferred to liquid nitrogen dewars. Retrieving frozen stocks involved thawing the samples to 37^{o}C, adding the sample to 2ml of its growth media in a 15ml falcon (Greiner) and then spinning down at 1500rpm for 5 minutes to pellet the cells. The pellet was re-suspended in the appropriate volume of growth media and the cells applied to tissue culture plastic.

Selection of Basal Epithelial Subpopulations

Six Collagen I coated 10cm dishes (Corning) were blocked with 3ml PBS – 0.3% BSA (that had been heat treated at 80^{o}C for 10 minutes followed by vacuum filtration) for 1 hour at 37^{o}C. Whilst the plates were blocking, the whole population cultures (≥6x10cm confluent plates) were trypsinised, neutralised in R10 [RPMI-1640 (Gibco) supplemented with 1% L-glutamine (Gibco) and 10% FCS (Gibco)], spun down at 1500rpm for 5 minutes in the IEC CL30R centrifuge (Thermo Scientific) and then re-suspended in 9ml SCM. Blocked plates were removed after the elapsed time and washed in PBS. Blocked plates were then labelled; 3x SC/TA, 3x Intermediate. 3ml of cells were applied to each of the three SC/TA blocked plates and placed in the incubator for 5-10 minutes. The adherent cells after this time are the SC/TA population. Plates were removed from the incubator and the media containing non-adherent cells collected. Plates were then washed twice with 3ml PBS – that was also collected and placed into the media containing tube. The plates of adherent SC/TA cells were then trypsinised for 10 minutes. The cells in suspension were pelleted at 1500rpm for 5 minutes and then re-suspended in 9ml SCM. 3 ml of the suspended cells were added to each of the three remaining blocked plates and incubated for 30 minutes. The trypsinised SC/TA cells were neutralised in R10 and spun down at 1500rpm for 5 minutes. If any adherent cells remained they were removed with 10X trypsin-EDTA. The SC/TA cells were then re-suspended, in the amount of media required for the next assay, and counted. The second set of blocked plates were removed after 30 minutes and non-adherent CB cells collected, as before; removal of media and collection of two PBS washes. The adherent intermediate cells were trypisinised. CB cells were span down at 1500rpm for 5 minutes and counted. Intermediate cells were then collected in the same manner as the SC/TA population. SC/TA and CB populations were then either applied to plates or harvested immediately depending on the following treatment.

For gDNA; intermediate cells were pelleted in the Accuspin Micro microcentrifuge (Fisher Scientific) – 2 minutes at 6500rpm. Pellets were washed in 1ml PBS, and spun down at the same speed and time. The PBS was aspirated and the pellet frozen at -80^{o}C until gDNA extraction.

For RNA; cells were grown in 12 well plates with 100,000 cells per well in 1ml SCM. They were left to adhere overnight before treatment and harvesting, or harvested immediately by spinning down at 6500rpm for 2 minutes in the Accuspin Micro microcentrifuge (Fisher Scientific), washed in PBS and re-pelleted. PBS was aspirated and the pellet frozen at -80^{o}C until RNA extraction.

For Protein; cells were grown in 6 well plates with 500,000 cells per well in 2ml SCM. They were left to adhere overnight before treatment and harvesting. Harvesting was either as cell pellets or protein lysate in 4X SDS protein buffer – See SDS-PAGE and Western Blotting section.

For Chromatin; cells were re-suspended in 2ml SCM and 54µl formaldehyde (36.5-38%)(Sigma Aldrich) was added. The sample was incubated in the formaldehyde for 15 minutes and flicked to prevent the cells settling on the bottom of the tube. After the allotted time the formaldehyde was neutralised with 1M glycine for 5 minutes. The sample was then centrifuged for 5 minutes at 1000rpm at 4°C in the IEC CL30R centrifuge (Thermo Scientific). The pellet was rinsed twice in 4ml of ice cold PBS – both times the cells were spun down for 3 minutes at 2500rpm at 4°C. PBS was aspirated and the pellet frozen at -80°C before ChIP.

Cell line culture

See **Table 2** in **Section 1.7** for more details on prostate epithelial cell lines.

- BPH-1 cells were grown in R5 [RPMI-1640 (Gibco) media supplemented with 5% FCS and 1% L-glutamine (Gibco)].
- PNT1a cells were grown in R10 media.
- PNT2-C2 cells were grown in R10 media.
- P4E6 cells were grown in K2 [KSFM media (Gibco) supplemented with bovine pituitary extract, epidermal growth factor (Gibco), 2% FCS and 1% L-glutamine (Gibco)].
- PC3 cells were grown in H7 [Hams F-12 media (Lonza) supplemented with 7% FCS and 1% L-glutamine (Gibco)].
- LNCaP cells were grown in R10 media.
- Du145 cells were grown in R10 media.
- VCaP cells were grown in R10 media on Corning Cell Bind T25 flasks (Corning).

Cells were cultured in the absence of antibiotics and anti-mycotics on, unless specifically stated, standard tissue culture plastics supplied by Corning or Starstedt and incubated at 37°C with 5% CO_2.

3.2 – Molecular Analyses

RNA extraction

Cells were harvested by trypsinisation (1X Trypsin-EDTA (Gibco) and neutralised with equal volume of R10. They were then centrifuged for 5 minutes at 1500rpm in an IEC CL30R centrifuge (Thermo Scientific) then washed in 1ml PBS before final centrifugation at 6500rpm for 2 minutes to produce a cell pellet in an Accuspin Micro microcentrifuge (Fisher Scientific). RNA extractions were performed on fresh cell pellets, pellets previously stored at -80°C or by direct in-plate lysis (addition of complete RLT buffer followed by storage at -80°C overnight) using the RNeasy Micro Kit (Qiagen) following the manufacturer's instructions for the animal cell protocol that proceeds as follows.

One part B-mercaptoethanol (BioChemica) was added to one hundred parts RLT buffer, and 600µl of this mix was added to the cell pellet and mixed using a pipette. Lysates were then transferred into a QIAshredder column (Qiagen) in a 2ml collection tube and centrifuged for 2 minutes at 13,000rpm in the Accuspin Micro microcentrifuge (Fisher Scientific). 600µl of 70% ethanol was added to the flow-through, mixed by pipette until homogenous and then aliquoted into an RNeasy Mini column in a 2ml collection tube. These were centrifuged at 8000rpm for 15 seconds (s) and flow-through discarded. Genomic DNA contamination was removed by on-column application of the RNase-free DNase Set (Qiagen) – this involved a wash step of 350µl Buffer RW1 (8000rpm for 15s, flow-through discarded) before application of 70µl:10µl mix of Buffer RDD:DNase. Columns were left to stand at room temperature for 15 minutes before a second Buffer RW1 wash step as before. 500µl of Buffer RPE was then used to wash the column, 8000rpm for 15s and flow-through discarded. This step was repeated with a final 2-minute centrifugation. The column was transferred to a fresh collection tube and centrifuged at 13,000rpm for 1 minute. The collection tube and flow-through were discarded and the column placed in a 1.5ml labelled Eppendorf. RNA was eluted from the column with 30µl of PCR quality water (Sigma) directly pipetted onto the membrane and centrifuged for 1 minute at 8000rpm, this step was repeated for a total volume of 60µl RNA. Concentration was measured on the Nanodrop ND-1000 (Labtech) and either proceeded directly into cDNA synthesis or stored at -80^{o}C.

cDNA synthesis

cDNA was synthesised directly from purified RNA using either the iScript cDNA synthesis kit (BioRad) or Superscript III or IV kits (Invitrogen), depending on availability in the laboratory. All mastermixes (MMs) were made up in the Mini V/PCR hood (Telstar) and the RNA added on bench. cDNA was stored at -20^{o}C or used immediately in qRT-PCR assays or RT-PCR.

iScript

MM was made up of (for one reaction); 4µl iScript RT Supermix and 14µl of PCR quality water (Sigma). This was mixed with a pipette, pulse centrifuged and added to 2µl of template RNA (≤1µg). Reactions were then placed into the GeneAmp PCR System 9700 thermal cycler (Applied Biosystems) and entered into a program of; 25^{o}C for 5 minutes, 46^{o}C for 20 minutes and 95^{o}C for 1 minute. Sample cDNA concentration was assessed using the Nanodrop and diluted to stock and working concentrations in PCR quality water (Sigma).

Superscript III

All reagents marked with (*) are supplied in kit from Invitrogen and reactions carried out as per manufacturer's instructions. MM1 for each reaction consisted of; 1µl Random Hexamer* (50g/µl),

1µl dNTP* (10mM). This was mixed using a pipette and added to 10µl sample RNA (≤5µg) and reactions placed in GeneAmp PCR System 9700 thermal cycler (Applied Biosystems) for 5 minutes at 65°C followed by 2 minutes on ice. At this point MM2 was made. Each reaction contained; 4µl First Strand Buffer*, 2µl DTT* (100mM), 1µl RNase OUT* (40U) and 1µl Superscript III Reverse Transcriptase* – mixed using a pipette and then pulse centrifuged. 8µl of MM2 was then added to each reaction before the tubes were again placed in the thermocycler; 25°C for 10 minutes, 42°C for 50 minutes, 15 minutes at 72°C, hold at 4°C. cDNA was then isolated using the QIAquick PCR Clean up kit (Qiagen) as described in PCR Product Purification. Following clean up, sample cDNA concentration was assessed using the Nanodrop and diluted to working concentrations in PCR quality water (Sigma).

Superscript IV

All reagents marked with (*) are supplied in kit from Invitrogen and reactions carried out as per manufacturer's instructions. MM1 for each reaction consisted of; 1µl Random Primers* (50µM), 1µl dNTPs* (10mM), 2µl PCR quality water (Sigma). MM1 was mixed using a pipette, pulse centrifuged and 4µl added to 1.5µl of template RNA (≤5µg) in PCR tube. Tubes were placed in GeneAmp PCR System 9700 thermal cycler (Applied Biosystems) for 5 minutes at 65°C followed by 1 minute on ice. At this point MM2 was made. Each reaction was made up of; 4µl of 5X SSIV Buffer* (after vortexing and pulse centrifugation), 1µl DTT* (100mM), 1µl RNase OUT* (40U) and 1µl Superscipt IV Reverse Transcriptase*. MM2 was mixed using a pipette, pulse centrifuged and 7µl added to the MM1 + RNA on ice. The reactions were again placed in the thermal cycler on the following program; 23°C for 10 minutes, 50°C for 10 minutes and 80°C for 10 minutes. Each sample then had 1µl RNase H* added and placed back in the thermal cycler for 20 minutes at 37°C. cDNA concentration was measured on the Nanodrop and diluted in PCR quality water (Sigma) to appropriate working stock concentrations.

Quantitative Real Time PCR (qRT-PCR)

qRT-PCR was performed in FrameStar 96 qRT-PCR plates (4titude). Input cDNA was standardised at 30ng per well and biological samples averaged from technical triplicate measurements. MM was constituted in the Mini V/PCR hood (Telstar) and was added 7µl per well (giving a total volume of 10µl) before the wells were protected by a clear adhesive cover and the plate centrifuged at 1000rpm for 2 minutes in the Heraeus Megafuge 1.0R centrifuge (Thermo Fisher). TaqMan probes were purchased from Thermo Fisher and BioRad, and are listed in **Table 8.** qRT-PCR was performed using the C1000 Thermal Cycler and CFX96 Real-Time System (BioRad) under the following protocol for all applications; 95°C – 2 minutes, 39 cycles; 95°C for 5s, 60°C for 30s, 4°C Hold. When using TaqMan Fast Universal Master Mix (Applied Biosystems) the following PCR

was used; 95°C – 10 minutes, 39 cycles; 95°C for 15s, 60°C for 60s, 4°C Hold. Machine reader heads were configured to WHITE-ALL CHANNELS (Thermo Fisher Taqman & BioRad Taqman), or WHITE-FAM ONLY (Thermo Fisher Taqman) dependent on Taqman probes used. Data was annotated using the CFX Manager 2.0 (BioRad) and analysed using the $2^{-\Delta\Delta Ct}$ method in Microsoft Excel **(740)**.

Gene Target	Probe	Company	Code
HMOX1	FAM	BioRad	qHsaCIP0033307
HSPA1A	FAM	BioRad	aHsaCEP0040036
JUN	FAM	BioRad	qHsaCEP0032009
GAPDH	TexRed	BioRad	qHsaCEP0041396
SOD2	FAM	Thermo Fisher	Hs00167309_m1
GPX2	FAM	Thermo Fisher	Hs01591589_m1
NOS2	FAM	Thermo Fisher	Hs01075529_m1
RPLP0	FAM	Thermo Fisher	Hs99999902_m1
NRARP	FAM	Thermo Fisher	Hs04183811_s1
HES1	FAM	Thermo Fisher	Hs00172878_m1
SOX9	FAM	Thermo Fisher	Hs00165814_m1
IL6R	FAM	Thermo Fisher	Hs01075664_m1
NR4A1	FAM	Thermo Fisher	Hs00374226_m1
NR4A2	FAM	Thermo Fisher	Hs01117527_g1
NR4A3	FAM	Thermo Fisher	Hs00545009_g1
FOSB	FAM	Thermo Fisher	Hs00171851_m1
DUSP10	FAM	Thermo Fisher	Hs00200527_m1
SQSTM1	FAM	Thermo Fisher	Hs01061917_g1
JUN	FAM	Thermo Fisher	Hs01103582_s1
HMOX1	FAM	Thermo Fisher	Hs01110250_m1
18S	VIC	Thermo Fisher	Hs99999901_s1

TABLE 8 – TaqMan probes used in study.

SDS-PAGE and Western Blotting

Cell lysates were either prepared from frozen pellets or cells were directly lysed in 6-well plates following plasma treatment. Each individual protein lysate sample required $5x10^5$ cells.

Cell pellet lysates were prepared by resuspension in 80µL CytoBuster™ Protein Extraction Reagent (Novagen) with PhosStop phosphatase inhibitors (Roche), cell debris removed by centrifugation in the Accuspin Micro microcentrifuge (Fisher Scientific) (13,000rpm, 5 minutes) and protein content measured by Pierce™ BCA Protein Assay Kit (Thermo Fisher Scientific). BCA Assays were performed according to manufacturer's instruction in a 96 well plate (Starstedt). A 2mg/ml stock of Bovine Serum Albumin (Sigma) was prepared in CytoBuster™ Protein Extraction Reagent, this was then serially diluted in triplicate across the wells (10µl/well) of the 96 well plate to produce standards. 10µl of protein sample, unknown concentration, was then pipetted into separate wells before addition of 190µl of BCA reagent (1 part Reagent B to 50 parts Reagent A). The plate was incubated at 37°C for 30 minutes before absorbance at 562nm was measured using the POLARstar OPTIMA plate reader (BMG Labtech). Data collected by the FluoSTAR OPTIMA program and protein concentration of the unknown samples calculated using Microsoft Excel. 20µg of protein with the appropriate amount of 4X SDS protein sample buffer (40% glycerol, 240mM Tris-HCl pH 6.8, 8% SDS, 0.04% bromophenol blue, 15% beta-mercaptoethanol) was incubated at 95°C for 5 minutes before loading onto an acrylamide gel.

In-plate cell lysates were prepared by direct application of 200µL/well 4X SDS protein sample buffer followed by cell scraping. Samples were then sonicated for 3x 10s using the Soniprep 150 (MSE Sanyo) and incubated at 95°C for 5 minutes on a heatblock (Grant BT3). 40µL of lysate was loaded per well.

Protein samples were resolved on 10% acrylamide gels for 2 hours at 110V with 10µl Precision Plus Kaleidoscope Prestained Protein Standards (BioRad). Proteins were transferred onto PVDF Immobilon P membranes (Merck Millipore) for 1 hour at 100V, with ice-pack. The membrane was blocked for 1 hour in 5% milk-TBS at room temperature before primary antibody was applied in 1% milk-TBS overnight at 4°C. After overnight incubation the membrane was washed 3x 5 minutes in TBS-Tween and secondary antibody applied; either anti-mouse or anti-rabbit HRP, at 1:10,000 in 1% milk-TBS. The membrane was washed 3x 5 minutes in TBS-Tween and then developed, using BM Chemi-luminescence Western Blotting Substrate (POD)(Roche), and viewed on the GeneGnome XRQ (Syngene). For all primary and secondary antibodies used, see **Table 9.**

Target	Species	Dilution Used	Code	Company
Nrf2	Rabbit polyclonal	1:500^{WB}/1:100^{IF}	ab137550	Abcam
Keap1	Mouse monoclonal	1;500	ab119403	Abcam
Keap1 (IF)	Rabbit monoclonal	1:100	D6B12 #8047	Cell Signalling Technologies
Phospho-SAPK/JNK (Thr183/Tyr185)	Rabbit monoclonal	1:500	81E11, #4668	Cell Signalling Technologies
SAPK/JNK	Rabbit monoclonal	1:500	#9252	Cell Signalling Technologies
Phospho-cJun (Ser63)	Rabbit monoclonal	1:500	54B3, #2361	Cell Signalling Technologies
Phospho-cJun (Ser73) (IF)	Rabbit monoclonal	1:100	#9164	Cell Signalling Technologies
cJun	Rabbit monoclonal	1:500	60A8, #9165	Cell Signalling Technologies
Cleaved Notch1 (Val1744)	Rabbit monoclonal	1:500	D3B8 #4147	Cell Signalling Technologies
NOTCH1	Rabbit polyclonal	1:500^{WB}/1:100^{IF}	ab27526	Abcam
NF-kB (p65)	Rabbit monoclonal	1:500	D14E12 #8242	Cell Signalling Technologies
NF-kB (p65) (IF)	Rabbit monoclonal	1:400	D14E12 #8242	Cell Signalling Technologies
IkBα	Rabbit monoclonal	1:500	[E130] ab32518-100	Abcam
Phospho-IkBα (Ser32)	Rabbit monoclonal	1:500	14D4 #2859	Cell Signalling Technologies
CD49b-FITC (IF)	Mouse polyclonal	1:800	MCA743F	Serotec
NIK	Rabbit polyclonal	1:500	#4994	Cell Signalling Technologies
Actin	Rabbit monoclonal	1:10,000	04-1040, clone EP184E	Merck-Millipore
GAPDH	Rabbit polyclonal	1:10,000	ab9485	Abcam
Anti-Mouse HRP	Goat	1:10,000	115-035-003	Affinipure
Anti-Rabbit HRP	Goat	1:10,000	7074P2	Cell Signalling Technologies
Anti-Rabbit AlexaFluor 568 (IF)	Goat	1:1000	A11036	Life Technologies
Anti-Mouse AlexaFluor 568 (IF)	Goat	1:1000	A11031	Invitrogen

TABLE 9 – Antibodies used in study.

IF – Immunofluorescence, WB – Western blot. Antibodies that have no notation after their name were used in western blotting experiments.

Densitometry Analysis

All western blot images were edited on GIMP 2.8 (GNU Image Manipulation Program) prior to densitometry analysis. In GIMP, the image colour output levels were reduced to avoid saturating the image analyser in the next step. Densitometry acquisition was performed using Image Studio Lite 5.2 (Licor). Using the analysis tools, a box was drawn around the band and the box copied (to not allow for any change in area affecting densitometry analysis) and pasted to surround adjacent bands. The readout from the densitometry then allowed results to be analysed using Excel 2010 (Microsoft).

In Excel, house-keeping gene normalisation as a loading control formed the first step of analysis. The lowest densitometry score for a house-keeping band was used to normalise the other house-keeping gene bands (division of the band score by the lowest score) – so that the lowest score was 1 and the other bands scored ≥1. The other protein bands in the lane were then divided by this score, for example proteins in the same lane as the lowest house-keeping gene band densitometry scores went unchanged as they were just divided by 1. Treatment induced changes in the levels of protein were then determined by dividing the normalised score of treated densitometry by the normalised untreated densitometry. This allowed for absolute protein level changes to be calculated but not phosphorylation of cleavage events.

Phosphorylation events were calculated from the house-keeping normalised scores in the following equation;

$$\frac{\left[\frac{phosphoProtein_{Treated}}{phosphoProtein_{Untreated}}\right]}{\left[\frac{Total\ Protein_{Treated}}{Total\ Protein_{Untreated}}\right]}$$

This allowed for changes in the total level of the protein to be taken into account as this could affect the level of phosphorylation seen by Western Blot. The same equation was applied to calculate Notch activation – here cleaved protein substituted phosphoprotein.

Statistical Analysis of Data

All analyses were performed using the statistical analysis platform on Prism 7 (GraphPad). Unpaired t tests (one-tailed) were performed on biological triplicate measurements of epithelial subpopulation gene expression data. All statistical tests, error bar parameters and biological repeats (n values) are included in the figure or figure legend.

Genomic DNA extraction

Genomic DNA was extracted from frozen cell pellets using the Qiagen DNeasy Blood and Tissue Kit protocol for cultured cells, detailed below.

Cell pellets were allowed to thaw on ice. Pellets were loosened by gentle flicking of the tube. 220µl of a solution constituted by 200µl PBS and 20µl Proteinase K (20mg/ml)(Qiagen) was used to break up the pellet – mixed using the pipette. 4µl of RNase A (100mg/ml) (Sigma) was added and each sample incubated at room temperature for 2 minutes. 200µl of ATL buffer was applied and mixed by pipette until the solution was homogeneous. The sample was then incubated at 56^{o}C for 10 minutes in a water bath. 200µl of ethanol (96-100%) was then added and again mixed to a homogeneous solution before being transferred to the DNeasy Mini spin column in a 2ml collection tube. The sample was then centrifuged in the Accuspin Micro microcentrifuge (Fisher Scientific) at 8000rpm for 1 minute with flow-through and collection tube discarded after the spin. The column was then placed into a new collection tube and 500µl of AW1 buffer was added before being centrifuged again for 1 minute at 8000rpm. Flow-through and collection tube were discarded again and the column placed in a fresh collection tube. 500µl of AW2 buffer was added and the sample centrifuged for 3 minutes at 13,000rpm. Again both flow-through and collection tube were discarded and the column placed in a 1.5ml Eppendorf tube. 50µl of PCR quality water (Sigma) was pipetted directly onto the membrane in the column and allowed to stand for 1 minute. The sample was then centrifuged for 1 minute at 8000rpm. The elution step was repeated so that genomic DNA was in a final total volume of 100µl – sample concentration was determined on the Nanodrop ND-1000 (Labtech) and gDNA stored at -20^{o}C.

Polymerase Chain Reaction

PCR product was amplified using two different polymerase systems, GoTaq Flexi G2 (Promega) and Phusion (NEB). All reactions were performed in the GeneAmp PCR System 9700 thermal cycler (Applied Biosystems). Reactions had 50ng total of gDNA or cDNA as template material (typically as 5µl at 10ng/µl). For negative reactions (no template controls) this was replaced by 5µl of PCR quality water (Sigma Aldrich). Before separation, products were combined with 6X Purple Loading Dye (NEB). Products were separated on a 1-3% agarose 1X TAE gel containing 1:20,000 GelRed Nucleic Acid Gel Stain (Biotium) alongside, unless stated, Quick-Load Purple 2log DNA Ladder (NEB). Gels were immersed in 1X TAE buffer and electrophoresed for 90 minutes at 90V, unless stated. Products were visualised under UV using the PXi Touch (Syngene).

GoTaq Flexi G2

All reagents marked with (*) are supplied in kit from Promega and reactions carried out as per manufacturer's instructions.

The MM was made up on ice in the Mini V/PCR hood (Telstar). For a single PCR tube; 10µl 5X Clear Flexi Buffer*, 6µl $MgCl_2$* (25mM), 2µl dNTP mix (10mM) (Invitrogen), 1µl forward primer, 1µl

reverse primer, 0.5µl GoTaq G2 Polymerase*, 26.5µl PCR quality water (Sigma). 45µl of the MM was added to 0.2ml PCR tubes followed by 5µl of DNA (10ng/µl).

The reactions were added to the thermocycler and ran; 94°C – 2 minutes, 35 cycles [94°C – 30 sec, (variable annealing temperature, see **Table 10**)– 30 sec, 72°C – 30 sec], 72°C – 5 minutes, 4°C – hold.

Phusion

All reagents marked with (*) are supplied in kit from NEB and reactions carried out as per manufacturer's instructions.

Phusion requires two MMs, both of which were made up on ice in the Mini V/PCR hood (Telstar). For a single PCR tube, MM1 contained; 28.75µl PCR quality water (Sigma), 1µl dNTP mix* (10mM), 2.5µl forward primer and 2.5µl reverse primer. 34.25µl of MM1 was added to the tubes in hood. MM2 was then made up of 0.25µl Phusion Polymerase* and 10µl HF Buffer*.

Tubes were taken out of the hood and 50ng of DNA was added to each sample on bench. The thermocycler was heated to 98°C and then paused before 10.25µl of MM2 was added to each tube and mixed. The reaction was placed directly into the thermocycler on the following program; 98°C – 30 sec, 35 cycles [98°C – 10 sec, (variable annealing temperature)– 30 sec, 72°C – 20 sec], 72°C – 5 minutes, 4°C – hold.

Target	Primer Sequence	Annealing Temperature (^{O}C)	Product Size (bp)	Template material
SPOP exon 6 & 7	FP: TTCTATGGGGCCTGCATTT	62 (Phusion)	429	gDNA
	RP: CTCCACTTGGGGCTTTTTCT			
IDH1 exon 6	FP: ATATTCTGGGTGGCACGGTC	62 (Phusion)	456	gDNA
	RP: TGCAGCCAGTGTTGAAAACC			
PTEN exon 5	FP: ACCTGTTAAGTTTGTATGCAAC	56 (Phusion)	385	gDNA
	RP: TCCAGGAAGAGGAAAGGAAA			
PTEN intron 8	FP: CATTCTTCATACCAGGACCAG	60 (GoTaq)	354	gDNA
	RP: TCATGTTACTGCTACGTAAAC			
TMPRSS2 exon 6	FP: CTGTTACTGTCACTCGGCGG	60 (GoTaq)	174	gDNA
	RP: CTCGTGCAGTTCGCCTCTAC			
TMPRSS2-ERG Outer	FP: CGCGAGCTAAGCAGGAGGC	70 (Phusion)	Variable	cDNA
	RP: GGCGTTGTAGCTGGGGGTGAG			
TMPRSS2-ERG Inner	FP: GGAGCGCCGCCTGGAG	71 (Phusion)	Variable	cDNA
	RP: CCATATTCTTTCACCGCCCACTCC			
GAPDH	FP: GCTCTCTGCTCCTCCTGTTC	63 (Phusion)	357	cDNA
	RP: AAATGAGCCCCAGCCTTCTC			

TABLE 10 – PCR information

FP – forward primer, RP – reverse primer, bp – base pairs.

PCR Product Purification

PCR products were purified for sequencing using an on-column method, extraction from gel fragments or DNA precipitation. Standard on-column purification was used for bulk PCR reactions. Gel extraction was used to separate unknown DNA fragments for sequencing and BLAST identification. DNA precipitation was used as an alternate method to on-column purification to confirm PCR product sequences.

On-column Purification

All reagents marked with (*) are supplied in the QIAquick PCR Purfication kit (Qiagen) and the purification carried out as per manufacturer's instructions. 200µl of Buffer PB* was added to the 40µl of remaining PCR product (10µl had been previously ran on a gel) and mixed by pipette. If the colour of the solution had turned from the yellow of Buffer PB* to an orange or violet then 10µl of 3M sodium acetate (pH 5.0) was added and mixed by pipette. The solution was then transferred to a QIAquick column* in 2ml collection tube and centrifuged at 13,000rpm for 1 minute in the Accuspin Micro microcentrifuge (Fisher Scientific). Flow-through was discarded and 750µl Buffer PE* applied to the column. The column was centrifuged at 13,000rpm for 1 minute and flow-through discarded. The tube was then centrifuged again for 1 minute at 13,000rpm to remove any residual buffer. The collection tube was discarded and the column placed in a clean 1.5ml tube. 30µl of PCR quality water (Sigma) was added to the membrane of the column and left to stand for 1 minute before being centrifuged at 13,000rpm. The elution step was repeated, making the final volume of gDNA; 60µl. The sample concentrations were measured on the Nanodrop ND-1000 (Labtech) and then stored at -20^{o}C.

Gel Extraction

All reagents marked with (*) are supplied in the QIAquick Gel Extraction kit (Qiagen) and the purification carried out as per manufacturer's instructions. The entire PCR reaction was loaded onto a 1% agarose TAE gel with 1:10,000 SYBRsafe DNA gel stain (Invitrogen) and ran at 90V for 90 minutes. Following this the gel was placed on the Safe Imager^{TM} (Invitrogen) and the band of interest excised using a scalpel. The gel fragment was then placed in a colourless 1.5ml tube and weighed on the Sartorius LE244S balance. 3 volumes of Buffer QG* was added to the single volume of gel, where 100mg of gel is a single volume of 100µl QG*. The gel in buffer was then incubated at 50^{o}C in a heatblock (Grant BT3) for 10 minutes and the tube vortexed briefly every 3 minutes to aid the dissolving of the gel fragment. If the colour of the solution had turned from the yellow of Buffer QG* to an orange or violet then 10µl of 3M sodium acetate (pH 5.0) was added and mixed by pipette. A single gel volume of isopropanol was then added to the solution and mixed. The gel solution was then transferred to the QIAquick spin column* in a 2ml collection

tube and centrifuged for 1 minute at 13,000rpm in the Accuspin Micro microcentrifuge (Fisher Scientific). 500µl of Buffer QG* was added to the column which was then centrifuged at 13,000rpm for 1 minute. Flow-through was discarded and 750µl Buffer PE* applied to the column which was centrifuged again at 13,000rpm for 1 minute. Flow-through was discarded and the column centrifuged at 13,000rpm to remove residual buffer from the membrane. The collection tube was discarded and the column placed in a 1.5ml tube. 30µl of PCR quality water (Sigma) was added to the membrane of the column and left to stand for 1 minute before being centrifuged at 13,000rpm. The elution step was repeated, making the final volume of gDNA; 60µl. The samples concentration was measured on the Nanodrop ND-1000 (Labtech) and then stored at -20^{o}C.

DNA Precipitation

Protocol adapted from **Collas 2011 (741)**.

400µl of PCR quality water (Sigma) was added to the 50µl PCR reaction in a 2ml tube. 44µl of sodium acetate (3M, pH5.2), 5µl linear acrylamide carrier (Ambion) and 1ml of 96% ethanol at -20^{o}C was added to the DNA and the solution mixed thoroughly. The tube was then incubated at -80^{o}C overnight. The next day, the tube was thawed and centrifuged at 14,000rpm for 15 minutes at 4^{o}C in the Mikro 220R (Hettich). The supernatant was removed using a pipette and 1ml of 70% ethanol at -20^{o}C was added. The tube was, again, centrifuged at 14,000rpm for 15 minutes at 4^{o}C in the Mikro 220R (Hettich) and supernatant removed. The pellet was dried using the Concentrator 5301 (Eppendorf) at 30^{o}C for 10 minutes with brake on. The DNA pellet was dissolved in 30µl PCR quality water (Sigma) and the concentration measured on the Nanodrop ND-1000 (Labtech).

PCR Product Sequencing

PCR products were Sanger sequenced in the departmental technology facility by a staff member. Each reaction was submitted as 5µl at 5ng/µl – making 25ng of DNA in total – sequencing primer or forward primer was supplied at a concentration of 3.2µM - 1µl per reaction. Trace files were analysed using the MegAlign and SeqMan II analysis software (DNA Star).

3.3 - Low Temperature Plasma Treatments

Dielectric Barrier Discharge LTP Jet Setup and Cell Treatments

The LTP jet consisted of a quartz glass tube of inner/outer diameter 4/6mm, with two copper tape electrodes 20mm apart. One electrode was powered (6kV sinusoidal voltage at 30kHz) and the other grounded. Helium, the carrier gas, flowed at 2 standard litres per minute and was fed with 0.3% molecular oxygen admixture. 1-5x10^{5} cells were used for each treatment condition, cell number varied, dependent upon assay used. Cells were exposed to the LTP jet at a distance of

15mm from the end of the bottom electrode for 180s in 1.5ml centrifuge tubes, suspended in 1.5ml of respective media or directly in 6-well (cells in 2ml SCM) or 12-well (cells in 1ml SCM) plates (Corning or Sarstedt). The distance between the end of the glass tube and the media surface was ~2mm. Treatment times up to 600s did not raise the surface temperature of culture media above 36.5^{o}C, measured using a thermocouple. The temperature and relative humidity of the laboratory were ~20^{o}C and ~25% respectively.

RT^2-PCR Oxidative Stress Profiler Arrays

Oxidative stress arrays (Qiagen) are 96 well plates consisting of 84 wells containing gene-specific primers to transcripts responsive to oxidative stress, 5 wells for house-keeping genes (HPRT1, GAPDH, B2M, RPLP0, B-ACT) for relative fold change quantification, PCR control wells in triplicate, reverse transcription control wells in triplicate and a single genomic DNA contamination control well. 1µg of RNA (8µl of 125ng/µl) was used as input for reverse transcription to cDNA with the RT^2 First Strand Synthesis kit (Qiagen). The cDNA was combined with SYBR Safe Mastermix (Qiagen) and aliquoted across the array plate. All array plate qRT-PCR was performed using the C1000 Thermal Cycler and CFX96 Real-Time System (BioRad) under the RT^2 Array qRT-PCR protocol; 95^{o}C – 10 minutes, 39 cycles of 95^{o}C for 10s, 60^{o}C for 1 minute (Qiagen). Data was assimilated using the CFX Manager 2.0 (BioRad) and analysed using the Qiagen's online Data Analysis Center (http://www.qiagen.com/gb/shop/genes-and-pathways/data-analysis-center-overview-page/)**(742)**. Gene expression scatterplots generated in the software were of the Log_{10} $2^{-\Delta\Delta Ct}$ values plotted against each other (treated/untreated), upregulation was marked as ≥2 fold change in expression.

Clariom D Affymetrix Microarray

Microarray analysis was outsourced and performed by Eurofins on RNA harvested from six primary samples before (untreated) and 2 hours (treated) after LTP treatment.

Meta-analysis of All Samples Treated against Untreated

Initial microarray analysis was performed using the Transcriptome Analysis Console ver3 (Affymetrix) set up with the Clariom_D_Human.na36.hg38.probeset. All samples were grouped Untreated against Treated and that dataset was used for all subsequent analysis.

LIMMA (Linear Models for Microarray and RNA-seq Data), GO (Gene Ontology) enrichment and KEGG pathway analysis were performed by Dr Alistair Droop. LIMMA Analysis Pre-processed data were analysed using the LIMMA **(743)** within the R numerical environment **(744)**. Cell of origin and treatment type was modelled in the design matrix. Significant results after empirical Bayes

smoothing of the standard errors were extracted using a false discovery rate threshold of 0.025. No log fold change threshold was applied.

Results were also analysed using gene set enrichment. The topGO package **(745)** was used. GO testing was performed using the "weight01" algorithm with Fisher's statistics. A threshold of 0.05 was used to select significant results.

Pathway analysis was performed against the KEGG **(746)** pathways. Significant results from the LIMMA analysis were analysed with a p-value threshold of 0.05.

Immunofluorescence

Cultured primary cells were trypsinised into chamber slides. These were BioCoat Collagen I 8-well plates (Corning) – 10,000 cells per well, or 2-well Nunc Lab-Tek chamber slides (Sigma Aldrich) – 300,000 cells per well.

Cells were left overnight before being treated in-well by plasma. A plasma dose of 1.5-minutes was used for 8 well chamber slides and 3-minutes for 2 well chamber slides. Following treatment, cells were fixed at either 0.5 hours or 2 hours post-treatment using 4% PFA (Paraformaldehyde) - 100µl for 8 well and 500µl for 2 well. Wells were then washed 3x for 5 minutes in PBS (equivalent to the volume of PFA). Chamberslides were then stored at 4^{o}C with the equivalent volume of PBS in well or carried forward into permeabilisation.

Cells were permeabilised for 10 minutes in 0.5% Triton X-100 (Sigma) in PBS (at a volume equivalent to that used for PFA). Triton X-100 was tipped off and cells washed in PBS 3x 5 minutes. Cells were then blocked in 10% goat serum (Sigma) in PBS for 1 hour. Goat serum was then removed and primary antibody applied. See **Table 9** for more information. Primary antibody was diluted in 10% goat serum in PBS. The chamber slides were left in the fridge overnight (~16 hours) at 4^{o}C on orbital shaker (Stuart SSM3) at 50rpm.

After overnight incubation the primary antibody **(Table 9)** was removed and cells washed 3x 5 minutes in PBS. The secondary Alexafluor 568 antibody **(Table 9)** diluted in 10% goat serum was then applied for 1 hour at room temperature. This incubation step was performed beneath a plastic box lid to prevent loss of Alexafluor signal. Secondary antibody was removed and cells washed 3x 5 minutes in PBS.

The chamber of the slides was now removed. For the BioCoat 8-well slides, the tool accompanying the slides was used, for the 2 well Nunc Lab-Tek slides the chamber was lifted off and the adhesive removed using forceps. 4 drops of Vectashield with DAPI (Vector, H-1200) was applied to the slide and a coverslip added on top. Excess Vectashield was wiped away and any air bubbles were removed before being sealed with nail varnish and left to dry for 15 minutes in the dark.

Slides were either stored at 4^{o}C in the dark or imaged immediately on the DM IL LED Microscope (Leica) with the DFC365 FX Camera (Leica), equipped with DAPI and Cy3 filter blocks. Images were viewed and stored using the LAS X program (Leica).

SmartFlares

SmartFlares were prepared from lyophilised stock by addition of 50µl Nuclease Free Water (Merck-Millipore). This was mixed by pipette and then vortexed to assure that there was no biphasic separation of the probes. The SmartFlares were then stored at room temperature away from light.

SmartFlare (Merck Millipore) experiments were attempted in two variations, with treatment before and following SmartFlare addition. SmartFlares used in the experiment were; Uptake-Cy3, Scrambled-Cy5 and HMOX1-Cy3 (discontinued).

LTP Treatment Before Application of SmartFlares

5x10^{5} cells suspended in 1.5ml growth media were treated with LTP. The cells were then added to a 48 well plate - 40,000 cells per well in 500µl media. SmartFlares were diluted 1:20 in PBS and 4µl added to each well. Plates were monitored and pictures taken 24 hours after addition of SmartFlare on DM IL LED Microscope (Leica) with the DFC365 FX Camera (Leica). Images were viewed and stored using the LAS X program (Leica).

LTP Treatment After Application of SmartFlares

100,000 cells were aliquoted across a 24 well plate and left to adhere for 6 hours in 1ml of media. SmartFlares were diluted 1:20 in PBS and 10µl added to each well. Cells were then treated with the appropriate plasma dose and pictures taken 24 hours after LTP treatment with the DM IL LED Microscope (Leica) uing the DFC365 FX Camera (Leica). Images were viewed and stored on the LAS X program (Leica).

Arsenite Treatments of Cell Lines

Sodium meta-arsenite 0.05M (Merck Millipore) was diluted to the appropriate concentration in K2 or R10 medium directly before treatment. Cells were exposed to arsenite-containing media for the allotted time, up until harvesting. Following treatment, cells were washed twice with PBS to maximise the removal of arsenite and pelleted.

3.4 - Allelic Expression Experiments

SURVEYOR

The SURVEYOR system detects mutation or SNPs by first forming heteroduplexes of wildtype and variant strands before the SURVEYOR nuclease is added. This enzyme can recognise regions of mismatch or ≤12bp indels and upon recognition; cleaves the duplex. This allows the fragments to then be separated by gel electrophoresis. Reagents marked with a (*) were supplied in the Integrated DNA Technologies kit.

Each reaction contained; 200-300ng purified PCR product (>10ng/µl), 2µl 0.5M KCl and PCR quality water (Sigma) to a final consistent volume between 20-30µl. The reactions were placed in a thermocycler (Applied Biosystems) on the following program to allow for heteroduplex formation; 95°C – 10 minutes, 85°C – 1 minute, 75°C – 1 minute, 65°C – 1 minute, 55°C – 1 minute, 45°C – 1 minute, 35°C – 1 minute, 25°C – 1 minute, 4°C – hold.

SURVEYOR nuclease was then added to these reactions in the following MM. For one reaction; 2.5µl 0.15M $MgCl_2$*, 1µl SURVEYOR nuclease*, 1µl ENHANCER*. 4.5µl was added to each reaction, mixed by pipette and incubated at 42°C for 1 hour in a thermocycler (Applied Biosystems). After incubation 2.5µl of STOP solution* was added.

The entire reaction was then loaded onto a 2% agarose 1X TAE gel with 1:20,000 GelRed and electrophoresed at 80V for 100 minutes. Bands were visualised under UV on the PXi Touch (Syngene)

PTEN Intron 8 LOH HincII Restriction Digests

The solution used for restriction digest was constituted of; 0.4µl of HincII (NEB), 2.5µl 3.1 restriction buffer (NEB) and 17.1µl of PCR quality water (Sigma). Following PCR of the intronic region, 20µl of HincII MM was added to 30µl of un-purified PCR product. Reactions were incubated at 37°C for 30 minutes and then at 65°C for 25 minutes in separate water baths. Reactions were combined with 10µl of 6X DNA loading dye and then 20µl loaded onto a 3% agarose 1X TAE gel alongside 10µl of undigested PCR product. Gels were ran at 100V for 1 hour and products visualised on the PXi Touch (Syngene).

4. Results – Determination if common tumourigenic alterations to genes in prostate cancers alters their allelic expression

Large scale genome sequencing studies often assume mutations to be expressed. Yet evidence of said expression is rarely provided through use of matched transcriptomic or proteomic data. **(330, 497)** This assumption is naïve in the common knowledge that many pre- and post-transcriptional mechanisms exist in cells, above the level of genetic alterations, that can significantly impact final and functional protein expression (or lack thereof) which affects the cancer phenotype. These include epigenetic modifications, which can promote or silence transcription, and nonsense mediated decay; that acts as a mRNA quality control mechanism. Most mutations and chromosomal alterations are heterozygous and cells retain a functional wildtype allele that, unless levels of the protein are critical and haploinsufficiency results, should be able to rescue the usual loss-of-function effects that such genomic alterations result in. Changes in the expression of disease or wildtype alleles therefore may have measurable molecular and cell fate outcomes in prostate cancer. The flowcharts, provided in **Figures 28 & 34**, show the plan of study progression in determining the effects on allelic expression made by gene alterations in prostate cancer.

4.1 – Heterozygosity in TMPRSS2 is common in primary prostate epithelial cultures

TMPRSS2 is monoallelically expressed in human tissues, including that of the prostate **(246, 518)**. The prostate cancer unique TMPRSS2-ERG fusion is also selectively expressed at an allelic level in CSCs **(246)**. To reproduce previous work, and show monoallelic expression in primary prostate cultures, heterozygosity had to be established so that the expression of each TMPRSS2 allele could be measured. Patient culture information on TMPRSS2 heterozygotes from previous work was compiled in **Table 11**. This data allowed for the selection of known heterozygous primary samples alongside the testing of recently harvested genomic DNA stocks for heterozygosity at SNP rs12329760, located in exon 6 of the TMPRSS2 gene **(Figure 29A)**. In total, thirty-six primary cultures (from thirty-four patients) were tested and nine rs12329760 heterozygotes were identified, at a minor allele frequency (MAF) of 0.125 (9/72) half of the expected global MAF 0.25 **(Figure 29B + 30)**. Sequence traces for all samples can be found in the **Appendix – 9.1**. From these findings, fourteen patient samples were grown from liquid nitrogen stocks and the cultures subsequently fractionated into epithelial subpopulations **(Figure 31)** where RNA, genomic DNA (gDNA) and chromatin were harvested. After this, the rs12329760 state of the freshly grown samples was confirmed by PCR **(Figure 32A)** and Sanger sequencing of the product **(Figure 32B)**. The second round of sequencing identified that YO47/09 and H329/13 LB were not A (minor allele) homozygotes, as was previously identified.

4.2 – The TMPRSS2-ERG fusion is expressed in primary prostate epithelial cultures

The advantage of fusion positive samples is that monoallelic expression can be established by RT-PCR. The fused and unfused TMPRSS2 alleles are inequivalent therefore expression of both can be assessed independently. Analysis of fusion expression in the primary cultures was achieved using a nested RT-PCR method (previously developed by **Polson 2013 (246)**) where outer and inner forward primers were located in TMPRSS2 exon 1 and the reverse primers in ERG exon 6, allowing for the amplification of all major fusion mRNA products **(596)**. Product from PCR 1, using the outer primers, was immediately entered into PCR 2, using the inner primers, to achieve specificity and minimise off target amplification of any other cDNAs **(Figure 33A)**. The strategy was confirmed to work using VCaP, a prostate cancer cell line with a confirmed TMPRSS2-ERG fusion, **(351)** to produce a PCR product that was identified as fusion mRNA by BLAST **(Figure 33B)**. A total of seventeen patients, with various whole population and subpopulation cultures, were tested for presence of the fusion. Three patient prostate cancer cultures; H434/14 RM, H116/11 RA and H050/11 RA, were TMPRSS2-ERG^{+} **(Figure 33C)**. Assessment of the unfused TMPRSS2 allele in the TMPRSS2-ERG^{+} cultures wasn't carried out at this stage as the cellular heterogeneity present in the primary cultures would prevent determination of monoallelic fusion transcript expression **(246)**.

From the combined work on TMPRSS2 heterozygosity and fusion status of the primary samples, twelve cultures were fractionated into epithelial subpopulations, and RNA, gDNA and chromatin were collected **(Table 12)**. These samples were to be analysed for allelic asymmetry in TMPRSS2 expression and promoter/gene body histone trimethylations.

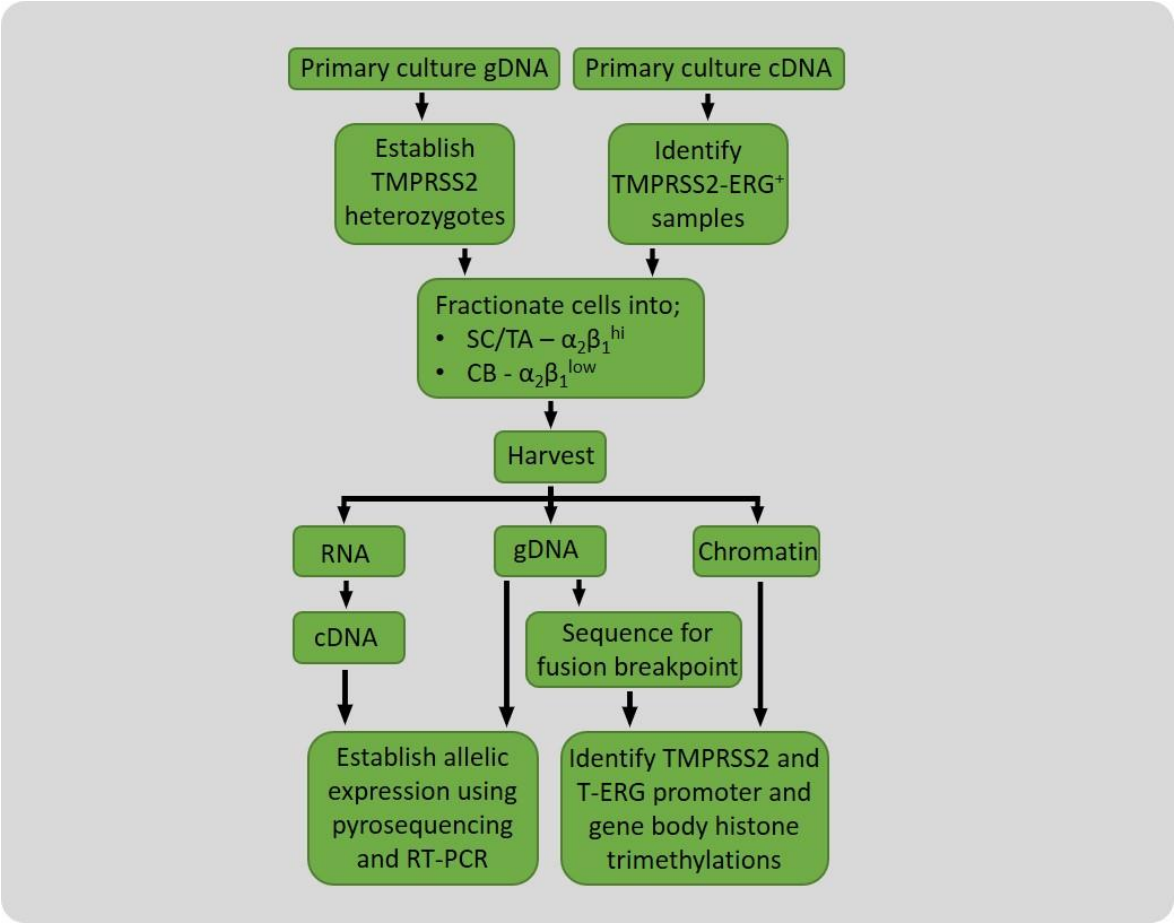

FIGURE 28 – Allelic expression of TMPRSS2 study structure and the primary cultures assessed for heterozygosity of the gene.

Flowchart detailing the workflow for the determination of allelic expression and assessment of the factors governing the expression of TMPRSS2 in primary prostate basal epithelial cultures.

Patient	Pathology	SNP rs12329760
Y023/09	BPH	G
Y006/09	BPH	G/A
Y012/09	BPH	G
Y013/09	BPH	G
Y025/09	BPH	G/A
YO29/09	BPH	G
YO30/09	BPH	G
YO40/10	BPH	G/A
YO47/09	BPH	A
YO26/09	BPH	G
PE667	Gleason 6 (3+3)	G
YO08/06	Gleason 6 (3+3)	G/A
H016/09	Gleason 7	G
PE665	Gleason 7 (3+4)	G/A
PE671	Gleason 7 (3+4)	G
PE659	Gleason 8 (4+4)	G
PE434	Gleason 8/9	G
YO46/09	CRPC	G
YO11/09	Gleason 8 (3+5)	G
YO21/09	Gleason 9 (4+5)	G

TABLE 11 – Primary samples with known rs12329760 status.

Data was compiled from **(Polson 2013) (246)** and lab books.

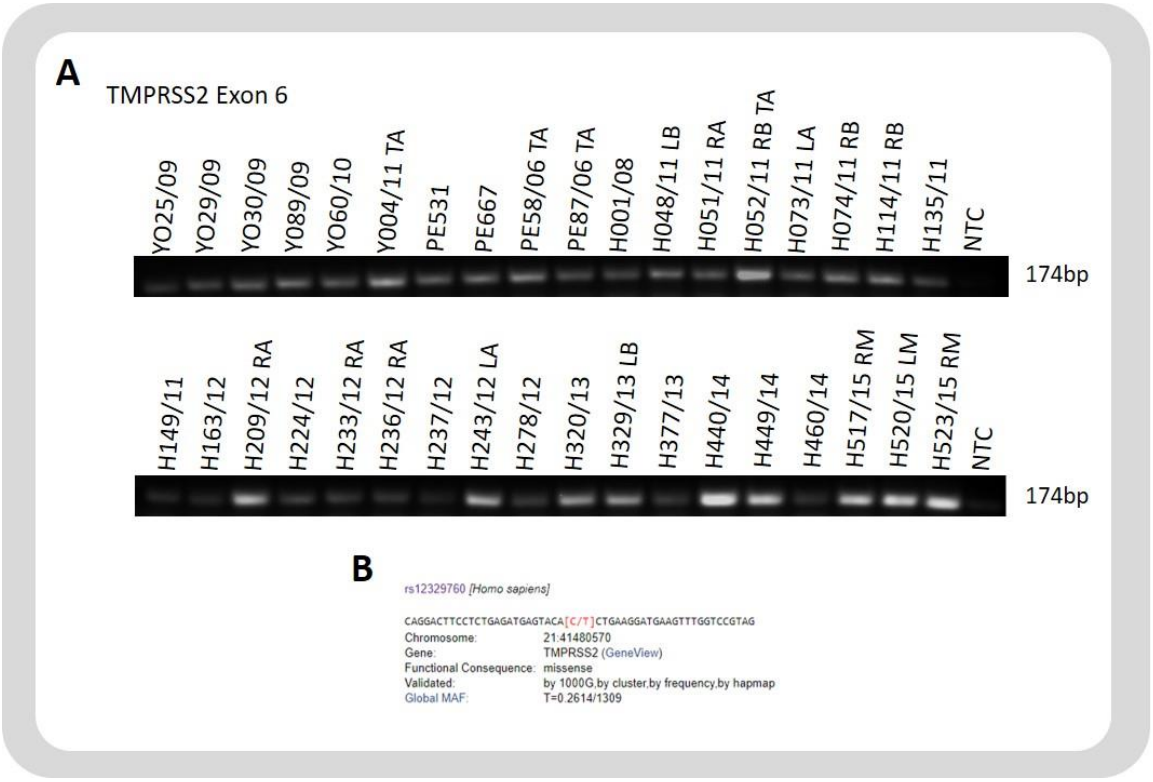

FIGURE 29 – Analysis of TMPRSS2 exon 6 DNA from primary prostate cultures for the SNP rs12329760.

A) TMPRSS2 exon 6 PCR products from primary prostate epithelial cultures. **B)** The coding SNP - rs12329760 C/T. Taken from the NCBI SNP database **(747)**.

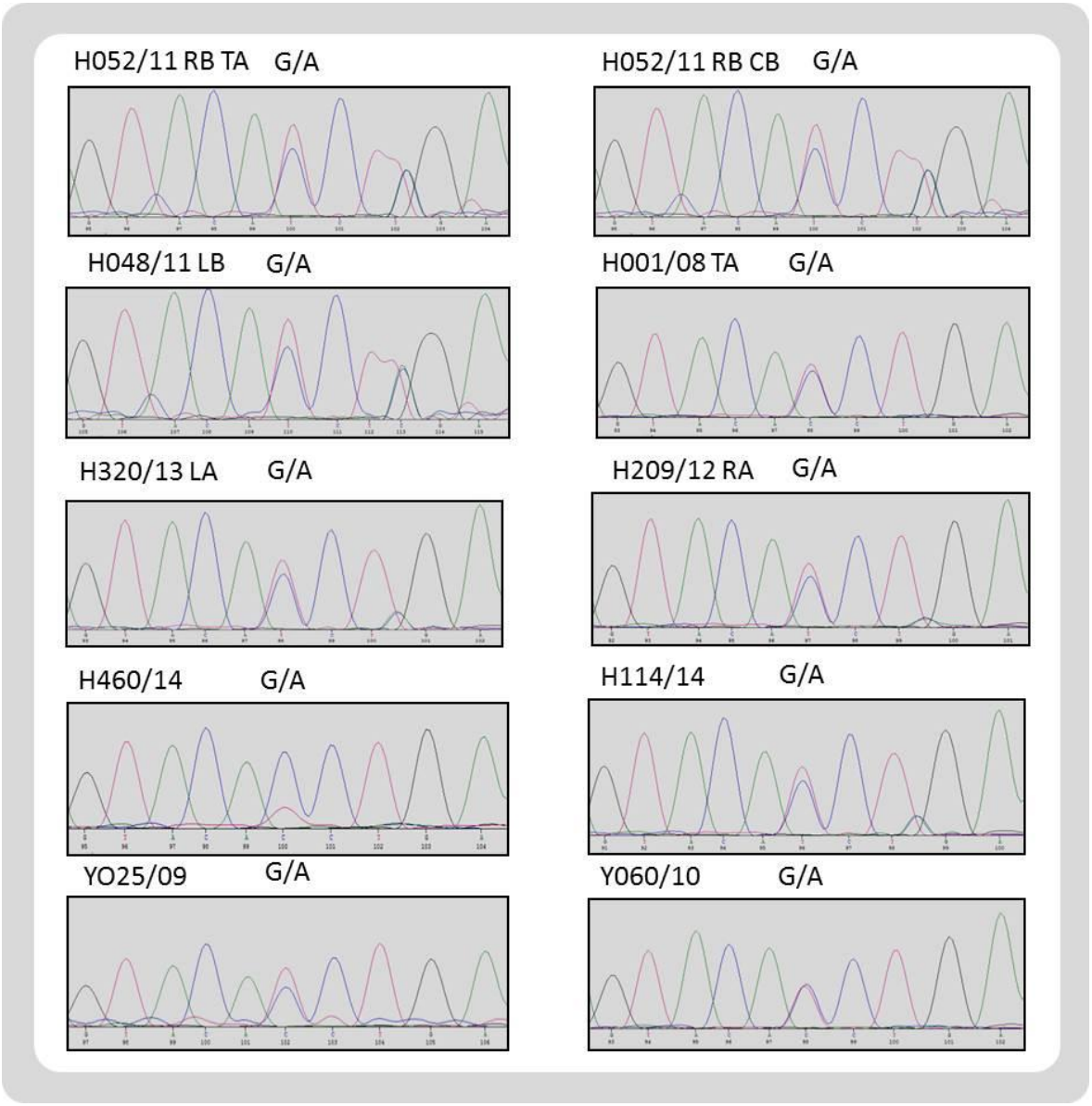

FIGURE 30 - Sanger sequencing traces of rs12329760 heterozygotes in TMPRSS2 exon 6 of primary cultures.

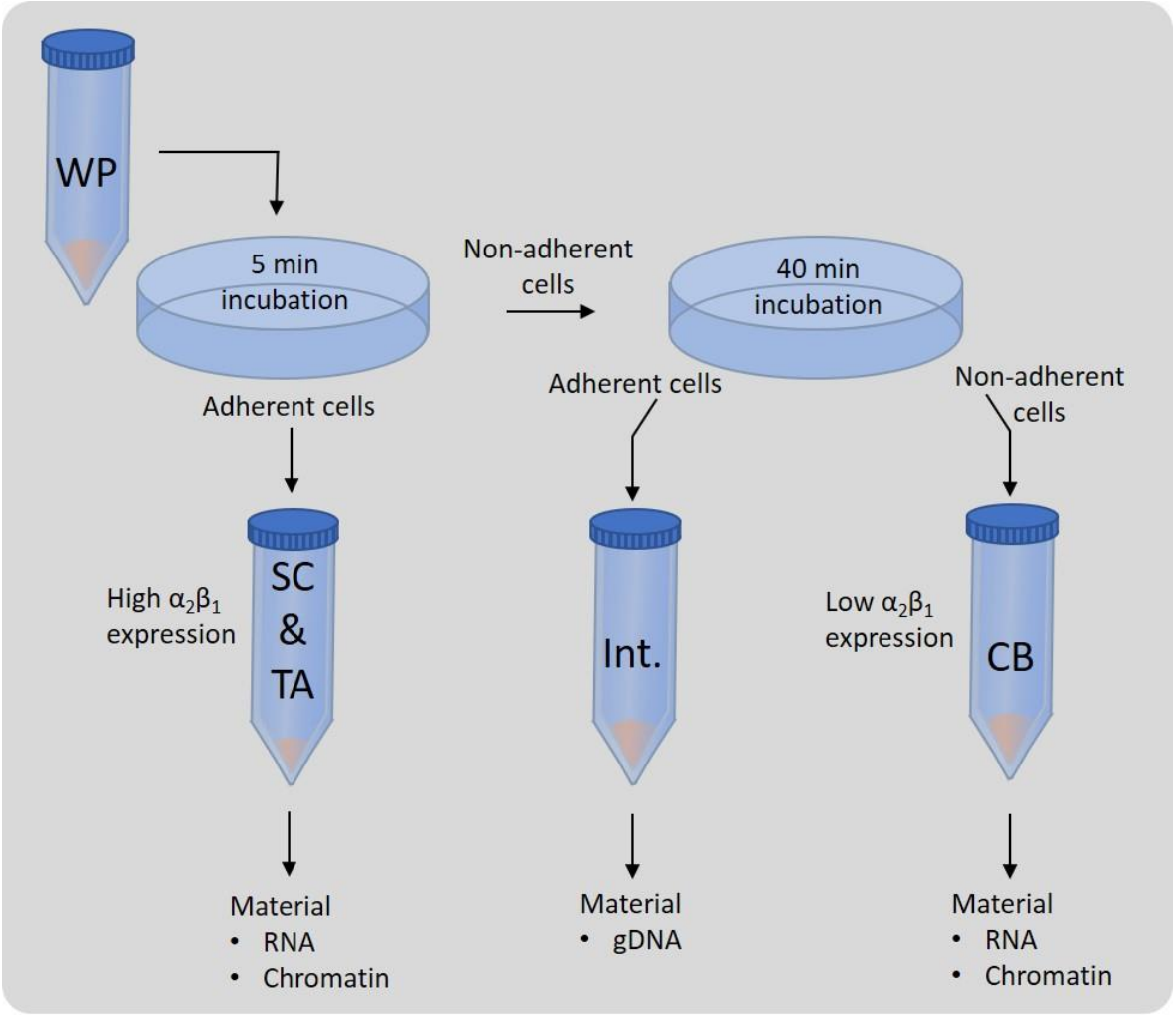

FIGURE 31 – Selection of prostate basal epithelial subpopulations by collagen I adhesion.

Diagrammatic representation of whole population (WP) primary culture fractionation protocol used to isolate; stem and transit amplifying (SC & TA), intermediate (Int.) and committed basal (CB) cell subpopulations in the TMPRSS2 allelic expression study.

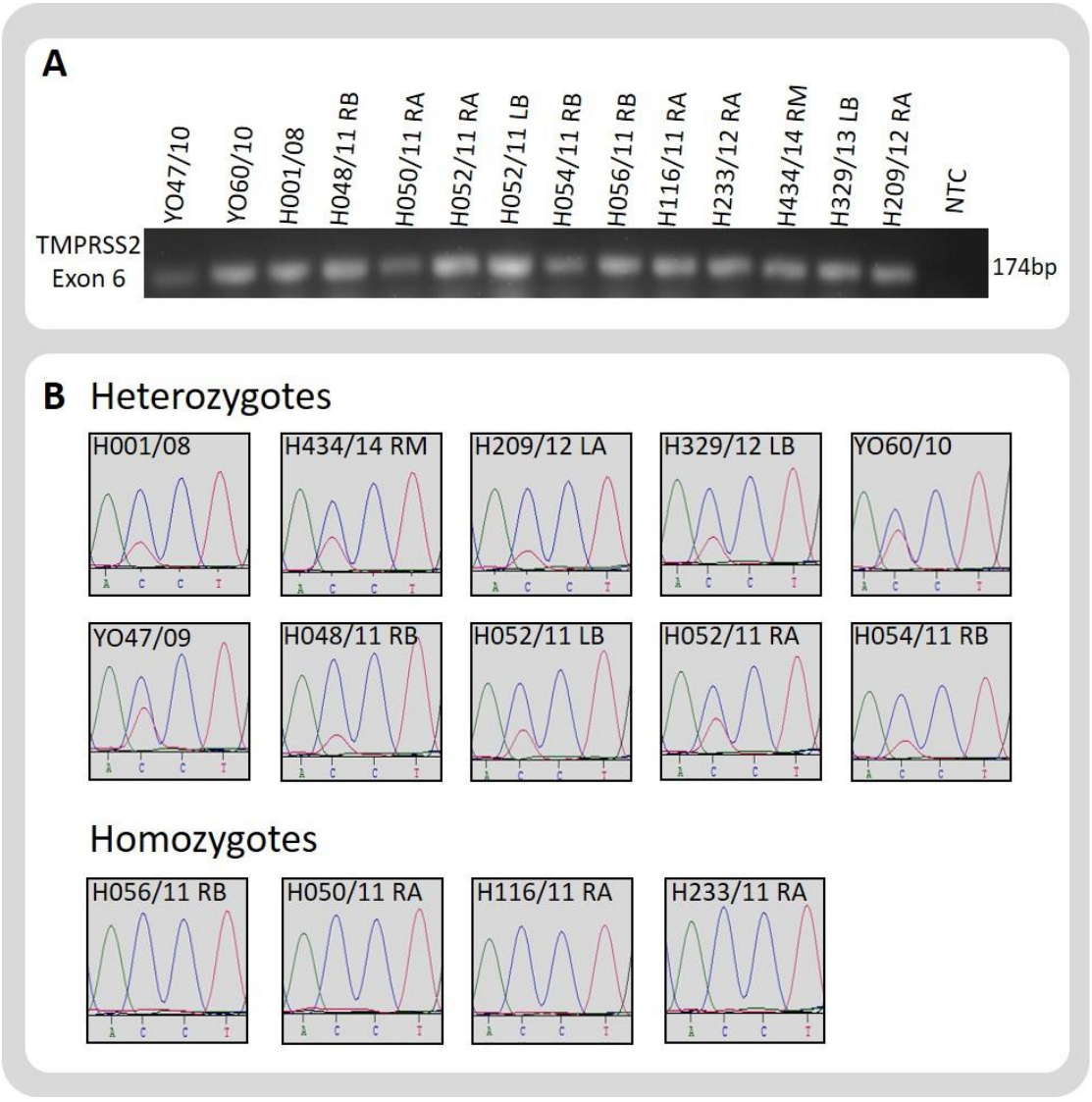

FIGURE 32 – Confirmation of rs12329760 SNP status in fractionated primary culture samples.

A) PCR products of TMPRSS2 exon 6 in chosen samples. **B)** Sanger sequence traces of rs12329760 in the fractionated samples, grouped as hetero- or homozygotes.

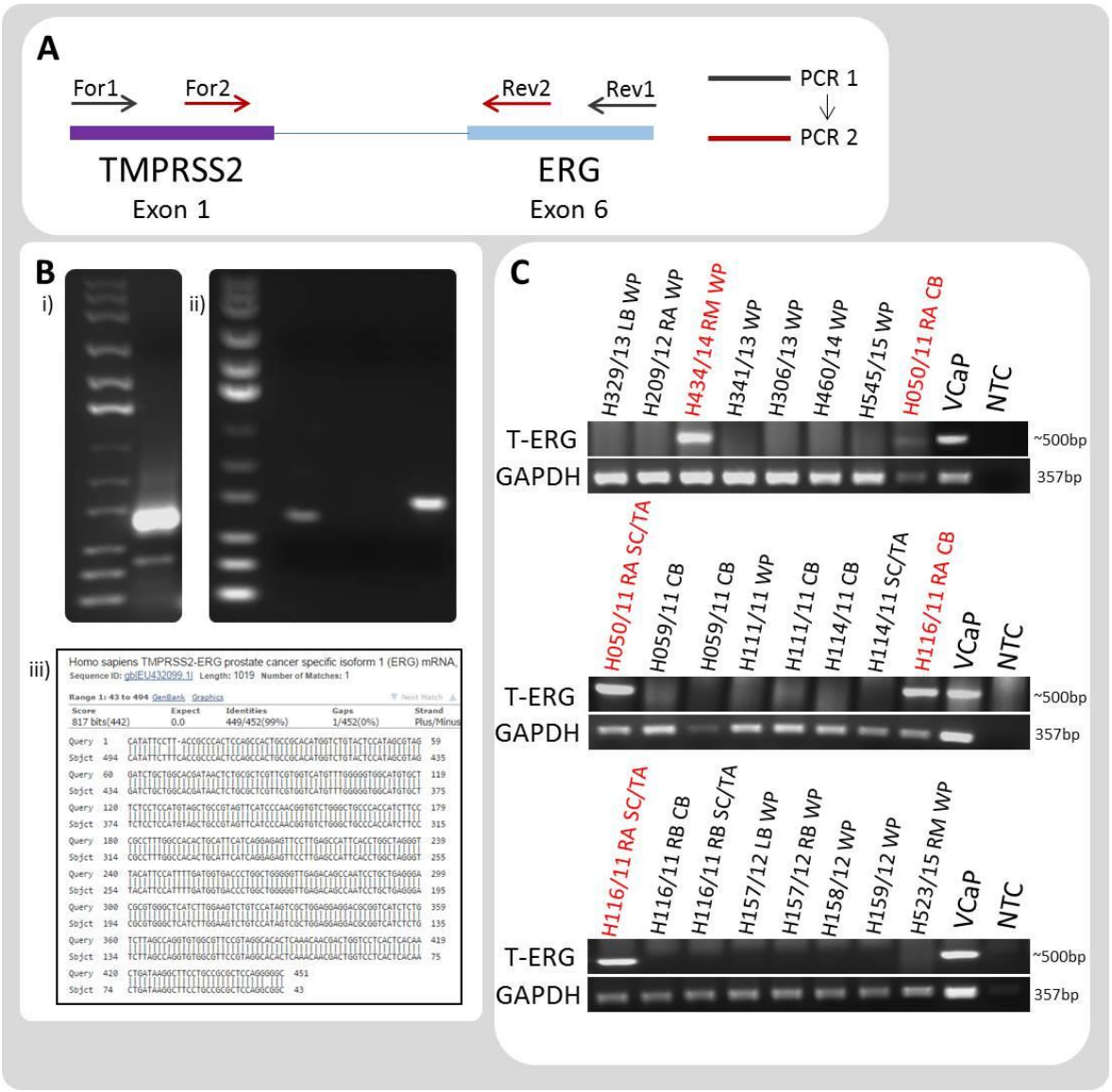

FIGURE 33 – Identification of TMPRSS2-ERG fusion expression in primary prostate cultures.

A) Nested PCR strategy for analysing TMPRSS2-ERG expression in primary sample cDNA. The analysis allowed detection of the most common fusion products; TMPRSS2 exon 1 to ERG exons 2, 4 and 5. **B)** i) VCaP TMPRSS2-ERG RT-PCR product amplified by the nested PCR strategy, ii) Small and large products isolated from the bright band in i. iii) Top BLAST result from the Sanger sequence consensus derived from both large and small products. **C)** TMPRSS2-ERG expression in primary prostate cultures.

Sample	Pathology	SNP rs12329760	Fusion status	Passage
H001/08	Gleason 6 (3+3)	G/A	-ve	3
H434/14 RM	Gleason 7 (4+3)	G/A	**+ve**	3
H209/12 LA	Normal	G/A	-ve	WP - RNA/gDNA
H329/13 LB	Gleason 7 (3+4)	G/A	-ve	WP - RNA/gDNA
Y047/09	BPH	G/A	-ve	5
H048/11 RB	Gleason 6 (3+3)	G/A	-ve	3
H052/11 LB	Gleason 7 (3+4)	G/A	**+ve**	2
H052/11 RA	Gleason 7 (3+4)	G/A	-ve	2
YO60/10	BPH	G/A	-ve	3
Y025/09	BPH	G/A	-ve	Didn't Grow
H054/11 RB	Gleason 7 (3+4)	G/A	-ve	3
H056/11 RB	Gleason 7 (4+3)	G	-ve	4
H050/11 RA	Gleason 7 (3+4)	G	**+ve**	3
H116/11 RA	Gleason 7 (4+3)	G	**+ve**	4
H233/12 RA	Gleason 8 (4+4)	G	-ve	3

TABLE 12 - Primary samples selected for further study of TMPRSS2 allelic expression in fractionated populations.

Samples were grouped on rs12329760 heterozygote status. TMPRSS2-ERG fusion status of samples is included. Passage number was that of the sample at harvest of RNA, gDNA and chromatin.

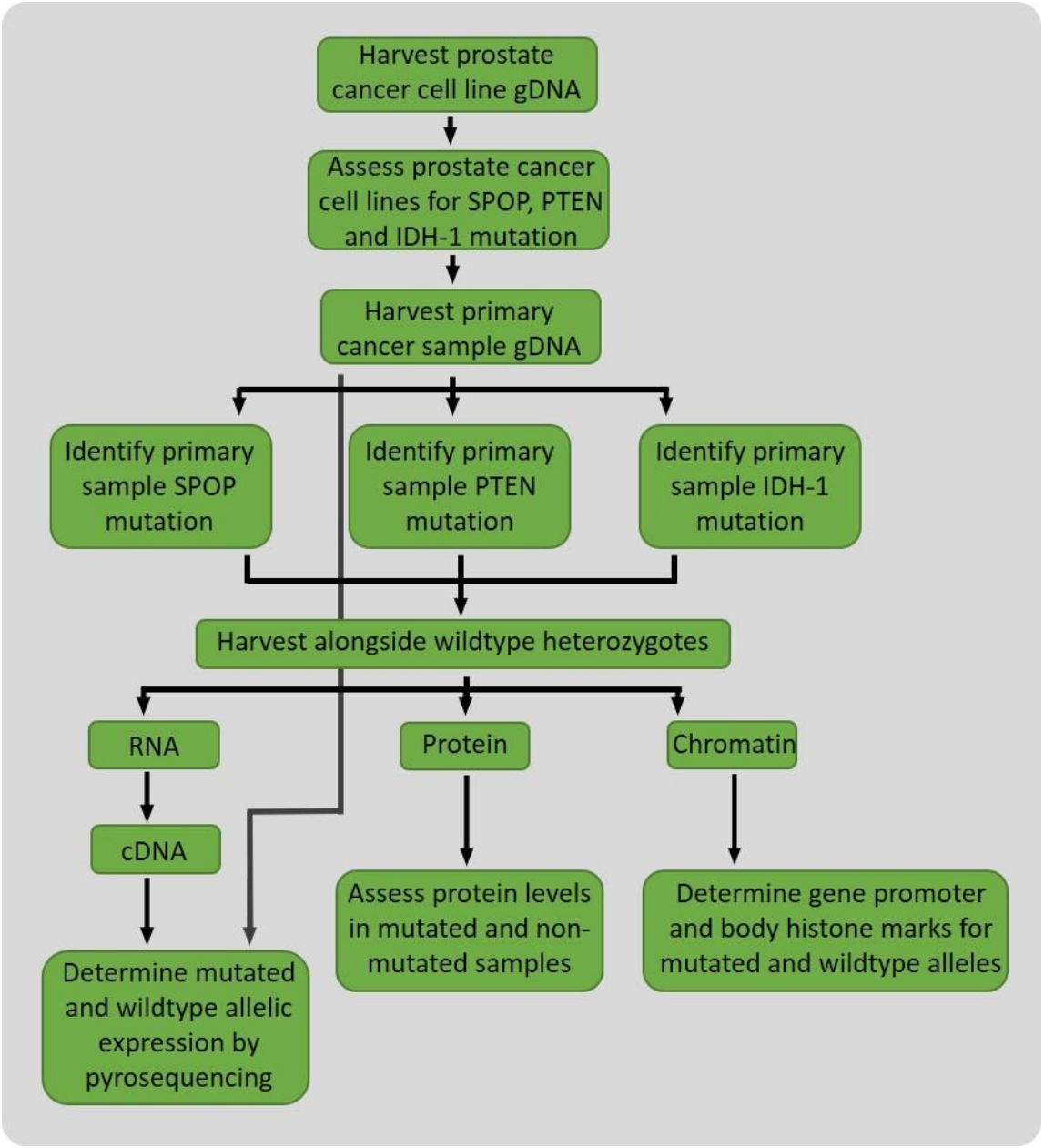

FIGURE 34 – Study plan - Does point mutation in prostate cancer genes affect allelic expression?

Flow chart of experiments to determine if and how mutation could affect allelic expression in prostate cancer.

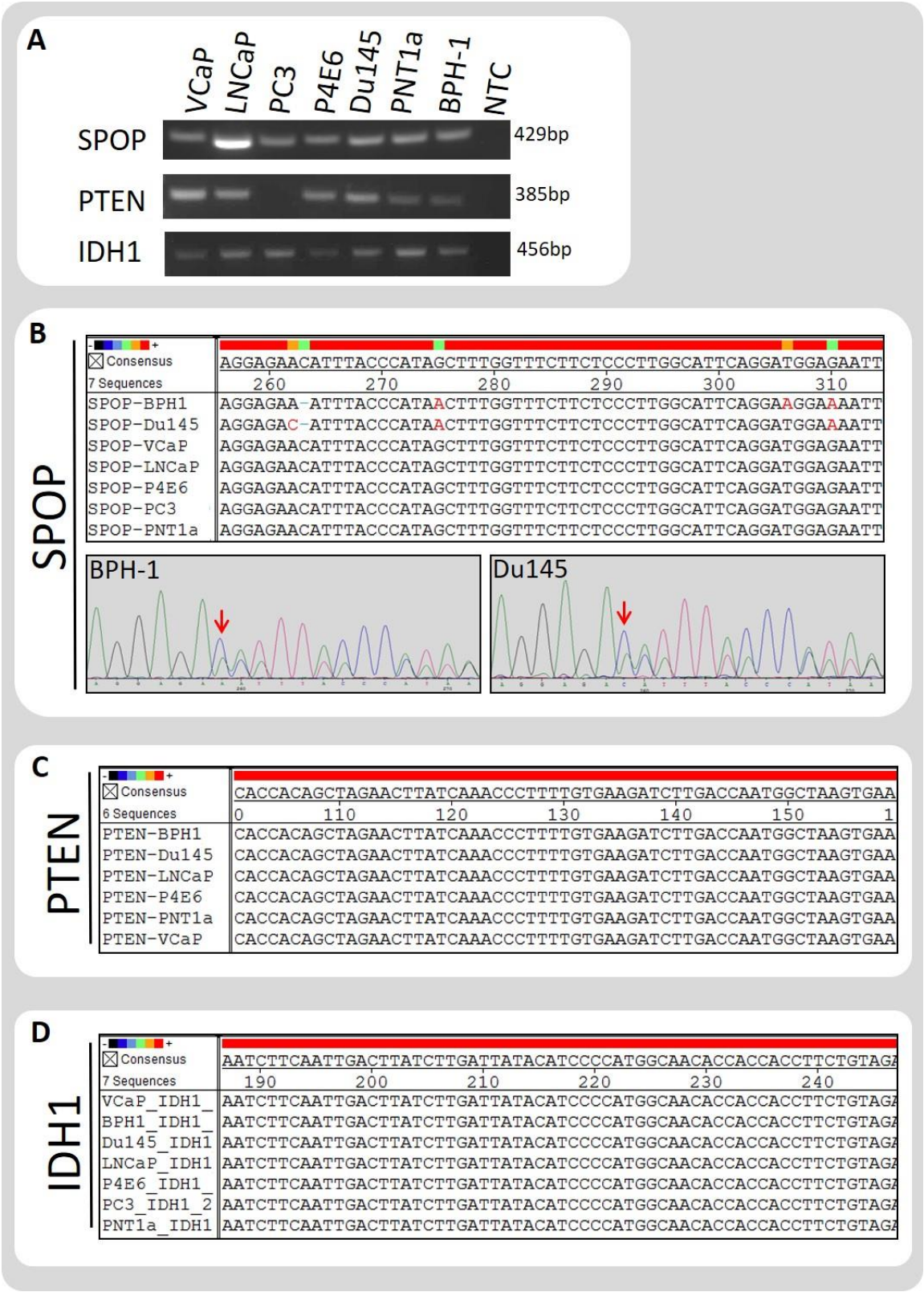

FIGURE 35 – SPOP, PTEN and IDH-1 aren't mutated in prostate cell lines.

A) PCR products of SPOP exon 6+7, PTEN exon 5 and IDH-1 exon 6 in prostate cell lines. **B)** Alignment of cell line SPOP exon 6+7 PCR product Sanger sequences and traces highlighting presence of the SNP; rs2066747 in the BPH-1 and Du145 cell lines. **C)** Alignment of cell line PTEN exon 5 PCR product Sanger sequences. **D)** Alignment of cell line IDH1 exon 6 PCR product Sanger sequences.

4.3 – Mutations observed in primary prostate cancers aren't represented in current cell lines

Mutational "hotspots" in the three genes chosen for allelic analysis; SPOP exon 6+7, PTEN exon 5 and IDH1 exon 6, were amplified in seven prostate cell lines **(Figure 35A)**. No mutations were observed in the SPOP amplicon yet two of the cell lines; BPH-1 and Du145, had an intronic SNP – rs2066747 **(Figure 35B)**. Both PTEN and IDH1 in the cell lines were wildtype **(Figure 35C+D)**. PC3 cells showed no PCR product for PTEN exon 5 as the cell line has a homozygous deletion of the gene **(451)**.

4.4 – PTEN heterozygous deletion is represented in primary prostate cancer cultures

Deletion of PTEN is a common event in primary prostate cancers **(345)**. To ascertain the effect of mutation on the allelic expression of PTEN, the gene needs to have both alleles intact. Heterozygous deletion would produce a situation that mimics monoallelic expression, therefore establishing that relevant samples had both alleles of PTEN was necessary in this study. Loss of heterozygosity (LOH) was determined in primary cancer cultures using a SNP (rs555895) in intron 8 of PTEN, the T allele of which provides a restriction site for the HincII enzyme. G/T heterozygotes produce a three-band pattern detectable by electrophoresis **(Figure 36A)**. Twenty-two patient lymphocyte (normal, with both alleles) and matched tumour samples were tested for LOH in the cancer PTEN gene. In four of the tested tumours, the uncut PTEN allele was deleted **(Figure 36B)**. In this small sample cohort, the LOH was 18% with a MAF of 0.45. A frequency comparable to the European MAF of 0.37 **(Figure 36C)**. Differences in banding intensities between tumour and lymphocyte DNA is due to there being more starting material in the lymphocyte PCR.

4.5 – Mutations observed in primary tumours aren't observed in primary prostate cancer cultures

The mutational status of 55 primary prostate cultures, taken from 49 patients, including 5 PDXs, was assessed. SPOP, PTEN and IDH1 were amplified in all cancer samples **(Figure 37)**. Some of the samples appeared under-represented in the SPOP and PTEN PCR products, however this was deemed to be technical variation upon repeat and not reflective of LOH status. After PCR, mutation of the genes was analysed either using the SURVEYOR nuclease assay or by Sanger sequencing.

The SURVEYOR assay allows mutations to be easily visualised by firstly denaturing and then re-annealing heterozygous PCR products to form heteroduplexes. The SURVEYOR nuclease is then applied to the products that can recognise and cut at the mismatched sites in formed heteroduplexes, allowing the different sized fragments to be separated by gel electrophoresis **(Figure 38A)**. The assay was first optimised by increasing the PCR product input over that of the

manufacturer's recommendation **(Figure 38B)** before being tested on the primary samples. SPOP heterozygotes were detected in tumour DNA by SURVEYOR, however the allelic difference was not due to mutation rather a germline SNP (rs2066747) as shown by the identical banding pattern produced by SPOP SURVEYOR in patient matched lymphocyte DNA **(Figure 38C)**.

PTEN and SPOP intronic heterozygotes were found, however no allelic differences were detected in IDH1. No tumour culture samples were mutated in the three chosen genes. SPOP Sanger sequence traces of all heterozygote samples are provided in **Figure 39**, PTEN in **Figure 40** and IDH1 (examples of homozygotes) in **Figure 41**. Sequence traces for all samples can be found in the **Appendix – 9.1.**

The goal of the study was to establish whether heterozygous mutation in prostate cancer altered the allelic expression of the affected gene and its wildtype copy. As no mutations of SPOP, PTEN or IDH1 were detected in either cell line or primary prostate cancer culture this goal could not be met. The models used in the study and that are currently available to researchers do not represent the full spectrum of disease that falls under the umbrella heading of prostate cancer.

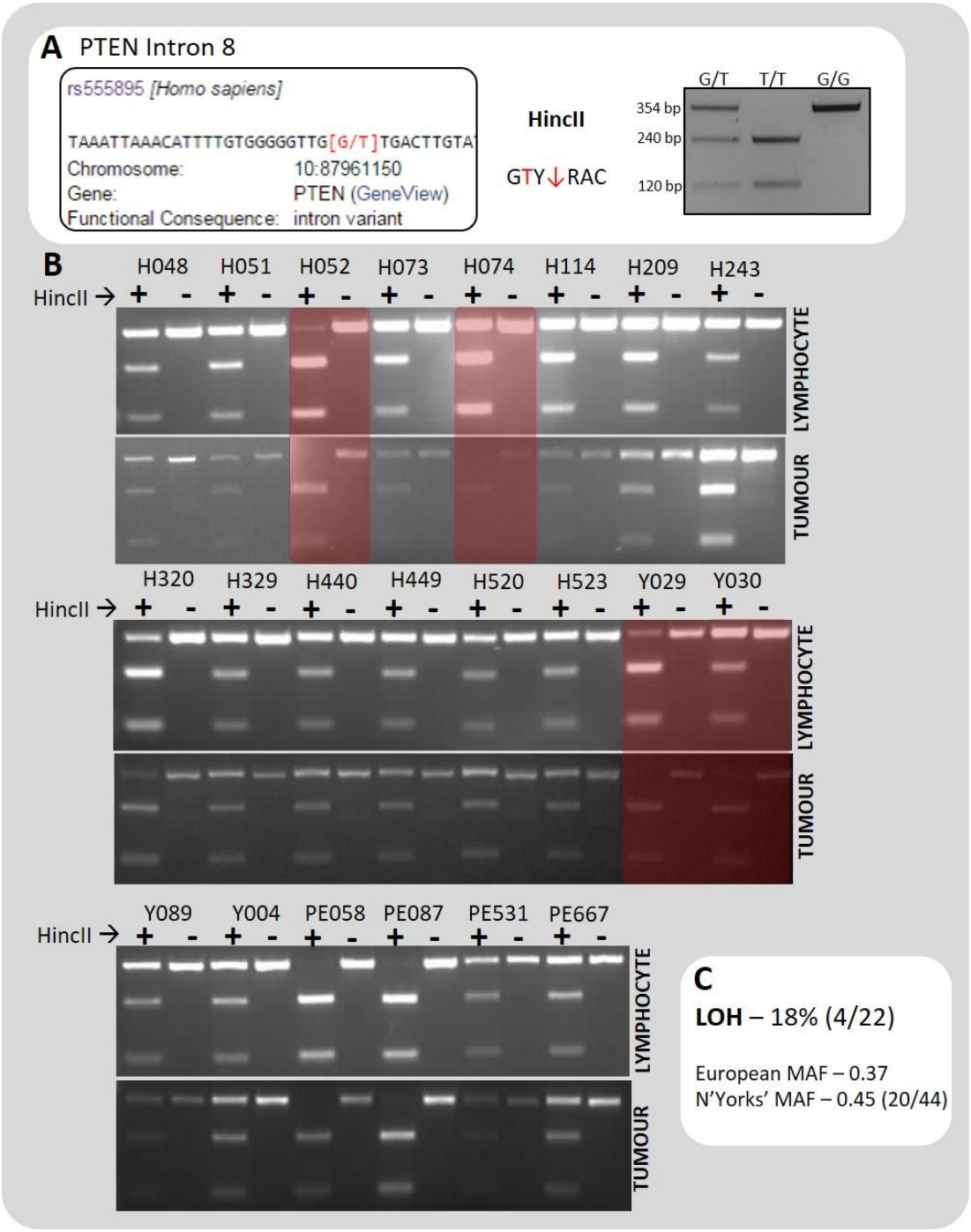

FIGURE 36 – Detection of PTEN Loss of Heterozygosity in prostate cancer primary cultures.

A) LOH of PTEN using the rs555895 SNP located in intron 8 of the gene that can act as a restriction site for HincII. **B)** LOH of primary prostate culture PTEN using HincII digests of patient matched tumour and lymphocyte DNA. LOH samples are highlighted. **C)** LOH percentages of primary samples with matching lymphocyte DNA. Minor allele frequency (MAF) of SNP in the tested samples compared to publicly available (NCBI SNP database **(747)**) MAF of European samples.

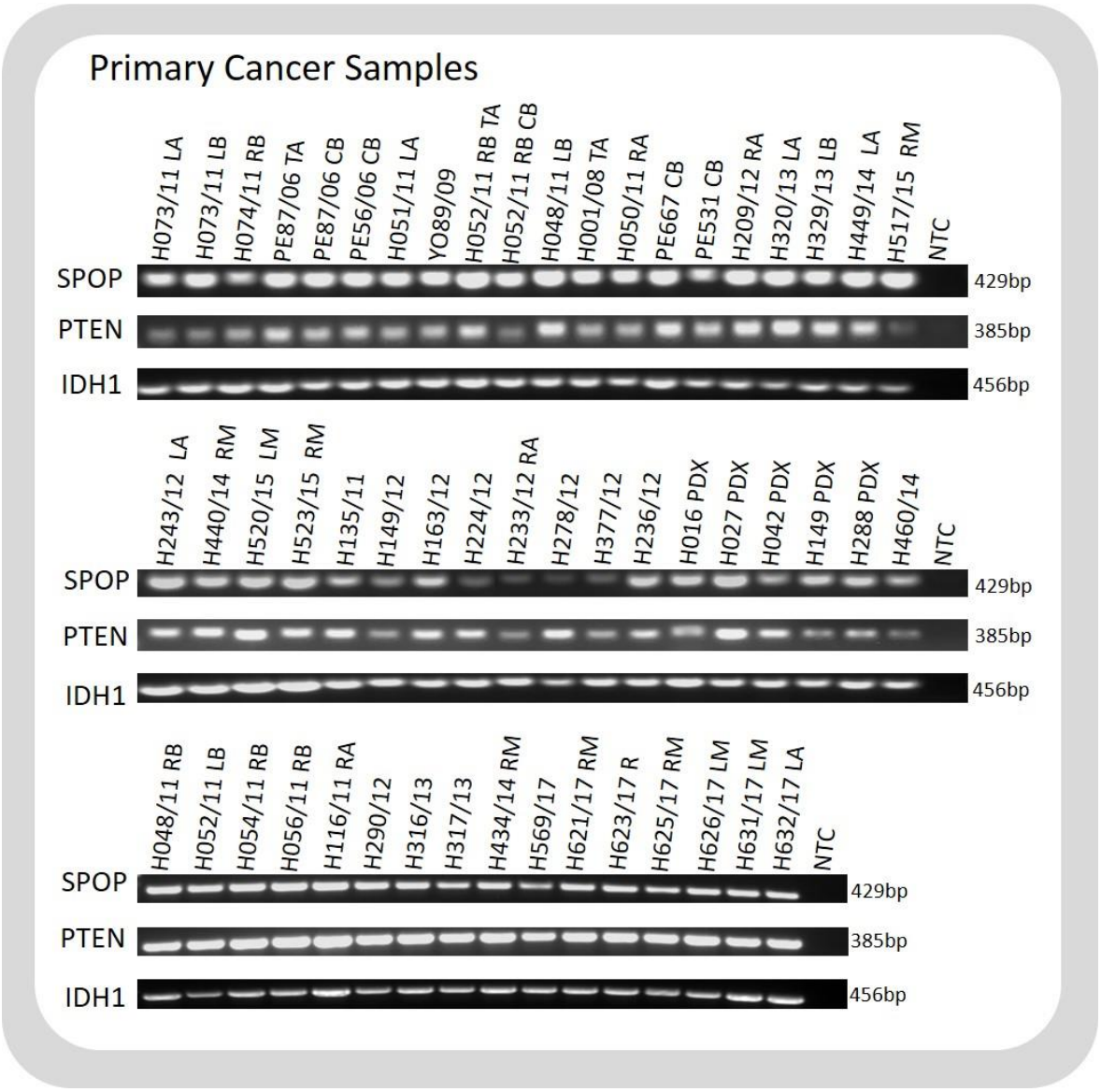

FIGURE 37 – Primary prostate culture SPOP exon 6+7, PTEN exon 5 and IDH1 exon 6 PCR products.

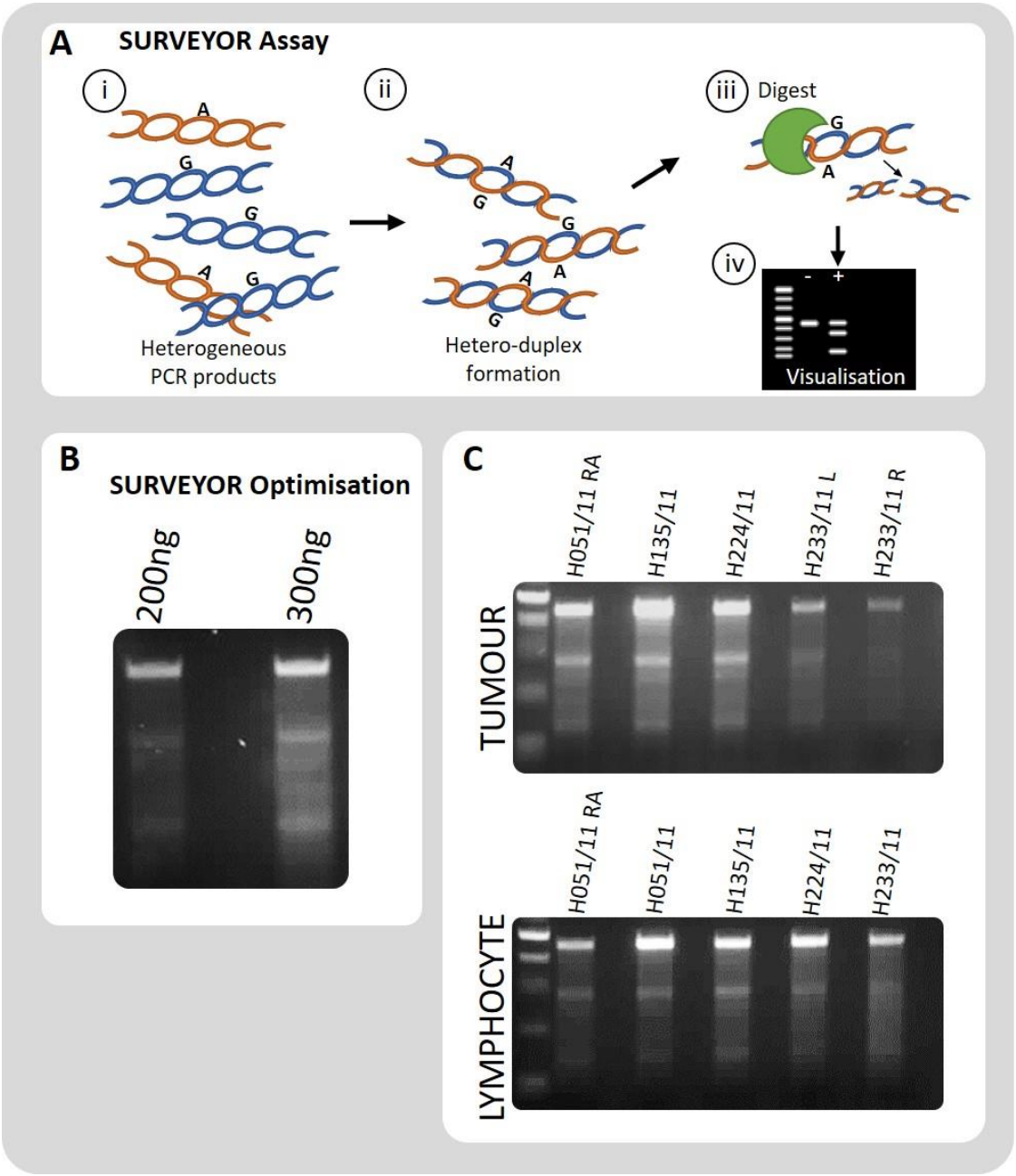

FIGURE 38 – SURVEYOR detection of primary prostate culture SPOP heterozygotes.

A) Diagrammatic process of the SURVEYOR nuclease assay. i) PCR is performed on the heterozygous amplicon to produce a mixture of allelic PCR products with variance at heterozygous nucleotide position/s, ii) products are denatured and then re-annealed allowing heteroduplexes (and homoduplexes) to form between heterozygous products, iii) SURVEYOR nuclease recognises mismatches (and indels of ≤12bp) and cleaves dsDNA to leave different sized fragments, iv) gel electrophoresis allows separation of the variant SURVEYOR cleavage products to detect heterozygosity. **B)** Optimisation of SURVEYOR assay with varying amounts of SPOP PCR product. **C)** Identification of germline SNP in SPOP prostate tumour and patient lymphocyte gDNA using SURVEYOR**.**

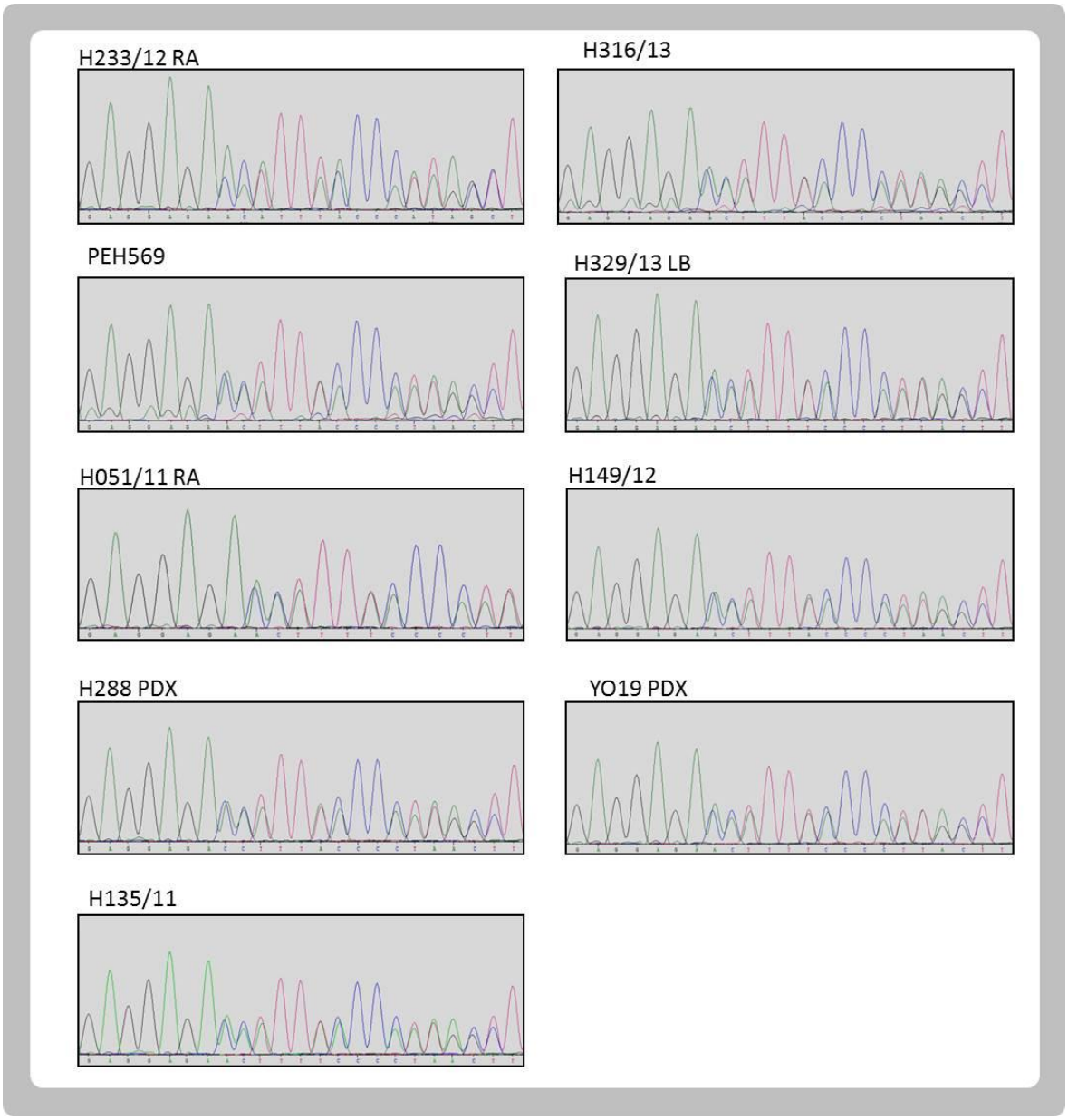

FIGURE 39 – SPOP Sanger sequence traces of heterozygote primary prostate cancer cultures.

SNP detected in the PCR product is rs2066747.

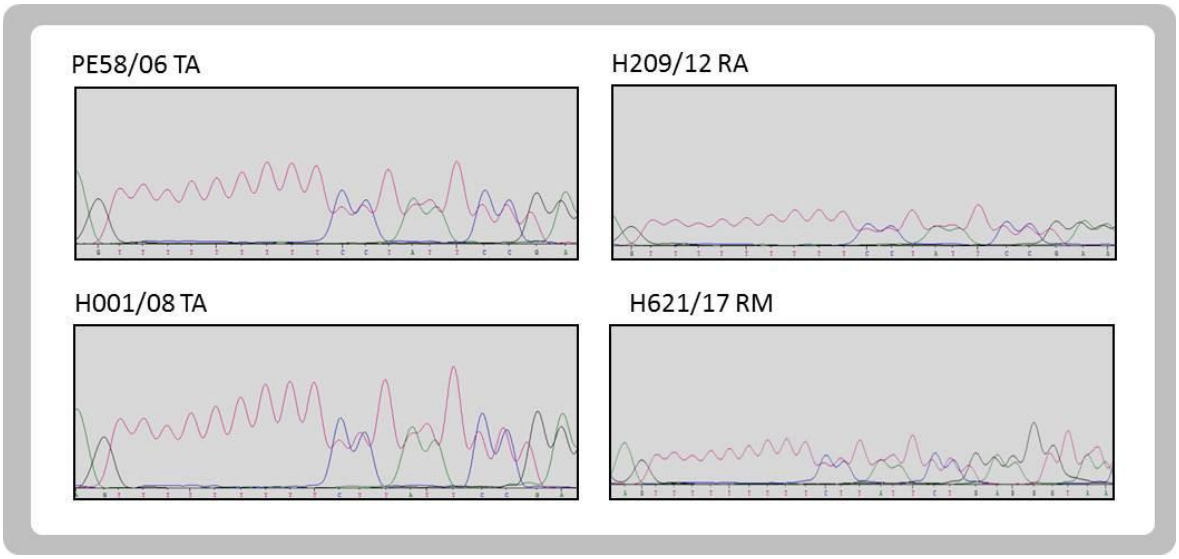

FIGURE 40 – PTEN Sanger sequence traces of heterozygote primary prostate cancer cultures.

SNP detected in the PCR product is rs398123319.

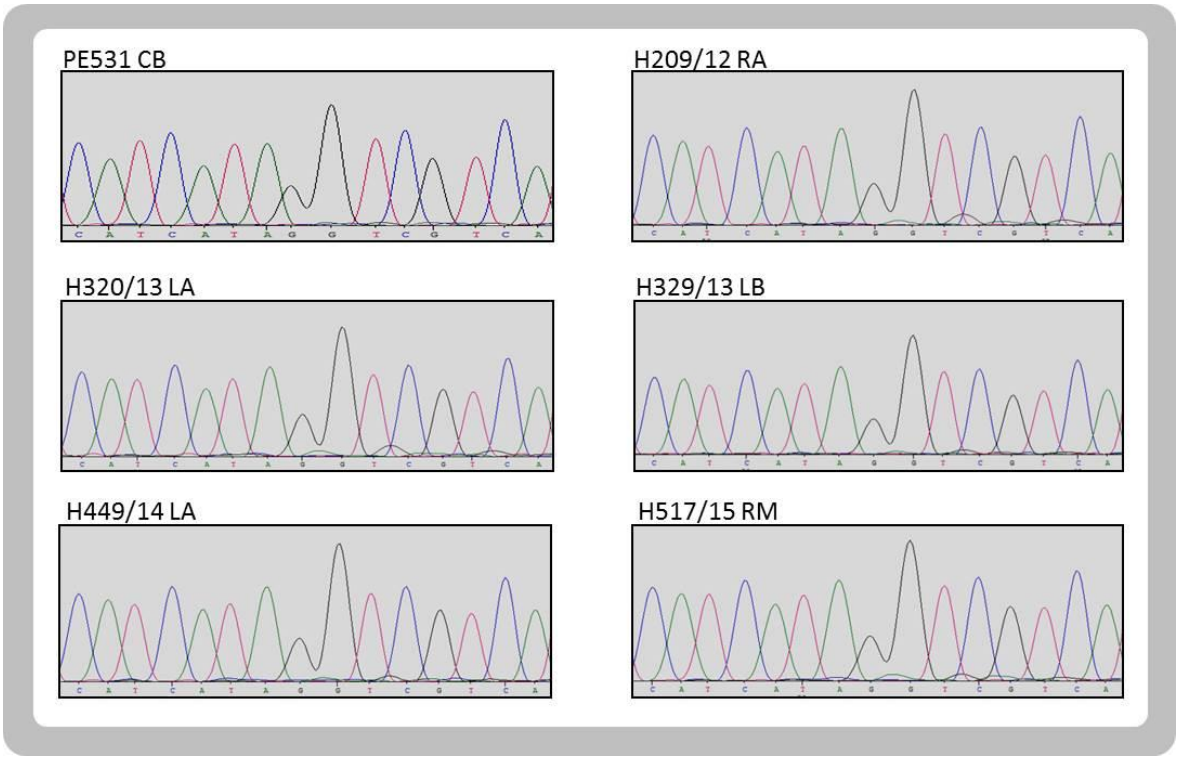

FIGURE 41- IDH1 Sanger sequence traces of primary prostate cancer cultures.

Examples of sequence traces taken from six primary prostate culture samples with wildtype IDH1. The traces show the location of the most frequent mutation (R132H) in the IDH1 gene.

5. Results– Oxidative stress response signalling in LTP treated primary prostate basal epithelial cells

5.1 – Optimisation of plasma dose and post-treatment assessment of gene expression

To investigate the immediate signalling events following LTP treatment of prostate basal epithelial cells **(Table 13)**, optimisation of both plasma dose and the post-treatment time-point at which gene expression changes became apparent were required.

The intention was to profile the antioxidant response of primary cells using the Qiagen Oxidative Stress Profiler Arrays which can simultaneously assess the expression of 84 genes. Genes common to the array plates were chosen for initial qRT-PCR analysis to establish both the time-point at which responsive gene expression was assessed and the time period of plasma treatment. Firstly, four prostate cell lines were assessed for their expression of the mitochondrial ROS scavenging enzyme SOD2 at 2, 4, 6 and 8 hours after a 10-minute plasma dose (post-treatment time-points and LTP dose were informed by previous work **(304)**) **(Figure 42)**. PC3 and PNT2 lines weren't responsive in their SOD2 expression, whereas both BPH-1 and LNCaP showed an increase in the transcript over the time-course.

From this initial data, 4 and 6 hour time-points were chosen and the number of array genes assessed was expanded. Expression of SOD2, GPX2 (peroxide scavenging enzyme) and NOS2 (reactive nitrogen species generating enzyme) was analysed in three primary cultures **(Figure 43)**. This experiment also included a 3-minute plasma dose and a 1mM hydrogen peroxide treatment. The peroxide treatment had previously been used as a positive control for both oxidative damage effects and cell fate responses in prostate primary cultures **(304)**, its inclusion in gene expression analysis was to provide the same positive inductive effect on cellular antioxidant response networks. The 3-minute plasma dose was the most effective in raising gene expression. SOD2 expression was marginally upregulated in cultures at the 4 hour time-point. GPX2 expression was largely unchanged by plasma and NOS2 also didn't appear to have a patterned upregulation in the cultures assessed.

As the primary cells didn't respond to plasma like the cell lines, post treatment time-points were tested directly on the Qiagen Oxidative Stress Response Profiler arrays. This included 0.5 and 2 hour time-points to monitor rapid response and the later snapshots of 4 and 8 hours to observe prolonged transcriptional change **(Figure 44)**. We observed, across multiple cultures, that the 2 hour post-LTP time-point was optimal for monitoring primary cell transcriptional response and that very few changes in gene expression were observed at 4 and 8 hours. The 3-minute plasma dose was chosen for the study as it produced a wider expressional response than the longer

treatment of 10 minutes **(Figure 45A)**. An H_2O_2 treatment also produced a robust induction of oxidative stress response genes, including catalase, at the 2 hour time-point. The peroxide response was similar to that of the 3-minute LTP dose in the H209/12 LA culture **(Figure 45C)**.

5.2 – A central oxidative stress response is triggered by LTP in cultures, regardless of pathology

Oxidative stress transcriptional response was assessed with Qiagen Oxidative Stress Profiler Array qRT-PCR plates. These monitored 84 literature-defined genes linked to oxidative stress, 5 house-keeping genes for normalisation and internal reverse transcriptase, PCR and genomic DNA contamination controls. All RNA samples used passed these internal quality controls. To see whether LTP response was determined by tissue pathology, three separate patient cultures from four different disease states were used; normal, BPH, Gleason 7 and Gleason 9 **(Table 14)**. For added comparative power, the normal and Gleason 7 tissues came from the same patient – a Patient Matched Pair – allowing a true comparison of normal and cancer that doesn't require adjustment for known inter-patient heterogeneity **(304)**.

Sample Identifier	Tissue Type	Biopsy Core Positivity	Tumour palpable?	Operation	Age of Patient
YO68/09	BPH	/	/	TURP	N/A
H221/12	BPH	/	/	TURP	77
H229/12	BPH	/	/	TURP	69
H249/12	BPH	/	/	TURP	83
H209/12 LA	Normal	0/5	No	LRP	64
H209/12 RA	Gleason 7 (4+3)	4/5	Yes		
H329/13 LB	Gleason 7 (3+4)	3/5	Yes	ORP	53
H329/13 R	Normal	0/5	No		
H341/13 LB	Gleason 7 (3+4)	3/5	Yes	LRP	52
H341/13 R	Normal	0/5	No		
H434/14 LM	Normal	0/6	No	ORP	68
H434/14 RM	Gleason 7 (4+3)	4/4	Yes		
H523/13 LM	Normal	0/5	No	LRP	66
H523/13 RM	Gleason 7(4+3)	4/5	Yes		
H641/17 L	Normal	0/5	No	RRP	64
H641/17 R	Gleason 9(4+5)	4/7	Yes		
H643/17 LM	Normal	No cores	No	RRP	78
H643/17 RM	Gleason 7(3+4)	5/5	No		
H646/17 LM	Gleason 7(3+4)	8/8	No	RRP	67
H646/17 RM	Normal	0/5	No		
H594/17 L	Gleason 7(3+4)	8/5	Yes	RRP	61
H637/17 L	Gleason 7(3+4)	7/14	Yes	RRP	52
H652/17b R	Gleason 7(3+4)	4/4	Yes	RRP	57
H306/13	Gleason 9 (5+4)	6/6	NA	chTURP	60
H460/14	Gleason 9 (4+5)	No cores	NA	chTURP	76
H545/15 RM	Gleason 9 (4+5)	4/5	Yes	ORP	69

TABLE 13 – Sample information of all patient cultures used in LTP study.

The letters after the anonymous patient identifier inform on the biopsy site of the originating tissue. L – left, R – right, A – apex, M – mid and B – base. Operations included Robotic Radical Prostatectomy (RRP), Open Radical Prostatectomy (ORP), Laparascopic Radical Prostatectomy (LRP) and channel (ch)/TURP – Transurethral Resection of the Prostate.

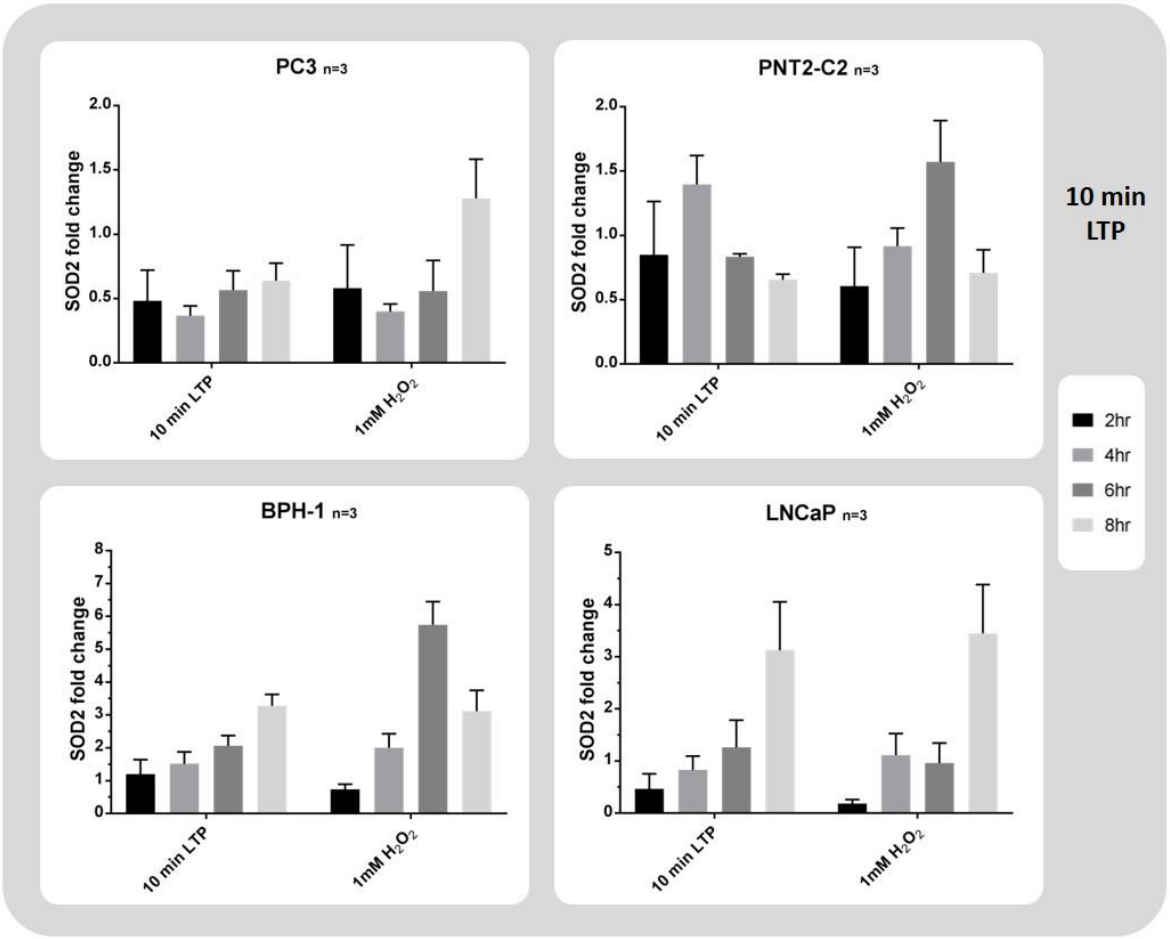

FIGURE 42 – Prostate cell line expression of SOD2 in response to LTP is varied.

Expression of SOD2 was measured at 2, 4, 6 and 8 hour time-points following application of a 10-minute LTP dose in four prostate cell lines. Note that y axis scales are different. Graph error bars represent the standard error of the mean (SEM) of the biological triplicates.

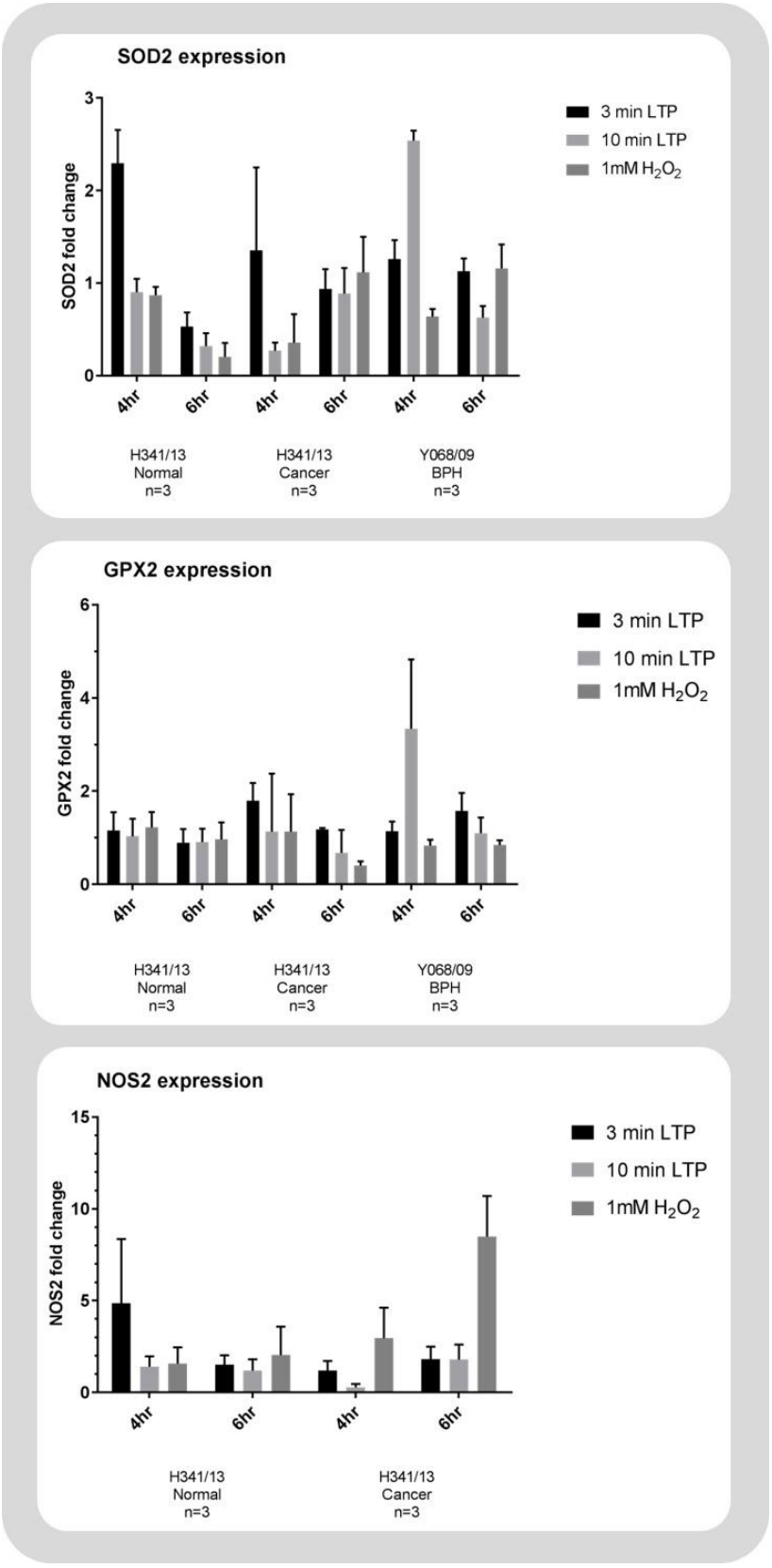

FIGURE 43 - Primary culture stress response gene expression following oxidative treatment.

Expression of SOD2, GPX2 and NOS2 was measured at 4 and 6 hour time-points following an LTP dose of 3 or 10-minutes and 1mM H_2O_2 treatment. Note that y axis scales are different. Graph error bars represent the SEM of the biological triplicates.

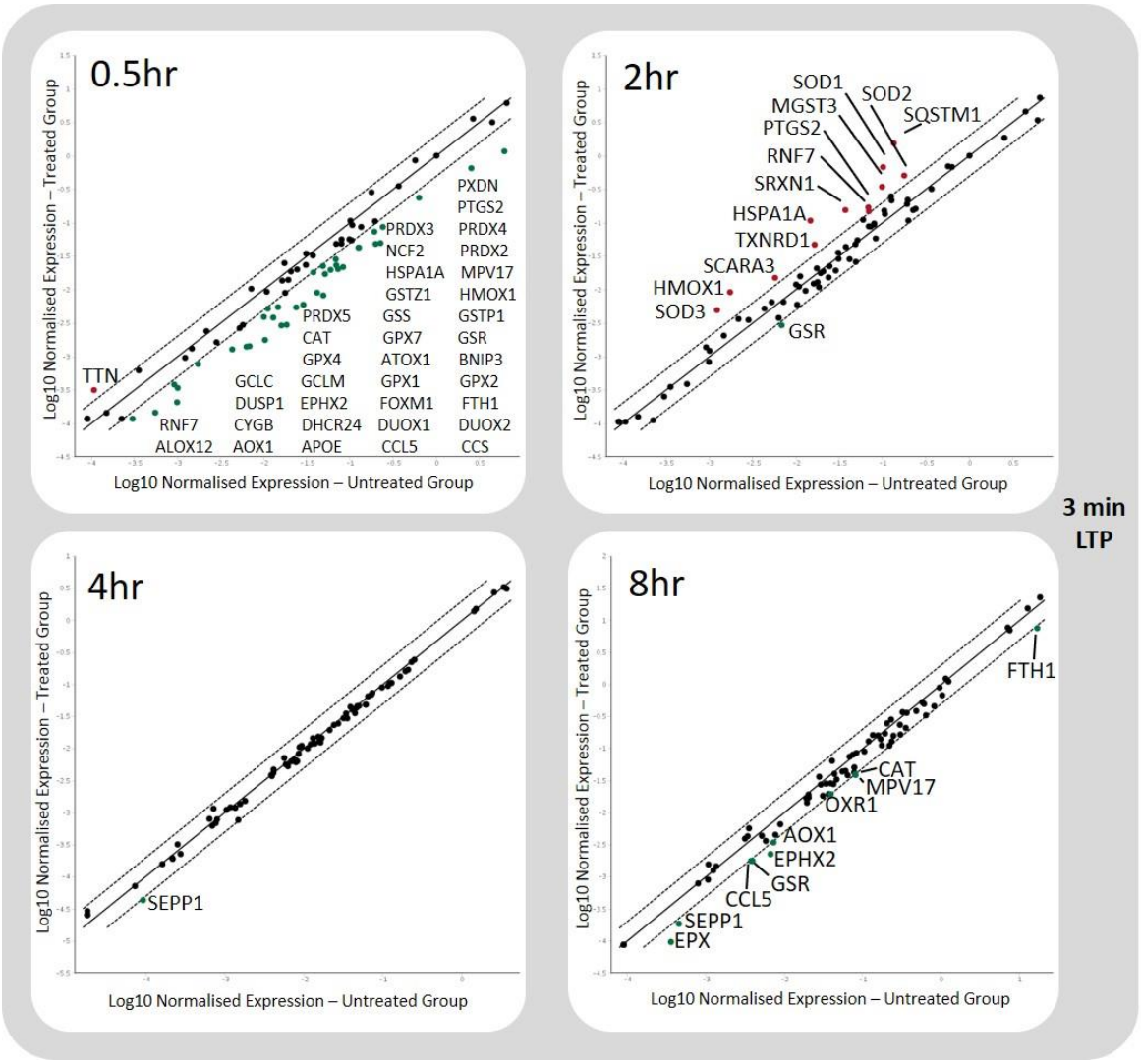

FIGURE 44 - Oxidative stress response array time-point optimisation using the H329/13 LB primary culture.

Gene expression analysis using the Oxidative Stress Profiler Arrays shows the upregulation of genes 2 hours after LTP dose. Black solid line denotes “no change” between untreated and treated gene expression, the dashed line (above and below the black solid line) signifies a 2-fold change in gene expression. Upregulated genes are red dots, unchanged genes are black dots and downregulated genes are green dots. Scatterplots prepared using Qiagen’s online data analysis tool **(742)**.

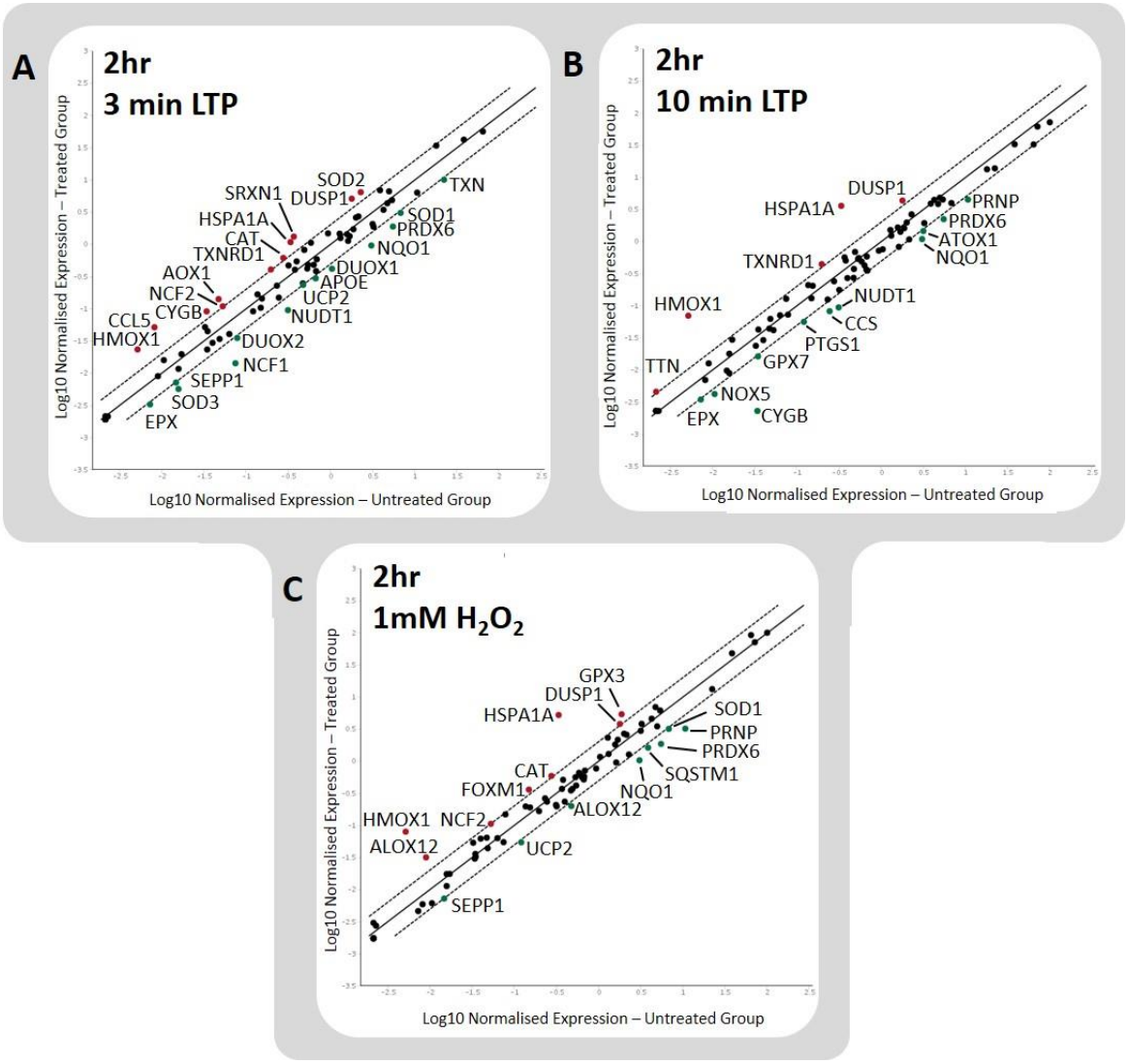

FIGURE 45 - Oxidative stress response array dose optimisation using the H209/12 LA primary culture. Gene expression at 2 hours post LTP using the treatments of **A)** 3-minutes LTP, **B)** 10-minutes LTP and **C)** 1mM H2O2. Black solid line denotes "no change" between untreated and treated gene expression, the dashed line (above and below the black solid line) signifies a 2-fold change in gene expression. Upregulated genes are red dots, unchanged genes are black dots and downregulated genes are green dots.

Tissue	Sample	Treatment	Time-point (hr)
BPH	H221/12	Untreated	0
		3 min LTP	0.5
			2
	H229/12	Untreated	0
		3 min LTP	0.5
			2
	H249/12	Untreated	0
		3 min LTP	0.5
			2
Normal	H209/12 LA	Untreated	0
		3 min LTP	0.5
			2
			2 (repeat)
		10 min LTP	0.5
			2
		H2O2	2
	H329/13 R	Untreated	0
		3 min LTP	0.5
			2
	H434/14 LM	Untreated	0
		3 min LTP	0.5
			2
Gleason 7 Cancer	H209/12 RA	Untreated	0
		3 min LTP	0.5
			2
	H329/13 LB	Untreated	0
		3 min LTP	0.5
			2
			4
			8
		10 min LTP	4
			8
	H434/14 RM	Untreated	0
		3 min LTP	0.5
			2
Gleason 9 Cancer	H306/13	Untreated	0
		3 min LTP	0.5
			2
	H460/14	Untreated	0
		3 min LTP	0.5
			2
	H545/15	Untreated	0
		3 min LTP	0.5
			2
			TOTAL – 44 Arrays

TABLE 14 – Summary of conditions and samples used for Oxidative Stress Profiler Arrays

The H434/14 normal culture rapidly responded to plasma treatment with an increase in the number of genes upregulated at the 2 hour mark. The Gleason 7 of the patient matched pair was muted in its response at 0.5 hours and had only a few upregulated genes at the later time-point **(Figure 46)**. Both cultures of the H329/13 patient matched pair showed an initial downregulation of genes followed by an upregulation of multiple genes at 2 hours, here the cancer had a greater number of responsive genes than the normal culture **(Figure 47)**. The H209/12 normal culture showed the usual response of initial gene downregulation and upregulation at the later time-point yet the cancer culture had a greatly reduced output at 2 hours with upregulation of only three genes **(Figure 48)**. Through averaging the responses of the three patient matched pairs it was possible to identify common genes that were either up or downregulated across patients. At the earlier time-point of 0.5 hours, the Gleason 7 cultures downregulated a number of genes, a response that wasn't observed in the other tissue pathologies **(Figure 49A)**. At 2 hours, the patient matched pair cultures had a very similar expression profile; sharing upregulation of HMOX1, TXNRD1, HSPA1A and SQSTM1, with the normal epithelia additionally expressing SRXN1 and DUSP1 – which were both recurrently upregulated by LTP in the other pathologies **(Figure 50A+B)**.

The patient matched pairs also afforded the ability to explore whether or not the cancer cultures expressed oxidative stress genes to a greater extent over normal counterparts with no treatment. Each patient's cancer varied in the composition of genes that were over or under-expressed in the disease state, yet the mean expression response highlighted that a few genes were consistently upregulated in Gleason 7 disease over normal epithelia, including HMOX1 and HSPA1A **(Figure 51)**.

BPH cultures, with the exception of H249/12, were the most responsive of the tissue types half an hour after treatment and showed a similar expression signature to the other pathologies at the later time-point **(Figure 52)**. The average expression profile of BPH showed the upregulation of HMOX1, HSPA1A and DUSP1 at 2 hours, similar to normal prostate epithelia **(Figure 50C)**.

The Gleason 9 samples also showed marked variability between patients that was observed amongst the other tissue pathologies. All cultures had a minimal response at 0.5 hours followed by a pronounced upregulation of genes at the 2 hour time-point. H306/13 showed huge upregulation of DUOX1 and GPX4 at both time-points in response to plasma **(Figure 53)**. The pathology average for the Gleason 9 patients showed upregulation of HMOX1, HSPA1A and SRXN1, with DUOX1 and GPX4 included due to the magnitude of both gene's expression in response to LTP in H306/13 **(Figure 50D)**.

Validation of the results obtained using the arrays was carried out by TaqMan qRT-PCR. The expression of four genes (SOD2, GPX2, HMOX1 and HSPA1A) was tested using this method across the four tissue pathologies; H229/12 – BPH, H329/13 R – normal, H329/13 LB – Gleason 7 and H545/15 – Gleason 9, with both SYBR green and TaqMan qRT-PCR producing similar results **(Figure 54A)**. Melt curve analysis of the array plates following the PCR showed that the array primers were specific as the PCR product generated in each well was a single species **(Figure 54B)**.

Assessment of real-time upregulation of the top hit from the arrays; HMOX1, was attempted using SmartFlares. These are gold nanoparticles coated in oligonucleotides specific to the mRNA of interest which are taken up indiscriminately by cells. Bound to these oligonucleotides are complementary fluorescent probes which are quenched when in close proximity to the gold particle. When the target mRNA increases it specifically displaces the probes on the gold particle and thus fluorescence increases **(Figure 55A)**. SmartFlares were chosen as they would permit simultaneous observation of close to real time increases in mRNA transcript and allow for assessment of cell population transcriptional heterogeneity. However, no change in HMOX1 fluorescence was observed in response to treatment in the PC3 cell line **(Figure 55B)** or primary cells **(Figure 55C)**. HMOX1 expression, as measured by the SmartFlares, did not match the accompanying qRT-PCR data.

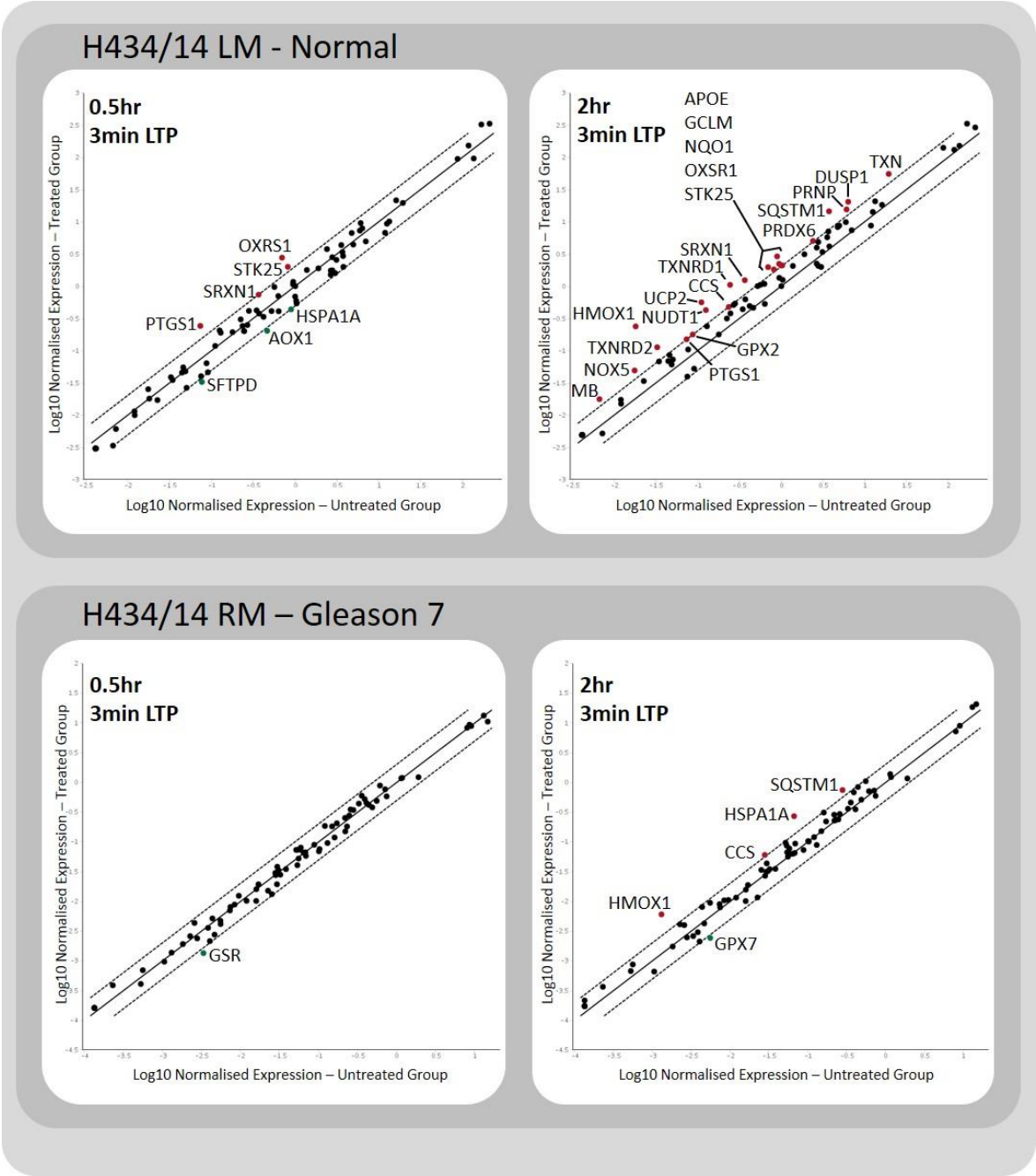

FIGURE 46 - Oxidative stress gene response in the H434/14 patient matched pair.

Oxidative stress transcriptional response in normal and Gleason 7 cultures from patient H434/14. Expression was assessed 0.5 and 2 hours after a 3-minute LTP dose. Black solid line denotes “no change” between untreated and treated gene expression, the dashed line (above and below the black solid line) signifies a 2-fold change in gene expression. Upregulated genes are red dots, unchanged genes are black dots and downregulated genes are green dots

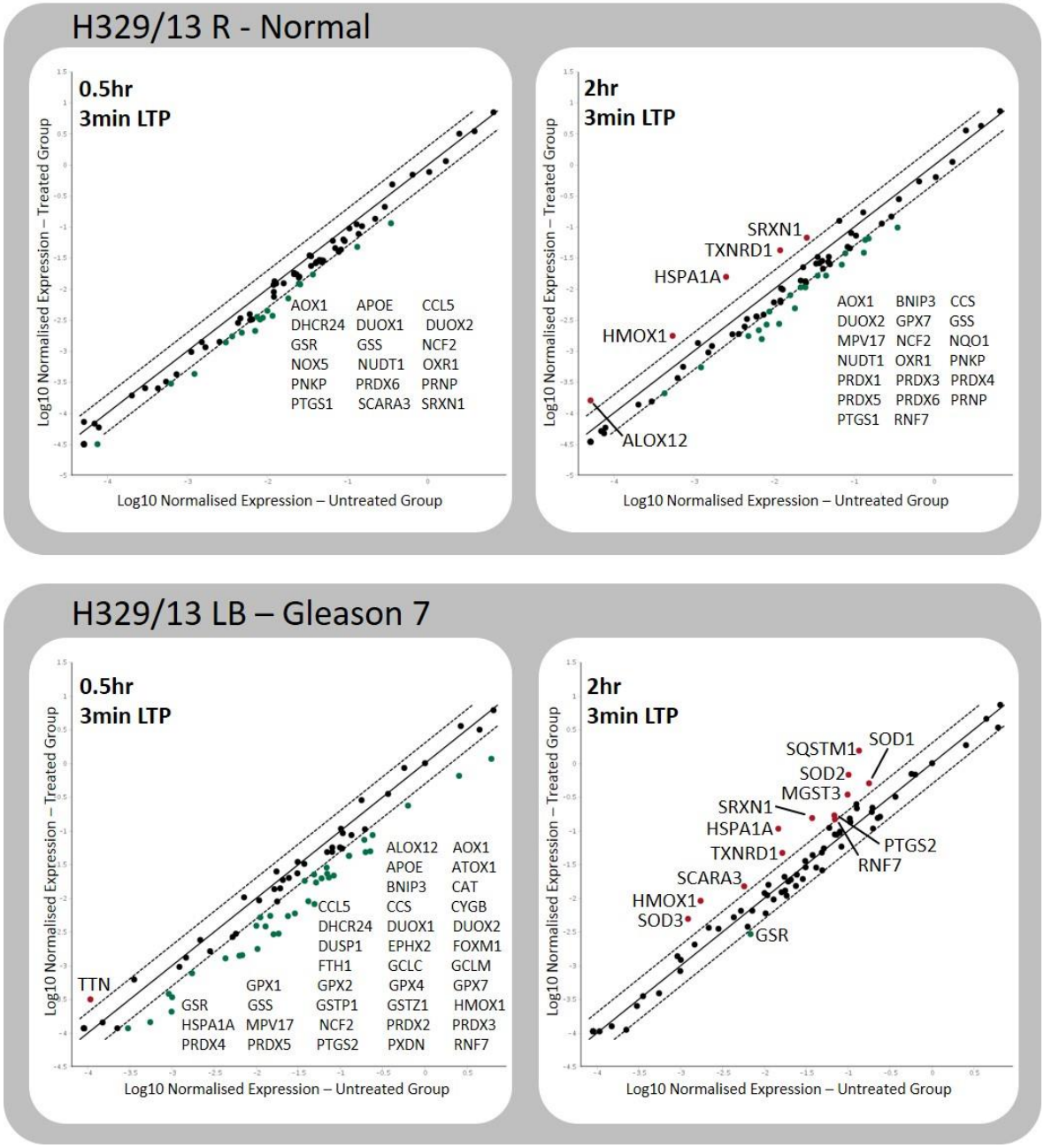

FIGURE 47 - Oxidative stress gene response in the H329/13 patient matched pair.

Oxidative stress transcriptional response in normal and Gleason 7 cultures from patient H329/13. Expression was assessed 0.5 and 2 hours after a 3-minute LTP dose. Black solid line denotes “no change” between untreated and treated gene expression, the dashed line (above and below the black solid line) signifies a 2-fold change in gene expression. Upregulated genes are red dots, unchanged genes are black dots and downregulated genes are green dots.

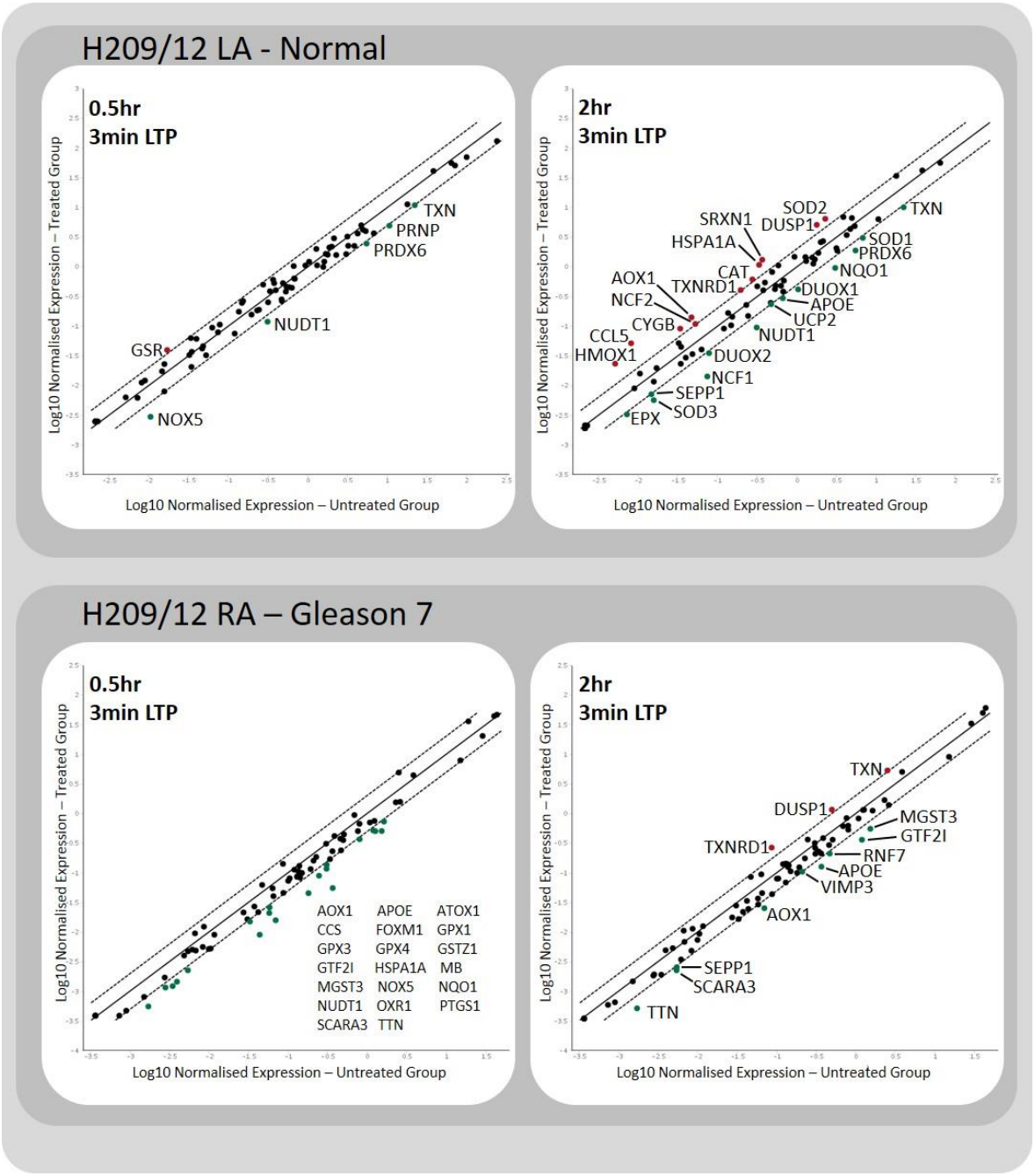

FIGURE 48 - Oxidative stress gene response in the H209/12 patient matched pair.

Oxidative stress transcriptional response in normal and Gleason 7 cultures from patient H209/12. Expression was assessed 0.5 and 2 hours after a 3-minute LTP dose. Black solid line denotes “no change” between untreated and treated gene expression, the dashed line (above and below the black solid line) signifies a 2-fold change in gene expression. Upregulated genes are red dots, unchanged genes are black dots and downregulated genes are green dots.

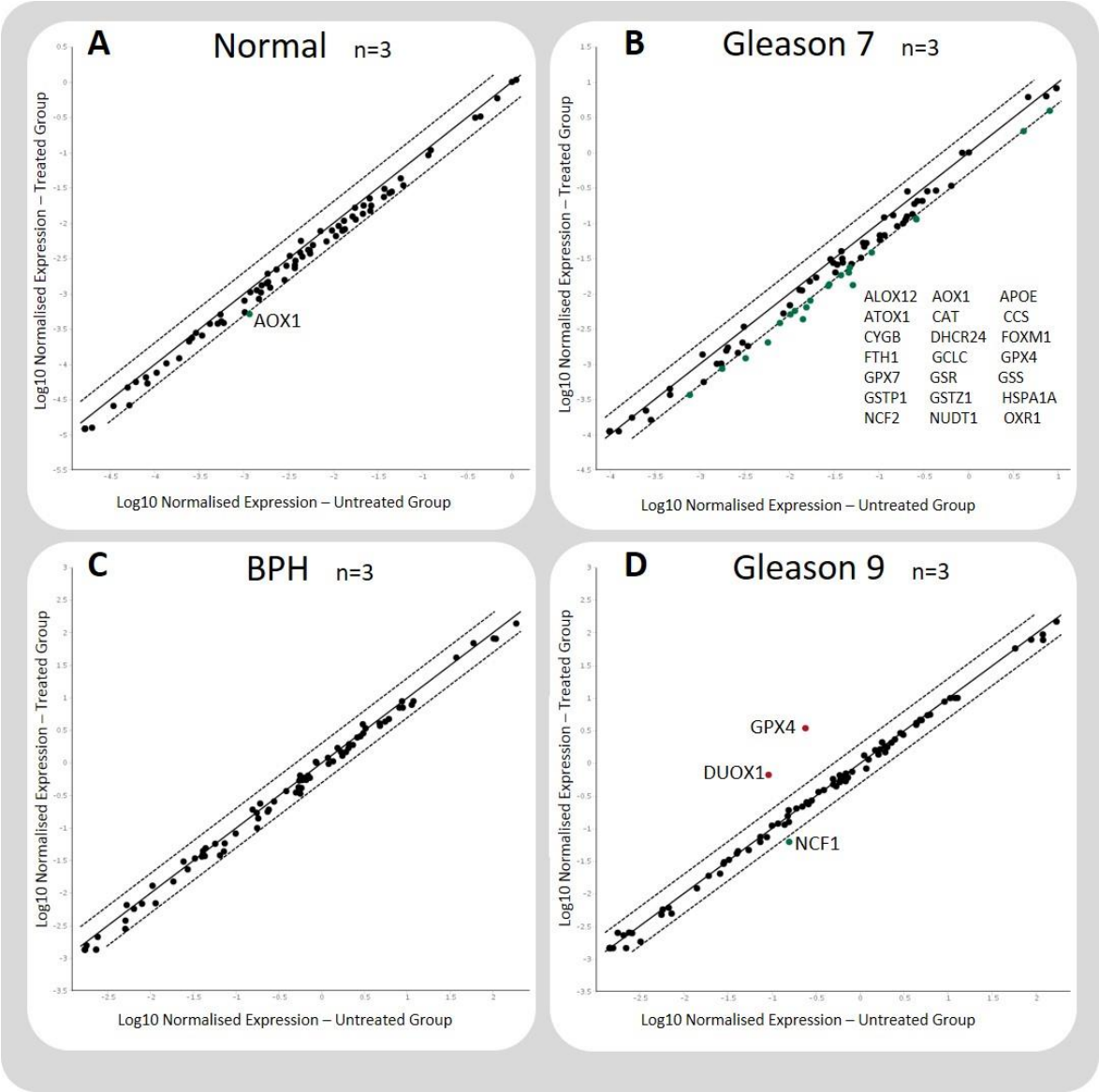

FIGURE 49 - Tissue pathology average of oxidative stress response gene expression at 0.5 hours post-LTP.

Average gene expression taken from the three cultures of **A)** Normal prostate, **B)** Gleason 7 cancer, **C)** Benign prostatic hyperplasia and **D)** Gleason 9 cancer, at 0.5 hours after a 3-minute LTP dose. Black solid line denotes “no change” between untreated and treated gene expression, the dashed line (above and below the black solid line) signifies a 2-fold change in gene expression. Upregulated genes are red dots, unchanged genes are black dots and downregulated genes are green dots.

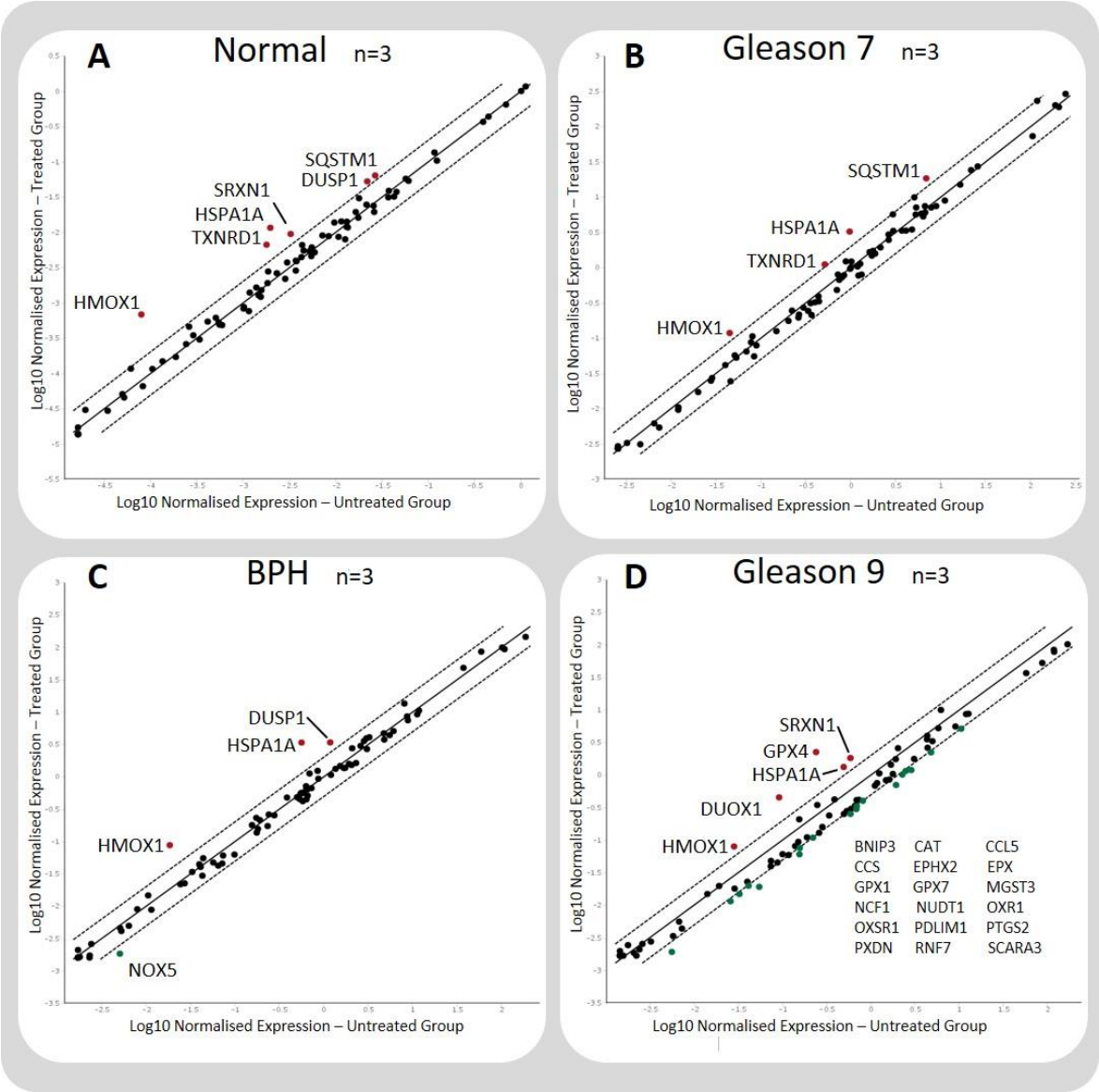

FIGURE 50 - Tissue pathology average of oxidative stress response gene expression at 2 hours post-LTP.

Average gene expression taken from the three cultures of **A)** Normal prostate, **B)** Gleason 7 cancer, **C)** Benign prostatic hyperplasia and **D)** Gleason 9 cancer, at 2 hours after a 3-minute LTP dose. Black solid line denotes “no change” between untreated and treated gene expression, the dashed line (above and below the black solid line) signifies a 2-fold change in gene expression. Upregulated genes are red dots, unchanged genes are black dots and downregulated genes are green dots.

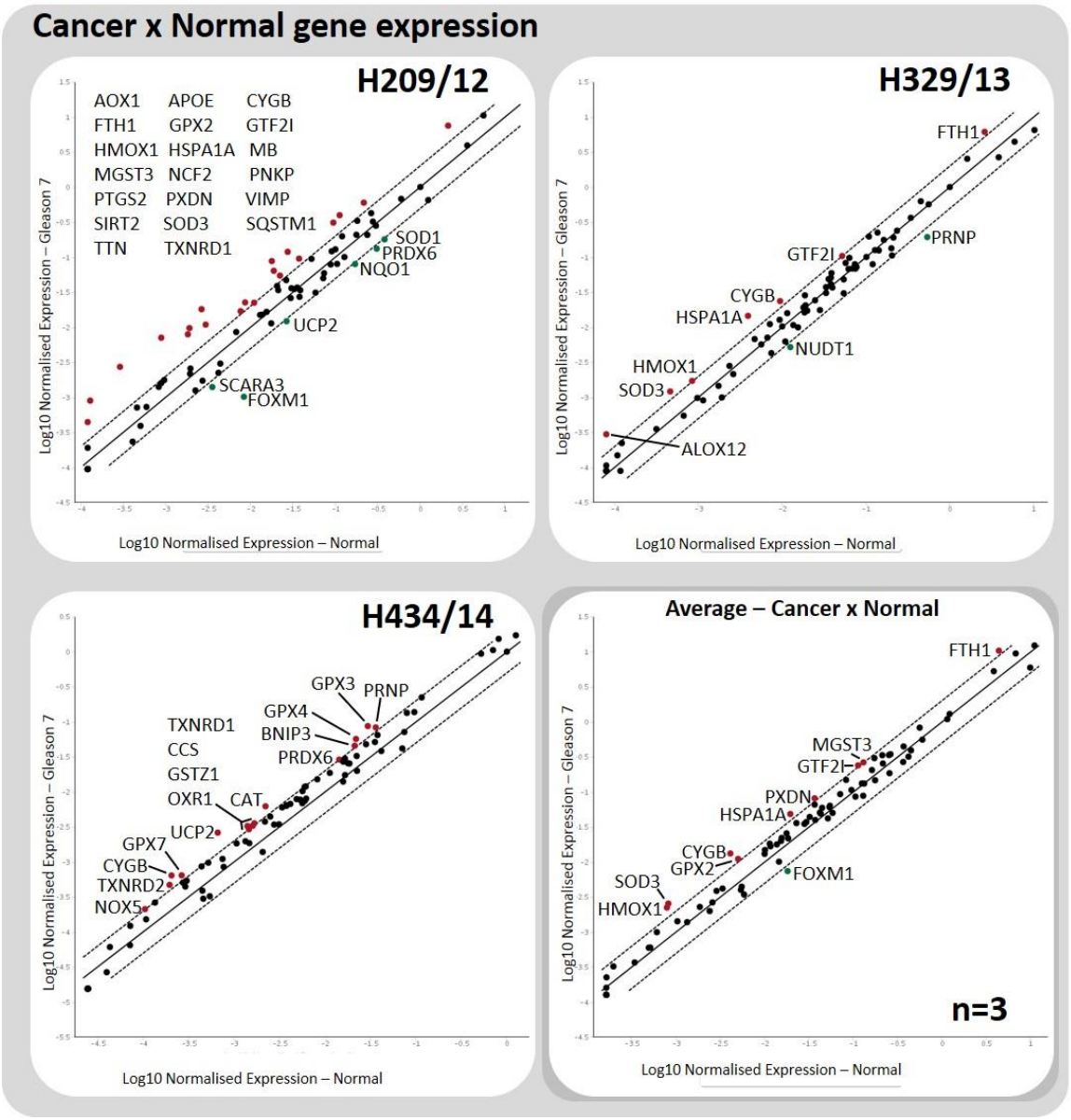

FIGURE 51 - Oxidative stress response genes are expressed at higher basal levels in Gleason 7 cultures of patient matched pairs.

Patient matched pair cancer and normal gene expression from untreated cultures were compared. The patient is marked on each scatterplot, the lower right panel shows the average expression of the three patients. Black solid line denotes “no change” between untreated and treated gene expression, the dashed line (above and below the black solid line) signifies a 2-fold change in gene expression. Upregulated genes are red dots, unchanged genes are black dots and downregulated genes are green dots.

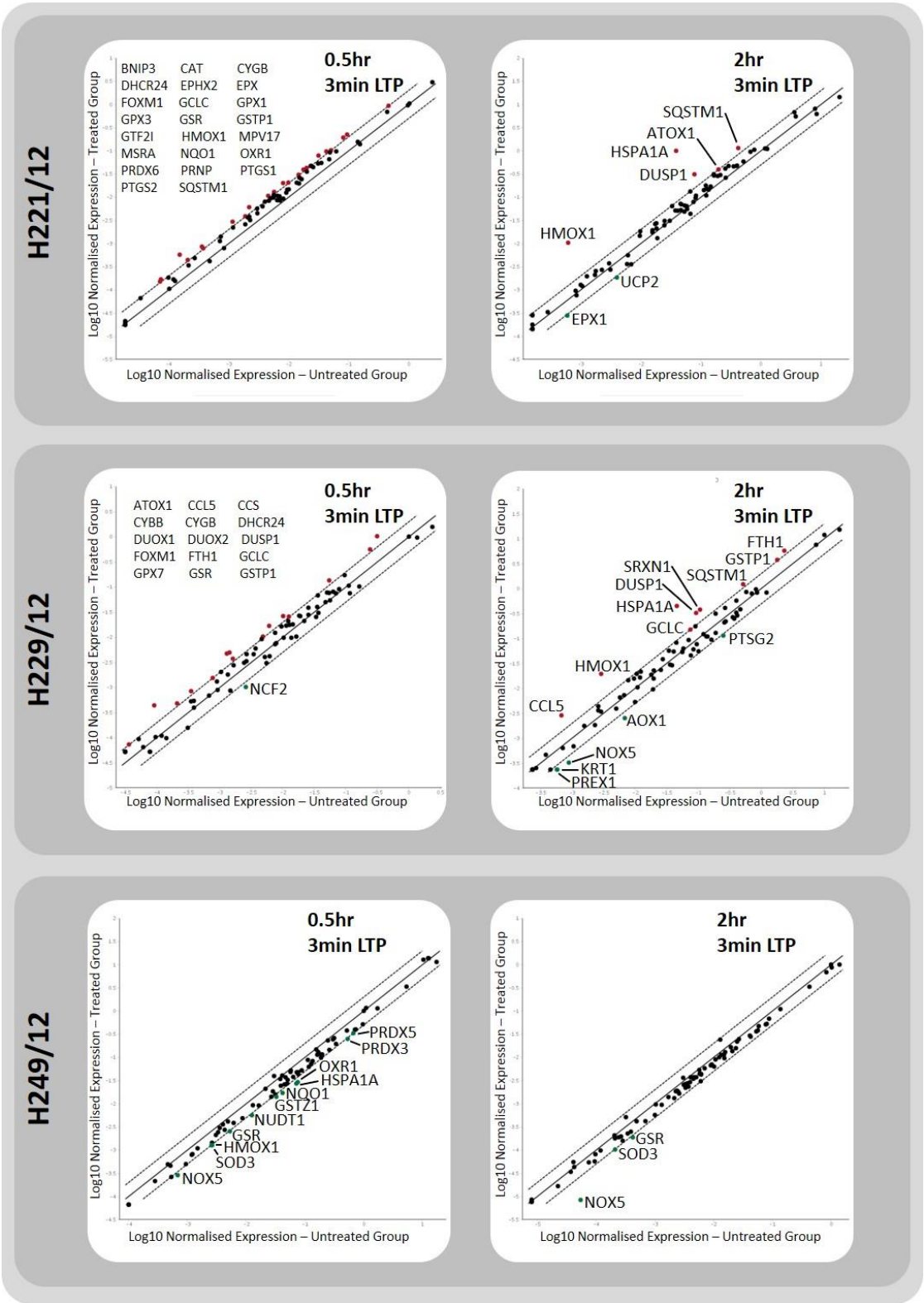

FIGURE 52 - Oxidative stress gene response in three BPH primary cultures.

Oxidative stress transcriptional response in cultures from patients H221/12, H229/12 and H249/12. Expression was assessed 0.5 and 2 hours after a 3-minute LTP dose. Black solid line denotes “no change” between untreated and treated gene expression, the dashed line (above and below the black solid line) signifies a 2-fold change in gene expression. Upregulated genes are red dots, unchanged genes are black dots and downregulated genes are green dots.

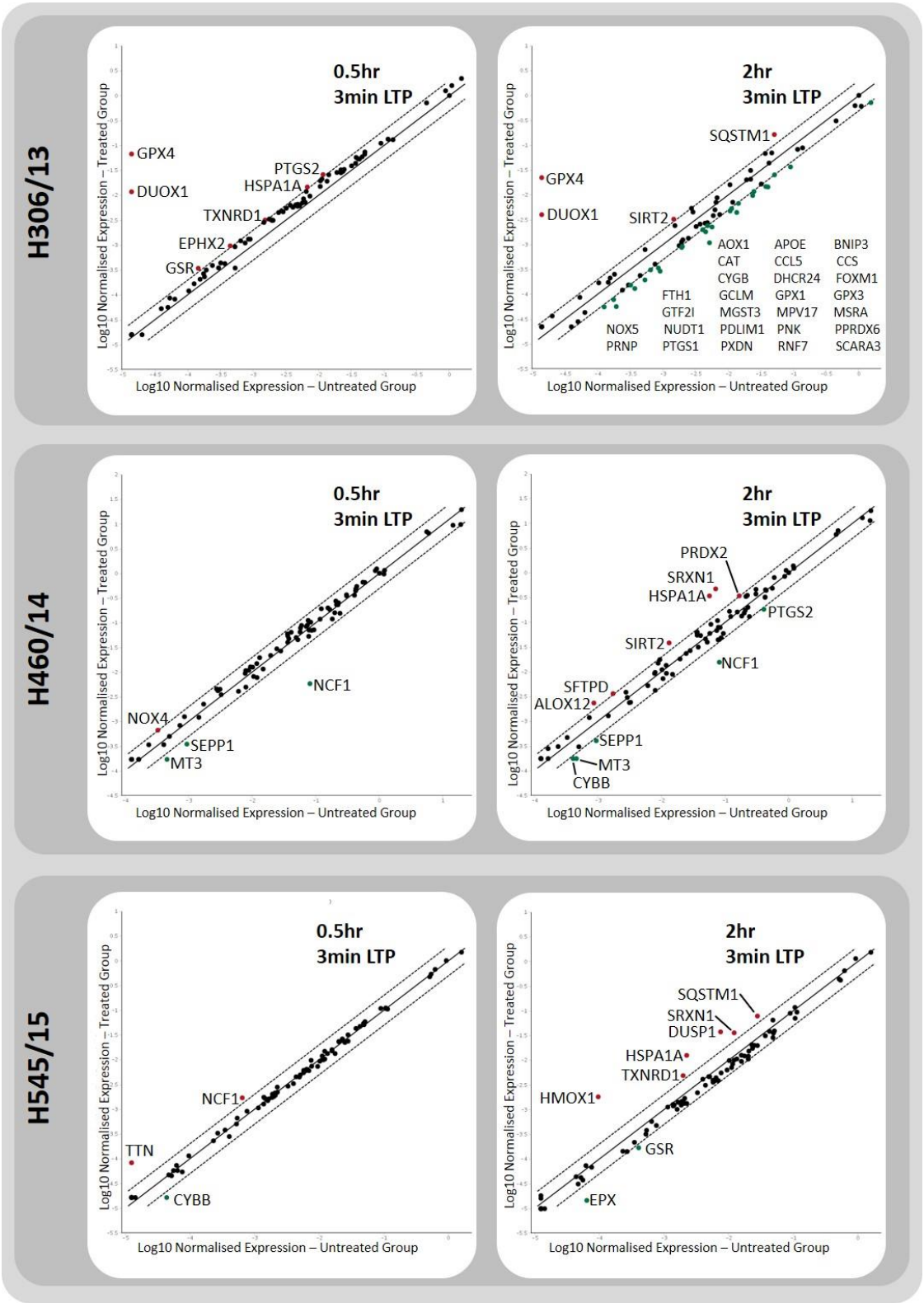

FIGURE 53 - Oxidative stress gene response in three Gleason 9 primary cultures.

Oxidative stress transcriptional response in cultures from patients H306/13, H460/14 and H545/15. Expression was assessed 0.5 and 2 hours after a 3-minute LTP dose. Black solid line denotes “no change” between untreated and treated gene expression, the dashed line (above and below the black solid line) signifies a 2-fold change in gene expression. Upregulated genes are red dots, unchanged genes are black dots and downregulated genes are green dots.

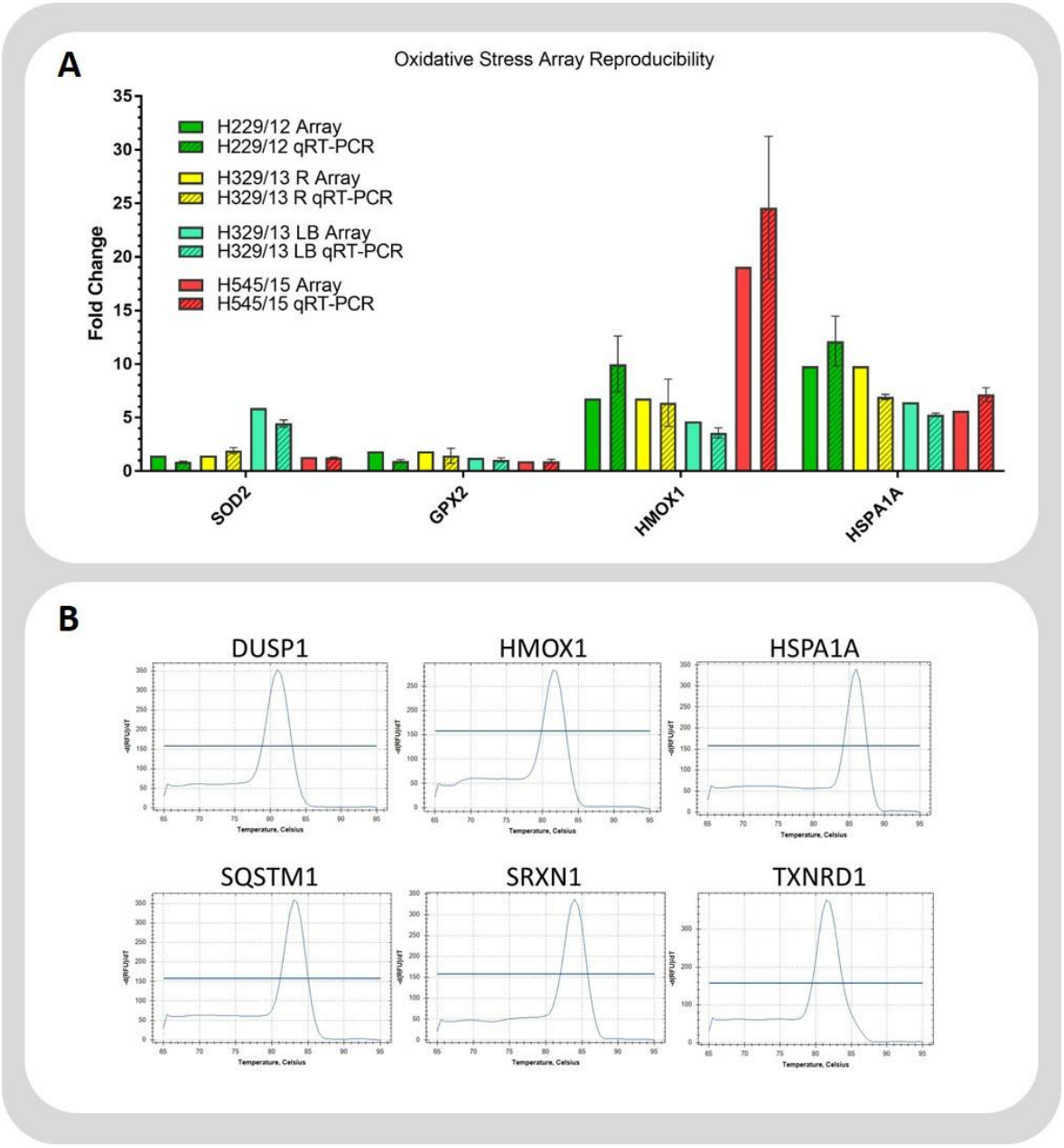

FIGURE 54 - Oxidative stress gene expression qRT-PCR array data was reproducible and robust.

A) Primary culture expression of four genes included on the arrays was measured using TaqMan qRT-PCR 2 hours after LTP treatment. Error bars of qRT-PCR measurements represent SEM of biological triplicates. **B)** Melt curve analysis of recurrently upregulated gene products on the array plates reveals amplification of a single product.

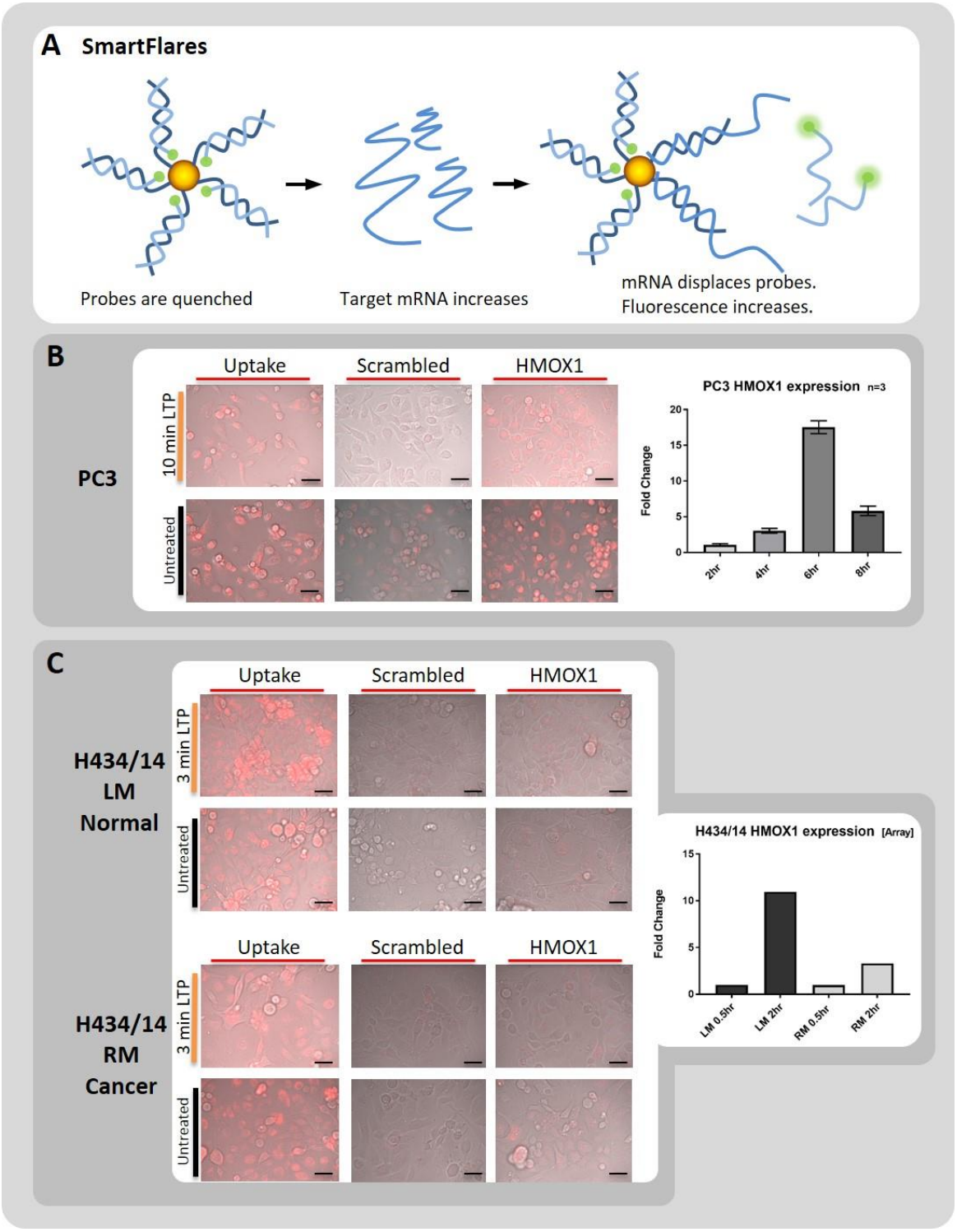

FIGURE 55 - SmartFlares do not accurately represent transcriptional changes in HMOX1 gene expression.

A) Diagrammatic depiction of how mRNA changes can be assessed in real time by fluorescence using SmartFlare gold particles. **B)** HMOX1 SmartFlare fluorescence in the PC3 cell line and comparison to transcript levels detected by TaqMan qRT-PCR. Error bars are representative of the SEM of biological triplicate measurements. **C)** SmartFlare fluorescence in the H434/14 patient matched pair with comparison to HMOX1 mRNA levels detected by Array qRT-PCR. Note different y axis scales in the HMOX1 expression graphs. Black scale bars are 75µm.

5.3 – LTP stimulated the respective activation and accumulation of AP-1 and Nrf2 transcription factors in prostate epithelial cells

The recurrent upregulation of several antioxidant genes by LTP across several tissue pathologies suggested involvement of a common upstream transcription factor/s. Literature supported the involvement of Nrf2 and AP-1 **(709-712, 726, 748)**, both canonical oxidative stress responders, in the induction of gene expression. The activation of both transcription factors following LTP exposure was assessed in patient matched pair cultures. Following 3-minute plasma treatment, the oxidative stress transcription factor Nrf2 accumulated in primary cultures **(Figure 56A+B)**. This effect, determined by densitometry, was more pronounced in the normal tissues of the patient matched pairs, compared to the accumulation of the transcription factor in the Gleason 7 cultures **(Figure 56C+D)**. Levels of Keap1, the protein responsible for Nrf2 turnover in non-stressed cells, were unchanged by treatment **(Figure 56)**. The AP-1 factor Jun was potently activated half an hour after plasma treatment, shown by the phosphorylation (pJun) in treated cells across all cultures of the three patient matched pairs. Activation of the AP-1 signalling axis was further confirmed by congruent activation (by phosphorylation) of Jun's upstream kinase; JNK, by LTP **(Figure 56A+B)**.

Attempts to view Nrf2 translocation from the cytoplasm to the nucleus after LTP treatment were hampered by the discovery that the transcription factor was located in the nucleus of untreated cultures, at least in the two patient matched pairs that were used. Only H209/12 RA showed expected cytosolic staining for Nrf2 in non-stress conditions **(Figure 57A)**. However, upon testing if treatment altered Nrf2 localisation, the initial result could not be reproduced and, in untreated cells, Nrf2 was nuclear as for the other cultures **(Figure 57B)**.

Jun phosphorylation was increased by LTP treatment in all cultures, with typical nuclear localisation of the transcription factor observed **(Figure 58A)**. The same was true of the active transcription factor in the basal epithelial subpopulations (SC/TA and CB). For several cultures (H594/17, H643/17 RM, H646/17 RM) pJun staining after treatment was more intense in the progenitor SC/TA fraction than in the more differentiated CB cells **(Figure 58B)**.

5.4 – Development of a cell line model of primary LTP stress response

Primary prostate cultures can rarely be grown to cell numbers adequate for assessment of transcription factor-response element binding by ChIP. As IF had failed to establish Nrf2-ARE binding after plasma treatment, a cell line model of primary prostate cancer was required to establish whether LTP altered both Nrf2 and Jun response element occupancy and whether this binding to chromatin caused transactivation of genes.

Two cell lines; P4E6 (cancer) and PNT1a (normal) were treated with the stress inducing chemical; sodium meta-arsenite (arsenite). P4E6 cells were more sensitive to the arsenite, with cell death obvious at 10µm dose and, using HMOX1 transcription as a readout, maximum gene expression reached levels four times those observed in the PNT1a cells **(Figure 59A)**. PNT1a also appeared more resistant in cellular morphology, with no obvious increase in cell death, even at the higher doses **(Figure 59B)**.

To map the timing of transcriptional stress response in the cell lines, HMOX1 was used. Following arsenite treatment, P4E6 showed a gradual production of transcript whereas LTP produced a delayed, but, peaked response **(Figure 60A)**. The PNT1a cell line showed the opposite response, with a peaked arsenite response and gradual HMOX1 expression after plasma treatment. The cell line was also much more sensitive to arsenite than plasma **(Figure 60C)**. Transcriptional output of HMOX1 reached greater levels than in the dose-response experiment **(Figure 59B)**. JUN transcription was also assessed in treated P4E6 cells. mRNA levels of the AP-1 factor reacted much quicker than that of HMOX1 and displayed a wave-like curve in response to both treatments **(Figure 60B)**.

LTP was shown to induce a robust and recurrent oxidative stress transcriptional response in primary prostate epithelial cultures which was confirmed by upstream involvement of classical stress-activated transcription factors Nrf2 and AP-1. Cell lines also responded to plasma yet had a longer refractory period than the patient cultures to the reactive species, something which may be attributable to "culture shock"**(reviewed in (749))** where the demands of adapting to the plastic environment have increased capacity to scavenge damaging ROS. As this focused approach had shown that primary cells responded to LTP, global transcriptional changes in treated cells were assessed using a micro-array based approach.

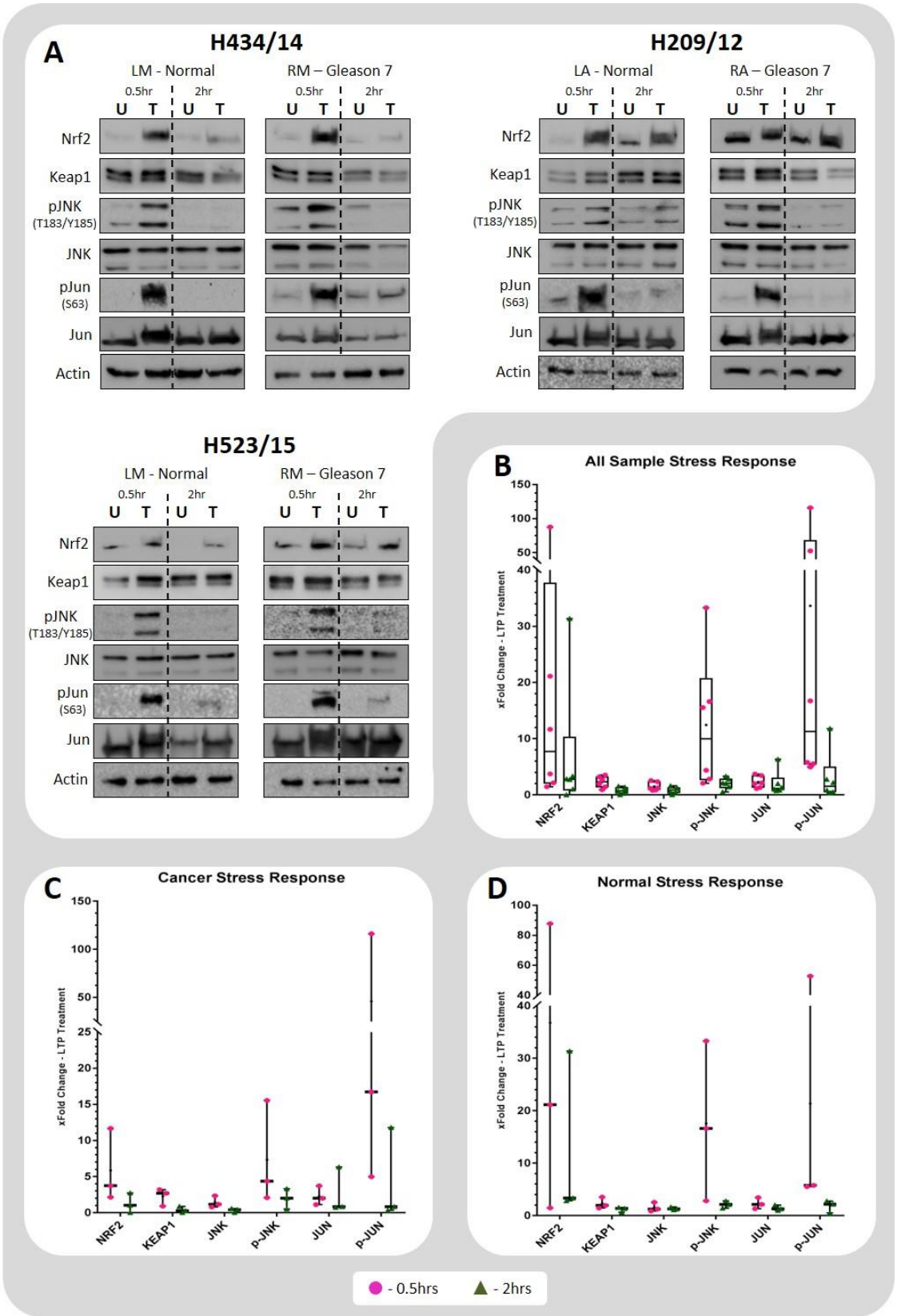

FIGURE 56 -LTP caused accumulation of Nrf2 and activation of AP-1 within 0.5 hours of treatment.

A) Oxidative stress response pathway protein analysis at 0.5 and 2 hours after a 3-minute plasma dose in three patient matched pairs. **B)** Densitometry analysis of LTP induced protein changes in all six cultures (n=6). Each sample's LTP induced fold change is plotted as a single pink circle (0.5hrs) and green triangle (2hrs) on the boxplot. Mean of measurements is plotted as a small (+)

in the boxplots. **C)** Densitometry analysis of LTP induced protein changes in the three normal prostate cultures (n=3) **D)** Densitometry analysis of LTP induced protein changes in the three Gleason 7 cultures (n=3). Note that y axis scales of densitometry boxplots are different.

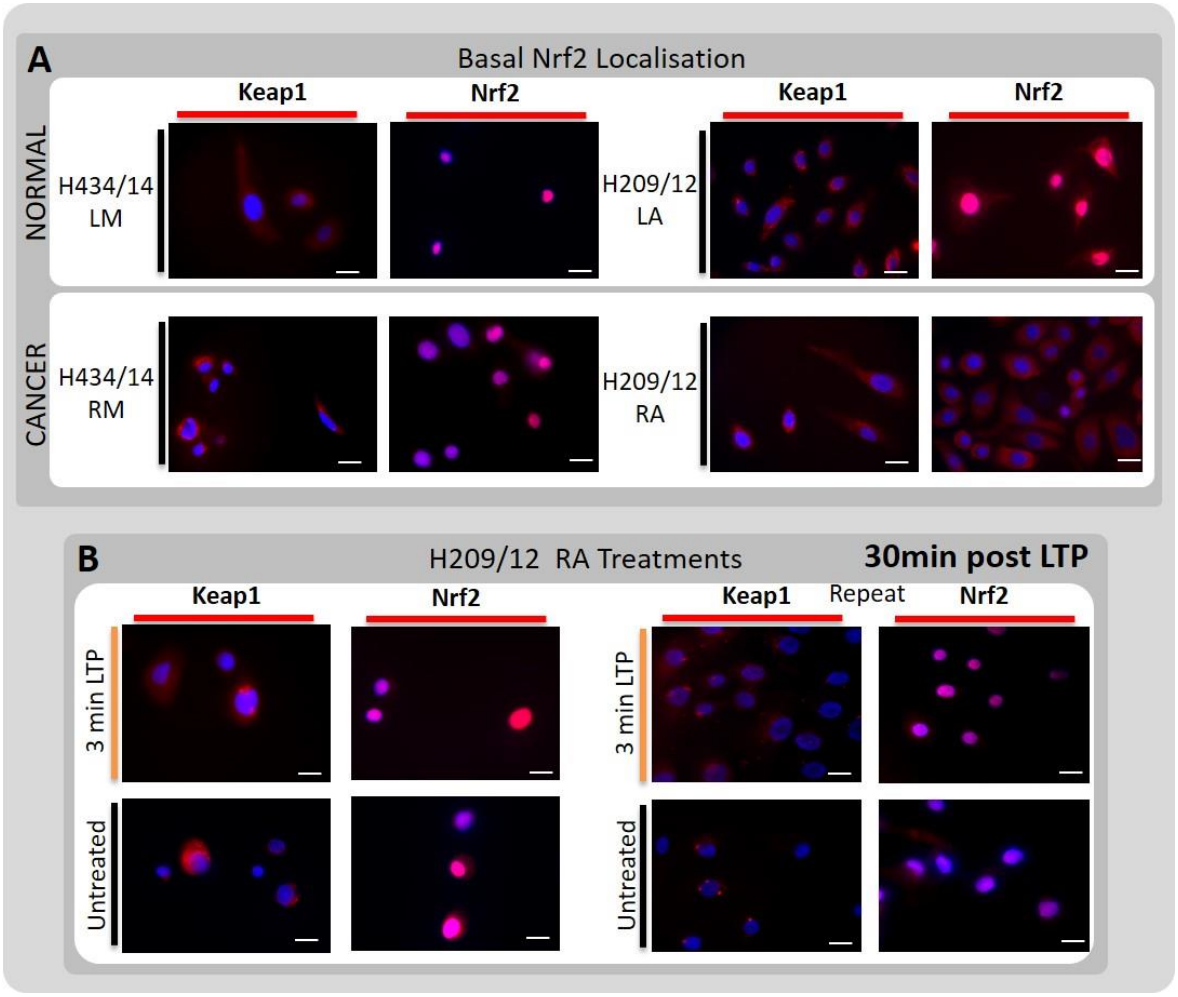

FIGURE 57 - Nrf2 is located in the nucleus of primary prostate basal epithelial cultures.

A) Assessment of Nrf2 and Keap1 localisation in the H209/12 and H434/14 patient matched pairs.

B) Repeat assessment of Nrf2 and Keap1 localisation in the H209/12 RA culture before and 30-minutes after 3-minute LTP treatment. All white scale bars are 100µm.

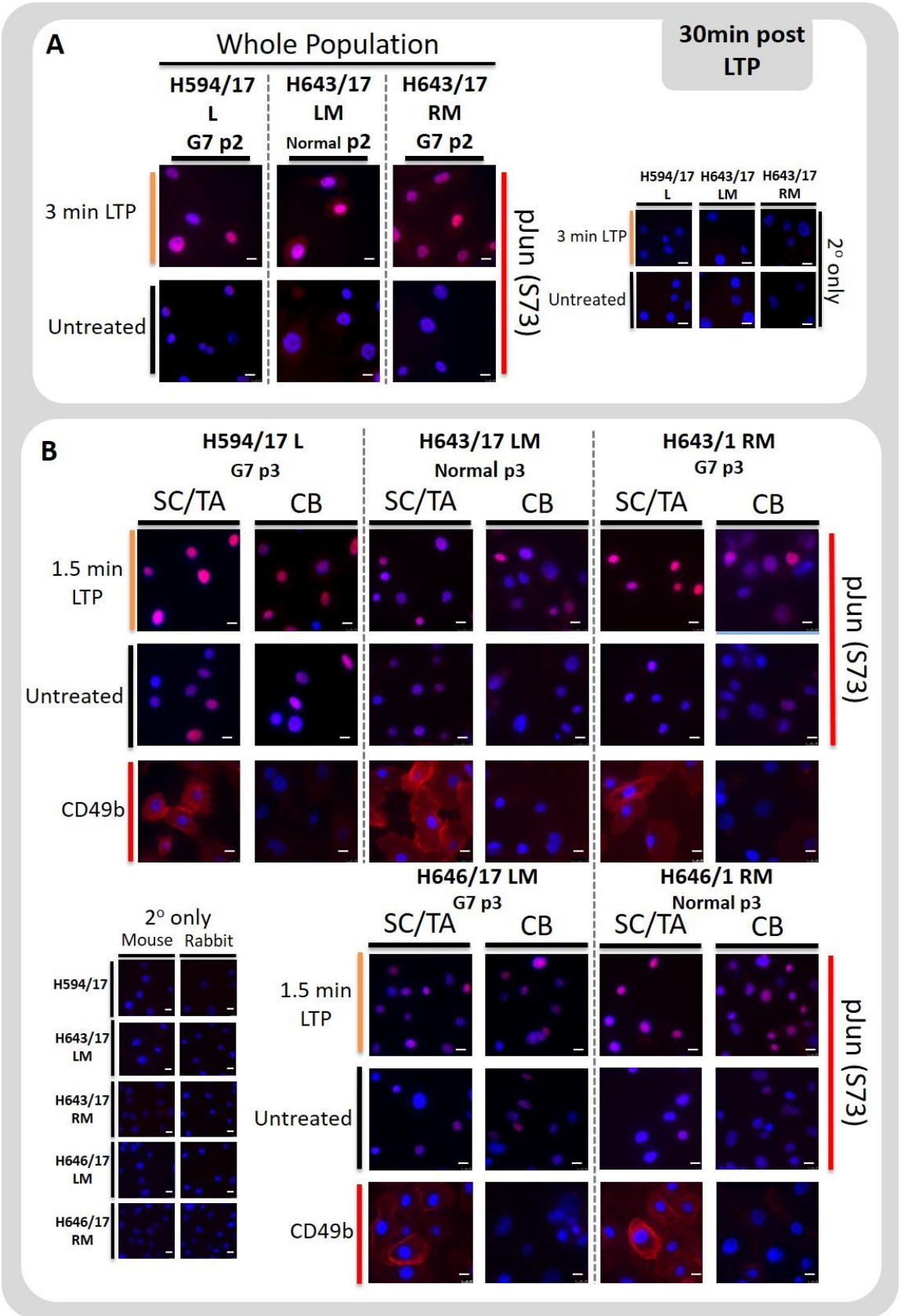

FIGURE 58 - pJun is nuclear in primary prostate cultures and phosphorylation was increased by LTP treatment.

A) Assessment of pJun localisation in three patient's primary prostate cultures 30-minutes after LTP treatment. **B)** Assessment of pJun localisation in the basal epithelial subpopulations of five

patient cultures 30-minutes after LTP. CD49b (α2 integrin) levels indicates a successful separation of SC/TA (high CD49b) and CB (low CD49b) populations. All white scale bars are 100μm.

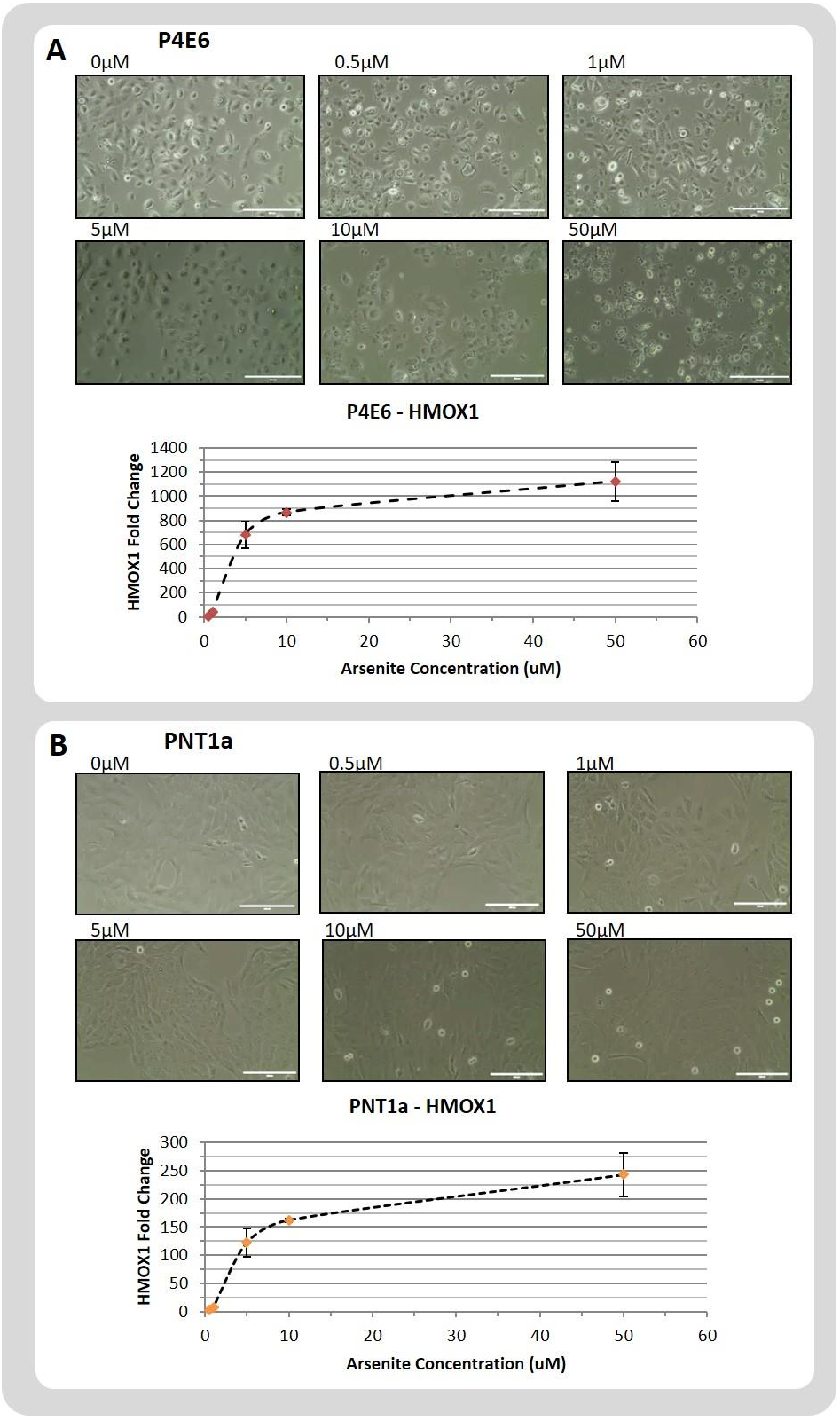

FIGURE 59 - Arsenite dose response in P4E6 and PNT1a prostate cell lines.

A) P4E6 morphology and HMOX1 transcription at increasing doses of sodium meta-arsenite. **B)** PNT1a morphology and HMOX1 transcription at increasing doses of sodium meta-arsenite. All white scale bars are 200µm. Note different y axis scales of the HMOX1 expression graphs. The error bars represent SEM of biological triplicates.

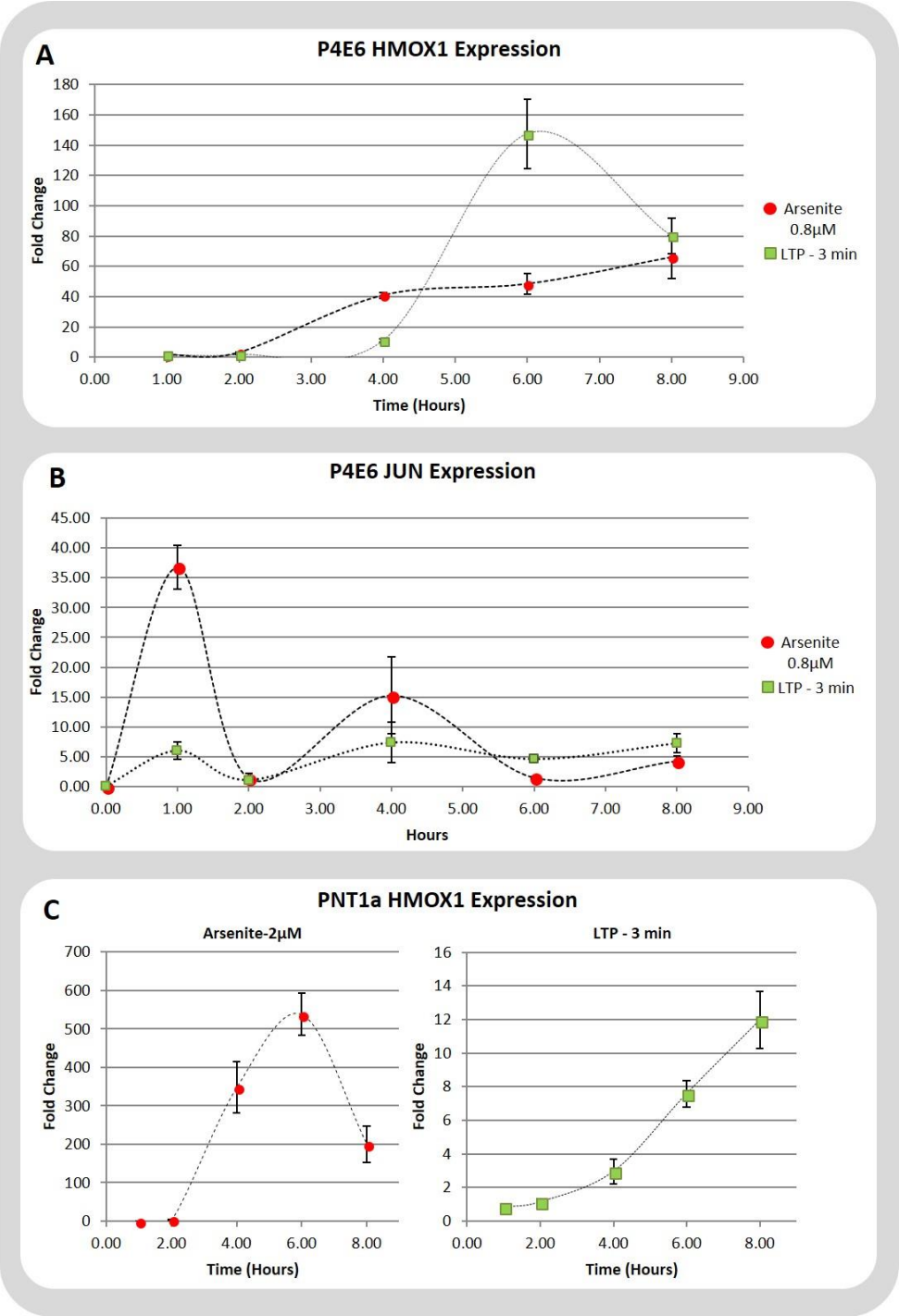

FIGURE 60 – HMOX1 and JUN transcript levels in Arsenite and Plasma treated P4E6 and PNT1a prostate cell lines.

A) P4E6 8 hour time-course of HMOX1 mRNA abundance following treatment with either 3-minute LTP dose or 0.8µM arsenite. **B)** P4E6 8 hour time-course of JUN mRNA amount following treatment with either 3-minute LTP dose or 0.8µM arsenite. **C)** PNT1a 8 hour time-course of HMOX1 mRNA following treatment with either 3-minute LTP dose or 2µM arsenite. The graph is split as LTP-induced expression wouldn't be visible if included with arsenite-induced HMOX1 expression. Note different y axis scales of expression graphs. Error bars of all graphs are representative of the SEM of the biological triplicates.

6. Results– Microarray analysis revealed rapid activation of Notch and AP-1 by LTP

6.1 – Microarray data identified activation of multiple signalling pathways by LTP in prostate primary cultures

As the qRT-PCR Profiler arrays had identified that LTP elicited a recurrent gene expression response in the primary prostate cultures, whole transcriptome analysis of LTP-treated cells was performed to gain a complete picture of the transcriptional changes caused by the treatment.

RNA was harvested from six untreated and treated primary prostate cultures 2 hours after a 3-minute plasma dose. The RNA was taken from two patient matched pairs and two Gleason 9 cancers. Quality of all RNA samples was excellent; with each sample earning a perfect RIN score of 10 and showing strong 28S and 18S rRNA banding in the accompanying electrophoresis images **(Figure 61A)**. Multidimensional scaling (MDS) using the Euclidean distance of each point of transcript expression was able to successfully separate the primary epithelial culture transcriptomes from those of two prostate cell lines; BPH-1 and PC3, that were also submitted for analysis in a separate experiment **(Figure 61B)**. Comparison of treated against untreated samples observed that LTP treatment altered the expression of 645, out of a total 540,000, transcripts on the Clariom D microarray. 544 were upregulated and 101 were downregulated 2 hours after a 3-minute plasma dose **(Figure 61C)**.

Focusing on the upregulated transcripts, it was immediately apparent that genes involved in **NF-kB** (NR4A1-3, RIPK1+4, IL6R, TNFS13B, TNFAIP3, IRAK2, SQSTM1, NFKBIA, REL, NFKB2), **AP-1** (JUN, JUND, FOSB, FOSL1, DUSP5, DUSP10, MAP3K8, MAP2K3) and **Notch** signalling (NRARP, HES1, HEY1, SOX9, ID2, ID3) were activated by the plasma alongside upregulation of many transcription factor genes. (ATF3, EGR2+3, KLF4,9+10) **(Figure 62)**. LIMMA analysis, which accounts for inherent biological variability in gene expression and removes genes that have a wide range of transcriptional variability in untreated samples from further analysis, **(743)** was applied to the 544 LTP-upregulated transcripts and returned 89 upregulated probe-sets, of which 42 were annotated genes **(Figure 63)**. This further confirmed involvement of Notch and AP-1 with a responsive expression of several previously identified transcription factors.

Expression of twelve genes in four independent primary cultures following LTP was assessed by qRT-PCR to validate the signalling pathways implicated in microarray analysis. NRARP was the only tested gene of those chosen to represent Notch signalling to pass validation **(Figure 64)**. The two AP-1 factors JUN and FOSB were expressed consistently following plasma treatment whereas the negative regulator DUSP10 was not **(Figure 64)**. IL6R also failed to pass validation. SQSTM1 and

HMOX1 were upregulated 2 hours post-LTP across the four samples, as were the three NR4A isoforms **(Figure 64)**.

6.2 – Upstream transcription factors Notch1 and Jun are activated by plasma

The transcription factors indicated to be initiating the transcriptional response to LTP in the primary cultures; Notch, NF-kB and AP-1, were assessed in two patient matched pairs over a 2 hour time-course. Nrf2 was also included **(Figure 65 & 66A)**.

Canonical NF-kB signalling was not universally activated by the plasma. IkBα levels remained stable and phosphorylation of the inhibitory protein only occurred in the Gleason 7 cultures of the patient matched pairs **(Figure 65 & 66B)**. Non-canonical NF-kB signalling however, was activated. Following LTP treatment, NIK protein accumulated over the time-course, an effect most obvious in the H646/17 LM culture **(Figure 65 & 66C)**.

Notch signalling was activated in the primary cultures after plasma treatment, which caused a release of the Notch1 intracellular domain (NICD). This cleavage event was most clearly observed in patient H646/17 **(Figure 65)**. Cleavage of Notch1 was initiated almost immediately by LTP and mean levels of the transcription factor peaked 1 hour after plasma dose **(Figure 66D)**.

AP-1 signalling was activated in all of the patient matched pairs **(Figure 65)**. The maximum intensity of Jun phosphorylation occurred, like Notch activation, 1 hour after LTP treatment **(Figure 66E)**. Nrf2 was present at high basal levels in the patient matched pair cultures, and no change in the amount of the transcription factor or its negative regulator, Keap1, was observed across the time-course, with the exception of Keap1 in the H643/17 RM culture **(Figure 65 & 66A)**.

Further analysis of canonical NF-kB signalling found that plasma treatment resulted in no change in the localisation of NF-kB p65, which remained cytosolic; in both whole population (WP) culture **(Figure 67A)** and in the basal epithelial subpopulations **(Figure 67B)**. Western blot data also showed no alteration in NF-kB p65 levels by LTP across four primary cultures. IkBα phosphorylation remained unchanged, yet total protein was reduced by treatment after 2 hours in the H523/15 matched pair – suggesting activation of the transcription factor in this patient **(Figure 67C)**.

Notch signalling was further assessed in three patients, 0.5 hours and 2 hours after LTP. In the majority of these cultures, Notch1 proteolytic activation was increased 0.5 hours after treatment **(Figure 68A+B)**.

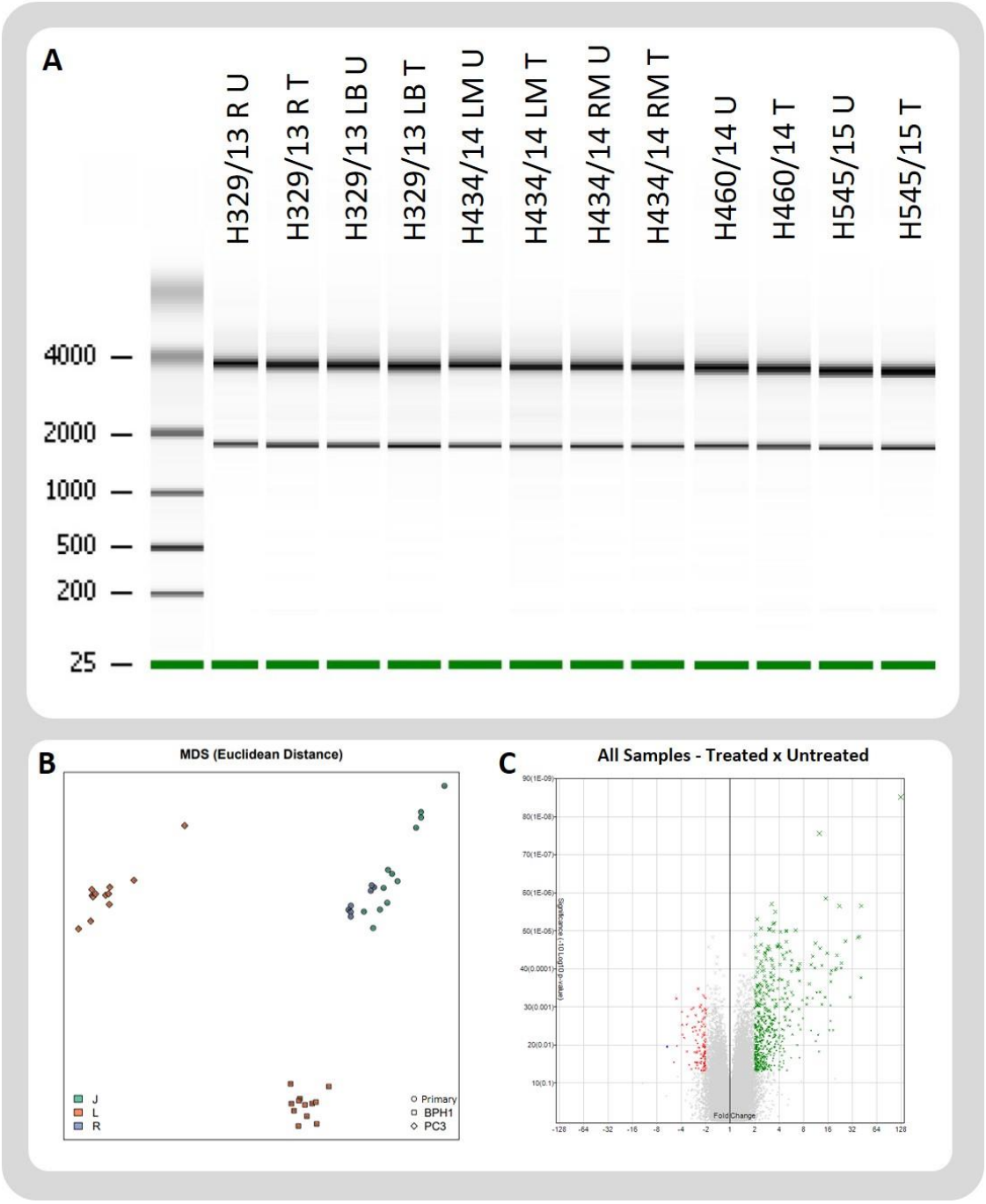

FIGURE 61 - Microarray RNA sample integrity and initial microarray data showed that LTP treatment alters gene expression.

A) Agilent electrophoretic image shows the intact ribosomal RNA in all samples sent for microarray analysis. All samples achieved a perfect RNA integrity score of 10. **B)** Multi-dimensional scaling of all transcripts expressed in the samples, as detected by microarray analysis, was able to separate two prostate cell lines and the primary cultures (top right) into three distinct clusters. **C)** Volcano plot showing significant fold changes in transcript expression at 2 hours post 3-minutes LTP dose in primary prostate epithelial cultures. All samples (2x normal, 2x Gleason 7 and 2x Gleason 9) were grouped and treated was compared to untreated. In total 645 transcripts were altered by LTP; 544 upregulated and 101 downregulated.

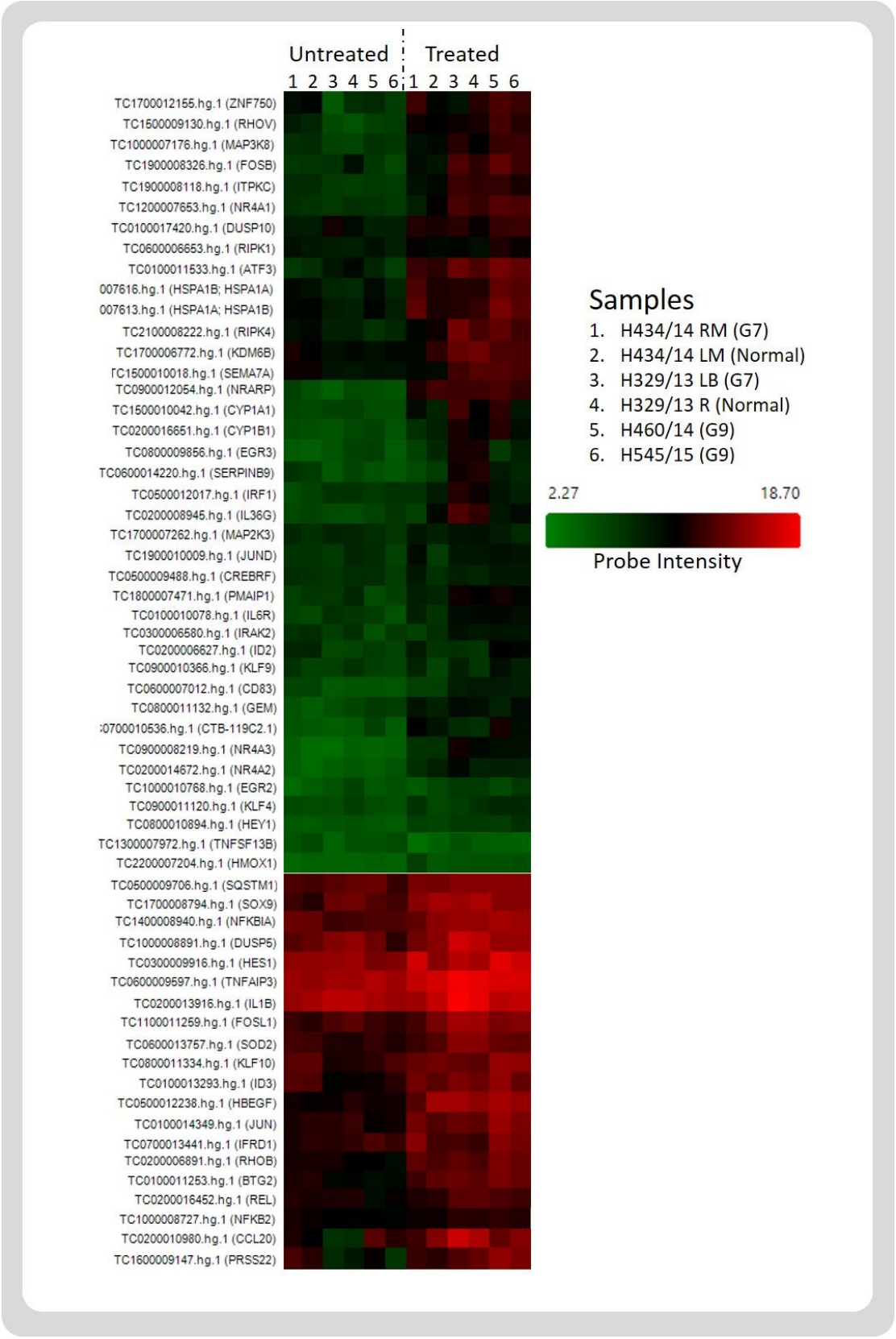

FIGURE 62 - Heatmap of annotated gene expression changes following LTP treatment.

Expression intensity in untreated and LTP-treated samples for genes of interest in the six primary prostate cultures. The heatmap was constructed on Affymetrix Transcriptome Analysis Console 3 and the genes chosen due to relation to activation of related pathways and magnitude of significant expression change.

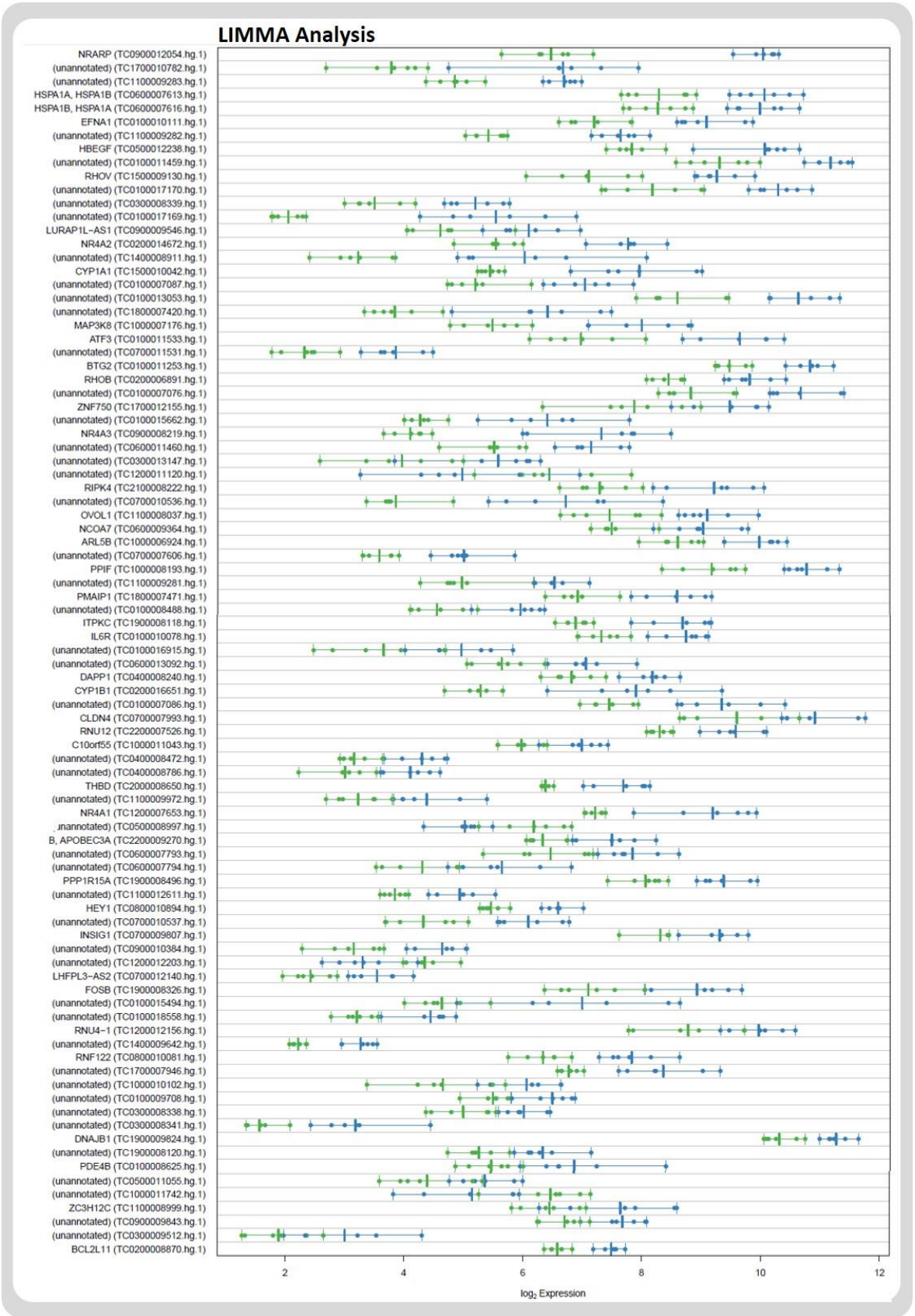

FIGURE 63 - Linear Models for Microarray Data (LIMMA) analysis found 89 transcripts were significantly altered by LTP in primary prostate cultures.

Each sample's expression of the transcript is plotted as a single dot, mean of total population (n=6) expression is represented by the vertical line. Green dots represent untreated, and blue are the treated samples.

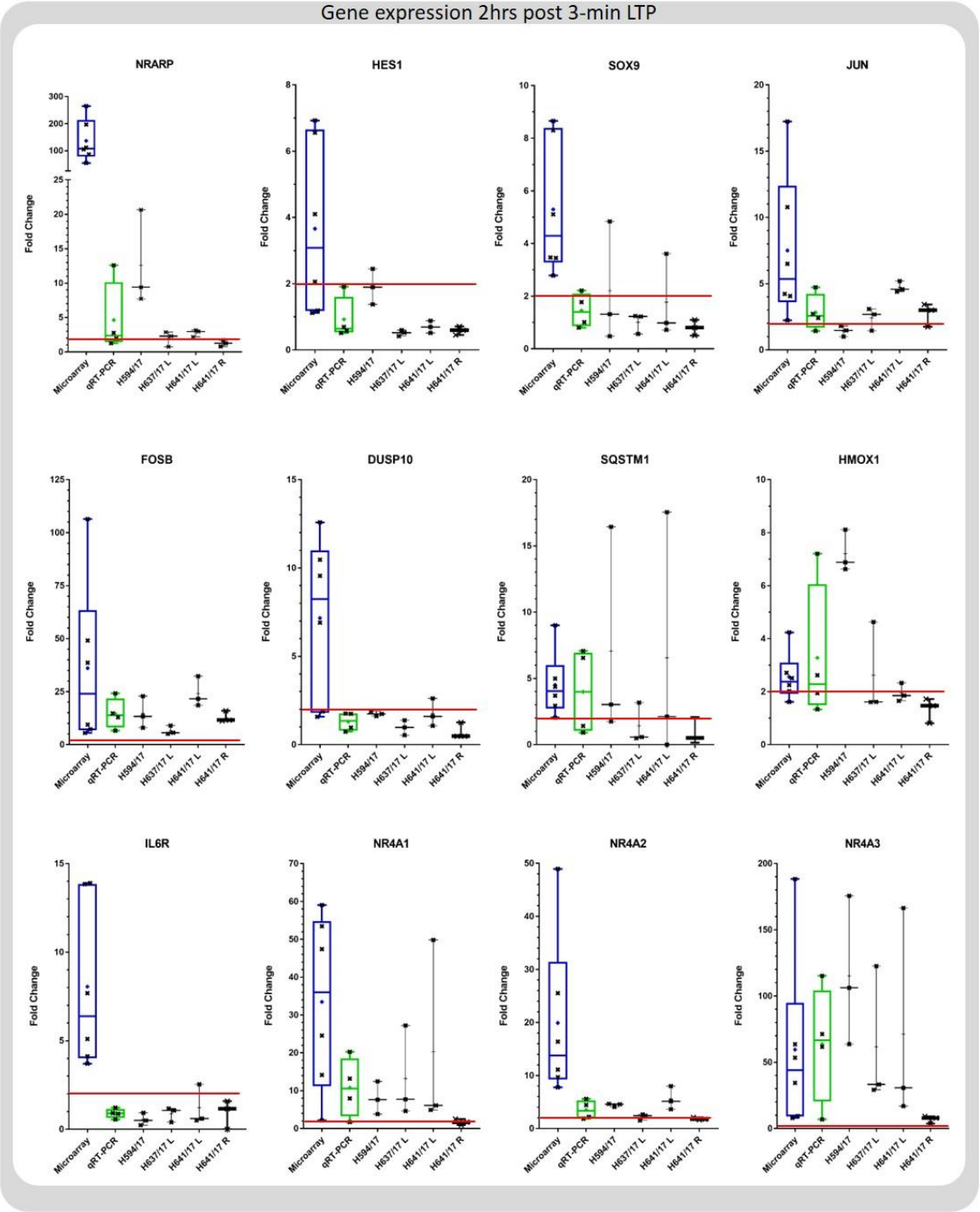

FIGURE 64 - Validation of 12 genes from initial analysis confirmed robustness of the microarray dataset.

Genes were chosen from the Notch (NRARP, HES1, SOX9), AP-1 (JUN, FOSB, DUSP10) Stress response (HMOX1, SQSTM1) and NF-kB (NR4A1-3, IL6R) signalling pathways. The blue boxplot shows gene expression of the six microarray samples, the green boxplot shows average gene expression of the four validation samples, with the individual biological replicates of the validation samples also plotted. 2-fold upregulation is marked by the solid red line across the gene expression data. Mean of sample box plots is indicated by (+). Note that y axis scales of gene expression boxplots are different.

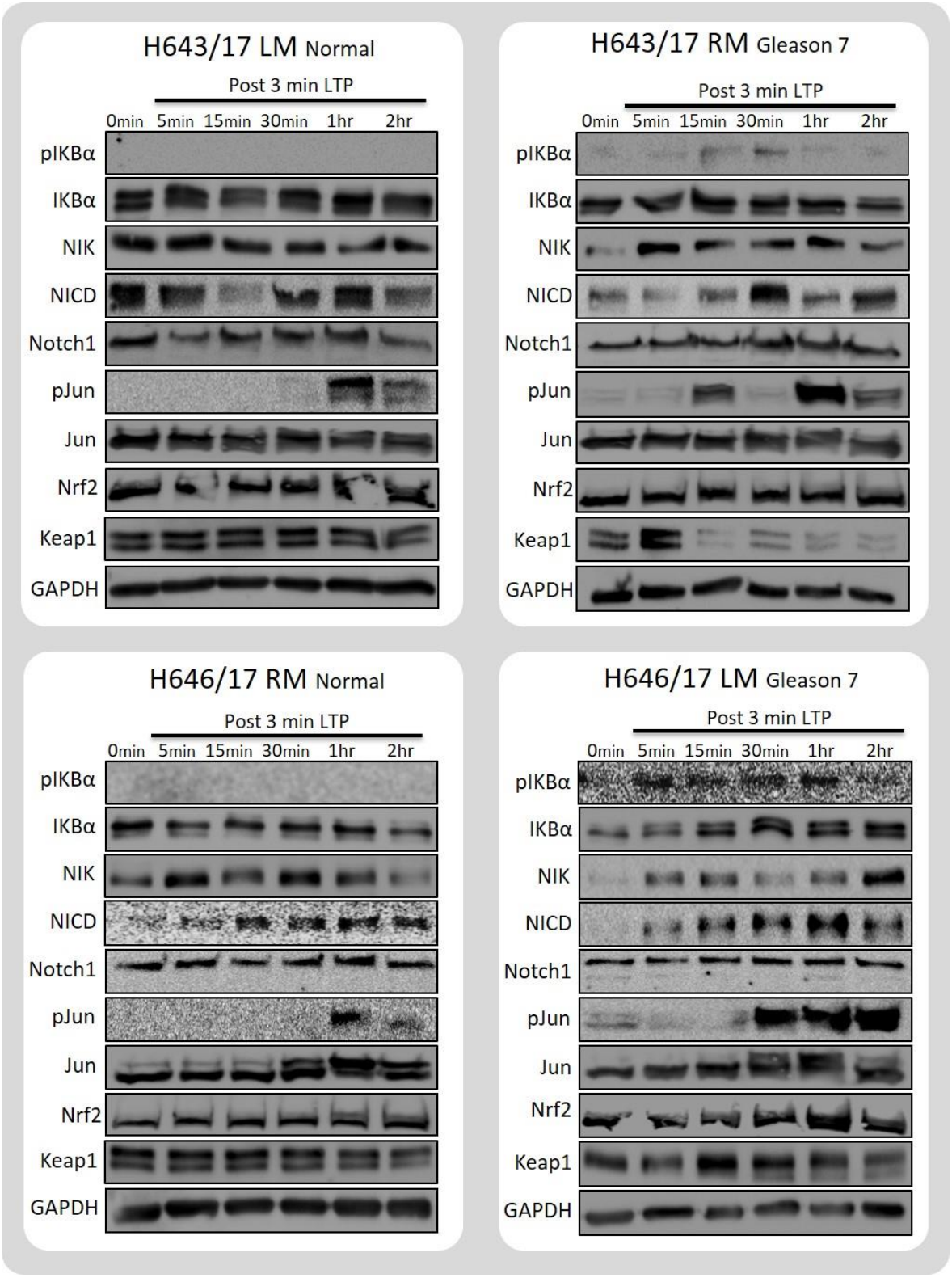

FIGURE 65 - LTP activated Notch and AP-1 signalling in primary prostate epithelial cultures.

Western blot time-course analysis of NF-kB, Notch, AP-1 and Nrf2 signalling in two LTP-treated patient matched pairs.

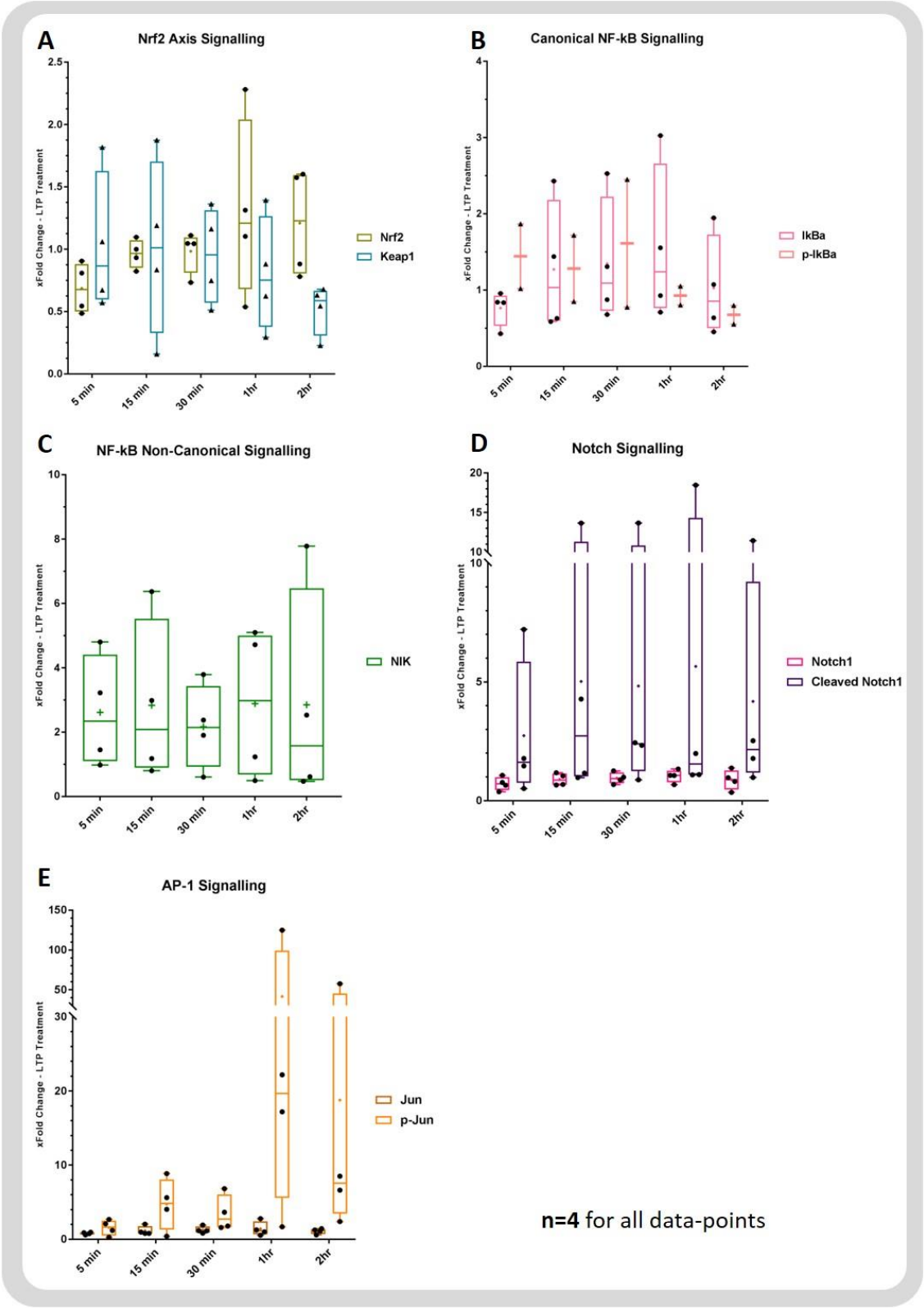

FIGURE 66 - Densitometry analysis of LTP treatment time-course showed activation of Notch, AP-1 and non-canonical NF-kB signalling.

Total protein and activation densitometry analysis of Figure 65 Western Blots. **A)** Nrf2 and Keap1, **B)** Total IkBα and phospho-IkBα, **C)** NIK, **D)** Notch1 and Cleaved Notch1, and **E)** Total Jun and phospho-Jun. Each sample's fold change is plotted with the group mean represented by a + within the boxplot. Note that y axis scales of the densitometry boxplots are different.

6.3 – Stem and transit amplifying cells are the plasma-responsive fraction in primary cultures

As all previous analysis had been conducted in heterogeneous cultures where epithelial subpopulations may have contributed differently to the LTP response, WP cells were separated on their expression of $\alpha_2\beta_1$ integrin. This yielded an $\alpha_2\beta_1^{hi}$ population consisting of prostate progenitors (SC/TA) and an $\alpha_2\beta_1^{lo}$ population of differentiated CB cells. The SC/TA population were the most responsive to LTP **(Figure 69)**. Mean upregulation of the NR4A isoforms in the progenitor population was higher than in both WP and CB cells, with only two exceptions (NR4A3 in H643/17 LM WP & NR4A1 in H594/17 WP). LTP upregulated NR4A1 and 3 in the progenitors to a significantly higher level than that observed in the more differentiated CB cell population.

AP-1 was also more readily activated by plasma in SC/TA cells **(Figure 70A)**. Average Jun phosphorylation in the SC/TA pool was three times that observed in the more differentiated CB cells **(Figure 70B)**. JUN mRNA was increased in all populations by LTP but there was no significant difference in upregulation of the gene between the SC/TA and CB epithelial subpopulations **(Figure 70C)**.

Notch1 signalling was constitutively active in the H646/17 patient matched pair and responsive to LTP in H652b/17 SC/TA. Densitometry analysis revealed that NICD release after plasma treatment was also greatest in the SC/TA pool **(Figure 70E)**. The progenitor subpopulation also had higher levels of the Notch1 receptor than CB cells **(Figure 70D)**. Significant upregulation of NRARP was seen 2 hours after LTP treatment in SC/TA cells but not CB cells from the same patients **(Figure 70F)**. Notch1 staining of plasma treated epithelial subpopulations revealed changes to cellular morphology and contact; some cells rounded up after LTP was administered and most treated cell-sheets were disrupted by the treatment **(Figure 71A)**. LTP altered Notch localisation in four of the five primary prostate cultures treated. Nuclear foci of Notch1 were observed exclusively in the LTP-treated SC/TA subpopulation, 30 minutes after plasma dose **(Figure 71B)**.

The microarray highlighted the diverse molecular response produced by LTP in the primary prostate cultures which was further characterised by validation of the upstream protein components. Activation of stress response pathways of AP-1 and NF-kB was expected, the global approach highlighted the involvement of Notch, a signalling network critical to epithelial differentiation and the human prostate stem cell population **(53)**. Separation of the basal cell populations revealed a heterogeneous response in both the transduction of the signal and the transcriptional output of primary prostate cells following plasma treatment. The activation of Notch and non-canonical NF-kB may prove to be hallmarks of the LTP-resistant population, something which requires further investigation.

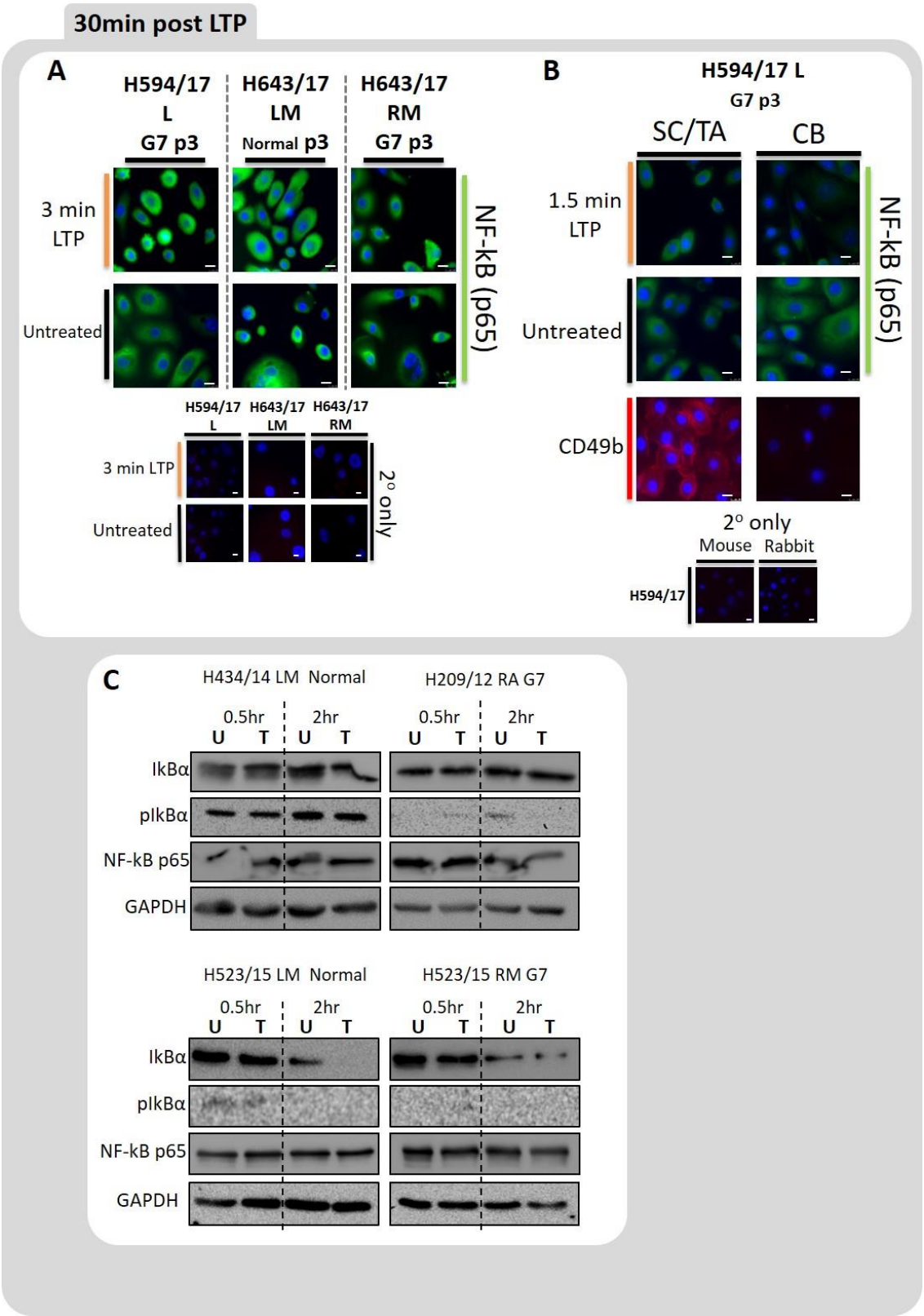

FIGURE 67 - Canonical NF-kB signalling in primary prostate cultures is unaffected by LTP.

A) Immunofluorescence of NF-kB p65 30-minutes post-LTP in treated and untreated cultures. **B)** Immunofluorescence of NF-kB p65 30-minutes post-LTP in H594/17 L epithelial subpopulations. CD49b (α2 integrin) levels indicate a successful separation of SC/TA (high CD49b) and CB (low CD49b) populations. White scale bar is 100μm. **C)** Canonical NF-kB activation protein analysis in four primary prostate cultures.

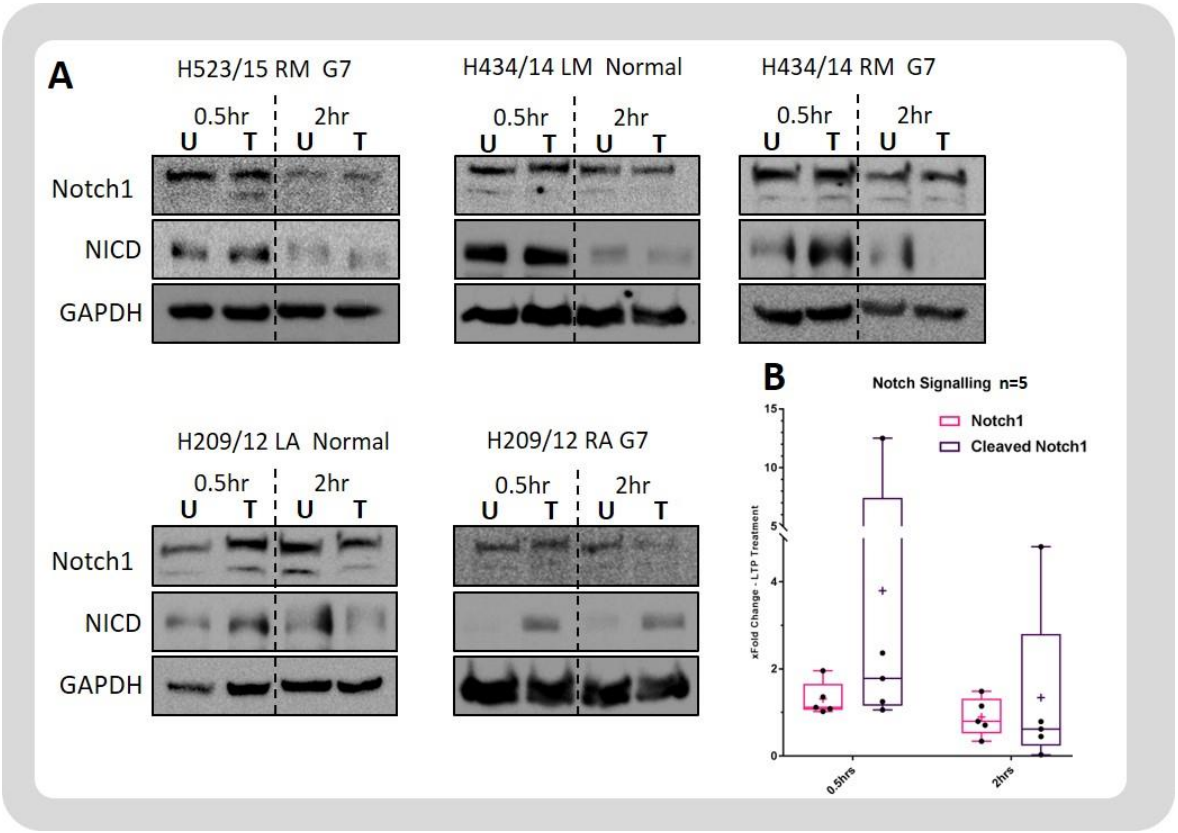

FIGURE 68 - Notch1 is activated by LTP in primary prostate epithelial cultures.

A) Assessment of LTP induced changes to Notch1 receptor total amount and its activation by proteolysis to produce the NICD 0.5 and 2 hours after a 3-minute LTP dose. **B)** Densitometry analysis of Notch1 receptor changes following LTP treatment. Each sample's LTP induced fold change is plotted and the mean is represented by the + inside the boxplot.

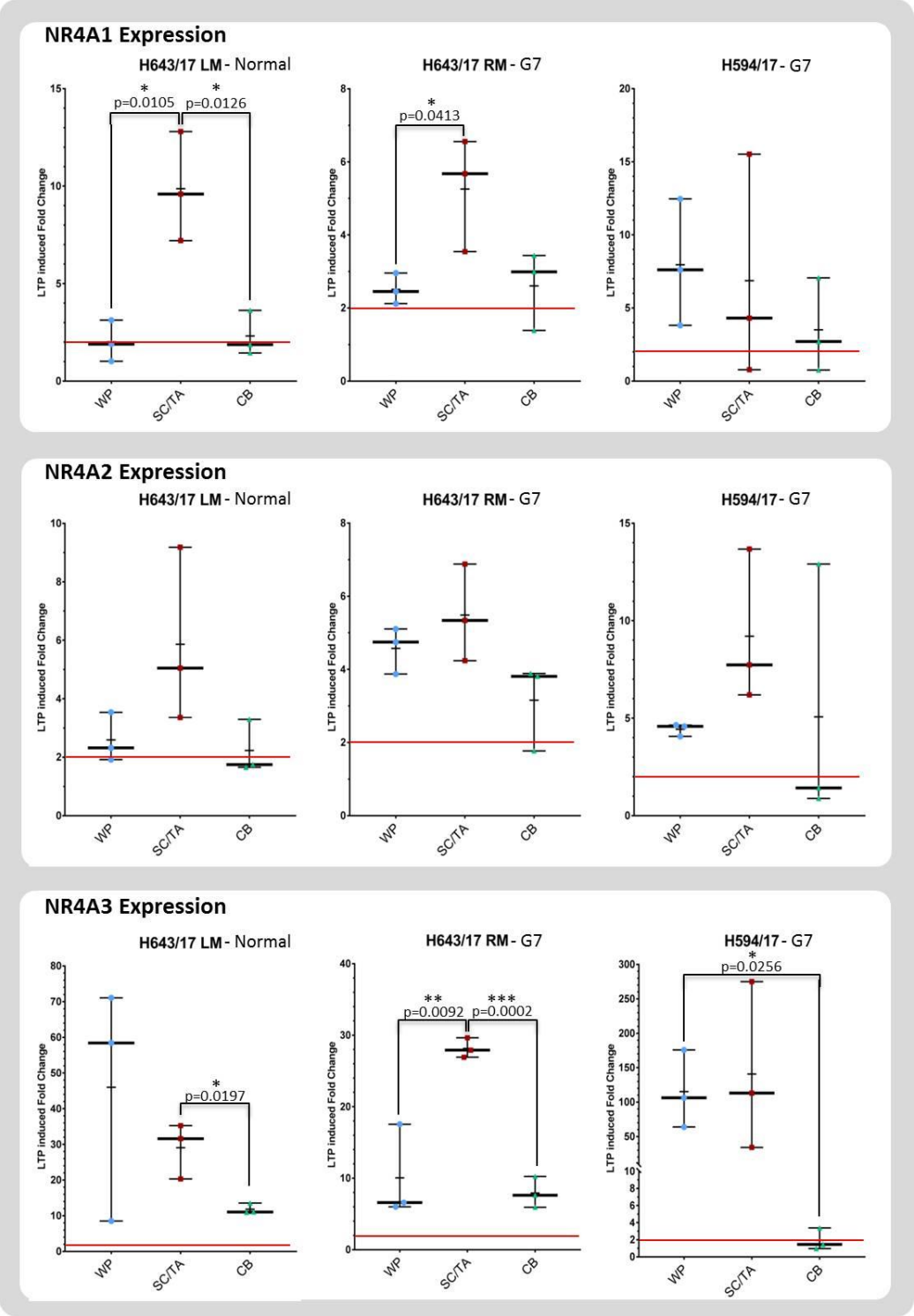

FIGURE 69 - NR4A isoform upregulation by LTP was more potent in the SC/TA subpopulation of primary prostate cultures.

NR4A1, 2 & 3 gene expression in the epithelial subpopulations from three primary prostate epithelial cultures. Individual biological replicates are plotted. The red lines highlight the 2-fold increase required for the gene to be designated “upregulated”. The mean of biological triplicates is represented by a (+) Note that y axis scales of the gene expression boxplots are different. Unpaired t-tests were performed between subpopulation gene expression – significant differences are shown in the figure.

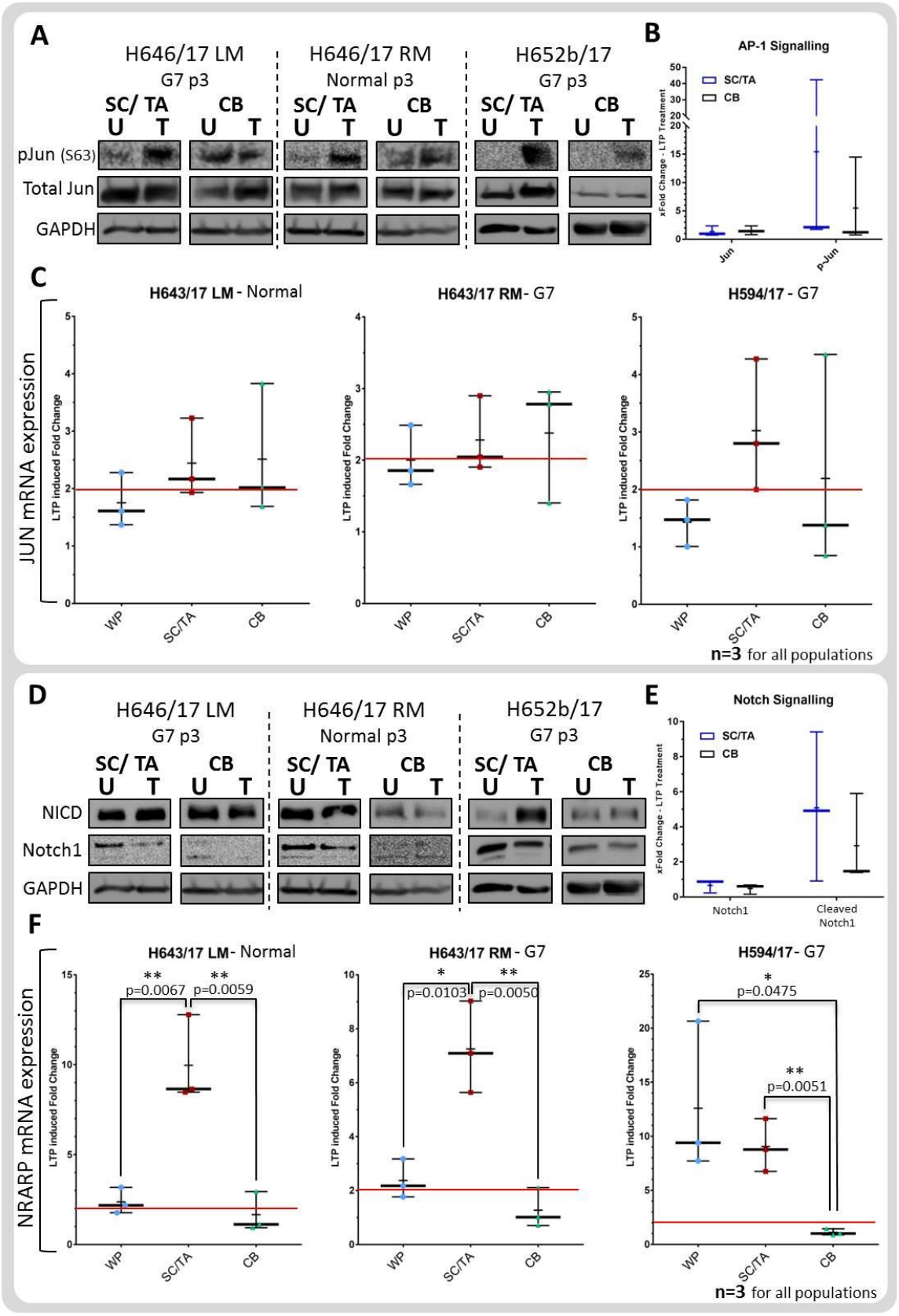

FIGURE 70 - Epithelial subpopulation analysis of LTP-induced AP-1 and Notch signalling.

A) Protein analysis of Jun activation 30-minutes post 3-minute LTP dose in the epithelial subpopulations of three primary cultures. **B)** Densitometry analysis of change in Jun activation in

LTP treated prostate epithelial subpopulations. Individual samples are plotted. Mean of the samples is represented by +. **C)** JUN expression 2 hours post 3-minute LTP dose in the epithelial subpopulations of three primary cultures. Individual biological replicates are plotted. 2-fold upregulation is marked by a solid red line. Mean of biological triplicates is represented as a (+). Note that y axis scales are different. Unpaired t-tests were performed between subpopulation gene expression – significant differences are shown in the figure. **D)** Protein analysis of Notch1 activation 30-minutes post 3-minute LTP dose in three primary cultures subpopulations. **E)** Densitometry analysis of Notch1 cleavage in LTP treated prostate epithelial subpopulations. Individual samples are plotted. Mean of the samples is represented by +. **F)** NRARP expression 2 hours post 3-minute LTP dose in the epithelial subpopulations of three primary cultures. Individual biological replicates are plotted. 2-fold upregulation is marked by a solid red line. Mean of biological triplicates is represented as a (+). Note that y axis scales are different between the patients. Unpaired t-tests were performed between subpopulation gene expression – significant differences are shown in the figure.

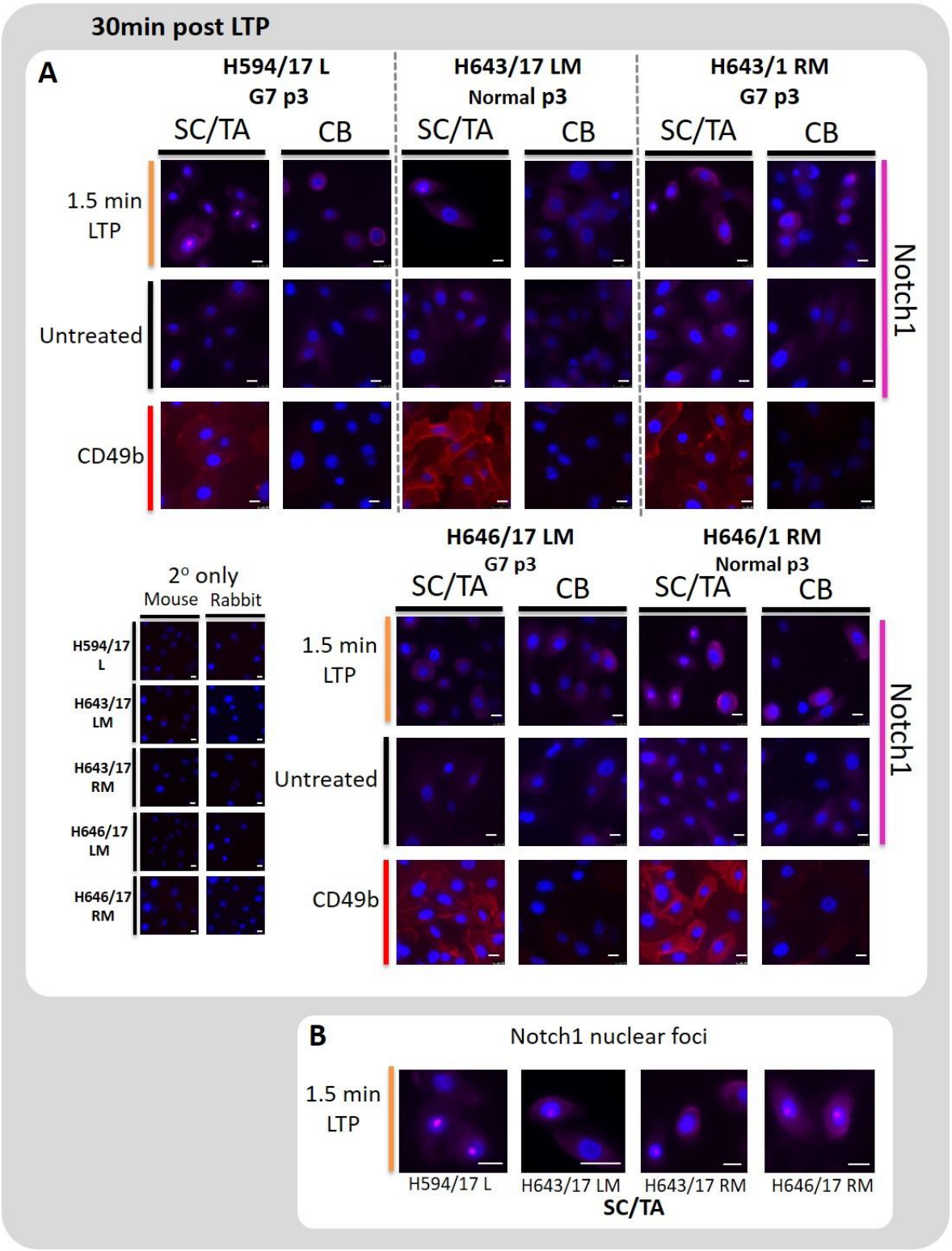

FIGURE 71 - Notch1 was nuclear in LTP-treated SC/TA cells.

A) Immunofluorescence of Notch1 in epithelial subpopulations of five primary prostate cultures. CD49b (α2 integrin) panel indicates a successful separation of SC/TA and CB populations. **B)** Larger images of Notch1 nuclear foci in SC/TA cells of four cultures. White scale bar is 100µm in all images.

7.1 Discussion – Alterations in allelic expression of genes involved in the molecular pathogenesis of prostate cancer

7.1 – Do current cell lines and the primary prostate basal epithelial cultures adequately represent modern prostate cancers?

Mutation is an infrequent event in prostate cancer with most genomic changes achieved by chromosomal rearrangements such as fusions of TMPRSS2 and ERG, and deletions in the PTEN gene **(90)**. AR is the most commonly mutated gene in prostate cancer, yet this molecular aberration only occurs in advanced disease and is selected for by hormonal treatments **(73)**. In primary prostate cancer, SPOP is the most commonly affected gene with publications citing mutation frequencies between of 5-15% in patient tumours. PTEN and IDH1 mutation are even less frequent, observed in ~1% of all tumours **(330, 618)**. In a recent global study of prostate cancer genomes, SPOP and IDH1 mutation defined subclasses of prostate cancers and therefore will have independent disease features and treatment susceptibilities. In order to recapitulate the heterogeneity of prostate cancer we must have models of these disease variants rather than project an all-encompassing conclusion of a treatment outcome or molecular aberration on a single model of disease. Especially now we have knowledge that a significant proportion of patient disease does not readily fall into a single category of prostate cancer or, even with the combined power of whole genomic, transcriptomic and epigenetic data-sets, is able to be grouped at all **(330)**.

7.1.1 - Cell lines

Current commercially available prostate cell lines are limited and most represent the advanced stage of disease with VCaP, Du145, LNCaP and PC3 having all been isolated from metastatic tissue. Whilst common molecular defects such as the TMPRSS2-ERG fusion (VCaP) and PTEN aberration (LNCaP, PTEN, Du145) are represented in cell lines, mutation of SPOP, PTEN or IDH-1 wasn't detected in the panel of seven lines **(351, 451, 453)(Figure 35)**.

SPOP mutation has only been documented in a single cell line isolated in 2014 **(241)**. However, the model hasn't been widely distributed. There is no documented production of an IDH1 mutant prostate cancer cell line, probably due to the low frequency of this mutation in tumours.

7.1.2 - Primary basal epithelial cultures

The primary basal cultures are grown from tissue biopsies isolated from radical prostatectomies. Cancerous tissue biopsies are informed by palpation (feeling the tumour in the organ at time of removal) and assessment of tissue pathology. Palpable tumours with a high rate of Gleason grade

positivity give the greatest chance of growing cultures that originate from cancerous cells. Biopsy cores, harvested with this criteria, typically contain >70% cancer cells **(Unpublished data from 1996)**.

The data collected from the primary prostate cancer cultures show that they mirror population diversity well in regards to minor allele frequency of SNPs and that molecular changes attributed to prostate cancer are present, such as LOH in the PTEN gene **(Figure 36)** and expression of the highly prostate cancer specific TMPRSS2-ERG fusion **(Figure 33)**.

The lack of observable IDH1 and PTEN mutation in the patient population assessed is reasonable due to the expected low frequency of both mutations identified in much larger studies **(330)**. However, not a single SPOP mutation was found in the 55 cancer cultures tested **(Figure 39)**. Although this isn't a large patient group it would be expected that, even at the lower end of mutational frequency (~5%); 2-3 patients would harbour point mutations. There are several other groups that have reported a lack of SPOP mutants in patient cohorts, including that of Guido Jenster in Rotterdam.

Aside from the possibility that SPOP mutations are entirely absent in the tumours from which we have grown the primary cultures used in this study, there are several other possibilities as to why no SPOP point mutants were detected.

Genomic differences between prostate cancers of variant racial/ethnic groups.

Genomic disparities exist between prostate cancers diagnosed in patient cohorts of different races **(750)**. For example, prostate cancers in Chinese men have low frequencies of TMPRSS2-ERG fusions (~6%) and divergent driver chromosomal alterations such as PCDH9 deletions (32%) and amplification of PLXNA1 (23%) **(751)**. The mortality and diagnostic figures based on geography show that different populations of men vary greatly in their disease outcomes **(73)**. Geographical environmental factors also play a significant role in disease outcome, and perhaps molecular pathology **(144)**. The first major SPOP mutation studies **(133)** were conducted in New York/Boston, cities that have far greater racial and ethnic diversity than North Yorkshire where my laboratory sources it's samples from. However this may not be such a decisive factor as a previous study has found that SPOP mutation varied little across ethnically diverse patient cohorts **(618)**.

Outgrowth of normal epithelia.

Although unlikely, it is a possibility that some samples may have had an outgrowth of normal prostate epithelia. Methods are in place to reduce the percentage of normal tissue included in the cancer biopsies, yet in all cases it is impossible to completely remove normal prostate epithelia from the biopsy. Biopsy core cancer positivity is monitored by tissue pathology and most tumour

biopsy sites are palpable through the prostate capsule. The harvesting of sample DNA at low passage limited the chance that normal outgrowth may have occurred and simultaneously will have retained cancer cells in which mutation would be detectable by a sensitive molecular technique such as PCR. Normal cells may out-compete cancerous epithelia in some patient samples, as adaptation to culture is determined on a patient-by-patient basis. Some samples don't grow at all. Therefore it is possible, although highly unlikely due to the presence of PTEN deletion and TMPRSS2-ERG expression in the same cultures, that primary "cancer" cultures may be normal epithelia and thus SPOP mutation wasn't detected.

Mutation is cell type dependent.

SPOP mutations have been detected by studies that process whole-prostate tissue sections **(133, 175)**. This identifies that a mutation is present in the prostate, yet not which cell type it occurs in. Some efforts have been made to identify cell-type using laser capture microdissection. However, due to the skewed epithelial proportions in cancer, this is likely to be a signature dominated by the luminal cells of the tumour **(133)**. A less likely hypothesis is that the mutation is exclusive to stromal cells. Stromal mutations are known to occur in epithelial cancers and aberrant signatures assigned to cancers have later been determined to be stromal, highlighting the difficulties of dissecting information provided by whole-tissue processing **(752)**. The more plausible scenario, as our cultures are grown from prostate basal epithelia, is that the SPOP mutation is in the luminal cells of tumours which do not grow in the culture environment. This would be interesting as it would imply that a separate lineage incurs the SPOP mutation that is then carried into advanced metastatic disease **(73)**.

7.2 Discussion - Stress signalling in LTP treated primary prostate basal epithelial cells

7.2.1 - Primary cultures respond more rapidly to plasma treatment than prostate cell lines

All of the cell lines tested **(Figure 42)** exhibited a delayed transcriptional response to LTP over that seen in the primary cultures. The genomic, transcriptomic and proteomic separation of cell line and primary cultures is well documented **(753, 754)**. Currently, the metastatic stage of disease is over-represented in prostate cancer cell lines **(450, 452, 455, 457, 459)** whereas our primary cultures have been taken and grown from organ confined tumours, the disease state for which LTP if successful, could provide a future treatment. The stark separation of the primary culture transcriptome from that of two basal prostate cell lines in Euclidean analysis of the samples used in this study gives further evidence of the distance from which cell lines can accurately re-capitulate disease, or even "normal", pathologies **(Figure 63B)**. The transcriptional response of the cell lines, peaking 4-8 hours after treatment, was misleading with respect to the primary culture experiments. Some cultures responded within half an hour of treatment (H221/12, H229/12 and H306/13) **(Figure 52 & 53)** with widespread reactionary transcription observed at the 2 hour time-point **(Figure 50)**.

7.2.2 - Oxidative stress is initiated by LTP in prostate primary cultures

Previous work has observed that ROS are generated in primary culture growth medium by low temperature plasma **(304)** with characteristic DNA damage following the induction of the reactive species. This work identified a robust gene expression response is triggered by the plasma, which is very similar to that generated by hydrogen peroxide treatment – implying that this particular species may be a major contributor to the damage initiated by LTP **(Figure 45C)**.

All cultures tested (with the exception of H249/12) robustly express genes involved in oxidative stress response. From the averaged expression data based on tissue type, six genes were highlighted as a core plasma response; HMOX1, HSPA1A, TXNRD1, SRXN1, DUSP1 and SQSTM1 **(Figure 50)**.

HMOX1 and HSPA1A are present in the mean expression data of all four pathologies **(Figure 50)**. HMOX1 translates as the inducible Haem Oxygenase 1 enzyme that permits intracellular ROS scavenging via catalysis of haem metabolism reactions **(755)** and HSPA1A (Heat Shock Protein A1A); a protein folding chaperone (autophagy and ER stress) **(756, 757)** that also has a negative feedback role in NF-kB signalling **(758)**.

SQSTM1 was upregulated in normal and Gleason 7 tissue averages and appears in individual BPH and Gleason 9 samples **(Figure 50)**. The gene encodes an autophagy chaperone protein called Sequestosome 1 or p62. SQSTM1 escorts misfolded protein aggregates to the autophagosome **(724, 759)**. Autophagy is activated in plasma treated prostate basal epithelial cells, so an increase in the molecular effectors of this response was not unexpected **(304)**. The activation of autophagic processes in LTP-response was further confirmed by pathway analysis highlighting enrichment in unfolded protein and ER stress signalling responses in treated cells **(Table 16)**. The misfolding and subsequent aggregation of proteins alongside potential oxidative damage to organelles would initiate autophagy in cells attempting to survive LTP.

Like SQSTM1, DUSP1 upregulation was observed in all tissue pathologies and appeared in the mean expression plots of normal and BPH patient cultures **(Figure 9)**. This gene encodes Dual Specificity Phosphatase 1, a MAPK phosphatase that acts as a pan-specific negative regulator of p38, JNK and ERK activation **(760)**. DUSP1 is classically upregulated in response to stress stimuli **(761)** and functions as an "off-switch" for AP-1 signalling.

SRXN1 was upregulated in all tissue types by LTP and appeared in the mean expression data of both the normal and Gleason 9 samples **(Figure 50)**. Sulfiredoxin 1 acts as a redox regulator in oxidative stress by recycling peroxiredoxins **(762, 763)**. The peroxiredoxins, in their recycled form are responsible for the detoxification of hydrogen peroxide, **(764)** thus a rise in SRXN levels allows cells to buffer an increase in H_2O_2 and ROS. This again suggested, alongside the H_2O_2 treatment data **(Figure 45C)(304)** that peroxide is a major active species induced within cells by the plasma.

Although TXNRD1 (thioredoxin reductase 1) wasn't upregulated in BPH cultures, **(Figure 52)** the enzyme was expressed in response to plasma in the other pathologies and was consistently expressed in the patient matched pair cultures **(Figure 50)**. The TXN system is a major cellular anti-oxidant defence which resolves inappropriate disulphide bridges in proteins that have sustained oxidative damage and restores them to native and functional state. However, in the process TXN itself becomes reduced with its active form being regained through enzymatic action of TXNRD1 **(765)**. Upregulation of this redox regulator suggests that cells enter a state of oxidative stress following LTP treatment and require a larger turnover of active TXN.

The upregulation of the above genes after LTP treatment indicates a state of oxidative stress was produced in primary prostate cultures. Activation of genes involved in protein misfolding, autophagy and ROS scavenging suggests that cells sustain oxidative damage and attempt to respond via a transcriptional response.

7.2.3 - Gleason 7 cultures have elevated expression of oxidative stress genes over their normal counterparts

The relative expression change of genes in response to plasma was measured using treated and untreated cells. Through comparison of both untreated normal and cancerous gene expression from the patient matched pairs it was, firstly, obvious that patient cultures had a divergent expression signature from one another and, secondly, that the Gleason 7 cultures had an elevated expression of several important oxidative stress response genes. For example, the Gleason 7 culture of patient H209/12 shows elevated expression HMOX1, HSPA1A, SQSTM1 and TXNRD1 over its corresponding normal epithelia **(Figure 51)**. By combining the data from the three patients, the prostate cancers again show a heightened expression of several well-known antioxidant genes, including; HMOX1, HSPA1A, GPX2 and SOD3. Prostate cancers do have an inflammatory aetiology that relies upon the control of oxidative species to promote hallmark genomic rearrangements in prostate cells **(72, 73, 666)**.

Metabolic changes in cancer cells are well studied and tumours are known to utilise different energy systems to normal tissues **(766)**. Indeed some cancers have hallmark defects in response to oxidative stress, with allelic variants or mutational expression pre-disposing carcinogenesis **(767, 768)** and transcriptional profiles indicating a higher expression of antioxidant genes **(769)**. Mutation or epigenetic changes in antioxidant transcription factors are also common in cancers, such as those observed for Nrf2 and the transcription factor's associated regulatory network which typically increase baseline levels of Nrf2 in cancer cells to increase their innate ROS scavenging capacity **(770)**. The pathology-dependent transcriptional separation identified in the base expression of the patient matched pairs agrees with previously published differential expression of antioxidant response genes in primary prostate cancer and normal cultures **(771)**.

7.2.4 - The HMOX1 SmartFlare fluorescence doesn't match transcript levels of its target

From the expression data of HMOX1, the gene was upregulated over 20-fold in some cultures after plasma treatment and was the obvious candidate for real-time monitoring of mRNA increases in cells. However, there was no change in SmartFlare fluorescence post LTP, relative to untreated cultures. This was surprising as HMOX1 is an inducible enzyme and therefore its basal/non-stress levels in the cell are low. The generation of ROS by LTP stimulates HMOX1 production in treated cells, as shown by the matched qRT-PCR data, and thus SmartFlare fluorescence should increase **(Figure 55B+C)**. A lack of response was also observed with the other SmartFlare probe being used in our laboratory at the same time. The ineffectiveness of the probes was further confirmed by a recent publication **(772)**. The paper observed that fluorescence variations produced by the HMOX1 SmartFlare were dependent on cellular uptake of the gold particles and not the amount of target transcript in cells. Testing of four other gene probes

achieved the same result; changes in fluorescence didn't match that of true transcript levels. SmartFlares therefore, fundamentally do not work and/or the quality control applied by the distributor, Merck-Millipore, was inadequate. Indeed, the number of commercially available SmartFlares in their inventory has dropped from ~1700 target transcripts to just 6 at present.

7.2.5 - The transcription factors Nrf2 and AP-1 are activated by Low Temperature Plasma in patient cultures

Due to the consistent transcriptional response of the recurrently upregulated genes across the primary cultures it was reasonable to assume that a common upstream regulator/s was activated by the plasma. The involvement of HMOX1 in the response, suggested a role for the redox active transcription factor Nrf2. In fact, upon further literature analysis, all six identified genes had Nrf2 consensus AREs in their promoters **(709-712, 726, 748)**. Nrf2 is activated by LTP in colorectal cancer, keratinocyte and fibroblast cell lines whereupon it aids cell survival **(715, 716)** through transactivation of a cytoprotective expression response initiated by binding to upstream AREs **(714)(Figure 72A)**.

Following plasma treatment, Nrf2 protein levels rose as expected **(Figure 56A+B)**. This was a rapid response, with a snapshot at half an hour post-treatment showing an obvious increase that was then reduced by the 2 hour time-point. This suggests that in the prostate epithelia, LTP induces oxidative stress that facilitates Nrf2 accumulation by redox alteration of Nrf2-bound Keap1. The constant levels of Keap1 in all cultures mean that the observed increase of Nrf2 protein is due to oxidative stress and not a decrease in its negative regulator **(Figure 56A+B)**. The transcription factor is then free to activate gene expression observed at the 2 hour time-point following LTP. The reduction in oxidative stress caused by the gene expression response causes the degradation of the transcription factor, as Keap1 is no longer modified by ROS and can be recycled to its reduced form, facilitating direction of Nrf2 to the proteasome, as is normal in non-stress conditions **(Figure 56)**.

The activation of Nrf2 is more pronounced in normal prostate epithelia than in the cancer cultures as shown by the densitometry analysis **(Figure 56C+D)**. This may imply that normal cultures can respond to oxidative stress better than their corresponding Gleason 7 cancers, however follow up work tracking the outcome and cellular fate of this antioxidant signalling is required before any conclusion can be drawn from this data. Basal levels of Nrf2 protein are higher in the cancer cultures (H209/12 RA and H523/15 RM) thus a less potent activation is expected. This observation also highlights that prostate cancers do have alterations in their base antioxidant levels and activities, also shown in the elevated expression of oxidative stress response genes in Gleason 7 cultures **(See Section 1.9 & Figure 51)**.

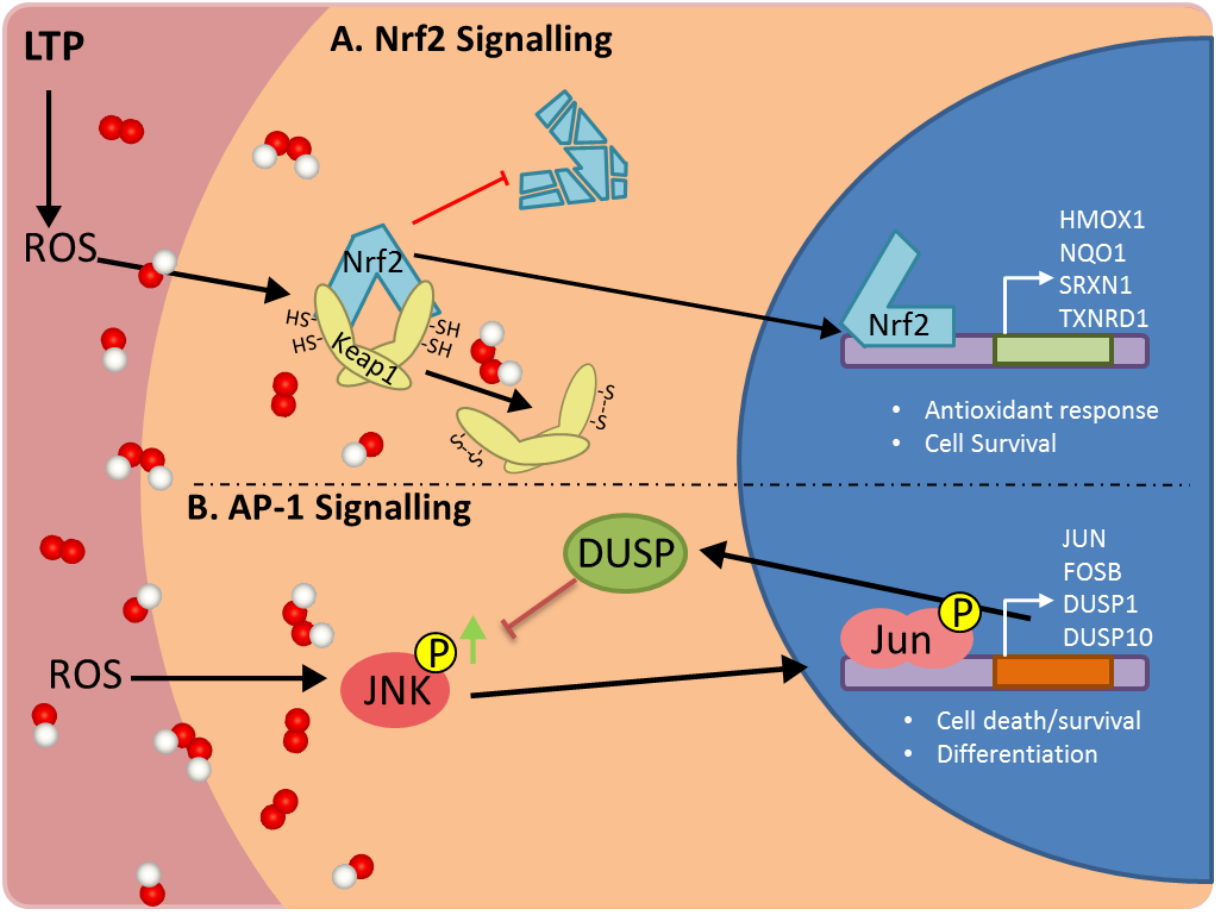

FIGURE 72 – Stress induced Nrf2 and AP-1 Signalling.

A) In non-stress conditions, binding of Keap1 to Nrf2 promotes the proteasomal degradation of the transcription factor. In oxidative stress, ROS modify key cysteine sulphydryl groups on Keap1 causing a conformational change in the protein. This prevents Keap1 binding of Nrf2 and frees the transcription factor. Nrf2 translocates to the nucleus and affects antioxidant gene expression to promote cell survival. **B)** The stress activated protein kinases, including JNK, are activated by ROS. JNK then activates the AP-1 transcription factor Jun, by phosphorylation, to promote gene expression. AP-1 signalling can affect multiple cell fate outcomes.

It was hypothesised that LTP treatment would cause translocation of Nrf2 from the cytosol into the nucleus of cells. However, the immunofluorescence data showed that Nrf2 is already localised in the nucleus in untreated cultures **(Figure 57A)** with perhaps a slight increase in nuclear intensity upon plasma treatment **(Figure 57B)**. Nuclear localisation does not necessarily determine functionality. It is entirely possible that nuclear Nrf2 in untreated cells is not bound to AREs, with a switch being made upon LTP treatment. To test this directly using chromatin immunoprecipitation (ChIP) however is extremely challenging due to the low cell numbers of primary cultures. Native ChIP, that is primarily used for detection of histone tri-methylations (and a limited repertoire of transcription factors), has been reported, for whole genome analyses, at cell counts of <1000 **(741, 773)**. X-ChIP a method that crosslinks the DNA to transiently bound transcription factors however requires an input of much larger cell numbers. The protocol attempted in our laboratory needed ~$20x10^6$ cells **(774)** and current leading techniques require 100,000 cells **(775)**. Adaptation of new techniques will require optimisation in the primary cells but, in future, should remove the limitations of working with low amounts of cellular material.

Although Nrf2 represented the most obvious transcription factor to be activated by plasma in the primary cultures from the gene expression analysis, recurrent DUSP1 upregulation was a major clue to AP-1 activation **(Figure 50)**. The DUSP1 gene is responsive to oxidative stress and the protein product; dual specificity phosphatase 1, a MAPK phosphatase, acts as a negative regulator of p38 and JNK, the stress-activated protein kinases **(776)**. Effectively, DUSP1 is an "off-switch" for AP-1 signalling **(Figure 72B)**.

AP-1 factors and upstream kinases, like the Nrf2 response, have previously been observed to be affected by LTP. Cell line studies have reported phosphorylation of JNK, p38 and ERK in response to plasma, **(679, 687, 716, 777)** with an increase in the protein expression of Jun and Fos also resulting from the treatment **(717)**.

The AP-1 axis of prostate epithelial cells is activated by plasma, with rapid phosphorylation of the DUSP1 substrate; JNK, followed by phospho-activation of the AP-1 factor Jun **(Figure 56A+B & 72B)**. The pJun immunofluorescence confirmed the AP-1 activation observed by Western blot. Nuclear localisation of the active transcription factor was observed only after treatment in whole cultures **(Figure 58A)**. This study is the first to establish Jun phosphorylation as an outcome of plasma treatment. The response is conserved across the patient matched pairs where the activation of Jun is amplified by active JNK in the signal transduction process **(Figure 56B)**. This signal amplification appears to be larger in the cancer cultures, which is attributable to the high base levels of pJNK in the H209/12 and H434/14 Gleason 7 cultures **(Figure 56 A,C+D)**. Elevated pJNK is a requirement for some cancers that rely on Jun for oncogenesis and growth **(778)**. A high base tumoural level of active JNK or Jun may be a hallmark of that patient's disease.

7.2.6 - Interpatient heterogeneity, and not tissue pathology, is the main generator of variability between the oxidative stress transcriptional response in primary cultures

There exists in the field of LTP treatment of cancer, a contentious theory; that cancerous cells have an increased sensitivity to LTP compared to their normal counterparts **(779)**. There are now many papers dedicated to this phenomenon; however all of them probably include some misinterpretations. Some studies use, for comparison, a normal cell line derived from a separate organ site **(696, 780-782)** or use cultures derived from separate lineages (such as epithelial and mesenchymal cells) **(715)**. Inter-patient heterogeneity is also neglected as a determining factor in treatment response when cell lines from the same organ and cell type are compared **(777)**.

There is a possibility that the selective effect does exist, as some cancers do have recurrent and hallmarked defects in antioxidant defences **(783)** and plasmas may exploit this Achilles heel in localised treatments. However, no study has provided sufficient evidence to make such a bold claim. Obvious variables in cell studies have not been accounted for and other alterations in cell culture biology such as the imposed immortalisation of "normal" cell lines aren't acknowledged. Differences in culture medium constitution also impose further artefacts upon conclusions drawn from these studies.

In this study of LTP response in normal and cancerous prostate epithelia, the heterogeneity evident in the gene composition, timing of response and in the magnitude of individual gene expression meant that individual patients, regardless of disease pathology, couldn't provide a divisive signature. The experiment was designed to include four states of prostate tissue; normal, BPH, Gleason 7 and Gleason 9 cancer to discern if there was a difference in how they responded to the same plasma dose. However, in the primary prostate basal epithelial cultures, there was no clear divergence of gene expression response at the 2 hour time-point. Instead a core group of six LTP-induced genes was identified across the four tissue pathologies **(Figure 50)**. No great variance in the LTP-response transcriptional profile was expected between disease states as previous work showed little difference in downstream damage and salvage pathways initiated by the treatment in patient matched pair cultures **(304)**.

This work represents a true normal/cancer comparison with the patient matched pairs supplying tissue isolated from the same individual yet with different disease pathology. There is extensive work detailing prostate cancer associated genomic and transcriptomic differences between normal and cancer primary cultures **(66, 246, 323, 771)**. Cultures were grown in the same medium and were not immortalised. There are no differences apparent between normal and cancer in cellular viability or colony forming efficiency **(304)** after an LTP dose**.** The same is true at the molecular level of gene expression **(Figure 50)** and protein response, **(Figure 46 & 65)** where no

recurrent differences can distinguish between the tissue pathology. The main generator of variance appears to be the biology of each individual patient's prostate.

If tissue pathology was unknown for the individual patient 2 hours post-LTP scatterplots, any attempt to sort the patients (on the basis of gene expression response) into the four separate tissue pathologies using the average gene expression profiles **(Figure 50)** would be completely unsuccessful. No divisive signature in the gene expression response is apparent across the individual scatterplots **(Figure 46, 47, 48, 52 & 53)**. The only near match of an individual patient to any of the tissue pathology 2 hour average gene expression signatures produced by LTP is H545/15 (Gleason 9), which would be identified as a normal prostate epithelial culture **(Figure 53)**.

The protein data draws the same conclusion; that cancer and normal cannot be separated based upon their LTP response, with slight differences only evident between individual patients. The stress signalling of Nrf2 and AP-1 are interchangeable between disease state and to a degree, between patients **(Figure 56)**. Notch signalling is also extremely variable between normal and cancer and seems to be determined by the patient of origin. For example, in the time-course Western blots, NICD activation is more similar between the cultures from the same patient than the disease state of normal or Gleason 7 **(Figure 65)**. This implies that a patient's background biology, rather than that of the disease seems to be driving the heterogeneity observed in transcription factor responses.

7.2.7 - A model of a model; using P4E6 to map LTP induced stress responses in the prostate

Primary cultures are a useful model of patient disease, which they mimic more closely than cell lines can achieve, however they are slow growing, difficult to transfect and have a limited life-span in culture. This hampers analysis using methods that require high cell numbers or those that alter cell biology using plasmids. As Nrf2 localisation in cells post LTP treatment was ambiguous in the primary cells, testing of Nrf2 occupancy and activation of AREs following plasma was attempted using ChIP and reporter luciferase assays in the P4E6 cell line. The same experiments were chosen to assess Jun activity in the prostate cancer cell line following plasma treatment.

P4E6 are a cell line which models localised prostate cancer that was generated from a primary culture grown in my laboratory. Immortalisation was achieved using the HPV 16 E6 protein **(449)**. The cell line has a basal morphology and behave extremely similarly to the primary epithelial cultures. Current work using ptychographic live cell imaging has given insight into the morphology, migration, size and other cellular variables of primary and cell line cultures **(784)**. Of the cell lines used, P4E6 is the closest representation of primary prostate epithelial cells. By using

P4E6 the limitations of the primary cultures can be avoided, whilst utilising a cell line model that resembles patient disease. PNT1a were chosen simply as they could be used as a “normal” cell line control to the induced stress responses of the study.

As the oxidative stress produced by LTP in the primary cultures was transduced through Nrf2 and AP-1 transcription factors; arsenite was selected as a chemical inducer that could generate a similar stress response in prostate cells. This chemical has been used previously to activate both Jun **(785, 786)** and Nrf2 **(710)**. In cell line studies of oxidative stress, arsenite could be used to stimulate a like-response in P4E6 and PNT1a cells. From initial dose curve analysis, it was immediately apparent that P4E6 were much more sensitive to arsenite than PNT1a cells. This was visible both in cellular morphology (appearance of vacuoles and abnormal processes in all arsenite concentrations) and apoptosis evident from ≥1μM, and in HMOX1 expression, with 1000-fold upregulation at higher doses **(Figure 59A)**. In comparison PNT1a cells were resistant to arsenite, with no obvious increase in cell death in culture and a, still potent, yet greatly reduced HMOX1 transcriptional response **(Figure 59B)**.

From this experiment, **(Figure 59)** a dose of 0.8μM for P4E6 and 2μM for PNT1a were chosen for ChIP and luciferase assays as they produced a ~50-fold upregulation in HMOX1 in each cell type, according to the dose curve, a response comparable to the 20-fold change following plasma in the primary cultures.

The timing of both plasma and arsenite responses was measured over an 8 hour time-course to find the optimum window to conduct Nrf2 and AP-1 ChIP analysis. Nrf2 timing was estimated by using HMOX1 transcription as a readout of activity. In P4E6, the cumulative response of gene expression produced over the 8 hours by arsenite was expected due to the cells constant exposure to the dose over the treatment course **(Figure 60A)**. HMOX1 transcript levels reached those previously observed in the dose response experiment **(Figure 59A)**. The HMOX1 response to plasma also proceeded as expected and the single “hit” treatment produced a peak of gene expression at 6 hours **(Figure 60A)**. This again shows that even for the P4E6 cell line, which has been generated from a primary culture, the speed of transcriptional response is much slower than that observed in primary cells. For the PNT1a cell line, the results were quite puzzling. HMOX1 transcriptional levels reached much higher magnitude than was observed in the dose response experiment and the cumulative and peaked curves were reversed. The intensity of response between arsenite and plasma treatments were also very different, with the PNT1a appearing to be resistant to the 3-minute plasma dose **(Figure 60C)**. This may be due to particular antioxidant levels in the cell line that are able to buffer the effects of the arsenite whilst the plethora of reactive species induced by plasma treatment caused damage that wasn’t able to be reconciled over the frame of the time-course. It also serves to highlight that the complexities of a cell-wide

and context dependent response cannot be equated to the transcriptional readout of a single gene. AP-1 response was also measured in reaction to both arsenite and plasma in the P4E6 cell line using JUN transcription. The transcription factor is known to trigger an autoregulatory feedback loop once activated **(787)** and produces a wave-like pattern suggestive of JUN positive feedback in the P4E6 cells **(Figure 60B)**. The response is also much more rapid than that resulting in HMOX1 transcription, citing that AP-1 acts as a very quick responder in P4E6 – and by projection; prostate epithelia **(Figure 65)**.

Initial work developing the P4E6 cell line into a model of stress response for LTP was promising, however unforeseen complications in the transfection of the cell line and time pressure meant that the work is incomplete. Finishing the designed experiments, alongside additional protein work to determine transcription factor localisation using IF and the activation/accumulation of Jun and Nrf2 respectively by Western blot would provide a robust characterisation of the cell line's response to LTP. Development of this model is discussed further in the **Appendix – 9.2**. As the cell line is easier to handle and grow than primary cultures any preliminary work could then be optimised using P4E6. Obviously, results would have to be extrapolated carefully into working with primaries for this approach to be successful, yet in doing so this would save time and avoid wasting the valuable, and finite, resource of the primary cells.

7.3 Discussion - Microarray analysis reveals rapid activation of Notch and AP-1 by LTP

7.3.1 - Microarray analysis reveals that Low Temperature Plasma significantly alters the expression of multiple genes involved in stress response and cellular fate

The microarray data of six prostate primary culture samples revealed that a large number of genes were central in the response to plasma, with significant alteration of over 600 transcripts following treatment **(Figure 61C)**. These fold-changes were consistently observed across all samples and the three chosen tissue pathologies; normal, Gleason 7 and Gleason 9 cancer. Genes could be grouped into functional pathways and it was apparent that plasma altered several signalling networks, the most obvious being Notch, NF-kB and AP-1 **(Figure 62)**. These pathways are very much context-dependent and can determine cell death, growth and differentiation state, the fluctuation of which will be occurring simultaneously amongst treated culture cell populations. The activation of transcription does, simply and as expected, infer that cells survive treatment and that cell death isn't an instant response – an attempt to recover from LTP-induced stress is initiated by primary cultures.

Similar global gene expression signatures were obtained in studies that manipulated Notch **(788)** and HIF1α expression **(789)**. The second group also observed comparable transcriptomic changes in cells exposed to the Na^+/K^+ ATPase inhibitor, ouabain. LTP may alter the transcriptional profiles of these transcription factors and influence membrane polarisation in prostate epithelial cells. This may be through the oxidative modification of cell surface proteins or be produced by electroporative effects associated with some plasma devices **(790, 791)**.

As interpatient heterogeneity is common in the primary patient cultures, this presented a limitation in the analysis of a single snapshot of gene expression. The time-point of 2 hours post-treatment was well considered and optimised across a range of primary cultures **(Figure 44 + 45)** isolated from a variety of tissue pathologies. However, the lack of gene expression changes observed in some cultures in response to LTP, combined with huge variance in upregulated genes at both 0.5 hour and 2 hour post-treatment highlights that transcription was induced as a peak by the "single-hit" therapy. Due to differences in cellular adaptation to culture and also epi/genetic and patient-based biological variance between cultures, response timing varied around the chosen time-point and peak expression in some instances may have been missed altogether by analysis. Whilst peripheral response genes may have been "missed" due to patient-patient heterogeneity, it strengthens the positive identification of the six central response genes in the oxidative stress arrays **(Figure 50)** and the 545 transcripts in the microarray that, even with

variables of interpatient variance in gene expression, were still recurrently and robustly upregulated by LTP across the six patient samples.

Whilst primary cultures are more physiologically relevant and representative of modern prostate cancers than cell lines, **(Figure 61B)** the plastic environment and growth medium change of cell culture still shifts the transcriptomes of primary cultures away from that of *in-situ* populations **(445)**. Acknowledgement of these differences in model systems must be made by studies before extrapolation of therapeutic results into clinical application – whilst the majority of upregulation observed in the prostate cultures by LTP is probably accurate of epithelial tissue response there will be a cohort of genes that are altered due to the cellular adaptation to culture environment.

7.3.2 – Low Temperature Plasma activates Notch-directed gene expression in primary prostate cultures

Notch signalling in the prostate

Notch signalling regulates cell fate decisions **(249)**, through establishment of asymmetrical division **(792)**, cell patterning events such as lateral inhibition **(793, 794)** and the maintenance of stem cell pools by enhancing the self-renewal capabilities of progenitor populations **(248, 795, 796)(Figure 73)**. As Notch signalling can achieve these functional outcomes, the pathway is often misappropriated by tumour initiating cells, such as in breast cancer **(797, 798)** and glioma **(799)**. Notch activation by mutation is classically observed in over half of all T cell acute lymphoblastic leukaemias (ALLs) **(800)**.

The receptor family also plays a regulatory role in the prostate. Notch signalling directs the development, and differentiation of the gland as well as formation of the organ itself **(801)**. Notch can repress AR dependent gene expression **(802)** and regulate the PI3K/AKT signalling axis through modulation of PTEN levels **(803, 804)**. Both of these signalling networks are important for development and differentiation of the normal prostate and in cancer progression. Immunohistochemical and gene expression analyses of patient tumour tissue found that Notch signalling components are increased in higher Gleason grade cancers, **(805, 806)** showing that Notch signalling plays a role in advancing disease and possibly reverts cancer cells to a favourable dedifferentiated state **(807, 808)**.The Notch receptors are direct transcriptional targets of ERG and the signalling pathway becomes critical to the survival of fusion positive prostate cancers **(663, 809)**.

Some members of the Notch signalling pathway (NOTCH1, HES1) are enriched in prostate epithelial SCs over their more differentiated progeny **(66)(Figure 74)**. The pathway appears to be critical to the identity of multipotent basal progenitors in the human prostate **(53)**. Notch

receptors and ligands are also expressed at the protein level in primary prostate cultures, where a reduction of signalling molecules was observed following treatment with gamma secretase inhibitors (GSI) **(Adamson unpublished data, Figure 75A)**. Inhibition of Notch, using GSIs, reduced prostate epithelial stem cell self-renewal capabilities in colony forming efficiency assays, both alone and in synergy with ionising radiation **(Figure 75B)**. GSI treatment of patient-derived prostate cancer xenograft cells found that Notch inhibition slowed tumour growth and could, at lower inoculation numbers, ablate tumour formation/initiation altogether **(Figure 75C)**. After removal from mice that had been treated with GSIs, basal cells from human prostate cancers expressed PAP, a protein marker of luminal differentiation **(Figure 75D)**. This suggests that inhibition of Notch signalling in the basal epithelia of the prostate pushes cells towards a luminal and terminally differentiated state where they are more susceptible to radiation **(Figure 75C+D)**. A similar killing effect is observed by targeting Notch in conjunction with radiation in glioma stem cells **(810)**. In future, use of antibodies specific to the tumour-associated Notch receptor isoform in treatments rather than non-specific GSIs could reduce toxicity towards other somatic stem cell pools, allowing for a more targeted treatment in cancers that misappropriate the signalling pathway **(811, 812)**.

Activation of Notch signalling in plasma treated cells, as indicated by initial findings of the microarray, **(Figure 62)** was surprising. Notch signalling has not been implicated in any previous work utilising LTP treatment of cells. This study therefore documented the first observed activation of the pathway by LTP. Transcriptional responders such as NF-kB and AP-1 were anticipated, in relation to the ROS induced stress, but the inclusion of a pathway linked heavily to stem cell function and epithelial cell fate determination in the microarray was unexpected The top hit of transcriptional and subsequent LIMMA analysis was the NRARP gene; a direct negative regulator of the NICD **(813)**. Interestingly, the constitutive expression of Notch1 in ESCs identified a similar transcriptional signature to that which was observed in the LTP treated prostate epithelial cells. Convergent hits included the ID proteins, NRARP, HEY1, HES1, BTG2, GADD45B, SOX9, RHOV, EFNA1, HBEGF **(814)**, ITPKC, RIPK4, ATF3 and the EGR proteins **(788).** This implicates that Notch directly, by causing transactivation of the expressed gene, or indirectly, through augmentation of other transcription factor activities, may alter the expression of these genes in prostate epithelial cells following plasma treatment.

Notch is responsive to oxidative stress **(815)**. Hydrogen peroxide activates Notch1 and initiates downstream gene expression in mesenchymal stem cells whilst the NICD can inhibit apoptosis induction upstream of SAPK activation to promote cell survival **(816)**. ROS, induced by application of the plasma, may therefore be the initiating factor of the Notch pathway in the primary prostate epithelial cultures.

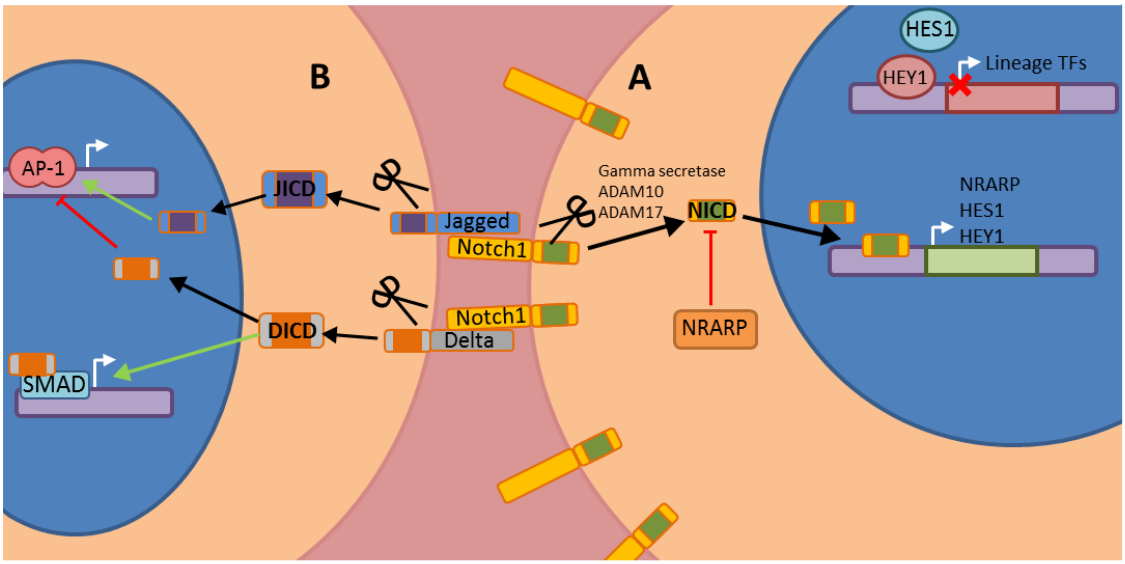

FIGURE 73 - Notch signalling

A) Canonical Notch signalling. Notch receptors are stimulated by binding of ligand receptor; Jagged or Delta. This initiates a series of proteolytic events that releases the Notch Intracellular Domain (NICD) into the cell. Here the NICD acts as a transcription factor and increases canonical gene expression of Hes1 and Hes1 transcriptional repressors that suppress differentiation by silencing lineage defining transcriptional programs. **B) Bi-directional Notch signalling.** The Notch ligand receptors Jagged and Delta are also internalised following receptor-receptor binding and the ICDs can also initiate gene expression changes. Delta ICD can synergise with SMAD proteins and inhibit AP-1 transcription, whilst Jagged ICD can promote AP-1 mediated gene expression.

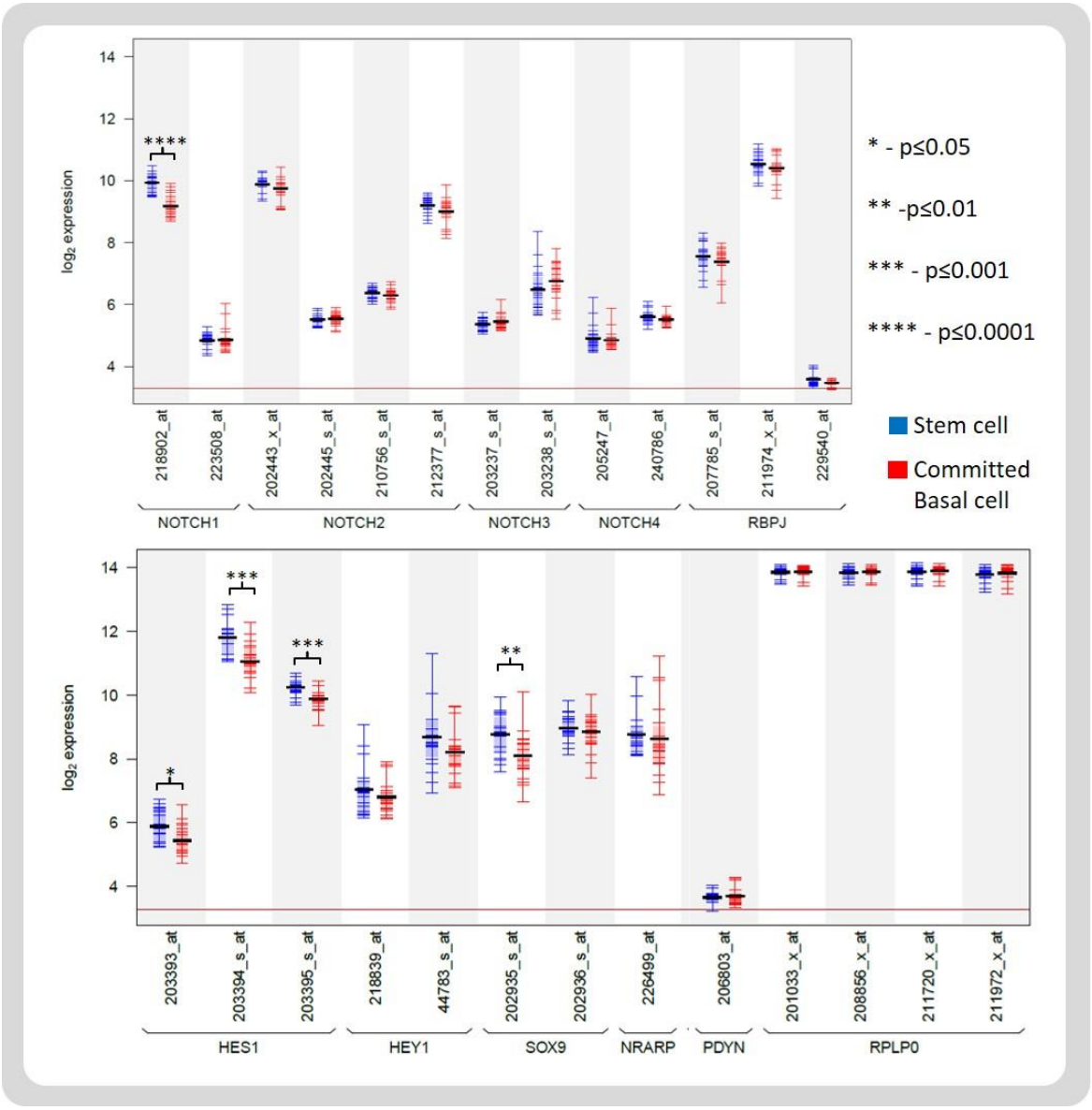

FIGURE 74 – Notch signalling molecule mRNA expression in prostate basal epithelial subpopulations. Notch signalling elements are elevated in prostate basal epithelial stem cells over their more differentiated progeny; committed basal cells. Figure produced from microarray data in **Birnie 2008 (66)**.

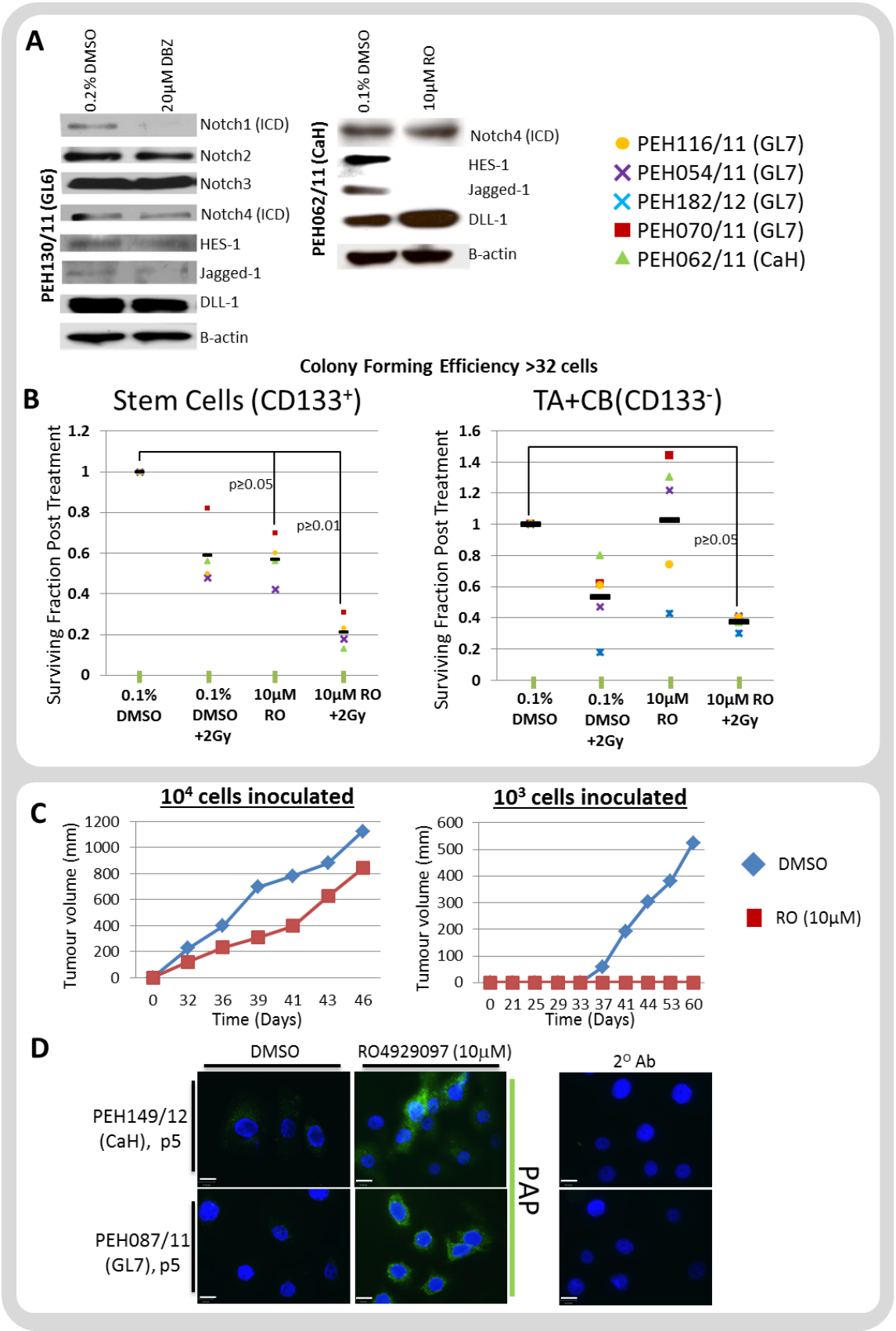
A
0.2% DMSO
20µM DBZ
PEH130/11 (GL6)
Notch1 (ICD)
Notch2
Notch3
Notch4 (ICD)
HES-1
Jagged-1
DLL-1
B-actin
0.1% DMSO
10µM RO
PEH062/11 (CaH)
Notch4 (ICD)
HES-1
Jagged-1
DLL-1
B-actin
PEH116/11 (GL7)
PEH054/11 (GL7)
PEH182/12 (GL7)
PEH070/11 (GL7)
PEH062/11 (CaH)
Colony Forming Efficiency >32 cells
B
Stem Cells (CD133+)
TA+CB(CD133-)
Surviving Fraction Post Treatment
p≥0.05
p≥0.01
p≥0.05
0.1% DMSO
0.1% DMSO +2Gy
10µM RO
10µM RO +2Gy
C
10⁴ cells inoculated
10³ cells inoculated
Tumour volume (mm)
Time (Days)
DMSO
RO (10µM)
D
DMSO
RO4929097 (10µM)
2° Ab
PEH149/12 (CaH), p5
PEH087/11 (GL7), p5
PAP

FIGURE 75 - Inhibition of Notch signalling in primary prostate cultures promoted epithelial differentiation.

A) Protein analysis showed that gamma secretase inhibitors DBZ and RO4929097 decreased levels of Notch signalling members in primary cultures. **B)** Gamma secretase inhibitor RO4929097 (and radiation - 2Gy) decreased prostate stem cell colony forming efficiency. **C)** Gamma secretase inhibitor RO4929097 decreased tumour formation in prostate cancer xenografts. **D)** Extracted xenograft tumour cells treated with RO4929097 were positive for the Prostatic Acid Phosphatase (PAP) differentiation marker. White scale bar - 15µm. Images were adapted from unpublished work completed by Rachel Adamson.

	Gene	H434/14 LM	H434/14 RM	H329/13 LB	H329/13 R	H460/14	H545/15	Average Fold Change	ANOVA p-value
Notch	NRARP	105.6	86.73	265.23	111.49	54.78	197.11	126.92	3.04E-09
	SOX9	8.66	5.11	2.78	3.45	3.47	8.3	4.67	0.000321
	ID1	1.6	1.89	3.05	2.18	4.63	4.05	2.53	0.213964
	ID2	3.95	5.51	3.22	2.06	4.55	2.15	4	0.044476
	ID3	1.54	3.94	18.44	9.14	9.29	2.97	5.8	0.00132
	HES1	4.1	6.56	2.06	1.12	6.93	1.19	2.99	0.00924
	HEY1	6.95	3.67	3.57	3.13	2.77	2.93	3.52	0.000006
AP-1	DUSP1	4.2	3.84	1.26	1.46	2.87	5.93	1.82	0.02892
	DUSP5	2.76	4.14	5.67	2.51	1.08	7.83	2.81	0.023169
	DUSP6	2.71	1.23	1.74	1.88	-4.23	2.28	2.55	0.56087
	DUSP10	12.59	10.47	1.58	1.88	9.56	6.91	7.75	0.000669
	FOSB	38.67	106.39	49.13	5.56	7.28	9.45	29.86	0.000557
	FOSL1	7.48	4.16	6.98	4.24	1.23	5.23	4.8	0.002221
	FOS	2.13	4.54	-2.4	-6.24	1.26	-1.19	-1.16	0.927986
	JUNB	2.1	4.22	1.88	1.31	1.19	1.81	1.27	0.160081
	JUN	6.5	17.24	4.23	2.23	10.78	4.07	5.62	0.000081
	JUND	3.77	5.08	4.56	1.95	4.24	1.27	4.07	0.012237
NF-kB	REL	2.23	2.49	4.03	3.89	3.3	2.18	2.38	0.004957
	NFKB1	1.46	1.59	4.08	3.11	-1.26	1.79	1.87	0.038902
	NFKB2	1.6	1.72	2.54	2.31	1.42	1.67	2.12	0.00357
	NFKBIA	3.16	3.42	7.58	6.05	1.46	3.85	4.84	0.001085
	NR4A1	53.43	47.41	59.06	24.55	2.18	14.15	40.94	0.000172
	NR4A2	25.53	16.39	48.97	11.12	7.77	9.68	14.99	0.000001
	NR4A3	63.63	34.45	188.37	53.5	9.47	7.95	39.07	0.000014
	HSPA1A	7.94	17.59	6.56	12.88	9.92	6.95	9.47	0.000249
	HSPA1B	12.35	12.09	11.42	12.4	8.47	9.96	11.02	0.000094
	RIPK1	3.36	3.89	2.84	2.17	2.39	2.73	2.84	0.001091
	RIPK4	5.63	15.84	55.83	18.33	7.39	7.37	14.71	0.000561
	TNFAIP3	5.13	4.1	6.35	5.3	1.47	3.36	3.89	0.000026
	MAP3K8	22.25	25.75	45.19	19.55	4.48	7.81	15.64	0.000039
Cytokine	IL1B	1.98	2.16	4.32	2.94	-1.25	2.53	2.05	0.041643
	IRAK2	2.86	3.72	7.64	2.93	2.06	1.52	4.1	0.027495
	IL6	4.09	5.35	22.22	7.32	-1.72	2.27	5.24	0.268214
	IL6R	13.9	13.84	5.1	7.69	3.71	4.12	10.35	0.000594
Stress	SQSTM1	4.37	9.01	2.94	2.04	4.99	3.7	3.13	0.000354
	HMOX1	2.25	2.71	2.02	2.51	4.24	1.61	2.56	0.00031

TABLE 15 – Signalling Pathway upregulated genes indicated by initial microarray analysis.

Validation of Notch target genes upregulated by LTP in microarray analysis

See **Table 15.**

NRARP

The top upregulated transcript in plasma treated cells was Notch Regulated Ankyrin Repeat Protein (126.92-fold, $p=3.04x10^{-9}$). NRARP is directly induced by Notch **(813)** and provides a negative feedback loop which causes loss of the NICD **(817, 818)**. The gene is recurrently overexpressed in breast, liver and thyroid cancers and is required for the maintenance of liver CSC stemness **(819-821)**. NRARP was an obvious choice in the validation of microarray results and plasma activation of the gene's expression passed the cut-off of a two-fold increase in three of the four samples chosen for qRT-PCR **(Figure 64)**. Upregulation in a further patient matched pair highlights that NRARP is recurrently expressed in response to LTP in prostate basal epithelia **(Figure 70F)**.

HES1 and HEY1

These canonical Notch targets are basic-helix-loop-helix (bHLH) transcriptional repressor proteins that maintain cells in a dedifferentiated state through silencing of multiple targets – many of which haven't yet been characterised **(822)**. They co-ordinately repress lineage transcription factors and other genes that can trigger differentiation, to assert Notch's control on stem cell fate dynamics **(823)**. Both were upregulated across the six treated samples; HEY1 - 3.52-fold ($p=6x10^{-6}$) and HES1 – 2.99-fold (p=0.00924). Associated transcriptional co-repressors TLE3 (2.11-fold, p=0.0005) and TLE4 (2.01-fold, p=0.0011) were also upregulated by LTP, these proteins aid the silencing of developmental genes by associating with Hes1 and Hey1 **(824, 825)**.

Hes1 is a negative regulator of PTEN, **(803)** Wnt3, Wnt4 **(826)** and the CDK inhibitors; p21 and p57 **(827)**. Expression of the protein is also inducible by oxidative stress **(828)**. HES1 was selected for validation as it's mRNA is differentially expressed at higher levels in prostate epithelial stem cells over more differentiated progeny **(66)(Figure 74)** and it is a Notch specific gene. It failed to pass validation cut-offs, with only mild upregulation observed in H594/17 **(Figure 64)**. However, HES1 is commonly subject to transcriptional oscillation, therefore peak expression may be missed by the single snapshot of gene expression afforded by qRT-PCR. Further time-points of analysis would be required to definitively rule out HES1 as a LTP responsive gene **(829)**.

HEY1 negatively regulates ID1 **(830)** and AR, **(802)** which is particularly relevant in prostate epithelial progenitors. Interestingly, Hey1 can be, in certain cellular contexts, upregulated by Jun **(831)** which is also activated and upregulated by plasma **(Figure 46 & 64)**. HEY1 was confirmed by

LIMMA analysis as a LTP responsive gene. Expression should be validated in future work, along with changes in protein levels of both Notch signalling effectors **(Figure 63)**.

ID2 and ID3

The ID (inhibitors of differentiation) proteins are also associated with stem-like cells and belong to the same family of bHLH transcriptional repressors as HES1 and HEY1 **(832)**. Like HES1 and HEY1, the ID proteins maintain a primitive cellular state with aberrancy in regulation and expression also defining CSC pools **(reviewed in (822))**. These genes, depending upon cellular context, can be directly upregulated by the NICD **(788, 833-835)**. Both ID2 (4.00-fold, p=0.044) and ID3 (5.8-fold, p=0.0013) are significantly increased by plasma treatment in the six sample group, with ID1 also observed to be upregulated in individual samples (2.53-fold, p=0.214).

SOX9

Another Notch interacting gene, upregulated by LTP (4.67-fold, $p=3.21x10^{-4}$), is Sox9; a member of the SRY box family of transcription factors that classically maintain stemness by inhibiting differentiation. Interplay of Sox9 and Notch has been observed in pancreatic progenitor cells **(836)**. Notch causes parallel HES1 and SOX9 expression in these pancreatic ductal cells, showing that the Sox9 transcription factor is a target of the NICD, either directly or through secondary effectors – an observation supported by other studies **(788, 837-839)**. SOX9 was selected for further validation as, like HES1, it was elevated in prostate stem cells **(Figure 74)** and was an intriguing Notch target gene. Even though some biological replicates showed upregulation of the transcription factor, the gene failed validation as a plasma responsive gene **(Figure 64)**.

The failure of some Notch signalling components in the validation process may be due to variable/unfavourable relative percentages of progenitor and CB cell populations in the patient cultures used. As shown for the NR4A isoforms and NRARP, the more differentiated cells can mask responsive expression of the gene in the SC/TA cells, **(Figure 69 & 70F)** especially if the LTP-induced upregulation of the gene is subtle.

<u>Bi-directional Notch signalling; a lesser studied phenomenon</u>

Although much study has been directed at canonical Notch receptor signalling, little research has focused on the activation of signalling by the reciprocal ligand receptors; Jagged and Delta-like. Jagged and Delta both release intracellular domains (JICD & DICD) that subsequently localise to the nucleus after binding Notch **(840-842)**. The ligand receptor ICDs can physically interact with the NICD and prevent formation of the active Notch ternary complex. The JICD can also stimulate proteasomal degradation of the Notch transcription factor **(843, 844)**.

Delta ICD can promote growth arrest in cells, independent of nuclear localisation of the protein **(845)**. The intracellular fragment can also bind to transcription factors which mediate gene expression through protein-protein interaction. DICD binding to Smad proteins can promote neural differentiation by augmentation of TGFβ signalling **(846)**. A similar interaction with Jun causes inhibition of AP-1 dependent transcription in endothelial cells **(847)**.

The reverse is observed for the JICD, which can increase AP-1 transcriptional activity. Again, the downstream signalling initiated by the active ligand receptor is not wholly dependent on nuclear localisation and could be nullified by the NICD **(841)**. Jagged overexpression can transform cells, an outcome attributable to a PDZ (PSD-95/Dlg/Zo1) ligand sequence in the JICD. This facilitates protein-protein binding to alter cellular gene expression and promote oncogenesis **(848).**

There may be functionally relevant bidirectional Notch signalling occurring in the LTP treated samples, however the cellular context for this is yet to be determined **(Figure 73)**. Further work would need to establish which Notch and ligand receptor isoforms were present in the signalling cascades initiated by LTP exposure in prostate epithelia. Whilst it is an attractive prospect that the JICD plays a role in the Jun signalling observed in plasma treated prostate epithelia, upstream SAPK signalling is likely to be the main contributor to AP-1 activation **(Figure 56)**. Indeed, other functional signalling pathways may be downstream targets of ligand receptor ICDs in the prostate lineage, yet no prior studies exist that have investigated signalling of the Notch ligands in this cellular context. Bi-directional Notch signalling is not apparent in every cellular situation, hinting again at a context dependency of this pathway **(849)**.

Upstream protein analysis shows Notch1 activation in prostate basal epithelia by LTP

Although only one of the three genes chosen for validation of activated Notch signalling by plasma passed the criteria, analysis of protein lysates treated with LTP were assessed for presence of the Notch1 receptor and the activate NICD **(Figure 65 & 68)**.

Cleavage of the Notch1 receptor, due to LTP treatment, to release the active NICD (distinguished in Western blot analysis by the proteolytically revealed Val1744 epitope) was observed in seven cultures taken from five separate patients, with densitometry analysis confirming the activation apparent in qualitative blotting images **(Figure 65 & 68)**. Time course analysis showed a rapid and incremental increase of the NICD in both the normal and cancer cultures of H646/17. Release of the intracellular fragment was also apparent at 30 minutes post treatment in H643/17 RM **(Figure 65)**. This body of evidence indicates that Notch activation by LTP is a conserved event in prostate basal epithelial cells. The context of the signalling and the cellular background make it very difficult to hypothesise the outcome of NICD release, but the answer may lie in the differential activation of Notch in the epithelial subpopulations, discussed further in **Section 7.3.8**.

7.3.3 - Further evidence of AP-1 signalling in plasma treated primary cultures

AP-1 target genes were noticeably altered in the microarray data. Upregulation was observed of the factors themselves, negative feedback regulators and genes involved in upstream kinase signalling nodes.

The microarray highlighted the autoregulatory effects of the AP-1 transcription factors **(787, 850)** that had been observed for Jun in the P4E6 cell line **(Figure 60B)**. Application of plasma caused significant upregulation of four AP-1 factors; FOSB (29.86-fold, $p=5.57x10^{-4}$), FOSL1 (4.8-fold, $p=2.22x10^{-3}$), JUN (5.62-fold, $p=8.1x10^{-5}$), and JUND (4.07-fold, p=0.012) **(Table 15)**. FOSB was included in the gene-set approved by the more stringent LIMMA analysis **(Figure 63)** and both FOSB and JUN passed qRT-PCR validation with consistent upregulation at levels similar to that observed in the microarray **(Figure 64)**.

DUSP1 was identified, by the targeted oxidative stress response gene arrays, as a plasma upregulated negative controller of MAPK activation **(Figure 50)**. The microarray approach found other DUSP family phosphatases to be expressed in response to LTP, presumably to further attenuate AP-1 activation.

DUSP5 expression was elevated modestly by plasma (2.81- fold, p=0.023). This phosphatase is a direct transcriptional target of Jun **(851)** and, like DUSP1, has pan-selectivity for p38, ERK and JNK **(852)**. Other DUSP isoforms were upregulated across individual samples, showing that negative regulation of AP-1 signalling was an important pathway induced by plasma **(Table 15)**. The highest upregulation observed for a MAPK phosphatase following LTP was that of the DUSP10 gene (7.75-fold, $p=6.69x10^{-4}$). This phosphatase has specificity for the SAPKs; JNK and p38, **(853, 854)** which have previously been identified to be activated by LTP **(679, 717)** (including JNK in prostate epithelia) **(Figure 56)**. Although upregulation of DUSP10 by plasma was expected as it provides negative feedback for stress activated AP-1 signalling, the gene did not pass the validation criteria in any of the four treated primary cultures **(Figure 64)**.

The use of more frequent intervals in the time-course experiment allowed a more accurate assessment of AP-1 activation timing **(Figure 65)**. For the two normal samples of the patient matched pairs Jun phosphorylation was delayed in comparison to the Gleason 7 cultures, taking an hour to be activated following LTP. More samples would need to be tested over this time frame to ascertain if this was common to all prostate cancers as H209/12, H434/14 and H545/15 normal cultures do show an activation of Jun at 30 minutes post-LTP **(Figure 56)**.

Activation of AP-1 directed gene expression and the phosphorylation of transcription factor proteins are a common denominator in plasma treated prostate cells, of both benign and cancerous origin. However, like Notch signalling, the problem of context-dependent signalling is, as yet, unresolved. Activated Jun could be promoting cell death in cultures or it may be coordinating an oxidative stress survival response. To ascertain the functionality of pJun in the setting of plasma treatment, future work is required in the monitoring of primary culture cell death and survival following LTP exposure with additional molecular dissection of the AP-1 response with small molecule inhibitors, such as JNK inhibition **(855)** and si/shRNAs (short-interfering/short-hairpin RNAs) to individual proteins. This would tease out the consequences of AP-1 activation from the complex milieu of signalling presented in the microarray analysis, discussed further in **Section 8.2.**

7.3.4 - Activation of NF-kB is not consistently observed in plasma treated cultures

NF-kB Signalling

The importance NF-kB signalling in primary prostate cultures is well established, with survival and malignancy of the prostate epithelial CSC population reliant upon the transcription factor **(66)**. Appearance of the pathway in the microarray data was expected due to its combined involvement in stress-response signalling and in the maintenance of prostate epithelial cell populations.

The NF-kB family is made up of two separate classes of proteins; Rel (c-Rel, RelA and RelB) and NF-KB (NFKB1 p50/p105 and NFKB2 p52/p100) that form homo (with the exception of RelB) or heterodimers to affect transcription. In the canonical signalling pathway; NF-kB complexes are held inactive in the cytosol by IkB proteins (α, β, γ, ε and ζ isoforms). Upon activation of upstream signalling, the sequestering IkB protein is phosphorylated, (signalling for its ubiquitination and degradation) permitting NF-kB dissociation and nuclear translocation **(Figure 76A)**. The upstream effectors are typically cell surface receptors, such as the tumour necrosis factor receptor (TNFR). Receptor activation then permits recruitment of TRAF and RIP proteins that subsequently activate the IKK complex responsible for IkB phosphorylation **(856)**.

NF-kB triggered gene expression can also occur through a non-canonical route. Here, activation relies upon signals passing through NIK (MAP3K14) or NF-kB-inducing kinase **(Figure 76B)**. NIK is constitutively degraded in unstimulated cells by a ubiquitin ligase complex containing TRAF3. Upon cell surface receptor activation, the TRAF proteins are recruited and degraded in-complex by the cognate E3 ligase; allowing NIK protein levels to rise. The kinase is then able to activate IKKα by phosphorylation and subsequently permit the processing of NF-kB p100, to its active form; p52. The increase in p52 is dependent thereupon the transcription and translation of the NFKB2 gene that encodes p100 and takes place over hours rather than minutes **(857)**.

The importance of the NF-kB proteins as master regulators of cellular stress and inflammation response is reliant upon complex modulating factors in every situation, which dictate the multifaceted and context dependent outcome of NF-kB signalling.

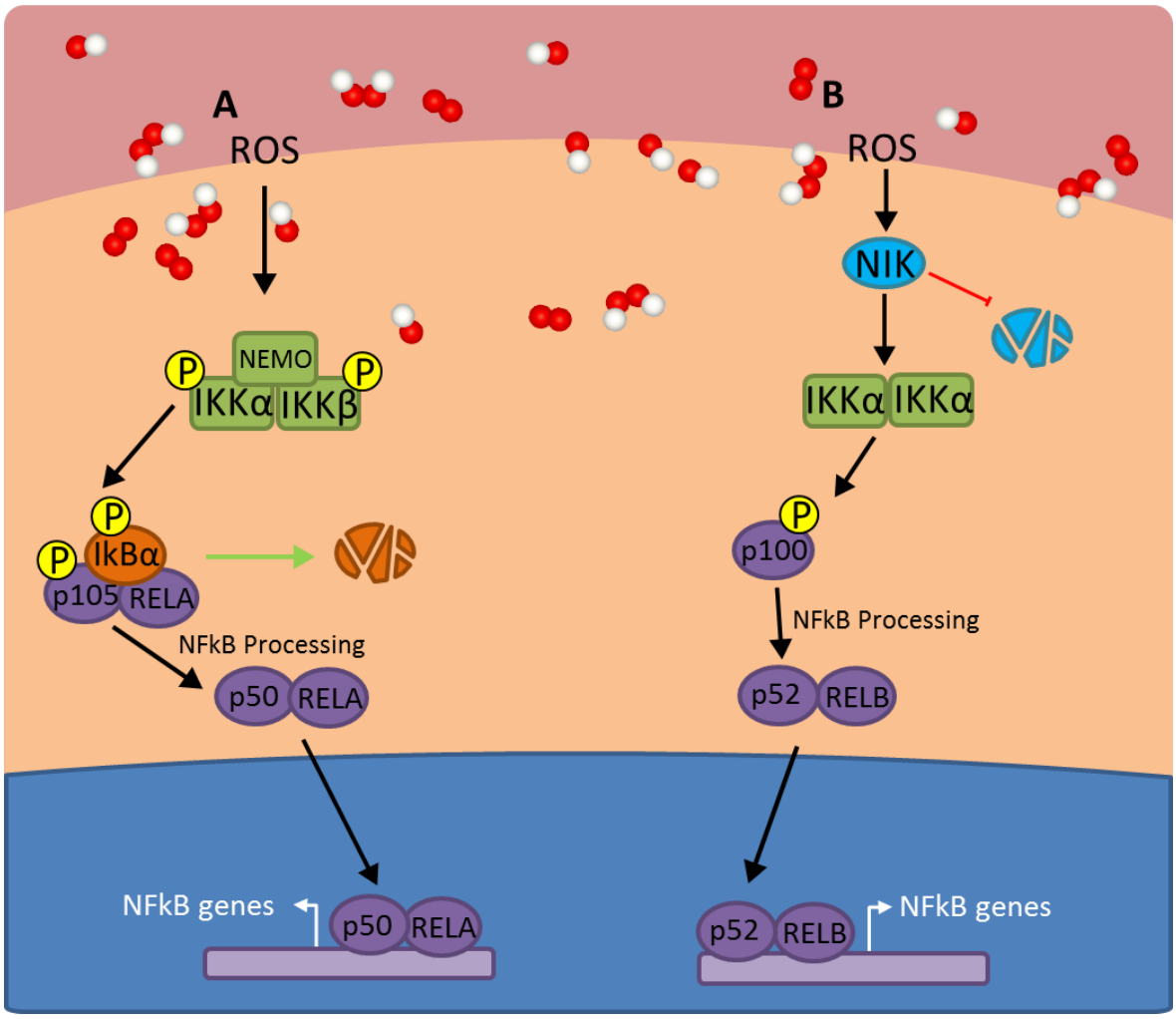

FIGURE 76 – Canonical and Non-canonical NF-kB signalling elements.

A) Canonical signalling. Cellular stress activates the IKK complex (IKKα:IKKβ:NEMO). IKK then phosphorylates IkBα, which sequesters NF-kB factors in the cytosol, stimulating the subsequent ubiquitination and degradation of the protein. The NF-kB proteins (RELA:p105) can then be processed, translocate to the nucleus and effect gene expression. **B) Non-canonical signalling.** Oxidative stress inhibits the constitutive degradation of NIK (NF-kB inducing kinase). Stabilised NIK activates the IKKα complex by phosphorylation which permits processing of p100 to active p52. p52 heterodimerises with RELB to promote the transcription of NF-kB genes

Validation of NF-kB genes upregulated by LTP in microarray analysis

See **Table 15**.

Direct NF-kB genes – NFKB2, REL, NFKBIA

Two subunits of NF-kB were upregulated by plasma treatment; c-Rel (2.38-fold, p=0.005) and NFKB2 (2.12-fold, p=0.0036). The seemingly modest upregulation of these genes was significant as they were already expressed at mid to high levels in untreated epithelial cultures **(Figure 62)**. The NFKBIA gene that encodes the IkBα inhibitory protein was also upregulated (4.84-fold, p=0.001) in plasma treated cultures.

NR4A isoforms

The orphan nuclear receptor 4A (NR4A) family is comprised of three members NR4A1 (Nur77), NR4A2 (Nurr1) and NR4A3 (Nor-1). All were upregulated by LTP treatment in the prostate epithelial cultures; NR4A1 (40.9-fold, $p=1.7x10^{-4}$), NR4A2 (14.99-fold, $p=1x10^{-6}$) and NR4A3 (39.07-fold, $p=1.4x10^{-5}$) **(Figure 64 & Table 15)**. The transcription factors are constitutively active, with control of function being achieved through a variety of mechanisms including the subcellular localisation and post-translational modification (PTM) of the receptors **(858)**. The role of the receptors is cell- and tissue dependent. They have a multitude of functions from pro-apoptotic signalling to DNA repair **(859)**. NR4A proteins have a large interactome and are modulated by a diverse range of proteins and transcription factors including NF-kB, AP-1 and Notch **(860)**. NR4A1 can be phosphorylated by active JNK to promote apoptosis **(861)**, whilst Notch is able to both inhibit NR4A1 transcription **(862)** and to physically inhibit **(863)** the receptor, preventing the initiation of apoptotic signalling. In the myeloid lineage, NR4As are upregulated by NF-kB and feedback to have effects on the transactivation of the transcription factor itself **(864, 865)**.

The receptors can act as negative regulators of the NF-kB network; NR4A1 and NR4A3 deficient cells have increased NF-kB target gene expression and phosphorylation of the p65 NF-kB subunit **(864, 866, 867)**. Depletion of NR4A2 results in the same phenotype, as the receptor acts as a NF-kB inhibitor through accrued PTMs,**(868)** NR4A3 can act on multiple levels of NF-kB signalling by limiting initial activation, translocation of the factor to the nucleus and downstream gene expression of NF-kB **(869)**.

The effect of the NR4A receptors however is entirely context dependent and synergistic activation of NF-kB gene expression has also been reported **(865, 870, 871)**. The orphan receptors can simultaneously attenuate and promote NF-kB signalling in the same cell type, **(872)** highlighting the dynamic and diverse signal modulation of this response network, probably to fine tune the potent NF-kB response in plasma treated prostate epithelial cells.

The three isoforms were chosen for further validation as they were all highly upregulated in the microarray data and they held an intriguing possibility of NF-kB modulatory differences between epithelial subpopulations, (discussed in **Section 7.3.7**) where one receptor may promote a certain cell fate that is abrogated by another. All NR4A genes were recurrently upregulated by LTP in the validation samples to similar fold changes observed on the array **(Figure 64)**. NR4A3 showed high biological variability due to transcript levels being almost undetectable in untreated prostate basal epithelia.

Upstream effectors of NF-kB signalling

Expression levels of receptor interacting serine/threonine protein kinases (RIPK) 1 and 4 were responsive to plasma treatment; RIPK1 (2.84-fold, p=0.001) and RIPK4 (14.71-fold, $p=5.61x10^{-4}$). RIPK1 associates with upstream cell surface receptors to activate the IKK complex. The formation of these receptor signalling-complexes is facilitated by ubiquitin chains, linked through variant lysine residues, regulated by ubiquitin editing enzymes. One such editing ligase is TNFAIP3. This protein acts as a negative regulator of NF-kB, that can simultaneously disrupt the ubiquitin scaffold and target RIPK for proteasomal degradation **(873)**. TNFAIP3 (3.89-fold, $p=2.6x10^{-5}$) was also upregulated in treated primary cultures by LTP. This suggests that immediate transduction of NF-kB signals into the cell is important following exposure to LTP. Response applied to this point in the cascade would provide an immediate opportunity to either, completely abrogate the signal through disruption of the signalling scaffolds, or amplify it by upregulation of the RIP kinases.

In activation of NF-kB; RIPK1 can interact with SQSTM1 (implicated in the qRT-PCR arrays and also upregulated in the microarray data; 3.13-fold, $p=4x10^{-4}$) to facilitate atypical PKC activation of the IKK complex **(874)**. RIPK1 is also required for activation of MAP3K8, a kinase that functions as an upstream hub of MAPK and NF-kB signalling, **(875)** and was also responsive to plasma treatment (15.64-fold, $p=3.9x10^{-5}$) implying that this node of signal transduction may be important in LTP-treated cells.

RIPK1 is also a regulator of both apoptosis and necroptosis (programmed necrosis following caspase inhibition) **(876)**. Necrosis is the dominant cell death response observed in our primary cultures treated with LTP, **(304)** the implication that this response may be regulated by RIPK1 could warrant further investigation in future experiments which can assign cell fate consequences to the signalling pathways activated.

RIPK4, like RIPK1, can activate NF-kB signalling **(877)** and interacts with PKC **(878)**. It is a downstream target gene of NF-kB, MAPK **(879)** and p63, **(880)** a classical marker of prostate basal epithelia.

SQSTM1 and HMOX1 were chosen as genes for further validation to confirm previous identification as plasma-responsive genes in qRT-PCR arrays and the microarray (HMOX1, 2.16-fold, p=0.0003). Both genes passed stipulated cut-offs yet there was significant biological and intra-patient variability in plasma responsive expression **(Figure 64)**.

Interleukin receptor signalling was also triggered by plasma treatment. Upregulation of the agonist, IL1B (2.05-fold, p=0.042) and signal transducer; IRAK2 (4.1-fold, p=0.027), a protein that can activate both NF-KB and JNK, was observed **(881)**. Plasma also enhances gene expression of IL6 signalling proteins – this pathway is particularly important in maintenance of the CSC population of the prostate though JAK-STAT signalling **(253)**. The cytokine itself was upregulated in the cultures but not to significant levels (IL6, 5.24-fold, p=0.29) whilst its cognate receptor IL6R (10.35-fold, $p=5.9x10^{-4}$) was differentially expressed in treated cells.

IL6R was a gene of interest due to previous association with prostate CSCs and its upregulation by plasma on the microarray **(66, 253)**. The gene was included by LIMMA analysis **(Figure 63)** yet did not pass validation, **(Figure 64**) appearing to be almost unresponsive to LTP treatment in four primary cultures.

LIMMA analysis and protein data conflict with initial microarray findings

From the initial microarray data, discussed above, NF-kB activation by LTP in the primary cultures appeared to be certain, with both intrinsic proteins and modulating regulators upregulated following treatment with the plasma. However, LIMMA analysis **(Figure 63 & Table 16)** removed most NF-kB transcripts (apart from RIPK4, MAP3K8 and the NR4A genes) suggesting that the high background of cyclic NF-kB signalling present in the cultures may have been picked up in microarray analysis rather than LTP enforcing a functional activation of the transcription factor **(66)**.

Assessing the upstream activation of NF-kB proteins returned results that also suggested a lack of pathway activation by plasma. The time-course experiment showed that IkBα protein content was not changed in treated cells with phosphorylation of the inhibitory protein only observed in the Gleason 7 cultures of the patient matched pairs **(Figure 65 & 66B)**. This cancer-specific phosphorylation of IkBα was only seen in patients H643/17 and H646/17. The signalling event was also observed to occur in normal cultures and was absent in some Gleason 7 samples following LTP treatment **(Figure 67C)**. This again highlights that interpatient heterogeneity and not the tissue pathology of the primary prostate cultures is the variable that determines molecular response to LTP.

If canonical activation was observed, there would have been a rapid phosphorylation of IkBα followed by loss of total protein, which would permit liberation of the NF-kB transcription factor. Phosphorylation without the expected decrease in NF-kB-bound inhibitor suggests that NF-kB remains inactive in LTP-treated primary prostate cultures. This was confirmed by the lack of nuclear translocation of the NF-kB factor; p65, in whole and subpopulation cultures, **(Figure 67A+B)** further evidence of cytosolic sequestration by IkBα. Patient H523/15 cultures were the only samples to respond to LTP, with a loss of IkBα at 2 hours post-treatment **(Figure 67C)**. Phosphorylation of the protein wasn't observed at the earlier time-point yet may still have occurred after this snapshot of cellular protein levels was taken. In any case, NF-kB activation doesn't appear to be a widespread consequence of LTP in primary prostate epithelial cultures.

The slight increase in NFKB2 gene (which encodes NF-kB p100/p52) expression following treatment with LTP implied that non-canonical signalling may be activated in LTP-treated prostate epithelium. The rise in NIK levels following treatment **(Figure 65 & 66C)** would suggest a role for this signalling in LTP response. Extension of the time course to assess the processing of NF-kB p100 to p52 would be required to confirm that the non-canonical signalling arm was truly having an effect in treated cells. The outcome of the signalling is again unknown but would be expected to be present in surviving cells as the stimulation of NF-kB processing requires time. Fresh protein synthesis of the NF-kB p100 protein has to occur for the effects of non-canonical signalling to take place, a process which is longer than the latency period of cell death mechanisms.

Initial impressions from the microarray data was that NF-kB must react rapidly via the canonical arm of signalling. However, activation of the slower non-canonical pathway may be an initial indicator of signalling in surviving cells as the full outcome of NIK accumulation and downstream signalling would take longer than the cell death mechanisms that would remove ROS damaged cells. Implying that cells which accumulate NIK may form an LTP-resistant population. Further investigation into how and if activation of non-canonical NF-kB associates with LTP-resistance is required.

7.3.5 – Gene Ontology and KEGG metadata confirms pathway activation and highlights the unfolded protein response, ER stress and a balancing of apoptotic signalling processes in LTP treated prostate epithelia

See **Table 17** for all GO and KEGG terms enriched in LTP-treated primary prostate basal epithelial cells.

Gene ontology (GO) and KEGG analysis are useful analytical tools as they provide a broad stroke picture of gene expression and activated pathways. However sole use of these tools without validation of individual gene and protein changes can detract from informing upon the finer

workings of molecular responses as unfocused background noise can be assigned to the gene signatures by numerous irrelevant annotations on genes, particularly as the collection of publicly available microarray datasets grows. To this end, the metadata from the LTP treated microarrays is discussed here, following the validation of both gene upregulation and signal pathway activation indicated by the patterns of individual annotated transcripts in the initially generated dataset and by LIMMA analysis.

Firstly, an LTP-induced state of oxidative stress was implied in the treated prostate primary cells by inclusion of GO terms; cellular response to oxidative stress (p=0.0002) and cellular response to hydrogen peroxide (p=0.0003), a reactive species known to be important in the cocktail of molecules activated by LTP **(Figure 45)**. There was also negative regulation of the cell cycle (p=0.003) which would be expected in cells that encounter LTP-induced DNA damage observed in the primary cultures following treatment **(304)**.

Other known signalling pathways were enriched in the GO and KEGG terms, expanding upon the immediately obvious gene regulation from initial array data **(Figure 64 & Table 15)**. NF-kB signalling appeared throughout the GO terms, including; positive regulation of tumour necrosis factor mediated signalling pathway ($p=7.2x10^{-5}$) and NF-kB transcription factor activity (p=0.003). There was also extensive sequence-specific transcription factor (activator and repressor) and coactivator binding terms. Selective terms for AP-1 signalling were also apparent; MAPK3 activity (p=0.048) and MAPK signalling pathway (p=0.01). IL-6 signalling was also observed to be significantly activated in the microarray data; interleukin-6 binding (p=0.004), receptor activity (p=0.004) and receptor binding (p=0.015).

Primary prostate cultures don't undergo apoptosis following LTP treatment and instead die via necrosis **(304)**. However the cells appeared to orchestrate a wide array of apoptotic signalling processes, apparent in the metadata generated from the microarray. The KEGG pathway hit of; Apoptosis – multiple species (p=0.006), was reinforced by multiple GO terms suggesting apoptotic cell death was occurring, including; positive regulation of cytochrome c from mitochondria ($p=3.5x10^{-5}$) and positive regulation of protein insertion into mitochondrial membrane involved in apoptotic signalling pathway (p=0.002). However, there were a significant amount of negative regulatory processes involved in apoptosis also enriched in the GO terms (negative regulation of mitochondrial outer membrane permeabilisation involved in apoptotic signalling pathway, p=0.0001, and negative regulation of extrinsic apoptotic signalling pathway in absence of ligand, p=0.002). This suggested that LTP may initiate an apoptotic response in primary cells which is then aborted by activation of reciprocal signalling pathway or that the heterogeneous cell populations in the primary cultures have variant apoptotic signalling responses to LTP.

Probably the major finding from the metadata was the initiation of an unfolded protein response and ER stress by LTP. Both processes were heavily enriched throughout the GO term processes and KEGG analysis. ER stress is linked directly to the unfolded protein response. This was observed in the upregulation of genes such as the heat shock proteins HSPA1A (9.47-fold, $p=2.49x10^{-4}$) and HSPA1B (11.02-fold, $p=9.4x10^{-5}$) that are stress responsive and act as protein folding chaperones and characteristic upregulation of ATF4 in four of the six samples. In conditions of ER stress, the ER transmembrane protein PERK phosphorylates the translation initiation factor, eIF2α. Phospho-eIF2α then causes upregulation of ATF4 to aid cellular anti-oxidant response and alleviation of ER stress **(reviewed in (882))**. The accumulation of unfolded proteins after LTP-induced oxidative damage upsets ER homeostasis and can initiate a diverse range of molecular responses such as JNK activation, NF-kB signalling, Nrf2 accumulation and autophagy **(883)**. All of which are implicated in the LTP response of prostate epithelia **(Figure 46)(304)**. The ER is also involved in Ca^{2+} homeostasis that affects a multitude of signalling pathways if disrupted. In relation to the microarray data; NR4A isoforms are upregulated by Ca^{2+} changes **(884)** and ITPKC is a modulator of extracellular signal-initiated calcium response **(885)**.

Another finding that was specific enough to warrant further analysis was the GO term enrichment in steroid hormone receptor activity (p=0.0003), highlighting glucocorticoid (p=0.0004) and retinoid X receptor binding (p=0.03) in treated cells. The signalling initiated by the hormone receptors will be context dependent in prostate epithelia but may be indicators of renewal processes following LTP treatment.

Symbol	Gene	Fold Change	ANOVA p-value	LIMMA p-value
NRARP	Notch regulated ankyrin repeat protein	126.92	3.04E-09	5.0759E-10
HSPA1A	Heat shock protein A1A	9.47	0.000249	1.25377E-08
HSPA1B	Heat shock protein A1B	11.02	0.000094	1.50624E-08
EFNA1	Ephrin A1	9.98	0.000078	2.2241E-08
HBEGF	Heparin binding EGF like growth factor	22.22	0.000002	5.72194E-08
RHOV	Ras homologue family member V	20.72	0.000044	8.03929E-08
NR4A2	Nuclear receptor 4A2	14.99	0.000001	2.03093E-07
CYP1A1	Cytochrome P450 family 1 subfamily A member 1	20.3	0.000099	2.32924E-07
MAP3K8	Mitogen activated protein kinase kinase kinase 8	15.64	0.000039	2.86501E-07
ATF3	Activating transcription factor 3	37.37	0.000015	3.38407E-07
BTG2	BTG anti-proliferation factor 2	12.74	0.000029	4.3246E-07
RHOB	Ras homology family member V	6.39	0.00001	5.36957E-07
NR4A3	Nuclear receptor 4A3	39.07	0.000014	6.76664E-07
RIPK4	Receptor interacting protein kinase 4	14.71	0.000561	8.20509E-07
OVOL1	Ovo like transcriptional repressor 1	8.74	0.000855	9.05974E-07
ARL5B	ADP ribosylation factor like GTPase 5B	4.95	0.000037	1.03334E-06
PPIF	Peptidylprolyl isomerase F	7.14	0.000211	1.32265E-06
PMAIP1	Phorbol-12-myristate-13-acetate-induced protein 1	11.66	0.000416	1.54963E-06
ITPKC	Inositol-triphosphate3-kinase C	26.33	0.000019	1.79006E-06
IL6R	Interleukin 6 receptor	10.35	0.000594	1.81086E-06
DAPP1	Dual adaptor of phosphotyrosine and 3-phosphoinositides 1	4.91	0.000019	2.51189E-06
CYP1B1	Cytochrome P450 family 1 subfamily B member 1	19.78	0.000108	2.90671E-06
RNU12	RNA, U12 small nuclear	6.92	0.000098	4.28598E-06
THBD	Thrombomodulin	3.08	0.005813	5.29702E-06
NR4A1	Nuclear receptor 4A1	40.94	0.000172	5.55242E-06
PPP1R15A	Protein phosphatase 1 regulatory subunit 15A	5.16	0.000269	6.54149E-06
HEY1	Hes related family bHLH transcription factor with YRPW motif 1	3.52	0.000006	6.73261E-06
INSIG1	Insulin induced gene 1	3.25	0.002229	7.11905E-06
LHFPL3-AS2	LHFPL3 antisense RNA 2	2.67	0.000037	8.16209E-06
RNU4-1	RNA, U4 small nuclear 1	5.6	0.021446	9.17945E-06
RNF122	Ring finger protein 122	5.45	0.000034	9.61055E-06
BCL2L11	BCL2 like 11	2.51	0.000865	1.55846E-05

TABLE 16 – LIMMA-specified and range-separated LTP-upregulated genes

Table includes the annotated transcripts identified as upregulated by LTP treatment. These all passed LIMMA analysis and the further constraint that expression ranges in the untreated and treated samples had no overlap. Genes are ranked by LIMMA p values, the most significant at the top.

GO - Biological Process

GO ID	Term	Annotated	Significant	Expected	score
GO:1904722	positive regulation of mRNA endonucleolytic cleavage involved in unfolded protein response	2	2	0	4.80E-06
GO:0090200	positive regulation of release of cytochrome c from mitochondria	29	3	0.06	3.50E-05
GO:0000122	negative regulation of transcription from RNA polymerase II promoter	752	13	1.67	5.70E-05
GO:1903265	positive regulation of tumor necrosis factor-mediated signaling pathway	6	2	0.01	7.20E-05
GO:1901029	negative regulation of mitochondrial outer membrane permeabilization involved in apoptotic signaling pathway	8	2	0.02	0.00013
GO:1902237	positive regulation of endoplasmic reticulum stress-induced intrinsic apoptotic signaling pathway	10	2	0.02	0.00021
GO:0034599	cellular response to oxidative stress	248	7	0.55	0.00023
GO:0070301	cellular response to hydrogen peroxide	82	4	0.18	0.00025
GO:0042026	protein refolding	24	3	0.05	0.0006
GO:0051131	chaperone-mediated protein complex assembly	19	2	0.04	0.0008
GO:1902236	negative regulation of endoplasmic reticulum stress-induced intrinsic apoptotic signaling pathway	20	2	0.04	0.00089
GO:1900740	positive regulation of protein insertion into mitochondrial membrane involved in apoptotic signaling pathway	29	2	0.06	0.00187
GO:1903917	positive regulation of endoplasmic reticulum stress-induced eIF2 alpha dephosphorylation	1	1	0	0.00222
GO:2001240	negative regulation of extrinsic apoptotic signaling pathway in absence of ligand	33	2	0.07	0.00242
GO:0045786	negative regulation of cell cycle	586	5	1.3	0.00275
GO:0051092	positive regulation of NF-kappaB transcription factor activity	134	3	0.3	0.00323
GO:0060734	regulation of endoplasmic reticulum stress-induced eIF2 alpha phosphorylation	2	1	0	0.00443
GO:0061394	regulation of transcription from RNA polymerase II promoter in response to arsenic-containing substance	2	1	0	0.00443

GO - Molecular Function

GO ID	Term	Annotated	Significant	Expected	score
GO:0031249	denatured protein binding	2	2	0	4.50E-06
GO:0001106	RNA polymerase II transcription corepressor activity	28	3	0.06	2.90E-05
GO:0001077	transcriptional activator activity, RNA polymerase II core promoter proximal region sequence-specific binding	257	5	0.55	0.00021
GO:0003707	steroid hormone receptor activity	59	3	0.13	0.00028
GO:0035259	glucocorticoid receptor binding	13	2	0.03	0.00035
GO:0070330	aromatase activity	23	2	0.05	0.00111
GO:0044183	protein binding involved in protein folding	27	2	0.06	0.00153
GO:0051082	unfolded protein binding	108	3	0.23	0.00161
GO:0001078	transcriptional repressor activity, RNA polymerase II core promoter proximal region sequence-specific binding	117	3	0.25	0.00202
GO:0097718	disordered domain specific binding	32	2	0.07	0.00215
GO:0004879	RNA polymerase II transcription factor activity, ligand-activated sequence-specific DNA binding	48	3	0.1	0.00333
GO:0019981	interleukin-6 binding	2	1	0	0.00431
GO:0004915	interleukin-6 receptor activity	2	1	0	0.00431
GO:0019825	oxygen binding	47	2	0.1	0.0046
GO:0001046	core promoter sequence-specific DNA binding	112	3	0.24	0.00534
GO:0000978	RNA polymerase II core promoter proximal region sequence-specific DNA binding	332	4	0.72	0.00548
GO:0047844	deoxycytidine deaminase activity	3	1	0.01	0.00646
GO:0031072	heat shock protein binding	96	3	0.21	0.00726
GO:0005138	interleukin-6 receptor binding	7	1	0.02	0.015
GO:0072542	protein phosphatase activator activity	8	1	0.02	0.01713
GO:0000988	transcription factor activity, protein binding	602	6	1.3	0.0172
GO:0046982	protein heterodimerization activity	468	4	1.01	0.01769
GO:0016679	oxidoreductase activity, acting on diphenols and related substances as donors	9	1	0.02	0.01925
GO:0004126	cytidine deaminase activity	9	1	0.02	0.01925
GO:0042826	histone deacetylase binding	103	2	0.22	0.02073
GO:0008440	inositol-1,4,5-trisphosphate 3-kinase activity	10	1	0.02	0.02137
GO:0020037	heme binding	127	2	0.27	0.03058
GO:0004115	3',5'-cyclic-AMP phosphodiesterase activity	15	1	0.03	0.03188
GO:0046965	retinoid X receptor binding	15	1	0.03	0.03188
GO:0008157	protein phosphatase 1 binding	18	1	0.04	0.03814
GO:0001223	transcription coactivator binding	19	1	0.04	0.04022
GO:0005525	GTP binding	371	3	0.8	0.04531
GO:0005506	iron ion binding	158	2	0.34	0.04548
GO:0000983	transcription factor activity, RNA polymerase II core promoter sequence-specific	22	1	0.05	0.04642
GO:0004709	MAP kinase kinase kinase activity	23	1	0.05	0.04848

KEGG Pathway analysis

	Pathway	n.pathway	n.seen	p.value
path:hsa04141	Protein processing in endoplasmic reticulum	166	4	0.00227184
path:hsa04215	Apoptosis - multiple species	33	2	0.00560536
path:hsa04010	MAPK signaling pathway	255	4	0.01042539
path:hsa00980	Metabolism of xenobiotics by cytochrome P450	74	2	0.02631755
path:hsa04151	PI3K-Akt signaling pathway	342	4	0.02774234
path:hsa05204	Chemical carcinogenesis	82	2	0.03182386

TABLE 17 – Gene Ontology and KEGG Pathway annotations of microarray data

7.3.6 - Plasma responsive genes of biological interest highlighted by LIMMA analysis

LIMMA analysis reduced the initial data-set of 645 differentially expressed transcripts in treated cells to 89 **(Figure 63)**. Only 42 of the 89 transcripts were annotated genes, which were then further concentrated by excluding transcripts that had any point of overlap in expression range between LTP treated and untreated cohorts. This yielded 32 genes that were; i) significantly upregulated in LTP treated cells when accounting for the transcript's inherent expressional variability and ii) completely separated on terms of expression between untreated and treated groups across all six samples **(Table 16)**.

Although no further investigation was directed for the majority of the genes included by this analysis, several of the transcripts with high scoring p-values such as ATF3, EFNA1, RHOV and HBEGF could be followed up with further study of context specific function in the prostate epithelia and the role that they play in LTP-induced stress response. If they are able to distinguish between resistant and susceptible populations, they may also have future significance if utilised as biomarkers of LTP response through tests of pre and post-treatment urinary RNA levels. Whilst the LIMMA analysis is a powerful tool in determining possible functionally significance of gene expression differences in the LTP treated cells, it is not infallible. IL6R signalling was highlighted in the GO terms **(Table 17)** and was already noted by previous work done in our laboratory as a gene important in the signalling of prostate basal epithelial cells **(253)**. However, IL6R didn't pass the validation criteria in qRT-PCR testing of LTP treated cultures **(Figure 64)**. This means that all genes that passed stringent LIMMA analysis would still have to be independently verified to confirm whether they are critical in the transcriptional response to LTP.

7.3.7 - Basal epithelial subpopulations differ in their molecular responses to plasma

Heterogeneity in primary prostate cultures is well documented. Previous studies have observed both differential gene expression **(66)** and treatment response **(323, 771)** among the basal subpopulations. Therefore, differences in how SC/TA and CB cells responded to plasma were expected.

NF-kB signalling plays a significant role in primary culture cell survival, **(66)** therefore changes in signal modulation in epithelial subpopulations following LTP treatment could impact cell fate dramatically. The NR4A orphan receptors are known to both attenuate and promote NF-kB signalling, and can do so simultaneously in cells **(872)**. The end consequence of their upregulation in LTP treated prostate cells is unknown, yet the progenitor SC/TA population consistently responds with greater upregulation of each NR4A isoform than that observed in CB cells **(Figure 69)**. This correlates with the increased requirement of NF-kB signalling in the stem cells over their more differentiated progeny **(66)** and may be because modulation of the pathway requires a

greater degree of control here, than in the CB cells; where upregulation of isoform expression is observed, just at more modest levels. The context-dependence of the NR4A receptors means that further work is required to discern their exact function in LTP response. Firstly, the background context of NR4A protein expression and localisation in the primary basal epithelial cells should be deduced to properly assess the changes impacted upon the receptor isoforms by LTP. Previously observed protein interactions such as those between NR4A1 and the NICD, **(863)** and whether the receptors are targets of JNK phosphorylation **(861)** warrant further investigation, alongside wider cell fate processes such as apoptosis and DNA damage repair **(859)** – both of which LTP induces **(304)** and the NR4A receptors are involved in.

The pattern provided by the expression of the NR4A receptors **(Figure 69)** and NRARP **(Figure 70F)** in the prostate epithelial subpopulations also highlights one of the limitations of the WP array. This data suggests that the LTP response is mainly elicited by the SC/TA cells, however this population constitutes 25-50% of the whole culture population (with the remainder of cells being CB cells). This means that the transcriptional response coordinated in the progenitor population is diluted by the more differentiated cells and the expression signature is masked. The effect is seen clearly in the NRARP and NR4A1 expression of both cultures from patient H643/17 where WP expression has just passed the threshold of 2-fold upregulation, matching that of the less-responsive CB fraction, yet the transcript is robustly expressed in the SC/TA population **(Figure 69 & 70F)**. Responsiveness of the progenitor population in the primary cultures allowed the effects of LTP to be observed in the whole culture microarray, however genes that may still be upregulated in a single subpopulation yet to a lesser extent (than observed for NRARP and NR4A isoforms) will be lost in the dominant non-responsive signature. To assess these "lost" genes, microarray analysis of individual subpopulation responses to plasma would have to be carried out where cultures are first separated into SC/TA and CB cells, treated with plasma and then gene expression assessed. The reduction of heterogeneity would afford a clearer view into the effects of LTP on the individual subpopulations and may allow true differences to be more readily established between the response of normal and cancerous prostate epithelium.

Similar to members of the Notch signalling pathway, Jun mRNA is consistently expressed at a higher level in prostate epithelial stem cells than in the CB population, **(66)(Figure 77A)** with my own data confirming that the transcription factor's base expression was higher in the progenitors **(Figure 77B)**. The protein levels of Jun were also elevated in the SC/TA population of H643/17 LM and H652b/17 cultures, **(Figure 70A)** and the activation of the transcription factor was also more potent in the progenitors **(Figure 70B)**. With an increased amount of active Jun, the progenitor population would be expected to have a higher upregulation of JUN, through the transcription factor's autoregulatory effects **(787)**. However, no significant difference was observed between

SC/TA and CB upregulation of the AP-1 factor gene **(Figure 70C)**. AP-1 signalling is entirely context dependent, with activation initiating signalling cascades for both cell death and survival in alternate circumstances. The downstream functionality of LTP-stimulated phospho-Jun in the progenitor population of the primary cultures is unknown. LTP affects the colony forming efficiency of primary prostate cells, reasoning that the oxidative stress induced by the treatment must abrogate stem cell function, possibly by killing this population. Whilst previous studies could find no apoptotic cell death in primary cultures after LTP **(304)** the enrichment of apoptotic pathways in GO terms **(Table 17)** and active AP-1 suggests that this mode of cell death may also occur in some cells.

From the transcriptional data alone it is difficult to ascertain what cell populations are resistant and which are susceptible to LTP. For example; are the CB cells dying (or becoming senescent? **(688)**) and therefore have a reduced transcriptional output or just non-responsive as LTP-stimulated ROS simply aren't affecting critical cellular processes. The final consequences of AP-1 cell fate determination will only be discernible after further study. Assessment of cell viability and death after plasma treatment in conjunction with pathway inhibitors will reveal if Jun phosphorylation is a LTP-resistance mechanism or a harbinger of cell death. Through the monitoring of these cell fate dynamics in both SC/TA and CB populations, the differential transcriptional responses may be linked to a functional outcome; the death or survival of a particular subpopulation.

7.3.8 - Stem and transit amplifying cells selectively activate Notch signalling in response to plasma treatment

As discussed previously in **Section 7.3.2**; Notch signalling is enriched in prostate epithelial stem cells and is important for maintenance of their dedifferentiated state **(Figure 73)**. This data was confirmed by assessment of Notch signalling following LTP in fractionated prostate epithelial subpopulations **(Figure 70 D-F)**. The Notch1 receptor was more highly expressed in the SC/TA fraction than in the CB cells **(Figure 72D & 74)** and, although Notch signalling was active to some degree in all patient cultures, densitometry analysis showed that the progenitor population activated Notch1 receptor cleavage more readily than the more differentiated CB cells **(Figure 70E)**. The significance of this selective activation was further increased by discovery that the receptor was internalised and translocated to the nucleus *only* in LTP-treated SC/TA cells **(Figure 71)**. The nuclear foci of the Notch1 receptor were not observed in treated CB cells nor in the untreated cells of either population. This suggests that LTP initiates a rapid response in the progenitor population Notch signalling network, a conclusion supported by the exclusive upregulation of the negative regulator NRARP ~10-fold caused by LTP in the SC/TA cells; whilst transcription of the Notch target gene is unchanged in the CB population **(Figure 70F)**. The Notch1

antibody used in the study is polyclonal and has been approved for ChIP meaning that it can detect both the receptor and it's intracellular fragment.

Notch signalling is classically activated to retain cellular identity and a dedifferentiated state **(249, 823)**. This poses three questions; i) could LTP-induced ROS provide a differentiation-promoting stimulus to the prostate epithelial stem cell population? ii) do the progenitors trigger Notch signalling in attempt to retain their stemness? And, iii) is the activation in Notch signalling critical in LTP resistance and regeneration of the epithelial hierarchy following treatment?

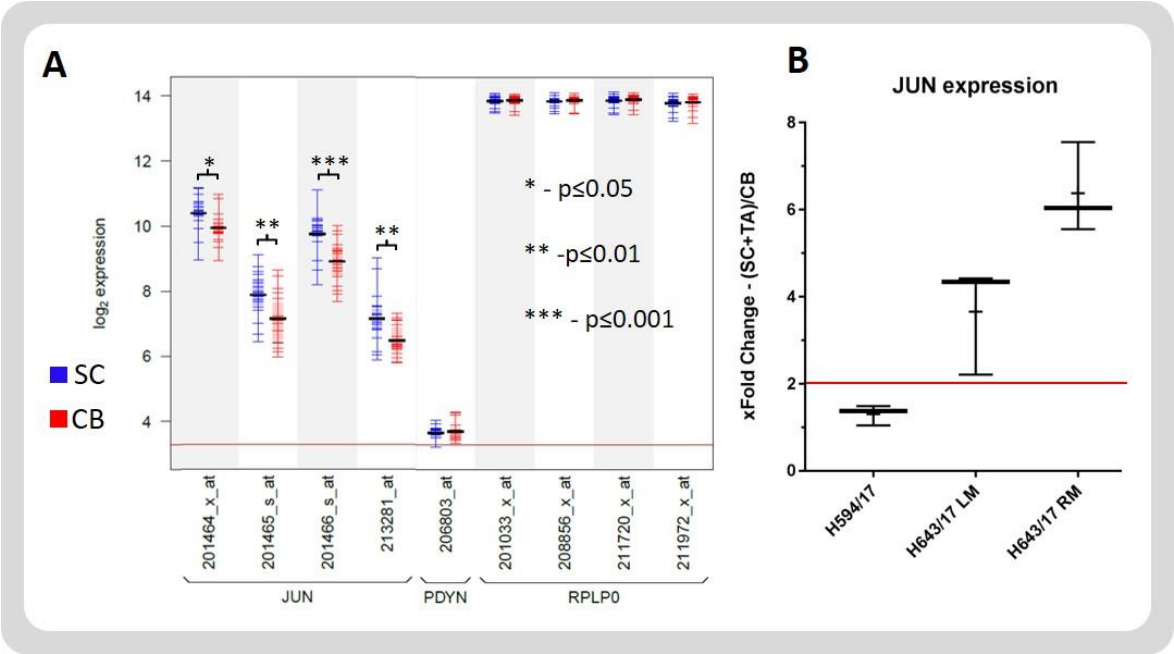

FIGURE 77 – Prostate epithelial progenitors express JUN to greater levels than differentiated committed basal cells.

A) Microarray data from comparison of SC and CB JUN expression. Across all four gene probes, JUN expression is significantly higher in the stem cells. Produced from data gathered in **Birnie 2008 (66)**. **B)** qRT-PCR data taken from fractionated epithelial cultures shows that the SC/TA population express equal or higher levels of the JUN transcription factor mRNA.

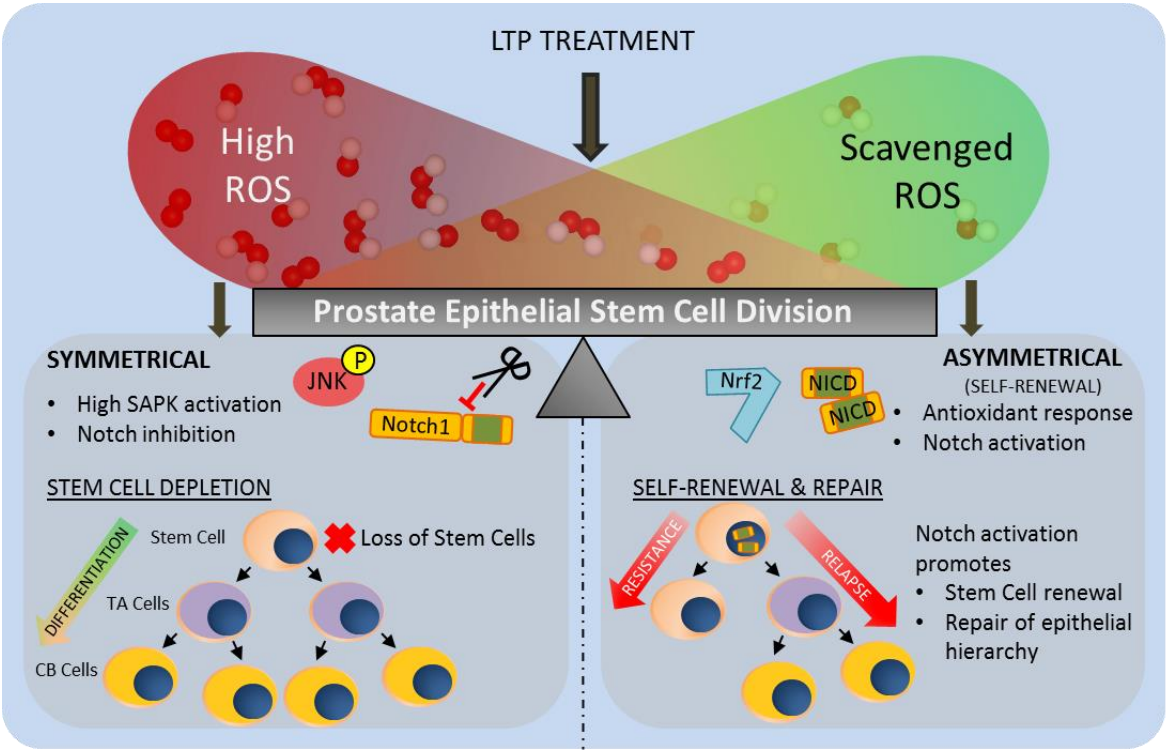

FIGURE 78 – Model of Notch signalling and the balance of prostate epithelial stem cell decision.

High ROS levels can promote a cellular environment favourable to stem cell depletion through symmetric division and forced differentiation. Activation of Notch signalling can aid ROS scavenging and promote self-renewal of the stem cell pool to give LTP resistance whilst also repairing the prostate epithelial hierarchy, allowing for relapse.

ROS are observed to stimulate differentiation in human ESCs **(886)** and glioma CSCs **(887)** through SAPK activation. The same process also occurs in prostate stromal cells **(888).** Notch is known to maintain low ROS levels in cells and is activated, in some contexts, by elevated ROS **(815, 816)**. In *Drosophila*, Notch signalling is activated to prevent lammellocyte stem cell differentiation in high ROS concentrations to prevent loss of niche integrity **(889)**. Airway basal stem cells activate Notch through Nrf2 in high levels of ROS to enhance self-renewal and allow for the repair of the epithelial hierarchy, whilst Nrf2 antioxidant signalling protected the stem cell pool from oxidative damage and differentiation **(890)**. The same situation has been observed in LTP-treated prostate epithelial cells where active SAPKs, Nrf2 and Notch have all been observed **(Figure 56 & 65)**.

It is therefore possible that prostate epithelial stem cells (in both normal and cancer cultures) initiate Notch signalling to both prevent depletion of the progenitor population, through high ROS promoting symmetrical division of the stem cells and subsequent differentiation; and replace dead cells further down the epithelial hierarchy by increasing self-renewal capabilities (asymmetrical divisions) **(Figure 78)**. If reactive species stimulated by LTP are promoting differentiation of the epithelial cultures this could be monitored through tracking loss and gain of epithelial differentiation markers – appearance of PSA, PAP, CK8 and CK18, with loss of CD133, $\alpha_2\beta_1$ integrin, CK5 and CK14 – following treatment. The colony forming efficiency of prostate basal epithelial cells is diminished by LTP **(304)** suggesting that self-renewal is impaired, and combination of LTP treatment with Notch inhibition, using GSIs or Notch receptor antibodies, may reveal the true importance of the Notch pathway to the surviving fraction of cells. Differentiation therapy, the pushing of stem cells into cycle to promote depletion of the progenitor population whilst increasing the number of therapeutically targetable differentiated cells, has already been discussed with respect to prostate cancer **(236)**.

There remains the problem that Notch activation by LTP is not exclusive to cancer cells as normal epithelia rely on the same signalling pathway to, presumably, retain stem cell numbers. This may also be an epithelial tissue regeneration response in the prostate, initiated by therapeutic insult **(891)**. Off-target inhibition of Notch in the prostate epithelial stem cell niche of normal tissue would be detrimental to acinar integrity **(892)**. Multiple Notch receptors and ligands are expressed in primary prostate cultures **(Figure 74 & 75A)**. However, only the LTP-response of Notch1 was examined. Further work is required to discern the full repertoire of Notch receptors and ligand-receptors in both normal and cancerous epithelia (including subpopulations) and how different isoforms respond to treatment. Any differences in cancer cell Notch signalling that can be targeted using receptor isoform specific antibodies in conjunction with LTP treatments could provide an enhanced killing effect in the tumour over surrounding normal tissue. This result

would be a significant advance towards the clinical implementation of the plasma-device as a possible focal therapy option in the treatment of localised prostate cancers.

8. Future work

8.1 – Determination of allelic expression changes in prostate cancer

This study attempted to assess any allelic expression changes produced by mutations in the SPOP, PTEN and IDH1 genes. There is a common assumption by cancer genome studies that detected heterozygous mutations are always expressed; biallelic expression would thus produce a mix of wildtype and non-functional or neomorphic protein product that enforces the molecular pathology of the tumour. Studies that have combined genomic and transcriptomic data have observed that some cancers do not express the mutated allele **(497, 553, 555)**. Combined datasets have been acquired from prostate cancers, **(330)** however the appropriate analysis of the data to the level of allelic expression hasn't been conducted.

One of the main purposes of the study was to determine whether the presence of a mutated allele affected the expression of the gene. Would the allele be continually expressed, or would it be silenced? There are several functional implications of heterozygous mutation in the context of allelic expression due to the plastic nature of epigenetic control. For example;

- The disease allele may be silenced and not expressed at all as it is simply disadvantageous to the cancer.
- The disease allele may be silenced to be later expressed. This may be due to a shift in microenvironmental stimuli, a permissive mutation/s is accrued that allows the silenced allele to be expressed without killing the cell, or possibly a differentiation stimulus, followed by a change in transcription factor regimens permits disease allele expression.
- The disease allele may be expressed biallelically alongside the wildtype.
- The disease allele may be selectively expressed whilst wildtype is silenced to give a population of affected protein that can cause carcinogenesis without the effect being "diluted" by wildtype protein.

Due to the heterogeneity in primary prostate cultures, any of the above hypotheticals could be occurring exclusively or simultaneously in different epithelial subpopulations. This was observed to be the case for the allelic expression of TMPRSS2-ERG. The fused allele was selectively expressed in the stem cell fraction of the prostate tumour epithelia and the "choice" of allele then relaxed throughout differentiation. The unit of heterozygosity between the alleles needed to be a relevant point mutation, a SNP wouldn't create a "disease" allele and therefore it would be assumed to have no bearing upon allelic gene expression. SNPs would have been used to determine true biallelic expression of SPOP, PTEN and IDH1 in wildtype cultures as reading the pyrosequencing trace of the mutated nucleotide position in a wildtype homozygous cDNA sample

would always show a 100% distribution of the nucleotide, without informing on the different contributions of the two wildtype alleles to that nucleotide position's 100% total. However, only IDH1 has a suitable coding synonymous SNP; rs11554137 that occurs at a population frequency of ~6%. A more laborious way to ascertain allelic expression of the genes would be to use single molecule FISH techniques that can detect intronic SNP expression in nascent mRNA **(893, 894)**. SPOP (rs6504618 in intron 8), PTEN (rs555895 in intron 8) and IDH1 (rs1437410 in intron 4) would be the appropriate heterozygous markers.

The primary aim of the study was to determine if the allelic restriction of TMPRSS2 and that of the TMPRSS2-ERG fusion observed in primary prostate cultures was imposed by either gene body or promoter deposition of asymmetrical activating and silencing histone trimethylations **(489, 526)**. This was due to the switching of allelic expression through differentiation. Fluctuations that were unable to be associated to promoter methylation status in the various epithelial subpopulations **(246)**. Although understanding of epigenetics has increased significantly over the last 20 years, it is still difficult to ascertain whether histone modifications determine the transcriptional state of associated chromatin or are deposited for transcriptional memory to mark a neighbourhood that is silent or active **(895)**. For example, RNA Polymerase II associated Set1 and 2 enzymes methylate histones as the polymerase transcribes the gene – these particular methylations are a consequence of transcription **(896, 897)**. Until recently the simplest way to alter histone modifications would be the application of an inhibitor targeting the enzyme responsible for deposition and removal of the marks. This changes the global chromatin state, therefore any alteration in gene expression associated could be due to a number of factors other than the single histone mark deemed to have been removed or deposited at the locus of interest. These include activation or repression of master regulator transcription factors that can alter the global transcriptome and the alteration of genomic neighbourhood structuring which can repress of activate genes depending on the re-ordering of long and short-range chromatin loops.

The development of CRISPR-Cas9 technology now affords researchers the opportunity to position Cas9 anywhere in the genome. The sequence-specific targeting of Cas9 has allowed precise modification of the cellular epigenome. Catalytically deactivated Cas9 (dCas9) has been fused to p300 H3K27acetyltransferase **(898)**, LSD1 histone demethylase **(899)**, Tet1 DNA demethylase and Dnmt3a DNA methyltransferase **(900)**. These studies have shown that removal or deposition of epigenetic marks at key loci can activate or silence protein expression which then impacts cellular identity. This can be solely attributed to the placement of the dCas9 construct and not any off-target effects associated with enzyme inhibition. Use of these (and future) dCas9 systems alongside techniques that allow unbiased identification of proteins at specific genomic loci **(901-**

903) will further identification of protein factors and post-translational modifications that determine the transcriptional state of genes.

Unlike previously reported RME, **(487)** expression of the TMPRSS2 allele wasn't held to initial choice in the stem cell; allelic expression was switched during epithelial differentiation. This finding has implications in our understanding of the complexity of cancer heterogeneity, which is rooted in genomic studies rather than mRNA and protein expression variability, and could also act as a gateway for emergent expression of a previously silenced fusion allele in a more differentiated cell type whereupon tumourigenesis can occur alongside accumulation of other epigenetic and genetic defects. Promoter and gene body histone trimethylation status would have also been ascertained if SPOP, IDH1 and PTEN allelic expression had been identified. Through the TMPRSS2-ERG work, fourteen primary samples were fractionated in to SC/TA and CB subpopulations from which RNA and chromatin were isolated. This material is sufficient for further study of histone modifications and the impact that they may have upon allelic expression in prostate cancers.

Transcriptional bursting would have to be accounted for in further studies and remains a blight on otherwise powerful transcriptional datasets produced by microarrays and RNA-seq **(486)**. Due to the temporally asynchronous production of mRNA product, techniques that rely on a single snapshot in analysis are incapable of determining stable RME in the absence of other methodologies or repeated time-points. Transcriptional bursting of TMPRSS2 is unlikely as ERG protein levels and localisation were assessed in fusion positive cells by IF **(246)**. Subpopulations that expressed only the fused allele expressed the ERG protein and in cultures that exclusively expressed unfused TMPRSS2 mRNA, the transcription factor protein was absent. ERG half-life in prostate cells is longer than typical bursts of allelic transcription **(904)** yet this may vary in the primary cultures meaning that, either ERG protein turnover is rapid (in this microenvironmental context) or there is a stability in allelic expression of the gene beyond that of transcriptional bursting in the epithelial subpopulations of primary prostate epithelial cells.

The impact of selective allelic expression in cancer is vast as it allows flexible expression of disease genes in varying contexts of differentiation and carcinogenesis. To gain further knowledge into the pervasiveness of this phenomenon would only serve to deepen our understanding of the disease and inform future treatment choices as clinicians progress towards the ultimate goal of personalised prostate cancer medicine; tailored treatment of each and every man's cancer at an individual level.

8.2 – LTP induced signalling and cell fate outcomes in prostate epithelial subpopulations

Investigation of the transcriptional response to LTP treatment in the primary culture system revealed induction of stress signalling and activation of multiple pathways that can impact cell fate decisions. Analysis of how individual cell populations contribute to whole culture response and how cell fate outcomes are reached by the signalling networks initiated by plasma are required to ascertain pathways that are treatment-actionable.

To confirm that the reactive species created by LTP were the primary agent in the induction of cellular transcriptional response, experiments using ROS scavengers, such as the vitamin E analogue trolox or N-actelycysteine **(905, 906)** would allow rescue of signal transduction through AP-1 and cleavage of the Notch receptor if reactive species were responsible. There is also the possibility that the electroporative effects of LTP **(790, 791)** may cause mechanical release of the NICD by disrupting the cell membrane. Use of the scavenging molecules should ascertain if Notch cleavage is a ROS-independent event or whether reactive species are responsible for the upregulation of Notch target genes.

As previously discussed, the mixing of progenitor and more differentiated cells can dilute the transcriptional signature produced by either cell pool if the other in non-responsive. To fully appreciate the differences between the cell populations in which resistance may either be inherent or develop following LTP, signatures (both transcriptional and in signalling intermediates) from separate epithelial subpopulations need to be established. WP cultures fractionated into SC/TA and CB cells would be treated with LTP and the subpopulation response measured using microarray and protein analysis. The reduction in cellular heterogeneity should allow transcriptional signatures to be viewed more clearly – such as Notch signalling in the SC/TA cells.

From the knowledge of varying responses in the subpopulations, indicators of the different signalling pathways activated (AP-1, Nrf2, Notch, NF-kB) would be chosen. Ideally this would be in conjunction with live cell imaging to map changes in responsive cell populations over a longer time-course – ie. does the pJun population die after 24 hours? Monitoring protein levels/subcellular localisation of the responsive mRNA transcripts such as the NR4A isoforms and those of the Notch signalling pathway; NRARP, HES1 and HEY1, could be useful here and would allow the initiated transcriptional response to be resolved in cells. The appropriate marking of positive Notch response, positive Jun response and positive Nrf2 response would allow tracking of populations of cells, from initial signalling to final cell fate outcome. To this end, SmartFlares would have been the ideal experimental tool as they would allow real time activation of specific signalling pathways to be viewed due to gene expression changes following LTP treatment. In the failure to mark signalling intermediates, specific si/shRNA or small molecule inhibition of individual pathways, up- and downstream of transactivation, will be sufficient to tease apart the

pathways critical in LTP resistance and survival, from those that direct cell death or are completely inconsequential in the determination of cell fate. In the case of Notch signalling, particular monitoring of differentiation antigens before and after plasma exposure (with and without Notch receptor inhibition) would be interesting in validating whether LTP-induced ROS impact balances within the epithelial hierarchy of the prostate.

Appendices

A.1 – Complete Sanger sequence traces of all samples; TMPRSS2, SPOP, PTEN & IDH1

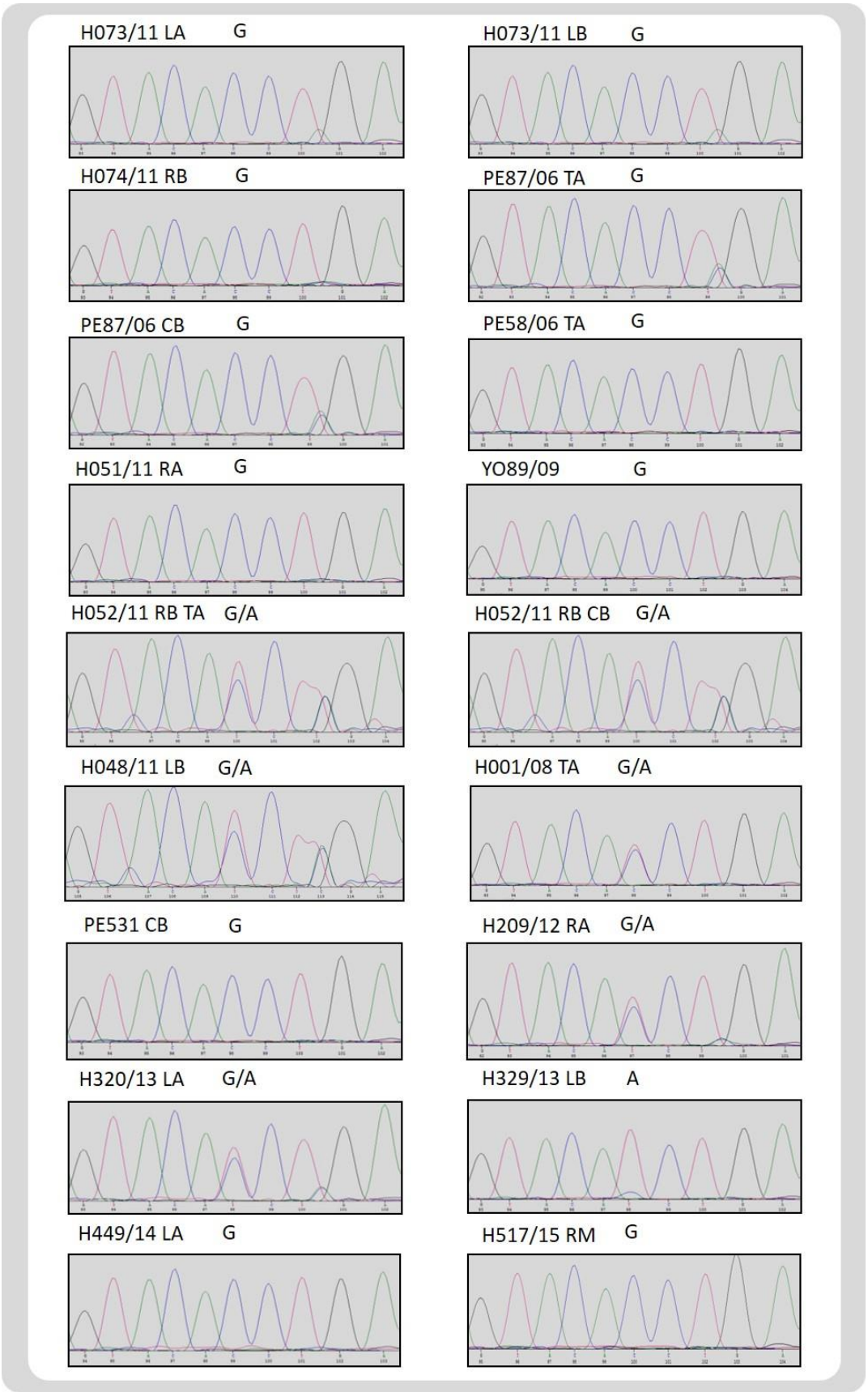

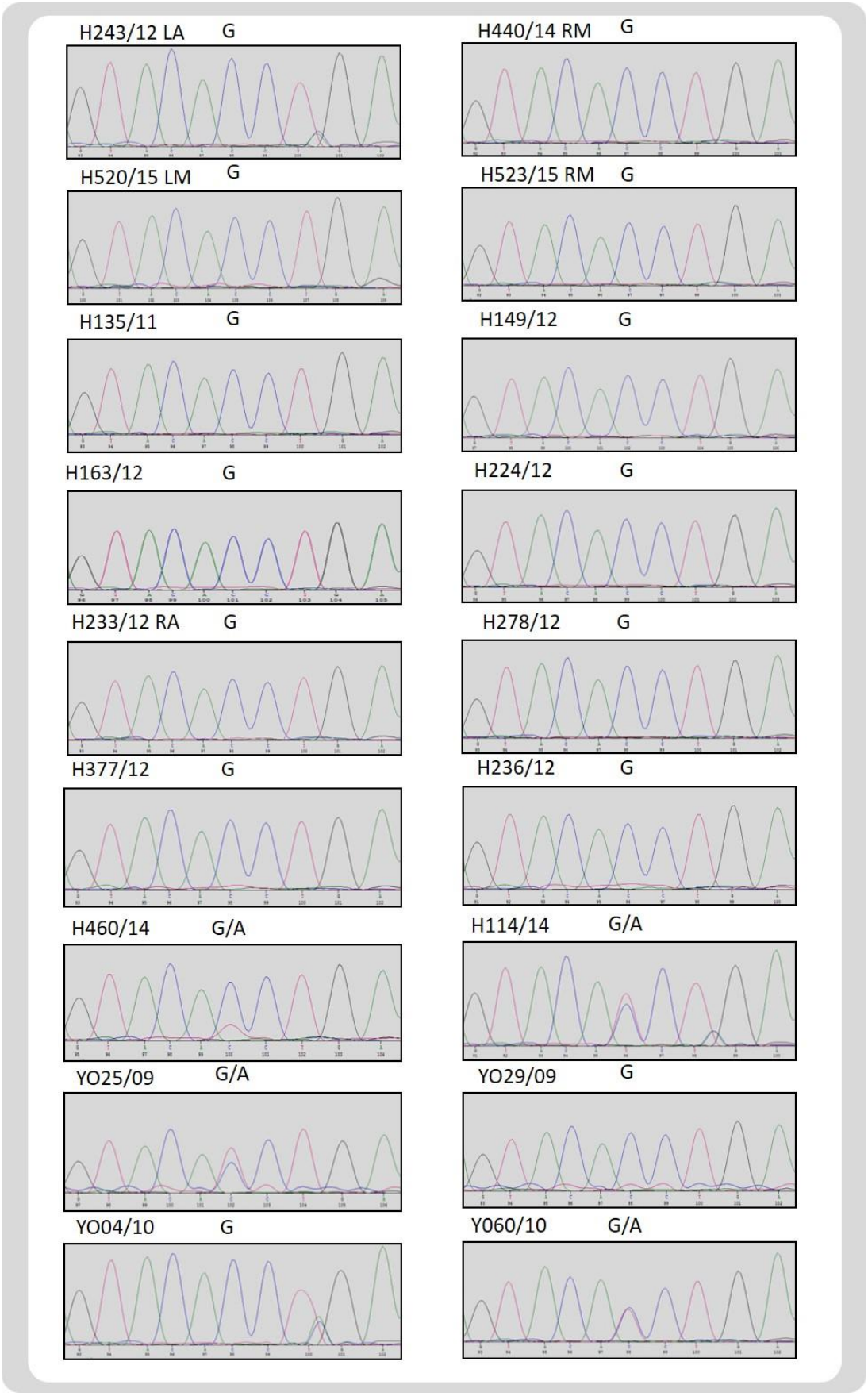

FIGURE 79 – TMPRSS2 exon 6 Sanger sequence traces.

Heterozygosity at the rs12329760 position detected in the PCR product is displayed in, and marked above traces.


H073/11 LA
H073/11 LB
H074/11 RB
PE87/06 TA
PE87/06 CB
PE58/06 TA
H051/11 RA
rs2066747
YO89/09
H052/11 RB TA
H052/11 RB CB
H048/11 LB
H001/08 TA
H050/11 RA
PE667 CB


PE531 CB
H209/12 RA
H320/13 LA
H329/13 LB
rs2066747
H449/14 LA
H517/15 RM
H243/12 LA
H440/14 RM
H520/15 LM
H523/15 RM
H135/11
rs2066747
H149/12
rs2066747
H163/12
H224/12


H233/12 RA rs2066747
H278/12
H377/12
H236/12
H016 PDX
H027 PDX
H042 PDX
H149 PDX
H288 PDX rs2066747
YO19 PDX rs2066747
H460/14
H048/11 RB
H052/11 LB
H054/11 RB

FIGURE 80 – SPOP exon 6 and 7 Sanger sequence traces of all samples.

The rs2066747 SNP status of the sample is displayed in, and marked above traces.

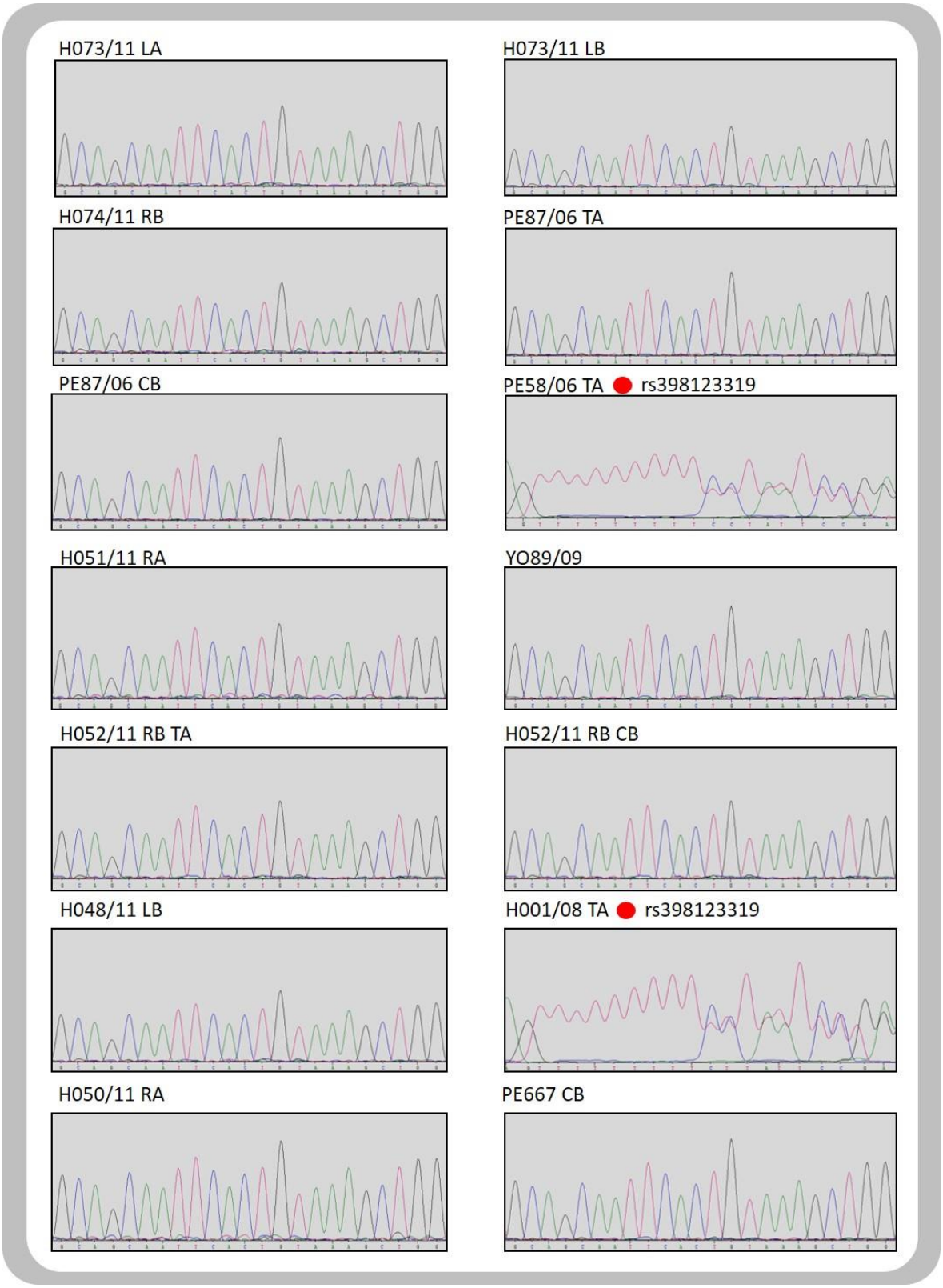
H073/11 LA
H073/11 LB
H074/11 RB
PE87/06 TA
PE87/06 CB
PE58/06 TA
rs398123319
H051/11 RA
YO89/09
H052/11 RB TA
H052/11 RB CB
H048/11 LB
H001/08 TA
rs398123319
H050/11 RA
PE667 CB

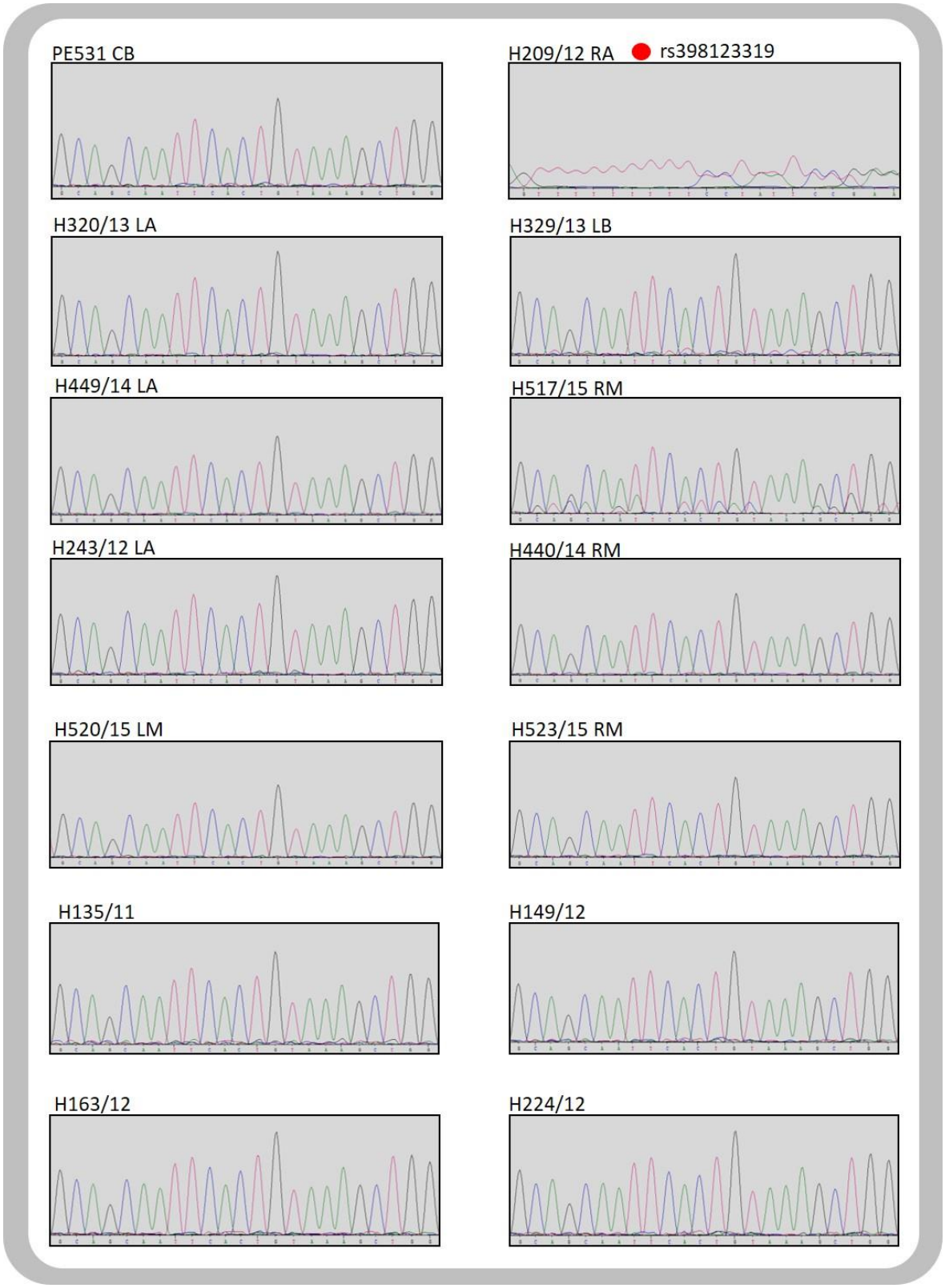
PE531 CB
H209/12 RA
rs398123319
H320/13 LA
H329/13 LB
H449/14 LA
H517/15 RM
H243/12 LA
H440/14 RM
H520/15 LM
H523/15 RM
H135/11
H149/12
H163/12
H224/12

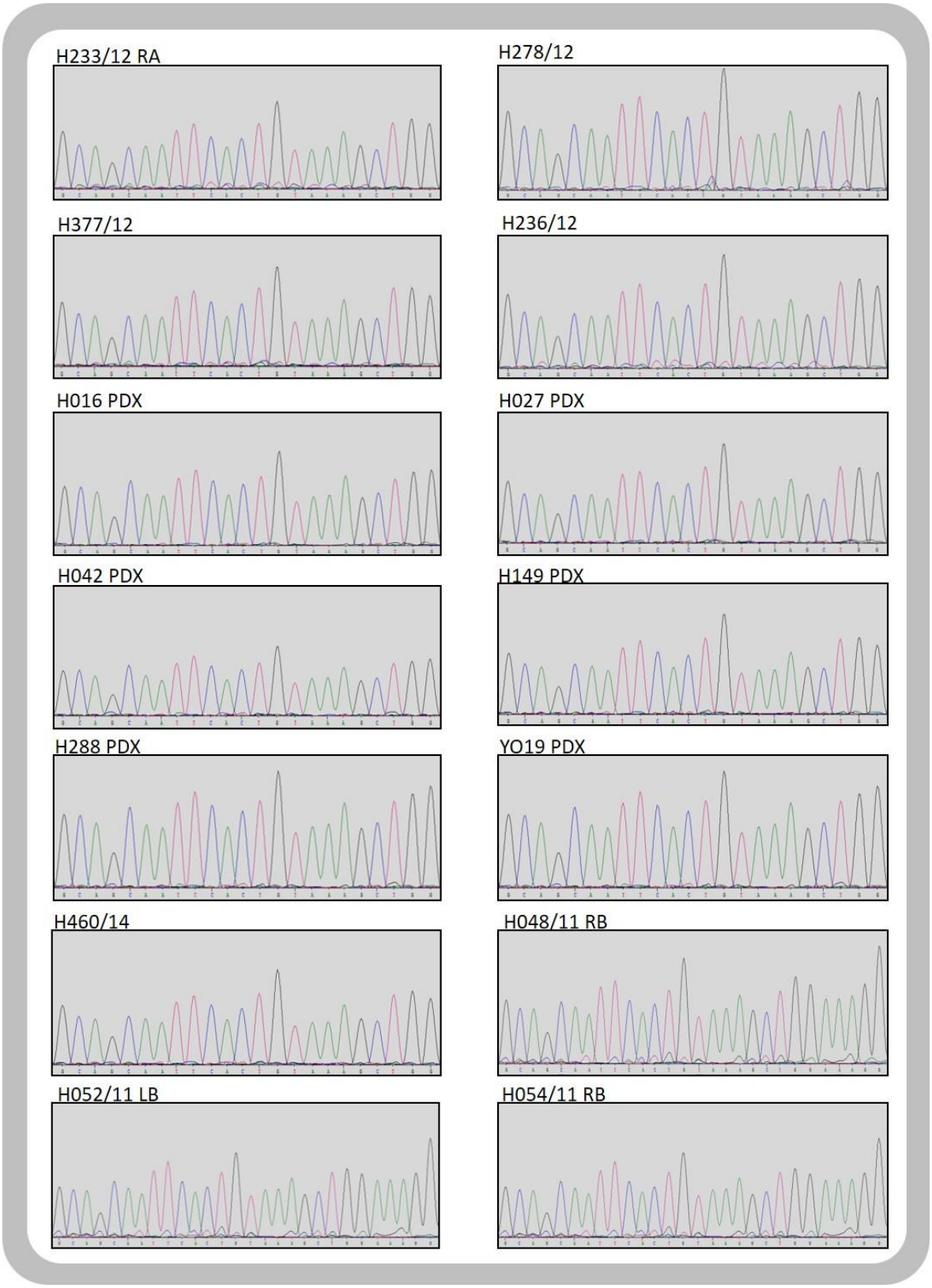
H233/12 RA
H278/12
H377/12
H236/12
H016 PDX
H027 PDX
H042 PDX
H149 PDX
H288 PDX
YO19 PDX
H460/14
H048/11 RB
H052/11 LB
H054/11 RB

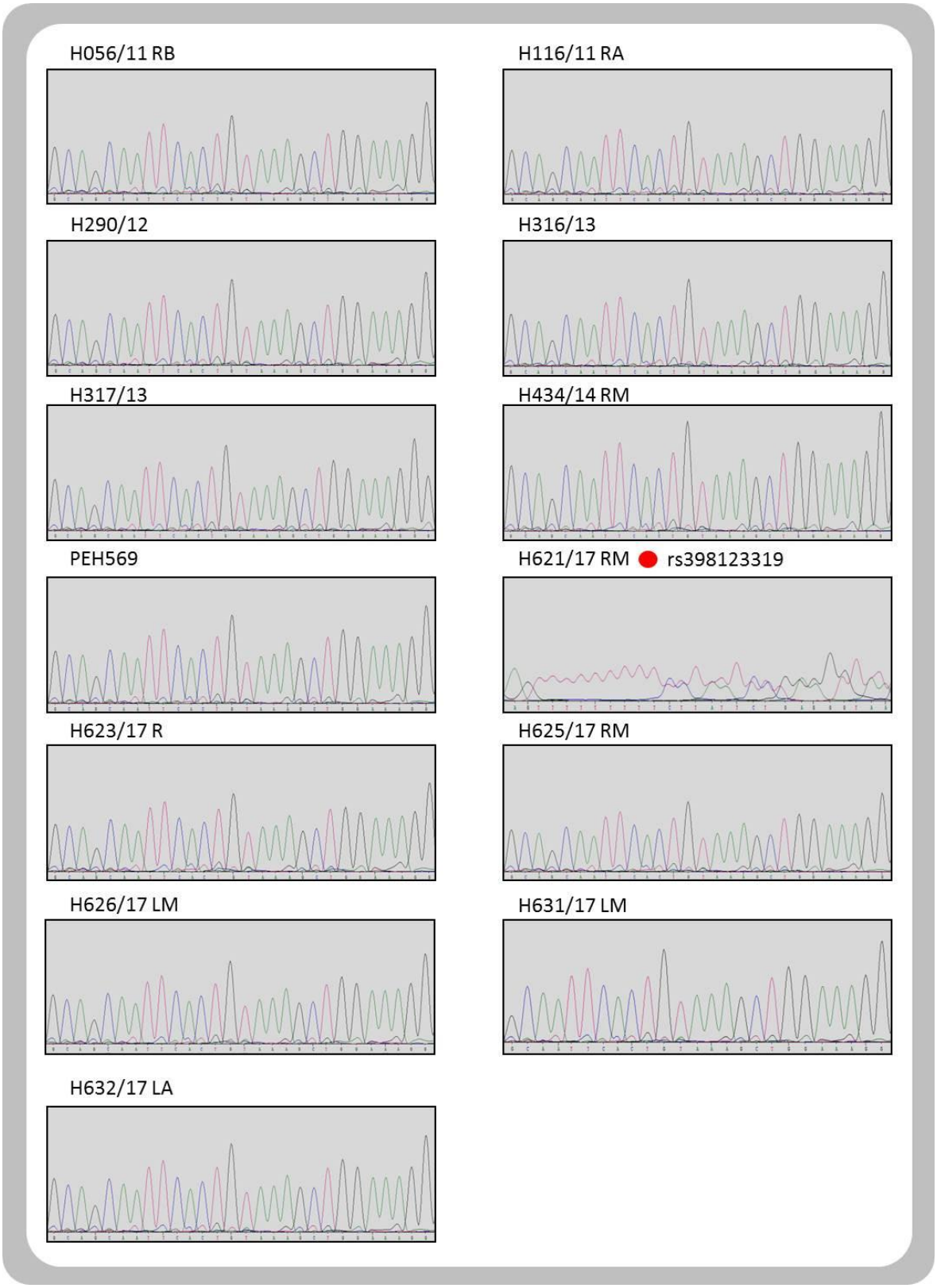

FIGURE 81 – PTEN exon 5 Sanger sequence traces of all samples.

The rs398123319 SNP status of the sample is displayed in, and marked above traces.

H073/11 LA

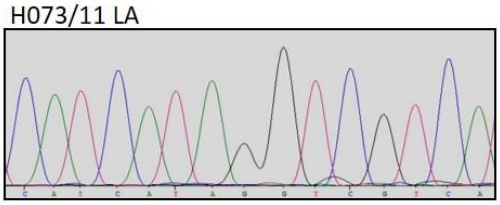

H073/11 LB

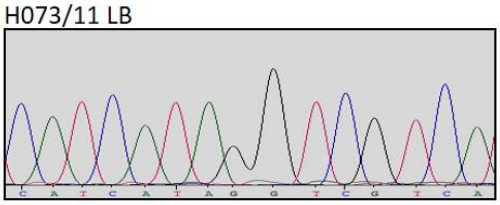

H074/11 RB

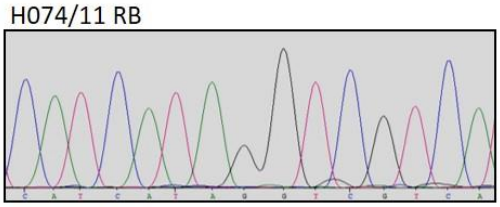

PE87/06 TA

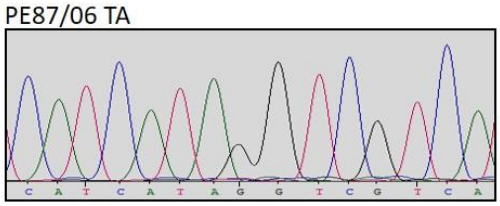

PE87/06 CB

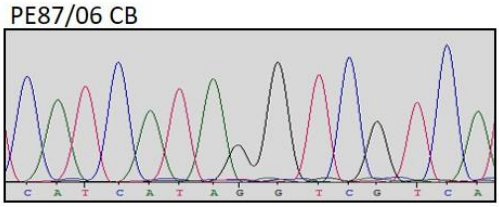

PE58/06 TA

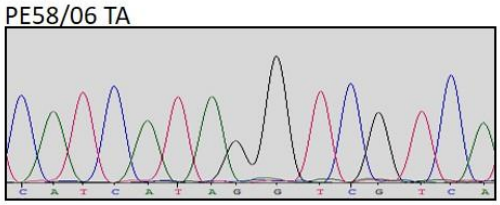

H051/11 RA

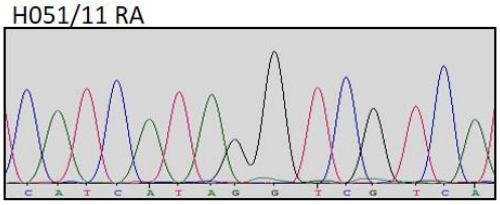

YO89/09

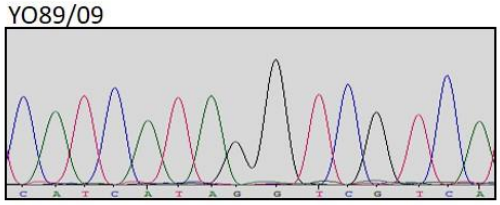

H052/11 RB TA

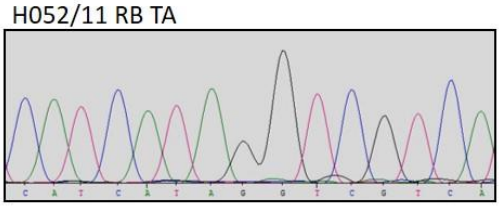

H052/11 RB CB

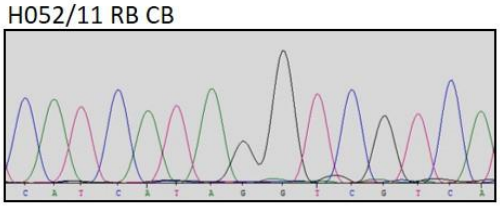

H048/11 LB

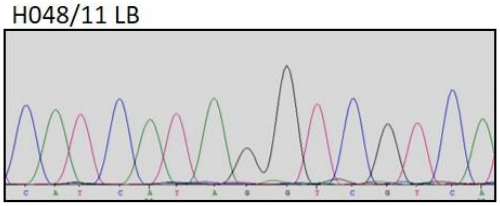

H001/08 TA

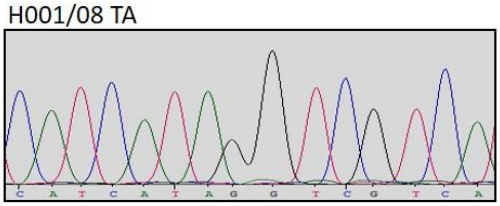

H050/11 RA

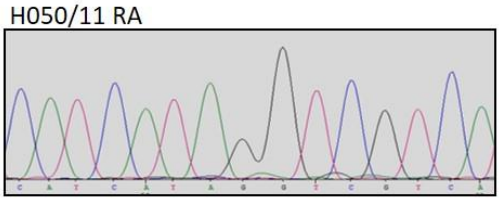

PE667 CB

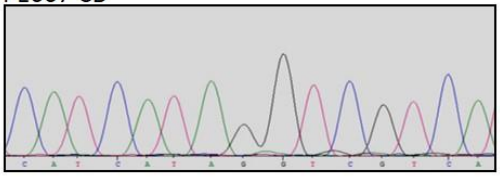

PE531 CB

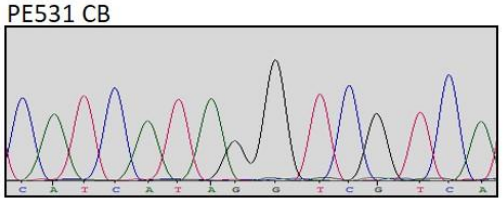

H209/12 RA

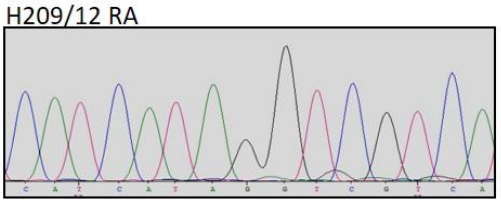

H320/13 LA

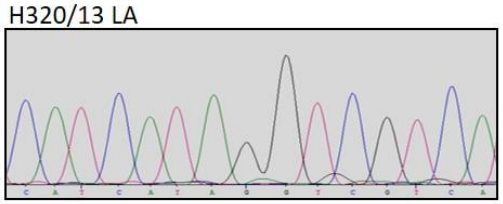

H329/13 LB

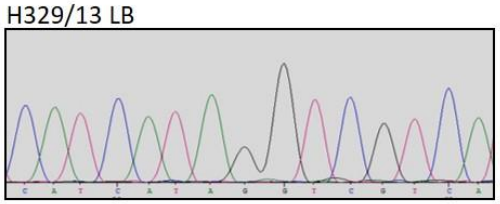

H449/14 LA

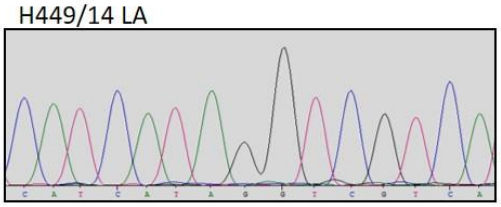

H517/15 RM

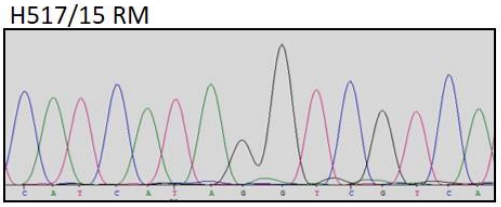

H243/12 LA

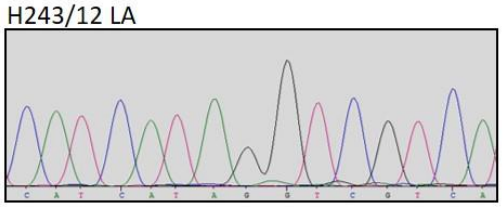

H440/14 RM

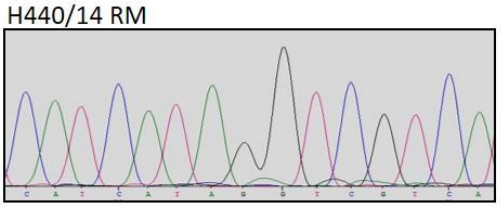

H520/15 LM

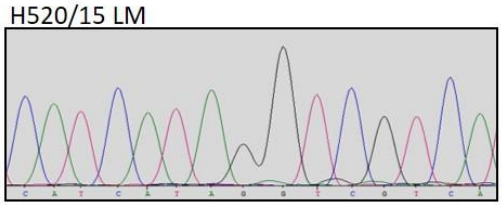

H523/15 RM

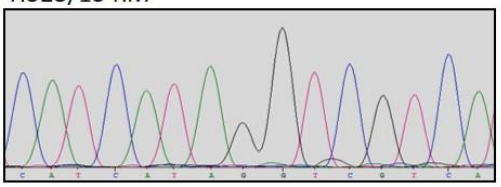

H135/11

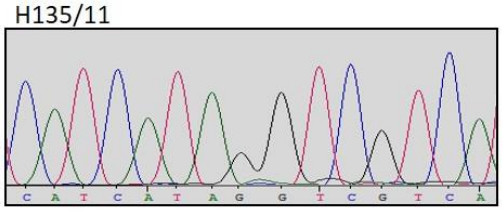

H149/12

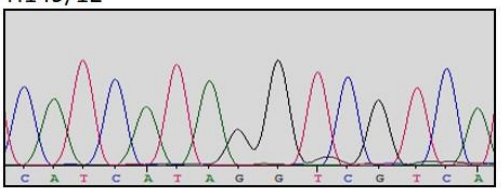

H163/12

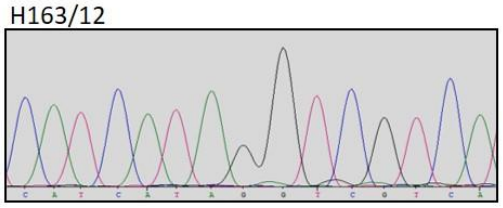

H224/12

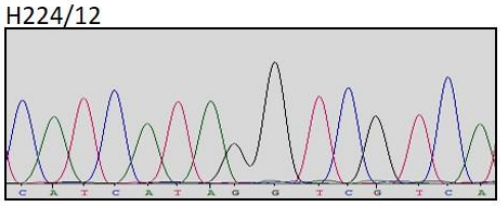

H233/12 RA

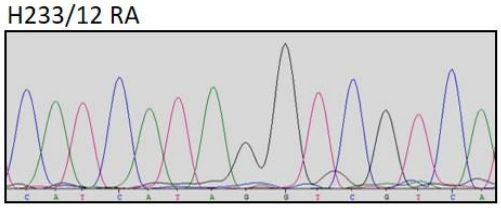

H278/12

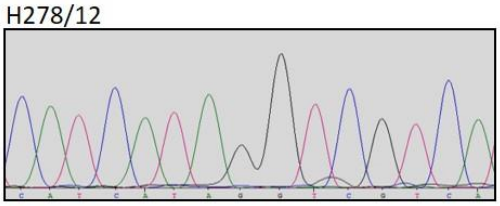

H377/12

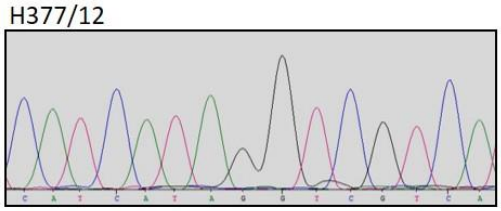

H236/12

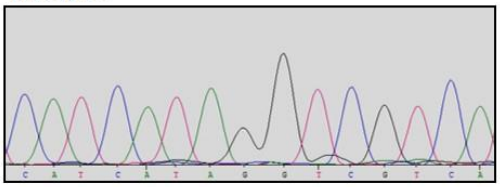

H016 PDX

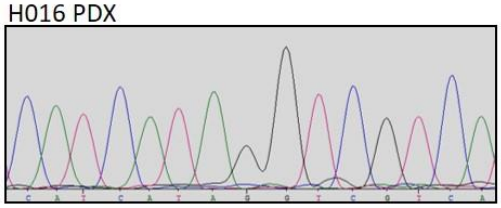

H027 PDX

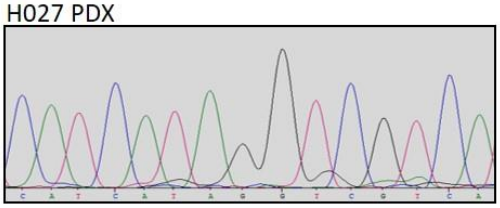

H042 PDX

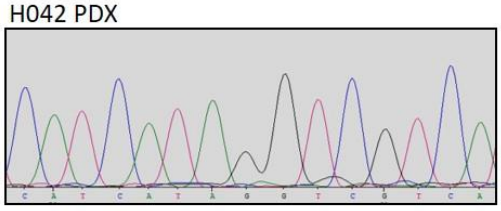

H149 PDX

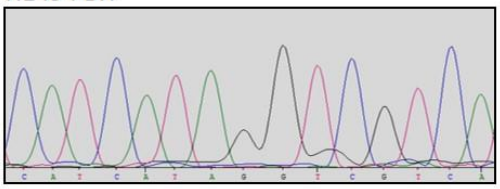

H288 PDX

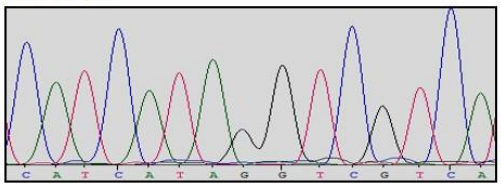

YO19 PDX

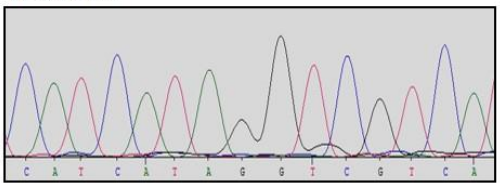

H460/14

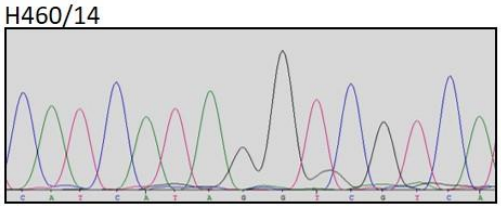

H048/11 RB

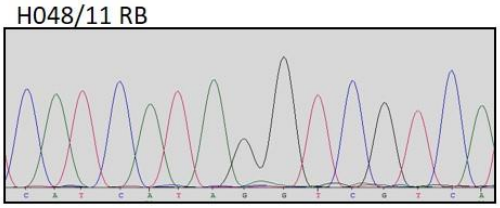

H052/11 LB

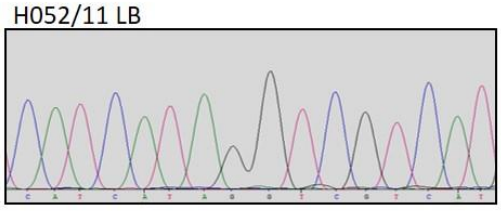

H054/11 RB

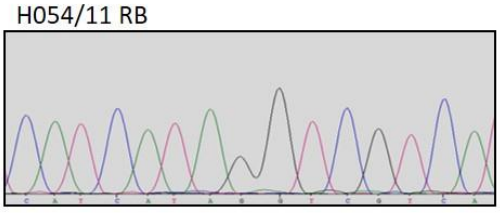

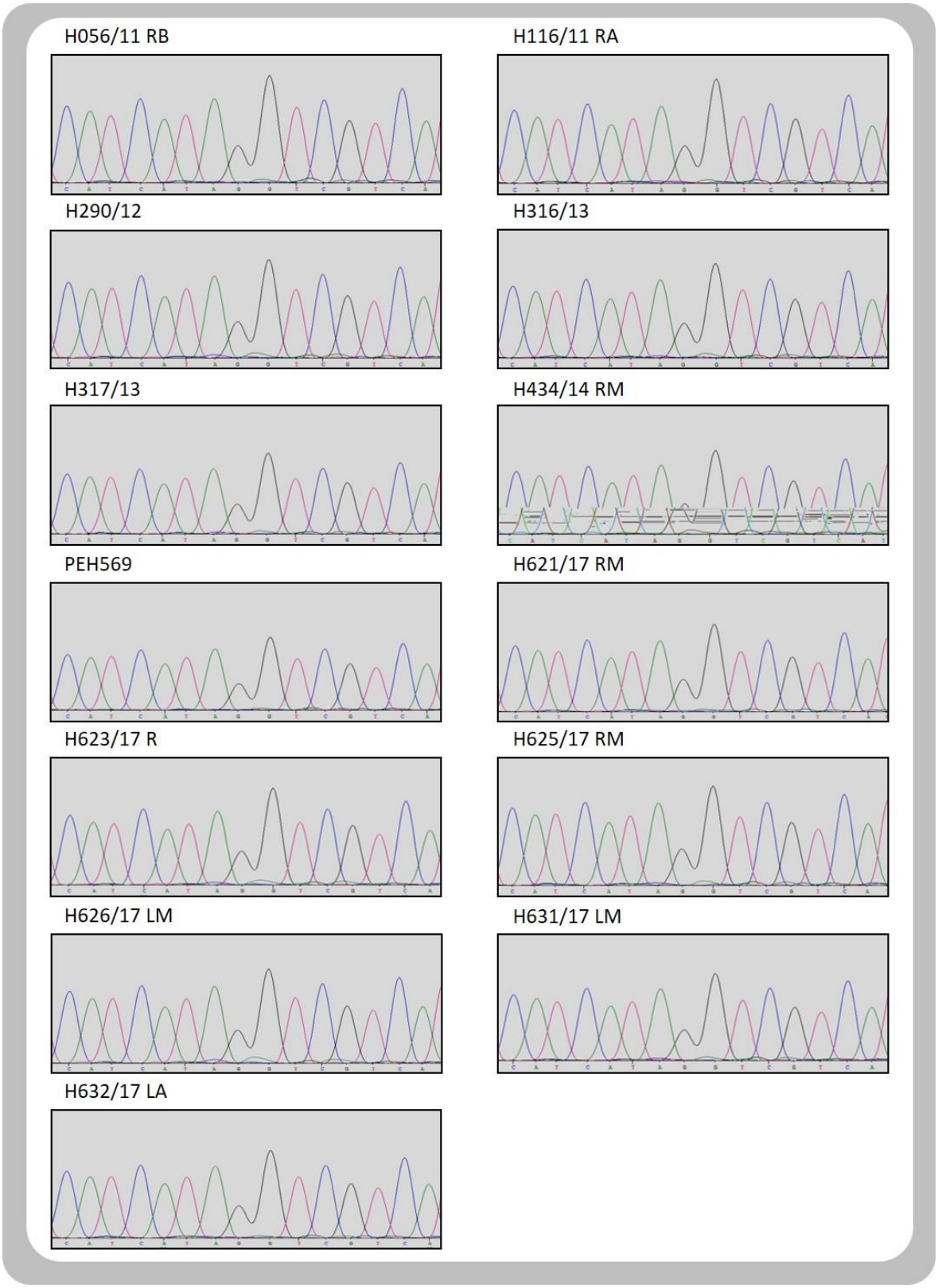

FIGURE 82 – IDH1 exon 6 Sanger sequence traces of all samples.

Traces show the location of the most frequent IDH1 mutation; R132H.

A.2 - Development of P4E6 as a stress signalling model of prostate cancer

Primary cultures have limitations in biological research as they are difficult to transfect and also don't grow to cell numbers large enough for some analytical techniques. Access to an easy-to-use model of LTP induced stress signalling would be advantageous in discerning some of the molecular details in the response.

Luciferase assays allow an accurate assessment of stress pathway transcriptional activation by measuring luminescence initiated by reporter Luciferase expression. In this context, the Luciferase gene has been placed downstream of a series of transcription factor elements on a plasmid. Promega supply a number of stress-reporter luciferase constructs. AP-1 and ARE (Nrf2) stress-reporter *Firefly* luciferase plasmids were acquired alongside constitutive Thymidine Kinase (TK) and CMV *Renilla* luciferase constructs. The constitutive reporters allow transfection efficiency to be estimated and normalised between conditions. The CMV promoter was used to optimise initial transfection of the cell lines and the TK for use in the stress reporter dual luciferase assay as CMV promoters can be transactivated by SAPKs such as JNK **(907)**. Vectors were prepared in competent bacteria and their identity confirmed by double restriction digest using the publicly available vector sequences provided by Promega **(Figure 83A)**. Optimising the transfection of the BPH-1 and P4E6 cell lines was attempted using a GFP plasmid. BPH-1 cells are usually easy to transfect however, using the XtremeGene reagent and varying seeding densities, transfection efficiency didn't exceed 30% **(Figure 83B)**. As the XtremeGene system was unsuccessful, Lonza Nucleofection – which had previously been used in my laboratory to achieve ~70% transfection efficiency in the P4E6 line – was used instead. However, even with varying input plasmid amount and seeding density transfection efficiency was poor **(Figure 83C)**. As a result of this and the prioritisation of other experiments, the luciferase reporter work was left incomplete. Inclusion of Notch reporter luciferase plasmids in future study would ascertain whether P4E6 also show an activation of the pathway by LTP.

P4E6 grow more quickly than primary cultures and have higher replicative longevity meaning that the cell numbers needed for transcription factor ChIP could be reached. $20x10^6$ cells were to be used for each condition; untreated, arsenite and LTP treated. Sonication cycles were tested on P4E6 chromatin. A program of 45 cycles was used to concentrate fragments between 200-1000bp **(Figure 84)**. Post-treatment time-points for the cross-linking of chromatin in treated P4E6 cells was determined using the HMOX1 and JUN expression time-courses, **(Figure 60A+B)** 0.5 hours following treatment was chosen for Jun and the 4 hour time-point for Nrf2 – as the transcription factors would be expected to be bound to promoter elements here to cause the rise in target gene expression. Unfortunately, due to prioritisation of other work, the ChIP experiments, like the luciferase work was unable to be completed.

A continuation of both streams of study and adaptation of new ChIP techniques to reduce cell number requirements is required to characterise LTP stress signalling in the P4E6 cell line and determine whether it is a faithful representation of primary cell LTP response.

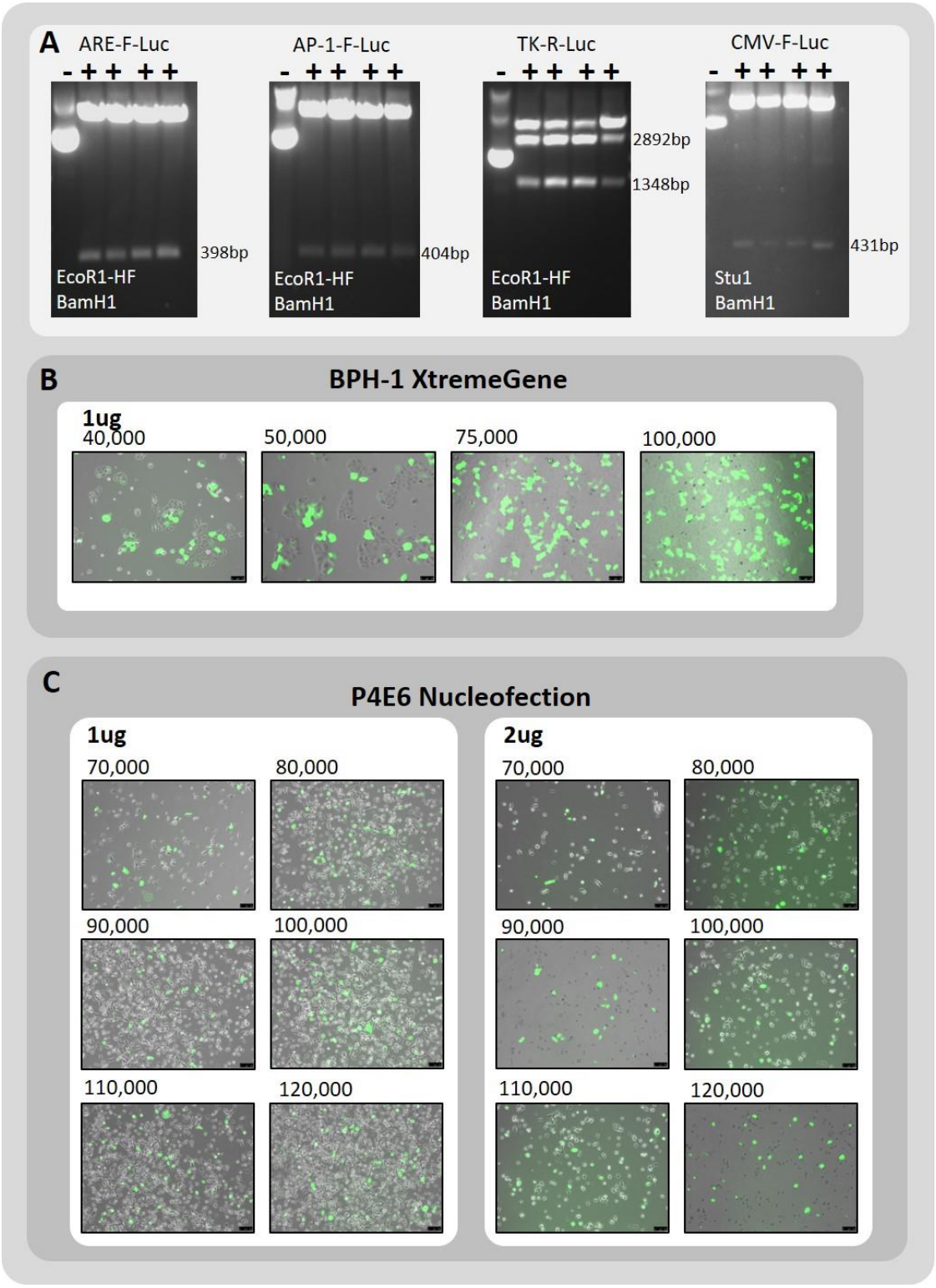

FIGURE 83 - Stress-reporter Luciferase vector preparation and optimisation of P4E6 transfection.

A) Double restriction digest of stress and constitutive reporter *Firefly* (F) and *Renilla* (R) Luciferase (Luc) plasmids to confirm construct identity. **B)** Transfection of the BPH-1 cell line, seeded at increasing densities, with GFP using the XtremeGene reagent. Black scale bar is 25µm. **C)** Transfection of the P4E6 cell line with GFP by Nucleofection. Cells were seeded at increasing densities and amount of input plasmid was either 1 or 2µg. Black scale bar is 100µm.

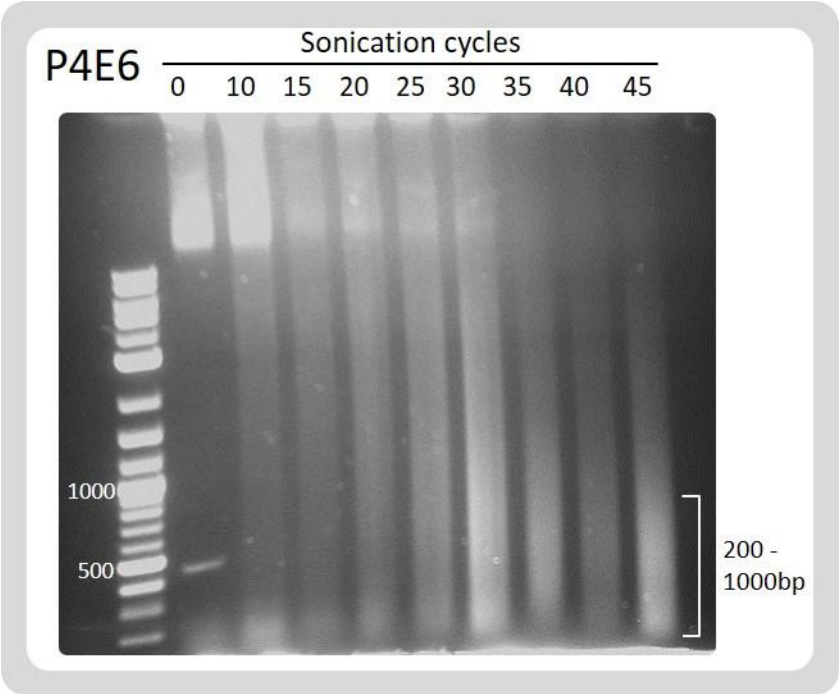

FIGURE 84 - Optimisation of P4E6 chromatin sonication.

Increasing sonication cycle number produce fragmentation of the chromatin until an enrichment of fragments less than 1000bp was produced at 45 sonication cycles.

List of Abbreviations used

2-HG – 2-hydroxygluturate

ADT – Androgen Deprivation Therapy

ALL – Acute Lymphoblastic Leukaemia

AML – Acute Myeloid Leukaemia

AP-1 – Activator Protein 1

AR – Androgen Receptor

ARE – Antioxidant Response Element

AR-V – Androgen Receptor splice variant

ASAR – Asynchronous Replication and Autosomal RNAs

AZ – Anterior Zone

BCA -Bicinchoninic Acid

BET – Bromodomain and Extraterminal

bHLH – basic Helix-Loop-Helix

BLAST – Basic Local Alignment Search Tool

BM – Basement Membrane

bp – base pair

BPH -Benign Prostatic Hyperplasia

BSA – Bovine Serum Albumin

BTB – Bric-a-brac/Tramtrack/Broad

CB – Committed Basal cell

CDK – Cyclin Dependent Kinase

ChIP – Chromatin Immunoprecipitation

CK - Cytokeratin

CLL – Chronic Lymphoblastic Leukaemia

CMV – Cytomegalo Virus

COSMIC – Catalogue Of Somatic Mutation In Cancer

COX – Cytochrome c Oxidase

CRISPR – Clustered Regularly Interspaced Palindromic Repeats

CRL3 - Cullin3-RING E3 ligase

CRPC – Castrate Resistant Prostate Cancer

CRUK – Cancer Research United Kingdom

CSC – Cancer Stem Cell

Ct – Threshold Cycle value

CTC – Circulating Tumour Cell

CZ – Central Zone

DAH – Differentiation Associated Hypermethylated

DAPK1 – Death Associated Protein Kinase 1

DBD – DNA Binding Domain

dCas9 – deactivated Cas9

DHT – Dihydrotestosterone

DICD – Delta Intracellular Domain

DLL- Delta-Like

DNA – Deoxyribo Nucleic Acid // c (prefix) – copy // g (prefix) - genomic

DNMT – DNA Methyltransferase

DRE – Digital Rectal Exam

DSB – Double Strand Break

DTT – Dithiothreiotol

DUSP1 – Dual Specificity Phosphatase 1

EBV - Epstein-Barr Virus

EGF – Epidermal Growth Factor

EMT – Epithelial to Mesenchymal Transition

ER – Endoplasmic Reticulum

ER – Estrogen Receptor

ESC – Embryonic Stem Cell

FAK – Focal Adhesion Kinase

FC – Field Cancerisation

FCS – Foetal Calf Serum

FGF – Fibroblast Growth Factor

FISH – Fluorescent In Situ Hybridisation

FP – Forward Primer

G – (prefix to a number) Gleason

GF – Growth Factor

GO – Gene Ontology

GPX – Glutathione Peroxidase

GR – Glucocorticoid Receptor

GSH – Glutathione

GSI – Gamma Secretase Inhibitor

GSR – Glutathione Reductase

H – followed by 1,2,3 or 4 – Histone

HCA – Heterocyclic Amines

HDAC – Histone Deacetylase

HIFU – High Intensity Focused Ultrasound

HMOX - Haem Oxygenase

HMT – Histone Methyltransferase

HPV – Human Papillomavirus

hr – hour/s

HRR – Homologous Recombination Repair

HSC – Haematopoietic Stem Cell

HSPA1A – Heat Shock Protein A1A

ICR – Imprinting Control Region

ID – Inhibitors of Differentiation

IDH1 – Isocitrate Dehydrogenase 1

IF – Immunofluorescence

IGF – Insulin-like Growth Factor

IL – Interleukin

JAG – Jagged

JICD – Jagged Intracellular Domain

LA – Left Apex

LB – Left Base

LBD – Ligand Binding Domain

LH – Luteinising Hormone

LHRH – Luteinising Hormone Releasing Hormone

LIMMA - Linear Models for Microarray and RNA-seq Data

LM – Left Mid

LOH – Loss of Heterozygosity

LRP – Laparascopic Radical Prostatectomy

LTP – Low Temperature Plasma

MAF – Minor Allele Frequency

MAPK – Mitogen Activated Protein Kinase

MATH – Meprin and TRAF homology

MDS – Multidimensional Scaling

MET – Mesenchymal to Epithelial Transition

min – minute/s

MM – Master Mix

MMP – Matrix Metalloproteinase

mpMRI – multi-parametric Magnetic Resonance Imaging

NEPC – Neuroendocrine Prostate Cancer

NHEJ – Non -homologous End Joining

NICD – Notch Intracellular Domain

NIK – NF-kB Inducing Kinase

NK – Natural Killer cells

NR4A – Nuclear Receptor 4 A

NRARP - Notch Regulated Ankyrin Repeat Protein

NRG - NOD-Rag1$^{-/-}$-ILR2γ$^{-/-}$

NSG – NOD-SCID-ILR2 γ$^{-/-}$

NTC – No Template Control

NTD – N Terminal Domain

ORP – Open Radical Prostatectomy

p – (prefix to number) passage

p – (prefix to protein) phoshpho-

PAP – Prostatic Acid Phosphatase

PBS – Phosphate Buffered Saline

PCR – Polymerase Chain Reaction // q (prefix) – quantitative // RT (prefix) – reverse transcriptase

PDGF – Platelet Derived Growth Factor

PDT – Photodynamic Therapy

PDX – Patient Derived Xenografts

PDZ - PSD-95/Dlg/Zo1

PFA – Paraformaldehyde

PHD – Prolyl Hydroxylase Domain containing protein

PhIP - 2-amino 1-methyl-6-phenylimidazo[4,5-b]pyridine

PIA – Prostatic Inflammatory Atrophy

PIN – Prostatic Intraepithelial Neoplasia // hg (prefix) – High Grade

PIP – Phosphatidylinositol phosphate

PLB – Passive Lysis Buffer

POZ - Pox virus and Zinc finger

PR – Progesterone Receptor

PRC2 – Polycomb Repressive Complex 2

PRDX – Peroxiredoxin

PSA – Prostate Specific Antigen // f (prefix) – Free // c (prefix) - Complexed

PTEN - Phosphatase and tensin homologue deleted on chromosome ten

PTM – Post Translational Modification

PTP – Protein Tyrosine Phosphatase

PZ - Peripheral Zone

RA – Right Apex

RAR/RXR – Retinoic Acid Receptor

RB – Right Base

RIPK - Receptor Interacting serine/threonine Protein Kinase

RM – Right Mid

RME – Random Monoallelic Expression

RNA – Ribo Nucleic Acid // m (prefix) – messenger // lnc (prefix) long non-coding // mi (prefix) – micro // si (prefix) - short-interfering // sh (prefix) - short-hairpin

RNS – Reactive Nitrogen Species

ROS – Reactive Oxygen Species

RP - Reverse Primer

RRP – Robotic Radical Prostatectomy

RT – Radiotherapy // EB (prefix) – External Beam

RT – Reverse Transcriptase **or** Room Temperature **or** Radiotherapy

SAPK – Stress Activated Protein Kinase

SBC – SPOP Binding Consensus

SC – Stem Cell

SCM – Stem Cell Media

SDO – Single Delta Oxygen

SDS – Sodium Dodecyl Sulphate

SEM – Standard Error of the Mean

SHH – Sonic Hedgehog

SNP – Single Nucleotide Polymorphism

SOD – Superoxide Dismutase

SOX9 – SRY box 9

SPOP - Speckled-type POZ protein

SQSTM1 – Sequestosome 1

SRXN – Sulfiredoxin

SSB – Single Strand Break

STHLM3 – Stockholm 3

STI – Sexually Transmitted Infection

T – Treated

TA – Transit Amplifying cell

TAE – Tris-Acetate-EDTA

TBS – Tris Buffered Saline

TCGA – The Cancer Genome Atlas

TERT – Telomerase Reverse Transcriptase

TET – Ten Eleven Translocase

TIC – Tumour Initiating Cell

TK – Thymidine Kinase

TNFR – Tumour Necrosis Factor Receptor

TNM – Tumour, Nodes, Metastases

TRUS – Transperineal Ultrasound

TSG – Tumour Suppressor Gene

TURP – Transurethral Resection of the Prostate // ch (prefix) – channel

TXN – Thioredoxin

TXNRD1 – Thioredoxin Reductase 1

TZ – Transitional Zone

U – Untreated

UGE – Urogenital Epithelia

UGM – Urogenital Mesenchyme

UGS – Urogenital Sinus

uPA – urokinase Plasminogen Activator

UTR – Untranslated Region

V - Volts

VEGF – Vascular Endothelial Growth Factor

WP – Whole Population

XCI – X Chromosome Inactivation

XIC – X chromosome Inactivation Centre

αKG – α-ketogluturate

References

1. Schauer IG, Rowley DR. The functional role of reactive stroma in benign prostatic hyperplasia. Differentiation; research in biological diversity. 2011;82(4-5):200-10.
2. Cohen RJ, Shannon BA, Phillips M, Moorin RE, Wheeler TM, Garrett KL. Central Zone Carcinoma of the Prostate Gland: A Distinct Tumor Type With Poor Prognostic Features. Journal of Urology. 2008;179(5):1762-7.
3. Akin O, Sala E, Moskowitz CS, Kuroiwa K, Ishill NM, Pucar D, et al. Transition zone prostate cancers: Features, detection, localization, and staging at endorectal MR imaging. Radiology. 2006;239(3):784-92.
4. McNeal JE. The zonal anatomy of the prostate. Prostate. 1981;2(1):35-49.
5. Risbridger GP, Almahbobi GA, Taylor RA. Early prostate development and its association with late-life prostate disease. Cell and Tissue Research. 2005;322(1):173-81.
6. Cunha GR. Tissue interactions between epithelium and mesenchyme of urogenital and integumental origin. Anatomical Record. 1972;172(3):529-41.
7. Cunha GR. The role of androgens in the epithelio-mesenchymal interactions involved in prostatic morphogenesis in embryonic mice. Anatomical Record. 1973;175(1):87-96.
8. Cunha GR, Lung B. The possible influence of temporal factors in androgenic responsiveness of urogenital tissue recombinants from wild-type and androgen-insensitive (Tfm) mice. Journal of Experimental Zoology. 1978;205(2):181-93.
9. Thomson AA, Marker PC. Branching morphogenesis in the prostate gland and seminal vesicles. Differentiation; research in biological diversity. 2006;74(7):382-92.
10. Wang Y, Hayward SW, Cao M, Thayer KA, Cunha GR. Cell differentiation lineage in the prostate. Differentiation; research in biological diversity. 2001;68(4-5):270-9.
11. Prins GS, Huang L, Birch L, Pu Y. The role of estrogens in normal and abnormal development of the prostate gland. Annals of the New York Academy of Sciences2006. p. 1-13.
12. Bonkhoff H, Wernert N, Dhom G, Remberger K. Basement membranes in fetal, adult normal, hyperplastic and neoplastic human prostate. Virchows Archiv A Pathological Anatomy and Histopathology. 1991;418(5):375-81.
13. Maitland NJ, Frame FM, Polson ES, Lewis JL, Collins AT. Prostate Cancer Stem Cells: Do They Have a Basal or Luminal Phenotype? Hormones and Cancer. 2011;2(1):47-61.
14. Berry PA, Maitland NJ, Collins AT. Androgen receptor signalling in prostate: Effects of stromal factors on normal and cancer stem cells. Molecular and Cellular Endocrinology. 2008;288(1-2):30-7.
15. Ayala G, Tuxhorn JA, Wheeler TM, Frolov A, Scardino PT, Ohori M, et al. Reactive Stroma as a Predictor of Biochemical-Free Recurrence in Prostate Cancer. Clinical Cancer Research. 2003;9(13):4792-801.
16. Hill R, Song Y, Cardiff RD, Van Dyke T. Selective evolution of stromal mesenchyme with p53 loss in response to epithelial tumorigenesis. Cell. 2005;123(6):1001-11.
17. Macintosh CA, Stower M, Reid N, Maitland NJ. Precise microdissection of human prostate cancers reveals genotypic heterogeneity. Cancer Research. 1998;58(1):23-8.
18. Hanson JA, Gillespie JW, Grover A, Tangrea MA, Chuaqui RF, Emmert-Buck MR, et al. Gene promoter methylation in prostate tumor-associated stromal cells. Journal of the National Cancer Institute. 2006;98(4):255-61.
19. Frame FM, Maitland NJ. Cancer stem cells, models of study and implications of therapy resistance mechanisms. Advances in Experimental Medicine and Biology2011. p. 105-18.
20. Oldridge EE, Pellacani D, Collins AT, Maitland NJ. Prostate cancer stem cells: Are they androgen-responsive? Molecular and Cellular Endocrinology. 2012;360(1-2):14-24.
21. Patrawala L, Calhoun-Davis T, Schneider-Broussard R, Tang DG. Hierarchical organization of prostate cancer cells in xenograft tumors: The CD44+α2β1+ cell population is enriched in tumor-initiating cells. Cancer Research. 2007;67(14):6796-805.
22. Grisanzio C, Signoretti S. p63 in prostate biology and pathology. Journal of Cellular Biochemistry. 2008;103(5):1354-68.

23. Bui M, Reiter RE. Stem cell genes in androgen-independent prostate cancer. Cancer and Metastasis Reviews. 1999;17(4):391-9.
24. Ruscica M, Dozio E, Motta M, Magni P. Role of neuropeptide Y and its receptors in the progression of endocrine-related cancer. Peptides. 2007;28(2):426-34.
25. Nelson EC, Cambio AJ, Yang JC, Ok JH, Lara PN, Evans CP. Clinical implications of neuroendocrine differentiation in prostate cancer. Prostate Cancer and Prostatic Diseases. 2007;10(1):6-14.
26. Beltran H, Beer TM, Carducci MA, De Bono J, Gleave M, Hussain M, et al. New therapies for castration-resistant prostate cancer: Efficacy and safety. European Urology. 2011;60(2):279-90.
27. Beltran H, Yelensky R, Frampton GM, Park K, Downing SR, MacDonald TY, et al. Targeted next-generation sequencing of advanced prostate cancer identifies potential therapeutic targets and disease heterogeneity. European Urology. 2013;63(5):920-6.
28. Collins AT, Berry PA, Hyde C, Stower MJ, Maitland NJ. Prospective identification of tumorigenic prostate cancer stem cells. Cancer Research. 2005;65(23):10946-51.
29. Rizzo S, Attard G, Hudson DL. Prostate epithelial stem cells. Cell Proliferation. 2005;38(6):363-74.
30. Bonkhoff H, Stein U, Remberger K. The proliferative function of basal cells in the normal and hyperplastic human prostate. Prostate. 1994;24(3):114-8.
31. Williamson SC, Hepburn AC, Wilson L, Coffey K, Ryan-Munden CA, Pal D, et al. Human α2β1HI CD133+VE Epithelial Prostate Stem Cells Express Low Levels of Active Androgen Receptor. PLoS ONE. 2012;7(11).
32. Bonkhoff H, Remberger K. Differentiation pathways and histogenetic aspects of normal and abnormal prostatic growth: A stem cell model. Prostate. 1996;28(2):98-106.
33. Jiao J, Hindoyan A, Wang S, Tran LM, Goldstein AS, Lawson D, et al. Identification of CD166 as a surface marker for enriching prostate stem/progenitor and cancer initiating cells. PLoS ONE. 2012;7(8).
34. Hansen AG, Arnold SA, Jiang M, Palmer TD, Ketova T, Merkel A, et al. ALCAM/CD166 is a TGF-b-responsive marker and functional regulator of prostate cancer metastasis to bone. Cancer Research. 2014;74(5):1404-15.
35. Burger PE, Gupta R, Xiong X, Ontiveros CS, Salm SN, Moscatelli D, et al. High aldehyde dehydrogenase activity: A novel functional marker of murine prostate stem/progenitor cells. Stem Cells. 2009;27(9):2220-8.
36. Magnen CL, Bubendorf L, Rentsch CA, Mengus C, Gsponer J, Zellweger T, et al. Characterization and clinical relevance of ALDH bright populations in prostate cancer. Clinical Cancer Research. 2013;19(19):5361-71.
37. Matsika A, Srinivasan B, Day C, Mader SA, Kiernan DM, Broomfield A, et al. Cancer stem cell markers in prostate cancer: An immunohistochemical study of ALDH1, SOX2 and EZH2. Pathology. 2015;47(7):622-8.
38. Watt FM, Hogan BLM. Out of eden: Stem cells and their niches. Science. 2000;287(5457):1427-30.
39. Pattabiraman DR, Weinberg RA. Tackling the cancer stem cells-what challenges do they pose? Nature Reviews Drug Discovery. 2014;13(7):497-512.
40. Hudson DL, O'Hare M, Watt FM, Masters JRW. Proliferative heterogeneity in the human prostate: Evidence for epithelial stem cells. Laboratory Investigation. 2000;80(8):1243-50.
41. Collins AT, Habib FK, Maitland NJ, Neal DE. Identification and isolation of human prostate epithelial stem cells based on α2β1-integrin expression. Journal of Cell Science. 2001;114(21):3865-72.
42. Li X, Placencio V, Iturregui JM, Uwamariya C, Sharif-Afshar AR, Koyama T, et al. Prostate tumor progression is mediated by a paracrine TGF-β/Wnt3a signaling axis. Oncogene. 2008;27(56):7118-30.
43. Guo M, Jan LY, Jan YN. Control of daughter cell fates during asymmetric division: Interaction of Numb and Notch. Neuron. 1996;17(1):27-41.

44. Reya T, Morrison SJ, Clarke MF, Weissman IL. Stem cells, cancer, and cancer stem cells. Nature. 2001;414(6859):105-11.
45. Baum CM, Weissman IL, Tsukamoto AS, Buckle AM, Peault B. Isolation of a candidate human hematopoietic stem-cell population. Proceedings of the National Academy of Sciences of the United States of America. 1992;89(7):2804-8.
46. Miller SJ, Lavker RM, Sun TT. Interpreting epithelial cancer biology in the context of stem cells: Tumor properties and therapeutic implications. Biochimica et Biophysica Acta - Reviews on Cancer. 2005;1756(1):25-52.
47. English HF, Santen RJ, Isaacs JT. Response of glandular versus basal rat ventral prostatic epithelial cells to androgen withdrawal and replacement. Prostate. 1987;11(3):229-42.
48. Isaacs JT, Coffey DS. Etiology and disease process of benign prostatic hyperplasia. The Prostate Supplement. 1989;2:33-50.
49. Patrawala L, Calhoun T, Schneider-Broussard R, Li H, Bhatia B, Tang S, et al. Highly purified CD44+ prostate cancer cells from xenograft human tumors are enriched in tumorigenic and metastatic progenitor cells. Oncogene. 2006;25(12):1696-708.
50. Richardson GD, Robson CN, Lang SH, Neal DE, Maitland NJ, Collins AT. CD133, a novel marker for human prostatic epithelial stem cells. Journal of Cell Science. 2004;117(16):3539-45.
51. Garraway IP, Sun W, Tran CP, Perner S, Zhang B, Goldstein AS, et al. Human prostate sphere-forming cells represent a subset of basal epithelial cells capable of glandular regeneration in vivo. Prostate. 2010;70(5):491-501.
52. Karthaus WR, Iaquinta PJ, Drost J, Gracanin A, Van Boxtel R, Wongvipat J, et al. Identification of multipotent luminal progenitor cells in human prostate organoid cultures. Cell. 2014;159(1):163-75.
53. Moad M, Hannezo E, Buczacki SJ, Wilson L, El-Sherif A, Sims D, et al. Multipotent Basal Stem Cells, Maintained in Localized Proximal Niches, Support Directed Long-Ranging Epithelial Flows in Human Prostates. Cell Reports. 2017;20(7):1609-22.
54. Frame FM, Hager S, Pellacani D, Stower MJ, Walker HF, Burns JE, et al. Development and limitations of lentivirus vectors as tools for tracking differentiation in prostate epithelial cells. Experimental Cell Research. 2010;316(19):3161-71.
55. Blackwood JK, Williamson SC, Greaves LC, Wilson L, Rigas AC, Sandher R, et al. In situ lineage tracking of human prostatic epithelial stem cell fate reveals a common clonal origin for basal and luminal cells. Journal of Pathology. 2011;225(2):181-8.
56. O'Sullivan RJ, Karlseder J. Telomeres: Protecting chromosomes against genome instability. Nature Reviews Molecular Cell Biology. 2010;11(3):171-81.
57. Urquidi V, Tarin D, Goodison S. Role of telomerase in cell senescence and oncogenesis. Annual Review of Medicine2000. p. 65-79.
58. Rane JK, Greener S, Frame FM, Mann VM, Simms MS, Collins AT, et al. Telomerase activity and telomere length in human benign prostatic hyperplasia stem-like cells and their progeny implies the existence of distinct basal and luminal cell lineages. European Urology. 2016;69(4):551-4.
59. Rane JK, Simms MS, Maitland NJ. Re: Yves Allorya, Willemien Beukers, Ana Sagrera, et al. Telomerase reverse transcriptase promoter mutations in bladder cancer: High frequency across stages, detection in urine, and lack of association with outcome. Eur Urol 2014;65:360-6: Telomerase expression and stem cells: Urologic epithelial perspective. European Urology. 2014;65(6):e85-e6.
60. Meeker AK, Hicks JL, Platz EA, March GE, De Marzo AM, Delannoy MJ. Telomere shortening is an early somatic DNA alteration in human prostate tumorigenesis. Cancer Research. 2002;62(22):6405-9.
61. Zhang W, Kapusta LR, Slingerland JM, Klotz LH. Telomerase activity in prostate cancer, prostatic intraepithelial neoplasia, and benign prostatic epithelium. Cancer Research. 1998;58(4):619-21.

62. Donaldson L, Fordyce C, Gilliland F, Smith A, Feddersen R, Joste N, et al. Association between outcome and telomere DNA content in prostate cancer. Journal of Urology. 1999;162(5):1788-92.
63. Sommerfeld HJ, Meeker AK, Piatyszek MA, Bova GS, Shay JW, Coffey DS. Telomerase activity: A prevalent marker of malignant human prostate tissue. Cancer Research. 1996;56(1):218-22.
64. Loeb S, Kettermann A, Carter HB, Ferrucci L, Metter EJ, Walsh PC. Prostate Volume Changes Over Time: Results From the Baltimore Longitudinal Study of Aging. Journal of Urology. 2009;182(4 SUPPL.):1458-62.
65. Fukuta F, Masumori N, Mori M, Tsukamoto T. Internal prostatic architecture on transrectal ultrasonography predicts future prostatic growth: Natural history of prostatic hyperplasia in a 15-year longitudinal community-based study. Prostate. 2011;71(6):597-603.
66. Birnie R, Bryce SD, Roome C, Dussupt V, Droop A, Lang SH, et al. Gene expression profiling of human prostate cancer stem cells reveals a pro-inflammatory phenotype and the importance of extracellular matrix interactions. Genome Biology. 2008;9(5).
67. Dermer GB. Basal cell proliferation in benign prostatic hyperplasia. Cancer. 1978;41(5):1857-62.
68. Maitland NJ, Collins AT. Inflammation as the primary aetiological agent of human prostate cancer: A stem cell connection? Journal of Cellular Biochemistry. 2008;105(4):931-9.
69. Roberts RO, Bergstralh EJ, Bass SE, Lieber MM, Jacobsen SJ. Prostatitis as a risk factor for prostate cancer. Epidemiology. 2004;15(1):93-9.
70. Sfanos KS, Hempel HA, De Marzo AM. The role of inflammation in prostate cancer. Advances in Experimental Medicine and Biology2014. p. 153-81.
71. Kawakami J, Siemens DR, Nickel JC. Prostatitis and prostate cancer: Implications for prostate cancer screening. Urology. 2004;64(6):1075-80.
72. De Marzo AM, Platz EA, Sutcliffe S, Xu J, Grönberg H, Drake CG, et al. Inflammation in prostate carcinogenesis. Nature Reviews Cancer. 2007;7(4):256-69.
73. Packer JR, Maitland NJ. The molecular and cellular origin of human prostate cancer. Biochimica et Biophysica Acta - Molecular Cell Research. 2016;1863(6):1238-60.
74. Krieger JN, Riley DE, Roberts MC, Berger RE. Prokaryotic DNA sequences in patients with chronic idiopathic prostatitis. Journal of Clinical Microbiology. 1996;34(12):3120-8.
75. Weinberger M, Cytron S, Servadio C, Block C, Rosenfeld JB, Pitlik SD. Prostatic abscess in the antibiotic era. Clinical Infectious Diseases. 1988;10(2):239-49.
76. Hrbacek J, Urban M, Hamsikova E, Tachezy R, Eis V, Brabec M, et al. Serum antibodies against genitourinary infectious agents in prostate cancer and benign prostate hyperplasia patients: A case-control study. BMC Cancer. 2011;11.
77. Caini S, Gandini S, Dudas M, Bremer V, Severi E, Gherasim A. Sexually transmitted infections and prostate cancer risk: A systematic review and meta-analysis. Cancer Epidemiology. 2014;38(4):329-38.
78. Perry A, Lambert P. Propionibacterium acnes: Infection beyond the skin. Expert Review of Anti-Infective Therapy. 2011;9(12):1149-56.
79. Chen Y, Wei J. Identification of pathogen signatures in prostate cancer using RNA-seq. PLoS ONE. 2015;10(6).
80. Cohen RJ, Shannon BA, McNeal JE, Shannon T, Garrett KL. Propionibacterium acnes associated with inflammation in radical prostatectomy specimens: A possible link to cancer evolution? Journal of Urology. 2005;173(6):1969-74.
81. Fassi Fehri L, Mak TN, Laube B, Brinkmann V, Ogilvie LA, Mollenkopf H, et al. Prevalence of Propionibacterium acnes in diseased prostates and its inflammatory and transforming activity on prostate epithelial cells. International Journal of Medical Microbiology. 2011;301(1):69-78.
82. Shinohara DB, Vaghasia AM, Yu SH, Mak TN, Brüggemann H, Nelson WG, et al. A mouse model of chronic prostatic inflammation using a human prostate cancer-derived isolate of Propionibacterium acnes. Prostate. 2013;73(9):1007-15.

83. Pascale M, Pracella D, Barbazza R, Marongiu B, Roggero E, Bonin S, et al. Is human papillomavirus associated with prostate cancer survival? Disease Markers. 2013;35(6):607-13.
84. Singh N, Hussain S, Kakkar N, Singh SK, Sobti RC, Bharadwaj M. Implication of high risk human papillomavirus HR-HPV infection in prostate cancer in Indian population--a pioneering case-control analysis. Scientific reports. 2015;5:7822.
85. Anderson M, Handley J, Hopwood L, Murant S, Stower M, Maitland NJ. Analysis of prostate tissue DNA for the presence of human papillomavirus by polymerase chain reaction, cloning, and automated sequencing. Journal of Medical Virology. 1997;52(1):8-13.
86. Bergh J, Marklund I, Gustavsson C, Wiklund F, Grönberg H, Allard A, et al. No link between viral findings in the prostate and subsequent cancer development. British Journal of Cancer. 2007;96(1):137-9.
87. Strickler HD, Schiffman MH, Shah KV, Rabkin CS, Schiller JT, Wacholder S, et al. A survey of human papillomavirus 16 antibodies in patients with epithelial cancers. European Journal of Cancer Prevention. 1998;7(4):305-13.
88. Thompson MP, Kurzrock R. Epstein-Barr Virus and Cancer. Clinical Cancer Research. 2004;10(3):803-21.
89. Whitaker NJ, Glenn WK, Sahrudin A, Orde MM, Delprado W, Lawson JS. Human papillomavirus and Epstein Barr virus in prostate cancer: Koilocytes indicate potential oncogenic influences of human papillomavirus in prostate cancer. Prostate. 2013;73(3):236-41.
90. Taylor BS, Schultz N, Hieronymus H, Gopalan A, Xiao Y, Carver BS, et al. Integrative Genomic Profiling of Human Prostate Cancer. Cancer Cell. 2010;18(1):11-22.
91. Das D, Wojno K, Imperiale MJ. BK virus as a cofactor in the etiology of prostate cancer in its early stages. Journal of Virology. 2008;82(6):2705-14.
92. Zambrano A, Kalantari M, Simoneau A, Jensen JL, Villarreal LP. Detection of human polyomaviruses and papillomaviruses in prostatictissue reveals the prostate as a habitat for multipleviral infections. Prostate. 2002;53(4):263-76.
93. Keller XE, Kardas P, Acevedo C, Sais G, Poyet C, Banzola I, et al. Antibody response to BK polyomavirus as a prognostic biomarker and potential therapeutic target in prostate cancer. Oncotarget. 2015;6(8):6459-69.
94. Krieger JN, Riley DE, Vesella RL, Miner DC, Ross SO, Lange PH. Bacterial DNA sequences in prostate tissue from patients with prostate cancer and chronic prostatitis. Journal of Urology. 2000;164(4):1221-8.
95. Riley DE, Berger RE, Miner DC, Krieger JN. Diverse and related 16S rRNA-encoding DNA sequences in prostate tissues of men with chronic prostatitis. Journal of Clinical Microbiology. 1998;36(6):1646-52.
96. Sfanos KS, Sauvageot J, Fedor HL, Dick JD, De Marzo AM, Isaacs WB. A molecular analysis of prokaryotic and viral DNA sequences in prostate tissue from patients with prostate cancer indicates the presence of multiple and diverse microorganisms. Prostate. 2008;68(3):306-20.
97. Michaud DS, Augustsson K, Rimm EB, Stampfer MJ, Willet WC, Giovannucci E. A prospective study on intake of animal products and risk of prostate cancer. Cancer Causes and Control. 2001;12(6):557-67.
98. Norrish AE, Ferguson LR, Knize MG, Felton JS, Sharpe SJ, Jackson RT. Heterocyclic amine content of cooked meat and risk of prostate cancer. Journal of the National Cancer Institute. 1999;91(23):2038-44.
99. Sugimura T, Wakabayashi K, Nakagama H, Nagao M. Heterocyclic amines: Mutagens/carcinogens produced during cooking of meet and fish. Cancer Science. 2004;95(4):290-9.
100. Inaguma S, Takahashi S, Ohnishi H, Suzuki S, Cho YM, Shirai T. High susceptibility of the ACI and spontaneously hypertensive rat (SHR) strains to 2-amino-1-methyl-6-phenylimidazo[4,5-b]pyridine (PhIP) prostate carcinogenesis. Cancer Science. 2003;94(11):974-9.
101. Nakai Y, Nelson WG, De Marzo AM. The dietary charred meat carcinogen 2-amino-1-methyl-6-phenylimidazo[4,5-b] pyridine acts as both a tumor initiator and promoter in the rat ventral prostate. Cancer Research. 2007;67(3):1378-84.

102. Patel SAA, Gooderham NJ. Interleukin-6 promotes dietary carcinogen-induced DNA damage in colorectal cancer cells. Toxicology Research. 2015;4(4):858-66.
103. Sfanos KS, Canene-Adams K, Hempel H, Yu SH, Simons BW, Schaeffer AJ, et al. Bacterial prostatitis enhances 2-amino-1-methyl-6-phenylimidazo[4,5-b]pyridine (PhIP)-induced cancer at multiple sites. Cancer Prevention Research. 2015;8(8):683-92.
104. Johnson JJ, Bailey HH, Mukhtar H. Green tea polyphenols for prostate cancer chemoprevention: A translational perspective. Phytomedicine. 2010;17(1):3-13.
105. Xu X, Li J, Wang X, Wang S, Meng S, Zhu Y, et al. Tomato consumption and prostate cancer risk: A systematic review and meta-analysis. Scientific Reports. 2016;6.
106. Higdon JV, Delage B, Williams DE, Dashwood RH. Cruciferous vegetables and human cancer risk: epidemiologic evidence and mechanistic basis. Pharmacological Research. 2007;55(3):224-36.
107. Yan L, Spitznagel EL. Soy consumption and prostate cancer risk in men: A revisit of a meta-analysis. American Journal of Clinical Nutrition. 2009;89(4):1155-63.
108. Adhami VM, Khan N, Mukhtar H. Cancer chemoprevention by pomegranate: laboratory and clinical evidence. Nutrition and cancer. 2009;61(6):811-5.
109. Krieger JN. Classification, epidemiology and implications of chronic prostatitis in North America, Europe and Asia. Minerva Urologica e Nefrologica. 2004;56(2):99-107.
110. Strasner A, Karin M. Immune infiltration and prostate cancer. Frontiers in Oncology. 2015;5(MAY).
111. Sfanos KS, Bruno TC, Meeker AK, De Marzo AM, Isaacs WB, Drake CG. Human prostate-infiltrating CD8+ T lymphocytes are oligoclonal and PD-1+. Prostate. 2009;69(15):1694-703.
112. Ebelt K, Babaryka G, Frankenberger B, Stief CG, Eisenmenger W, Kirchner T, et al. Prostate cancer lesions are surrounded by FOXP3+, PD-1+ and B7-H1+ lymphocyte clusters. European Journal of Cancer. 2009;45(9):1664-72.
113. Nonomura N, Takayama H, Nakayama M, Nakai Y, Kawashima A, Mukai M, et al. Infiltration of tumour-associated macrophages in prostate biopsy specimens is predictive of disease progression after hormonal therapy for prostate cancer. BJU International. 2011;107(12):1918-22.
114. Woo JR, Liss MA, Muldong MT, Palazzi K, Strasner A, Ammirante M, et al. Tumor infiltrating B-cells are increased in prostate cancer tissue. Journal of Translational Medicine. 2014;12(1).
115. Gannon PO, Poisson AO, Delvoye N, Lapointe R, Mes-Masson AM, Saad F. Characterization of the intra-prostatic immune cell infiltration in androgen-deprived prostate cancer patients. Journal of Immunological Methods. 2009;348(1-2):9-17.
116. Ammirante M, Kuraishy AI, Shalapour S, Strasner A, Ramirez-Sanchez C, Zhang W, et al. An IKKAα-E2F1-BMI1 cascade activated by infiltrating B cells controls prostate regeneration and tumor recurrence. Genes and Development. 2013;27(13):1435-40.
117. Birkeland SA, Storm HH, Lamm LU, Barlow L, Blohmé I, Forsberg B, et al. Cancer risk after renal transplantation in the nordic countries, 1964–1986. International Journal of Cancer. 1995;60(2):183-9.
118. Jafari S, Etminan M, Afshar K. Nonsteroidal anti-inflammatory drugs and prostate cancer: A systematic review of the literature and meta-analysis. Journal of the Canadian Urological Association. 2009;3(4):323-30.
119. Mahmud S, Franco E, Aprikian A. Prostate cancer and use of nonsteroidal anti-inflammatory drugs: Systematic review and meta-analysis. British Journal of Cancer. 2004;90(1):93-9.
120. Platz EA, Rohrmann S, Pearson JD, Corrada MM, Watson DJ, De Marzo AM, et al. Nonsteroidal anti-inflammatory drugs and risk of prostate cancer in the Baltimore Longitudinal Study of Aging. Cancer Epidemiology Biomarkers and Prevention. 2005;14(2):390-6.
121. Gurel B, Lucia MS, Thompson Jr IM, Goodman PJ, Tangen CM, Kristal AR, et al. Chronic inflammation in benign prostate tissue is associated with high-grade prostate cancer in the

placebo arm of the prostate cancer prevention trial. Cancer Epidemiology Biomarkers and Prevention. 2014;23(5):847-56.
122. Putzi MJ, De Marzo AM. Morphologic transitions between proliferative inflammatory atrophy and high-grade prostatic intraepithelial neoplasia. Urology. 2000;56(5):828-32.
123. Tomlins SA, Mehra R, Rhodes DR, Cao X, Wang L, Dhanasekaran SM, et al. Integrative molecular concept modeling of prostate cancer progression. Nature Genetics. 2007;39(1):41-51.
124. Bethel CR, Faith D, Li X, Guan B, Hicks JL, Lan F, et al. Decreased NKX3.1 protein expression in focal prostatic atrophy, prostatic intraepithelial neoplasia, and adenocarcinoma: Association with gleason score and chromosome 8p deletion. Cancer Research. 2006;66(22):10683-90.
125. Ruska KM, Sauvageot J, Epstein JI. Histology and cellular kinetics of prostatic atrophy. American Journal of Surgical Pathology. 1998;22(9):1073-7.
126. Vral A, Magri V, Montanari E, Gazzano G, Gourvas V, Marras E, et al. Topographic and quantitative relationship between prostate inflammation, proliferative inflammatory atrophy and low-grade prostate intraepithelial neoplasia: A biopsy study in chronic prostatitis patients. International Journal of Oncology. 2012;41(6):1950-8.
127. Bostwick DG, Qian J. High-grade prostatic intraepithelial neoplasia. Modern Pathology. 2004;17(3):360-79.
128. Shen MM, Abate-Shen C. Molecular genetics of prostate cancer: New prospects for old challenges. Genes and Development. 2010;24(18):1967-2000.
129. Sakr WA, Haas GP, Cassin BF, Pontes JE, Crissman JD. The frequency of carcinoma and intraepithelial neoplasia of the prostate in young male patients. Journal of Urology. 1993;150(2):379-85.
130. Qian J, Wollan P, Bostwick DG. The extent and multicentricity of high-grade prostatic intraepithelial neoplasia in clinically localized prostatic adenocarcinoma. Human Pathology. 1997;28(2):143-8.
131. Haffner MC, Weier C, Xu MM, Vaghasia A, Gürel B, Gümüşkaya B, et al. Molecular evidence that invasive adenocarcinoma can mimic prostatic intraepithelial neoplasia (PIN) and intraductal carcinoma through retrograde glandular colonization. Journal of Pathology. 2016;238(1):31-41.
132. Gao X, Li LY, Zhou FJ, Xie KJ, Shao CK, Su ZL, et al. ERG rearrangement for predicting subsequent cancer diagnosis in high-grade prostatic intraepithelial neoplasia and lymph node metastasis. Clinical Cancer Research. 2012;18(15):4163-72.
133. Barbieri CE, Baca SC, Lawrence MS, Demichelis F, Blattner M, Theurillat JP, et al. Exome sequencing identifies recurrent SPOP, FOXA1 and MED12 mutations in prostate cancer. Nature Genetics. 2012;44(6):685-9.
134. Herawi M, Kahane H, Cavallo C, Epstein JI. Risk of prostate cancer on first re-biopsy within 1 year following a diagnosis of high grade prostatic intraepithelial neoplasia is related to the number of cores sampled. Journal of Urology. 2006;175(1):121-4.
135. Prostate Cancer Incidence Statistics: Cancer Research UK; 2014 [updated 11/06/2014. Available from: http://www.cancerresearchuk.org/cancer-info/cancerstats/types/prostate/incidence/.
136. Lilja H, Ulmert D, Vickers AJ. Prostate-specific antigen and prostate cancer: Prediction, detection and monitoring. Nature Reviews Cancer. 2008;8(4):268-78.
137. Ohori M, Wheeler TM, Scardino PT. The new American Joint Committee on Cancer and International Union Against Cancer TNM classification of prostate cancer: Clinicopathologic correlations. Cancer. 1994;74(1):104-14.
138. UK CR. Prostate Cancer Statistics 2017 [Available from: http://www.cancerresearchuk.org/health-professional/cancer-statistics/statistics-by-cancer-type/prostate-cancer#heading-Five.
139. Siegel R, Naishadham D, Jemal A. Cancer statistics, 2013. CA Cancer Journal for Clinicians. 2013;63(1):11-30.

140. Stanford JL, Ostrander EA. Familial prostate cancer. Epidemiologic Reviews. 2001;23(1):19-23.
141. Ito K. Prostate cancer in Asian men. Nature Reviews Urology. 2014;11(4):197-212.
142. Powell IJ, Bollig-Fischer A. Minireview: The molecular and genomic basis for prostate cancer health disparities. Molecular Endocrinology. 2013;27(6):879-91.
143. Lloyd T, Hounsome L, Mehay A, Mee S, Verne J, Cooper A. Lifetime risk of being diagnosed with, or dying from, prostate cancer by major ethnic group in England 2008-2010. BMC Medicine. 2015;13(1).
144. Peto J. Cancer epidemiology in the last century and the next decade. Nature. 2001;411(6835):390-5.
145. Nelson WG, Demarzo AM, Yegnasubramanian S. The diet as a cause of human prostate cancer. Cancer Treatment and Research2014. p. 51-68.
146. Hong D, Gupta R, Ancliff P, Atzberger A, Brown J, Soneji S, et al. Initiating and cancer-propagating cells in TEL-AML1-associated childhood leukemia. Science. 2008;319(5861):336-9.
147. Pierce GB, Speers WC. Tumors as Caricatures of the Process of Tissue Renewal: Prospects for Therapy by Directing Differentiation. Cancer Research. 1988;48(8):1996-2004.
148. Hanahan D, Weinberg RA. Hallmarks of cancer: The next generation. Cell. 2011;144(5):646-74.
149. Sabbath KD, Ball ED, Larcom P, Davis RB, Griffin JD. Heterogeneity of clonogenic cells in acute myeloblastic leukemia. Journal of Clinical Investigation. 1985;75(2):746-53.
150. Gerlinger M, Rowan AJ, Horswell S, Larkin J, Endesfelder D, Gronroos E, et al. Intratumor heterogeneity and branched evolution revealed by multiregion sequencing. New England Journal of Medicine. 2012;366(10):883-92.
151. Visvader JE, Lindeman GJ. Cancer stem cells in solid tumours: Accumulating evidence and unresolved questions. Nature Reviews Cancer. 2008;8(10):755-68.
152. Fearon ER, Vogelstein B. A genetic model for colorectal tumorigenesis. Cell. 1990;61(5):759-67.
153. Nowell PC. The clonal evolution of tumor cell populations. Acquired genetic lability permits stepwise selection of variant sublines and underlies tumor progression. Science. 1976;194(4260):23-8.
154. Tamborero D, Gonzalez-Perez A, Perez-Llamas C, Deu-Pons J, Kandoth C, Reimand J, et al. Comprehensive identification of mutational cancer driver genes across 12 tumor types. Scientific Reports. 2013;3.
155. Haffner MC, Mosbruger T, Esopi DM, Fedor H, Heaphy CM, Walker DA, et al. Tracking the clonal origin of lethal prostate cancer. Journal of Clinical Investigation. 2013;123(11):4918-22.
156. Stratton MR, Campbell PJ, Futreal PA. The cancer genome. Nature. 2009;458(7239):719-24.
157. Vogelstein B, Papadopoulos N, Velculescu VE, Zhou S, Diaz Jr LA, Kinzler KW. Cancer genome landscapes. Science. 2013;340(6127):1546-58.
158. Feinberg AP, Ohlsson R, Henikoff S. The epigenetic progenitor origin of human cancer. Nature Reviews Genetics. 2006;7(1):21-33.
159. Goldstein AS, Huang J, Guo C, Garraway IP, Witte ON. Identification of a cell of origin for human prostate cancer. Science. 2010;329(5991):568-71.
160. Park JW, Lee JK, Phillips JW, Huang P, Cheng D, Huang J, et al. Prostate epithelial cell of origin determines cancer differentiation state in an organoid transformation assay. Proceedings of the National Academy of Sciences of the United States of America. 2016;113(16):4482-7.
161. Armitage PD, R. The age distribution of cancer and a multi-stage theory of carcinogenesis. British Journal of Cancer. 1954;8(1):1-12.
162. Tomasetti C, Marchionni L, Nowak MA, Parmigiani G, Vogelstein B. Only three driver gene mutations are required for the development of lung and colorectal cancers. Proceedings of the National Academy of Sciences of the United States of America. 2015;112(1):118-23.

163. Fialkow PJ, Jacobson RJ, Papayannopoulou T. Chronic myelocytic leukemia: Clonal origin in a stem cell common to the granulocyte, erythrocyte, platelet and monocyte/macrophage. The American Journal of Medicine. 1977;63(1):125-30.
164. Valastyan S, Weinberg RA. Tumor metastasis: Molecular insights and evolving paradigms. Cell. 2011;147(2):275-92.
165. Aguirre-Ghiso JA. Models, mechanisms and clinical evidence for cancer dormancy. Nature Reviews Cancer. 2007;7(11):834-46.
166. Rosa Mendoza ES, Moreno E, Caguioa PB. Predictors of early distant metastasis in women with breast cancer. Journal of Cancer Research and Clinical Oncology. 2013;139(4):645-52.
167. Kim R, Emi M, Tanabe K. Cancer immunoediting from immune surveillance to immune escape. Immunology. 2007;121(1):1-14.
168. Lee SJ, Cho YS, Cho MC, Shim JH, Lee KA, Ko KK, et al. Both E6 and E7 oncoproteins of human papillomavirus 16 inhibit IL-18-induced IFN-γ production in human peripheral blood mononuclear and NK cells. Journal of Immunology. 2001;167(1):497-504.
169. Munger K, Phelps WC, Bubb V, Howley PM. The E6 and E7 genes of the human papillomavirus type 16 together are necessary and sufficient for transformation of primary human keratinocytes. Journal of Virology. 1989;63(10):4417-21.
170. Slaughter DP, Southwick HW, Smejkal W. “Field cancerization” in oral stratified squamous epithelium. Clinical implications of multicentric origin. Cancer. 1953;6(5):963-8.
171. Mohan M, Jagannathan N. Oral field cancerization: An update on current concepts. Oncology Reviews. 2014;8(1):13-9.
172. Nonn L, Ananthanarayanan V, Gann PH. Evidence for field cancerization of the prostate. Prostate. 2009;69(13):1470-9.
173. Mehrotra J, Varde S, Wang H, Chiu H, Vargo J, Gray K, et al. Quantitative, spatial resolution of the epigenetic field effect in prostate cancer. Prostate. 2008;68(2):152-60.
174. Berger MF, Lawrence MS, Demichelis F, Drier Y, Cibulskis K, Sivachenko AY, et al. The genomic complexity of primary human prostate cancer. Nature. 2011;470(7333):214-20.
175. Cooper CS, Eeles R, Wedge DC, Van Loo P, Gundem G, Alexandrov LB, et al. Analysis of the genetic phylogeny of multifocal prostate cancer identifies multiple independent clonal expansions in neoplastic and morphologically normal prostate tissue. Nature Genetics. 2015;47(4):367-72.
176. Barker N, Ridgway RA, Van Es JH, Van De Wetering M, Begthel H, Van Den Born M, et al. Crypt stem cells as the cells-of-origin of intestinal cancer. Nature. 2009;457(7229):608-11.
177. Clevers H. The cancer stem cell: Premises, promises and challenges. Nature Medicine. 2011;17(3):313-9.
178. Visvader JE, Lindeman GJ. Cancer stem cells: Current status and evolving complexities. Cell Stem Cell. 2012;10(6):717-28.
179. Calabrese P, Tavaré S, Shibata D. Pretumor Progression: Clonal Evolution of Human Stem Cell Populations. American Journal of Pathology. 2004;164(4):1337-46.
180. Furth J, Kahn MC. The transmission of leukemia of mice with a single cell. American Journal of Cancer. 1937;31(2):276-82.
181. Chury Z, Tobiska J. Clinical findings & results of culture in a case of stem-cell leukemia with pluripotential properties of the stem cells. Neoplasma. 1958;5(3):220-31.
182. Cairns J. Mutation selection and the natural history of cancer. Nature. 1975;255(5505):197-200.
183. Hamburger AW, Salmon SE. Primary bioassay of human tumor stem cells. Science. 1977;197(4302):461-3.
184. Bonnet D, Dick JE. Human acute myeloid leukemia is organized as a hierarchy that originates from a primitive hematopoietic cell. Nature Medicine. 1997;3(7):730-7.
185. Al-Hajj M, Wicha MS, Benito-Hernandez A, Morrison SJ, Clarke MF. Prospective identification of tumorigenic breast cancer cells. Proceedings of the National Academy of Sciences of the United States of America. 2003;100(7):3983-8.
186. Singh SK, Clarke ID, Terasaki M, Bonn VE, Hawkins C, Squire J, et al. Identification of a cancer stem cell in human brain tumors. Cancer Research. 2003;63(18):5821-8.

187. Matsui W, Huff CA, Wang Q, Malehorn MT, Barber J, Tanhehco Y, et al. Characterization of clonogenic multiple myeloma cells. Blood. 2004;103(6):2332-6.
188. Fang D, Nguyen TK, Leishear K, Finko R, Kulp AN, Hotz S, et al. A tumorigenic subpopulation with stem cell properties in melanomas. Cancer Research. 2005;65(20):9328-37.
189. Li C, Lee CJ, Simeone DM. Identification of human pancreatic cancer stem cells. Methods in molecular biology (Clifton, NJ). 2009;568:161-73.
190. Ma S, Chan K, Hu L, Lee TK, Wo JY, Ng IO, et al. Identification and Characterization of Tumorigenic Liver Cancer Stem/Progenitor Cells. Gastroenterology. 2007;132(7):2542-56.
191. Ricci-Vitiani L, Lombardi DG, Pilozzi E, Biffoni M, Todaro M, Peschle C, et al. Identification and expansion of human colon-cancer-initiating cells. Nature. 2007;445(7123):111-5.
192. Prince ME, Sivanandan R, Kaczorowski A, Wolf GT, Kaplan MJ, Dalerba P, et al. Identification of a subpopulation of cells with cancer stem cell properties in head and neck squamous cell carcinoma. Proceedings of the National Academy of Sciences of the United States of America. 2007;104(3):973-8.
193. Eramo A, Lotti F, Sette G, Pilozzi E, Biffoni M, Di Virgilio A, et al. Identification and expansion of the tumorigenic lung cancer stem cell population. Cell Death and Differentiation. 2008;15(3):504-14.
194. Zhang S, Balch C, Chan MW, Lai HC, Matei D, Schilder JM, et al. Identification and characterization of ovarian cancer-initiating cells from primary human tumors. Cancer Research. 2008;68(11):4311-20.
195. Rutella S, Bonanno G, Procoli A, Mariotti A, Corallo M, Prisco MG, et al. Cells with characteristics of cancer stem/progenitor cells express the CD133 antigen in human endometrial tumors. Clinical Cancer Research. 2009;15(13):4299-311.
196. He X, Marchionni L, Hansel DE, Yu W, Sood A, Yang J, et al. Differentiation of a highly tumorigenic basal cell compartment in urothelial carcinoma. Stem Cells. 2009;27(7):1487-95.
197. Feng D, Peng C, Li C, Zhou Y, Li M, Ling B, et al. Identification and characterization of cancer stem-like cells from primary carcinoma of the cervix uteri. Oncology Reports. 2009;22(5):1129-34.
198. Brinckerhoff CE. Cancer Stem Cells (CSCs) in melanoma: There's smoke, but is there fire? Journal of Cellular Physiology. 2017;232(10):2674-8.
199. Maitland NJ, Collins AT. The Hallmarks of Prostate Cancer Stem Cells. Cancer Stem Cells: John Wiley & Sons; 2014. p. 17-37.
200. Dylla SJ, Beviglia L, Park IK, Chartier C, Raval J, Ngan L, et al. Colorectal cancer stem cells are enriched in xenogeneic tumors following chemotherapy. PLoS ONE. 2008;3(6).
201. Calcagno AM, Salcido CD, Gillet JP, Wu CP, Fostel JM, Mumau MD, et al. Prolonged drug selection of breast cancer cells and enrichment of cancer stem cell characteristics. Journal of the National Cancer Institute. 2010;102(21):1637-52.
202. Tomasetti C, Vogelstein B. Variation in cancer risk among tissues can be explained by the number of stem cell divisions. Science. 2015;347(6217):78-81.
203. Potter JD, Prentice RL. Cancer risk: Tumors excluded. Science. 2015;347(6223):727.
204. Song M, Giovannucci EL. Cancer risk: many factors contribute. Science (New York, NY). 2015;347(6223):728-9.
205. Albini A, Cavuto S, Apolone G, Noonan DM. Strategies to Prevent "bad Luck" in Cancer. Journal of the National Cancer Institute. 2015;107(10).
206. Wild C, Brennan P, Plummer M, Bray F, Straif K, Zavadil J. Cancer risk: Role of chance overstated. Science. 2015;347(6223):728.
207. IACR. Most types of cancer not due to 'bad luck' IARC responds to scientific article claiming that environmental and lifestyle factors account for less than one third of cancers. Central European journal of public health. 2015;23(1):87.
208. Gotay C, Dummer T, Spinelli J. Cancer Risk: Prevention is crucial. Science. 2015;347(6223):728.
209. Tomlinson I, Bodmer W. Selection, the mutation rate and cancer: Ensuring that the tail does not wag the dog. Nature Medicine. 1999;5(1):11-2.

210. Tomlinson I, Sasieni P, Bodmer W. How many mutations in a cancer? American Journal of Pathology. 2002;160(3):755-8.
211. Johnston MD, Edwards CM, Bodmer WF, Maini PK, Chapman SJ. Mathematical modeling of cell population dynamics in the colonic crypt and in colorectal cancer. Proceedings of the National Academy of Sciences of the United States of America. 2007;104(10):4008-13.
212. Greaves M, Maley CC. Clonal evolution in cancer. Nature. 2012;481(7381):306-13.
213. Williams MJ, Werner B, Barnes CP, Graham TA, Sottoriva A. Identification of neutral tumor evolution across cancer types. Nature Genetics. 2016;48(3):238-44.
214. Jones DL, Wagers AJ. No place like home: Anatomy and function of the stem cell niche. Nature Reviews Molecular Cell Biology. 2008;9(1):11-21.
215. Hjelmeland AB, Wu Q, Heddleston JM, Choudhary GS, MacSwords J, Lathia JD, et al. Acidic stress promotes a glioma stem cell phenotype. Cell Death and Differentiation. 2011;18(5):829-40.
216. Wang R, Chadalavada K, Wilshire J, Kowalik U, Hovinga KE, Geber A, et al. Glioblastoma stem-like cells give rise to tumour endothelium. Nature. 2010;468(7325):829-35.
217. Ricci-Vitiani L, Pallini R, Biffoni M, Todaro M, Invernici G, Cenci T, et al. Tumour vascularization via endothelial differentiation of glioblastoma stem-like cells. Nature. 2010;468(7325):824-30.
218. Lang SH, Stower M, Maitland NJ. In vitro modelling of epithelial and stromal interactions in non-malignant and malignant prostates. British Journal of Cancer. 2000;82(4):990-7.
219. Shiozawa Y, Pedersen EA, Havens AM, Jung Y, Mishra A, Joseph J, et al. Human prostate cancer metastases target the hematopoietic stem cell niche to establish footholds in mouse bone marrow. Journal of Clinical Investigation. 2011;121(4):1298-312.
220. Cairns J. Cancer and the immortal strand hypothesis. Genetics. 2006;174(3):1069-72.
221. Rando TA. The Immortal Strand Hypothesis: Segregation and Reconstruction. Cell. 2007;129(7):1239-43.
222. Lark KG, Consigli RA, Minocha HC. Segregation of Sister Chromatids in Mammalian Cells. Science. 1966;154(3753):1202.
223. Conboy MJ, Karasov AO, Rando TA. High incidence of non-random template strand segregation and asymmetric fate determination in dividing stem cells and their progeny. PLoS biology. 2007;5(5).
224. Potten CS, Owen G, Booth D. Intestinal stem cells protect their genome by selective segregation of template DNA strands. Journal of Cell Science. 2002;115(11):2381-8.
225. Kiel MJ, He S, Ashkenazi R, Gentry SN, Teta M, Kushner JA, et al. Haematopoietic stem cells do not asymmetrically segregate chromosomes or retain BrdU. Nature. 2007;449(7159):238-42.
226. Steinhauser ML, Bailey AP, Senyo SE, Guillermier C, Perlstein TS, Gould AP, et al. Multi-isotope imaging mass spectrometry quantifies stem cell division and metabolism. Nature. 2012;481(7382):516-9.
227. Tomasetti C, Bozic I. The (not so) immortal strand hypothesis. Stem Cell Research. 2015;14(2):238-41.
228. Merok JR, Lansita JA, Tunstead JR, Sherley JL. Cosegregation of chromosomes containing immortal DNA strands in cells that cycle with asymmetric stem cell kinetics. Cancer Research. 2002;62(23):6791-5.
229. Essers MAG, Trumpp A. Targeting leukemic stem cells by breaking their dormancy. Molecular Oncology. 2010;4(5):443-50.
230. Murphy WM, Soloway MS, Barrows GH. Pathologic changes associated with androgen deprivation therapy for prostate cancer. Cancer. 1991;68(4):821-8.
231. Westin P, Bergh A, Damber JE. Castration rapidly results in a major reduction in epithelial cell numbers in the rat prostate, but not in the highly differentiated dunning R3327 prostatic adenocarcinoma. The Prostate. 1993;22(1):65-74.
232. Westin P, Stattin P, Damber JE, Bergh A. Castration therapy rapidly induces apoptosis in a minority and decreases cell proliferation in a majority of human prostatic tumors. American Journal of Pathology. 1995;146(6):1368-75.

233. Ewald JA, Desotelle JA, Church DR, Yang B, Huang W, Laurila TA, et al. Androgen deprivation induces senescence characteristics in prostate cancer cells in vitro and in vivo. Prostate. 2013;73(4):337-45.
234. Chakkalakal JV, Jones KM, Basson MA, Brack AS. The aged niche disrupts muscle stem cell quiescence. Nature. 2012;490(7420):355-60.
235. Ghajar CM. Metastasis prevention by targeting the dormant niche. Nature Reviews Cancer. 2015;15(4):238-47.
236. Maitland NJ, Collins AT. Prostate cancer stem cells: A new target for therapy. Journal of Clinical Oncology. 2008;26(17):2862-70.
237. Trumpp A, Essers M, Wilson A. Awakening dormant haematopoietic stem cells. Nature Reviews Immunology. 2010;10(3):201-9.
238. Leong KG, Wang BE, Johnson L, Gao WQ. Generation of a prostate from a single adult stem cell. Nature. 2008;456(7223):804-10.
239. Wang X, Julio MKD, Economides KD, Walker D, Yu H, Halili MV, et al. A luminal epithelial stem cell that is a cell of origin for prostate cancer. Nature. 2009;461(7263):495-500.
240. Chua CW, Shibata M, Lei M, Toivanen R, Barlow LJ, Bergren SK, et al. Single luminal epithelial progenitors can generate prostate organoids in culture. Nature Cell Biology. 2014;16(10):951-61.
241. Gao D, Vela I, Sboner A, Iaquinta PJ, Karthaus WR, Gopalan A, et al. Organoid cultures derived from patients with advanced prostate cancer. Cell. 2014;159(1):176-87.
242. Hurt EM, Kawasaki BT, Klarmann GJ, Thomas SB, Farrar WL. CD44+CD24- prostate cells are early cancer progenitor/stem cells that provide a model for patients with poor prognosis. British Journal of Cancer. 2008;98(4):756-65.
243. Qin J, Liu X, Laffin B, Chen X, Choy G, Jeter CR, et al. The PSA-/lo prostate cancer cell population harbors self-renewing long-term tumor-propagating cells that resist castration. Cell Stem Cell. 2012;10(5):556-69.
244. Trerotola M, Rathore S, Goel HL, Li J, Alberti S, Piantelli M, et al. CD133, Trop-2 and α2β1 integrin surface receptors as markers of putative human prostate cancer stem cells. American Journal of Translational Research. 2010;2(2):135-44.
245. Taylor RA, Toivanen R, Frydenberg M, Pedersen J, Harewood L, Collins AT, et al. Human epithelial basal cells are cells of origin of prostate cancer, independent of CD133 status. Stem Cells. 2012;30(6):1087-96.
246. Polson ES, Lewis JL, Celik H, Mann VM, Stower MJ, Simms MS, et al. Monoallelic expression of TMPRSS2/ERG in prostate cancer stem cells. Nature Communications. 2013;4.
247. Butler DE, Marlein C, Walker HF, Frame FM, Mann VM, Simms MS, et al. Inhibition of the PI3K/AKT/mTOR pathway activates autophagy and compensatory Ras/Raf/MEK/ERK signalling in prostate cancer. Oncotarget. 2017;8(34):56698-713.
248. Ranganathan P, Weaver KL, Capobianco AJ. Notch signalling in solid tumours: A little bit of everything but not all the time. Nature Reviews Cancer. 2011;11(5):338-51.
249. Fortini ME. Notch Signaling: The Core Pathway and Its Posttranslational Regulation. Developmental Cell. 2009;16(5):633-47.
250. Adler HL, McCurdy MA, Kattan MW, Timme TL, Scardino PT, Thompson TC. Elevated levels of circulating interleukin-6 and transforming growth factor-β1 in patients with metastatic prostatic carcinoma. Journal of Urology. 1999;161(1):182-7.
251. Nakashima J, Tachibana M, Horiguchi Y, Oya M, Ohigashi T, Asakura H, et al. Serum interleukin 6 as a prognostic factor in patients with prostate cancer. Clinical Cancer Research. 2000;6(7):2702-6.
252. Twillie DA, Eisenberger MA, Carducci MA, Hseih WS, Kim WY, Simons JW. Interleukin-6: A candidate mediator of human prostate cancer morbidity. Urology. 1995;45(3):542-9.
253. Kroon P, Berry PA, Stower MJ, Rodrigues G, Mann VM, Simms M, et al. JAK-STAT blockade inhibits tumor initiation and clonogenic recovery of prostate cancer stem-like cells. Cancer Research. 2013;73(16):5288-98.

254. Iliopoulos D, Hirsch HA, Struhl K. An Epigenetic Switch Involving NF-κB, Lin28, Let-7 MicroRNA, and IL6 Links Inflammation to Cell Transformation. Cell. 2009;139(4):693-706.
255. Schroeder A, Herrmann A, Cherryholmes G, Kowolik C, Buettner R, Pal S, et al. Loss of androgen receptor expression promotes a stem-like cell phenotype in prostate cancer through STAT3 signaling. Cancer Research. 2014;74(4):1227-37.
256. Guryanova O, Wu Q, Cheng L, Lathia J, Huang Z, Yang J, et al. Nonreceptor Tyrosine Kinase BMX Maintains Self-Renewal and Tumorigenic Potential of Glioblastoma Stem Cells by Activating STAT3. Cancer Cell. 2011;19(4):498-511.
257. Han Z, Wang X, Ma L, Chen L, Xiao M, Huang L, et al. Inhibition of STAT3 signaling targets both tumor-initiating and differentiated cell populations in prostate cancer. Oncotarget. 2014;5(18):8416-28.
258. Don-Doncow N, Escobar Z, Johansson M, Kjellström S, Garcia V, Munoz E, et al. Galiellalactone is a direct inhibitor of the transcription factor STAT3 in prostate cancer cells. Journal of Biological Chemistry. 2014;289(23):15969-78.
259. Greaves M. Cancer stem cells as 'units of selection'. Evolutionary Applications. 2013;6(1):102-8.
260. Hudson MA, Bahnson RR, Catalona WJ. Clinical use of prostate specific antigen in patients with prostate cancer. Journal of Urology. 1989;142(4):1011-7.
261. Sävblom C, Malm J, Giwercman A, Nilsson JÅ, Berglund G, Lilja H. Blood levels of free-PSA but not complex-PSA significantly correlates to prostate release of PSA in semen in young men, while blood levels of complex-PSA, but not free-PSA increase with age. Prostate. 2005;65(1):66-72.
262. Thompson IM, Ankerst DP, Chi C, Goodman PJ, Tangen CM, Lucia MS, et al. Assessing prostate cancer risk: Results from the Prostate Cancer Prevention Trial. Journal of the National Cancer Institute. 2006;98(8):529-34.
263. Catalona WJ, Partin AW, Slawin KM, Brawer MK, Flanigan RC, Patel A, et al. Use of the percentage of free prostate-specific antigen to enhance differentiation of prostate cancer from benign prostatic disease: A prospective multicenter clinical trial. Journal of the American Medical Association. 1998;279(19):1542-7.
264. Smith MR, Biggar S, Hussain M. Prostate-specific antigen messenger RNA is expressed in non-prostate cells: Implications for detection of micrometastases. Cancer Research. 1995;55(12):2640-4.
265. Marks LS, Bostwick DG. Prostate Cancer Specificity of PCA3 Gene Testing: Examples from Clinical Practice. Reviews in Urology. 2008;10(3):175-81.
266. Tomlins SA, Aubin SMJ, Siddiqui J, Lonigro RJ, Sefton-Miller L, Miick S, et al. Urine TMPRSS2:ERG fusion transcript stratifies prostate cancer risk in men with elevated serum PSA. Science translational medicine. 2011;3(94):94ra72-94ra72.
267. Cui Y, Cao W, Li Q, Shen H, Liu C, Deng J, et al. Evaluation of prostate cancer antigen 3 for detecting prostate cancer: a systematic review and meta-analysis. Scientific Reports. 2016;6:25776.
268. Pellegrini KL, Patil D, Douglas KJS, Lee G, Wehrmeyer K, Torlak M, et al. Detection of prostate cancer-specific transcripts in extracellular vesicles isolated from post-DRE urine. The Prostate. 2017;77(9):990-9.
269. Koo KM, Wee EJH, Mainwaring PN, Trau M. A simple, rapid, low-cost technique for naked-eye detection of urine-isolated TMPRSS2:ERG gene fusion RNA. Scientific Reports. 2016;6:30722.
270. Grönberg H, Adolfsson J, Aly M, Nordström T, Wiklund P, Brandberg Y, et al. Prostate cancer screening in men aged 50–69 years (STHLM3): a prospective population-based diagnostic study. The Lancet Oncology. 2015;16(16):1667-76.
271. Eklund M, Nordström T, Aly M, Adolfsson J, Wiklund P, Brandberg Y, et al. The Stockholm-3 (STHLM3) Model can Improve Prostate Cancer Diagnostics in Men Aged 50–69 yr Compared with Current Prostate Cancer Testing. European Urology Focus. 2016.

272. Ström P, Nordström T, Grönberg H, Eklund M. The Stockholm-3 Model for Prostate Cancer Detection: Algorithm Update, Biomarker Contribution, and Reflex Test Potential. European Urology. 2018.
273. Ghai S, Haider MA. Multiparametric-MRI in diagnosis of prostate cancer. Indian Journal of Urology : IJU : Journal of the Urological Society of India. 2015;31(3):194-201.
274. Panebianco V, Barchetti F, Sciarra A, Ciardi A, Indino EL, Papalia R, et al. Multiparametric magnetic resonance imaging vs. standard care in men being evaluated for prostate cancer: A randomized study. Urologic Oncology: Seminars and Original Investigations. 2015;33(1):17.e1-.e7.
275. Kasivisvanathan V, Rannikko AS, Borghi M, Panebianco V, Mynderse LA, Vaarala MH, et al. MRI-targeted or standard biopsy for prostate-cancer diagnosis. New England Journal of Medicine. 2018;378(19):1767-77.
276. Ahmed HU, El-Shater Bosaily A, Brown LC, Gabe R, Kaplan R, Parmar MK, et al. Diagnostic accuracy of multi-parametric MRI and TRUS biopsy in prostate cancer (PROMIS): a paired validating confirmatory study. The Lancet. 2017;389(10071):815-22.
277. Gleason DF. Classification of prostatic carcinomas. Cancer chemotherapy reports Part 1. 1966;50(3):125-8.
278. Albertsen PC, Hanley JA, Gleason DF, Barry MJ. Competing risk analysis of men aged 55 to 74 years at diagnosis managed conservatively for clinically localized prostate cancer. Journal of the American Medical Association. 1998;280(11):975-80.
279. Epstein JI, Allsbrook Jr WC, Amin MB, Egevad LL, Bastacky S, López Beltrán A, et al. The 2005 International Society of Urological Pathology (ISUP) consensus conference on Gleason grading of prostatic carcinoma. American Journal of Surgical Pathology. 2005;29(9):1228-42.
280. Epstein JI. An Update of the Gleason Grading System. Journal of Urology. 2010;183(2):433-40.
281. Epstein JI, Egevad L, Amin MB, Delahunt B, Srigley JR, Humphrey PA. The 2014 international society of urological pathology (ISUP) consensus conference on gleason grading of prostatic carcinoma definition of grading patterns and proposal for a new grading system. American Journal of Surgical Pathology. 2016;40(2):244-52.
282. Kulac I, Haffner MC, Yegnasubramanian S, Epstein JI, De Marzo AM. Should Gleason 6 be labeled as cancer? Current Opinion in Urology. 2015;25(3):238-45.
283. True L, Coleman I, Hawley S, Huang CY, Gifford D, Coleman R, et al. A molecular correlate to the Gleason grading system for prostate adenocarcinoma. Proceedings of the National Academy of Sciences of the United States of America. 2006;103(29):10991-6.
284. Cohen MS, Hanley RS, Kurteva T, Ruthazer R, Silverman ML, Sorcini A, et al. Comparing the Gleason Prostate Biopsy and Gleason Prostatectomy Grading System: The Lahey Clinic Medical Center Experience and an International Meta-Analysis. European Urology. 2008;54(2):371-81.
285. Lavery HJ, Droller MJ. Do gleason patterns 3 and 4 prostate cancer represent separate disease states? Journal of Urology. 2012;188(5):1667-75.
286. Penney KL, Stampfer MJ, Jahn JL, Sinnott JA, Flavin R, Rider JR, et al. Gleason grade progression is uncommon. Cancer Research. 2013;73(16):5163-8.
287. Eggener SE, Scardino PT, Walsh PC, Han M, Partin AW, Trock BJ, et al. Predicting 15-year prostate cancer specific mortality after radical prostatectomy. Journal of Urology. 2011;185(3):869-75.
288. Hernandez DJ, Nielsen ME, Han M, Trock BJ, Partin AW, Walsh PC, et al. Natural History of Pathologically Organ-Confined (pT2), Gleason Score 6 or Less, Prostate Cancer After Radical Prostatectomy. Urology. 2008;72(1):172-6.
289. Trock BJ, Guo CC, Gonzalgo ML, Magheli A, Loeb S, Epstein JI. Tertiary Gleason Patterns and Biochemical Recurrence After Prostatectomy: Proposal for a Modified Gleason Scoring System. Journal of Urology. 2009;182(4 SUPPL.):1364-70.
290. Kovtun IV, Cheville JC, Murphy SJ, Johnson SH, Zarei S, Kosari F, et al. Lineage relationship of gleason patterns in gleason score 7 prostate cancer. Cancer Research. 2013;73(11):3275-84.

291. Dall'Era MA, Konety BR, Cowan JE, Shinohara K, Stauf F, Cooperberg MR, et al. Active surveillance for the management of prostate cancer in a contemporary cohort. Cancer. 2008;112(12):2664-70.
292. Bill-Axelson A, Holmberg L, Ruutu M. Radical prostatectomy versus watchful waiting in early prostate cancer. New England Journal of Medicine. 2005;352(19):2038.
293. Hirst AM, Frame FM, Maitland NJ, O'Connell D. Low temperature plasma: A novel focal therapy for localized prostate cancer? BioMed Research International. 2014;2014.
294. Ter Haar GR, Clarke RL, Vaughan MG, Hill CR. Trackless surgery using focused ultrasound: Technique and case report. Minimally Invasive Therapy. 1992;1(1):13-9.
295. Bomers JGR, Sedelaar JPM, Barentsz JO, Fütterer JJ. MRI-guided interventions for the treatment of prostate cancer. American Journal of Roentgenology. 2012;199(4):714-20.
296. Nomura T, Mimata H. Focal therapy in the management of prostate cancer: An emerging approach for localized prostate cancer. Advances in Urology. 2012.
297. De La Taille A, Benson MC, Bagiella E, Burchardt M, Shabsigh A, Olsson CA, et al. Cryoablation for clinically localized prostate cancer using an argon-based system: Complication rates and biochemical recurrence. BJU International. 2000;85(3):281-6.
298. Xie Y, Djajaputra D, King CR, Hossain S, Ma L, Xing L. Intrafractional Motion of the Prostate During Hypofractionated Radiotherapy. International Journal of Radiation Oncology Biology Physics. 2008;72(1):236-46.
299. Katz AJ, Santoro M, Diblasio F, Ashley R. Stereotactic body radiotherapy for localized prostate cancer: disease control and quality of life at 6 years. Radiation Oncology. 2013;8(1):118.
300. Park DS. Current status of brachytherapy for prostate cancer. Korean Journal of Urology. 2012;53(11):743-9.
301. Oleinick NL, Morris RL, Belichenko I. The role of apoptosis in response to photodynamic therapy: What, where, why, and how. Photochemical and Photobiological Sciences. 2002;1(1):1-21.
302. Arumainayagam N, Moore CM, Ahmed HU, Emberton M. Photodynamic therapy for focal ablation of the prostate. World Journal of Urology. 2010;28(5):571-6.
303. Azzouzi A-R, Vincendeau S, Barret E, Cicco A, Kleinclauss F, van der Poel HG, et al. Padeliporfin vascular-targeted photodynamic therapy versus active surveillance in men with low-risk prostate cancer (CLIN1001 PCM301): an open-label, phase 3, randomised controlled trial. The Lancet Oncology. 2017;18(2):181-91.
304. Hirst AM, Simms MS, Mann VM, Maitland NJ, O'Connell D, Frame FM. Low-temperature plasma treatment induces DNA damage leading to necrotic cell death in primary prostate epithelial cells. British Journal of Cancer. 2015;112(9):1536-45.
305. Hirst AM, Frame FM, Maitland NJ, O'Connell D. Low temperature plasma causes double-strand break DNA damage in primary epithelial cells cultured from a human prostate Tumor. IEEE Transactions on Plasma Science. 2014;42(10):2740-1.
306. Peeling WB. Phase III studies to compare goserelin (Zoladex) with orchiectomy and with diethylstilbestrol in treatment of prostatic carcinoma. Urology. 1989;33(5 SUPPL.):45-52.
307. Andriole GL, Humphrey P, Ray P, Gleave ME, Trachtenberg J, Thomas LN, et al. Effect of the dual 5α-reductase inhibitor dutasteride on markers of tumor regression in prostate cancer. Journal of Urology. 2004;172(3):915-9.
308. Labrie F, Dupont A, Cusan L, Gomez J, Emond J, Monfette G. Combination therapy with flutamide and medical (LHRH agonist) or surgical castration in advanced prostate cancer: 7-year clinical experience. Journal of Steroid Biochemistry and Molecular Biology. 1990;37(6):943-50.
309. Iversen P, Tyrrell CJ, Kaisary AV, Anderson JB, Van Poppel H, Tammela TLJ, et al. Bicalutamide monotherapy compared with castration in patients with nonmetastatic locally advanced prostate cancer: 6.3 years of followup. Journal of Urology. 2000;164(5):1579-82.
310. Furr BJA, Tucker H. The preclinical development of bicalutamide: Pharmacodynamics and mechanism of action. Urology. 1995;47(1 SUPPL. A):13-25.

311. Tran C, Ouk S, Clegg NJ, Chen Y, Watson PA, Arora V, et al. Development of a second-generation antiandrogen for treatment of advanced prostate cancer. Science. 2009;324(5928):787-90.
312. Scher HI, Fizazi K, Saad F, Taplin ME, Sternberg CN, Miller K, et al. Increased survival with enzalutamide in prostate cancer after chemotherapy. New England Journal of Medicine. 2012;367(13):1187-97.
313. De Bono JS, Logothetis CJ, Molina A, Fizazi K, North S, Chu L, et al. Abiraterone and increased survival in metastatic prostate cancer. New England Journal of Medicine. 2011;364(21):1995-2005.
314. Antonarakis ES, Lu C, Wang H, Luber B, Nakazawa M, Roeser JC, et al. AR-V7 and resistance to enzalutamide and abiraterone in prostate cancer. New England Journal of Medicine. 2014;371(11):1028-38.
315. Li Y, Chan SC, Brand LJ, Hwang TH, Silverstein KAT, Dehm SM. Androgen receptor splice variants mediate enzalutamide resistance in castration-resistant prostate cancer cell lines. Cancer Research. 2013;73(2):483-9.
316. Joseph JD, Lu N, Qian J, Sensintaffar J, Shao G, Brigham D, et al. A clinically relevant androgen receptor mutation confers resistance to second-generation antiandrogens enzalutamide and ARN-509. Cancer Discovery. 2013;3(9):1020-9.
317. Korpal M, Korn JM, Gao X, Rakiec DP, Ruddy DA, Doshi S, et al. An F876l mutation in androgen receptor confers genetic and phenotypic resistance to MDV3100 (Enzalutamide). Cancer Discovery. 2013;3(9):1030-43.
318. Duff J, McEwan IJ. Mutation of histidine 874 in the androgen receptor ligand-binding domain leads to promiscuous ligand activation and altered p160 coactivator interactions. Molecular Endocrinology. 2005;19(12):2943-54.
319. Tannock IF, De Wit R, Berry WR, Horti J, Pluzanska A, Chi KN, et al. Docetaxel plus prednisone or mitoxantrone plus prednisone for advanced prostate cancer. New England Journal of Medicine. 2004;351(15):1502-12.
320. Patterson SG, Wei S, Chen X, Sallman DA, Gilvary DL, Zhong B, et al. Novel role of Stat1 in the development of docetaxel resistance in prostate tumor cells. Oncogene. 2006;25(45):6113-22.
321. Zemskova M, Sahakian E, Bashkirova S, Lilly M. The PIM1 kinase is a critical component of a survival pathway activated by docetaxel and promotes survival of docetaxel-treated prostate cancer cells. Journal of Biological Chemistry. 2008;283(30):20635-44.
322. Sissung TM, Baum CE, Deeken J, Price DK, Aragon-Ching J, Steinberg SM, et al. ABCB1 genetic variation influences the toxicity and clinical outcome of patients with androgen-independent prostate cancer treated with docetaxel. Clinical Cancer Research. 2008;14(14):4543-9.
323. Frame FM, Pellacani D, Collins AT, Simms MS, Mann VM, Jones G, et al. HDAC inhibitor confers radiosensitivity to prostate stem-like cells. British Journal of Cancer. 2013;109(12):3023-33.
324. Bao S, Wu Q, McLendon RE, Hao Y, Shi Q, Hjelmeland AB, et al. Glioma stem cells promote radioresistance by preferential activation of the DNA damage response. Nature. 2006;444(7120):756-60.
325. Schatton T, Murphy GF, Frank NY, Yamaura K, Waaga-Gasser AM, Gasser M, et al. Identification of cells initiating human melanomas. Nature. 2008;451(7176):345-9.
326. Piccirillo SGM, Reynolds BA, Zanetti N, Lamorte G, Binda E, Broggi G, et al. Bone morphogenetic proteins inhibit the tumorigenic potential of human brain tumour-initiating cells. Nature. 2006;444(7120):761-5.
327. Pham PV, Phan NLC, Nguyen NT, Truong NH, Duong TT, Le DV, et al. Differentiation of breast cancer stem cells by knockdown of CD44: Promising differentiation therapy. Journal of Translational Medicine. 2011;9(1).
328. Nowak D, Stewart D, Koeffler HP. Differentiation therapy of leukemia: 3 decades of development. Blood. 2009;113(16):3655-65.

329. Huggins C, Stevens RE, Jr, Hodges CV. Studies on prostatic cancer: Ii. the effects of castration on advanced carcinoma of the prostate gland. Archives of Surgery. 1941;43(2):209-23.
330. Abeshouse A, Ahn J, Akbani R, Ally A, Amin S, Andry CD, et al. The Molecular Taxonomy of Primary Prostate Cancer. Cell. 2015;163(4):1011-25.
331. Robinson D, Van Allen EM, Wu YM, Schultz N, Lonigro RJ, Mosquera JM, et al. Integrative clinical genomics of advanced prostate cancer. Cell. 2015;161(5):1215-28.
332. Fraser M, Sabelnykova VY, Yamaguchi TN, Heisler LE, Livingstone J, Huang V, et al. Genomic hallmarks of localized, non-indolent prostate cancer. Nature. 2017;541(7637):359-64.
333. Beltran H, Prandi D, Mosquera JM, Benelli M, Puca L, Cyrta J, et al. Divergent clonal evolution of castration-resistant neuroendocrine prostate cancer. Nature Medicine. 2016;22(3):298-305.
334. Baca SC, Prandi D, Lawrence MS, Mosquera JM, Romanel A, Drier Y, et al. Punctuated evolution of prostate cancer genomes. Cell. 2013;153(3):666-77.
335. Grasso CS, Wu YM, Robinson DR, Cao X, Dhanasekaran SM, Khan AP, et al. The mutational landscape of lethal castration-resistant prostate cancer. Nature. 2012;487(7406):239-43.
336. Hong MKH, Macintyre G, Wedge DC, Van Loo P, Patel K, Lunke S, et al. Tracking the origins and drivers of subclonal metastatic expansion in prostate cancer. Nature Communications. 2015;6.
337. Pritchard CC, Morrissey C, Kumar A, Zhang X, Smith C, Coleman I, et al. Complex MSH2 and MSH6 mutations in hypermutated microsatellite unstable advanced prostate cancer. Nature Communications. 2014;5.
338. Wedge DC, Gundem G, Mitchell T, Woodcock DJ, Martincorena I, Ghori M, et al. Sequencing of prostate cancers identifies new cancer genes, routes of progression and drug targets. Nature Genetics. 2018;50(5):682-92.
339. Heaphy CM, Yoon GS, Peskoe SB, Joshu CE, Lee TK, Giovannucci E, et al. Prostate cancer cell telomere length variability and stromal cell telomere length as prognostic markers for metastasis and death. Cancer Discovery. 2013;3(10):1130-41.
340. Karanika S, Karantanos T, Li L, Corn PG, Thompson TC. DNA damage response and prostate cancer: Defects, regulation and therapeutic implications. Oncogene. 2015;34(22):2815-22.
341. Leongamornlert D, Mahmud N, Tymrakiewicz M, Saunders E, Dadaev T, Castro E, et al. Germline BRCA1 mutations increase prostate cancer risk. British Journal of Cancer. 2012;106(10):1697-701.
342. Van Asperen CJ, Brohet RM, Meijers-Heijboer EJ, Hoogerbrugqe N, Verhoef S, Vasen HFA, et al. Cancer risks in BRCA2 families: Estimates for sites other than breast and ovary. Journal of Medical Genetics. 2005;42(9):711-9.
343. Dong X, Wang L, Taniguchi K, Wang X, Cunningham JM, McDonnell SK, et al. Mutations in CHEK2 associated with prostate cancer risk. American Journal of Human Genetics. 2003;72(2):270-80.
344. Park JY, Huang Y, Sellers TA. Single nucleotide polymorphisms in DNA repair genes and prostate cancer risk. Methods in Molecular Biology2009. p. 361-85.
345. Yoshimoto M, Ding K, Sweet JM, Ludkovski O, Trottier G, Song KS, et al. PTEN losses exhibit heterogeneity in multifocal prostatic adenocarcinoma and are associated with higher Gleason grade. Modern Pathology. 2013;26(3):435-47.
346. Karantanos T, Corn PG, Thompson TC. Prostate cancer progression after androgen deprivation therapy: Mechanisms of castrate resistance and novel therapeutic approaches. Oncogene. 2013;32(49):5501-11.
347. Schiewer MJ, Goodwin JF, Han S, Chad Brenner J, Augello MA, Dean JL, et al. Dual roles of PARP-1 promote cancer growth and progression. Cancer Discovery. 2012;2(12):1134-49.
348. Goodwin JF, Schiewer MJ, Dean JL, Schrecengost RS, de Leeuw R, Han S, et al. A hormone-DNA repair circuit governs the response to genotoxic insult. Cancer Discovery. 2013;3(11):1254-71.

349. Luedeke M, Linnert CM, Hofer MD, Surowy HM, Rinckleb AE, Hoegel J, et al. Predisposition for TMPRSS2-ERG fusion in prostate cancer by variants in DNA repair genes. Cancer Epidemiology Biomarkers and Prevention. 2009;18(11):3030-5.
350. Lin C, Yang L, Tanasa B, Hutt K, Ju Bg, Ohgi K, et al. Nuclear Receptor-Induced Chromosomal Proximity and DNA Breaks Underlie Specific Translocations in Cancer. Cell. 2009;139(6):1069-83.
351. Tomlins SA, Rhodes DR, Perner S, Dhanasekaran SM, Mehra R, Sun XW, et al. Recurrent fusion of TMPRSS2 and ETS transcription factor genes in prostate cancer. Science. 2005;310(5748):644-8.
352. Huang S, Gulzar ZG, Salari K, Lapointe J, Brooks JD, Pollack JR. Recurrent deletion of CHD1 in prostate cancer with relevance to cell invasiveness. Oncogene. 2012;31(37):4164-70.
353. Burkhardt L, Fuchs S, Krohn A, Masser S, Mader M, Kluth M, et al. CHD1 Is a 5q21 tumor suppressor required for ERG rearrangement in prostate cancer. Cancer Research. 2013;73(9):2795-805.
354. Ross-Adams H, Lamb AD, Dunning MJ, Halim S, Lindberg J, Massie CM, et al. Integration of copy number and transcriptomics provides risk stratification in prostate cancer: A discovery and validation cohort study. EBioMedicine. 2015;2(9):1133-44.
355. Lapointe J, Li C, Higgins JP, Van De Rijn M, Bair E, Montgomery K, et al. Gene expression profiling identifies clinically relevant subtypes of prostate cancer. Proceedings of the National Academy of Sciences of the United States of America. 2004;101(3):811-6.
356. Gao J, Arnold JT, Isaacs JT. Conversion from a paracrine to an autocrine mechanism of androgen-stimulated growth during malignant transformation of prostatic epithelial cells. Cancer Research. 2001;61(13):5038-44.
357. Heinlein CA, Chang C. Androgen receptor in prostate cancer. Endocrine Reviews. 2004;25(2):276-308.
358. Waltering KK, Urbanucci A, Visakorpi T. Androgen receptor (AR) aberrations in castration-resistant prostate cancer. Molecular and Cellular Endocrinology. 2012;360(1-2):38-43.
359. Thompson J, Hyytinen ER, Haapala K, Rantala I, Helin HJ, Jänne OA, et al. Androgen Receptor Mutations in High-Grade Prostate Cancer before Hormonal Therapy. Laboratory Investigation. 2003;83(12):1709-13.
360. Tilley WD, Buchanan G, Hickey TE, Bentel JM. Mutations in the androgen receptor gene are associated with progression of human prostate cancer to androgen independence. Clinical Cancer Research. 1996;2(2):277-85.
361. Chen CD, Welsbie DS, Tran C, Baek SH, Chen R, Vessella R, et al. Molecular determinants of resistance to antiandrogen therapy. Nature Medicine. 2004;10(1):33-9.
362. Grad JM, Lyons LS, Robins DM, Burnstein KL. The androgen receptor (AR) amino-terminus imposes androgen-specific regulation of AR gene expression via an exonic enhancer. Endocrinology. 2001;142(3):1107-16.
363. Sharma A, Yeow WS, Ertel A, Coleman I, Clegg N, Thangavel C, et al. The retinoblastoma tumor suppressor controls androgen signaling and human prostate cancer progression. Journal of Clinical Investigation. 2010;120(12):4478-92.
364. Zhang L, Altuwaijri S, Deng F, Chen L, Lal P, Bhanot UK, et al. NF-κB regulates androgen receptor expression and prostate cancer growth. American Journal of Pathology. 2009;175(2):489-99.
365. Gao L, Schwartzman J, Gibbs A, Lisac R, Kleinschmidt R, Wilmot B, et al. Androgen Receptor Promotes Ligand-Independent Prostate Cancer Progression through c-Myc Upregulation. PLoS ONE. 2013;8(5).
366. Visakorpi T, Hyytinen E, Koivisto P, Tanner M, Keinanen R, Palmberg C, et al. In vivo amplification of the androgen receptor gene and progression of human prostate cancer. Nature Genetics. 1995;9(4):401-6.
367. Bubendorf L, Kononen J, Koivisto P, Schraml P, Moch H, Gasser TC, et al. Survey of gene amplifications during prostate cancer progression by high-throughput fluorescence in situ hybridization on tissue microarrays. Cancer Research. 1999;59(4):803-6.

368. Culig Z, Hobisch A, Cronauer MV, Cato ACB, Hittmair A, Radmayr C, et al. Mutant androgen receptor detected in an advanced-stage prostatic carcinoma is activated by adrenal androgens and progesterone. Molecular Endocrinology. 1993;7(12):1541-50.
369. Culig Z, Hoffmann J, Erdel M, Eder IE, Hobisch A, Hittmair A, et al. Switch from antagonist to agonist of the androgen receptor blocker bicalutamide is associated with prostate tumour progression in a new model system. British Journal of Cancer. 1999;81(2):242-51.
370. Haapala K, Hyytinen ER, Roiha M, Laurila M, Rantala I, Helin HJ, et al. Androgen receptor alterations in prostate cancer relapsed during a combined androgen blockade by orchiectomy and bicalutamide. Laboratory Investigation. 2001;81(12):1647-51.
371. Sack JS, Kish KF, Wang C, Attar RM, Kiefer SE, An Y, et al. Crystallographic structures of the ligand-binding domains of the androgen receptor and its T877A mutant complexed with the natural agonist dihydrotestosterone. Proceedings of the National Academy of Sciences of the United States of America. 2001;98(9):4904-9.
372. Suzuki H, Sato N, Watabe Y, Masai M, Seino S, Shimazaki J. Androgen receptor gene mutations in human prostate cancer. Journal of Steroid Biochemistry and Molecular Biology. 1993;46(6):759-65.
373. Taplin ME, Bubley GJ, Shuster TD, Frantz ME, Spooner AE, Ogata GK, et al. Mutation of the androgen-receptor gene in metastatic androgen-independent prostate cancer. New England Journal of Medicine. 1995;332(21):1393-8.
374. Goker E, Waltham M, Kheradpour A, Trippett T, Mazumdar M, Elisseyeff Y, et al. Amplification of the dihydrofolate reductase gene is a mechanism of acquired resistance to methotrexate in patients with acute lymphoblastic leukemia and is correlated with p53 gene mutations. Blood. 1995;86(2):677-84.
375. Beltran H, Wyatt AW, Chedgy EC, Donoghue A, Annala M, Warner EW, et al. Impact of therapy on genomics and transcriptomics in high-risk prostate cance treated with neoadjuvant docetaxel and androgen deprivation therapy. Clinical Cancer Research. 2017;23(22):6802-11.
376. Wang Q, Li W, Zhang Y, Yuan X, Xu K, Yu J, et al. Androgen Receptor Regulates a Distinct Transcription Program in Androgen-Independent Prostate Cancer. Cell. 2009;138(2):245-56.
377. Dehm SM, Schmidt LJ, Heemers HV, Vessella RL, Tindall DJ. Splicing of a novel androgen receptor exon generates a constitutively active androgen receptor that mediates prostate cancer therapy resistance. Cancer Research. 2008;68(13):5469-77.
378. Guo Z, Yang X, Sun F, Jiang R, Linn DE, Chen H, et al. A novel androgen receptor splice variant is up-regulated during prostate cancer progression and promotes androgen depletion-resistant growth. Cancer Research. 2009;69(6):2305-13.
379. Hu R, Dunn TA, Wei S, Isharwal S, Veltri RW, Humphreys E, et al. Ligand-independent androgen receptor variants derived from splicing of cryptic exons signify hormone-refractory prostate cancer. Cancer Research. 2009;69(1):16-22.
380. Tepper CG, Boucher DL, Ryan PE, Ma AH, Xia L, Lee LF, et al. Characterization of a novel androgen receptor mutation in a relapsed CWR22 prostate cancer xenograft and cell line. Cancer Research. 2002;62(22):6606-14.
381. Watson PA, Chen YF, Balbas MD, Wongvipat J, Socci ND, Viale A, et al. Constitutively active androgen receptor splice variants expressed in castration-resistant prostate cancer require full-length androgen receptor. Proceedings of the National Academy of Sciences of the United States of America. 2010;107(39):16759-65.
382. An J, Wang C, Deng Y, Yu L, Huang H. Destruction of Full-Length Androgen Receptor by Wild-Type SPOP, but Not Prostate-Cancer-Associated Mutants. Cell Reports. 2014;6(4):657-69.
383. Chan SC, Li Y, Dehm SM. Androgen receptor splice variants activate androgen receptor target genes and support aberrant prostate cancer cell growth independent of canonical androgen receptor nuclear localization signal. Journal of Biological Chemistry. 2012;287(23):19736-49.
384. Sun S, Sprenger CCT, Vessella RL, Haugk K, Soriano K, Mostaghel EA, et al. Castration resistance in human prostate cancer is conferred by a frequently occurring androgen receptor splice variant. Journal of Clinical Investigation. 2010;120(8):2715-30.

385. COSMIC. Androgen Receptor Somatic Mutations 2018 [Available from: https://cancer.sanger.ac.uk/cosmic/gene/analysis?ln=AR&ln1=AR&start=1&end=921&coords=AA%3AAA&dis_sn=prostate&sn=prostate&ss=&hn=&sh=&wgs=off&id=2916.
386. Harris WP, Mostaghel EA, Nelson PS, Montgomery B. Androgen deprivation therapy: Progress in understanding mechanisms of resistance and optimizing androgen depletion. Nature Clinical Practice Urology. 2009;6(2):76-85.
387. Bergerat JP, Céraline J. Pleiotropic functional properties of androgen receptor mutants in prostate cancer. Human Mutation. 2009;30(2):145-57.
388. Gingrich JR, Barrios RJ, Kattan MW, Nahm HS, Finegold MJ, Greenberg NM. Androgen-independent prostate cancer progression in the TRAMP model. Cancer Research. 1997;57(21):4687-91.
389. Craft N, Chhor C, Tran C, Belldegrun A, DeKernion J, Witte ON, et al. Evidence for clonal outgrowth of androgen-independent prostate cancer cells from androgen-dependent tumors through a two-step process. Cancer Research. 1999;59(19):5030-6.
390. Smith BA, Sokolov A, Uzunangelov V, Baertsch R, Newton Y, Graim K, et al. A basal stem cell signature identifies aggressive prostate cancer phenotypes. Proceedings of the National Academy of Sciences of the United States of America. 2015;112(47):E6544-E52.
391. Mattie MD, Benz CC, Bowers J, Sensinger K, Wong L, Scott GK, et al. Optimized high-throughput microRNA expression profiling provides novel biomarker assessment of clinical prostate and breast cancer biopsies. Molecular Cancer. 2006;5.
392. Östling P, Leivonen SK, Aakula A, Kohonen P, Mäkelä R, Hagman Z, et al. Systematic analysis of microRNAs targeting the androgen receptor in prostate cancer cells. Cancer Research. 2011;71(5):1956-67.
393. Ozen M, Creighton CJ, Ozdemir M, Ittmann M. Widespread deregulation of microRNA expression in human prostate cancer. Oncogene. 2008;27(12):1788-93.
394. Porkka KP, Pfeiffer MJ, Waltering KK, Vessella RL, Tammela TLJ, Visakorpi T. MicroRNA expression profiling in prostate cancer. Cancer Research. 2007;67(13):6130-5.
395. Shi XB, Xue L, Yang J, Ma AH, Zhao J, Xu M, et al. An androgen-regulated miRNA suppresses Bak1 expression and induces androgen-independent growth of prostate cancer cells. Proceedings of the National Academy of Sciences of the United States of America. 2007;104(50):19983-8.
396. Sun Y, Niu J, Huang J. Neuroendocrine differentiation in prostate cancer. American Journal of Translational Research. 2009;1(2):148-62.
397. Varambally S, Cao Q, Mani RS, Shankar S, Wang X, Ateeq B, et al. Genomic loss of microRNA-101 leads to overexpression of histone methyltransferase EZH2 in cancer. Science. 2008;322(5908):1695-9.
398. Song C, Chen H, Wang T, Zhang W, Ru G, Lang J. Expression profile analysis of microRNAs in prostate cancer by next-generation sequencing. Prostate. 2015;75(5):500-16.
399. Rane JK, Scaravilli M, Ylipää A, Pellacani D, Mann VM, Simms MS, et al. MicroRNA expression profile of primary prostate cancer stem cells as a source of biomarkers and therapeutic targets. European Urology. 2015;67(1):7-10.
400. Nguyen HCN, Xie W, Yang M, Hsieh CL, Drouin S, Lee GSM, et al. Expression differences of circulating microRNAs in metastatic castration resistant prostate cancer and low-risk, localized prostate cancer. Prostate. 2013;73(4):346-54.
401. Kong D, Banerjee S, Ahmad A, Li Y, Wang Z, Sethi S, et al. Epithelial to mesenchymal transition is mechanistically linked with stem cell signatures in prostate cancer cells. PLoS ONE. 2010;5(8).
402. Hermann PC, Huber SL, Herrler T, Aicher A, Ellwart JW, Guba M, et al. Distinct Populations of Cancer Stem Cells Determine Tumor Growth and Metastatic Activity in Human Pancreatic Cancer. Cell Stem Cell. 2007;1(3):313-23.
403. Têtu B, Ro JY, Ayala AG, Johnson DE, Logothetis CJ, Ordonez NG. Small cell carcinoma of the prostate Part I. A clinicopathologic study of 20 cases. Cancer. 1987;59(10):1803-9.

404. Abrahamsson A. Neuroendocrine differentiation in prostatic carcinoma. Prostate. 1999;39(2):135-48.
405. Tanaka M, Suzuki Y, Takaoka K, Suzuki N, Murakami S, Matsuzaki O, et al. Progression of prostate cancer to neuroendocrine cell tumor. International Journal of Urology. 2001;8(8):431-6.
406. Spiotto MT, Chung TDK. STAT3 mediates IL-6-induced neuroendocrine differentiation in prostate cancer cells. Prostate. 2000;42(3):186-95.
407. Hansel DE, Nakayama M, Luo J, Abukhdeir AM, Park BH, Bieberich CJ, et al. Shared TP53 gene mutation in morphologically and phenotypically distinct concurrent primary small cell neuroendocrine carcinoma and adenocarcinoma of the prostate. Prostate. 2009;69(6):603-9.
408. Lohr JG, Adalsteinsson VA, Cibulskis K, Choudhury AD, Rosenberg M, Cruz-Gordillo P, et al. Whole-exome sequencing of circulating tumor cells provides a window into metastatic prostate cancer. Nature Biotechnology. 2014;32(5):479-84.
409. Menon R, Deng M, Rüenauver K, Queisser A, Pfeifer M, Offermann A, et al. Somatic copy number alterations by whole-exome sequencing implicates YWHAZ and PTK2 in castration-resistant prostate cancer. Journal of Pathology. 2013;231(4):505-16.
410. Rajan P, Sudbery IM, Villasevil MEM, Mui E, Fleming J, Davis M, et al. Next-generation sequencing of advanced prostate cancer treated with androgen-deprivation therapy. European Urology. 2014;66(1):32-9.
411. Carreira S, Romanel A, Goodall J, Grist E, Ferraldeschi R, Miranda S, et al. Tumor clone dynamics in lethal prostate cancer. Science Translational Medicine. 2014;6(254).
412. Miyamoto DT, Zheng Y, Wittner BS, Lee RJ, Zhu H, Broderick KT, et al. RNA-Seq of single prostate CTCs implicates noncanonical Wnt signaling in antiandrogen resistance. Science. 2015;349(6254):1351-6.
413. Zhao XY, Malloy PJ, Krishnan AV, Swami S, Navone NM, Peehl DM, et al. Glucocorticoids can promote androgen-independent growth of prostate cancer cells through a mutated androgen receptor. Nature Medicine. 2000;6(6):703-6.
414. Benhar M, Dalyot I, Engelberg D, Levitzki A. Enhanced ROS production in oncogenically transformed cells potentiates c-Jun N-terminal kinase and p38 mitogen-activated protein kinase activation and sensitization to genotoxic stress. Molecular and Cellular Biology. 2001;21(20):6913-26.
415. Gundem G, Van Loo P, Kremeyer B, Alexandrov LB, Tubio JMC, Papaemmanuil E, et al. The evolutionary history of lethal metastatic prostate cancer. Nature. 2015;520(7547):353-7.
416. Fong PC, Boss DS, Yap TA, Tutt A, Wu P, Mergui-Roelvink M, et al. Inhibition of poly(ADP-ribose) polymerase in tumors from BRCA mutation carriers. New England Journal of Medicine. 2009;361(2):123-34.
417. Mateo J, Carreira S, Sandhu S, Miranda S, Mossop H, Perez-Lopez R, et al. DNA-repair defects and olaparib in metastatic prostate cancer. New England Journal of Medicine. 2015;373(18):1697-708.
418. Sandhu SK, Schelman WR, Wilding G, Moreno V, Baird RD, Miranda S, et al. The poly(ADP-ribose) polymerase inhibitor niraparib (MK4827) in BRCA mutation carriers and patients with sporadic cancer: A phase 1 dose-escalation trial. The Lancet Oncology. 2013;14(9):882-92.
419. Xiang Y, Zhu Z, Han G, Lin H, Xu L, Chen CD. JMJD3 is a histone H3K27 demethylase. Cell Research. 2007;17(10):850-7.
420. Cloos PAC, Christensen J, Agger K, Maiolica A, Rappsilber J, Antal T, et al. The putative oncogene GASC1 demethylates tri- and dimethylated lysine 9 on histone H3. Nature. 2006;442(7100):307-11.
421. Ke X, Qu Y, Cheng Y, Li W, Rotter V, Øyan AM, et al. Global profiling of histone and DNA methylation reveals epigenetic-based regulation of gene expression during epithelial to mesenchymal transition in prostate cells. BMC Genomics. 2010;11(1).
422. Ke XS, Qu Y, Rostad K, Li WC, Lin B, Halvorsen OJ, et al. Genome-wide profiling of histone H3 lysine 4 and lysine 27 trimethylation reveals an epigenetic signature in prostate carcinogenesis. PLoS ONE. 2009;4(3).

423. Pellacani D, Kestoras D, Droop AP, Frame FM, Berry PA, Lawrence MG, et al. DNA hypermethylation in prostate cancer is a consequence of aberrant epithelial differentiation and hyperproliferation. Cell Death and Differentiation. 2014;21(5):761-73.
424. Bubendorf L, Schöpfer A, Wagner U, Sauter G, Moch H, Willi N, et al. Metastatic patterns of prostate cancer: An autopsy study of 1,589 patients. Human Pathology. 2000;31(5):578-83.
425. Chambers AF, Groom AC, MacDonald IC. Dissemination and growth of cancer cells in metastatic sites. Nature Reviews Cancer. 2002;2(8):563-72.
426. Braun S, Vogl FD, Naume B, Janni W, Osborne MP, Coombes RC, et al. A pooled analysis of bone marrow micrometastasis in breast cancer. New England Journal of Medicine. 2005;353(8):793-802.
427. Tomlins SA, Laxman B, Varambally S, Cao X, Yu J, Helgeson BE, et al. Role of the TMPRSS2-ERG gene fusion in prostate cancer. Neoplasia. 2008;10(2):177-88.
428. Thiery JP, Acloque H, Huang RYJ, Nieto MA. Epithelial-Mesenchymal Transitions in Development and Disease. Cell. 2009;139(5):871-90.
429. Carmeliet P, Jain RK. Molecular mechanisms and clinical applications of angiogenesis. Nature. 2011;473(7347):298-307.
430. Ghossein RA, Scher HI, Gerald WL, Kelly WK, Curley T, Amsterdam A, et al. Detection of circulating tumor cells in patients with localized and metastatic prostatic carcinoma: Clinical implications. Journal of Clinical Oncology. 1995;13(5):1195-200.
431. Shaffer DR, Leversha MA, Danila DC, Lin O, Gonzalez-Espinoza R, Gu B, et al. Circulating tumor cell analysis in patients with progressive castration-resistant prostate cancer. Clinical Cancer Research. 2007;13(7):2023-9.
432. Attard G, Swennenhuis JF, Olmos D, Reid AHM, Vickers E, A'Hern R, et al. Characterization of ERG, AR and PTEN gene status in circulating tumor cells from patients with castration-resistant prostate cancer. Cancer Research. 2009;69(7):2912-8.
433. Guo W, Giancotti FG. Integrin signalling during tumour progression. Nature Reviews Molecular Cell Biology. 2004;5(10):816-26.
434. Joyce JA, Pollard JW. Microenvironmental regulation of metastasis. Nature Reviews Cancer. 2009;9(4):239-52.
435. Nguyen DX, Bos PD, Massagué J. Metastasis: From dissemination to organ-specific colonization. Nature Reviews Cancer. 2009;9(4):274-84.
436. Psaila B, Lyden D. The metastatic niche: Adapting the foreign soil. Nature Reviews Cancer. 2009;9(4):285-93.
437. Weilbaecher KN, Guise TA, McCauley LK. Cancer to bone: A fatal attraction. Nature Reviews Cancer. 2011;11(6):411-25.
438. Yachida S, Jones S, Bozic I, Antal T, Leary R, Fu B, et al. Distant metastasis occurs late during the genetic evolution of pancreatic cancer. Nature. 2010;467(7319):1114-7.
439. Kim TM, Jung SH, Baek IP, Lee SH, Choi YJ, Lee JY, et al. Regional biases in mutation screening due to intratumoural heterogeneity of prostate cancer. Journal of Pathology. 2014;233(4):425-35.
440. Lee J, Kotliarova S, Kotliarov Y, Li A, Su Q, Donin NM, et al. Tumor stem cells derived from glioblastomas cultured in bFGF and EGF more closely mirror the phenotype and genotype of primary tumors than do serum-cultured cell lines. Cancer Cell. 2006;9(5):391-403.
441. Izadpanah R, Kaushal D, Kriedt C, Tsien F, Patel B, Dufour J, et al. Long-term in vitro expansion alters the biology of adult mesenchymal stem cells. Cancer Research. 2008;68(11):4229-38.
442. Meissner A, Mikkelsen TS, Gu H, Wernig M, Hanna J, Sivachenko A, et al. Genome-scale DNA methylation maps of pluripotent and differentiated cells. Nature. 2008;454(7205):766-70.
443. Horbach SPJM, Halffman W. The ghosts of HeLa: How cell line misidentification contaminates the scientific literature. PLoS ONE. 2017;12(10).
444. Yang J, Battacharya P, Singhal R, Kandel ES. Xenotropic murine leukemia virus-related virus (XMRV) in prostate cancer cells likely represents a laboratory artifact. Oncotarget. 2011;2(5):358-62.

445. Rane JK, Droop AP, Maitland NJ. A Detailed Analysis of Gene Expression in Human Basal, Luminal, and Stromal Cell Populations from Benign Prostatic Hyperplasia Tissues and Comparisons with Cultured Basal Cells. European Urology. 2017;72(1):157-9.
446. Berthon P, Cussenot O, Hopwood L, Le Duc A, Maitland NJ. Functional expression of SV40 in normal human prostatic epithelial and fibroblastic cells: Differentiation pattern of non-tumorigenic cell lines. International Journal of Oncology. 1995;6(2):333-43.
447. Cussenot O, Berthon P, Berger R, Mowszowicz I, Faille A, Hojman F, et al. Immortalization of human adult normal prostatic epithelial cells by liposomes containing large T-SV40 gene. Journal of Urology. 1991;146(3):881-6.
448. Hayward SW, Dahiya R, Cunha GR, Bartek J, Deshpande N, Narayan P. Establishment and characterization of an immortalized but non-transformed human prostate epithelial cell line: BPH-1. In Vitro Cellular & Developmental Biology - Animal. 1995;31(1):14-24.
449. Maitland NJ, Macintosh CA, Hall J, Sharrard M, Quinn G, Lang S. In vitro models to study cellular differentiation and function in human prostate cancers. Radiation Research. 2001;155(1):133-42.
450. Stone KR, Mickey DD, Wunderli H, Mickey GH, Paulson DF. Isolation of a human prostate carcinoma cell line (DU 145). International Journal of Cancer. 1978;21(3):274-81.
451. Fraser M, Zhao H, Luoto KR, Lundin C, Coackley C, Chan N, et al. PTEN deletion in prostate cancer cells does not associate with loss of RAD51 function: Implications for radiotherapy and chemotherapy. Clinical Cancer Research. 2012;18(4):1015-27.
452. Kaighn ME, Narayan KS, Ohnuki Y, Lechner JF, Jones LW. Establishment and characterization of a human prostatic carcinoma cell line (PC-3). Investigative Urology. 1979;17(1):16-23.
453. Vlietstra RJ, Van Alewijk DCJG, Hermans KGL, Van Steenbrugge GJ, Trapman J. Frequent inactivation of PTEN in prostate cancer cell lines and xenografts. Cancer Research. 1998;58(13):2720-3.
454. Marcias G, Erdmann E, Lapouge G, Siebert C, Lémy PB, Duclos B, et al. Identification of novel truncated Androgen Receptor (AR) mutants including unreported pre-mRNA splicing variants in the 22Rv1 hormone-refractory Prostate Cancer (PCa) cell line. Human Mutation. 2010;31(1):74-80.
455. Sramkoski RM, Pretlow Ii TG, Giaconia JM, Pretlow TP, Schwartz S, Sy MS, et al. A new human prostate carcinoma cell line, 22Rv1. In Vitro Cellular and Developmental Biology - Animal. 1999;35(7):403-9.
456. Veldscholte J, Berrevoets CA, Brinkmann AO, Grootegoed JA, Mulder E. Anti-androgens and the mutated androgen receptor of LNCaP cells: Differential effects on binding affinity, heat-shock protein interaction, and transcription activation. Biochemistry. 1992;31(8):2393-9.
457. Horoszewicz JS, Leong SS, Chu TM, Wajsman ZL, Friedman M, Papsidero L, et al. The LNCaP cell line--a new model for studies on human prostatic carcinoma. Progress in clinical and biological research. 1980;37:115-32.
458. Saramäki OR, Harjula AE, Martikainen PM, Lvessella R, Tammela TLJ, Visakorpi T. TMPRSS2.ERG fusion identifies a subgroup of prostate cancers with a favorable prognosis. Clinical Cancer Research. 2008;14(11):3395-400.
459. Korenchuk S, Lehr JE, McLean L, Lee YG, Whitney S, Vessella R, et al. VCaP, a cell-based model system of human prostate cancer. In Vivo. 2001;15(2):163-8.
460. Tomlins SA, Rhodes DR, Yu J, Varambally S, Mehra R, Perner S, et al. The Role of SPINK1 in ETS Rearrangement-Negative Prostate Cancers. Cancer Cell. 2008;13(6):519-28.
461. Maini A, Archer C, Wang CY, Haas GP. Comparative pathology of benign prostatic hyperplasia and prostate cancer. In Vivo. 1997;11(4):293-9.
462. Sharma P, Schreiber-Agus N. Mouse models of prostate cancer. Oncogene. 1999;18(38):5349-55.
463. Maitland NJ. Stem Cells in the Normal and Malignant Prostate. In: Tindall DJ, editor. Prostate Cancer - Biochemistry, Molecular Biology and Genetics. New York: Springer 2013. p. pp 3-41.

464. Valkenburg KC, Williams BO. Mouse Models of Prostate Cancer. Prostate Cancer. 2011;2011:895238.
465. Wu X, Gong S, Roy-Burman P, Lee P, Culig Z. Current mouse and cell models in prostate cancer research. Endocrine-Related Cancer. 2013;20(4):R155-R70.
466. Toivanen R, Taylor RA, Pook DW, Ellem SJ, Risbridger GP. Breaking through a roadblock in prostate cancer research: An update on human model systems. Journal of Steroid Biochemistry and Molecular Biology. 2012;131(3-5):122-31.
467. Bondarenko G, Ugolkov A, Rohan S, Kulesza P, Dubrovskyi O, Gursel D, et al. Patient-derived tumor xenografts are susceptible to formation of human lymphocytic tumors. Neoplasia. 2015;17(9):735-41.
468. Nguyen HM, Vessella RL, Morrissey C, Brown LG, Coleman IM, Higano CS, et al. LuCaP Prostate Cancer Patient-Derived Xenografts Reflect the Molecular Heterogeneity of Advanced Disease an--d Serve as Models for Evaluating Cancer Therapeutics. Prostate. 2017;77(6):654-71.
469. Wetterauer C, Vlajnic T, Schüler J, Gsponer JR, Thalmann GN, Cecchini M, et al. Early development of human lymphomas in a prostate cancer xenograft program using triple knock-out Immunocompromised mice. Prostate. 2015;75(6):585-92.
470. Taurozzi AJ, Beekharry R, Wantoch M, Labarthe M-C, Walker HF, Seed RI, et al. Spontaneous development of Epstein-Barr Virus associated human lymphomas in a prostate cancer xenograft program. PLOS ONE. 2017;12(11):e0188228.
471. Wang ZA, Mitrofanova A, Bergren SK, Abate-Shen C, Cardiff RD, Califano A, et al. Lineage analysis of basal epithelial cells reveals their unexpected plasticity and supports a cell-of-origin model for prostate cancer heterogeneity. Nature Cell Biology. 2013;15(3):274-83.
472. Gleave ME, Hsieh JT, von Eschenbach AC, Chung LW. Prostate and bone fibroblasts induce human prostate cancer growth in vivo: implications for bidirectional tumor-stromal cell interaction in prostate carcinoma growth and metastasis. Journal of Urology. 1992;147(4):1151-9.
473. Tuxhorn JA, McAlhany SJ, Dang TD, Ayala GE, Rowley DR. Stromal cells promote angiogenesis and growth of human prostate tumors in a differential reactive stroma (DRS) xenograft model. Cancer Research. 2002;62(11):3298-307.
474. El-Alfy M, Pelletier G, Hermo LS, Labrie F. Unique features of the basal cells of human prostate epithelium. Microscopy Research and Technique. 2000;51(5):436-46.
475. Tsujimura A, Koikawa Y, Salm S, Takao T, Coetzee S, Moscatelli D, et al. Proximal location of mouse prostate epithelial stem cells: A model of prostatic homeostasis. Journal of Cell Biology. 2002;157(7):1257-65.
476. Lo HS, Wang Z, Hu Y, Yang HH, Gere S, Buetow KH, et al. Allelic variation in gene expression is common in the human genome. Genome Research. 2003;13(8):1855-62.
477. Brown CJ, Ballabio A, Rupert JL, Lafreniere RG, Grompe M, Tonlorenzi R, et al. A gene from the region of the human X inactivation centre is expressed exclusively from the inactive X chromosome. Nature. 1991;349(6304):38-44.
478. Brown CJ, Hendrich BD, Rupert JL, Lafrenière RG, Xing Y, Lawrence J, et al. The human XIST gene: Analysis of a 17 kb inactive X-specific RNA that contains conserved repeats and is highly localized within the nucleus. Cell. 1992;71(3):527-42.
479. Zhao J, Sun BK, Erwin JA, Song JJ, Lee JT. Polycomb proteins targeted by a short repeat RNA to the mouse X chromosome. Science. 2008;322(5902):750-6.
480. Barlow DP. Genomic imprinting: A mammalian epigenetic discovery model. Annual Review of Genetics2011. p. 379-403.
481. Lee JT, Bartolomei MS. X-inactivation, imprinting, and long noncoding RNAs in health and disease. Cell. 2013;152(6):1308-23.
482. Latos PA, Pauler FM, Koerner MV, Şenergin HB, Hudson QJ, Stocsits RR, et al. Airn transcriptional overlap, but not its lncRNA products, induces imprinted Igf2r silencing. Science. 2012;338(6113):1469-72.
483. Pandey RR, Mondal T, Mohammad F, Enroth S, Redrup L, Komorowski J, et al. Kcnq1ot1 Antisense Noncoding RNA Mediates Lineage-Specific Transcriptional Silencing through Chromatin-Level Regulation. Molecular Cell. 2008;32(2):232-46.

484. Kanduri C. Long noncoding RNAs: Lessons from genomic imprinting. Biochimica et Biophysica Acta - Gene Regulatory Mechanisms. 2016;1859(1):102-11.
485. Gimelbrant A, Hutchinson JN, Thompson BR, Chess A. Widespread monoallelic expression on human autosomes. Science. 2007;318(5853):1136-40.
486. Eckersley-Maslin MA, Spector DL. Random monoallelic expression: Regulating gene expression one allele at a time. Trends in Genetics. 2014;30(6):237-44.
487. Gendrel AV, Attia M, Chen CJ, Diabangouaya P, Servant N, Barillot E, et al. Developmental dynamics and disease potential of random monoallelic gene expression. Developmental Cell. 2014;28(4):366-80.
488. Jeffries AR, Uwanogho DA, Cocks G, Perfect LW, Dempster E, Mill J, et al. Erasure and reestablishment of random allelic expression imbalance after epigenetic reprogramming. RNA. 2016;22(10):1620-30.
489. Nag A, Savova V, Fung HL, Miron A, Yuan GC, Zhang K, et al. Chromatin signature of widespread monoallelic expression. eLife. 2013;2013(2).
490. Nag A, Vigneau S, Savova V, Zwemer LM, Gimelbrant AA. Chromatin signature identifies monoallelic gene expression across mammalian cell types. G3: Genes, Genomes, Genetics. 2015;5(8):1713-20.
491. Jeffries AR, Collier DA, Vassos E, Curran S, Ogilvie CM, Price J. Random or stochastic monoallelic expressed genes are enriched for neurodevelopmental disorder candidate genes. PLoS ONE. 2013;8(12).
492. Voutsinas GE, Stavrou EF, Karousos G, Dasoula A, Papachatzopoulou A, Syrrou M, et al. Allelic imbalance of expression and epigenetic regulation within the alpha-synuclein wild-type and p.Ala53Thr alleles in Parkinson disease. Human Mutation. 2010;31(6):685-91.
493. Raval A, Tanner SM, Byrd JC, Angerman EB, Perko JD, Chen SS, et al. Downregulation of Death-Associated Protein Kinase 1 (DAPK1) in Chronic Lymphocytic Leukemia. Cell. 2007;129(5):879-90.
494. Eckersley-Maslin MA, Thybert D, Bergmann JH, Marioni JC, Flicek P, Spector DL. Random monoallelic gene expression increases upon embryonic stem cell differentiation. Developmental Cell. 2014;28(4):351-65.
495. Gui B, Slone J, Huang T. Perspective: Is random monoallelic expression a contributor to phenotypic variability of autosomal dominant disorders? Frontiers in Genetics. 2017;8(NOV).
496. Zhao D, Lin M, Pedrosa E, Lachman HM, Zheng D. Characteristics of allelic gene expression in human brain cells from single-cell RNA-seq data analysis. BMC Genomics. 2017;18(1).
497. Rashid NU, Sperling AS, Bolli N, Wedge DC, Van Loo P, Tai YT, et al. Differential and limited expression of mutant alleles in multiple myeloma. Blood. 2014;124(20):3110-7.
498. Kreso A, O'Brien CA, Van Galen P, Gan OI, Notta F, Brown AMK, et al. Variable clonal repopulation dynamics influence chemotherapy response in colorectal cancer. Science. 2013;339(6119):543-8.
499. Klein AM, Mazutis L, Akartuna I, Tallapragada N, Veres A, Li V, et al. Droplet barcoding for single-cell transcriptomics applied to embryonic stem cells. Cell. 2015;161(5):1187-201.
500. Macosko EZ, Basu A, Satija R, Nemesh J, Shekhar K, Goldman M, et al. Highly parallel genome-wide expression profiling of individual cells using nanoliter droplets. Cell. 2015;161(5):1202-14.
501. Marinov GK, Williams BA, McCue K, Schroth GP, Gertz J, Myers RM, et al. From single-cell to cell-pool transcriptomes: Stochasticity in gene expression and RNA splicing. Genome Research. 2014;24(3):496-510.
502. Lee MCW, Lopez-Diaz FJ, Khan SY, Tariq MA, Dayn Y, Vaske C, et al. Single-cell analyses of transcriptional heterogeneity during drug tolerance transition in cancer cells by RNA sequencing. Proceedings of the National Academy of Sciences of the United States of America. 2014;111(44):E4726-E35.
503. Patel AP, Tirosh I, Trombetta JJ, Shalek AK, Gillespie SM, Wakimoto H, et al. Single-cell RNA-seq highlights intratumoral heterogeneity in primary glioblastoma. Science. 2014;344(6190):1396-401.

504. Ting DT, Wittner BS, Ligorio M, Vincent Jordan N, Shah AM, Miyamoto DT, et al. Single-cell RNA sequencing identifies extracellular matrix gene expression by pancreatic circulating tumor cells. Cell Reports. 2014;8(6):1905-18.
505. Bapat SA, Jin V, Berry N, Balch C, Sharma N, Kurrey N, et al. Multivalent epigenetic marks confer microenvironment-responsive epigenetic plasticity to ovarian cancer cells. Epigenetics. 2010;5(8):717-30.
506. Dar RD, Razooky BS, Singh A, Trimeloni TV, McCollum JM, Cox CD, et al. Transcriptional burst frequency and burst size are equally modulated across the human genome. Proceedings of the National Academy of Sciences of the United States of America. 2012;109(43):17454-9.
507. Miyanari Y, Torres-Padilla ME. Control of ground-state pluripotency by allelic regulation of Nanog. Nature. 2012;483(7390):470-3.
508. Faddah DA, Wang H, Cheng AW, Katz Y, Buganim Y, Jaenisch R. Single-cell analysis reveals that expression of nanog is biallelic and equally variable as that of other pluripotency factors in mouse escs. Cell Stem Cell. 2013;13(1):23-9.
509. Deng Q, Ramsköld D, Reinius B, Sandberg R. Single-cell RNA-seq reveals dynamic, random monoallelic gene expression in mammalian cells. Science. 2014;343(6167):193-6.
510. Jeffries AR, Perfect LW, Ledderose J, Schalkwyk LC, Bray NJ, Mill J, et al. Stochastic choice of allelic expression in human neural stem cells. Stem Cells. 2012;30(9):1938-47.
511. Reinius B, Mold JE, Ramsköld D, Deng Q, Johnsson P, Michaëlsson J, et al. Analysis of allelic expression patterns in clonal somatic cells by single-cell RNA-seq. Nature Genetics. 2016;48(11):1430-5.
512. Borel C, Ferreira PG, Santoni F, Delaneau O, Fort A, Popadin KY, et al. Biased allelic expression in human primary fibroblast single cells. American Journal of Human Genetics. 2015;96(1):70-80.
513. Metsalu T, Viltrop T, Tiirats A, Rajashekar B, Reimann E, Kõks S, et al. Using RNA sequencing for identifying gene imprinting and random monoallelic expression in human placenta. Epigenetics. 2014;9(10):1397-409.
514. Gutierrez-Arcelus M, Lappalainen T, Montgomery SB, Buil A, Ongen H, Yurovsky A, et al. Passive and active DNA methylation and the interplay with genetic variation in gene regulation. eLife. 2013;2013(2).
515. Wang J, Valo Z, Bowers CW, Smith DD, Liu Z, Singer-Sam J. Dual DNA methylation patterns in the CNS reveal developmentally poised chromatin and monoallelic expression of critical genes. PLoS ONE. 2010;5(11).
516. Xu J, Carter AC, Gendrel A-V, Attia M, Loftus J, Greenleaf WJ, et al. Landscape of monoallelic DNA accessibility in mouse embryonic stem cells and neural progenitor cells. Nature Genetics. 2017;49:377.
517. Savova V, Chun S, Sohail M, McCole RB, Witwicki R, Gai L, et al. Genes with monoallelic expression contribute disproportionately to genetic diversity in humans. Nature Genetics. 2016;48(3):231-7.
518. Savova V, Patsenker J, Vigneau S, Gimelbrant AA. dbMAE: The database of autosomal monoallelic expression. Nucleic Acids Research. 2016;44(D1):D753-D6.
519. Donley N, Stoffregen EP, Smith L, Montagna C, Thayer MJ. Asynchronous Replication, Mono-Allelic Expression, and Long Range Cis-Effects of ASAR6. PLOS Genetics. 2013;9(4):e1003423.
520. Donley N, Smith L, Thayer MJ. ASAR15, A cis-Acting Locus that Controls Chromosome-Wide Replication Timing and Stability of Human Chromosome 15. PLoS Genetics. 2015;11(1).
521. Shema E, Jones D, Shoresh N, Donohue L, Ram O, Bernstein BE. Single-molecule decoding of combinatorially modified nucleosomes. Science. 2016;352(6286):717.
522. Sen S, Block KF, Pasini A, Baylin SB, Easwaran H. Genome-wide positioning of bivalent mononucleosomes. BMC Medical Genomics. 2016;9(1).
523. Weiner A, Lara-Astiaso D, Krupalnik V, Gafni O, David E, Winter DR, et al. Co-ChIP enables genome-wide mapping of histone mark co-occurrence at single-molecule resolution. Nature Biotechnology. 2016;34(9):953-61.

524. Delachat AMF, Guidotti N, Bachmann AL, Meireles-Filho ACA, Pick H, Lechner CC, et al. Engineered Multivalent Sensors to Detect Coexisting Histone Modifications in Living Stem Cells. Cell Chemical Biology. 2018;25(1):51-6.e6.
525. Kochat V, Equbal Z, Baligar P, Kumar V, Srivastava M, Mukhopadhyay A. JMJD3 aids in reprogramming of bone marrow progenitor cells to hepatic phenotype through epigenetic activation of hepatic transcription factors. PLoS ONE. 2017;12(3).
526. Bernstein BE, Mikkelsen TS, Xie X, Kamal M, Huebert DJ, Cuff J, et al. A Bivalent Chromatin Structure Marks Key Developmental Genes in Embryonic Stem Cells. Cell. 2006;125(2):315-26.
527. Vincent A, Kazmierczak C, Duchêne B, Jonckheere N, Leteurtre E, Van Seuningen I. Cryosectioning the intestinal crypt-villus axis: An ex vivo method to study the dynamics of epigenetic modifications from stem cells to differentiated cells. Stem Cell Research. 2015;14(1):105-13.
528. Xu J, Carter AC, Gendrel AV, Attia M, Loftus J, Greenleaf WJ, et al. Landscape of monoallelic DNA accessibility in mouse embryonic stem cells and neural progenitor cells. Nature Genetics. 2017;49(3):377-86.
529. Jadhav U, Nalapareddy K, Saxena M, O'Neill NK, Pinello L, Yuan GC, et al. Acquired tissue-specific promoter bivalency is a basis for PRC2 necessity in adult cells. Cell. 2016;165(6):1389-400.
530. Hahn MA, Li AX, Wu X, Yang R, Drew DA, Rosenberg DW, et al. Loss of the polycomb mark from bivalent promoters leads to activation of cancer-promoting genes in colorectal tumors. Cancer Research. 2014;74(13):3617-29.
531. Chapman-Rothe N, Curry E, Zeller C, Liber D, Stronach E, Gabra H, et al. Chromatin H3K27me3/H3K4me3 histone marks define gene sets in high-grade serous ovarian cancer that distinguish malignant, tumour-sustaining and chemo-resistant ovarian tumour cells. Oncogene. 2013;32(38):4586-92.
532. Ohm JE, McGarvey KM, Yu X, Cheng L, Schuebel KE, Cope L, et al. A stem cell-like chromatin pattern may predispose tumor suppressor genes to DNA hypermethylation and heritable silencing. Nature Genetics. 2007;39(2):237-42.
533. Tan J, Yang X, Jiang X, Zhou J, Li Z, Lee PL, et al. Integrative epigenome analysis identifies a polycomb-targeted differentiation program as a tumor-suppressor event epigenetically inactivated in colorectal cancer. Cell Death and Disease. 2014;5(7).
534. Deneberg S, Guardiola P, Lennartsson A, Qu Y, Gaidzik V, Blanchet O, et al. Prognostic DNA methylation patterns in cytogenetically normal acute myeloid leukemia are predefined by stem cell chromatin marks. Blood. 2011;118(20):5573-82.
535. Iliou MS, Lujambio A, Portela A, Brüstle O, Koch P, Andersson-Vincent PH, et al. Bivalent histone modifications in stem cells poise miRNA loci for CpG Island hypermethylation in human cancer. Epigenetics. 2011;6(11):1344-53.
536. Lin B, Lee H, Yoon JG, Madan A, Wayner E, Tonning S, et al. Global analysis of H3K4me3 and H3K27me3 profiles in glioblastoma stem cells and identification of SLC17A7 as a bivalent tumor suppressor gene. Oncotarget. 2015;6(7):5369-81.
537. Rodriguez J, Muñoz M, Vives L, Frangou CG, Groudine M, Peinado MA. Bivalent domains enforce transcriptional memory of DNA methylated genes in cancer cells. Proceedings of the National Academy of Sciences of the United States of America. 2008;105(50):19809-14.
538. Chen Y, Breeze CE, Zhen S, Beck S, Teschendorff AE. Tissue-independent and tissue-specific patterns of DNA methylation alteration in cancer. Epigenetics & Chromatin. 2016;9(1):10.
539. Court F, Arnaud P. An annotated list of bivalent chromatin regions in human ES cells: A new tool for cancer epigenetic research. Oncotarget. 2017;8(3):4110-24.
540. Prickaerts P, Adriaens ME, Beucken TVD, Koch E, Dubois L, Dahlmans VEH, et al. Hypoxia increases genome-wide bivalent epigenetic marking by specific gain of H3K27me3. Epigenetics and Chromatin. 2016;9(1):1-19.
541. Taube JH, Sphyris N, Johnson KS, Reisenauer KN, Nesbit TA, Joseph R, et al. The H3K27me3-demethylase KDM6A is suppressed in breast cancer stem-like cells, and enables the resolution of bivalency during the mesenchymal-epithelial transition. Oncotarget. 2017;8(39):65548-65.

542. Yu J, Yu J, Mani RS, Cao Q, Brenner CJ, Cao X, et al. An Integrated Network of Androgen Receptor, Polycomb, and TMPRSS2-ERG Gene Fusions in Prostate Cancer Progression. Cancer Cell. 2010;17(5):443-54.
543. Kunderfranco P, Mello-Grand M, Cangemi R, Pellini S, Mensah A, Albertini V, et al. ETS transcription factors control transcription of EZH2 and epigenetic silencing of the tumor suppressor gene Nkx3.1 in prostate cancer. PLoS ONE. 2010;5(5).
544. Navarro JM, Touzart A, Pradel LC, Loosveld M, Koubi M, Fenouil R, et al. Site- and allele-specific polycomb dysregulation in T-cell leukaemia. Nature Communications. 2015;6.
545. Huijts PEA, van Dongen M, de Goeij MCM, van Moolenbroek AJ, Blanken F, Vreeswijk MPG, et al. Allele-specific regulation of FGFR2 expression is cell type-dependent and may increase breast cancer risk through a paracrine stimulus involving FGF10. Breast Cancer Research. 2011;13(4).
546. Meyer KB, Maia AT, O'Reilly M, Teschendorff AE, Chin SF, Caldas C, et al. Allele-specific up-regulation of FGFR2 increases susceptibility to breast cancer. PLoS Biology. 2008;6(5):1098-103.
547. Killela PJ, Reitman ZJ, Jiao Y, Bettegowda C, Agrawal N, Diaz Jr LA, et al. TERT promoter mutations occur frequently in gliomas and a subset of tumors derived from cells with low rates of self-renewal. Proceedings of the National Academy of Sciences of the United States of America. 2013;110(15):6021-6.
548. Kinde I, Munari E, Faraj SF, Hruban RH, Schoenberg M, Bivalacqua T, et al. TERT Promoter Mutations Occur Early in Urothelial Neoplasia and Are Biomarkers of Early Disease and Disease Recurrence in Urine. Cancer Research. 2013;73(24):7162.
549. Vinagre J, Almeida A, Pópulo H, Batista R, Lyra J, Pinto V, et al. Frequency of TERT promoter mutations in human cancers. Nature Communications. 2013;4:2185.
550. Horn S, Figl A, Rachakonda PS, Fischer C, Sucker A, Gast A, et al. TERT promoter mutations in familial and sporadic melanoma. Science. 2013;339(6122):959-61.
551. Stern JL, Paucek RD, Huang FW, Ghandi M, Nwumeh R, Costello JC, et al. Allele-Specific DNA Methylation and Its Interplay with Repressive Histone Marks at Promoter-Mutant TERT Genes. Cell Reports. 2017;21(13):3700-7.
552. Stern JL, Theodorescu D, Vogelstein B, Papadopoulos N, Cech TR. Mutation of the TERT promoter, switch to active chromatin, and monoallelic TERT expression in multiple cancers. Genes and Development. 2015;29(21):2219-24.
553. Shah SP, Roth A, Goya R, Oloumi A, Ha G, Zhao Y, et al. The clonal and mutational evolution spectrum of primary triple-negative breast cancers. Nature. 2012;486(7403):395-9.
554. Govindan R, Ding L, Griffith M, Subramanian J, Dees ND, Kanchi KL, et al. Genomic landscape of non-small cell lung cancer in smokers and never-smokers. Cell. 2012;150(6):1121-34.
555. Parsons DW, Jones S, Zhang X, Lin JCH, Leary RJ, Angenendt P, et al. An integrated genomic analysis of human glioblastoma multiforme. Science. 2008;321(5897):1807-12.
556. Howell Jr PM, Liu Z, Khong HT. Demethylating agents in the treatment of cancer. Pharmaceuticals. 2010;3(7):2022-44.
557. Sonpavde G, Aparicio AM, Zhan F, North B, DeLaune R, Garbo LE, et al. Azacitidine favorably modulates PSA kinetics correlating with plasma DNA LINE-1 hypomethylation in men with chemonaïve castration-resistant prostate cancer. Urologic Oncology: Seminars and Original Investigations. 2011;29(6):682-9.
558. Li J, Yen C, Liaw D, Podsypanina K, Bose S, Wang SI, et al. PTEN, a putative protein tyrosine phosphatase gene mutated in human brain, breast, and prostate cancer. Science. 1997;275(5308):1943-7.
559. Maehama T, Dixon JE. The tumor suppressor, PTEN/MMAC1, dephosphorylates the lipid second messenger, phosphatidylinositol 3,4,5-trisphosphate. Journal of Biological Chemistry. 1998;273(22):13375-8.
560. Cantley LC, Neel BG. New insights into tumor suppression: PTEN suppresses tumor formation by restraining the phosphoinositide 3-kinase/AKT pathway. Proceedings of the National Academy of Sciences of the United States of America. 1999;96(8):4240-5.

561. Datta SR, Dudek H, Xu T, Masters S, Haian F, Gotoh Y, et al. Akt phosphorylation of BAD couples survival signals to the cell- intrinsic death machinery. Cell. 1997;91(2):231-41.
562. Shimura T, Noma N, Oikawa T, Ochiai Y, Kakuda S, Kuwahara Y, et al. Activation of the AKT/cyclin D1/Cdk4 survival signaling pathway in radioresistant cancer stem cells. Oncogenesis. 2012;1(6).
563. Agarwal A, Das K, Lerner N, Sathe S, Cicek M, Casey G, et al. The AKT/IκB kinase pathway promotes angiogenic/metastatic gene expression in colorectal cancer by activating nuclear factor-κB and β-catenin. Oncogene. 2005;24(6):1021-31.
564. Keniry M, Parsons R. The role of PTEN signaling perturbations in cancer and in targeted therapy. Oncogene. 2008;27(41):5477-85.
565. Song MS, Salmena L, Pandolfi PP. The functions and regulation of the PTEN tumour suppressor. Nature Reviews Molecular Cell Biology. 2012;13(5):283-96.
566. Mendes-Pereira AM, Martin SA, Brough R, McCarthy A, Taylor JR, Kim JS, et al. Synthetic lethal targeting of PTEN mutant cells with PARP inhibitors. EMBO Molecular Medicine. 2009;1(6-7):315-22.
567. Puc J, Keniry M, Li HS, Pandita TK, Choudhury AD, Memeo L, et al. Lack of PTEN sequesters CHK1 and initiates genetic instability. Cancer Cell. 2005;7(2):193-204.
568. Shen WH, Balajee AS, Wang J, Wu H, Eng C, Pandolfi PP, et al. Essential Role for Nuclear PTEN in Maintaining Chromosomal Integrity. Cell. 2007;128(1):157-70.
569. Tamura M, Gu J, Matsumoto K, Aota SI, Parsons R, Yamada KM. Inhibition of cell migration, spreading, and focal adhesions by tumor suppressor PTEN. Science. 1998;280(5369):1614-7.
570. Gu T, Zhang Z, Wang J, Guo J, Shen WH, Yin Y. CREB is a novel nuclear target of PTEN phosphatase. Cancer Research. 2011;71(8):2821-5.
571. Zhang S, Huang WC, Li P, Guo H, Poh SB, Brady SW, et al. Combating trastuzumab resistance by targeting SRC, a common node downstream of multiple resistance pathways. Nature Medicine. 2011;17(4):461-9.
572. Yadav SS, Li J, Lavery HJ, Yadav KK, Tewari AK. Next-generation sequencing technology in prostate cancer diagnosis, prognosis, and personalized treatment. Urologic oncology. 2015;33(6):267.e1-13.
573. COSMIC. Prostate Cancer - PTEN Somatic Mutations 2018 [Available from: http://cancer.sanger.ac.uk/cosmic/gene/analysis?coords=AA%3AAA&ln=PTEN&res_type=AA&all_data=&sn=prostate&seqlen=404&id=15&export=html&start=67&end=173.
574. Wang S, Gao J, Lei Q, Rozengurt N, Pritchard C, Jiao J, et al. Prostate-specific deletion of the murine Pten tumor suppressor gene leads to metastatic prostate cancer. Cancer Cell. 2003;4(3):209-21.
575. Knudson Jr AG. Mutation and cancer: statistical study of retinoblastoma. Proceedings of the National Academy of Sciences of the United States of America. 1971;68(4):820-3.
576. Zhou XP, Gimm O, Hampel H, Niemann T, Walker MJ, Eng C. Epigenetic PTEN silencing in malignant melanomas without PTEN mutation. American Journal of Pathology. 2000;157(4):1123-8.
577. Cairns P, Okami K, Halachmi S, Halachmi N, Esteller M, Herman JG, et al. Frequent inactivation of PTEN/MMAC1 in primary prostate cancer. Cancer Research. 1997;57(22):4997-5000.
578. Adamo P, Porazinski S, Rajatileka S, Jumbe S, Hagen R, Cheung MK, et al. The oncogenic transcription factor ERG represses the transcription of the tumour suppressor gene PTEN in prostate cancer cells. Oncology Letters. 2017;14(5):5605-10.
579. Kwabi-Addo B, Giri D, Schmidt K, Podsypanina K, Parsons R, Greenberg N, et al. Haploinsufficiency of the Pten tumor suppressor gene promotes prostate cancer progression. Proceedings of the National Academy of Sciences of the United States of America. 2001;98(20):11563-8.
580. Trotman LC, Niki M, Dotan ZA, Koutcher JA, Di Cristofano A, Xiao A, et al. Pten dose dictates cancer progression in the prostate. PLoS Biology. 2003;1(3).

581. De Muga S, Hernández S, Agell L, Salido M, Juanpere N, Lorenzo M, et al. Molecular alterations of EGFR and PTEN in prostate cancer: Association with high-grade and advanced-stage carcinomas. Modern Pathology. 2010;23(5):703-12.
582. Dong JT, Sipe TW, Hyytinen ER, Li CL, Heise C, McClintock DE, et al. PTEN/MMAC1 is infrequently mutated in pT2 and pT3 carcinomas of the prostate. Oncogene. 1998;17(15):1979-82.
583. Kan Z, Jaiswal BS, Stinson J, Janakiraman V, Bhatt D, Stern HM, et al. Diverse somatic mutation patterns and pathway alterations in human cancers. Nature. 2010;466(7308):869-73.
584. Suzuki H, Freije D, Nusskern DR, Okami K, Cairns P, Sidransky D, et al. Interfocal heterogeneity of PTEN/MMAC1 gene alterations in multiple metastatic prostate cancer tissues. Cancer Research. 1998;58(2):204-9.
585. Dong JT, Li CL, Sipe TW, Frierson H.F, Jr. Mutations of PTEN/MMAC1 in primary prostate cancers from Chinese patients. Clinical Cancer Research. 2001;7(2):304-8.
586. COSMIC. Prostate Adenocarcinoma - UK: Wellcome Trust Sanger Institute, Genome Research Limited 2016 [Available from: http://cancer.sanger.ac.uk/cosmic/study/overview?study_id=538.
587. Feilotter HE, Nagai MA, Boag AH, Eng C, Mulligan LM. Analysis of PTEN and the 10q23 region in primary prostate carcinomas. Oncogene. 1998;16(13):1743-8.
588. Furukawa M, He YJ, Borchers C, Xiong Y. Targeting of protein ubiquitination by BTB-Cullin 3-Roc1 ubiquitin ligases. Nature Cell Biology. 2003;5(11):1001-7.
589. Xu L, Wei Y, Reboul J, Vaglio P, Shin TH, Vidal M, et al. BTB proteins are substrate-specific adaptors in an SCF-like modular ubiquitin ligase containing CUL-3. Nature. 2003;425(6955):316-21.
590. Nagai Y, Kojima T, Muro Y, Hachiya T, Nishizawa Y, Wakabayashi T, et al. Identification of a novel nuclear speckle-type protein, SPOP. FEBS Letters. 1997;418(1-2):23-6.
591. Jeong EK, La M, Kyu HO, Young MO, Gi RK, Jae HS, et al. BTB domain-containing speckle-type POZ protein (SPOP) serves as an adaptor of Daxx for ubiquitination by Cul3-based ubiquitin ligase. Journal of Biological Chemistry. 2006;281(18):12664-72.
592. Theurillat JPP, Udeshi ND, Errington WJ, Svinkina T, Baca SC, Pop M, et al. Ubiquitylome analysis identifies dysregulation of effector substrates in SPOP-mutant prostate cancer. Science. 2014;346(6205):85-9.
593. Mani RS. The emerging role of speckle-type POZ protein (SPOP) in cancer development. Drug Discovery Today. 2014.
594. Van Geersdaele LK, Stead MA, Harrison CM, Carr SB, Close HJ, Rosbrook GO, et al. Structural basis of high-order oligomerization of the cullin-3 adaptor SPOP. Acta Crystallographica Section D: Biological Crystallography. 2013;69(9):1677-84.
595. Zhuang M, Calabrese MF, Liu J, Waddell MB, Nourse A, Hammel M, et al. Structures of SPOP-Substrate Complexes: Insights into Molecular Architectures of BTB-Cul3 Ubiquitin Ligases. Molecular Cell. 2009;36(1):39-50.
596. An J, Ren S, Murphy SJ, Dalangood S, Chang C, Pang X, et al. Truncated ERG Oncoproteins from TMPRSS2-ERG Fusions Are Resistant to SPOP-Mediated Proteasome Degradation. Molecular Cell. 2015;59(6):904-16.
597. Gan W, Dai X, Lunardi A, Li Z, Inuzuka H, Liu P, et al. SPOP Promotes Ubiquitination and Degradation of the ERG Oncoprotein to Suppress Prostate Cancer Progression. Molecular Cell. 2015;59(6):917-30.
598. Hernández-Muñoz I, Lund AH, Van Der Stoop P, Boutsma E, Muijrers I, Verhoeven E, et al. Stable X chromosome inactivation involves the PRC1 Polycomb complex and requires histone MACROH2A1 and the CULLIN3/SPOP ubiquitin E3 ligase. Proceedings of the National Academy of Sciences of the United States of America. 2005;102(21):7635-40.
599. Wang C, Pan Y, Wang B. Suppressor of fused and Spop regulate the stability, processing and function of Gli2 and Gli3 full-length activators but not their repressors. Development. 2010;137(12):2001-9.

600. Zhu K, Lei PJ, Ju LG, Wang X, Huang K, Yang B, et al. SPOP-containing complex regulates SETD2 stability and H3K36me3-coupled alternative splicing. Nucleic Acids Research. 2017;45(1):92-105.
601. Dai X, Gan W, Li X, Wang S, Zhang W, Huang L, et al. Prostate cancer-Associated SPOP mutations confer resistance to BET inhibitors through stabilization of BRD4. Nature Medicine. 2017;23(9):1063-71.
602. Janouskova H, El Tekle G, Bellini E, Udeshi ND, Rinaldi A, Ulbricht A, et al. Opposing effects of cancer-Type-specific SPOP mutants on BET protein degradation and sensitivity to BET inhibitors. Nature Medicine. 2017;23(9):1046-54.
603. Zhang P, Wang D, Zhao Y, Ren S, Gao K, Ye Z, et al. Intrinsic BET inhibitor resistance in SPOP-mutated prostate cancer is mediated by BET protein stabilization and AKT-mTORC1 activation. Nature Medicine. 2017;23(9):1055-62.
604. Jin X, Wang J, Gao K, Zhang P, Yao L, Tang Y, et al. Dysregulation of INF2-mediated mitochondrial fission in SPOP-mutated prostate cancer. PLoS Genetics. 2017;13(4).
605. Boysen G, Barbieri CE, Prandi D, Blattner M, Chae SS, Dahija A, et al. SPOP mutation leads to genomic instability in prostate cancer. eLife. 2015;4(September).
606. Zhang D, Wang H, Sun M, Yang J, Zhang W, Han S, et al. Speckle-type POZ protein, SPOP, is involved in the DNA damage response. Carcinogenesis. 2014;35(8):1691-7.
607. Zhu H, Ren S, Bitler BG, Aird KM, Tu Z, Skordalakes E, et al. SPOP E3 Ubiquitin Ligase Adaptor Promotes Cellular Senescence by Degrading the SENP7 deSUMOylase. Cell Reports. 2015;13(6):1183-93.
608. Palapattu GS, Salami SS, Cani AK, Hovelson DH, Lazo de la Vega L, Vandenberg KR, et al. Molecular Profiling to Determine Clonality of Serial Magnetic Resonance Imaging/Ultrasound Fusion Biopsies from Men on Active Surveillance for Low-Risk Prostate Cancer. Clinical Cancer Research. 2017;23(4):985.
609. Kim MS, Je EM, Oh JE, Yoo NJ, Lee SH. Mutational and Expressional Analyses Of SPOP, A Candidate Tumor Suppressor Gene, In Prostate, Gastric and Colorectal Cancers. APMIS. 2013;121(7):626-33.
610. Xu J, Wang F, Jiang H, Jiang Y, Chen J, Qin J. Properties and Clinical Relevance of Speckle-Type POZ Protein in Human Colorectal Cancer. Journal of Gastrointestinal Surgery. 2015;19(8):1484-96.
611. Huang Y, Tan N, Jia D, Jing Y, Wang Q, Li Z, et al. Speckle-type POZ protein is negatively associated with malignancies and inhibits cell proliferation and migration in liver cancer. Tumor Biology. 2015;36(12):9753-61.
612. Yoo SK, Lee S, Kim SJ, Jee HG, Kim BA, Cho H, et al. Comprehensive Analysis of the Transcriptional and Mutational Landscape of Follicular and Papillary Thyroid Cancers. PLoS Genetics. 2016;12(8).
613. Li C, Ao J, Fu J, Lee DF, Xu J, Lonard D, et al. Tumor-suppressor role for the SPOP ubiquitin ligase in signal-dependent proteolysis of the oncogenic co-activator SRC-3/AIB1. Oncogene. 2011;30(42):4350-64.
614. Li G, Ci W, Karmakar S, Chen K, Dhar R, Fan Z, et al. SPOP promotes tumorigenesis by acting as a key regulatory hub in kidney cancer. Cancer Cell. 2014;25(4):455-68.
615. Liu J, Ghanim M, Xue L, Brown CD, Iossifov I, Angeletti C, et al. Analysis of Drosophila segmentation network identifies a JNK pathway factor overexpressed in kidney cancer. Science. 2009;323(5918):1218-22.
616. Guo ZQ, Zheng T, Chen B, Luo C, Ouyang S, Gong S, et al. Small-Molecule Targeting of E3 Ligase Adaptor SPOP in Kidney Cancer. Cancer Cell. 2016;30(3):474-84.
617. COSMIC. Prostate Cancer - SPOP Somatic Mutations 2018 [Available from: https://cancer.sanger.ac.uk/cosmic/gene/analysis?coords=AA%3AAA&sn=prostate&wgs=off&samps=1001&id=6661&ln=SPOP&start=1&end=375.
618. Blattner M, Lee DJ, O'Reilly C, Park K, MacDonald TY, Khani F, et al. SPOP mutations in prostate cancer across demographically diverse patient cohorts. Neoplasia (United States). 2014;16(1):14-20.

619. Buckles E, Qian C, Tadros A, Majumdar S, Cvitanovic J, Zabaleta J, et al. Identification of speckle-type POZ protein somatic mutations in African American prostate cancer. Asian Journal of Andrology. 2014;16(6):829-32.
620. Saar M, Zhao H, Nolley R, Young SR, Coleman I, Nelson PS, et al. Spheroid culture of LuCaP 147 as an authentic preclinical model of prostate cancer subtype with SPOP mutation and hypermutator phenotype. Cancer letters. 2014;351(2):272-80.
621. COSMIC. Prostate Adenocarcinoma - CA: Wellcome Trust Sanger Institute, Genome Research Limited; 2016 [Available from: http://cancer.sanger.ac.uk/cosmic/study/overview?study_id=537.
622. García-Flores M, Casanova-Salas I, Rubio-Briones J, Calatrava A, Domínguez-Escrig J, Rubio L, et al. Clinico-pathological significance of the molecular alterations of the SPOP gene in prostate cancer. European Journal of Cancer. 2014.
623. Lee SH, Jung SH, Shin S, Kim MS, Baek IP, Lee JY, et al. Genetic Progression of High Grade Prostatic Intraepithelial Neoplasia to Prostate Cancer. European Urology. 2016;69(5):823-30.
624. Wu F, Dai X, Gan W, Wan L, Li M, Mitsiades N, et al. Prostate cancer-associated mutation in SPOP impairs its ability to target Cdc20 for poly-ubiquitination and degradation. Cancer Letters. 2017;385:207-14.
625. Geng C, He B, Xu L, Barbieri CE, Eedunuri VK, Chew SA, et al. Prostate cancer-associated mutations in speckle-type POZ protein (SPOP) regulate steroid receptor coactivator 3 protein turnover. Proceedings of the National Academy of Sciences of the United States of America. 2013;110(17):6997-7002.
626. Groner AC, Cato L, de Tribolet-Hardy J, Bernasocchi T, Janouskova H, Melchers D, et al. TRIM24 Is an Oncogenic Transcriptional Activator in Prostate Cancer. Cancer Cell. 2016;29(6):846-58.
627. Zhang P, Gao K, Jin X, Ma J, Peng J, Wumaier R, et al. Endometrial cancer-associated mutants of SPOP are defective in regulating estrogen receptor-α protein turnover. Cell death & disease. 2015;6:e1687.
628. Shoag J, Liu D, Blattner M, Sboner A, Park K, Deonarine L, et al. SPOP mutation drives prostate neoplasia without stabilizing oncogenic transcription factor ERG. Journal of Clinical Investigation. 2018;128(1):381-6.
629. Zhang J, Bu X, Wang H, Zhu Y, Geng Y, Nihira NT, et al. Cyclin D-CDK4 kinase destabilizes PD-L1 via cullin 3-SPOP to control cancer immune surveillance. Nature. 2018;553(7686):91-5.
630. Blattner M, Liu D, Robinson BD, Huang D, Poliakov A, Gao D, et al. SPOP Mutation Drives Prostate Tumorigenesis In Vivo through Coordinate Regulation of PI3K/mTOR and AR Signaling. Cancer Cell. 2017;31(3):436-51.
631. Zuhlke KA, Johnson AM, Tomlins SA, Palanisamy N, Carpten JD, Lange EM, et al. Identification of a novel germline SPOP mutation in a family with hereditary prostate cancer. Prostate. 2014;74(9):983-90.
632. Cairns RA, Mak TW. Oncogenic isocitrate dehydrogenase mutations: Mechanisms, models, and clinical opportunities. Cancer Discovery. 2013;3(7):730-41.
633. Cerami E, Gao J, Dogrusoz U, Gross BE, Sumer SO, Aksoy BA, et al. The cBio Cancer Genomics Portal: An open platform for exploring multidimensional cancer genomics data. Cancer Discovery. 2012;2(5):401-4.
634. Watanabe T, Nobusawa S, Kleihues P, Ohgaki H. IDH1 mutations are early events in the development of astrocytomas and oligodendrogliomas. American Journal of Pathology. 2009;174(4):1149-53.
635. Johnson BE, Mazor T, Hong C, Barnes M, Aihara K, McLean CY, et al. Mutational analysis reveals the origin and therapy-driven evolution of recurrent glioma. Science. 2014;343(6167):189-93.
636. Dang L, White DW, Gross S, Bennett BD, Bittinger MA, Driggers EM, et al. Cancer-associated IDH1 mutations produce 2-hydroxyglutarate. Nature. 2009;462(7274):739-44.
637. Penard-Lacronique V, Bernard OA. IDH1, Histone Methylation, and So Forth. Cancer Cell. 2016;30(2):192-4.

638. Gilbert MR, Liu Y, Neltner J, Pu H, Morris A, Sunkara M, et al. Autophagy and oxidative stress in gliomas with IDH1 mutations. Acta Neuropathologica. 2014;127(2):221-33.
639. Figueroa ME, Abdel-Wahab O, Lu C, Ward PS, Patel J, Shih A, et al. Leukemic IDH1 and IDH2 Mutations Result in a Hypermethylation Phenotype, Disrupt TET2 Function, and Impair Hematopoietic Differentiation. Cancer Cell. 2010;18(6):553-67.
640. Turcan S, Rohle D, Goenka A, Walsh LA, Fang F, Yilmaz E, et al. IDH1 mutation is sufficient to establish the glioma hypermethylator phenotype. Nature. 2012;483(7390):479-83.
641. Flavahan WA, Drier Y, Liau BB, Gillespie SM, Venteicher AS, Stemmer-Rachamimov AO, et al. Insulator dysfunction and oncogene activation in IDH mutant gliomas. Nature. 2016;529(7584):110-4.
642. Xu W, Yang H, Liu Y, Yang Y, Wang P, Kim SH, et al. Oncometabolite 2-hydroxyglutarate is a competitive inhibitor of α-ketoglutarate-dependent dioxygenases. Cancer Cell. 2011;19(1):17-30.
643. Inoue S, Li WY, Tseng A, Beerman I, Elia AJ, Bendall SC, et al. Mutant IDH1 Downregulates ATM and Alters DNA Repair and Sensitivity to DNA Damage Independent of TET2. Cancer Cell. 2016;30(2):337-48.
644. Kivirikko KI, MyllylÄ R. Post-Translational Processing of Procollagens. Annals of the New York Academy of Sciences1985. p. 187-201.
645. Myllyharju J, Kivirikko KI. Collagens, modifying enzymes and their mutations in humans, flies and worms. Trends in Genetics. 2004;20(1):33-43.
646. Sasaki M, Knobbe CB, Itsumi M, Elia AJ, Harris IS, Chio IIC, et al. D-2-hydroxyglutarate produced by mutant Idh1 perturbs collagen maturation and basement membrane function. Genes and Development. 2012;26(18):2038-49.
647. Tarpey PS, Behjati S, Cooke SL, Van Loo P, Wedge DC, Pillay N, et al. Frequent mutation of the major cartilage collagen gene COL2A1 in chondrosarcoma. Nature Genetics. 2013;45(8):923-6.
648. Zhao S, Lin Y, Xu W, Jiang W, Zhai Z, Wang P, et al. Glioma-derived mutations in IDH1 dominantly inhibit IDH1 catalytic activity and induce HIF-1α. Science. 2009;324(5924):261-5.
649. Aydin H, Yalaza C, Ak H, Cagli M, Ozgiray E, Atay S. Association of IDH1 Gene R132H Mutation and Increased Tumor HIF1-α and Serum VEGF Levels in Primary Glioblastoma Multiforme. The FASEB Journal. 2015;29(1 Supplement).
650. Koivunen P, Lee S, Duncan CG, Lopez G, Lu G, Ramkissoon S, et al. Transformation by the (R)-enantiomer of 2-hydroxyglutarate linked to EGLN activation. Nature. 2012;483(7390):484-8.
651. Kickingereder P, Sahm F, Radbruch A, Wick W, Heiland S, Von Deimling A, et al. IDH mutation status is associated with a distinct hypoxia/angiogenesis transcriptome signature which is non-invasively predictable with rCBV imaging in human glioma. Scientific Reports. 2015;5.
652. COSMIC. Prostate Cancer - IDH1 Somatic Mutations 2018 [Available from: https://cancer.sanger.ac.uk/cosmic/gene/analysis?coords=AA%3AAA&sn=prostate&wgs=off&samps=1001&id=5136&ln=IDH1&start=1&end=415.
653. Kang MR, Kim MS, Oh JE, Kim YR, Song SY, Seo SI, et al. Mutational analysis of IDH1 codon 132 in glioblastomas and other common cancers. International Journal of Cancer. 2009;125(2):353-5.
654. Ghiam AF, Cairns RA, Thoms J, Dal Pra A, Ahmed O, Meng A, et al. IDH mutation status in prostate cancer. Oncogene. 2012;31(33):3826-.
655. Barnett CM, Heinrich MC, Lim J, Nelson D, Beadling C, Warrick A, et al. Genetic profiling to determine risk of relapse-free survival in high-risk localized prostate cancer. Clinical Cancer Research. 2014;20(5):1306-12.
656. Kim YH, Pierscianek D, Mittelbronn M, Vital A, Mariani L, Hasselblatt M, et al. TET2 promoter methylation in low-grade diffuse gliomas lacking IDH1/2 mutations. Journal of Clinical Pathology. 2011;64(10):850-2.
657. Kumar A, Coleman I, Morrissey C, Zhang X, True LD, Gulati R, et al. Substantial interindividual and limited intraindividual genomic diversity among tumors from men with metastatic prostate cancer. Nature Medicine. 2016;22(4):369-78.

658. Patnaik MM, Hanson CA, Hodnefield JM, Lasho TL, Finke CM, Knudson RA, et al. Differential prognostic effect of IDH1 versus IDH2 mutations in myelodysplastic syndromes: A Mayo Clinic Study of 277 patients. Leukemia. 2012;26(1):101-5.
659. Chen J, Yang J, Cao P. The evolving landscape in the development of isocitrate dehydrogenase mutant inhibitors. Mini-Reviews in Medicinal Chemistry. 2016;16(16):1344-58.
660. Okoye-Okafor UC, Bartholdy B, Cartier J, Gao EN, Pietrak B, Rendina AR, et al. New IDH1 mutant inhibitors for treatment of acute myeloid leukemia. Nature Chemical Biology. 2015;11(11):878-86.
661. Lin B, Ferguson C, White JT, Wang S, Vessella R, True LD, et al. Prostate-localized and androgen-regulated expression of the membrane- bound serine protease TMPRSS2. Cancer Research. 1999;59(17):4180-4.
662. Perner S, Demichelis F, Beroukhim R, Schmidt FH, Mosquera JM, Setlur S, et al. TMPRSS2:ERG fusion-associated deletions provide insight into the heterogeneity of prostate cancer. Cancer Research. 2006;66(17):8337-41.
663. Kron KJ, Murison A, Zhou S, Huang V, Yamaguchi TN, Shiah YJ, et al. TMPRSS2-ERG fusion co-opts master transcription factors and activates NOTCH signaling in primary prostate cancer. Nature Genetics. 2017;49(9):1336-45.
664. Weier C, Haffner MC, Mosbruger T, Esopi DM, Hicks J, Zheng Q, et al. Nucleotide resolution analysis of TMPRSS2 and ERG rearrangements in prostate cancer. Journal of Pathology. 2013;230(2):174-83.
665. Li X, Baek G, Ramanand SG, Sharp A, Gao Y, Yuan W, et al. BRD4 Promotes DNA Repair and Mediates the Formation of TMPRSS2-ERG Gene Rearrangements in Prostate Cancer. Cell Reports. 2018;22(3):796-808.
666. Mani RS, Amin MA, Li X, Kalyana-Sundaram S, Veeneman BA, Wang L, et al. Inflammation-Induced Oxidative Stress Mediates Gene Fusion Formation in Prostate Cancer. Cell Reports. 2016;17(10):2620-31.
667. Gerrin SJ, Sowalsky AG, Balk SP, Ye H. Mutation Profiling Indicates High Grade Prostatic Intraepithelial Neoplasia as Distant Precursors of Adjacent Invasive Prostatic Adenocarcinoma. Prostate. 2016;76(13):1227-36.
668. Clark J, Merson S, Jhavar S, Flohr P, Edwards S, Foster CS, et al. Diversity of TMPRSS2-ERG fusion transcripts in the human prostate. Oncogene. 2007;26(18):2667-73.
669. Kabbout M, Garcia MM, Fujimoto J, Liu DD, Woods D, Chow CW, et al. ETS2 mediated tumor suppressive function and MET oncogene inhibition in human non-small cell lung cancer. Clinical Cancer Research. 2013;19(13):3383-95.
670. Mani R-S, Tomlins SA, Callahan K, Ghosh A, Nyati MK, Varambally S, et al. Induced Chromosomal Proximity and Gene Fusions in Prostate Cancer. Science. 2009;326(5957):1230.
671. Haffner MC, Aryee MJ, Toubaji A, Esopi DM, Albadine R, Gurel B, et al. Androgen-induced TOP2B-mediated double-strand breaks and prostate cancer gene rearrangements. Nature Genetics. 2010;42(8):668-75.
672. Casey OM, Fang L, Hynes PG, Abou-Kheir WG, Martin PL, Tillman HS, et al. TMPRSS2-driven ERG expression in vivo increases self-renewal and maintains expression in a castration resistant subpopulation. PLoS ONE. 2012;7(7).
673. Brase JC, Johannes M, Mannsperger H, Fälth M, Metzger J, Kacprzyk LA, et al. TMPRSS2-ERG -specific transcriptional modulation is associated with prostate cancer biomarkers and TGF-β signaling. BMC Cancer. 2011;11.
674. Ratz L, Laible M, Kacprzyk LA, Wittig-Blaich SM, Tolstov Y, Duensing S, et al. TMPRSS2: ERG gene fusion variants induce TGF-β signaling and epithelial to mesenchymal transition in human prostate cancer cells. Oncotarget. 2017;8(15):25115-30.
675. Magistroni V, Mologni L, Sanselicio S, Reid JF, Redaelli S, Piazza R, et al. ERG deregulation induces PIM1 over-expression and aneuploidy in prostate epithelial cells. PLoS ONE. 2011;6(11).
676. Wang X, Qiao Y, Asangani IA, Ateeq B, Poliakov A, Cieślik M, et al. Development of Peptidomimetic Inhibitors of the ERG Gene Fusion Product in Prostate Cancer. Cancer Cell. 2017;31(4):532-48.e7.

677. Sartor AO, Hricak H, Wheeler TM, Coleman J, Penson DF, Carroll PR, et al. Evaluating Localized Prostate Cancer and Identifying Candidates for Focal Therapy. Urology. 2008;72(6 SUPPL.):S12-S24.
678. Jones JS. Radiorecurrent prostate cancer: An emerging and largely mismanaged epidemic. European Urology. 2011;60(3):411-2.
679. Kang SU, Cho JH, Chang JW, Shin YS, Kim KI, Park JK, et al. Nonthermal plasma induces head and neck cancer cell death: The potential involvement of mitogen-activated protein kinase-dependent mitochondrial reactive oxygen species. Cell Death and Disease. 2014;5(2).
680. Knake N, Niemi K, Reuter S, Schulz-Von Der Gathen V, Winter J. Absolute atomic oxygen density profiles in the discharge core of a microscale atmospheric pressure plasma jet. Applied Physics Letters. 2008;93(13).
681. Ma Y, Ha CS, Hwang SW, Lee HJ, Kim GC, Lee KW, et al. Non-thermal atmospheric pressure plasma preferentially induces apoptosis in p53-mutated cancer cells by activating ROS stress-response pathways. PLoS ONE. 2014;9(4).
682. Ninomiya K, Ishijima T, Imamura M, Yamahara T, Enomoto H, Takahashi K, et al. Evaluation of extra- and intracellular OH radical generation, cancer cell injury, and apoptosis induced by a non-thermal atmospheric-pressure plasma jet. Journal of Physics D: Applied Physics. 2013;46(42).
683. Wagenaars E, Gans T, O'Connell D, Niemi K. Two-photon absorption laser-induced fluorescence measurements of atomic nitrogen in a radio-frequency atmospheric-pressure plasma jet. Plasma Sources Science and Technology. 2012;21(4).
684. Waskoenig J, Niemi K, Knake N, Graham LM, Reuter S, Schulz-von Der Gathen V, et al. Atomic oxygen formation in a radio-frequency driven micro-atmospheric pressure plasma jet. Plasma Sources Science and Technology. 2010;19:045018--11.
685. Avery SV. Molecular targets of oxidative stress. Biochemical Journal. 2011;434(2):201-10.
686. Klaunig JE, Kamendulis LM, Hocevar BA. Oxidative stress and oxidative damage in carcinogenesis. Toxicologic Pathology. 2010;38(1):96-109.
687. Ahn HJ, Kim KI, Hoan NN, Kim CH, Moon E, Choi KS, et al. Targeting cancer cells with reactive oxygen and nitrogen species generated by atmospheric-pressure air plasma. PLoS ONE. 2014;9(1).
688. Arndt S, Wacker E, Li YF, Shimizu T, Thomas HM, Morfill GE, et al. Cold atmospheric plasma, a new strategy to induce senescence in melanoma cells. Experimental Dermatology. 2013;22(4):284-9.
689. Fridman G, Shereshevsky A, Jost MM, Brooks AD, Fridman A, Gutsol A, et al. Floating electrode dielectric barrier discharge plasma in air promoting apoptotic behavior in Melanoma skin cancer cell lines. Plasma Chemistry and Plasma Processing. 2007;27(2):163-76.
690. Barekzi N, Laroussi M. Dose-dependent killing of leukemia cells by low-temperature plasma. Journal of Physics D: Applied Physics. 2012;45(42).
691. Iseki S, Nakamura K, Hayashi M, Tanaka H, Kondo H, Kajiyama H, et al. Selective killing of ovarian cancer cells through induction of apoptosis by nonequilibrium atmospheric pressure plasma. Applied Physics Letters. 2012;100(11).
692. Kalghatgi S, Kelly CM, Cerchar E, Torabi B, Alekseev O, Fridman A, et al. Effects of non-thermal plasma on mammalian cells. PLoS ONE. 2011;6(1).
693. Wang M, Holmes B, Cheng X, Zhu W, Keidar M, Zhang LG. Cold atmospheric plasma for selectively ablating metastatic breast cancer cells. PLoS One. 2013;8(9):e73741.
694. Kaushik NK, Kim YH, Han YG, Choi EH. Effect of jet plasma on T98G human brain cancer cells. Current Applied Physics. 2013;13(1):176-80.
695. Vandamme M, Robert E, Dozias S, Sobilo J, Lerondel S, Le Pape A, et al. Response of human glioma U87 xenografted on mice to non thermal plasma treatment. Plasma Medicine. 2011;1(1):27-43.
696. Kaushik NK, Kaushik N, Park D, Choi EH. Altered antioxidant system stimulates dielectric barrier discharge plasma-induced cell death for solid tumor cell treatment. PLoS ONE. 2014;9(7).

697. Panngom K, Baik KY, Nam MK, Han JH, Rhim H, Choi EH. Preferential killing of human lung cancer cell lines with mitochondrial dysfunction by nonthermal dielectric barrier discharge plasma. Cell Death and Disease. 2013;4(5).
698. Kim CH, Kwon S, Bahn JH, Lee K, Jun SI, Rack PD, et al. Effects of atmospheric nonthermal plasma on invasion of colorectal cancer cells. Applied Physics Letters. 2010;96(24).
699. Yan X, Xiong Z, Zou F, Zhao S, Lu X, Yang G, et al. Plasma-induced death of HepG2 cancer cells: Intracellular effects of reactive species. Plasma Processes and Polymers. 2012;9(1):59-66.
700. Kim GJ, Kim W, Kim KT, Lee JK. DNA damage and mitochondria dysfunction in cell apoptosis induced by nonthermal air plasma. Applied Physics Letters. 2010;96(2).
701. Kaushik N, Kumar N, Kim CH, Kaushik NK, Choi EH. Dielectric barrier discharge plasma efficiently delivers an apoptotic response in human monocytic lymphoma. Plasma Processes and Polymers. 2014;11(12):1175-87.
702. Reuter S, Gupta SC, Chaturvedi MM, Aggarwal BB. Oxidative stress, inflammation, and cancer: How are they linked? Free Radical Biology and Medicine. 2010;49(11):1603-16.
703. Snyder SH, Barañano DE. Heme oxygenase: A font of multiple messengers. Neuropsychopharmacology. 2001;25(3):294-8.
704. Jönsson TJ, Lowther WT. The peroxiredoxin repair proteins. Sub-cellular biochemistry. 2007;44:115-41.
705. Monteiro G, Horta BB, Pimenta DC, Augusto O, Netto LES. Reduction of 1-Cys peroxiredoxins by ascorbate changes the thiol-specific antioxidant paradigm, revealing another function of vitamin C. Proceedings of the National Academy of Sciences of the United States of America. 2007;104(12):4886-91.
706. Rhee SG, Kang SW, Chang TS, Jeong W, Kim K. Peroxiredoxin, a novel family of peroxidases. IUBMB Life. 2001;52(1-2):35-41.
707. Vaz M, Machireddy N, Irving A, Potteti HR, Chevalier K, Kalvakolanu D, et al. Oxidant-induced cell death and Nrf2-dependent antioxidative response are controlled by Fra-1/AP-1. Molecular and Cellular Biology. 2012;32(9):1694-709.
708. Cullinan SB, Gordan JD, Jin J, Harper JW, Diehl JA. The Keap1-BTB protein is an adaptor that bridges Nrf2 to a Cul3-based E3 ligase: Oxidative stress sensing by a Cul3-Keap1 ligase. Molecular and Cellular Biology. 2004;24(19):8477-86.
709. Hensen SMM, Heldens L, Van Enckevort CMW, Van Genesen ST, Pruijn GJM, Lubsen NH. Activation of the antioxidant response in methionine deprived human cells results in an HSF1-independent increase in HSPA1A mRNA levels. Biochimie. 2013;95(6):1245-51.
710. Reichard JF, Motz GT, Puga A. Heme oxygenase-1 induction by NRF2 requires inactivation of the transcriptional repressor BACH1. Nucleic Acids Research. 2007;35(21):7074-86.
711. Zakkar M, Van Der Heiden K, Luong LA, Chaudhury H, Cuhlmann S, Hamdulay SS, et al. Activation of Nrf2 in endothelial cells protects arteries from exhibiting a proinflammatory state. Arteriosclerosis, Thrombosis, and Vascular Biology. 2009;29(11):1851-7.
712. Zhou Y, Duan S, Zhou Y, Yu S, Wu J, Wu X, et al. Sulfiredoxin-1 Attenuates Oxidative Stress via Nrf2/ARE Pathway and 2-Cys Prdxs After Oxygen-Glucose Deprivation in Astrocytes. Journal of Molecular Neuroscience. 2015;55(4):941-50.
713. Kwak MK, Wakabayashi N, Itoh K, Motohashi H, Yamamoto M, Kensler TW. Modulation of gene expression by cancer chemopreventive dithiolethiones through the Keap1-Nrf2 pathway: Identification of novel gene clusters for cell survival. Journal of Biological Chemistry. 2003;278(10):8135-45.
714. Horiba M, Kamiya T, Hara H, Adachi T. Cytoprotective effects of mild plasma-activated medium against oxidative stress in human skin fibroblasts. Scientific Reports. 2017;7.
715. Ishaq M, Evans MDM, Ostrikov KK. Atmospheric pressure gas plasma-induced colorectal cancer cell death is mediated by Nox2-ASK1 apoptosis pathways and oxidative stress is mitigated by Srx-Nrf2 anti-oxidant system. Biochimica et Biophysica Acta - Molecular Cell Research. 2014;1843(12):2827-37.

716. Schmidt A, Dietrich S, Steuer A, Weltmann KD, Von Woedtke T, Masur K, et al. Non-thermal plasma activates human keratinocytes by stimulation of antioxidant and phase II pathways. Journal of Biological Chemistry. 2015;290(11):6731-50.
717. Hou J, Ma J, Yu KN, Li W, Cheng C, Bao L, et al. Non-thermal plasma treatment altered gene expression profiling in non-small-cell lung cancer A549 cells. BMC Genomics. 2015;16(1).
718. Karin M, Hunter T. Transcriptional control by protein phosphorylation: signal transmission from the cell surface to the nucleus. Current Biology. 1995;5(7):747-57.
719. Karin M, Shaulian E. AP-1: Linking hydrogen peroxide and oxidative stress to the control of cell proliferation and death. IUBMB Life. 2001;52(1-2):17-24.
720. Birben E, Sahiner UM, Sackesen C, Erzurum S, Kalayci O. Oxidative stress and antioxidant defense. World Allergy Organization Journal. 2012;5(1):9-19.
721. Melino G, Bernassola F, Knight RA, Corasaniti MT, Nistico G, Finazzi-Agro A. S-nitrosylation regulates apoptosis. Nature. 1997;388(6641):432-3.
722. Ozben T. Oxidative stress and apoptosis: Impact on cancer therapy. Journal of Pharmaceutical Sciences. 2007;96(9):2181-96.
723. Glick D, Barth S, Macleod KF. Autophagy: Cellular and molecular mechanisms. Journal of Pathology. 2010;221(1):3-12.
724. Pankiv S, Clausen TH, Lamark T, Brech A, Bruun JA, Outzen H, et al. p62/SQSTM1 binds directly to Atg8/LC3 to facilitate degradation of ubiquitinated protein aggregates by autophagy*[S]. Journal of Biological Chemistry. 2007;282(33):24131-45.
725. Duran A, Linares JF, Galvez AS, Wikenheiser K, Flores JM, Diaz-Meco MT, et al. The Signaling Adaptor p62 Is an Important NF-κB Mediator in Tumorigenesis. Cancer Cell. 2008;13(4):343-54.
726. Jain A, Lamark T, Sjøttem E, Larsen KB, Awuh JA, Øvervatn A, et al. p62/SQSTM1 is a target gene for transcription factor NRF2 and creates a positive feedback loop by inducing antioxidant response element-driven gene transcription. Journal of Biological Chemistry. 2010;285(29):22576-91.
727. Lee J, Giordano S, Zhang J. Autophagy, mitochondria and oxidative stress: Cross-talk and redox signalling. Biochemical Journal. 2012;441(2):523-40.
728. Taguchi K, Motohashi H, Yamamoto M. Molecular mechanisms of the Keap1-Nrf2 pathway in stress response and cancer evolution. Genes to Cells. 2011;16(2):123-40.
729. Anastasiou D, Poulogiannis G, Asara JM, Boxer MB, Jiang JK, Shen M, et al. Inhibition of pyruvate kinase M2 by reactive oxygen species contributes to cellular antioxidant responses. Science. 2011;334(6060):1278-83.
730. Fiaschi T, Marini A, Giannoni E, Taddei ML, Gandellini P, De Donatis A, et al. Reciprocal metabolic reprogramming through lactate shuttle coordinately influences tumor-stroma interplay. Cancer Research. 2012;72(19):5130-40.
731. Diehn M, Cho RW, Lobo NA, Kalisky T, Dorie MJ, Kulp AN, et al. Association of reactive oxygen species levels and radioresistance in cancer stem cells. Nature. 2009;458(7239):780-3.
732. Zhang P, Singh A, Yegnasubramanian S, Esopi D, Kombairaju P, Bodas M, et al. Loss of kelch-like ECH-associated protein 1 function in prostate cancer cells causes chemoresistance and radioresistance and promotes tumor growth. Molecular Cancer Therapeutics. 2010;9(2):336-46.
733. Frohlich DA, McCabe MT, Arnold RS, Day ML. The role of Nrf2 in increased reactive oxygen species and DNA damage in prostate tumorigenesis. Oncogene. 2008;27(31):4353-62.
734. Khor TO, Fuentes F, Shu L, Paredes-Gonzalez X, Yang AY, Liu Y, et al. Epigenetic DNA methylation of antioxidative stress regulator NRF2 in human prostate cancer. Cancer Prevention Research. 2014;7(12):1186-97.
735. Thomsen MK, Bakiri L, Hasenfuss SC, Wu H, Morente M, Wagner EF. Loss of JUNB/AP-1 promotes invasive prostate cancer. Cell Death and Differentiation. 2015;22(4):574-82.
736. Vivanco I, Palaskas N, Tran C, Finn SP, Getz G, Kennedy NJ, et al. Identification of the JNK Signaling Pathway as a Functional Target of the Tumor Suppressor PTEN. Cancer Cell. 2007;11(6):555-69.

737. Hübner A, Mulholland DJ, Standen CL, Karasarides M, Cavanagh-Kyros J, Barrett T, et al. JNK and PTEN cooperatively control the development of invasive adenocarcinoma of the prostate. Proceedings of the National Academy of Sciences of the United States of America. 2012;109(30):12046-51.
738. Edwards J, Krishna NS, Mukherjee R, Bartlett JMS. The role of c-Jun and c-Fos expression in androgen-independent prostate cancer. Journal of Pathology. 2004;204(2):153-8.
739. Ouyang X, Jessen WJ, Al-Ahmadie H, Serio AM, Lin Y, Shih WJ, et al. Activator protein-1 transcription factors are associated with progression and recurrence of prostate cancer. Cancer Research. 2008;68(7):2132-44.
740. Livak KJ, Schmittgen TD. Analysis of Relative Gene Expression Data Using Real-Time Quantitative PCR and the 2−ΔΔCT Method. Methods. 2001;25(4):402-8.
741. Collas P. A chromatin immunoprecipitation protocol for small cell numbers. Methods in Molecular Biology2011. p. 179-93.
742. Qiagen. Data Analysis Center 2018 [Available from: http://www.qiagen.com/gb/shop/genes-and-pathways/data-analysis-center-overview-page/.
743. Ritchie ME, Phipson B, Wu D, Hu Y, Law CW, Shi W, et al. Limma powers differential expression analyses for RNA-sequencing and microarray studies. Nucleic Acids Research. 2015;43(7):e47.
744. Team RC. R: A language and environment for statistical computing. Foundation for Statistical Computing, Vienna, Austria2017 [Available from: https://www.R-project.org/.
745. Rahnenfuhrer AAaJ. topGO: Enrichment Analysis for Gene Ontology. R package version 2.28.0 ed2016.
746. Kanehisa M, Furumichi M, Tanabe M, Sato Y, Morishima K. KEGG: New perspectives on genomes, pathways, diseases and drugs. Nucleic Acids Research. 2017;45(D1):D353-D61.
747. NCBI. SNP Database 2018 [Available from: https://www.ncbi.nlm.nih.gov/snp/.
748. Chorley BN, Campbell MR, Wang X, Karaca M, Sambandan D, Bangura F, et al. Identification of novel NRF2-regulated genes by ChiP-Seq: Influence on retinoid X receptor alpha. Nucleic Acids Research. 2012;40(15):7416-29.
749. Halliwell B. Oxidative stress in cell culture: an under-appreciated problem? FEBS Letters. 2003;540(1):3-6.
750. Castro P, Creighton CJ, Ozen M, Bcrel D, Mims MP, Ittmann M. Genomic profiling of prostate cancers from African American men 1. Neoplasia. 2009;11(3):305-12.
751. Ren S, Wei GH, Liu D, Wang L, Hou Y, Zhu S, et al. Whole-genome and Transcriptome Sequencing of Prostate Cancer Identify New Genetic Alterations Driving Disease Progression [Figure presented]. European Urology. 2018;73(3):322-39.
752. Kurose K, Gilley K, Matsumoto S, Watson PH, Zhou XP, Eng C. Frequent somatic mutations in PTEN and TP53 are mutually exclusive in the stroma of breast carcinomas. Nature Genetics. 2002;32(3):355-7.
753. Hughes P, Marshall D, Reid Y, Parkes H, Gelber C. The costs of using unauthenticated, over-passaged cell lines: How much more data do we need? BioTechniques. 2007;43(5):575-86.
754. Pan C, Kumar C, Bohl S, Klingmueller U, Mann M. Comparative proteomic phenotyping of cell lines and primary cells to assess preservation of cell type-specific functions. Molecular and Cellular Proteomics. 2009;8(3):443-50.
755. Ryter SW, Choi AMK. Heme oxygenase-1: Redox regulation of a stress protein in lung and cell culture models. Antioxidants and Redox Signaling. 2005;7(1-2):80-91.
756. Chakrabarti A, Chen AW, Varner JD. A review of the mammalian unfolded protein response. Biotechnology and Bioengineering. 2011;108(12):2777-93.
757. Witkin SS, Kanninen TT, Sisti G. The role of Hsp70 in the regulation of autophagy in gametogenesis, pregnancy, and parturition. Advances in Anatomy Embryology and Cell Biology2017. p. 117-27.
758. Kim N, Kim JY, Yenari MA. Anti-inflammatory properties and pharmacological induction of Hsp70 after brain injury. Inflammopharmacology. 2012;20(3):177-85.

759. Bjørkøy G, Lamark T, Brech A, Outzen H, Perander M, Øvervatn A, et al. p62/SQSTM1 forms protein aggregates degraded by autophagy and has a protective effect on huntingtin-induced cell death. Journal of Cell Biology. 2005;171(4):603-14.
760. Slack DN, Seternes OM, Gabrielsen M, Keyse SM. Distinct Binding Determinants for ERK2/p38α and JNK MAP Kinases Mediate Catalytic Activation and Substrate Selectivity of MAP Kinase Phosphatase-1. Journal of Biological Chemistry. 2001;276(19):16491-500.
761. Keyse SM, Emslie EA. Oxidative stress and heat shock induce a human gene encoding a protein-tyrosine phosphatase. Nature. 1992;359(6396):644-7.
762. Chang TS, Jeong W, Woo HA, Sun ML, Park S, Sue GR. Characterization of mammalian sulfiredoxin and its reactivation of hyperoxidized peroxiredoxin through reduction of cysteine sulfinic acid in the active site to cysteine. Journal of Biological Chemistry. 2004;279(49):50994-1001.
763. Hyun AW, Jeong W, Chang TS, Kwang JP, Sung JP, Jeong SY, et al. Reduction of cysteine sulfinic acid by sulfiredoxin is specific to 2-Cys peroxiredoxins. Journal of Biological Chemistry. 2005;280(5):3125-8.
764. Wood ZA, Schröder E, Harris JR, Poole LB. Structure, mechanism and regulation of peroxiredoxins. Trends in Biochemical Sciences. 2003;28(1):32-40.
765. Lee S, Kim SM, Lee RT. Thioredoxin and thioredoxin target proteins: From molecular mechanisms to functional significance. Antioxidants and Redox Signaling. 2013;18(10):1165-207.
766. Wu W, Zhao S. Metabolic changes in cancer: Beyond the Warburg effect. Acta Biochimica et Biophysica Sinica. 2013;45(1):18-26.
767. Jansen RJ, Robinson DP, Stolzenberg-Solomon RZ, Bamlet WR, Tan X, Cunningham JM, et al. Polymorphisms in metabolism/antioxidant genes may mediate the effect of dietary intake on pancreatic cancer risk. Pancreas. 2013;42(7):1043-53.
768. Oestergaard MZ, Tyrer J, Cebrian A, Shah M, Dunning AM, Ponder BAJ, et al. Interactions between genes involved in the antioxidant defence system and breast cancer risk. British Journal of Cancer. 2006;95(4):525-31.
769. Leone A, Roca MS, Ciardiello C, Costantini S, Budillon A. Oxidative Stress Gene Expression Profile Correlates with Cancer Patient Poor Prognosis: Identification of Crucial Pathways Might Select Novel Therapeutic Approaches. Oxidative Medicine and Cellular Longevity. 2017;2017.
770. Menegon S, Columbano A, Giordano S. The Dual Roles of NRF2 in Cancer. Trends in Molecular Medicine. 2016;22(7):578-93.
771. Frame FM, Savoie H, Bryden F, Giuntini F, Mann VM, Simms MS, et al. Mechanisms of growth inhibition of primary prostate epithelial cells following gamma irradiation or photodynamic therapy include senescence, necrosis, and autophagy, but not apoptosis. Cancer Medicine. 2016;5(1):61-73.
772. Czarnek M, Bereta J. SmartFlares fail to reflect their target transcripts levels. Scientific Reports. 2017;7(1).
773. Gilfillan GD, Hughes T, Sheng Y, Hjorthaug HS, Straub T, Gervin K, et al. Limitations and possibilities of low cell number ChIP-seq. BMC Genomics. 2012;13(1).
774. Brown S, Adrian TEO, Pauklin S, Hannan N, Cho CHH, Lim B, et al. Activin/nodal signaling controls divergent transcriptional networks in human embryonic stem cells and in endoderm progenitors. Stem Cells. 2011;29(8):1176-85.
775. Arrigoni L, Richter AS, Betancourt E, Bruder K, Diehl S, Manke T, et al. Standardizing chromatin research: A simple and universal method for ChIP-seq. Nucleic Acids Research. 2015;44(7).
776. Shepherd EG, Zhao Q, Welty SE, Hansen TN, Smith CV, Liu Y. The function of mitogen-activated protein kinase phosphatase-1 in peptidoglycan-stimulated macrophages. Journal of Biological Chemistry. 2004;279(52):54023-31.
777. Ishaq M, Kumar S, Varinli H, Han ZJ, Rider AE, Evans MDM, et al. Atmospheric gas plasma-induced ROS production activates TNF-ASK1 pathway for the induction of melanoma cancer cell apoptosis. Molecular Biology of the Cell. 2014;25(9):1523-31.

778. Bubici C, Papa S. JNK signalling in cancer: In need of new, smarter therapeutic targets. British Journal of Pharmacology. 2014;171(1):24-37.
779. Yan D, Sherman JH, Keidar M. Cold atmospheric plasma, a novel promising anti-cancer treatment modality. Oncotarget. 2017;8(9):15977-95.
780. Guerrero-Preston R, Ogawa T, Uemura M, Shumulinsky G, Valle BL, Pirini F, et al. Cold atmospheric plasma treatment selectively targets head and neck squamous cell carcinoma cells. International Journal of Molecular Medicine. 2014;34(4):941-6.
781. Ja Kim S, Min Joh H, Chung TH. Production of intracellular reactive oxygen species and change of cell viability induced by atmospheric pressure plasma in normal and cancer cells. Applied Physics Letters. 2013;103(15).
782. Kim SJ, Chung TH. Cold atmospheric plasma jet-generated RONS and their selective effects on normal and carcinoma cells. Scientific Reports. 2016;6.
783. Taguchi K, Yamamoto M. The KEAP1–NRF2 System in Cancer. Frontiers in Oncology. 2017;7:85.
784. Frame FM, Noble AR, Klein S, Walker HF, Suman R, Kasprowicz R, et al. Tumor heterogeneity and therapy resistance - implications for future treatments of prostate cancer. Journal of Cancer Metastasis and Treatment. 2017;3(12):302-14.
785. Cai B, Chang SH, Becker EBE, Bonni A, Xia Z. p38 MAP kinase mediates apoptosis through phosphorylation of Bim EL at Ser-65. Journal of Biological Chemistry. 2006;281(35):25215-22.
786. Cavigelli M, Li WW, Lin A, Su B, Yoshioka K, Karin M. The tumor promoter arsenite stimulates AP-1 activity by inhibiting a JNK phosphatase. EMBO Journal. 1996;15(22):6269-79.
787. Angel P, Hattori K, Smeal T, Karin M. The jun proto-oncogene is positively autoregulated by its product, Jun/AP-1. Cell. 1988;55(5):875-85.
788. Meier-Stiegen F, Schwanbeck R, Bernoth K, Martini S, Hieronymus T, Ruau D, et al. Activated Notch1 target genes during embryonic cell differentiation depend on the cellular context and include lineage determinants and inhibitors. PLoS ONE. 2010;5(7).
789. Koltsova SV, Shilov B, Birulina JG, Akimova OA, Haloui M, Kapilevich LV, et al. Transcriptomic changes triggered by hypoxia: Evidence for HIF-1α -independent, [Na+]<inf>i</inf>/[K+]<inf>i</inf>-mediated, excitation-transcription coupling. PLoS ONE. 2014;9(11).
790. Onik G, Mikus P, Rubinsky B. Irreversible electroporation: Implications for prostate ablation. Technology in Cancer Research and Treatment. 2007;6(4):295-300.
791. Xu D, Wang B, Xu Y, Chen Z, Cui Q, Yang Y, et al. Intracellular ROS mediates gas plasma-facilitated cellular transfection in 2D and 3D cultures. Scientific Reports. 2016;6:27872.
792. Greenwald IS, Sternberg PW, Robert Horvitz H. The lin-12 locus specifies cell fates in caenorhabditis elegans. Cell. 1983;34(2):435-44.
793. Doe CQ, Goodman CS. Early events in insect neurogenesis. I. Development and segmental differences in the pattern of neuronal precursor cells. Developmental Biology. 1985;111(1):193-205.
794. Hartenstein V, Campos-Ortega JA. The peripheral nervous system of mutants of early neurogenesis in Drosophila melanogaster. Roux's Archives of Developmental Biology. 1986;195(4):210-21.
795. Dontu G, Jackson KW, McNicholas E, Kawamura MJ, Abdallah WM, Wicha MS. Role of Notch signaling in cell-fate determination of human mammary stem/progenitor cells. Breast Cancer Research. 2004;6(6).
796. Koch U, Lehal R, Radtke F. Stem cells living with a Notch. Development (Cambridge). 2013;140(4):689-704.
797. Farnie G, Clarke RB. Mammary stem cells and breast cancer - Role of notch signalling. Stem Cell Reviews. 2007;3(2):169-75.
798. Hao L, Rizzo P, Osipo C, Pannuti A, Wyatt D, Cheung LWK, et al. Notch-1 activates estrogen receptor-α-dependent transcription via IKKα in breast cancer cells. Oncogene. 2010;29(2):201-13.

799. Zhang XP, Zheng G, Zou L, Liu HL, Hou LH, Zhou P, et al. Notch activation promotes cell proliferation and the formation of neural stem cell-like colonies in human glioma cells. Molecular and Cellular Biochemistry. 2008;307(1-2):101-8.
800. Weng AP, Ferrando AA, Lee W, Morris Iv JP, Silverman LB, Sanchez-Irizarry C, et al. Activating mutations of NOTCH1 in human T cell acute lymphoblastic leukemia. Science. 2004;306(5694):269-71.
801. Prins GS, Putz O. Molecular signaling pathways that regulate prostate gland development. Differentiation; research in biological diversity. 2008;76(6):641-59.
802. Belandia B, Powell SM, García-Pedrero JM, Walker MM, Bevan CL, Parker MG. Hey1, a mediator of Notch signaling, is an androgen receptor corepressor. Molecular and Cellular Biology. 2005;25(4):1425-36.
803. Palomero T, Dominguez M, Ferrando AA. The role of the PTEN/AKT pathway in NOTCH1-induced leukemia. Cell Cycle. 2008;7(8):965-70.
804. Whelan JT, Kellogg A, Shewchuk BM, Hewan-Lowe K, Bertrand FE. Notch-1 signaling is lost in prostate adenocarcinoma and promotes PTEN gene expression. Journal of Cellular Biochemistry. 2009;107(5):992-1001.
805. Hafeez BB, Adhami VM, Asim M, Siddiqui IA, Bhat KM, Zhong W, et al. Targeted knockdown of notchl inhibits invasion of human prostate cancer cells concomitant with inhibition of matrix metalloproteinase-9 and urokinase plasminogen activator. Clinical Cancer Research. 2009;15(2):452-9.
806. Ross AE, Marchionni L, Vuica-Ross M, Cheadle C, Fan J, Berman DM, et al. Gene expression pathways of high grade localized prostate cancer. Prostate. 2011;71(14):1568-78.
807. Deng G, Ma L, Meng Q, Ju X, Jiang K, Jiang P, et al. Notch signaling in the prostate: critical roles during development and in the hallmarks of prostate cancer biology. Journal of Cancer Research and Clinical Oncology. 2016;142(3):531-47.
808. Carvalho FLF, Simons BW, Eberhart CG, Berman DM. Notch signaling in prostate cancer: A moving target. Prostate. 2014;74(9):933-45.
809. Mohamed AA, Tan SH, Xavier CP, Katta S, Huang W, Ravindranath L, et al. Synergistic activity with NOTCH inhibition and androgen ablation in ERG-positive prostate cancer cells. Molecular Cancer Research. 2017;15(10):1308-17.
810. Wang J, Wakeman TP, Lathia JD, Hjelmeland AB, Wang XF, White RR, et al. Notch promotes radioresistance of glioma stem cells. Stem Cells. 2010;28(1):17-28.
811. Moellering RE, Cornejo M, Davis TN, Bianco CD, Aster JC, Blacklow SC, et al. Direct inhibition of the NOTCH transcription factor complex. Nature. 2009;462(7270):182-8.
812. Wu Y, Cain-Hom C, Choy L, Hagenbeek TJ, De Leon GP, Chen Y, et al. Therapeutic antibody targeting of individual Notch receptors. Nature. 2010;464(7291):1052-7.
813. Pirot P, Grunsven LAV, Marine JC, Huylebroeck D, Bellefroid EJ. Direct regulation of the Nrarp gene promoter by the Notch signaling pathway. Biochemical and Biophysical Research Communications. 2004;322(2):526-34.
814. MacGrogan D, D'Amato G, Travisano S, Martinez-Poveda B, Luxán G, Del Monte-Nieto G, et al. Sequential Ligand-Dependent Notch Signaling Activation Regulates Valve Primordium Formation and Morphogenesis. Circulation Research. 2016;118(10):1480-97.
815. Yang Y, Duan W, Liang Z, Yi W, Yan J, Wang N, et al. Curcumin attenuates endothelial cell oxidative stress injury through Notch signaling inhibition. Cellular Signalling. 2013;25(3):615-29.
816. Mo JS, Yoon JH, Ann EJ, Ahn JS, Baek HJ, Lee HJ, et al. Notch1 modulates oxidative stress induced cell death through suppression of apoptosis signal-regulating kinase 1. Proceedings of the National Academy of Sciences of the United States of America. 2013;110(17):6865-70.
817. Lamar E, Deblandre G, Wettstein D, Gawantka V, Pollet N, Niehrs C, et al. Nrarp is a novel intracellular component of the Notch signaling pathway. Genes and Development. 2001;15(15):1885-99.
818. Phng LK, Potente M, Leslie JD, Babbage J, Nyqvist D, Lobov I, et al. Nrarp Coordinates Endothelial Notch and Wnt Signaling to Control Vessel Density in Angiogenesis. Developmental Cell. 2009;16(1):70-82.

819. Imaoka T, Okutani T, Daino K, Iizuka D, Nishimura M, Shimada Y. Overexpression of NOTCH-regulated ankyrin repeat protein is associated with breast cancer cell proliferation. Anticancer Research. 2014;34(5):2165-72.
820. Zhang M, Qin Y, Zuo B, Gong W, Zhang S, Gong Y, et al. Overexpression of NOTCH-regulated Ankyrin Repeat Protein is associated with papillary thyroid carcinoma progression. PLoS ONE. 2017;12(2).
821. Zhu P, Wang Y, Du Y, He L, Huang G, Zhang G, et al. C8orf4 negatively regulates self-renewal of liver cancer stem cells via suppression of NOTCH2 signalling. Nature Communications. 2015;6.
822. Lasorella A, Benezra R, Iavarone A. The ID proteins: Master regulators of cancer stem cells and tumour aggressiveness. Nature Reviews Cancer. 2014;14(2):77-91.
823. Fischer A, Gessler M. Delta-Notch-and then? Protein interactions and proposed modes of repression by Hes and Hey bHLH factors. Nucleic Acids Research. 2007;35(14):4583-96.
824. Payankaulam S, Li LM, Arnosti DN. Transcriptional Repression: Conserved and Evolved Features. Current Biology. 2010;20(17):R764-R71.
825. Nakaya HI, Beckedorff FC, Baldini ML, Fachel AA, Reis EM, Verjovski-Almeida S. Splice variants of TLE family genes and up-regulation of a TLE3 isoform in prostate tumors. Biochemical and Biophysical Research Communications. 2007;364(4):918-23.
826. Devgan V, Mammucari C, Millar SE, Brisken C, Dotto GP. p21WAF1/Cip1 is a negative transcriptional regulator of Wnt4 expression downstream of Notch1 activation. Genes and Development. 2005;19(12):1485-95.
827. Riccio O, van Gijn ME, Bezdek AC, Pellegrinet L, van Es JH, Zimber-Strobl U, et al. Loss of intestinal crypt progenitor cells owing to inactivation of both Notch1 and Notch2 is accompanied by derepression of CDK inhibitors p27Kip1 and p57Kip2. EMBO Reports. 2008;9(4):377-83.
828. Xu L, Zhang Y, Guo R, Shen W, Qi Y, Wang Q, et al. HES1 promotes extracellular matrix protein expression and inhibits proliferation and migration in human trabecular meshwork cells under oxidative stress. Oncotarget. 2017;8(13):21818-33.
829. Kageyama R, Ohtsuka T, Kobayashi T. The Hes gene family: Repressors and oscillators that orchestrate embryogenesis. Development. 2007;134(7):1243-51.
830. Itoh F, Itoh S, Goumans MJ, Valdimarsdottir G, Iso T, Dotto GP, et al. Synergy and antagonism between Notch and BMP receptor signaling pathways in endothelial cells. EMBO Journal. 2004;23(3):541-51.
831. Elagib KE, Xiao M, Hussaini IM, Delehanty LL, Palmer LA, Racke FK, et al. Jun blockade of erythropoiesis: Role for repression of GATA-1 by HERP2. Molecular and Cellular Biology. 2004;24(17):7779-94.
832. Sikder HA, Devlin MK, Dunlap S, Ryu B, Alani RM. Id proteins in cell growth and tumorigenesis. Cancer Cell. 2003;3(6):525-30.
833. Reynaud-Deonauth S, Zhang H, Afouda A, Taillefert S, Beatus P, Kloc M, et al. Notch signaling is involved in the regulation of Id3 gene transcription during Xenopus embryogenesis. Differentiation; research in biological diversity. 2002;69(4-5):198-208.
834. Zhang P, Zhao Y, Sun XH. Notch-regulated periphery B cell differentiation involves suppression of E protein function. Journal of Immunology. 2013;191(2):726-36.
835. Chadwick N, Zeef L, Portillo V, Fennessy C, Warrander F, Hoyle S, et al. Identification of novel Notch target genes in T cell leukaemia. Molecular Cancer. 2009;8.
836. Seymour PA, Freude KK, Tran MN, Mayes EE, Jensen J, Kist R, et al. SOX9 is required for maintenance of the pancreatic progenitor cell pool. Proceedings of the National Academy of Sciences of the United States of America. 2007;104(6):1865-70.
837. Capaccione KM, Hong X, Morgan KM, Liu W, Bishop MJ, Liu L, et al. Sox9 mediates Notch1-induced mesenchymal features in lung adenocarcinoma. Oncotarget. 2014;5(11):3636-50.
838. Hosokawa S, Furuyama K, Horiguchi M, Aoyama Y, Tsuboi K, Sakikubo M, et al. Impact of Sox9 dosage and hes1-mediated notch signaling in controlling the plasticity of adult pancreatic duct cells in mice. Scientific Reports. 2014;5.

839. Kohn A, Rutkowski TP, Liu Z, Mirando AJ, Zuscik MJ, O'Keefe RJ, et al. Notch signaling controls chondrocyte hypertrophy via indirect regulation of Sox9. Bone Research. 2015;3.
840. Bland CE, Kimberly P, Rand MD. Notch-induced proteolysis and nuclear localization of the delta ligand. Journal of Biological Chemistry. 2003;278(16):13607-10.
841. LaVoie MJ, Selkoe DJ. The Notch Ligands, Jagged and Delta, Are Sequentially Processed by α-Secretase and Presenilin/γ-Secretase and Release Signaling Fragments. Journal of Biological Chemistry. 2003;278(36):34427-37.
842. Six E, Ndiaye D, Laâbi Y, Brou C, Gupta-Rossi N, Israël A, et al. The Notch ligand Delta1 is sequentially cleaved by an ADAM protease and γ-secretase. Proceedings of the National Academy of Sciences of the United States of America. 2003;100(13):7638-43.
843. Jung J, Mo JS, Kim MY, Ann EJ, Yoon JH, Park HS. Regulation of notch1 signaling by delta-like ligand 1 intracellular domain through physical interaction. Molecules and Cells. 2011;32(2):161-5.
844. Kim MY, Jung J, Mo JS, Ann EJ, Ahn JS, Yoon JH, et al. The intracellular domain of Jagged-1 interacts with Notch1 intracellular domain and promotes its degradation through Fbw7 E3 ligase. Experimental Cell Research. 2011;317(17):2438-46.
845. Kolev V, Kacer D, Trifonova R, Small D, Duarte M, Soldi R, et al. The intracellular domain of Notch ligand Delta1 induces cell growth arrest. FEBS Letters. 2005;579(25):5798-802.
846. Hiratochi M, Nagase H, Kuramochi Y, Koh CS, Ohkawara T, Nakayama K. The Delta intracellular domain mediates TGF-β/Activin signaling through binding to Smads and has an important bi-directional function in the Notch-Delta signaling pathway. Nucleic Acids Research. 2007;35(3):912-22.
847. Forghany Z, Robertson F, Lundby A, Olsen JV, Baker DA. Control of endothelial cell tube formation by Notch ligand intracellular domain interactions with activator protein 1 (AP-1). Journal of Biological Chemistry. 2018;293(4):1229-42.
848. Ascano JM, Beverly LJ, Capobianco AJ. The C-terminal PDZ-ligand of JAGGED1 is essential for cellular transformation. Journal of Biological Chemistry. 2003;278(10):8771-9.
849. Liebler SS, Feldner A, Adam MG, Korff T, Augustin HG, Fischer A. No Evidence for a Functional Role of Bi-Directional Notch Signaling during Angiogenesis. PLoS ONE. 2012;7(12).
850. Sassone-Corsi P, Sisson JC, Verma IM. Transcriptional autoregulation of the proto-oncogene fos. Nature. 1988;334(6180):314-9.
851. Nunes-Xavier C, Romá-Mateo C, Ríos P, Tárrega C, Cejudo-Marín R, Tabernero L, et al. Dual-specificity MAP kinase phosphatases as targets of cancer treatment. Anti-Cancer Agents in Medicinal Chemistry. 2011;11(1):109-32.
852. Caunt CJ, Keyse SM. Dual-specificity MAP kinase phosphatases (MKPs): Shaping the outcome of MAP kinase signalling. FEBS Journal. 2013;280(2):489-504.
853. Tanoue T, Moriguchi T, Nishida E. Molecular cloning and characterization of a novel dual specificity phosphatase, MKP-5. J Biol Chem. 1999;274.
854. Theodosiou A, Smith A, Gillieron C, Arkinstall S, Ashworth A. MKP5, a new member of the MAP kinase phosphatase family, which selectively dephosphorylates stress-activated kinases. Oncogene. 1999;18.
855. Zhang T, Inesta-Vaquera F, Niepel M, Zhang J, Ficarro SB, MacHleidt T, et al. Discovery of potent and selective covalent inhibitors of JNK. Chemistry and Biology. 2012;19(1):140-54.
856. Gilmore TD. Introduction to NF-κB: Players, pathways, perspectives. Oncogene. 2006;25(51):6680-4.
857. Sun SC. Non-canonical NF-κB signaling pathway. Cell Research. 2011;21(1):71-85.
858. Murphy EP, Crean D. Molecular Interactions between NR4A Orphan Nuclear Receptors and NF-κB Are Required for Appropriate Inflammatory Responses and Immune Cell Homeostasis. Biomolecules. 2015;5(3):1302-18.
859. Mohan HM, Aherne CM, Rogers AC, Baird AW, Winter DC, Murphy EP. Molecular pathways: The role of NR4A orphan nuclear receptors in cancer. Clinical Cancer Research. 2012;18(12):3223-8.

860. Kurakula K, Koenis DS, van Tiel CM, de Vries CJM. NR4A nuclear receptors are orphans but not lonesome. Biochimica et Biophysica Acta - Molecular Cell Research. 2014;1843(11):2543-55.
861. Han YH, Cao X, Lin B, Lin F, Kolluri SK, Stebbins J, et al. Regulation of Nur77 nuclear export by c-Jun N-terminal kinase and Akt. Oncogene. 2006;25(21):2974-86.
862. Jehn BM, Bielke W, Pear WS, Osborne BA. Cutting edge: Protective effects of Notch-1 on TCR-induced apoptosis. Journal of Immunology. 1999;162(2):635-8.
863. G RJ. Notch 1 Mediated Inhibition of Nur77-induced apoptosis: Implications for T-cell Leukemia. Open Access Dissertations2010.
864. Bonta PI, Van Tiel CM, Vos M, Pols TWH, Van Thienen JV, Ferreira V, et al. Nuclear receptors Nur77, Nurr1, and NOR-1 expressed in atherosclerotic lesion macrophages reduce lipid loading and inflammatory responses. Arteriosclerosis, Thrombosis, and Vascular Biology. 2006;26(10):2288-94.
865. Pei L, Castrillo A, Chen M, Hoffmann A, Tontonoz P. Induction of NR4A orphan nuclear receptor expression in macrophages in response to inflammatory stimuli. Journal of Biological Chemistry. 2005;280(32):29256-62.
866. Hanna RN, Shaked I, Hubbeling HG, Punt JA, Wu R, Herrley E, et al. NR4A1 (Nur77) deletion polarizes macrophages toward an inflammatory phenotype and increases atherosclerosis. Circulation Research. 2012;110(3):416-27.
867. Li L, Liu Y, Chen HZ, Li FW, Wu JF, Zhang HK, et al. Impeding the interaction between Nur77 and p38 reduces LPS-induced inflammation. Nature Chemical Biology. 2015;11(5):339-46.
868. Saijo K, Winner B, Carson CT, Collier JG, Boyer L, Rosenfeld MG, et al. A Nurr1/CoREST Pathway in Microglia and Astrocytes Protects Dopaminergic Neurons from Inflammation-Induced Death. Cell. 2009;137(1):47-59.
869. Calvayrac O, Rodríguez-Calvo R, Martí-Pamies I, Alonso J, Ferrán B, Aguiló S, et al. NOR-1 modulates the inflammatory response of vascular smooth muscle cells by preventing NFκB activation. Journal of Molecular and Cellular Cardiology. 2015;80:34-44.
870. Aherne CM, McMorrow J, Kane D, FitzGerald O, Mix KS, Murphy EP. Identification of NR4A2 as a transcriptional activator of IL-8 expression in human inflammatory arthritis. Molecular Immunology. 2009;46(16):3345-57.
871. Crean D, Cummins EP, Bahar B, Mohan H, McMorrow JP, Murphy EP. Adenosine modulates NR4A orphan nuclear receptors to attenuate hyperinflammatory responses in monocytic cells. Journal of Immunology. 2015;195(4):1436-48.
872. McEvoy C, de Gaetano M, Giffney HE, Bahar B, Cummins EP, Brennan EP, et al. NR4A receptors differentially regulate NF-κB signaling in myeloid cells. Frontiers in Immunology. 2017;8(JAN).
873. Wartz IE, O'Rourke KM, Zhou H, Eby M, Aravind L, Seshagiri S, et al. De-ubiquitination and ubiquitin ligase domains of A20 downregulate NF-κB signalling. Nature. 2004;430(7000):694-9.
874. Sanz L, Sanchez P, Lallena MJ, Diaz-Meco MT, Moscat J. The interaction of p62 with RIP links the atypical PKCs to NF-κB activation. EMBO Journal. 1999;18(11):3044-53.
875. Eliopoulos AG, Das S, Tsichlis PN. The tyrosine kinase Syk regulates TPL2 activation signals. Journal of Biological Chemistry. 2006;281(3):1371-80.
876. Newton K. RIPK1 and RIPK3: Critical regulators of inflammation and cell death. Trends in Cell Biology. 2015;25(6):347-53.
877. Moran ST, Haider K, Ow Y, Milton P, Chen L, Pillai S. Protein kinase C-associated kinase can activate NFκB in both a kinase-dependent and a kinase-independent manner. Journal of Biological Chemistry. 2003;278(24):21526-33.
878. Bahr C, Rohwer A, Stempka L, Rincke G, Marks F, Gschwendt M. DIK, a novel protein kinase that interacts with protein kinase Cδ: Cloning, characterization, and gene analysis. Journal of Biological Chemistry. 2000;275(46):36350-7.
879. Adams S, Munz B. RIP4 is a target of multiple signal transduction pathways in keratinocytes: Implications for epidermal differentiation and cutaneous wound repair. Experimental Cell Research. 2010;316(1):126-37.

880. Mitchell K, O'Sullivan J, Missero C, Blair E, Richardson R, Anderson B, et al. Exome sequence identifies RIPK4 as the Bartsocas-Papas syndrome locus. American Journal of Human Genetics. 2012;90(1):69-75.
881. Muzio M, Ni J, Feng P, Dixit VM. IRAK (Pelle) family member IRAK-2 and MyD88 as proximal mediators of IL- 1 signaling. Science. 1997;278(5343):1612-5.
882. Ron D, Walter P. Signal integration in the endoplasmic reticulum unfolded protein response. Nature Reviews Molecular Cell Biology. 2007;8(7):519-29.
883. Bravo R, Parra V, Gatica D, Rodriguez AE, Torrealba N, Paredes F, et al. Endoplasmic Reticulum and the Unfolded Protein Response. Dynamics and Metabolic Integration. International Review of Cell and Molecular Biology2013. p. 215-90.
884. Youn HD, Sun L, Prywes R, Liu JO. Apoptosis of T cells mediated by Ca2+-induced release of the transcription factor MEF2. Science. 1999;286(5440):790-3.
885. Alphonse MP, Duong TT, Shumitzu C, Hoang TL, McCrindle BW, Franco A, et al. Inositol-triphosphate 3-Kinase C mediates inflammasome activation and treatment response in Kawasaki disease. Journal of Immunology. 2016;197(9):3481-9.
886. Ji AR, Ku SY, Cho MS, Kim YY, Kim YJ, Oh SK, et al. Reactive oxygen species enhance differentiation of human embryonic stem cells into mesendodermal lineage. Experimental and Molecular Medicine. 2010;42(3):175-86.
887. Sato A, Okada M, Shibuya K, Watanabe E, Seino S, Narita Y, et al. Pivotal role for ROS activation of p38 MAPK in the control of differentiation and tumor-initiating capacity of glioma-initiating cells. Stem Cell Research. 2014;12(1):119-31.
888. Sampson N, Koziel R, Zenzmaier C, Bubendorf L, Plas E, Jansen-Dürr P, et al. ROS signaling by NOX4 drives fibroblast-to-myofibroblast differentiation in the diseased prostatic stroma. Molecular Endocrinology. 2011;25(3):503-15.
889. Small C, Ramroop J, Otazo M, Huang LH, Saleque S, Govind S. An unexpected link between notch signaling and ROS in restricting the differentiation of hematopoietic progenitors in Drosophila. Genetics. 2014;197(2):471-83.
890. Paul MK, Bisht B, Darmawan DO, Chiou R, Ha VL, Wallace WD, et al. Dynamic changes in intracellular ROS levels regulate airway basal stem cell homeostasis through Nrf2-dependent notch signaling. Cell Stem Cell. 2014;15(2):199-214.
891. Wakabayashi N, Chartoumpekis DV, Kensler TW. Crosstalk between Nrf2 and Notch signaling. Free Radical Biology and Medicine. 2015;88(Part B):158-67.
892. Wang XD, Leow CC, Zha J, Tang Z, Modrusan Z, Radtke F, et al. Notch signaling is required for normal prostatic epithelial cell proliferation and differentiation. Developmental Biology. 2006;290(1):66-80.
893. Levesque MJ, Ginart P, Wei Y, Raj A. Visualizing SNVs to quantify allele-specific expression in single cells. Nature Methods. 2013;10(9):865-7.
894. Levesque MJ, Raj A. Single-chromosome transcriptional profiling reveals chromosomal gene expression regulation. Nature Methods. 2013;10(3):246-8.
895. Dong X, Weng Z. The correlation between histone modifications and gene expression. Epigenomics. 2013;5(2):113-6.
896. Krogan NJ, Kim M, Tong A, Golshani A, Cagney G, Canadien V, et al. Methylation of histone H3 by Set2 in Saccharomyces cerevisiae is linked to transcriptional elongation by RNA polymerase II. Molecular and Cellular Biology. 2003;23(12):4207-18.
897. Krogan NJ, Dover J, Wood A, Schneider J, Heidt J, Boateng MA, et al. The Paf1 complex is required for histone H3 methylation by COMPASS and Dot1p: Linking transcriptional elongation to histone methylation. Molecular Cell. 2003;11(3):721-9.
898. Hilton IB, D'Ippolito AM, Vockley CM, Thakore PI, Crawford GE, Reddy TE, et al. Epigenome editing by a CRISPR-Cas9-based acetyltransferase activates genes from promoters and enhancers. Nature Biotechnology. 2015;33(5):510-7.
899. Kearns NA, Pham H, Tabak B, Genga RM, Silverstein NJ, Garber M, et al. Functional annotation of native enhancers with a Cas9-histone demethylase fusion. Nature Methods. 2015;12(5):401-3.

900. Liu XS, Wu H, Ji X, Stelzer Y, Wu X, Czauderna S, et al. Editing DNA Methylation in the Mammalian Genome. Cell. 2016;167(1):233-47.e17.
901. Déjardin J, Kingston RE. Purification of Proteins Associated with Specific Genomic Loci. Cell. 2009;136(1):175-86.
902. Ide S, Dejardin J. End-targeting proteomics of isolated chromatin segments of a mammalian ribosomal RNA gene promoter. Nature Communications. 2015;6.
903. Tsui C, Inouye C, Levy M, Lu A, Florens L, Washburn MP, et al. DCas9-targeted locus-specific protein isolation method identifies histone gene regulators. Proceedings of the National Academy of Sciences of the United States of America. 2018;115(12):E2734-E41.
904. Wang S, Kollipara RK, Humphries CG, Ma SH, Hutchinson R, Li R, et al. The ubiquitin ligase TRIM25 targets ERG for degradation in prostate cancer. Oncotarget. 2016;7(40):64921-31.
905. Harris IS, Treloar AE, Inoue S, Sasaki M, Gorrini C, Lee K, et al. Glutathione and Thioredoxin Antioxidant Pathways Synergize to Drive Cancer Initiation and Progression. Cancer Cell. 2015;27(2):211-22.
906. Halasi M, Wang M, Chavan TS, Gaponenko V, Hay N, Gartel AL. ROS inhibitor N-acetyl-L-cysteine antagonizes the activity of proteasome inhibitors. Biochemical Journal. 2013;454(2):201-8.
907. Bruening W, Giasson B, Mushynski W, Durham HD. Activation of stress-activated MAP protein kinases up-regulates expression of transgenes driven by the cytomegalovirus immediate/early promoter. Nucleic Acids Research. 1998;26(2):486-9.